ARISTOTLE UNIVERSITY OF THESSALONIKI
FACULTY OF SCIENCES
SCHOOL OF GEOLOGY

ANASTASIA G. GKEME
MSc Geologist

STUDY OF THE QUATERNARY EQUIDS OF GREECE: SYSTEMATICS, BIOSTRATIGRAPHY, PHYLOGENY, PALAEOECOLOGY

DISSERTATION THESIS

This research is co-financed by Greece and the European Union (European Social Fund-ESF) through the Operational Programme «Human Resources Development, Education and Lifelong Learning» in the context of the project "Strengthening Human Resources Research Potential via Doctorate Research - 2nd Cycle" (MIS-5000432), implemented by the State Scholarships Foundation (IKY).

THESSALONIKI
2023

ΑΡΙΣΤΟΤΕΛΕΙΟ ΠΑΝΕΠΙΣΤΗΜΙΟ ΘΕΣΣΑΛΟΝΙΚΗΣ
ΣΧΟΛΗ ΘΕΤΙΚΩΝ ΕΠΙΣΤΗΜΩΝ
ΤΜΗΜΑ ΓΕΩΛΟΓΙΑΣ

ΑΝΑΣΤΑΣΙΑ Γ. ΓΚΕΜΕ
MSc Γεωλόγος

ΜΕΛΕΤΗ ΤΩΝ ΤΕΤΑΡΤΟΓΕΝΩΝ ΙΠΠΟΕΙΔΩΝ ΤΗΣ ΕΛΛΑΔΑΣ: ΣΥΣΤΗΜΑΤΙΚΗ, ΒΙΟΣΤΡΩΜΑΤΟΓΡΑΦΙΑ, ΦΥΛΟΓΕΝΕΣΗ, ΠΑΛΑΙΟΟΙΚΟΛΟΓΙΑ

ΔΙΔΑΚΤΟΡΙΚΗ ΔΙΑΤΡΙΒΗ

Το έργο συγχρηματοδοτείται από την Ελλάδα και την Ευρωπαϊκή Ένωση (Ευρωπαϊκό Κοινωνικό Ταμείο) μέσω του Επιχειρησιακού Προγράμματος «Ανάπτυξη Ανθρώπινου Δυναμικού, Εκπαίδευση και Διά Βίου Μάθηση», στο πλαίσιο της Πράξης «Ενίσχυση του ανθρώπινου ερευνητικού δυναμικού μέσω της υλοποίησης διδακτορικής έρευνας - 2ος Κύκλος» (MIS-5000432), που υλοποιεί το Ίδρυμα Κρατικών Υποτροφιών (ΙΚΥ).

ΘΕΣΣΑΛΟΝΙΚΗ
2023

ANASTASIA G. GKEME
MSc Geologist

STUDY OF THE QUATERNARY EQUIDS OF GREECE: SYSTEMATICS, BIOSTRATIGRAPHY, PHYLOGENY, PALAEOECOLOGY

Prepared at the Department of Geology of the School of Geology of A.U.Th.
Submitted at the School of Geology of A.U.Th. on September 2023

Date of Oral Examination: 19/09/2023

Annex Number of the Scientific Annals of the School of Geology A.U.Th. N°: 236

Three-member Advisory Committee

Professor Emeritus George D. Koufos, Supervisor
Professor Dimitris S. Kostopoulos, Member of the Three-member Advisory Committee
Associate Professor Socrates Roussiakis, Member of the Three-member Advisory Committee

Examination Committee

Professor Emeritus George D. Koufos
Professor Dimitris S. Kostopoulos
Assoc. Professor Socrates Roussiakis
Former Professor Evangelia Tsoukala
Professor Dionisios Youlatos
CNRS Director Gildas Merceron
Assoc. Professor George Lyras

STUDY OF THE QUATERNARY EQUIDS OF GREECE: SYSTEMATICS, BIOSTRATIGRAPHY, PHYLOGENY, PALAEOECOLOGY – *Ph.D. Thesis*

ΜΕΛΕΤΗ ΤΩΝ ΤΕΤΑΡΤΟΓΕΝΩΝ ΙΠΠΟΕΙΔΩΝ ΤΗΣ ΕΛΛΑΔΑΣ: ΣΥΣΤΗΜΑΤΙΚΗ, ΒΙΟΣΤΡΩΜΑΤΟΓΡΑΦΙΑ, ΦΥΛΟΓΕΝΕΣΗ, ΠΑΛΑΙΟΟΙΚΟΛΟΓΙΑ. – *Διδακτορική Διατριβή*

Citation:
Gkeme A. G., 2023. Study of the Quaternary equids of Greece: systematics, biostratigraphy, phylogeny, palaeoecology. Ph.D. Thesis, School of Geology, Aristotle University of Thessaloniki, Annex Number of Scientific Annals of the School of Geology No 236, 289 pp.

Γκεμέ Α. Γ., 2023. Μελέτη των Τεταρτογενών ιπποειδών της Ελλάδας : συστηματική, βιοστρωματογραφία, φυλογένεση, παλαιοοικολογία. Διδακτορική Διατριβή, Τμήμα Γεωλογίας Α.Π.Θ., Αριθμός Παραρτήματος Επιστημονικής Επετηρίδας Τμ. Γεωλογίας Νο 236, 289 σελ.

Στην αδερφή μου και τη μητέρα μου

Preface

Equids are tremendously well documented in the fossil record, through time and space, with around 56 million years of evolutionary history. The evolution of the equids has been frequently cited as principal evidence of evolutionally history. In the past 40 years, many important discoveries have been made, which in conjunction with the new methods of precise geochronology, magnetostratigraphy and new cladistic methods, greatly improving the evolutionary trends of this group.

The arrival of the monodactyl equids in Eurasia, and their dispersion towards Europe, is one of the most important events that marks the lower boundary of the Quaternary (2.6 Ma). The first appearance of *Equus* in the Old World was contemporary with great climatic, environmental, and geological events that influenced *Equus* evolution, geographic dispersion, and adaptation. Thus, the study of *Equus* remains is essential for the interpretation of the palaeoenvironment and palaeobiology of the Pleistocene of Europe.

The present thesis synthesizes a great amount of data and research from several disciplines, including taxonomy, phylogeny, biostratigraphy, and palaeoecology. The author of the thesis revises old collections and studies new material of the Quaternary equids of Greece. How many species of equids have occupied Greece and Europe during the Early to Middle Pleistocene? What were their spatial and chronologic ranges? Palaeodietary, palaeohabitat and palaeoecological interpretations are arguing for understanding the evolution of *Equus*. The author presents an inventory of the progress of recent research on the taxonomy, biostratigraphy and palaeoecology mainly of the of non-caballine *Equus* in Greece and the rest of Europe. New hypotheses are presented concerning the dispersal and evolution of these equids (dating from the Early to Middle Pleistocene), focusing on recent discoveries, descriptions of taxa, and revised diagnoses. The thesis attempts to assemble equid knowledge of the Greek fossil record in order to improve the evolutionary history of the Quaternary *Equus* of Greece and hence Europe.

* * *

The most difficult part of writing a thesis, for me at least, was to finish it. I would like to express my deepest gratitude to my beloved professor, mentor and thesis supervisor, Prof. Emeritus George D. Koufos (Aristotle University of Thessaloniki), who guided me throughout this project, gave me freedom to work my own way and time, trusted

me all those years that we have been working together and for always believing in me. His guidance not only professionally, but also personally, was essential in my life and my prospective career. He has been like a father figure to me. This endeavor would not have been possible without the help and continuously support of my co-supervisor Prof. Dimitris S. Kostopoulos (Aristotle University of Thessaloniki), to whom I am deeply grateful. His guidance and advice carried me through all stages of this project. I thank him for the numerous revisions and suggestions on my manuscripts and analyses which have incredibly improving them. I thank both Prof. Emeritus, George D. Koufos and Prof. Dimitris S. Kostopoulos for their invaluable patience and feedback all those years; it was an amazing experience and great pleasure working by their side. They always had time to listen, whether or not the subject was equids.

Acknowledgements

Throughout the journey of my PhD research, I have received a great deal of encouragement and assistance. I would like to thank each and every one individually hoping that I will not forget anyone.

I am grateful to my co-supervisor, Associate Prof. Sokrates Roussiakis (National and Kapodistrian University of Athens) for his support and his valuable discussions throughout my Master and PhD studies. I also thank him for his suggestions that greatly improved this manuscript.

I am sincerely thankful to Dr. Gildas Merceron, Director of the PALEVOPRIM (Laboratory Palaeontology Evolution Palaeoecosystems Palaeoprimatology, University of Poitiers, France) for his guidance, help, feedback, and support during my PhD studies and especially when I worked at the PALEVOPRIM Lab with the Erasmus+ Program. It was a great pleasure working with him both on the field and at the lab. I am also grateful for the further financial support that he provided during my visit to some French Institutions/Museums.

I am extremely grateful to V*é*ra Eisenmann for sharing all of her data on extant and fossil equids on her public database. Such kind of access amazingly facilitated my work, especially in cases where either my scheduled visits were cancelled due to covid-19 restrictions, or when equid material was not accessible for me to study. I also thank her for our personal communication and help in some equid matters.

I also wish to thank Former Prof. Evangelia Tsoukala (Aristotle University of Thessaloniki) for giving me her permission to study the equid material from Petralona Cave and for her significant discussions on this project.

I would like to extend my gratitude to Dr. George E. Konidaris (University of Tübingen) for his invaluable help, support, and friendship during my PhD studies and also for the constructive advice that he gave my all those years. It was a great pleasure working with him both on the field and at the lab (LGPUT). I also thank him for being brave enough to read earlier versions of this manuscript.

I am grateful to Dr. Athanassios Athanassiou (Ministry of Culture, Ephorate of Palaeoanthropology-Speleology) not only for providing access to unpublished material from Sésklo, Alykes and Volos, but also for providing his personal data.

I sincerely thank Prof. Dr. Ralf-Dietrich Kahlke (Senckenberg Research Station of Quaternary Palaeontology, Weimar, Germany) not only for providing me access in such a short notice to the collection from Süssenborn, but also for the free accommodation in their facility. I also thank him for providing me the manuscripts from Süssenborn. I am also grateful to Gerald Utschig (Technical Assistant, Senckenberg Research Station of Quaternary Palaeontology) and Dennis Rössler (Preparator of Geosciences, Senckenberg Research Station of Quaternary Palaeontology) for their significant assistance and all three of them for their great hospitality in Weimar.

I would like to thank the Curators Elisabetta Cioppi and Luca Bellucci (Museo di Storia Naturale dell'Univerisità degli Studi di Firenze) for providing me access to the equid collections stored at the Natural History Museum in Florence and for their great assistance all the way. I also thank Dr. Omar Cirilli (University of Florence) for his assistance at the museum and for his significant discussions on several equid topics.

I thank Stéphane Madelaine, curator of Musée national de Préhistoire, Les Eyzies-de-Tayac-Sireuil (France), for providing access to the equid collections at his disposal and express my gratitude to Anne-Marie Gadioux for her essential assistance and great hospitality.

I also thank Dominique Armand (University of Bordeaux, France), Emmanuel Robert (Claude Bernard University Lyon 1, France) and Didier Berthet (Musée des Confluences, Lyon, France), for giving permission to study the collections at their disposal and François Vigouroux (Centre de Conservation du Musée des Confluences) for his essential assistance.

Many thanks to Christine Banassat (Mayor of Chilhac, Haute-Loire, France) and especially Véronique Brissaud (*Vacances* à *Chilhac)* for providing access to the equid collection stored at the Musée de Paléontologie Christian Guth de Chilhac and for such a great hospitality.

Many thanks to Dr. Loïc Costeur, Curator of the Vertebrate Palaeontology collections at the Natural History Museum in Basel (Switzerland), for providing access to the Early Pleistocene equid collections stored at the Natural History Museum Basel.

I also thank Dr. George Lyras (National and Kapodistrian University of Athens) for providing me access to the equid collection stored at the Natural History Museum of Vatera (Vrissa, Lesvos Inland).

I am incredibly thankful to Dr. Evangelos Vlachos, Researcher at CONICET and Museo Palaeontológico Egidio Feruglio, for his assistance in the phylogenetic analysis.

I would like to express my deepest gratitude to my dearest friend and colleague, Dr. Chris-Alexander Plastiras for his continuous support along the way and for sharing his knowledge on palaeoecological topics (microwear analysis among others).

I sincerely thank Dr. Ioanna Sylvestrou (Aristotle University of Thessaloniki) for her huge help and support during my Master and PhD studies.

I am grateful to Dr. Ioannis Maniakas for sharing a great number of palaeoecological information with me, for his continuous support and his numerous talks on several palaeontological topics.

I would like to thank MSc Evangelia Alifieri for sharing her data of extant species on the microwear analysis. Such kind of access significantly helped my work.

I would also like to thank the late Dr. Katerina Vasileiadou for her continuously support and friendship during my Master and PhD studies.

I would like to thank my friends and co-workers Dr. Chris-Alexander Plastiras, (the soon to be Dr.) Antriani Varnava, Dr. Ioannis Maniakas, Dr. Stratis Karantanelis, Katerina Kafetzidou, (the also soon to be Dr.) Aliki Kokkala, Krystallia Chitoglou, Konstantinos Laskos and Dr. Pavlos Piskoulis for the great times that we shared at the lab. It was an enjoyable experience spending long hours at the lab, even when the most challenging times occurred during lockdowns due to covid-19 restrictions.

I thank Erasmus+ for studies programme for their financial support and for giving me the opportunity to study at the PALEVOPRIM (University of Poitiers, France). Erasmus+ programme was an amazing experience that apart from the academic assets that I received, it taught me that one should never stop experiencing and learning. I

want also to express my gratitude to my "Greek squad", Dr. Chis-Alexander Plastiras, Anastasia Karakosta, and Nikoletta Kargopoulou and all the incredible Erasmus+ students-friends-colleagues that I had the chance to meet, work with and have fun. It was one of the best experiences of my career. I am especially thankful to both Anastasia Karakosta and Nikoletta Kargopoulou who helped me scan many of the dental molds at the PALEVOPRIM lab.

The Willy Hennig Society is thanked for sponsoring the free use of the TNT software.

The excavations in Tsiotra Vrysi (Mygdonia Basin) were supported by the ERC Consolidator Grant ERC-CoG-724703 ("CROSSROADS") and the ERC Starting Grant ERC-StG-283503 ("PaGe"), both awarded to Prof. Katerina Harvati. Research in Apollonia-1 (Mygdonia Basin) was supported by grants of the Research Committee of the Aristotle University of Thessaloniki (Projects 1396 and 87845) awarded to George D. Koufos and Dimitris S. Kostopoulos and by the European Research Council StG 283503 (PaGE) awarded to Katerina Harvati (University of Tübingen).

Excavations at Dafnero were supported by the Lab of Palaeontology, AUTh, the CNRS, France [grant number PICS5185; 2010-2013]; and the National Geographic Society [grant 9903-16; 2016-2017]. ALM studies were partly supported by the Austrian Science Fund [FWF grant number P29397] and ChAP studies by Eiffel scholarship program of excellence.

I am grateful to all the field members for their valuable contribution, and everyone who helped me with the preparation of the studied material at the LGPUT.

This research is co-financed by Greece and the European Union (European Social Fund – ESF) through the Operational Programme "*Human Resources Development, Education and Lifelong Learning*" in the context of the Project "Strengthening Human Resources Research Potential via Doctorate Research – 2nd Cycle" (MIS-5000432), implemented by the State Scholarships Foundation (IKY). This project would not have been possible without their financial support.

I am also thankful to Katerina Kyriakidou, Christina Ververidou, Marika Mple, and Panagiotis Dimitriadis for their support during the final year of my PhD.

I would like to express my deepest gratitude to my beloved friends Rania Karaisaridou, Evangelia Giannouli, Elena Vasilikari, Christos Donios, Elena Kyriazidou, Victoria Karagkouni and Anna-Maria Mpampatsikou for their huge encouragement and continuous support.

I am deeply grateful to Andreas Athanasiadis who supported and encouraged me during the last years of my research. He inspired me to always follow my dreams. I feel incredibly fortunate to have him by my side.

Finally, I would like to thank my family who helped financially all those years and supported me every step of this beautiful journey. I am thankful to my two beautiful kids (cats), Julio and Iraklis, for all the entertainment and for taking my anxiety away in great moments of stress. I am deeply grateful to my mum and my beloved sister, Maria: Thank you for *everything*. I dedicate this PhD thesis to both of you.

Anastasia G. Gkeme

Thessaloniki, September 2023

Organization of the Doctoral Thesis

CHAPTER 1 provides introductory information on fossil equids trying to answer the question *Why study fossil equids?* The main objectives of this study are stated briefly. This chapter also provides information on extant equids and a historical overview of the study of fossil equids in Greece.

CHAPTER 2 contains information on the Material and Methods used at the systematic analysis (2.1 and 2.2 respectively), at the phylogenetic analysis (2.3) and at the palaeoecological analysis (2.4) followed by abbreviations (2.5).

CHAPTER 3 provides briefly geological information for the localities/sites (3.1-3.8) from where the studied material in the thesis comes from and the equid species that have been acknowledged by earlier studies.

CHAPTER 4 contains information on the European Quaternary *Equus*; their nomenclatural history, systematic position and phylogenetic relationships are briefly discussed.

CHAPTER 5 contains the main information on the palaeontological results (taxonomy), such as, detailed anatomical description, photographic documentation, and some measurements. In this chapter, each equid species, dated from the Early to Middle Pleistocene of Greece, is being compared and redefined based on both morphological and morphometric characters on crania, mandibles, teeth, and postcranial remains from different localities. Bivariate and multivariate analyses were performed to estimate variation and differences in size and proportions between the species. At the end of this chapter, the palaeontological outcomes by the thesis are being discussed.

CHAPTER 6 analyzes and discusses the phylogenetic hypotheses on the Early Pleistocene equids based on morphological data.

CHAPTER 7 analyzes the dispersal events of the fossil equids and their relationship to the environmental changes.

CHAPTER 8 contains the results of the palaeoecological analysis conducted to Greek and European equids. Sub-chapter 8.1 contains the equine body masses that were calculated. In the sub-chapters 8.2 and 8.3 ancient feeding ecology is discussed based on mesowear and microwear analysis respectively. In the sub-chapters 8.3, metapodials (MCIII, MTIII) are used to quantify locomotor adaptations relevant to habitat preferences in order to imply palaeoecological inferences from ecomorphological patterns.

CHAPTER 9 summarizes the conclusions of this study.

ABSTRACT provides an extensive summary of this thesis.

ΠΕΡΙΛΗΨΗ provides an extensive summary of this thesis in Greek language.

At the end of this thesis, the full reference list is followed by an extensive Supplementary Material, with tables of measurements, photographic documentation, microwear results, and all data concerning the phylogenetic analysis.

TABLE OF CONTENTS

The evolutionary history of equids is one of the most captivating and intriguing among the Cenozoic large mammals. Because of their widespread distribution and their rich fossil record across America, Eurasia, and Africa over the past 56 Ma, their evolution has been one the most frequent cited examples of natural evolution interpreted from the fossil record (MacFadden 1992, 2005). Fossil equids are useful to express biological diversity, reconstruct palaeoenvironments and acknowledge the effects of climatic changes through time. Furthermore, equids have been associated to the human history with the earliest association between equids and primitive cultures to be found on the paintings of Middle and Upper Palaeolithic French and Spanish caves (MacFadden 1992; Prado and Alberdi 2017).

CHAPTER 1. INTRODUCTION

1.1 THE GENUS *EQUUS*

Over the past 20 years, the discovery of new fossils and the reconsideration of reference collections in conjunction with the progress of palaeogenetics has led to the revision of the taxonomy and evolutionary history of the Quaternary European *Equus* (Orlando et al. 2013; Jónsson et al. 2014; Bennett et al. 2017). Further, the intensified precision of the dating of certain deposits from key localities has led to the revision of their biochronology (Alberdi et al. 1998; Forstén 1999a; Eisenmann 2004a, 2006a, 2010; Alberdi and Palombo 2013; Palombo and Alberdi 2017; Van der Made et al. 2017).

A fundamental separation of *Equus* is into caballine (including the domesticated *Equus ferus caballus*) and non-caballine equids that include zebras and asses/donkeys. Recent studies consider seven valid living species of equids (Figure 1.1). *Equus ferus* (including the Mongolian Przewalski's horse) is the wild caballine equid of Eurasia. The wild asses from Asia (also known as Asiatic wild Asses) include the hemione *Equus hemionus* (ranging from Iran to China) and *Equus kiang* (Tibetan Plateau), while wild African asses are represented by *Equus asinus* (including *Equus asinus somaliensis* in Somali, Horn of Africa, and *Equus asinus africanus* in Ethiopia) from

which the domestic donkey has derived. The African zebras include three species: *Equus grevyi* (Ethiopia and Kenya), the plains zebra *Equus quagga* (south of Ethiopia to southern Africa) and the mountain zebra *Equus zebra* (southern Africa) (see George and Ryder 1986; Eisenmann 1980, 1981; Groves 2002; Weinstock et al. 2005; Orlando et al. 2009; Bernor et al. 2010; Jónsson et al. 2014).

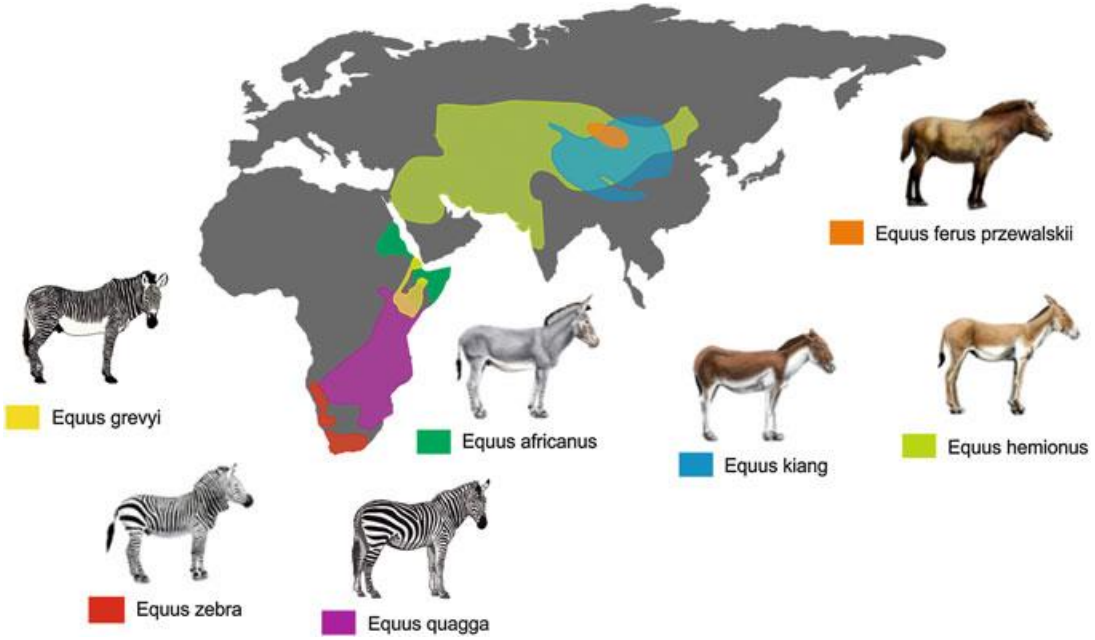

Figure 1.1. Distribution of the living equids in the world. Taken from Prado and Alberdi (2017).

The genus *Equus*, that most likely emerged at 4.0–4.5 Ma (Figure 1.2), is considered to include all monodactyl equids present in Europe, giving rise to all contemporary (true) horses, zebras, and asses/donkeys (Orlando et al. 2013). The first representative of the genus *Equus* (that is *Equus simplicidens* Cope, 1892) appeared in North America at about 3.5 Ma, according to the age of the Blancan fauna from the Hagerman Horse Quarry (Idaho) (Lundelius et al. 1987; Repenning 1987; McDonald 1996). Though, the first appearance of the genus may be older as proposed by the presence of ?*Equus* sp. reported by Lindsay and Jacobs (1985) in the Concha Fauna (Chihuahua, Mexico). *Equus simplicidens* (Skinner and Hibbard 1972) [=*Plesippus shoshonensis* in Gidley (1930) and Gazin (1936)] shows some affinities with the modern Grévy's zebra; it is considered the earliest common ancestor of *Equus,* and it is likely the first phylogenetic source for Old World stenonine equids (Azzaroli and Voorhies 1993). During the Pleistocene, representatives of the genus *Equus* extensively dispersed across America, Eurasia, and Africa, inhabiting a variety of palaeoenvironments, giving rise to different

lineages, which record radiative and anagenetic evolutionary processes (Palombo and Alberdi 2017).

The arrival of *Equus* in Eurasia through the Beringian Strait is one of the most significant events at the beginning of the Quaternary, marking an important faunal turnover caused by global environmental changes from humid-warm to cool-dry conditions (Azzaroli 1983; Alberdi et al. 1997; Bernor et al. 2019; Rook et al. 2019; Cirilli et al. 2020; Kahlke et al. 2011). The stenonid group (equids related to *Equus stenonis*) was the first to disperse at the Plio-Pleistocene boundary (previously called the *Equus-Elephant* event; Lindsay et al. 1980). The *Equus*-datum is calibrated at 2.58 Ma (base of the Middle Villafranchian) in Europe and 2.55 in China (*Equus qingyangensis*, Sun and Deng 2019), while it is slightly younger in the Subaharan Africa, 2.33 Ma. In the Mediterranean region, *Equus*-datum is traced in the Lower Pleistocene (MNQ 16) localities of Montopoli (Italy) and El Rincon-1 (Spain). In Western and Central Europe, the *Equus*-datum is recognized in the French locality Roca-Neyra, where *Equus* and *Hipparion* co-existed (Eisenmann and Brunet 1973; Cirilli et al. 2020). *Equus livenzovensis* from the Middle Villafranchian of Eurasia is recognized by some authors as the first Old World *Equus* species and it is considered as the phylogenetic root of all the European stenonoid species (Azzaroli 1992; Alberdi et al. 1998; Palombo and Alberdi 2017; Bernor et al. 2018).

During the late Villafranchian and Galerian of Europe, generally two different groups of equids are recognized: the "stenonoids" or else "stenonids" (after *E. stenonis* Cocchi, 1867, a typical Villafranchian representative of this group) and the "caballoids" (after *E. caballus* Linnaeus, 1758). The stenonoid equids are recognized by their V-shaped linguaflexid (zebrine feature) on the lower cheek teeth (Figure 1.3), while caballoids have a U-shaped linguaflexid (Hopwood 1936; McGrew 1944).

According to Eisenmann and Baylac (2000) and Eisenmann (2006, 2017) modern equids (true horses) are separated from the primitive *Allohippus* (taxon that is comprised from all stenonoid equids) and *Plesippus* (North American Pliocene equids, type species *E. simplicidens*) based on their basicranial proportions (discussed in detail later). Following on this outline, the Asian *E. nalaikhaensis* Kuznetsova and Zhegallo, 1996 from Nalaikha, Mongolia (0.9Ma, Kuznetsova and Zhegallo 2007) and *E. coliemensis* from Kolyma, Siberia (beginning of the Middle Pleistocene) are considered as true horses (Eisenmann and Kuznetsova 2004). In Europe the first cranium belonging to a true *Equus* (Eisenmann and Kuznetsova 2004) is from Apollonia-1, Greece (=*E.*

apolloniensis in Koufos et al. 1997; 1.2–0.9Ma, Koufos and Kostopoulos 2016), while the latest cranium belonging to stenonoid equids is the one from Ceyssaguet (1.2Ma, *E. stenonis* in Aouadi and Bonifay 2008). According to Eisenmann (2006a, 2010, 2017), some equids (*E. a. granatensis, E. altidens, E. hipparionoides, E. coliemensis, E. suessenbornensis*) suggest a common origin within the branch of *Equus* at least from 1.5 Ma and maybe soon before around 2.5Ma just above the Gauss-Matuyama limit (VAT-E, Vatera Formation, Greece).

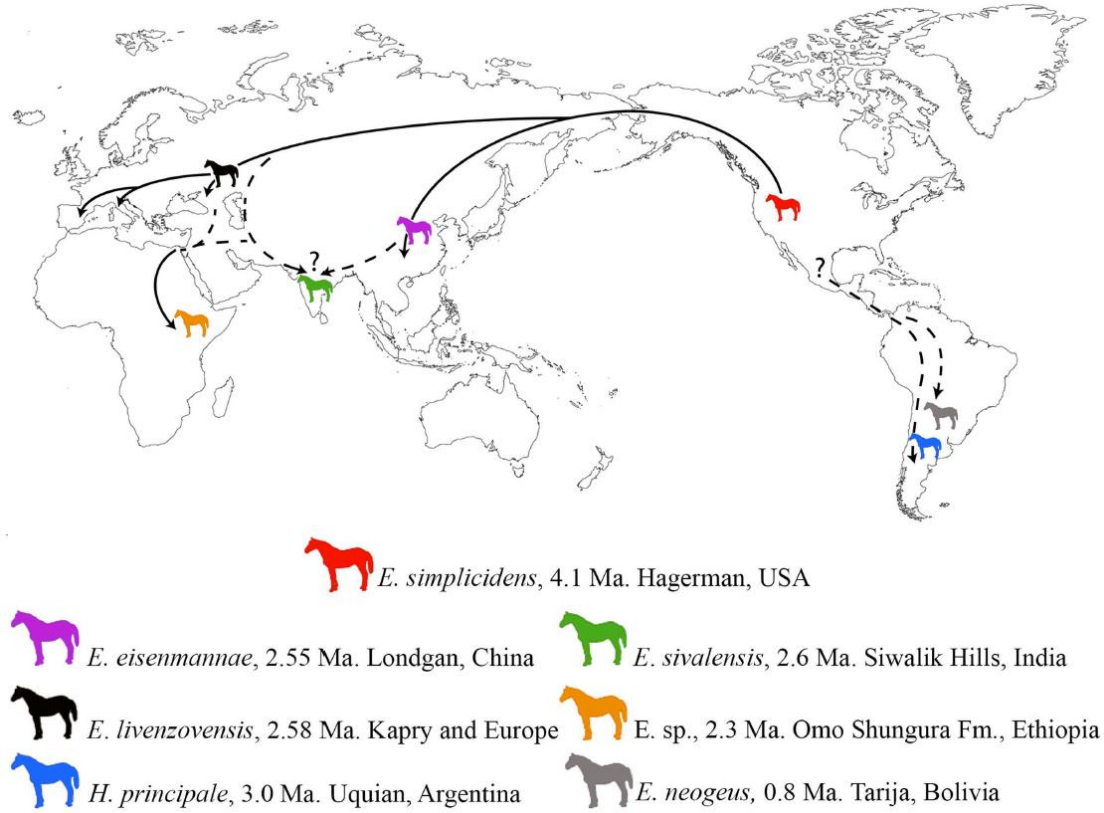

Figure 1.2. Biogeographic extension of early *Equus* species across the America, Eurasia and Africa including the timing of early record of those species. Taken from Rook et al. (2019).

Nevertheless, according to Palombo and Alberdi (2017) the separation of Eurasian Pleistocene equids in different genera/subgenera requires a great deal of caution, considering the homogeneity, but also the large intra- and low interspecific variation shown by fossil monodactyl equids (Boulbes and Van Asperen 2019). This argument is beyond the scope of the present thesis which aims to briefly discuss the debated scenarios and questions that still need to be answered (such as the number of lineages, the concrete taxonomical ranks of some alleged species or subspecies, phylogenetic relationships and more), mainly focusing on equids recorded in the late Villafranchian

and Epivillafranchian Local Faunal Assemblages (LFAs) of Greece and Central-South Europe.

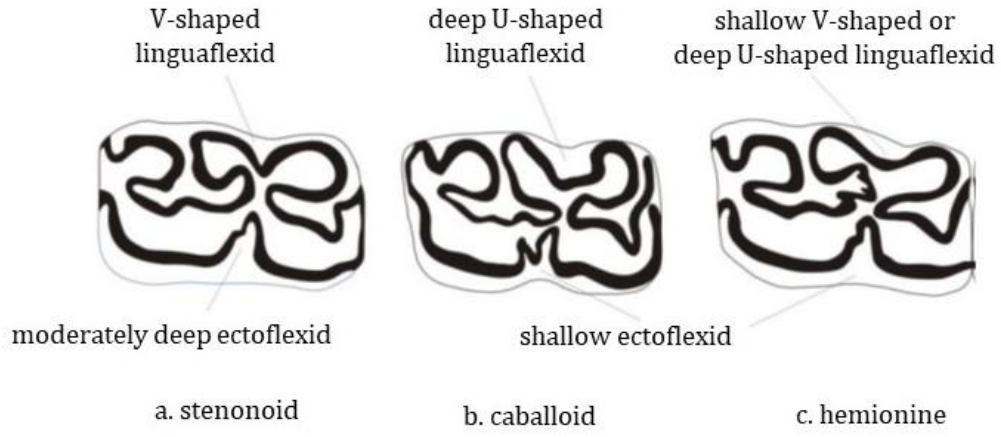

Figure 1.3. Discrimination of the genus *Equus* based on the morphology of the lower cheek teeth: a. stenonoid, b. caballoid, c. hemionine. Modified from MacFadden (1992).

1.2 GREEK QUATERNARY EQUID FOSSIL RECORD AND SCOPE OF THE THESIS

Since the beginning of the 1980's, few were known about the Pleistocene faunas of Greece. The most important publications were those referred to the fauna of Megalopolis in Peloponnese (Melentis 1961, 1963, 1965a, b; Sickenberg 1975). Sporadic articles describing or reporting the presence of some equid's remains were also known from northern Greece (e. g. Forsyth Major 1887; Paraskevaidis 1953, 1977; Brunn 1956; Marinos 1964; Sickenberg, 1971,1967, 1968). During the end of the 1970's - beginning of the 1980's, new localities have been discovered especially in northern Greece and new material has been unearthed (e. g. Sakellariou-Mane et al. 1979; Koufos 1981; Symeonidis and Tataris, 1982-83; Koufos and Melentis, 1983; Koufos et al. 1988, 1991, 1992). In the following years extensive field work in the new sites provided rich mammal collections. Thanks to several decades of excavations, notably the ones conducted by George D. Koufos (Aristotle University of Thessaloniki) in Northern Greece (Western and Central Macedonia), the Neogene assemblage of Greece has been established as one of the most up-to-date fossil collections in Europe. Several articles have been published, studying these faunas, and providing significant palaeontological and biochronological data for Greece and Eastern Mediterranean region (e.g. Steensma 1988; Tsoukala 1989; Symeonidis 1992; Koufos 1992a, b, 1993;

Koufos and Kostopoulos, 1993, 1997; Koliadimou 1996; Kostopoulos and Koufos 1994; Kostopoulos 1996, 1997a, b; Koufos and Vlachou 1997; Koufos et al. 1997, 2018; Athanassiou 1998, 2001, 2018; Tsoukala and Chatzopoulou 2005; Konidaris et al. 2015, 2020; Maniakas 2019). These Greek collections are used as reference for the scientific community to understand the evolution of these mammals from their first occurrence in Old World and as far equids are concerned from their dispersal from North America through the Bering Strait.

Equids are usually the most common fossils in the Pleistocene faunal assemblages, of Greece, often representing more than 50% of the palaeocenosis in terms of findings. The earliest evidence of *Equus* in Greece is traced in the locality Damatria in Rhodes Island and probably represented the first local appearance of the genus in this region (de Bruijn et al. 1970; Benda et al. 1977; Van der Meulen and Van Kolfschoten 1986; Koufos and Kostopoulos 2016 and ref. therein). Recently both hipparionine horses and equids were also recognized in the locality Sésklo (Thessaly, Central Greece). The fauna from the lower levels of the section, dated to early Villafranchian (MNQ 16, probably in its upper part), includes *Plesiohipparion* cf. *shanxiense*, while in the upper fauna (middle Villafranchian, MNQ 17), *Equus stenonis* is present; they did not occur sympatrically (Athanassiou 2018). The majority of *Equus* findings of Greece mainly originates from the middle-late Villafranchian and Epivillafranchian faunas (Figure 3.1). Several articles on Quaternary equids have been published over the years mainly focusing on their taxonomy (Melentis 1963; Steensma 1988; Tsoukala 1989; Koufos 1992a; Koufos and Vlachou 1997; Koufos et al. 1997; Athanassiou 1998, 2001; Tsoukala and Chatzopoulou 2005; Konidaris et al. 2015; Gkeme 2016; Gkeme et al. 2017; Gkeme et al. 2021; Koufos et al. 2022). The continuity of the research that led to the discovery of the new sites, as well as the numerous field campaigns, provided more material, enriching the old collections. Thus, a reconsideration of the old and the study of the new material is essential, providing new information on the taxonomy, phylogeny, biostratigraphy and palaeoecology of Greek *Equus*.

To untangle the taxonomy of earliest equids, different samples spread in time and space must be examined. How many species of equids occupied Eurasia during the Quaternary? What were their spatial and chronologic ranges? Such questions can be resolved by collecting data from other sites in Europe, notably the ones coming from key localities. France (sites: Saint Vallier, Chilhac, Senèze etc.), Germany (sites: Süssenborn, Untermassfeld), Italy (sites: Upper Valdarno, Casa Frata, Terranuova,

Montopoli, Pirro Nord among others), and Iberia (sites: Venta Micena, Cueva Victoria etc.) have yielded several rich fossil sites corresponding to the time window during which equids spread into Old World. These collections will be used for comparative anatomy and morphometry, on cranial, mandibular, dental, and postcranial material in order to better understand the taxonomy of the different species of *Equus* in Europe during the Quaternary. From this taxonomic work, the present author will be able to propose an up-to-date phylogeny.

Taxonomy and phylogeny apart, this thesis also aims at describing past environments between 2.5 and 0.4 Ma in Greece and consequently in Europe. As the occurrence of equids at a given fossil site cannot be used as a direct environmental proxy, the author will conduct two approaches in order to extract palaeoecological implications: assessing locomotor behaviors/locomotor substrates (using postcranial anatomy) and their feeding habits (dental wear analyses).

This thesis can be contextualized into human evolution. Indeed, equids are faunal elements found in many archaeological sites or faunal sites contemporaneous with the spread of the genus *Homo* out of Africa and into Eurasia. As environmental proxy, equids can be used to track hominid ecotypes in Eurasia. Do early humans occur with plain or forest dwelling ungulates such as equids or antelopes? To answer such a question requires long standing studies. The present thesis will contribute to this by studying taxonomy, phylogeny, biogeography, and ecology of the Quaternary Greek equids.

In summary, the present author aims to review and discuss the most recent knowledge of the Greek *Equus* fossil record with the following objectives:

-Provide a revision of the material from old collections and describe new material from known fossiliferous sites in order to systematically classify the Greek Quaternary equids and fill the gap in the knowledge of the Quaternary equids of Greece and, by extension, the Balkans and Europe,

-Further establish phylogenetic relationships of European Quaternary equids,

-Contribute to the chronological structure of the terrestrial deposits of the Quaternary of Greece and to the indirect dating of the fossiliferous sites on the basis of equids,

-Investigate the palaeoecological preferences and locomotor adaptations of the Quaternary equids in order to reconstruct the wider palaeoenvironment,

-Study the dispersal, disappearance, and temporal distribution of the Quaternary equids in Greece and rest of Europe, which, in conjunction to the delineation of major faunal

changes, will lead to the investigation to a possible correlation of them with other events, such as palaeogeographical and palaeoclimatic ones.

CHAPTER 2. MATERIAL AND METHODS

2.1 MATERIAL

The equid remains from Greece are given in detail before the description of each species. They come from several fossiliferous sites dating from the Early to Middle Pleistocene. Some of the material lacks a precise stratigraphical location/origin, because it comes from old collections, where only information about the locality is provided, but many times the stratigraphic level or date is not indicated. The studied material is stored in the following institutions/museums: Museum of Geology-Palaeontology-Palaeoanthropology of the Aristotle University of Thessaloniki (LGPUT, sites: Aggitis, Apollonia, Dafnero-1, 3, Gerakarou, Libakos, Kapetanios, Krimni-1,2,3, Petralona Cave (old collection), Platanochori-1, Polylakkos, Riza-1, Siatista-E, Tsiotra Vryssi, Vassiloudi, Volax); Museum of Palaeontology and Geology of the National and Kapodistrian University of Athens (AMPG, sites: Sésklo, Alykes, Volos); Vrissa Museum of Natural History, Lesvos Island (VM: Vatera).

Equid collections from late Villafranchian to middle Galerian were used as comparative material for the purposes of this thesis. The material has been studied by the author in the following museums and institutes: Italy: Museo di Storia Naturale dell'Univerisità degli Studi di Firenze [sites: Montopoli-Lower Valdarno, Upper Valdarno, Valdarno indet., Olivola, Matassino, Terranuova, Terranuova (L'inferno), Terranuova (L'infernuzzo), Le Ville, San Giovanni, Figline, Casa Frata, Pirro Nord, Grotta Romanelli]; France: Claude Bernard University Lyon 1 (sites: Senèze, Saint-Vallier); Musée des Confluences in Lyon (sites: Senèze, Saint-Vallier); University of Bordeaux (site: Saint-Vallier); Musée de Paléontologie Christian Guth, Chilhac (site: Chilhac-2,

3); Musée National de Préhistoire, Les Eyzies-de-Tayac-Sireuil (site: Ceyssaguet); Switzerland: Naturhistorisches Museum Basel (sites: Senèze, Saint-Vallier, Upper Valdarno); Germany: Senckenberg Research Station of Quaternary Palaeontology in Weimar (site: Süssenborn).

The remaining comparative data are from the literature, as follows:

E. stenonis from Kalamoto, Mygdonia Basin by Tsoukala and Chatzopoulou (2005), *E. hydruntinus* and *E. ferus* cf. *germanicus* from Agios Georgios, Kilkis by Tsoukala (1992); the German equids *E. wuesti* from Untermassfeld and *E. mosbachensis* from Mosbach by Eisenmann and Boulbes (2020) and Eisenmann (2011) respectively; the Spanish equids *E. a. granatensis* from Venta Micena and *E. stenonis pueblensis* from La Puebla de Valverde by Eisenmann (2007) and Eisenmann (1980) respectively, *E. livenzovensis* from El Rincon by Alberdi and Ruiz Bustos (1989); the French equids *E. major*/*bressanus* from Chagny and *E. mosbachensis micoquii* from La Micoque, Les Eyzies-de-Tayac-Sireuil by Eisenmann (2010) and Langlois (2005) respectively, *E. ferus gallicus* from Siréjol (Gignac) by Eisenmann (2008), *Equus mosbachensis palustris* from Lunel-Viel, Hérault by Bonifay (1980), *E. ferus gallicus* from Solutré, Saône-et-Loire by Guadelli (1989), *Equus mosbachensis tautavelensis* from Caune de l'Arago, Tautavel by Crégut (1980), *E. mosbachensis* from Biache-Saint-Vaast, Pas-de-Calais by Auguste (1995), *E. ferus piveteaui* from Abri Buard by Prat (1968), *E.* cf. *mosbachensis* from Achenheim and Montoussé by Prat (1968), *E. mosbachensis campdepeyri* from Camp-de-Peyre by Guadelli and Prat (1995); the Georgian equids *Equus stenonis* and *Equus altidens* from Dmanisi and *E. hipparionoides* and *E.* cf. *suessenbornensis* from Akhalkalaki by Bernor et al. (2019) and Eisenmann (2010) respectively; the Italian *E. stehlini* (additional material from Upper Valdarno Basin) by Cirilli (2022), *E. altidens* from Selvella-Gioiella and additional material from Pirro Nord by Alberdi and Palombo (2013) and *E. ferus malatestai* from Torre in Pietra, Rome by Caloi (1997); *E. simplicidens* from Hagerman Horse-Quarry, Idaho, North America by Eisenmann (2011); the Siberian equids *E. verae* from NE Siberia and *E. ovodovi* from Khakassia, SW Siberia by Eisenmann (2011, 2022) and Eisenmann and Sergej (2011) respectively; *E. livenzovensis* and *E.* aff. *major* from Liventsovka and other localities of the Khaprovskii Faunal Complex, Russia by Eisenmann (2011, 2022); *E. hydruntinus* (from several localities) by Eisenmann (2018a, b, c, d, e); the extant *E. hemionus onager*, *E. grevyi*, *E. africanus* by Eisenmann (2011).

2.2 METHODS

2.2.1 Descriptions and morphometric analysis

The descriptions and measurements follow the recommendations of the ‘‘*Hipparion Conference*’’, New York in Eisenmann et al. (1988). Further character nomenclature was taken from Eisenmann (1983, 2017) and Budras et al. (2012) and for comparative anatomical nomenclature from Smuts and Penzhorn (1988) and Bernor et al. (1997). As detailed descriptions of each studied bone are long and tiresome, descriptions were only focused on crania and teeth and on specific features on the limb bones with possible diagnostic value. To avoid repetition, descriptions were made on each species. All measurements are given in millimeters with an accuracy of two decimal digits for the teeth and one for the postcranial material (see Appendix 1). Inaccurate measurements are given in parentheses. Specimens belonging to juvenile individuals were excluded from the statistical analysis.

The nomenclature used for the morphological descriptions of the teeth is given in Figure 2.1. Measurements of length and breadth of the teeth were taken on the occlusal surface for both upper and lower teeth; cement and any stylids (on lower cheek teeth) were excluded from the measurement. However, since these measurements vary due to the degree of the attrition, additional measurements of isolated teeth were taken at 1 cm above the roots/crown junctions. On the upper cheek teeth, the shape of the protocone was described using the recommendations by Eisenmann et al. (1988) and Vlachou (2013); the shape varies with the degree of wear. The Protocone Index (PI) was calculated as Lp/Lo % ratio (PI = Lp/Lo %), where Lp is the occlusal length of the protocone and Lo the occlusal length of the tooth (Eisenmann 1986).

The plications on the anterior and posterior enamel borders of the fossettes were counted according to the formula: plis on the anterior wall of the prefossette - plis on its posterior wall - plis on the anterior wall of the postfossette - pli on its posterior wall - pli caballin (e.g., 2-7-3-1/1); (Figure 2.1). On lower cheek teeth, the presence of pli preflexid and caballinid was only counted, while the presence of any plications on postflexid was described as wrinkled or not. Also, the presence of pli protostylid was noted. Tooth height was measured from the uppermost margin of the anterior root to the anterostyle/paraconid of P2/p2 and the parastyle/parastylid on the other cheek teeth (P3-4/p3-4 and M1-3/m1-3). The height of unworn or slightly worn teeth was used to distinguish 4 stages of wear for each kind of tooth; 1. unworn or slightly worn teeth, 2

and 3 intermediate worn teeth, 4. very worn teeth. The determination of the stage of wear on a toothrow (inside a cranium/maxilla or mandible) is approximative. The Hypsodonty Index was calculated as H/Lb % ratio, where 'H' represents the maximal height of the tooth and 'Lb' maximal length at 1 cm above the base of the crown (Eisenmann et al. 1988; Alberdi 1974).

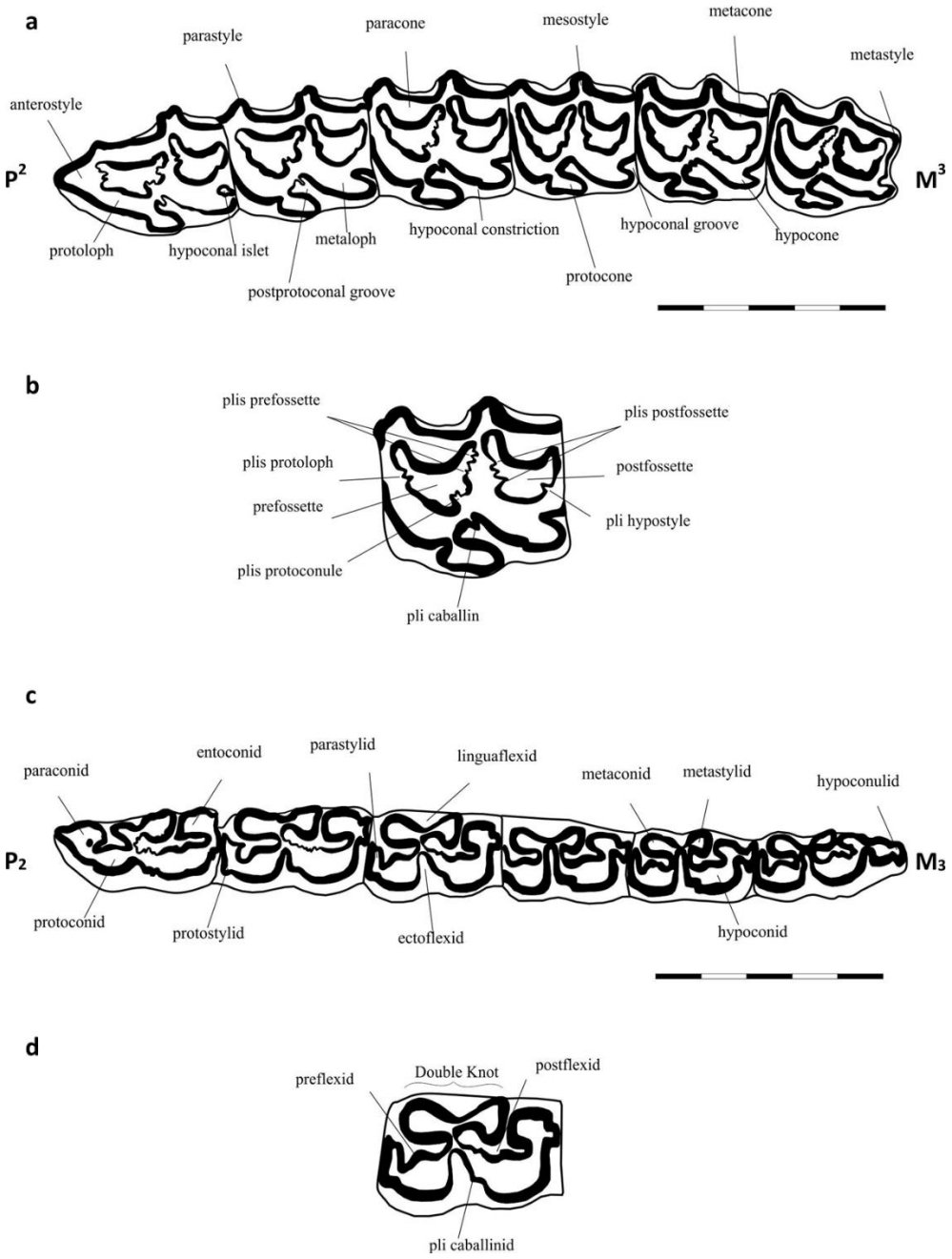

Figure 2.1. Nomenclature of the (a, b) upper and (c, d) lower cheek teeth morphology according to Eisenmann et al.'s (1988) recommendations. *Equus altidens granatensis* from Venta Micena: occlusal views of the a. Left upper cheek teeth row, VM 84-C3-E9-52 and b. Left lower cheek teeth row, VM 84-C3-B9-12. Modified from Eisenmann (1995).

For the metapodials, the following indices have been calculated (Boulbes and Van Asperen 2019): slenderness index 1 (SI 1): minimal breadth at the middle of the diaphysis (M3) / maximal length (M1) % (Alberdi et al., 1998; Eisenmann, 2002); slenderness index 2 (SI 2): maximal breadth at the distal articular end (M11) / maximal length (M1) (Koufos, 1992); diaphysis flatness (DF): anteroposterior diameter of diaphysis (M4) / minimal breadth of the diaphysis (M3) (Eisenmann, 2002); caballine index (CI): distal supra-articular breadth at tuberosities (M10) / distal articular breadth (M11) (Prat, 1980; Eisenmann, 2002); proximal flatness (PF): proximal articular breadth (M5) / proximal articular depth (M6). The development of the sagittal crest is expressed by the keel Index (KI) (Koufos and Sen 2016) as the distal maximal anteroposterior diameter of the keel (M12) / distal minimal DAP of the lateral condyle (M13) %.

Age determination. Age at death was estimated using the eruption-wear sequences for the ageing of equids provided by Levine (1982). Furthermore, the occlusal shape of incisors and the shape of infundibulum were used as an indicator of age (Penzhorn 1982); 1. worn (with infundibulum or oval infundibulum, 2. round infundibulum, 3. worn (with infundibulum), 4. very worn (without infundibulum), 5. extremely worn (labio-lingual diameter is greater than mesio-distal diameter). The incisive arcade which is the angle formed between upper and lower incisors becomes more acute with age. The presence or absence of the Galvayne's groove on I3 is also an age indicator; at ~10 years it appears at gum line, at ~15 years it extends halfway, at ~20 years is at its full length and extends to the end of the tooth, at ~25 years it disappears from half of the tooth.

Sex determination. The determination of the sex was based on the main sexual dimorphism in equids, the presence or absence of well-developed canines. In males, canines are stronger at least on the maxilla, while on females, they either are rudimentary or absent. Concerning the dimensions of the limb bones, the dimorphism is too weak to discriminate sexes; differences in size and proportions between males and females are lost within the general intraspecific variation in *Equus* species (Winans 1989).

2.2.2 Discrimination of equid crania

According to some authors, there are three types of crania belonging to the monodactyl horses in the Old World: *Plesippus, Allohippus* (e.g., *E. stenonis*), and *Equus* (Samson

1975; Forstén and Eisenmann 1995; Eisenmann and Baylac 2000; Eisenmann 2004; Eisenmann and Deng 2005). These names, either attributed to generic or subgeneric Villafranchian fossil equids, can only be used in cases of complete or almost complete crania. In equids, the axial lengths of the cranium seem to maintain stable reciprocal relations inside specific groups (Eisenmann 2006). The basicranial proportions (relations between two axial segments) have generally been proven reliable and possibly the only way to separate primitive equids (*Plesippus*, *Allohippus*) from the modern ones (*Equus*) (Eisenmann and Baylac 2000). *Equus* has longer post-vomerine length (M4) in relation to the overall palatal length (M2) than *Plesippus* and *Allohippus*, and the latter has a deeper naso-incisival notch (M30) in relation to the cheek teeth length than *Plesippus* and a shorter vomerine length (M3) relative to the palatal length (Eisenmann 2017) (see Figure 2.2).

The crania of extant and fossil caballines can be separated from the crania of asses using *Franck's Index* (aka Franck's vomer index in older literature) (Forstén and Eisenmann 1995; Eisenmann and Baylac 2000; Eisenmann 2002). The Franck's Index (Figure 2.2) compares the distance between the posterior border of palate (Staphylion) to the posterior border of vomer (Hormion) and the distance from the posterior border of vomer (Hormion) to the anterior border of foramen magnum (Basion) [F.I. = vomerine length (M3) / post-vomerine length (M4) %]. This relation is phylogenetically important (e.g., Osborn 1912); the index shows a decrease during the evolution of *Equus* with the decrease of the vomerine length (distance between Staphylion to Hormion) (Forstén and Eisenmann 1995) and instead of an increase of the post-vomerine length (distance between Hormion to Basion) as stated earlier by Samson (1975). In true horses (i.e., caballine), contrary to asses and donkeys, post-vomerine length is longer than the vomerine length. In plesippine equids, the vomer reaches far back than in living equids (Gromova 1949), representing the most primitive basicranial proportions: *Equus (Plesippus) simplicidens* from North America (Hagerman Horse-Quarry, Idaho) which is considered as the earliest common ancestor of *Equus* exhibits the longest vomerine length.

Franck's Index is not that good when it is used to caballines and other living equid species and thus it should be combined with the Palatal Index (Figure 2.2). The latter compares the palatal length (distance between the minimal length between the middle of the line connecting the anterior borders of the P2 and the Staphylion) to the vomer

length (like in Franck's Index): P.I. = palatal length (M2) / vomerine length (M3) %]. Caballines always exhibit longer palatal length that the vomer length.

However, when dealing with fossil equid crania, these indices cannot always be combined due to taphonomical deformations of the crania; Franck's Index can be used when the anterior cranial part is damaged or missing and, in the opposite, Palatal Index can be used when the distortion concerns the posterior part of the cranium. Thus, both indices can either be combined or alternatively be used individually in fragmentary crania.

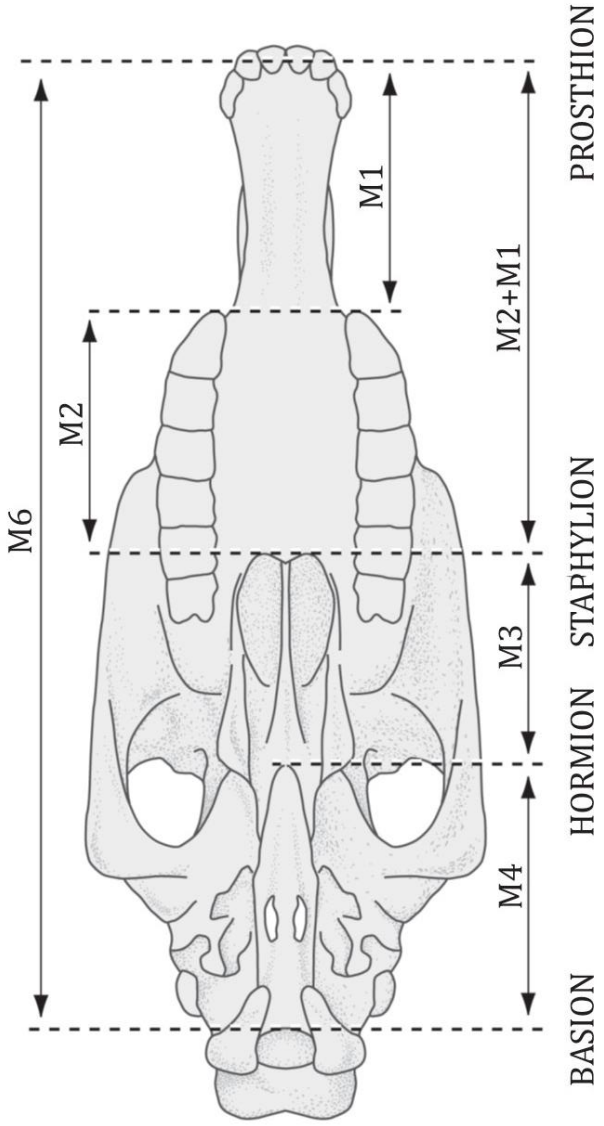

Figure 2.2. Ventral view of an *Equus* cranium. M1: muzzle length, from Prosthion to a line connecting the front of P2; M2: palatal length, from P2 to Staphylion; M2+M1: overall palatal length, from Prosthion to Staphylion; M3: vomero-palatal length, from Staphylion to Hormion; M4: cranial length, from Hormion to Basion; M6: basilar length, from Prosthion to Basion. Modified from Eisenmann and Baylac (2000) and Eisenmann (2002).

Muzzle. Other cranial differences on Pleistocene equid crania can be the variations on the proportions of the muzzle (Eisenmann 2014). These differences cannot be interpreted as evolutionary processes, but as an explanation of the adaptations in local climate conditions. However, it is not clear whether these differences derive from a micro-adaptive phenomenon or phenotypic plasticity (Boulbes and Van Asperen 2019). Following Allen's rule, short and broad muzzle could represent an adaptation on cold climate conditions and a grazer specialization, while more elongated muzzles (often associated with narrower proportions) could represent an adaptation to temperate climatic conditions. In the case of stenonoid Pleistocene equids, the typical *E. stenonis* and *E. s. vireti* exhibit long muzzles, while *E. stehlini*, *E. mygdoniensis*, *E. s. pueblensis* and *E. s. senezensis* exhibit short muzzles (Eisenmann 2017).

Preorbital Fossa. In modern *Equus*, preorbital fossae (POF) are poorly developed or absent at least virtually (expect for the fossil *E. simplicidens*). Although the function/cause of preorbital fossa is not clear, a possible cause at least on *Equus* could be the "caveing-in" in the maxillary region when cheek teeth are very worn (Eisenmann 2013). In fossil cases, it is rather difficult to distinguish with certainty the presence of POF and to measure its dimensions due to the deformations and poor preservations of crania. In the present study, the author refers the probable presence of a POF.

2.2.3 Correlation between crania and metapodials

In cases, where more than one species is recognized in the same stratigraphic layers of a certain fossiliferous locality, it can be rather tricky how to separate the material when it comes to two species of similar size. Basilar lengths can be corelated with the distal articular breadths of metapodials (M10 and M11). In most asses, hemiones, Grevy's and mountain zebras the proportions are similar, while most Prezwalskii equids and Burchell's zebra (plain zebra) have relatively wider metapodials especially on the distal articular breadth of the MTIII (Eisenmann 2016).

2.2.4 System of measurements

Measurements were taken to the nearest 0.1 mm using a digital caliper, following the system of measurements after Eisenmann et al. (1988) (Figures 2.3–2.9).

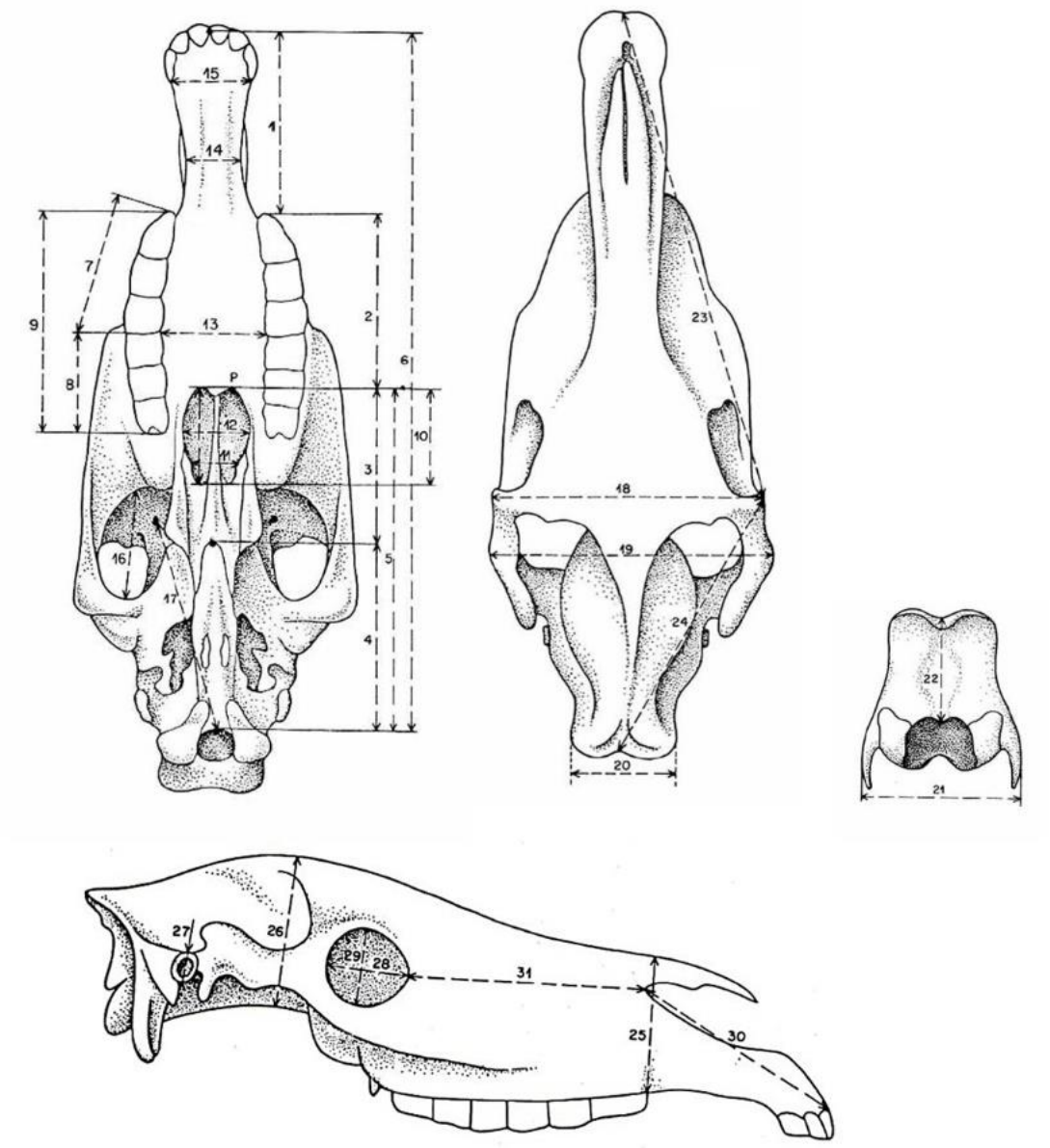

Figure 2.3. Measurements and figures of the cranium according to Eisenmann et al (1988). Ventral view (a): **M1** Muzzle length: from Prosthion (point situated between the bases of the I1) to the middle of the line connecting the anterior borders of the P2, **M2** Palatal length: minimal length between the middle of the line connecting the anterior borders of the P2 and the point P situated at the base of the Palatal spur, **M3** Vomerine length: from the same point P to the middle of the Vomerine notch, **M4** Post-vomerine length: from the middle of the Vomerine notch to Basion (point situated at the middle of the ventral border of the Foramen magnum), **M5** Post-palatal length: from the point P to Basion (5 is roughly equal to 3+4), **M6** Basilar length: from Prosthion to Basion, **M7** Premolar length: alveolar and on the vestibular side, without P1, if present, **M8** Molar length: alveolar and on the vestibular side, **M9** Upper check teeth length: alveolar without P1, if present, **M10** Choanal length: in projection from the point P to the point of meeting of the guttural and caudal parts of the Vomer (always approximative), **M11** Minimal breadth of the choanae, **M12** Maximal breadth of the choanae, **M13** Palatal

breadth: at the level of P4-M1, **M14** Minimal muzzle breadth: the points of the calliper on the premaxillary ridges, **M15** Muzzle breadth: between the posterior borders of the I3, **M16** Length of fossa temporalis: maximal, **M17** Length between Basion and the foramen ethmoidalis; Dorsal view (b): **M18** Frontal breadth: greatest breadth between orbital processes; compass, **M19** Bizygomatic breadth: greatest breadth between the most exterior points of the zygomatic arches; compass, **M20** Occipital breadth: greatest breadth of the supra-occipital crest; Occipital view (c): **M21** Basioccipital breadth: greatest breadth at the base of the paroccipital processes, **M22** Occipital height: from the middle of the dorsal border of the foramen magnum to the middle of the supra-occipital crest, **M23** Anterior ocular line: from Prosthion to the most exterior point of the orbital process, **M24** Posterior ocular line: from the most exterior point of the orbital process to the middle of the supra-occipital crest; Lateral view (d): **M25** Facial height: with the compass, in front of P2, **M26** Cranial height: with the compass at the level of the posterior margin of the orbital process, **M27** Exterior height of meatus acusticus; **M28** Anteroposterior diameter of the orbit; **M29** Dorsoventral diameter of the orbit (perpendicular to 28); **M30** Length of the naso-incisival notch: from prosthion to the posterior end of the narial opening; **M31** Cheek length: from the posterior end of the narial opening to the anterior border of the orbit.

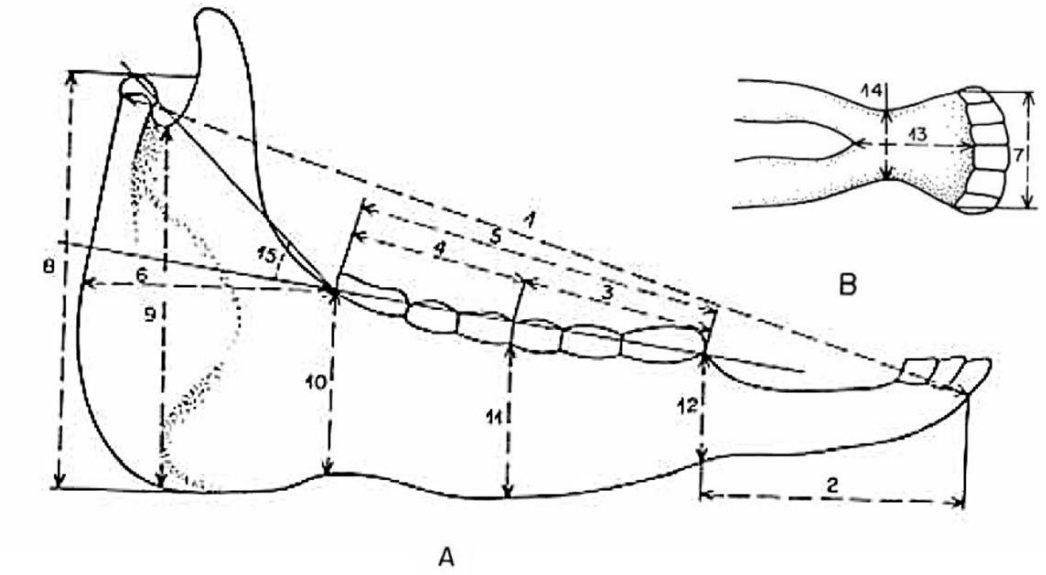

Figure 2.4. Measurements and figures of the mandible according to Eisenmann et al (1988). **M1** Length: from the point between the alveoles of i3 to the back of the condyle; **M2** Muzzle length: from the same point between the alveoles of i3 to the middle of the line connecting the anterior borders of the p2; **M3** Premolar length (alveolar); **M4** Molar length (alveolar); **M5** Tooth row length (alveolar); **M6** Distance between the back of the alveole of m3 and the posterior ascending ramus; **M7** Muzzle breadth: between the posterior alveolar borders of i3;

M8 Height of the mandible at the condyle: from the top of the condyle to the plane tangent to the horizontal ramus (perpendicular to the alveolar plane); **M9** Height of the ascending ramus: from the bottom of the depression between condyle and coronoid process to the same plane; **M10** Height of the jaw posterior to m3 (perpendicular to the alveolar plane); **M11** Height of the jaw between p4 and m1; **M12** Height of the jaw in front of p2; **M13** Length of the symphysis: from the pointed situated between the alveoles of i1 to the back of the symphysis; **M14** Minimal breadth of the symphysis.

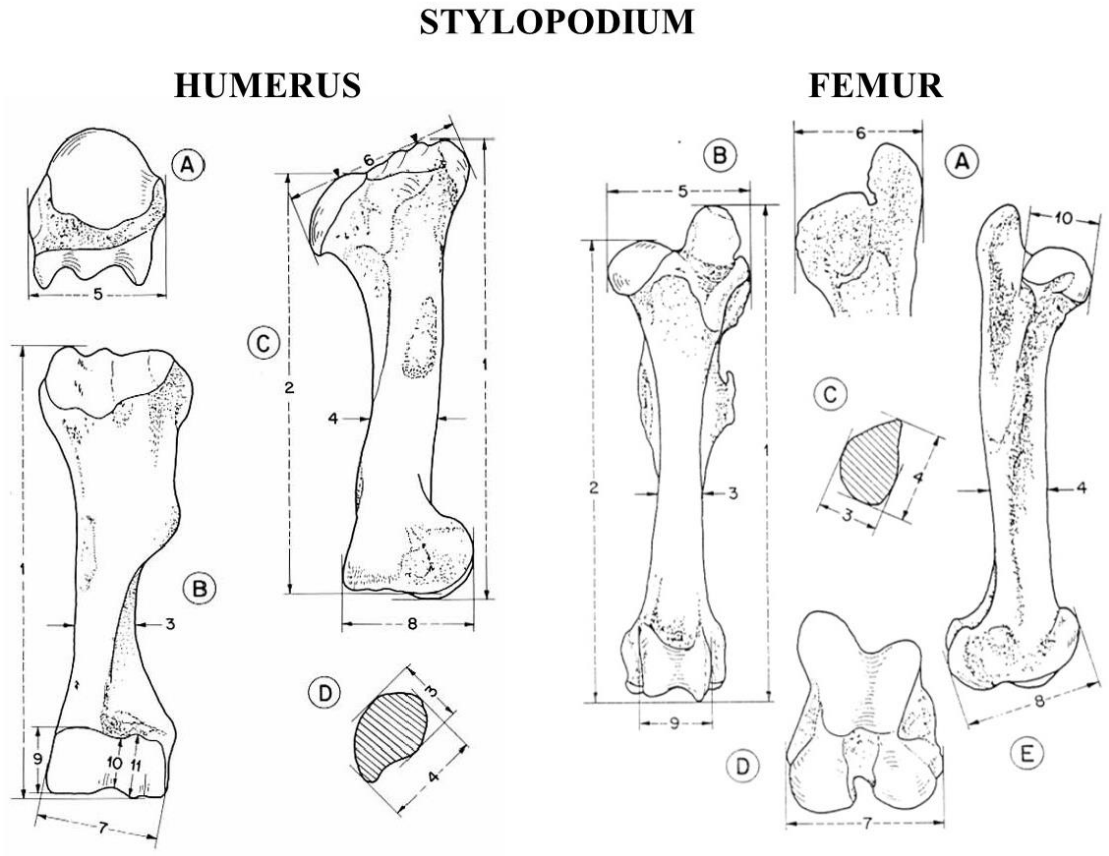

Figure 2.5. Measurements and figures of the humerus and femur according to Eisenmann et al (1988). **Humerus. M1** Maximal length; **M2** Maximal length from caput; **M3** Minimal breadth (oblique); **M4** Diameter perpendicular to, and at level of M3; **M5** Proximal articular breadth; **M6** Proximal depth at the level of the median tubercule; **M7** Maximal breadth of the trochlea; **M8** Distal maximal depth; **M9** Maximal trochlea height (medial); **M10** Minimal trochlea height (in the middle); **M11** Trochlear height at the sagittal crest (near the condyle). **Femur. M1** Maximal length; **M2** Length from caput femoris to lateral condyle; **M3** Minimal breadth (oblique); **M4** Diameter perpendicular to, and at level of M3; **M5** Proximal maximal breadth; **M6** Proximal maximal depth; **M7** Distal maximal breadth; **M8** Distal maximal depth (not at right angle with the long axis of the bone); **M9** Maximal breadth of the trochlea; **M10** Maximal depth of caput femoris.

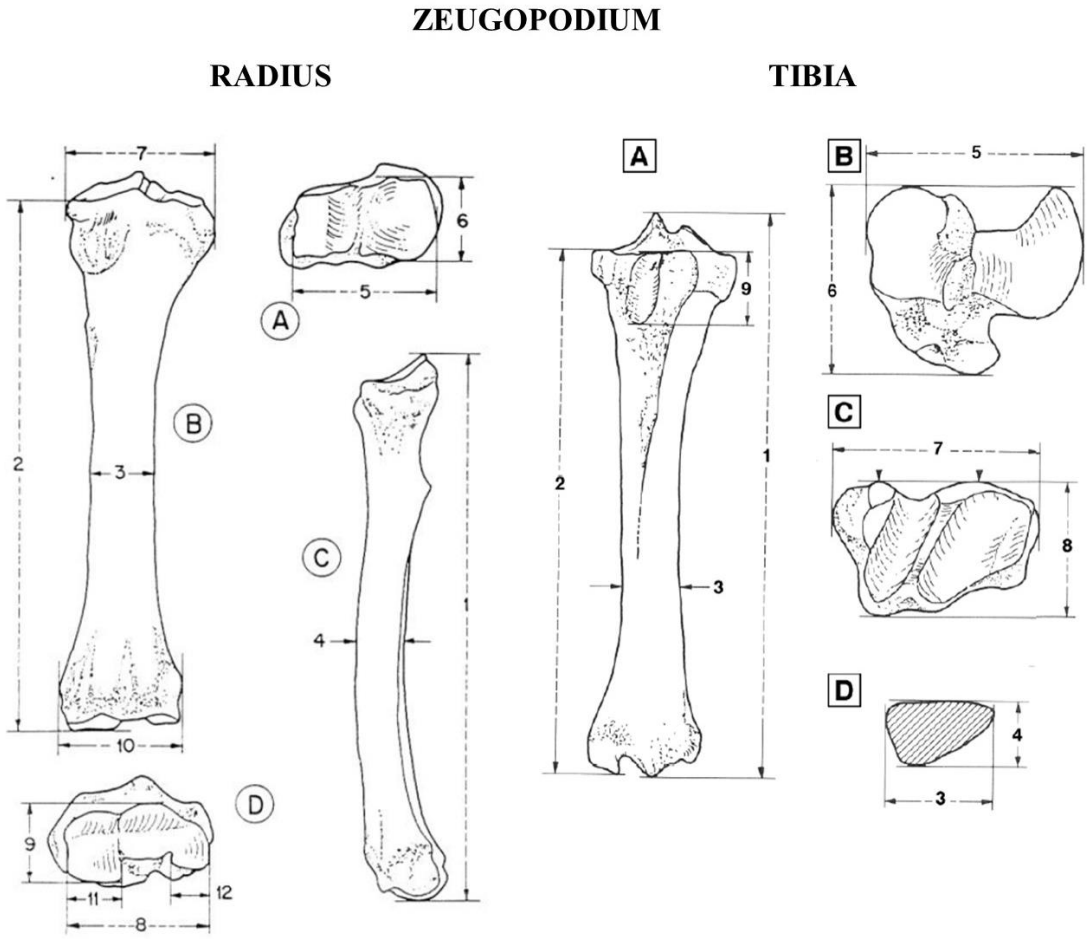

Figure 2.6. Measurements and figures of the radius according to Eisenmann et al (1988). **Radius. M1** Maximal length; **M2** Medial length; **M3** Minimal breadth; **M4** Diameter of diaphysis at level of M3; **M5** Proximal articular breadth; **M6** Proximal articular depth; **M7** Proximal maximal breadth; **M8** Distal articular breadth; **M9** Distal articular depth; **M10** Distal maximal breadth; **M11** Breadth of the radial condyle; **M12** Breadth of the ulnar condyle. **Tibia. M1** Maximal length; **M2** Medial length; **M3** Minimal breadth; **M4** Minimal depth of the diaphysis (more or less at level of M3); **M5** Proximal maximal breadth; **M6** Proximal maximal depth; **M7** Distal maximal breadth; **M8** Distal maximal depth; **M9** Length of the fossa digitalis.

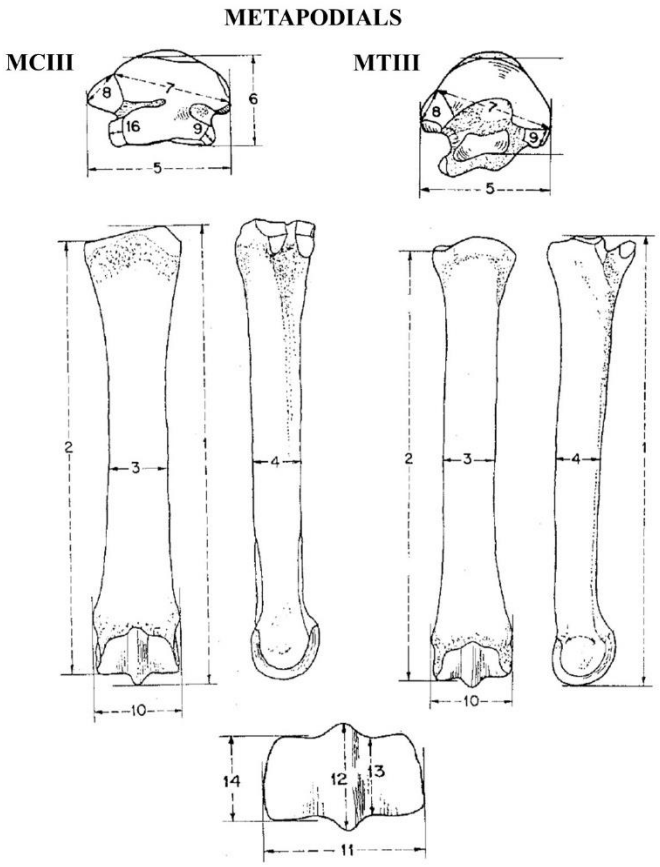

Figure 2.7. Measurements and figures of the third metacarpal (McIII) and third metatarsal (MtIII) according to Eisenmann et al (1988). **Third metacarpal. M1** Maximal length; **M2** Medial length; **M3** Minimal breadth (near the middle of the bone) **M4** Depth of the diaphysis at level of M3; **M5** Proximal articular breadth; **M6** Proximal articular depth; **M7** Maximal diameter of articular facet for the third carpal; **M8** Diameter of the anterior facet for the fourth carpal; **M9** Diameter of the anterior facet for the second carpal; **M10** Distal maximal supra-articular breadth; **M11** Distal maximal articular breadth; **M12** Distal maximal depth of the keel; **M13** Distal minimal depth of the lateral condyle; **M14** Distal maximal depth of the medial condyle; **M15** Angle measuring the dorso-volar development of the keel; **M16** Diameter of the posterior facet for the fourth carpal. **Third metatarsal. M1** Maximal length; **M2** Medial length; **M3** Minimal breadth (near the middle of the bone); **M4** Depth of the diaphysis at level of M3; **M5** Proximal articular breadth; **M6** Proximal articular depth; **M7** Maximal diameter of articular facet for the third tarsal; **M8** Diameter of the anterior facet for the fourth tarsal; **M9** Diameter of the anterior facet for the second tarsal; **M10** Distal maximal supra-articular breadth; **M11** Distal maximal articular breadth; **M12** Distal maximal depth of the keel; **M13** Distal minimal depth of the lateral condyle; **M14** Distal maximal depth of the medial condyle; **M15** Angle measuring the dorso-volar development of the keel.

TARSALS

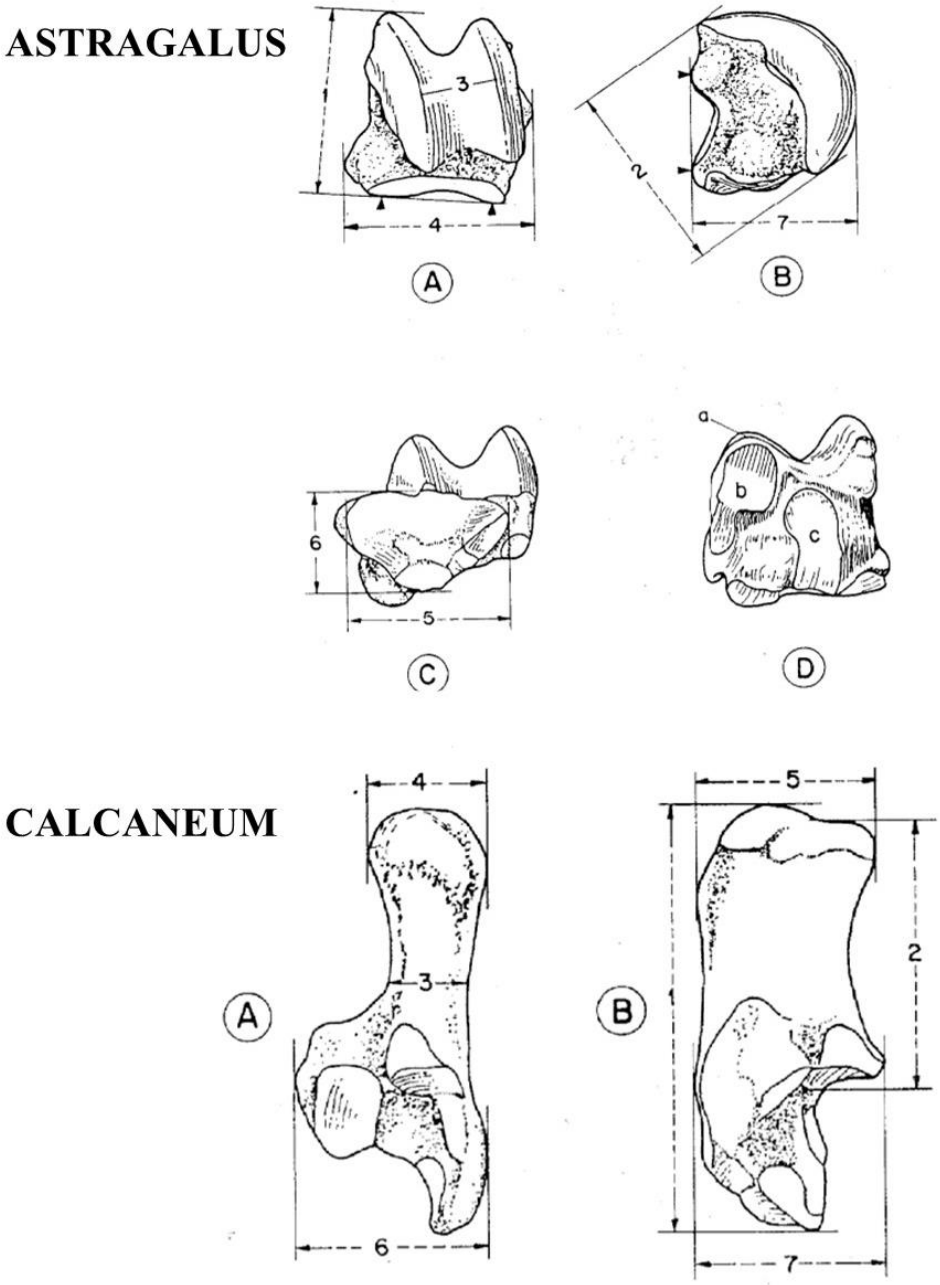

Figure 2.8. Measurements and figures of the astragalus and calcaneum according to Eisenmann et al (1988). **Astragalus. M1** Maximal length; **M2** Maximal diameter of the medial condyle; **M3** Breadth of the trochlea (at the apex of each condyle); **M4** Maximal breadth; **M5** Distal articular breadth; **M6** Distal articular depth; **M7** Maximal medial depth. **Calcaneum. M1** Maximal length; **M2** Length of the proximal part; **M3** Minimal breadth; **M4** Proximal maximal breadth; **M5** Proximal maximal depth; **M6** Distal maximal breadth; **M7** Distal maximal depth.

ACROPODIUM

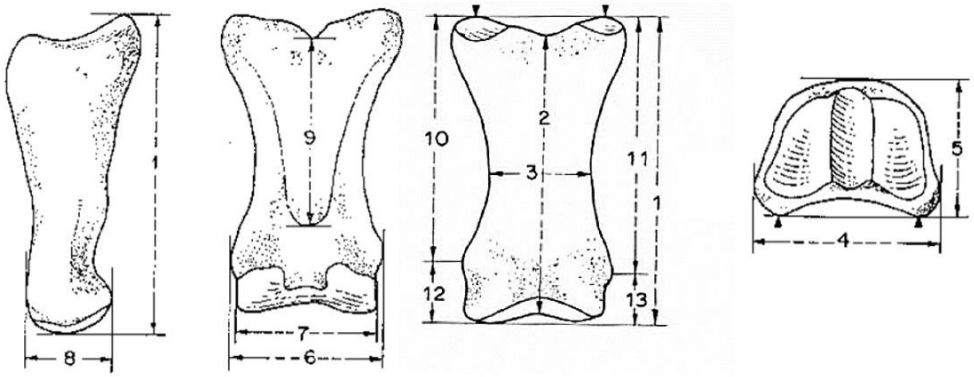

PHI

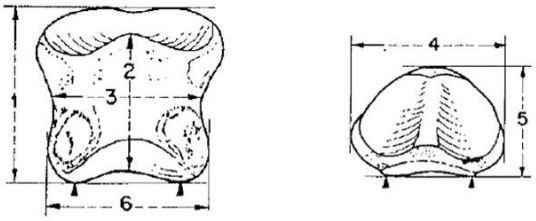

PHII

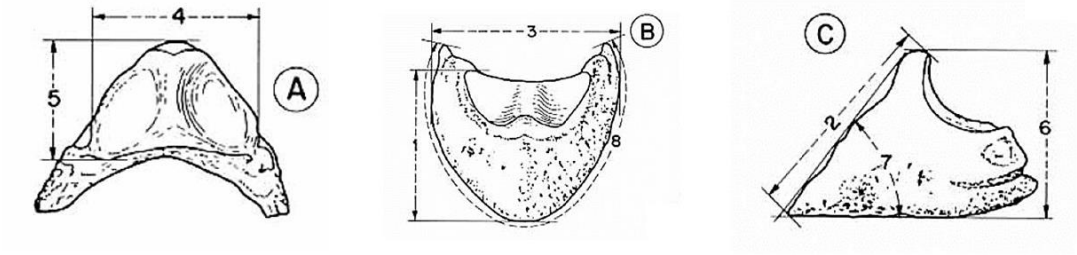

PHIII

Figure 2.9. Measurements and figures of the phalanges according to Eisenmann et al (1988). **First Phalanx. M1** Maximal length; **M2** Anterior length; **M3** Minimal breadth; **M4** Proximal breadth; **M5** Proximal depth; **M6** Distal breadth at the tuberosities; **M7** Distal articular breadth; **M8** Distal articular depth; **M9** Minimal length of the trigonum phalanges; **M10** Medial supratuberosital length; **M11** Lateral supratuberosital length; **M12** Medial infratuberosital length; **M13** Lateral infratuberosital length**. Second Phalanx. M1** Maximal length; **M2** Anterior length; **M3** Minimal breadth; **M4** Proximal maximal breadth; **M5** Proximal maximal depth; **M6** Distal articular maximal breadth**. Third Phalanx. M1** Length from the posterior edge of the articular surface to the tip of the phalanx; **M2** Anterior length; **M3** Maximal breadth; **M4** Articular breadth; **M5** Articular depth; **M6** Maximal height; **M7** Angle between the sole and the dorsal line; **M8** 'Circumference' of the sole.

2.2.5 Statistical analysis/comparisons

In order to characterize, compare, and possibly redefine each taxon, both morphological and morphometric features on crania, mandibles, teeth, and postcranial remains were used. Simpson's log ratio diagrams, box plots, bivariate and multivariate analyses were performed to estimate variation and differences in size and proportions. Differences between the morphology of the equids were further tested using either one-way analysis of variance (either one-way ANOVA or one-way PERMANOVA).

Separation of the material. Fossils from the same fossiliferous locality were separated based on some morphological differences and mainly size. Principal component analysis (PCA) and discriminant analysis (LDA) using PAST 4.15, Simpson's log ratio diagrams and scatter diagrams were used for the separation. These (or some of these) diagrams are not included in the thesis.

Simpson's log ratio diagrams

Simpson's log ratio diagrams (Simpson and Roe 1939) are widely used in equid comparisons. They provide a standard and adequate comparison for both size and shape, expressing differences in size and proportions at the same time among many specimens; if the size is different (e.g., between two crania) similarities in proportions can be easily traced when the curves are parallel to each other. Ratio diagrams are particularly useful because they can compare incomplete specimens on which multivariate analysis cannot be performed due to the possible missing measuring points (especially on fossil remains). Eisenmann (1982, 1995), Bernor et al. (2003), Bernor and Harris (2003) and others used Log10 ratio diagrams on postcranial elements (long bones) to evaluate differences among equids (*Hipparion* and *Equus*), their evolutionary trends and locomotor adaptations. Here, diagrams were created, for both cranial and postcranial material, using either individual specimens (from the same locality) or mean values of different species. *Equus hemionus onager* is used as a reference ('0' line) in all cases, as it is the most common reference (Eisenmann 1980). Excel 365 was used to compute the log10 ratio diagrams.

Box plots

Boxplots are undertaken on the maximal length (M1) and breadth of the diaphysis (M3) for MCIII and MTIII for the same species considered in Log10 ratios diagrams, in addition with *Equus grevyi* (Kenya, Africa), *Equus eisenmannae* from Longdan

(China), *Equus stenonis pueblensis* from La Puebla de Valverde (Spain) and *Equus major* from Senèze (France).

Bivariate Analysis

Scatter diagrams were produced by contrasting Length (Lb) versus Breadth (Bb) of the upper and lower cheek teeth (P2-4/p2-4 and M1-3/m1-3) at 1 cm above the roots. However, for teeth still within the maxilla or mandible, only occlusal surfaces were measured. In that case, length/protocone length ratio in upper teeth and length/double-knot ratio and length/postflexid ratio in lower teeth were used for additional discriminations. Bivariate diagrams were also performed on the metapodials and first phalanges using the maximal length (M1) and breadth of the diaphysis (M3) and on tibiae using the distal maximal breadth (M7) and distal maximal depth (M8). The scatter diagrams were constructed using PAST 4.05 (Hammer et al. 2001).

Multivariate Analysis

Statistical analyses were extended by using multivariate analyses on sets of limb bones measurements to identify groups in equids (third metacarpal, third metatarsal, astragalus, calcaneum, phalanges). Principal Components Analysis (PCA) has been applied on the postcranial material using the PAST 4.05 software (Hammer et al. 2001). PCAs are used to identify variabilities in a sample. The problem of missing data was dealt with the Iterative Imputation method. The third metacarpal and third metatarsal PCAs include the following measurements: M1, M3, M4, M5, M6, M10, M11, M12, M13, M14 (in Log10 ratio diagrams also M8 was included. The present author decided to use both raw measurements and also measurements for each element that were all divided by the geometric mean of the measurements for that element (GEOMEAN) and these GEOMEAN corrected measurements were used in the PCA (Jungers et al. 1995).

One-way ANOVA/One-way PERMANOVA

Analyses of variance were performed to test significant differences among equids. Both parametric and nonparametric tests were applied depending on the case. For normally distributed data ANOVA was performed and for non-normally distributed data the Krustal-Wallis test (PERMANOVA) was implemented. One-way ANOVA has been applied to test significant differences in mesowear and microwear patterns between the different teeth (M1-M2) (see in detail in palaeoecology of *Equus* section). Differences between metapodials of *Equus* were tested using one-way PERMANOVA. Statistical

analyses were performed with the Statistical Package for the Social Sciences (SPSS) version 15.0. Results for all the tests were considered as significant if $\alpha = 0.05$ (level of significance); significant comparisons are shown in bold on the tables. Missing data supported by pairwise deletion.

2.3 PHYLOGENY

The phylogenetic analysis of the Greek *Equus* focused only on taxa that include cranial, dental, and postcranial elements, i.e.: *Equus altidens* (Gerakarou, Krimni), *Equus apolloniensis* (Apollonia) and *Equus stenonis* (Sésklo, Dafnero). The present author adopted the data matrix constructed by Cirilli et al. (2021), that summarizes data matrices from previous publications (such as Bennett 1980; Antoine 2002, 2010; Sun and Deng 2019; Barron Ortiz et al. 2019; Table SI 1); Cirilli et al. (2021) included some additional characters and personal observations in the matrix. Some of the characters have been additionally coded by the present author by direct observations on fossil collections combined with other published fossil or extant specimens (e.g., *Equus stenonis*, *Equus senezensis*, *Equus asinus*, *Equus hydruntinus* among others, see SI 1, Appendix 1). *Equus stenonis* as handled here also includes the Greek populations studied (the author decided to not analyze them separately). The complete sample of the specimens coded in the cladistic matrix is presented in the Appendix 1 text. As a whole, the present cladistic analysis uses 33 taxa and 129 characters (46 cranial, 12 mandibular, 54 dental and 17 autopodial: taken from Cirilli et al. 2021) in order to explore the evolution of the Greek equids and their phylogenetic relationships with the North American Equidae and the early *Equus* from the Old World and China. 29 taxa form the ingroup and 4 (*Tapirus terrestris*, *Hyrachyus eximius*, *Trigonias osborni* and *Merychippus insignis*) the outgroup of the analysis: (Appendix 1 and SI 1) (Cirilli et al. 2021). The characters have been coded either by literature or by direct observations; 6 characters are ordered (5, 6, 91, 92, 113, 114, 129) and 123 characters remained unordered.

The matrix was created in Mesquite 3.81 software (Maddison and Maddison 2023). The cladistic analysis was performed using TNT 1.6 (Goloboff et al. 2008; Goloboff and Morales 2023) with a traditional search method, 1,000 replications and the trees-bisection-reconnection branch-swapping algorithm (TBR). All characters were equally weighted. Gaps are treated as “missing”. Character list and data matrix are presented in SI 1.

2.4 PALAEOECOLOGY OF *EQUUS*

Numerous excavations the past 40 years, especially in Northern Greece (Western and Central Macedonia), establish the Neogene assemblage of Greece to be one of the most up-to-date fossil collections in Europe. As equids are the most common element in these faunas, they are used as a reference not only to understand the taxonomy and evolution of *Equus* between 2.5 and 1.0 Ma in Europe, but also to reconstruct their ecological traits (diet and habitat preferences). Furthermore, as equids are also the most common element in archeological sites or faunal sites contemporaneous with the dispersion of *Homo* out of Africa, they can be used as an environmental proxy to track hominid ecotypes in Eurasia.

Modern equids, such as zebras, Prezwalskii horses or semi-wild horses, were often used as reference to reconstruct the ecology of extinct equids. This approach may lead to inaccurate results, as these living species are mostly grazers occupying open habitats. However, wild donkeys and asses are not exclusively grazers and may occupy dry bushlands in Middle East, Central Asia, or Africa. Thus, to consider the occurrence of equids at a given fossil site cannot be used as a direct environmental proxy.

To overpass this problem, inferences from both feeding habits of equids and locomotor behaviors/locomotor substrates have been combined to track palaeoenvironmental differences between *Equus* local samples from Greece (taxon-free approach: e.g., Reed 1997, 1998). Cursoriality and substrate preferences of equids can be reconstructed using postcranial anatomy mainly on metapodials. Robustness of the metapodials may depict palaeo-landscapes: equids occupying mountainous habitats would tend to have shorter and more robust metapodials than highly cursorial species occupying steppes.

Locomotion apart, diet is also a key parameter to reconstruct the palaeoenvironment of extinct equids. Tracing the dietary preferences of a given species is rather critical for the reconstruction of each ecology. Several methods have been developed over the years for palaeodietary analyses on mammals (Walker et al. 1978; Lee-Thorp and Van der Merwe 1987; Cerling et al. 1997; Hoffman et al. 2015; Fortelius and Solounias 2000; Kaiser and Solounias (2003); Evans et al. 2007; Rivals et al. 2007 and others). Herein, to reconstruct the diet, two methods will be combined with different temporal resolutions: 1) Hypsodonty index (crown height) which reflects the long-term adaptative response to tooth wear and, 2) Dental wear (mesowear and microwear analyses). These analyses can provide insights into equid's feeding behavior. These methods are noninvasive, so can be applied on large dental samples.

Data (post cranial anatomy, microwear and mesowear data) from all known Greek localities and from several French, German, Italian and Swiss institutions/universities were collected by the author.

2.4.1 Hypsodonty index

The index of hypsodonty was originally calculated on the m3, as the ratio of crown height to tooth width (Janis 1988). However, since m3 on equids is kind of the 'worst' cheek tooth to measure due to its great mesiodistal curvature, the index was calculated to the other cheek teeth. The Hypsodonty Index was calculated as H/Lb % ratio, where 'H' represents the maximal height of the tooth and 'Lb' the maximal length at 1 cm above the crown base (Eisenmann et al. 1988; Alberdi 1974). The index was also calculated for little worn teeth if no unworn teeth were available.

2.4.2 Dental wear analyses

The analysis of tooth wear at different scales has been used for nearly half a century in order to track dietary capabilities of species in the fossil record and thus to infer their habitat and climate preferences. Tooth wear reflects availabilities of food resources, individual senescence and can be used to investigate niche partitioning among species of mammals (Janis 1990; Scott et al. 2006; Ungar et al. 2007; Nussey et al. 2007; Kaiser et al. 2013; Calandra and Merceron 2016). There are two main types of tooth wear: attrition and abrasion. Dental attrition corresponds to the wear conducted by tooth-to-tooth contact forming acquired wear facets upon pristine enamel, while abrasion corresponds to food-to-tooth (foreign body to tooth, such as phytoliths or grit) contact and may obliterate wear patterns (Kaiser et al. 2013).

Dental wear analyses can be divided into two types, microwear and mesowear, that correspond to different time scales. Dental microwear analysis reflects short-term dietary signals (Teaford et al. 2020; Teaford and Oyen 1989; Winkler et al. 2020) whereas dental mesowear likely bears a longer time signal (Ackermans et al. 2020, 2021). Microwear analyses are used to correlate the pattern of scars in microscopic scale (such as pits and striations) imposed upon the dental enamel of teeth to the physical properties of the food ingested by the studied individuals just before dying. Herein, both mesowear and microwear analyses were combined to reconstruct the feeding habits of equids.

Due to several limitations at the visiting museums/institutions (giving emphasis on collecting as many morphometric data as possible), microwear analysis has only been

applied on specific European localities (mentioned later) and mesowear analysis has only been conducted on the Greek equids. Data from both Greek and other European equids were collected by the author. The author used extant species (Table D: SI 2) with known dietary habits as a reference to conjecture the equine feeding habits. The dietary preferences of these species are ranging from grazing to mixed feeding to browsing.

2.4.2.1 Dental Microwear Texture Analysis

Microwear analyses are used in the past few decades as a tool to correlate the pattern of the wear features (scratches and pits) with the physical properties of the food resources that were consumed by the studied individual in the days before it died (Walker et al 1978). Confocal microscopy (with its capability of collecting 3D surface data: Boyde and Fortelius 1991) together with scale–sensitive fractal analysis (SSFA) (Ungar et al. 2003) offered a more practical approach to characterize microwear surface textures, now known as dental microwear texture analysis (DMTA) (Scott et al. 2005, 2006). Dental Microwear Texture Analysis (DMTA) has proved to be a very useful tool for the reconstruction of the ecology of both extant and extinct species especially of mammals (Scott et al. 2006; Calandra and Merceron 2016; Haupt et al., 2013; Merceron et al. 2007, 2014; Scott et al. 2005, 2006; Souron et al. 2015; Ungar et al. 2007; Ungar and Evans 2016; Ungar and Zhou 2017) and to reconstruct palaeo-environments (e.g. Ungar et al., 2012; Merceron, Novello, et al., 2016; Berlioz et al. 2018; Blondel et al. 2018; Ungar et al. 2020). It is useful tool free of (inter- or intra-) observer measurements errors (DeSantis et al. 2013; Scott et al. 2005; Galbany et al. 2005; Mihlbacher and Beatty 2012; Mihlbacher et al. 2012) in assessing (palaeo-)diets (Calandra and Merceron 2016;).

Material used in the DMTA.

The material used in the DMTA comes from Quaternary key-localities from Greece and Europe. Data were collected by the author in the following museums and institutes: Greece: Laboratory of Geology and Palaeontology of University of Thessaloniki **(**LGPUT): *Equus stenonis* (Dafnero, Volax), '*Equus stenonis mygdoniensis'* (Gerakarou, Tsiotra Vrysi), *Equus apolloniensis* (Apollonia), *Equus petraloniensis* (Petralona); Museum of Palaeontology and Geology of the National and Kapodistrian University of Athens **(**AMPG): *Equus stenonis* (Sésklo), *Equus* cf. *apolloniensis* (Alykes). France: Centre de Conservation du Musée des Confluences, Lyon (CCMCL):

Equus stenonis vireti (Saint-Vallier), *Equus senezensis* (Senèze); Musée de Paléontologie Christian Guth, Chilhac: *Equus stenonis guthi* (Chilhac-2, 3); Musée National de Préhistoire, Les Eyzies-de-Tayac-Sireuil: *Equus* cf. *stenonis* (Ceyssaguet). Switzerland: Natural History Museum Basel (NMBS): *Equus stenonis* (Upper Valdarno), *Equus stenonis vireti* (Saint-Vallier) and *Equus senezensis* (Senèze). More than 340 dental molds have been scanned from the Greek sample, and more than 180 molds have been scanned from other European institutions/museums.

Extant species have been used as comparative material (Dataset on Table C, SI 2; Alifieri 2021). The dataset, taken from Alifieri (2021), includes wild-shot animals from several places: Bauges Natural Regional Park (BNRP; Alps; Merceron et al. 2021): *Ovis ammon*, *Rupicapra rupicapra*, *Cervus elaphus* and *Capreolus capreolus*; Biebrza marshes, Eastern Poland (Poland; Berlioz et al. 2022): *Alces alces*; Białowieża Primeval Forest in Poland (Hermier et al. 2020; Merceron et al. 2014): *Bison bonasus*; Camargue, Rhone Delta in France (Hermier et al. 2020): *Bos taurus*.

The red deer *Cervus elaphus* from BNRP is a mixed-feeding species with grazing habits (Merceron et al. 2021 and references therein). The species is mainly feeding herbaceous monocots (50-60%), forbs (20-6%) and fruits, acorns (up to 20%), as well as herbaceous dicots (up to 20%). The red deer from BNRP exhibits a seasonal shift from graze to browse from summer to winter (Suter et al. 2004). The roe deer *Capreolus capreolus* is a selective browser (Cibien 1984; Cornelis et al. 1999; Cransac et al. 2001; Storms et al. 2008; Tixier et al. 1997). The *C. capreolus* from BNRP is mainly feeding on evergreen shrubs (bramble leaves, 60-44%), forbs (22-10%) and very low number of fruits (3.4-5.8%) (Merceron et al. 2021). The chamois *Rupicapra rupicapra* and the mouflon *Ovis ammon* are mixed feeders, grazing and browsing depending on resources availabilities and energetic requirements, with *R. rupicapra* having a bigger percentage of grasses in its diet (42-50% vs 32-40%) (Pérez-Barberia et al. 1997; Marchand et al. 2013; Merceron et al. 2021 and references therein). The semi-wild cattle, *Bos taurus* from Camargues, is a variable grazer, feeding on tough vegetation (Hermier et al. 2020 and references therein). The European wood bison, *Bison bonasus* from the Białowieża Forest, is more of a mixed feeder than a grazer (Merceron et al. 2014 and references therein). The moose *Alces alces* from the Biebrza marshes is a selective browser with a diet dominated by hard tissues, feeding on buds, twigs, stems, fresh foliage, berries, bark, and leaf-litter (Berlioz et al. 2022 and references therein).

Sampling/Method. DMTA is preferentially applied on the second upper or lower molars. However, due to possibly post-mortem alterations, glue or limited number of samples can be applied to either third or first molar (upper and lower). When dealing with isolated equine teeth, it is rather difficult to distinguish first and second molars (neither upper, nor lower). Herein, isolated molars were acknowledged as M1,2 or m1,2; in the case of in situ molars, second molars were preferentially sampled otherwise first molars. Too much worn teeth or too recently erupted teeth have been excluded in all cases. The author sampled the antero-lingual facet of the paracone (blue circle, Figure 2.10a) and the lingual facet of the protoloph (antero-lingually of the protocone, red circle, Figure 2.10a) on the first and second upper molars and the antero-labial facet of the protoconid (green circle, Figure 2.10a) on the first and second lower molars.

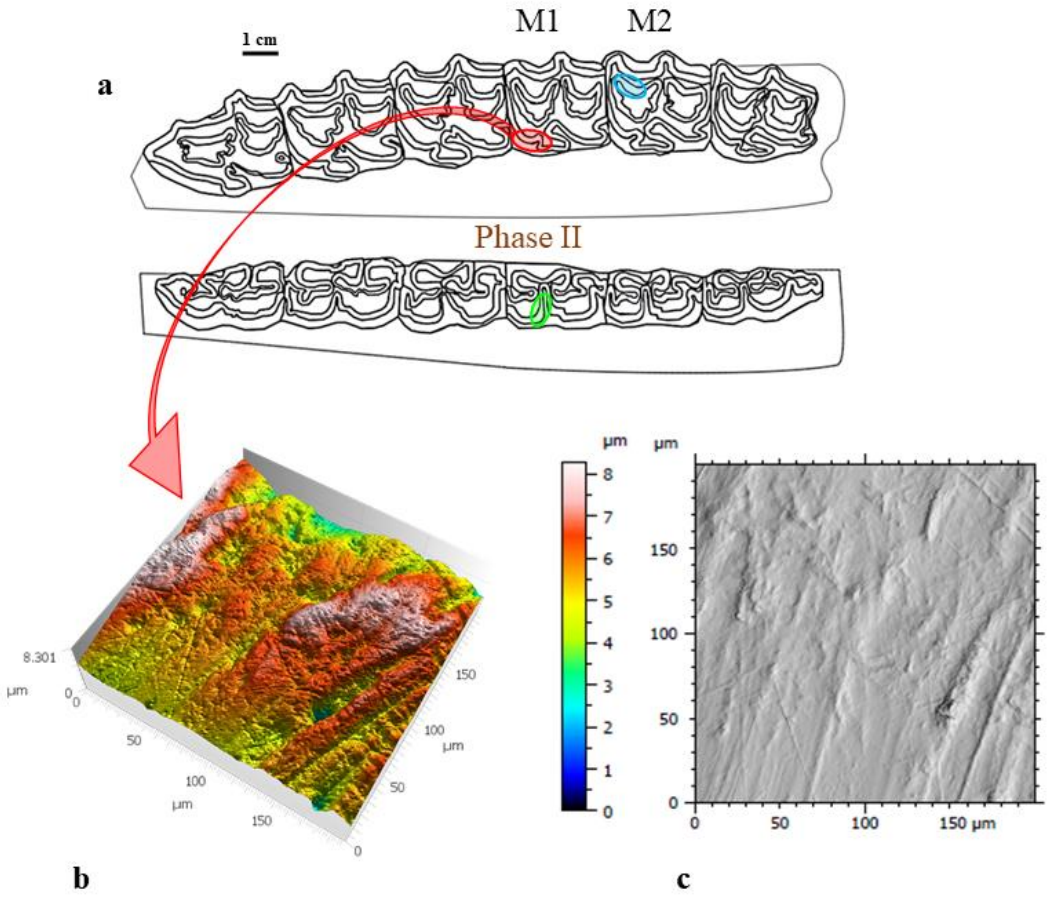

Figure 2.10. (a) Occlusal view of left upper and lower cheek teeth row of *Equus altidens granatensis* from Venta Micena, VM 84-C3-E9-52 (modified from Eisenmann 1995); *Equus apolloniensis* (b) APL-148, 3D surface simulation on shearing dental facet, (c) APL-148, photosimulation.

Teeth were prepared in the labs of the host institutions, following standard procedures, and were thoroughly cleaned with cotton swabs using acetone to remove glue and/or dust. Dental facets were molded (two to three molds per facet) with a blue polyvinyl siloxane silicone (Coltène Whaledent, President regular body). Scans were made directly on the molds (mirror image) using a surface profilometer confocal DCM8 Leica Microsystems (TRIDENT) producing inverse (negative) 3D models (point clouds) of wear surfaces at the Laboratory Palaeontology Evolution Palaeoecosystems Palaeoprimatology (PALEVOPRIM lab, CNRS, University of Poitiers, France). Molds were scanned by the present author, Dr. Gildas Merceron, Anastasia Karakosta and Nikoletta Kargopoulou. The surface profilometer was equipped with a 100× objective (Leica Microsystems; NA=0.90; working distance=0.9 mm; see also Merceron et al. 2016), extracting a 200 x 200 μm area and was saved to be used for DMTA. At that point, samples that were dusty, glued, with badly preserved enamel or with post-mortem alterations (features with unusual morphology or fresh features made during the collecting process or during storage) were excluded from the analysis following King et al. (1999). The resulting data were analysed in MountainsMap software v.7.0 and v.8.0 (Sensofar metrology) to export the Scale Sensitive Fractal Analyses (DMTA-SSFA).

Four (SSFA) variables were used to characterize microwear surface textures: complexity (area scale fractal complexity, *Asfc*), anisotropy (exact proportion of length scale anisotropy of relief, *epLsar*), heterogeneity (heterogeneity of the area scale of fractal complexity, *HAsfc* with 9, 36, 81 cells) and scale of maximal complexity (*Smc*) or scale of maximum fractal complexity (*Smfc*, in MountainsMap' s SSFA module). Textural fill volume (*Tfv*), also a SSFA variable, was not available in the versions 7.0 and 8.0 of Mountains (Calandra et al. 2022). When all these SSFA variables are combined, they provide a quantified characterization of the microwear surface features and a good dietary classification (DeSantis 2016; Merceron et al. 2021; Scott et al. 2005, 2006 among others). Their selection was done in regard to their statistical significance.

Complexity (Asfc) measures changes in surface roughness at different scales (hard and brittle foods from tough ones) (DeSantis 2016; Scott et al. 2012, 2006, 2005; Ungar et al. 2003). Complexity is positively correlated with mastication of browse and hard items, such as seeds, fruits, twigs, and bark (Scott, 2012; Merceron et al. 2014; Calandra and Merceron, 2016). Such foods give higher Asfc values (generate surface complexity)

as they require more crushing force to be reduced, forming pits (Merceron et al. 2014, 2012; Ramdarshan et al. 2016; Scott 2012; Scott et al. 2012; Solounias and Semprebon 2002; Ungar 2015; Ungar et al. 2007). Anisotropy (epLsar) is a measure of directionality, orientation of the surface relief. Anisotropy is positively correlated with grazing habits (DeSantis 2016; Merceron et al. 2016b, 2014; Schulz et al. 2010; Scott 2012; Scott et al., 2012) and also with tough leaf eating (leaf-dominated browsers; Fortelius et al. 2002; Hedberg and DeSantis 2017; Merceron et al. 2021, 2014, 2012, 2010; Ramdarshan et al. 2016). Both dietary preferences give surfaces dominated by aligned striations. When the surface is dominated by pits (browsing with consumption of hard foods) and when the scratches are not oriented (diet of soft, non-tough foods like forbs; Ungar 2015), the epLsar is low. The heterogeneities H9, H36 and H88 show the variety of the mechanical properties of the foods ingested in three different scales (3x3, 6x6 and 9X9 cells). They give higher values in polytypic diets than monotypic and seed-free ones (Ramdarshan et al. 2016).

Statistical analysis for DMTA.

Facets that have same functions during mastication (shearing phase II), that are the mesio-lingual protocone facets of the upper molars (Figure 2.10, red circle) and the disto-labial protoconid facets of the lower molars (Figure 2.10; green circle), according to Ramdarshan et al. (2017), they were grouped.

Statistical analysis was performed using the SPSS version 15.0 statistical software package and run the non-parametric Kruskal-Wallis tests for equal medians, because the data were not normally distributed. Followed by pairwise Dunn's post hoc (SI Appendix B2), used the Bonferroni p values, since they are more statistically constrained. Interspecific variations among the equine samples were also explored in order to track potential seasonal signal in the feeding habits.

2.4.2.2 Dental Mesowear Analysis

The mesowear method was developed by Fortelius and Solounias (2000). Mesowear describes the tooth wear patterns that are caused from an individual's diet over a large part of its lifetime (Fortelius and Solounias, 2000; Rivals et al., 2007). Mesowear is a macroscopic dietary proxy for ungulate in which worn molar cusps are characterized by two variables: their sharpness (sharp, round, blunt) and degree of (occlusal) relief (high, low) (Fortelius and Solounias 2000; Rivals et al. 2007; DeMiguel et al. 2008; Mihlbachler et al. 2006). Mesowear is observed by naked-eye or low magnification

(using hand lens). Mesowear was firstly applied only on upper molars (strictly on M2), examining the buccal edges of paracone or metacone (Fortelius and Solounias 2000). Kaiser and Solounias (2003) extended this method to four upper cheek teeth (P4–M3) on extinct and extant equids making available to include more isolated teeth from the studied assemblage. Two populations of the recent zebras *Equus quagga burchelli* Gray, 1824, and one large fossil with lots of isolated cheek teeth of *Hippotherium primigenium* Meyer, 1829, were used it their analysis. There are two protocols the original one by Fortelius and Solounias (2000) and the second one by Mihlbachler et al. (2011). The original method discriminates the buccal view of the molar cusp in 4 categories: 0 = high and sharp cusp, 1 = high and round cusp, 2 = low and sharp cusp, 3 = low and round cusp and 4 = low and blunt cusp. Herein, we apply Protocol 2 using the Mesowear Scale given by Mihlbachler et al. (2011) that categorises ungulates into four general groups; grazers, graze-dominated mixed feeders, browse-dominated mixed feeders, and browsers (Figure 2.11b). This scale was developed by Mihlbachler et al. (2011), dividing dental mesowear data from modern equids to seven stages representing seven cusp types (numbered from 0 to 6 with stage 0 for high and sharp (stage 0) to stage 6 completely blunt with no relief) (Figure 2.11a). In addition, "stage 7" is given to teeth with negative relief (e.g., a convex cusp apex), but it is not included in the ruler since it is rarely observed among equids (Mihlbachler et al. 2011). According to the Mesowear Scale, the earliest equids (~55 Ma) were browsers consuming fruits, while the Eocene and Oligocene equids were leafy browsers (Figure 1E in Mihlbachler et al. 2011). The lowest mesowear scores are in the earliest Oligocene suggesting low abrasion. The subfamily Equinae, that includes extant equids, appeared in the early Miocene (18 Ma) sugging s shift towards grazing (grass-eating) diets (Figure 1E in Mihlbachler et al. 2011).

Mesowear data collection. To score mesowear data, worn cusp apices were observed macroscopically, photos were taken (at the labial side of the upper molars and at the lingual side of the lower molars) and partitioned into categories based on their sharpness and degree of relief. In the present study, mesowear analysis has only been applied on the first and second upper and lower molars (M1, M2, m1, m2), and did not get extended on premolars, so that both mesowear and microwear results could be compared with each other. In cases where first and second molars where not well-preserved, the author used M3 and m3. Molars were examined in their occlusal relief (low or high) and cusp shape (sharp, rounded, or blunt) of the apex of the paracone or metacone and scored

were converted to a single mesowear score (MWS) following the mesowear "ruler" (Figure 2.11a) conducted by Mihlbachler et al. (2011). The mesowear score was calculated for all specimens that had at least one well-preserved cusp. Very early (unworn or little worn, stage 1) or very late (stage 4) worn teeth were excluded from the analysis. In cases that can be applied, the author observed at least 20 specimens as proposed by Fortelius and Solounias (2000) for a more accurate classification. However, when it comes to fossil remains that is not always possible. In these cases, the author observed as many molars as possible.

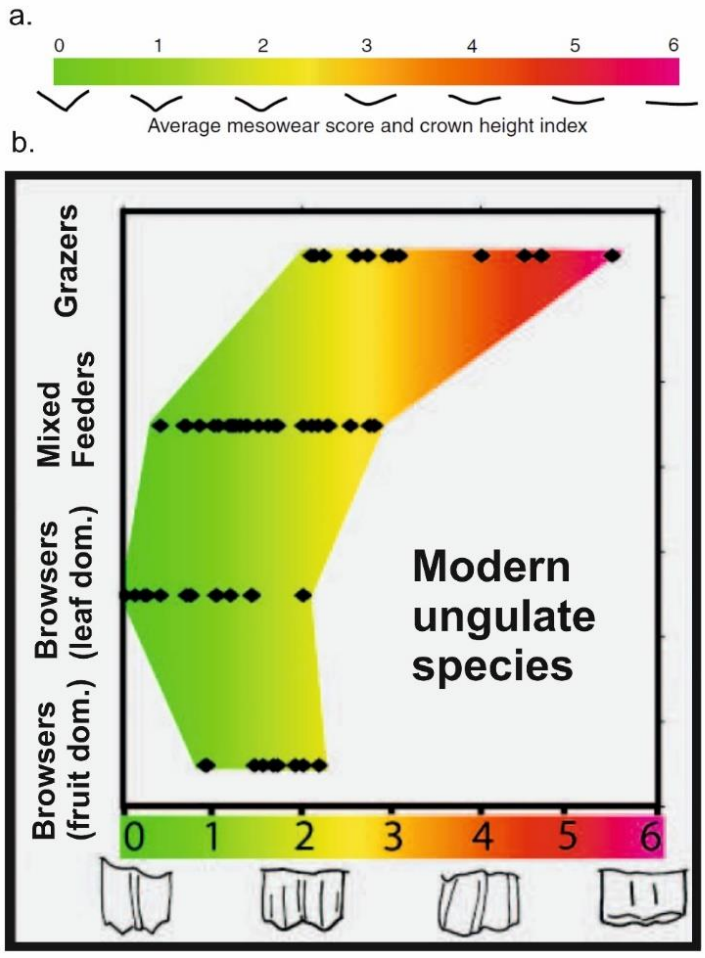

Figure 2.11. (a) Average mesowear score and crown height index, (b) Average mesowear values converted to a univariate scale for modern ungulate species arranged by diet. Taken from Mihlbachler et al. (2011).

The results of this method were compared to the results conducted by Uzunidis et al. (2017) (with the same method) on the Middle Pleistocene equids from Southern France: Camps-de-Peyre (*Equus mosbachensis campdepeyri*), La Micoque (*Equus*

mosbachensis micoquii), Lunel-Viel I and Lunel-Viel IV (*Equus mosbachensis palustris*) and Igue des Rameaux (*Equus mosbachensis* ssp.) and with the equine results of Semprebon et al. (2019). Also, they were compared to the extant and fossil ungulate species (SI 2) such as *Bison bonasus*, *Bison menneri*, *Bison priscus*, *Bos primigenius*, *Bison schoetensacki* and *Bison* cf. *degiulii* scored by Maniakas (2019), *Croizetoceros ramosus* and *Gazella bouvraine* from Gerakarou scored by Alifieri (2021) and the extant *Capreolus capreolus*, *Cervus elaphus*, *Ovis ammon* and *Rupicapra rupicapra* also scored by Alifieri (2021).

2.4.3 Ecomorphology–habitat analysis

Combining metric data (morphological characteristics) mainly from third metapodials with the studies of tooth characteristics (mesowear, microwear) is the best way to guarantee the robustness of palaeoecological implications from ecomorphological patterns and their use as a proxy. The abundance of the equid material from the Early and Middle Pleistocene European fossiliferous localities (faunas) and the large number of third metapodials (McIII and MtIII) gives the opportunity to quantify locomotor adaptations relevant to habitat preferences.

Habitat is associated with the length of third metapodials. According to Gregory (1952), relatively elongated third metapodials (in relation to body size) are adaptive to open landscapes and are associated with cursorial locomotion, while relatively broad (mediolaterally expanded third metapodials) are adaptive to closed or wet habitats (Gromova 1949, 1952). Following Gromova' s (1949) framework on the functional interpretation of the metapodials of hipparionine equids (Gromova 1949, 1952), Eisenmann (1995) is linking metapodial gracility to open and dry habitats. Increasing metapodial gracility is considered as a shift in the location of the lateral metapodials and the tridactyl foot (hipparionine) becomes functionally more monodactyl (equine); primitive equids are tied to rather wet and forested habitats, while modern ones to dry and open landscapes (Scott 2004). Furthermore, the midshaft-diaphysis dimensions of the metapodials are reduced in equids inhabiting in drier environments (Gromova 1949, 1952). Equids occupying mountainous habitats would tend to have shorter and more robust third metapodials than highly cursorial equids occupying open habitats (steppes) (Scott 2004).

Habitat analysis.

Habitat scores were originally developed for bovids, but also applied on hipparions and extant species of *Equus*. This analysis is size independent and taxon-free, and taxonomic identification is not needed for the determination of any morphological adaptations relevant to environment and ecology (Scott 2004).

Material and methods of habitat analysis.

The sample of *Equus* metapodials used in the analysis includes 280 third metacarpals and 320 third metatarsals from the Greek and European fossil record and extant *Equus asinus africanus* (Eisenmann 2007) and *Equus grevyi* (Eisenmann 2009). Ten standard measurements were taken on the third metapodials (MPIII) (M1, M3, M4, M5, M6, M10, M11, M12, M13 and M14) according to Eisenmann et al. (1988) and Bernor et al. (1997). Only metapodials with all ten measurements were considered complete and were included in the analysis. All these measurements were taken by the author of this thesis. Data from extant equids were taken from https://vera-eisenmann.com/.

The metapodials measured and analysed herein were gathered from five countries: Greece (Aggitis, Apollonia, Dafnero-1, 3, Gerakarou, Libakos, Kapetanios, Krimni-1,2,3, Petralona Cave, Platanochori-1, Polylakkos, Riza-1, Siatista-E, Tsiotra Vryssi, Vassiloudi, Volax, Sésklo, Alykes, Volos, Vatera); Italy (Montopoli-Lower Valdarno, Upper Valdarno, Olivola, Matassino, Casa Frata, Pirro Nord, Grotta Romanelli); France (Senèze, Saint-Vallier, Chilhac-2, 3, Ceyssaguet); Switzerland (Senèze, Saint-Vallier, Upper Valdarno); Germany (Süssenborn) (for information of the institutions see Chapter 2.1 Material).

The measurements are analogous for equids and bovids facilitating the comparisons between the two families and they were used to generate a common size variable that is referring as Metapodial Global Size Variable (MGSV). The MGSV was generated following Jungers et al. (1995) and Gordon (2002; 2003). For equids, this size variable is the geometric mean of nine variables: M3, M4, M5, M6, M10, M11, M12, M13, and M14 of Eisenmann et al. (1988).

$$MGSV = (M3 \times M4 \times M5 \times M6 \times M10 \times M11 \times M12 \times M13 \times M14)^{(1/9)}$$

Measurements were transformed to generate shape variables independent of size, so that the relationship between the morphology of the metapodials and habitat are uncorrelated with size. Each measurement is divided by the MGSV and resulting ratios were logged (see Scott 2004). The result is ten variables that are size independent. Each variable gets the prefix ‘si’ ‘for size independent’. For bovids and by extension for

equids, siM1 and siM3 variables are associated with habitat. These analogous variables are the morphological basis of the 'habitat score' (HS) (see Scott 2004).

2.4.4 Body mass estimation and limb proportion

The body mass was estimated following the recommendations of Saarinen et al. (2021). They proved that the better equations to estimate body mass were the ones published by Scott (1990) using the metapodials. In order to reconstruct body mass, the present author used measurements of the minimum midshaft width, maximum proximal width, and maximum distal width of third metacarpals and third metatarsals. Saarinen et al. (2021) defined body size classes: small (<380 kg), medium (380–450 kg), large (450–550 kg), and very large (>550 kg).

2.5 ABBREVIATIONS

Greek Locality Abbreviations.

Ag Aggitis (Drama Basin, Eastern Macedonia),

Al Alykes (Volos, Magnesia),

APL Apollonia (Mygdonia Basin, Central Macedonia),

AQP Aliakmon Q-Profil (Aliakmon Basin, Western Macedonia),

DFN/DFN3 Dafnero-1/3 (Aliakmon Basin, Western Macedonia),

E-SIA isolated surface specimens from Siatista (Aliakmon Basin, Western Macedonia),

GER Gerakarou (Mygdonia Basin, Central Macedonia),

KAL/KLT Kalamoto-1/-2 (Mygdonia Basin, Central Macedonia),

KPT Kapetanios (Aliakmon Basin, Western Macedonia),

KRI/KRM/KMN Krimni-1/2/3 (Mygdonia Basin, Central Macedonia),

LIB Libakos (Aliakmon Basin, Western Macedonia),

PEC Petralona Cave (Chalkidiki, Central Macedonia),

PLN Platanochori-1 (Mygdonia Basin, Central Macedonia)

POL Polylakkos (Aliakmon Basin, Western Macedonia),

PYR Pyrgos (Peloponnese),

RIZ Riza-1 (Mygdonia Basin, Central Macedonia),

RVL Ravin of Voulgarakis (Mygdonia Basin, Central Macedonia),

SES Sésklo (Volos, Magnesia),

TSR Tsiotra Vryssi (Mygdonia Basin, Central Macedonia)
VAT Vatera (Lesvos Island, Northeastern Aegean Sea),
Vo Volos (Volos, Magnesia).
VOL Volakas (Drama Basin, Eastern Macedonia),
VTR-E Vatera E-site (Lesvos Island, Northeastern Aegean Sea),
VTR-F Vatera F-site (Lesvos Island, Northeastern Aegean Sea).

European Locality Abbreviations.
Cey Ceyssaguet (France),
CF Casa Frata (Italy),
CH2A, CH2B, CH3 Chilhac (France),
Dm Dmanisi (Georgia),
GR Grotta Romanelli (Italy),
Li Liventsovka (Russia),
LPDV La Puebla de Valverde (Spain),
LV Lower Valdarno (Italy),
MAT Matassino (Italy),
MONT Montopoli (Italy),
OLI Olivola (Italy),
PN Pirro Nord (Italy),
SE, Se, SZ Senèze (France),
St.V. Saint-Vallier (France),
SUE, Süβ Süssenborn (Germany),
VA Upper Valdarno (Italy).

Museums/Institutions/Laboratories.
AMPG Museum of Palaeontology and Geology of the National and Kapodistrian University of Athens (Greece),
CCMCL Centre de Conservation du Musée des Confluences, Lyon (France),
GUL Laboratoire de Géologie, Université Claude-Bernard Lyon I (France),
IGF University of Florence (Italy),
LGPUT Museum of Geology-Palaeontology-Palaeoanthropology of the Aristotle University of Thessaloniki (Greece),
MNP Musée National de Préhistoire, Les Eyzies-de-Tayac-Sireuil (France),

MPCGC Musée de Paléontologie Christian Guth Chilhac (France),

NMBS Natural History Museum Basel (Switzerland),

PALEVOPRIM Laboratory Palaeontology Evolution Palaeoecosystems Palaeoprimatology, University of Poitiers (France),

SNRC Senckenberg Nature Research Society: Station of Quaternary Palaeontology, Weimar (Germany),

UB University of Bordeaux (France),

VM Vrissa Museum of Natural History (Lesvos Island).

Anatomical Abbreviations.

AST Astragalus/talus,

BA Basion,

BL Basilar length,

Bo ant. Breadth anteriorly,

Bo Occlusal breadth,

Bo post. Breadth posteriorly,

Bp Breadth of the protocone,

CAL Calcaneum,

H Maximal height,

HO Hormion,

Lb/Bb Length/Breadth at 1cm above the roots,

Lo Occlusal length,

Lp Length of the protocone,

Lprfl Length of the preflexid,

Lptfl Length of the postflexid,

MCIII Third metacarpal,

MCX Third metacarpal measurement X,

MpIII Third metapodial,

MTIII Third metatarsal,

MTX Third metatarsal measurement X,

PhI First phalanx,

PhAI First anterior phalanx,

PhII Second phalanx,

PhIII Third phalanx,

POF Preorbital fossa,
PR Prosthion,
Prfl Preflexid,
Prl Protoloph,
Pro Protocone,
Ptcd Protoconid,
Ptfl Postflexid.

Indices.
FI Franck's Index,
HI Hypsodonty Index,
KI Keel Index,
PaI Palatal Index,
PI Protocone Index.

Taxa used in DMTA.
AALC *Alces alces*,
BBONA *Bison bonasus*,
BTAUR *Bos taurus*,
CCAPRE *Capreolus capreolus*,
CELAPH *Cervus elaphus*,
CRUMGE *Croizetoceros ramosus gerakarensis*,
EAFFGRA *Equus* aff. *E. a. granatensis*,
EALTI *Equus altidens*,
EAPOL *Equus apolloniensis*,
ESENEZ *Equus senezensis*,
ESTE *Equus stenonis*,
EUTEGU *Eucladoceros tegulensis*,
GBOUVR *Gazella bouvrainae*,
OAMMO *Ovis ammon*,
RRUPI *Rupicapra rupicapra*.

Other Abbreviations.
Asfc area-scale fractal complexity,

BNRP Bauges Natural Regional Park,

CS Cusp shape,

DMTA Dental Microwear Texture Analysis,

epLsar exact proportion length-scale anisotropy of relief,

Fm Geological Formation,

HS Habitat score,

LFA Local Fauna Assemblage,

MX Measurements of the postcranial material,

MX/mX Upper and lower molar respectively,

OR Occlusal relief,

PCA Principal component analysis,

PX/pX Upper and lower premolar respectively,

s. l. Sensu lato.

CHAPTER 3. GEOLOGICAL FRAMEWORK OF THE FOSSILIFEROUS LOCALITIES

3.1 INTRODUCTION

Fossil Equidae (genus *Equus*, family Equidae), which admittedly constitute the overwhelming percentage of Greek mammal fauna of this period in number of finds, compose the subject of this doctoral thesis. More than 20 equid-bearing sites are studied. However, the actual number of Quaternary localities in Greece is much greater considering the remains from the archaeological sites (which is beyond the scope of the thesis). Equid remains (genus *Equus*) come from Quaternary deposits from all over Greece, mainly from the Greek mainland but also from islands (Kos, Rhodes, Lesvos, Crete). The Greek *Equus* fossil record starts from the early Villafranchian (Damatria, Epanomi) to Late Pleistocene-Holocene; however, most of the studied fossils come from the late Villafranchian localities and especially from Mygdonia Basin (Figure 3.1). Stratigraphical information of the studied fossiliferous localities is here presented based on their geological/geographical position, e.g., Mygdonia Basin, Chalkidiki Peninsula, Drama Basin, Aliakmon Basin, Peloponnese, Magnesia (Thessaly) and Lesvos Island. However, in some cases, detailed stratigraphy and dating are missing; some of the localities do not have a precise stratigraphical position because they come from old collections such as Libakos, Polylakkos, Kapetanios and Q-Profil from Western Macedonia and Pyrgos from Peloponnese (Steensma 1988; Van der Meulen and Van Kolfschoten, 1986).

3.2 MYGDONIA BASIN

Mygdonia Basin is situated in central Macedonia (Greece), northeastern of Thessaloniki, and represents an extensive and elongated east–west-trending tectonic depression. Its formation started during the Early/Middle Miocene forming the pre-

Mygdonian Basin. During the Neogene–Early Pleistocene, the basin was filled with fluvial-fluvioterrestrial and lacustrine deposits. At the beginning of the Middle Pleistocene new tectonic events subdivided the basin into smaller subbasins (Mygdonia, Zagliveri, Doubia, Marathoussa), which were filled mostly by lacustrine deposits. The current lakes Koronia and Volvi are the remnants of the original Mygdonia lake, which existed during the Pleistocene (Psilovikos 1977).

Figure 3.1 Map with the Greek localities where *Equus* has been recorded. **1.** Damatria, **2.** Epanomi, **3.** Tourkovounia, **4.** Dafnero sites, **5.** Sésklo, **6.** Volax, **7.** Vatera sites, **8.** Gerakarou, **9.** Vassiloudi, **10.** Pyrgos, **11.** Tsiotra Vrysi, **12.** Krimni sites, **13.** Libakos, **14.** Polylakkos, **15.** Kapetanios, **16.** Alykes, **17.** Apollonia, **18.** Ravin of Voulgarakis, **19.** Kalamoto sites , **20.** Platanochori, **21.** Riza-1, **22.** Volos, **23.** Q-Profil, **24.** Kos Island, **25.** Marathousa, **26.** Kyparissia, **27.** Petralona Cave, **28.** Megalopolis, **29.** Lerna, **30.** Franchthi Cave, **31.** Agios Georgios Cave, **32.**Aggitis Cave, **33.** Penios Valley. The map of Greece is taken from www.vemaps.com.

Since the middle of the 1970's few were known about the mammalian presence in the Mygdonia Basin. A handful of rhino teeth were only known from an old clay-pit, situated in the northwestern limit of the basin, near the village Chrysavgi (Figure 3.2). Some years later, mammal remains were found in the locality 'Krimni 1' (KRM) (Sakellariou-Mane et al. 1979).

After extensive investigations in the basin conducted by the LGPUT and international collaborations more mammal sites have been discovered in the Pleistocene deposits of the area which further enriched the fossil collections (Koufos and Melentis, 1983; Koufos et al. 1988, 1992; Konidaris et a. 2015). Several studies have been published during the last 40 years about the mammalian faunas of Mygdonia Basin, concerning their taxonomy, biochronology and palaeoecology (e. g. Koliadimou, 1996; Kostopoulos, 1996; Koufos, 1992a, b; Kostopoulos and Koufos 1994, 2000; Koufos et al; 1995, 1997, 2018; Tsoukala and Chatzopoulou 2005; Maniakas 2019; Kokotini 2020; Konidaris et al. 2015, 2020, 2021).

The Neogene/Quaternary deposits of the basin are divided in two main groups the Premygdonian and the Mygdonian Group (Psilovikos, 1977; Koufos et al. 1995). Three successive formations have been distinguished in the Premygdonian Group: Chrysavgi Fm, Gerakarou Fm and Platanochori Fm (Koufos et al., 1995).

Chrysavgi Formation. It is the oldest formation of the basin that directly overlies the pre-Neogene basement. It has limited exposure at the north-western part of the basin (north of Chrysavgi village) (Figure). It mainly consists of alternating lenses and lens-shaped intercalations of grey-white, loose, coarse conglomerates and sands with silty-clayey lenses; its thickness is estimated about 40–50 m. The lower part of Chrysavgi Fm is dominated by coarse conglomerates; a gradual decrease of the pebbles size is observed from the bottom to the top of the formation. In the upper part of the formation, lenses of silty sand and silty clays or lenticular intercalations are more frequent (Koufos et al. 1995). The fossiliferous locality ‘Chryssavgi-1’ (CHR) is situated into a clay pit in the upper part of this formation. The fauna mainly consists of micro-mammals and some large ones (*Brachypotherium brachypus*); the faunal assemblage suggests a Late Astaracian age (Middle Miocene), MN 7+8 for the fauna (Koliadimou 1996; Koliadimou and Koufos 1998; Koufos and Kostopoulos 2013).

Gerakarou Formation. This is the most widely exposed formation across the Mygdonia Basin, consisting of red beds, with typical exposures near Gerakarou Village. Its thickness exceeds more than 100 m. The red beds consist of alternating lenses and lens-shaped beds of loose gravels, coarse reddish-brown sands and reddish-brown silts and clays deposited in a fluvioterrestrial environment with a few lenses of sandstones and marls intercalated these beds. In the field, the red beds bare pyramidic erosion that makes them quite easy to recognize (Koufos et al. 1995).

Eight fossiliferous localities have been found in Gerakarou Fm: Gerakarou-1 (GER), Vassiloudi-1 (VSL), Krimni-1, 2 and 3 (KRI, KRM and KMN respectively), Kalamoto-2 (KLT), Krimni-stratified (K-S1, -S2 respectively) and Tsiotra Vryssi (TSR). All sites are situated in the upper levels of the Gerakarou Fm. Even though, the localities are not isochronous, the study of the material based on the large mammal faunas suggests a late Villafranchian age (Koufos 1992; Konidaris et al. 2015; 2021).

Platanochori Formation. It is the uppermost formation of the Pre-Mygdonian Group and it has small and limited occurrences restricted at the south-eastern part of the basin in the wider area of the villages Platanochori, Riza and Apollonia. It mainly consists of sands, sandstones, conglomerates, silty-sands, silts, clays, marls and marly limestones, deposited in fluvial, fluviolacustrine environment. Its thickness varies from 10-20 m. The deposits of Platanochori Fm indicate the development of small local lakes and marshes before the complete filling of the basin by water and the deposition of the Mygdonian Group. Thus, the formation is considered transitional from the fluvioterrestrial sediments of the Gerakarou Fm to the lacustrine depositional conditions of the Mygdonian Group (Koufos et al. 1988; Koufos et al. 1995).

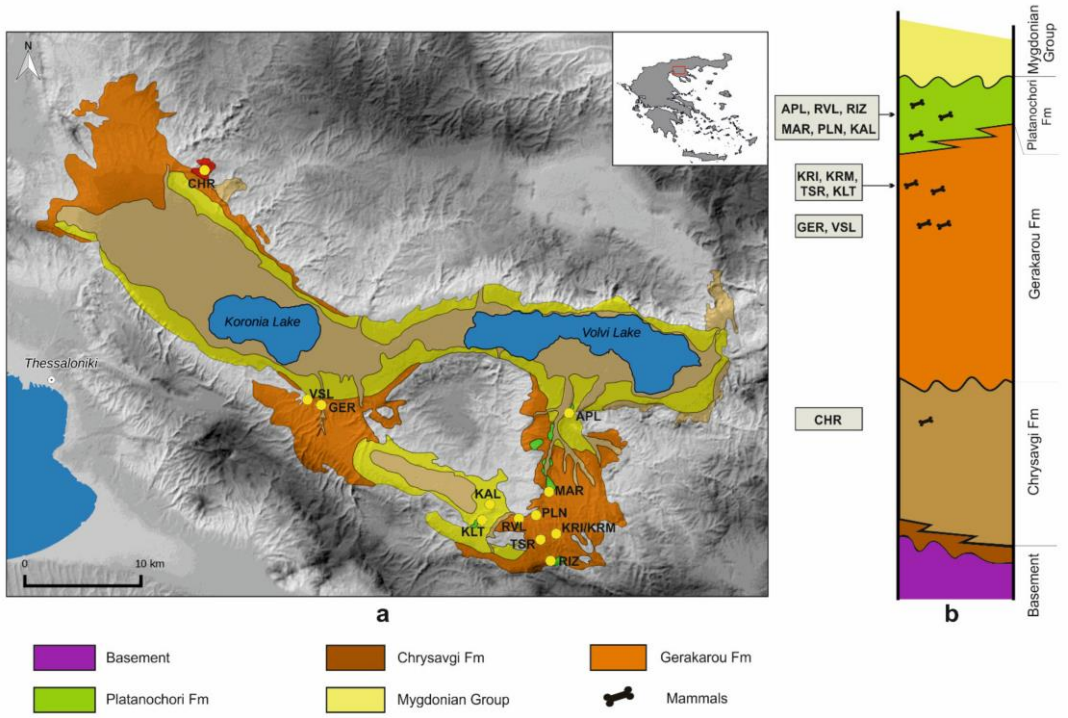

Figure 3.2. (a) Geological map of the Neogene and Quaternary lithostratigraphic units of the Mygdonia Basin; (b) simplified composite stratigraphic column of the Mygdonia Basin indicating the position of the fossiliferous localities. Map and data from Koufos et al. (1995); modified by Konidaris et al. (2015).

Seven fossiliferous localities have been found in Platanochori Fm: Kalamoto-1 (KAL), Ravin of Voulgarakis (RVL), Apollonia-1 (APL), Riza-1 (RIZ), Marathoussa (MAR) and Platanochori-1 (PLN). The study of the faunal assemblages suggests an Epivillafranchian (Latest Villafranchian) age (Koufos et al. 1988; Tsoukala and Chatzopoulou 2005; Konidaris et al. 2015; Koufos and Kostopoulos 2016).

Mygdonian Group. The Mygdonian Group overlies unconformably the Pre-Mygdonian Group. It mainly consists of lacustrine sediments. The lower part of the group consists of coarse clastic sediments that are followed by sands, clays, silts, and fine sands. The upper part of the group consists of silts, clays and sands, while in the uppermost part of it there are occurrences of sandstones, gravels, sands and travertines. The group is dated from the Middle Pleistocene to the Holocene. Only isolated fossils have been found in this group.

The studied localities from the Mygdonia Basin are:

Krimni, late Villafranchian

Several mammal localities were discovered in 1977, near the village Krimni. The localities were named after the so-called village, 'Krimni-1' (KRI) and 'Krimni-2' (KRM). Most of the material coming from KRI consists of equids. The equid material from KRM is incredibly scanty and it only consists of a few bones. Koufos (1992) described it as *Equus stenonis* cf. *mygdoniensis* in both sites. The collection is stored at the LGPUT. A third site near the village of Krimni was discovered in 2019 in the same ravine with KMN. After three years of subsequent excavations (2020-2022) in Krimni-3 (KMN), many large mammals were unearthed. The equid remains were attributed to *E. altidens* and *Equus* sp. (large size) (Kostopoulos et al. 2023). The most common element are equids. The collection is stored in the LGPUT. A few equid bones were also collected from the surrounding area from stratigraphic layers similar to the other sites, and they are referred to as Krimni-stratified (K-S1, -S2 respectively). The stratigraphic relationship of the different sites is not clear, due to the presence of many faults.

Gerakarou, late Villafranchian

Gerakarou-1 (GER) was discovered in 1978 after the great earthquake of Thessaloniki in 1978. The material was collected by Prof. Emeritus G.D. Koufos, during the following years (Koufos 1986a, b, 1988, 1992). The fauna is rich comprising of more than 18 taxa. The first local occurrence of *Canis*, marking the arrival of *Canis* in Europe

and the co-existence of *Pliocrocuta perrieri* and *Pachycrocuta brevirostris* gives a middle/late Villafranchian age to the large mammal assemblage (middle/late Villafranchian boundary, ~2 Ma) (Koufos and Melentis 1983; Koufos 1992; Koufos and Kostopoulos 2016). Equids are dominant in the related fauna. Koufos (1992) described a medium-sized stenonoid equid, resembling *E. stenonis* in the morphology, but smaller in size, and he erected a new subspecies of *E. stenonis* called *E. stenonis mygdoniensis*, which later was upgraded to species level, *Allohippus mygdoniensis*, in Eisenmann (2004).

Vassiloudi, late Villafranchian

The locality 'Vassiloudi' (VSL) was found in 1991 during a field survey conducted by the LGPUT, near the so-called village. Material was collected consisting of a few large mammals belonging to suids, equids and bovids. The equid material is incredibly scanty consisting of two(?) postcranial bones.

Tsiotra Vryssi, late Villafranchian

Tsiotra Vryssi (TSR), named after a local toponym, was discovered during a field survey in 2014 in Marathoussa basin. The site is located southwestern of Krimni and northern of Riza (northern Chalkidiki) (Konidaris et al. 2015, 2016). The material consists of more than 2000 specimens cranial and postcranial, and they are stored at the LGPUT. The faunal assemblage consists of large mammals and some micromammals, reptiles, and birds. The large mammal assemblage comprises of 14 species. Two species of equids are recognized in the assemblage: *Equus* sp. (medium-sized), which is similar to *E. stenonis mygdoniensis* and *Equus* sp. (large-sized) which similar to *E. apolloniensis* (Konidaris et al. 2015, 2016). Based on the magnetostratigraphy of the site and cosmogenic radionuclides, TSR is dated between 1.78 and ~1.5 Ma (within the first part of the late Villafranchian) (Konidaris et al. 2021).

Apollonia (Epivillafranchian)

One of the richest fossil equid collections in Greece is coming from the fossiliferous site Apollonia 1, framing a time period from pre-Olduvai to early Middle Pleistocene (Koufos et al. 1992). The site Apollonia 1 is situated near the village Nea Apollonia, about 45 Km northeast of Thessaloniki city within the Neogene-Quaternary deposits of Mygdonia Basin. Apollonia 1 (APL) was discovered during the summer of 1991 (Koufos et al., 1992) and after subsequent excavations until 1996, a great amount of fossil mammals was unearthed. Another series of field campaign was developed from 2012 to 2014 and from 2019-2022, which further enriched the collection (Koufos 2018,

Konidaris et al. 2020, present study). Apollonia 1 is a key fossil site in this area as it revealed an extremely well-preserved fossil mammal assemblage of high diversity and abundance. The collection is stored in the LGPUT, and it consists of more than 1000 specimens. The APL fauna contains more than 25 taxa suggesting an Epivillafranchian age (Koufos et al. 1995; Koufos and Kostopoulos 1997, 2016; Koufos 2001; Spassov 2003; Kahlke et al. 2011). Two species of equids are described, *Equus apolloniensis* and *Equus* sp. (Koufos et al. 1997; Gkeme et al. 2021).

Ravin of Voulgarakis (Epivillafranchian)

The locality of 'Ravin of Voulgarakis' (RVL) was discovered in 1986, near the village of Platanochori (Koufos et al. 1989). The RVL fauna is rich in micromammals, and only a few large mammals have been found (equids, hippos, carnivores). Equid fossils are scanty, and they were attributed to *E. stenonis* (Koufos 1992).

Platanochori-1 (Epivillafranchian)

Platonochori-1 (PLN) was discovered during a field survey in 2013 in Marathoussa basin, near the villages Platanochori and Krimni. No systematic excavations have been conducted due to the location of the site at the uppermost part of a vertical cliff. Fossil mammals were collected from large intact blocks of sediment that collapsed from the cliff. The material that was collected is stored in the LGPUT. The faunal assemblage consists of equids, bovids (genus *Bison*), antelopes, Proboscidea and rhinos. The most common element of the fauna are equids, belonging to a single large-sized species resembling *Equus apolloniensis* in size (Koufos et al. 1997; Konidaris et al. 2015). PLN is correlated with Apollonia, dating at the Latest Villafranchian (Epivillafranchian) (Konidaris et al. 2015).

Riza 1 (Villafranchian)

The Riza-1 (RIZ) locality was discovered in 1986 during the field campaigns in the Mygdonia Basin. The site is situated in a hard sandy sandstone near the village of Riza. Due to the hardness of the sediment, only a few bones were collected, with bad preservation. Koufos (1992) refers the equid material as *E. stenonis;* it resembles both *E. stenonis* and *E. stenonis mygdoniensis* in the morphology.

3.3 CHALKIDIKI PENINSULA

Petralona Cave, Middle/Late Pleistocene

Petralona Cave (PEC) is situated in Chalkidiki peninsula (Central Macedonia), about 50 km from Thessaloniki, close to the Triglia village. It is developed in Jurassic

limestone at the mountain 'Katsika', and it is filled by sediments dating up to 800.000 years (Papamarinopoulos et al. 1987). The cave is one of the richest palaeontological caves in terms of findings and it is well-known for the discovery of the almost complete cranium of *Homo heidelbergensis* stored in LGPUT (Stringer et al., 1979). The Pleistocene fauna consists of numerous fossils stored in LGPUT (old collection) and in the Petralona Museum (new collection). The faunal contains more than 20 taxa from three biostratigraphic groups based on the carnivore assemblages: early Middle Pleistocene, late Middle Pleistocene and Late Pleistocene (Crégut-Bonnoure and Tsoukala 2005; Baryshnikov and Tsoukala 2010; Tsoukala and Guérin 2016). However, these faunas are mixed due to the action of the flowing water in the cave. Two equids were determined in the fauna according to Tsoukala (1989), *Equus petraloniensis* and *Equus ferus piveteaui* [=*Equus caballus piveteaui* in Tsoukala (1989)], in the latest Middle-late Pleistocene fauna.

3.4 DRAMA BASIN

The Drama basin is trending NW-SE, parallel to the Strymon basin and it is surrounded Falakron, Pageon and Menikion mountains. The basin is covered by the Neogene and Quaternary deposits. The Neogene in the southern part of the basin, consists of three series (Melidonis 1969; Koufos 1981): (a) lower series consisting of conglomerates, sands and lacustrine marls and clays with lignites dating probably at the Late Miocene or Early Pliocene; (b) intermediate series consisting of a consolidated conglomerate and a sandy clay of fluvio-terrestrial origin and (c) upper series consisting of grey sandy marls with intercalations of clay and sand dated at the Pliocene.

The Pleistocene deposits mainly consist of red clays and loose fIuvio-lacustrine conglomerate. In the southern part of the basin, there is also a series of organic (turf-peat, soft lignite) and inorganic (clays, marls) sediments (Melidonis 1969), which overlaying the red clay and the conglomerate. The Holocene deposits are represented by lacustrine and fluvio-terrestrial formations.

There are two fossiliferous localities studied in the Drama Basin: Volax and Aggitis.

Volax, middle/late Villafranchian

The locality is situated near the village Volax about 10km north-western of Drama. The sites of 'Volax' (VOL) were discovered in the early '60s during the investigations for manganium deposits by Prof. H. Martini (University of Hannover). The locality was excavated by Prof. O. Sickenberg (University of Hannover) in association with Prof.

M. Mitzopoulos (Kapodistirian University of Athens) and Prof. G. Marinos (Aristotle University of Thessaloniki), and a part of the material was published (Sickenberg 1967, 1968a, b). The collection, also known as '*Sickenberg collection*', is housed in the LGPUT and AMPG; the equid material is housed in the LGPUT. Equids were studied by Koufos and Vlachou (1997); the authors identified *E. stenonis* cf. *vireti*. Volax is dated at the middle/late Villafranchian (MNQ17/18) (Koufos and Vlachou 1997).

Aggitis, Late Pleistocene

The locality 'Aggitis' (Ag) is situated in the northern part of Drama Basin, near the village Aggitis. The site is in an unconsolidated alluvial cone consisting of terra-rossa, conglomerate-breccia loosely cemented, pebbles, gravels, sand, and soil Koufos (1981). The fossils were found in lens-like accumulations in the upper part of the terra-rossa near the summit of the cone carried by water. The material is stored in the LGPUT and was originally studied by Koufos (1981); equids are represented by *E. caballus* (=*E. ferus* according to the guidelines of ICZN 2003).

3.5 ALIAKMON BASIN

Sporadic articles reporting the presence of some large mammals and equid's remains were known from the deposits near Neapolis (Gorceix 1873; Brunn, 1956, Marinos 1965); *Equus stenonis* and *Mammuthus meridionalis*, *Mastodon borsoni*, *Hipparion* sp. and Rhinocerotidae indet. were documented in the wider area. In the following years extensive field work has been conducted mainly by the LGPUT, new sites have been discovered and new material has been unearthed (e.g. Eltgen 1968; Tsoukala 2000; Koufos et al. 1991).

The Aliakmon Basin (also known as Grevena-Neapolis Basin) is developed between the cities of Grevena, Neapolis and Kozani (Western Macedonia). The basin is developed across the western part of the Mesohellenic Trough. The basement of the basin consists of metamorphic rocks belonging to the Pelagonian Zone and Triassic-Jurassic limestones (Brunn 1956). During the Late Eocene-Late Miocene, the region was filled by fluvial, lacustrine, and marine sediments (Brunn 1956, Vamvaka et al. 2006); the marine molassic deposition possibly continued until Lower Pliocene in the region north of Grevena (Fountoulis et al. 2001). The Pliocene and Quaternary sediments consist of Pliocene lacustrine deposits following by fluvial deposits that overlie uncomformably the older deposits and they are divided into three successive lithostratigraphic units (Faugères 1978):

Lower unit. It consists of conglomerates (with large pebbles, 30-40 cm composed of Pindos rocks), and some massive green sandy-silt deposits. Its thickness varies from 50 to 60 m and its major exposure is observed between Grevena city, Venetikos and Aliakmon rivers.

Intermediate unit. It is the most widely exposed across Grevena and Polylakkos and its thickness reaches up to 80 m in some places. It mainly consists of cross-bedding sands and pebbles at the lower part, while in its upper layers it consists of sands and clay.

Upper unit. It has limited exposure in the Grevena-Neapolis Basin, and its thickness does not exceed 20 m due to the erosion. It consists of small pebbles, gravels, cross-bedded red sands, and clays. Dafnero is situated in the lower part of this formation (Koufos and Kostopoulos 1993).

In the present thesis, we focus on the equid sample that comes from the fossiliferous localities: Dafnero (DFN, DFN3), Libakos (LIB) and Polylakkos (POL).

Dafnero, middle/late Villafranchian (MNQ 17/18)

The primate-bearing fossiliferous locality of Dafnero was discovered in the early 1990s (Koufos et al. 1991). The locality is situated in a ravine across Aliakmon River, at about 30 km from Kozani city, near the homonymous village. Until 1994, continuous excavations conducted by the LGPUT, yielded a significant yet poor faunal assemblage from the site 'Dafnero-1' (Koufos et al. 1991, Koufos and Kostopoulos 1993). Ever since 2010, extensive field work campaigns on the sites of Dafnero (DFN, DFN2, DFN3), have been conducted by the LGPUT and PALEVOPRIM (Laboratoire Paléontologie Evolution Palaeoecosystémes Paléoprimatologie, University of Poitiers, France) and new material has been unearthed which significantly enriched the DFN sample (more than 1000 fossils) and faunal assemblage. The most common element in terms of findings is equids; Koufos and Kostopoulos (1993) described *E. stenonis* cf. *vireti* in the associated fauna. Dafnero fauna is dated at 2.3 Ma (Middle Villafranchian) based on recent magnetostratigraphic data (Benammi et al. 2020).

Libakos – Polylakkos, late Villafranchian (MNQ 19)

The fossiliferous localities of Libakos (LIB), and Polylakkos (POL) are situated inside the Aliakmon basin along the banks of Libakos stream (tributary of Aliakmon River) southeastern of Neapolis. The sites were found in 1968, during a geological survey conducted by Prof. H. Eltgen (Clausthal University of Technology, Germany) in collaboration with the Institute of Geological and Mineral Exploration (I.G.M.E.). The

fossil collection stored in LGPUT, also known as '*Eltgen collection*' comes from several sites such as Libakos, Klima, Polylakkos, Kapetanios, Aliakmon Q-Profil and Trapezitsa, but most of the material originates from Libakos stream. The faunas were studied by Steensma (1988); however, the author does not give the exact stratigraphic position of the localities, or any kind of information regarding their stratigraphy. Investigations from the LGPUT in the area for the relocation of the fossiliferous sites were unsuccessful during the past years. However, Libakos and Polylakkos overlie Dafnero (Kostopoulos 1996), and they are possibly located in the upper part of the clay deposits in the Middle Formation. Steensma (1988) described the horse from Libakos and Polylakkos as *Equus stenonis* cf. *senezensis* and a second species was also described in POL fauna as *Equus stenonis* ssp. B. However, the material of these two localities is mixed. Koufos (1992) included the equid from Libakos in *E. stenonis mygdoniensis* and Gkeme (2016) in *E. altidens*. Libakos and Polylakkos are dated at the late Villafranchian (MNQ 18/19) based on their fauna assemblages.

3.6 LESVOS ISLAND

Vatera, Early Pleistocene

Vatera is located at the southern part of Lesvos Island. There are seven sites situated in the Vatera Formation with vertebrate remains in the area between the villages of Vrissa and Vatera (Lyras and Van der Geer 2007). The Vatera Fm consists of lacustrine (clayey, calcareous, and diatomaceous muds), brackish (claystone with sandstone and siltstone beds) and fluvial (conglomerates, sandy clays, sandy conglomerates, and silt) sediments which overlie conformably the volcanic rocks; these deposits represent the evolution from an open lacustrine environment to an alluvial fan system that filled the lake (Dermitzakis and Drinia 1999; Drinia et al. 2002). All vertebrate fossils were unearthed from the upper part of the Vatera Fm, apart from the proboscideans that were found inside the conglomerates. Initially de Vos et al. (2002) and later Lyras and Van der Geer (2007) described the faunal assemblage of vertebrate from Vatera. Equid remains were only found in the sites E and F. Two equids have been described from the material (Eisenmann 2002; de Vos et al. 2002); *E.* cf. *stenonis* and *Equus* sp. in de Vos et al. (2002), while Eisenmann (2002) does not give a specific name to neither equid. Later, Eisenmann (2017) included the large specimens from Vatera in the *E. suessenbornensis* group. De Vos et al. (2002) provided an approximate age between 2.7 – 1.8 Ma age, while Lyras and Van der Geer (2007) and Koufos and Kostopoulos (2016)

provided an age of ~2 Ma based on biochronological data. In any case, the Vatera locality is referred as Early Pleistocene.

3.7 MAGNESIA (THESSALY)

The province of Thessaly is a mainly plain geographical area. During the Middle Pleistocene, Thessaly was subsided into two grabens that formed the Larisa and Karditsa basins/plains (with NW-SE direction). Two smaller basins are formed, Volos and Almyros in south-eastern Thessaly. Alluvial sediments that are filling most of the central and eastern region and forming extensive plains, overlie the Palaeozoic and Mesozoic basement of the Pelagonian zone (Müller 1983; Symeonidis and Tataris 1983; Mastoras 1985). Several sites have been discovered in the wider area, either in the Quaternary deposits or in fissure fillings in karstified limestones and marbles. Most of the localities are found in the eastern part of the province. In the present study, we focus on the equid material from Sésklo, Alykes and Volos.

Sésklo, middle/late Villafranchian (MNQ 17/18)

The locality of Sésklo (SES) is situated in a basin filled with fluvio-lacustrine clay deposits lain on the Mesozoic basement, about 10km from the town of Volos. It is the richest locality in Magnesia. The site was found in 1971 during the works in a clay pit (Symeonidis and Tataris 1982). In the following years, other excavations were conducted, but not from the exact location of the first-findings area. The fauna was studied by Symeonidis (1992) and Athanassiou (1996, 2001); *E. stenonis* is referred in the associated fauna. Sésklo is dated in the middle/late Villafranchian (MNQ 17/18) (Athanassiou 2001).

Alykes – Volos, late Villafranchian (MNQ 19/20?)

Both localities come from fissure fillings from the wider area of the town Volos. The locality of Alykes (Αλ) is located near the village Alykes, in an old quarry of Mesozoic marbles. The site was found, in 1990, in fissure fillings filled with clay, by G. Theodorou (Kapodistrian University of Athens), who initially studied the fauna. Athanassiou (1996) extensively studied the material, describing *Equus* sp. [=*E.* cf. *stenonis* in Athanassiou (1994)] in the associated fauna. Later, the same author refers that the equid from Alykes is resembling *E. apolloniensis* (Athanassiou 2002).

Van der Meulen and Van Kolfschoten (1986) gave a faunal list from the locality of Volos, including *E.* cf. *marxi*, without however mentioning the exact location of the

site or describing any of the material. According to Athanassiou (2002), both localities should be the same age, probably late Villafranchian (MNQ 19/20), based on their geological similarity and rather similar faunas.

3.8 PELOPONNESE

Pyrgos, ?late Villafranchian (?MNQ 18)

The locality is situated in Peloponnese. The material is scanty, and fossils come from at least two different sites. Van der Meulen and Van Kolfschoten (1986) give a faunal list that includes two species of *Equus*: *E.* cf. *stehlini* and *E.* cf. *stenonis*. However, the authors neither describe the material, nor they provide any kind of information on their stratigraphy. The fauna of Pyrgos (Pg) suggests a possible late Villafranchian age similar to Gerakarou and Vassiloudi (Mygdonia Basin) (Koufos and Kostopoulos 1997).

CHAPTER 4. THE EUROPEAN *EQUUS*

During the Early Pleistocene various species and subspecies of *Equus* have been recorded in the European local faunal assemblages (LFAs). Despite the rich amount of equid remains in those sites as well as the great number of studies, the equine taxonomy and their phylogenetic relationships are still a matter of debate (see among others Azzaroli 1965, 1979, 1990, 1999; Boeuf 1986; Alberdi et al. 1988, 1998, 2001; Musil 1992, 2001; Eisenmann 1992, 2004, 2010; Eisenmann and Boulbes 2020; Caloi 1997; Guerrero-Alba and Palmqvist 1997; Forstén 1999; Alberdi and Palombo 2013a, b; Palombo et al. 2017; Gkeme et al. 2021; Bernor et al. 2021; Cirilli et al. 2020a, 2021, and references therein). The lack of complete or well-preserved crania (or any crania at all), as well as the lack of crania associated to limb bones from the Lower Pleistocene European localities can complicate things when it comes to taxonomic and phylogenetic analyses. Moreover, the possible mixing of the old collections from key localities could cause misclassification.

Over the last 20 years, new fossils have been unearthed and reference collections have been revised, leading to a reconsideration of the taxonomy (Alberdi et al. 1998; Forstén 1999a; Eisenmann 2004a, 2006a, 2010; Alberdi and Palombo 2013; Palombo and Alberdi 2017; Van der Made et al. 2017) and biochronology of the Pleistocene equids taking also advantage of the increased dating precision of developed. The palaeogenetics made it also possible to calibrate evolutionary models proposed by palaeontology (Orlando et al. 2013; Jónsson et al. 2014; Bennett et al. 2017).

The genus *Equus*, that most likely emerged at 4.0–4.5Ma, is considered to include all monodactyl equids present in Europe, giving rise to all contemporary horses, zebras, and donkeys (Orlando et al. 2013). The stenonid group (equids related to *E. stenonis*) was the first to disperse at the Plio-Pleistocene boundary (previously called the *Equus*-

Elephant event, Lindsay et al. 1980). For several researchers, *Equus livenzovensis* is supposed to be the first (*Equus*) species recognized in Eurasia and it is considered as ancestral stock of all the European stenonoid equids (Azzaroli 1992; Alberdi et al. 1998; Palombo and Alberdi 2017; Bernor et al. 2018). Nevertheless, the definition of this species remains uncertain due to the heterogeneity of the material coming from the type locality of Livenzovka (Rostov-Don, Russia), the uncertainties about its chronology (Forstén 1998a) and the conflict about the taxonomy of contemporaneous fossils recorded in Western Europe and attributed to this taxon (i.e., in Montopoli in Italy, and Huélago, El Rincón in Spain; Forstén 1999a; Eisenmann 2004a).

There are several taxonomical interpretations regarding the position of the Early-to-early Middle Pleistocene European non-caballine *Equus* related to the genus/subgenus *Allohippus* Kretzoi, 1938 (e.g., Gromova 1949a, Samson 1975, Prat 1980, Eisenmann and Baylac 2000, Eisenmann 2003, 2004, 2006 and others) and the extant equids. The name *Allohippus* Kretzoi 1938, which originally used at genus level, nowadays it is used at different levels of the taxonomic rank. *Allohippus* has been referred to some primitive equids (*E. stenonis*) from some key Early Pleistocene European faunas such as Saint-Vallier and Senèze (France), Olivola, Montopoli, Upper Valdarno (Italy), Huélago, El Rincón, and La Puebla de Valverde (Spain), Gerakarou and Vatera (Greece), Sarikol Tepe (Turkey) and Livenzovka (Russia) (Prat 1964, 1980; Azzaroli 1965, 1982, 1987; Azzaroli and Voorhies 1993; Bolomey 1965; De Giuli 1972; Bajgusheva 1978; Samson 1975; Alberdi and Ruiz Bustos 1985, 1989; Boeuf 1986; Forstén 1986; Bonadonna and Alberdi 1987b; Alberdi et al., 1991; Koufos 1992; Caloi 1997). Gromova (1949) and Azzaroli (1982) used *Allohippus* as a subgenus of *Equus*. According to Eisenmann and Baylac (2000), Eisenmann (2006, 2017) and Eisenmann and Deng (2005), modern equids -genus *Equus* or true *Equus*- is separated from the primitive equids *Allohippus* (taxon that is comprised from all stenonoid equids) and *Plesippus* based on their basicranial proportions: stenonine and plesippine equids are recognized as distinct linages from *Equus*. Barrón-Ortiz et al. (2019) also suggested that *Plesippus* and *Allohippus* should be elevated to generic rank. Based on this outline (Eisenmann and Kuznetsova 2004), the first cranium in Europe belonging to a true *Equus* is that described in Apollonia-1, Greece (=*E. apolloniensis* in Koufos et al. 1997; 1.2–0.9Ma, Koufos and Kostopoulos 2016), while the latest cranium belonging to stenonoid equids (genus *Allohippus* according to Eisenmann) is the one from Ceyssaguet (1.2Ma, *E. stenonis* in Aouadi and Bonifay 2008).

In 2010, Eisenmann erected a new subgenus "*Sussemionus*" including species with dental peculiarities such as *E. suessenbornensis*, *E. hipparionoides*, *E. coliemensis*, *E. altidens* and *E. a. granatensis*. In this hypothesis (cf. Introduction, Eisenmann 2010), these equids originated probably in North America and are not linked with the stenonid group (*Allohippus* according to Eisenmann). *Sussemionus* is defined based on the mixture of morphological characters shared in the fossil equids from Süssenborn and extant hemiones (deep postprotoconal groove, multiple plis caballin or with very large base, sometimes very short protocones on upper teeth, and elongated/bilobated metaconids, presence of stylids and deep ectoflexid on lowers) (Eisenmann 2010). As a result of this hypothesis, *Allohippus* and *Equus* could have co-occurred in Europe for more than 1.0 Ma (Boulbes and Van Asperen 2019). As these peculiarities are not constant, their presence is a good indicator of this taxon, but their absence is not because stenonine patterns may occur to sussemiones (Eisenmann and Boulbes 2020). This approach is not shared by other authors who consider the species *E. suessenbornensis*, *E. altidens* and *E. a. granatensis* stenonoid equids (Forstén 1986, 1999a; Azzaroli 1990, 1992; Alberdi et al. 1998; Alberdi and Palombo 2013; Palombo and Alberdi 2017). According to Palombo and Alberdi (2017) the separation of the European Pleistocene equids in different genera/subgenera names demands a great deal of caution, considering the homogeneity, due to the large intra- and interspecific variation in the fossil monodactyl equids.

Recently, Cirilli et al. (2021) conducted cladistic analysis combining both morphological and morphometrical cranial anatomy in order to assess the validity of the three different genera *Plesippus, Allohippus* and *Equus* proposed for the non-caballine Plio-Pleistocene Eurasian, African and North American equids. In their research, they reject the recognition of the taxa *Plesippus* and *Allohippus* (as either distinct genera or subgenera) and suggest that all Plio-Pleistocene species (mentioned above) can be grouped into the genus *Equus* as a single clade. This argument is beyond the scope of the present thesis which aims to briefly discuss (see Phylogeny Chapter) some of the debated scenarios that still need to be answered by equid specialists, mainly focusing on the phyletic relationships between the equids recorded in the late Villafranchian and Epivillafranchian LFAs of Greece and Europe. In this thesis, the author considers the genus *Equus* sensu lato taking into account the different points of view between equid specialists.

4.1 THE EARLY PLEISTOCENE AND GALERIAN EUROPEAN EQUIDS

Equus livenzovensis Baigusheva, 1978

It is the oldest monodactyl equid species to be recorded in the Early Pleistocene of Europe. *E. livenzovensis* was erected by Baigusheva (1978) based on the equid remains coming from the deposits of Liventsovka (Rostov-on-Don, Russia) that were initially been described as "*Equus stenonis var. major*" by Gromova (1949a). Recently, in her latest revision on the equids from Liventsovka and other localities of the Khaprovskii Complex (Russia), Eisenmann (2022) redefined the *E. livenzovensis* material (along with the other equid species) and provided the most complete information on the equid remains with measurements, photographs, and some additional descriptions.

Equus livenzovensis is a large-sized stenonoid equid, larger and heavier than *E. stenonis* with more elongated limb bones (Palombo and Alberdi 2017). The type cranium of *E. livenzovensis* (ROMK L 4; Eisenmann 2022a: fig. 7. A-D) exhibits a well-developed preorbital pit. The basilar length of the cranium is estimated at ~570-580 mm by Titov (2008) and ~550 mm by Eisenmann (2022). The species exhibits typical stenonine cheek teeth morphology, with short protocones on the upper teeth, short plis caballin and mesostyles without groove. The linguaflexid on the lower cheek teeth is V-shaped and shallow ectoflexid on premolars and consistently deep on the molars (Forstén 1998; Alberdi et al. 1998). The third metacarpals are long and slender with relatively deep diaphysis. The third metatarsals exhibit wide proximal epiphyses (M5) and shallow keels (M12) (Eisenmann 2022). Generally, the metapodials are longer than *E. stenonis* s. l., but shorter than *E. major* and *E. suessenbornensis* (Alberdi et al. 1998).

This species occurred in localities at the Plio/Pleistocene boundary (2.58 Ma). Apart from Liventsovka (Baigusheva 1978; Gromova 1949a; Azzaroli 1982; Forstén 1998; Eisenmann 2022), *E. livenzovensis* is also recorded in Roca-Neyra, France (*Equus* cf. *E. livenzovensis* in Cirilli et al. 2020), in Montopoli, Italy (*Equus* cf. *livenzovensis* in Bernor et al. 2018) and in Spain at El Rincón and Huélago (Alberdi and Ruiz Bustos 1989; Alberdi et al. 1997, 1998). In a chronotable (biostratigraphy of *Equus*) in Eisenmann's site (Eisenmann 2017), *E. livenzovensis* sensu lato is referred at Saint-Vallier LD2 (France). According to Alberdi et al. (1998), the species *Equus athanasiui* Samson, 1975, from Tetoiu (Romania, Radulesco and Samson 1990) may be considered as a junior synonym of *E. livenzovensis*. The chronological distribution of *E. livenzovensis* covers middle Villafranchian.

Equus stenonis Cocchi, 1867

Equus stenonis was erected by the Igino Cocchi in 1867 based on an almost complete, though strongly laterally compressed cranium (IGF-560; Azzaroli 1965: p. 5; tab. I, fig. 3; tab. II, fig. 1, 1a; tab. V, fig. 1, 1a) stored at the Palaeontological Museum of the University of Florence (Italy). The holotype cranium was recovered from Early Pleistocene site Terranuova Bracciolini (Upper Valdarno Basin, Italy), but Cocchi (1867) did not provide any formal description or diagnosis for the species. A preliminary description was later given by Forsyth (1885 or 77-80). Azzaroli (1965) described and figured cranial and postcranial remains from the Upper Valdarno (Florentine Collection), and finally provided a diagnosis of the species.

Equus stenonis is a large-sized and robust equid. A typical feature of this species is the deep indentation of the narial notch, which extends caudally above the third premolar. The great elongation of the narial notch is always apparent. *Equus stenonis* has a slender and elongated snout and the diastema is very long. The braincase is rather small in relation to the length of the face and is strongly deflected and the forehead is transversally undulated. *Equus stenonis* shares some common features of the forehead and braincase with *Equus livenzovensis*, but the preorbital fossa is poorly developed and the posterior palatine foramina are shifted caudally, opposite the M3/ on the holotype. The protocone on the upper cheek teeth is usually short, similar to *Equus livenzovensis*, but it tends to be more elongated in some subspecies (e. g. *E. stenonis vireti*). The enamel of the inner fossettes is richly plicated. The lower cheek teeth are typically stenonoid (zebrine) with V-shaped linguaflexid and the ectoflexid is either deep or shallow; in the type cranium it is shallow (Azzaroli 1965, 1982). *Equus stenonis* followed *E. livenzovensis* in time and represents an intermediate form between *E. livenzovensis* and *E. s. senezensis* (Azzaroli 1989). *Equus stenonis* is believed to have been replaced by smaller and more gracile species (*E. altidens*) and larger species (*E. suessenbornensis*), which often coexisted sometime during the Latest Villafranchian.

Equus stenonis sensu lato is recorded in Greece (Sésklo, Dafnero, Volax), France (Saint-Vallier, Chilhac, possibly Ceyssaguet), Italy (Terranuova, Olivola, Matassino, Upper Valdarno, Spain (La Puebla de Valverde), Turkey (Sarikol Tepe) and Georgia (Dmanisi). The chronological distribution of *Equus stenonis* s. l. could be from 2.5 Ma (Saint-Vallier and Chilhac, France; Nomade et al. 2014) to 1.2 Ma (Ceyssaguet, France; Aouadi and Bonifay 2008).

Subspecies or ecomorphotypes of *Equus stenonis*

The taxonomy and evolutionary history of *E. stenonis* has been extensively discussed by equid specialists. *E. stenonis* has been considered by many researchers as the most common equid species in the Early Pleistocene of Eurasia and has been referred to as '*E. stenonis* group' or '*E. stenonis* sensu lato' (Palombo and Alberdi 2017). Many stenonoid equids recorded from several European localities dated from the middle to late Villafranchian, have been identified over the years as different subspecies of *E. stenonis* (Prat 1964, 1980; Azzaroli 1965, 1982, 1987; Azzaroli and Voorhies 1993; Bolomey 1965; De Giuli 1972; Bajgusheva 1978; Samson 1975; Alberdi and Ruiz Bustos 1985, 1989; Boeuf 1986; Forstén 1986; Bonadonna and Alberdi 1987b; Alberdi et al., 1991; Koufos 1992; Caloi 1997). These subspecies were distinguished mostly based on size and proportions.

Prat (1964, 1980) distinguished two subspecies of *E. stenonis*, *E. stenonis vireti* from Saint Vallier (France), an equid with a heavy built and more robust metapodials than *E. stenonis* from Upper Valdarno and *E. stenonis senezensis* from Senèze (France), an equid smaller in size than *E. stenonis* with slenderer metapodials. De Giuli (1972) assigned the remains from the Italian Early Pleistocene faunas from Olivola and Upper Valdarno to *E. stenonis stenonis*. Samson (1975) gave rise to the subspecies *E. stenonis mitilanensis* [=*Plesippus (Allohippus) stenonis mitilanensis*] from the Lower Pleistocene of Romania. Boeuf (1986) described *E. stenonis guthi* from Chilhac (France), a large-sized equid with heavy built, more robust than *E. stenonis* and slenderer than *E. s. vireti*. Koufos (1992) erected '*E. stenonis mygdoniensis'* from Gerakarou-1 (Greece), an equid smaller in size with slenderer proportions than all former subspecies of *E. stenonis*. Azzaroli and Voorhies (1993) proposed the North American subspecies *E. stenonis anguinus* from the Idaho at about 2 Ma and *E. s. pamirensis* Sharapov 1986 from Kuruksay (Tajikistan). Caloi (1997) erected two subspecies of *E. stenonis*, the large-sized *E. stenonis pueblensis* from La Puebla de Valverde (Spain), an equid of similar size to *E. stenonis vireti,* but slenderer, and *E. stenonis olivolanus* ('partim *E. stenonis*') from Olivola and Matassino (Italy), an also large-sized equid, slenderer than *E. stenonis*.

The validity, taxonomy, and chronological distribution of (at least) the European subspecies of *E. stenonis* have been a matter of debate among equid specialists (Alberdi et al., 1998; Forstén, 1999; Athanassiou, 2001; Alberdi and Palombo, 2013a; Eisenmann 2004, 2010, 2017; Palombo and Alberdi, 2017; Bernor et al., 2019; Cirilli

et al., 2020a; Cirilli et al. 2021). The medium-sized equid from Senèze has been referred as *E. stenonis senezensis* by Prat (1964, 1968 and 1980), De Giuli (1972), and Azzaroli (1990). Alberdi et al. (1998) elevated it to the species rank *E. senezensis*, while Delson et al. (2006), following the classification of Eisenmann (using *Allohippus* at a genus level) referred to this equid as *Allohippus stenonis senezensis*. *Equus* from La Puebla de Valverde has been referred by Eisenmann (1980) as *E. stenonis* cf. *vireti*, by Caloi (1997) as *E. stenonis pueblensis* and Alberdi et al. (1998) as *E. stenonis guthi*. *Equus* from Gerakarou has been identified as a subspecies of *E. stenonis*, *E. stenonis mygdoniensis* by Koufos 1992, and as *E.* cf. *altidens* by Forstén (1999). Gkeme et al. (2017), Cirilli et al. (2020a), Bernor et al. (2021) and Koufos et al. (2022) have included this taxon to *E. altidens* (junior synonym of *E. altidens* in Bernor et al. 2021). Eisenmann elevated most of European subspecies of *E. stenonis* to the species rank (e.g., Eisenmann 2017): *Allohippus stenonis*, *Allohippus pueblensis*, *Allohippus mygdoniensis*, *Allohippus vireti*, *Allohippus senezensis*. In any case, '*E. s. mygdoniensis'* is not included in *E. stenonis* subspecies. Alberdi et al. (1998) recognized three subspecies of *E. stenonis* (*E. s. stenonis*, *E. s. vireti* and *E. s. guthi*). *Equus livenzovensis* (=*Equus stenonis livenzovensis* Bajgusheva, 1978 in Alberdi and Ruiz Bustos 1989, p. 243-248, pl. 1, figs. 1-8) from Livenzovka (Rostov, Russia) is considered a distinct species from *E. stenonis* but closely related to it, with the latter being smaller in general size and proportions, but same in dental morphology (Alberdi et al. 1998 among others).

In a recent review on *Equus stenonis*, Cirilli et al. (2021), following Forstén (1999), Athanassiou (2001), Alberdi and Palombo (2013a), Palombo and Alberdi (2017), Bernor et al. (2019), Cirilli et al. (2020a) and Cherin et al. (2021), consider *E. stenonis* as a monotypic species, and that the alleged subspecies *E. stenonis pueblensis*, *E. stenonis guthi*, *E. stenonis vireti*, *E. stenonis stenonis* and *E. stenonis olivolanus* do not merit any taxonomic distinction at the subspecies rank, suggesting they represent local ecomorphotypes of *E. stenonis*. In addition, Cirilli et al. (2021), following Alberdi et al. (1998) suggestions, consider *E. senezensis* as a distinct species from *E. stenonis*. Furthermore, Cherin et al. (2021), Cirilli et al. (2021) and Bernor et al. (2021) following Forstén (1999) and Gkeme et al. (2017) point out the difference of '*E. stenonis mygdoniensis*' with the other European *E. stenonis* subspecies/populations.

The role of the European Early Pleistocene *E. stenonis* in the evolutionary history of *Equus* and the origin of the zebra-ass clade is one of the most controversial issues.

Eisenmann (1980, 1983) and Azzaroli (1964) suggested a relationship between *E. stenonis* and the extant Grévy's zebra based on cranial and dental morphology. Other studies that have acknowledged cranial and dental similarities between *E. stenonis*, *E. koobiforensis* (Kenya, Africa, 1.9Ma) and *E. grevyi* (Eisenmann 1980), suggest that *E. koobiforensis* could be closely related to the European *E. stenonis* than the Chinese Early to Middle Pleistocene *E. sanmeniensis* (Deng and Xue 1999; Bernor et al. 2015). Similarities on the crania, mandible, and teeth of *E. stenonis* and *E. simplicidens*, suggest that *E. stenonis* presents an intermediate morphology between the North American *E. simplicidens* and the East African *E. koobiforensis* (Eisenmann 1980). Other hypotheses, however, suggest *E. stenonis* as a branch of the *E. simplicidens–E. sanmeniensis–E. koobiforensis–E. grevyi* evolutionary lineage (Azzaroli 1992; Cirilli et al. 2021).

The case of *'Equus stenonis mygdoniensis* Koufos, 1992*'*

'*E. stenonis mygdoniensis*' is a medium-sized stenonoid equid originally recorded in the late Villafranchian LFA of Gerakarou-1 (Greece) and other Greek localities e.g., Krimni sites, Libakos (see Koufos and Melentis 1983; Koufos 1992). It is larger than *E. stehlini* and smaller than *E. livenzovensis*, all subspecies of *E. stenonis*, including *E. senezensis*. The holotype of this subspecies (cranium LGPUT GER-8) is moderate in size with short muzzle and with the nasal notch retracted to P3 parastyle. The preorbital fossa is very shallow with no peripheral border. The cheek teeth are typically stenonoid (short triangular-shaped protocones, V-shaped linguaflexid, consistently deep ectoflexid on lower molars). The metapodials are short and slenderer than all *E. stenonis* subspecies, including *E. senezensis* (Koufos 1992).

The systematic position of *'E. stenonis mygdoniensis'* has been extensively debated by many equid specialists over the last 30 years (Koufos 1992; Forstén 1999; Eisenmann 2004, 2006, 2017; Gkeme et al. 2017; Palombo and Alberdi 2017; Cherin et al. 2020; Bernor et al. 2021; Cirilli et al. 2021; Cirilli 2022). The taxon was originally described by Koufos (1992), who erected it as a new subspecies of *E. stenonis* based on adequate cranial and postcranial elements from the type locality (GER). The subspecies' diagnosis was based on its much smaller size and slenderer metapodials than all the other *E. stenonis* subspecies, including *E. senezensis*. Koufos (1992) included into the subspecies the equid material from Libakos, described by Steensma (1988) as *E. stenonis* cf. *senezensis* and Krimni remains. In her review on *E. stenonis*, Forstén (1999)

acknowledged the similarities between the equid remains from Gerakarou and Libakos, although she questioned the validity of *'Equus stenonis mygdoniensis'*. More precisely, Forstén (1999) mentions about the Krimni (KRM, KRI) and Gerakarou-1 equids that: "With the possible exception of the horse from Riza, these finds evidently do not represent *E. stenonis*; they rather resemble *E. stehlini* or belong with the gracile horses from Libakos and Petralona here pooled under the name *E.* cf. *altidens*." Eisenmann (2004, 2017) elevated *E. stenonis mygdoniensis* to species rank (=*Allohippus mygdoniensis*). Moreover, Eisenmann (2017) supports the close relationship between the equids from Gerakarou (*Allohippus mygdoniensis*), Senèze (*Allohippus senezensis*) and those of Upper Valdarno -partim- (*Allohippus stehlini*) based on some common characteristics (e.g., short-muzzled skulls) but keeps them at a species level. In the chronotable composed by Eisenmann (2017: p. 12-13, Table 1), *Allohippus mygdoniensis* sensu lato is referred in Libakos (Greece), Upper Valdarno (partim, Italy) and Dmanisi IV-V (Georgia). Palombo et al. (2017) and Palombo and Alberdi (2017) included the equid from Gerakarou in the *E. senezensis* group. Gkeme (2016) and Gkeme et al. (2017) support Forstén' s (1999) opinion that *'E. stenonis mygdoniensis'* in closely related to *E. altidens*, including the equid remains from Libakos, and hence from Gerakarou, in the latter species. Moreover, Cherin et al. (2020) and Cirilli et al. (2021) support the closer relationship between '*E. stenonis mygdoniensis'* with *E. altidens* rather than *E. stenonis*, based on morphometric analyses. Bernor et al. (2021) and Cirilli et al., (2021a) concluded that *E. stenonis mygdoniensis* Koufos, 1992 is a junior synonym of *E. altidens*, thereby favoring Gkeme et al.'s (2017) preliminary work.

Equus senezensis Prat, 1964

Equus senezensis is a late Villafranchian medium-sized stenonoid equid. *Equus senezensis* was originally described from the French site of Senèze based on an upper cheek teeth-row, P2-M3 (Se 553 stored in the NMBS), and two metacarpals (Se 831 stored in the NMBS) by Prat (1964, pl.l, fig. C, and pl. 2, figs. D-E). It was originally described as a subspecies of *E. stenonis* (*E. stenonis senezensis*) (Prat 1964, 1980) that is smaller in size than *E. stenonis*, with slenderer metapodials. Later, Prat (1980) partially figured the skeleton Se 554 (paralectotype, stored in the NMBS) (Prat 1980, p. 108; figs. 16, 18.2, 19.4 and 30.3) and considered it as the holotype. *Equus senezensis*

is also figured and analyzed by Eisenmann (2017), who redefined the equid remains from Senèze.

The cranium is long and relatively narrow, with short muzzle and its average basilar length is 523 mm (taken from Eisenmann 2017) smaller than the other *E. stenonis* subspecies (including the crania from LPDV), but larger than '*E. stenonis mygdoniensis'* (mean = 471 mm, pers. data). The dental morphology of the species is typically stenonoid; the protocone is short on the upper cheek teeth and on the lower cheek teeth the linguaflexid is V-shaped. The metapodials are short and robust; they are slenderer than those of *E. stenonis* but more robust than those of '*E. stenonis mygdoniensis'* and *E. altidens*.

Equus senezensis is reported in France at the site of Senèze (dated at about 2.093 Ma±10 ka to 2.206 Ma± 21 ka by Nomade et al. 2014) and in Italy at the middle Villafranchian site of Vigna Nuova (Valdichiana Basin, Perugia: *E.* cf. *senezensis* in Azzarà et al. 2022). *E. senezensis* is possibly also present in Greece at the site of Pyrgos (*E.* cf. *senezensis* according to the present author) dated at the (?)late Villafranchian (Koufos and Kostopoulos 1997).

The systematic position of *E. senezensis* has been discussed by many researchers (Prat 1964, 1980; Alberdi et al. 1998; Palombo and Alberdi 2017; Eisenmann 2006, 2017; Cirilli et al. 2021a among others). In their quantitative review on the stenonoid equids, Alberdi et al. (1998) elevated the subspecies *E. stenonis senezensis* Prat, 1964, to species rank, recognizing two geographical subspecies, the nominotypical subspecies from Senèze (France), and *E. senezensis stehlini* from Upper Valdarno Basin (Italy). *E. senezensis* may be considered as a bona fide species (Alberdi et al. 1998; Palombo and Alberdi 2017). Cirilli et al. (2021a) embraced the idea of *E. stenonis senezensis* to be considered as a distinct species (*E. senezensis*), but also the same authors do not support the hypothesis that *E. stehlini* is a subspecies of *E. senezensis* (*E. stehlini* also in Cirilli 2022).

Equus stehlini Azzaroli, 1965

Equus stehlini was described and figured by Azzaroli (1965) based on a cranium retrieved from the late Villafranchian fauna of Terranuova (Upper Valdarno, Italy). The holotype cranium IGF-563 (Azzaroli 1965, pl. II, fig. 2, 2a; pl. III, fig. 2, 2a; pl. IV, fig. 3; pl. V, fig. 4).) belongs to an aged male individual and it is housed in the Florence Geological Institute Collection in Italy.

Revised by Azzaroli (1965, 1982) and Cirilli (2022), *Equus stehlini* is characterized by its much smaller size relative to *Equus stenonis* and even to *Equus senezensis*. It is the smallest Early Pleistocene stenonoid equid in overall proportions/dimensions (cranial, mandibular, metapodial and phalangeal). The cranium is smaller in size than *E. stenonis* and *E. senezensis*, it has slenderer muzzle, but shares many cranial specializations with both species, such as the depth of the narial notch (above the P3 mesostyle), shallow preorbital fossae and deep groove along the sagittal suture of the nasal (Azzaroli 1990). The braincase is small and deflected downward and the facial crest extends up to P4 mesostyle. The maxillary and mandibular cheek teeth are typically stenonoid (Figure 4.1l). The protocone is very short on the upper cheek teeth, the linguaflexid is V-shaped on the lower cheek teeth and the ectoflexid is consistently deep on the lower molars. The metapodials are short and robust and the phalanges are short and massive (Alberdi et al. 1998; Cirilli 2022 for detailed descriptions).

Equus stehlini is recorded in several late Villafranchian Italian faunas of fossiliferous localities such as Terranuova, Casa Frata, Le Ville, Inferno, Il Tasso, La Cicogna, Figline (Azzaroli 1965; Alberdi et al. 1998; Cirilli 2022). The species is probably also present in Coste San Giacomo (Anagni Basin, Italy) (*Equus senezensis* aff. *E. sen. stehlini* in Palombo et al. 2017). In France, the species has been reported in Montecarlo (ca. 2.2 Ma; Ghinassi et al. 2005; Fidolini et al. 2013) by Bernor et al. (2019), and possibly at Senèze (2.2-2.0 Ma, France; Delson et al. 2006). In Greece, *E. stehlini* is possibly recorded in Pyrgos, Peloponnese (?MNQ 18, Greece; Van der Meulen and Van Kolfschoten 1986).

The systematic position and evolutionary relationships of *E. stehlini* have been extensively debated by many researchers over the last 60 years (Azzaroli 1965, 1982, 1990, 1992, 2003; Alberdi et al. 1998; Alberdi and Palombo 2013a, b; Palombo et al. 2017; Palombo and Alberdi 2017; Bernor et al. 2019; Cirilli et al. 2020a; Cirilli et al. 2021c; Cirilli 2022). There are mainly two hypotheses on this topic. Azzaroli (1965, 1982, 1990) considers *E. stehlini* a distinct species closely related to *E. stenonis* from which it may originated by cladogenesis. In their revision on the European Early Pleistocene stenonoid equids, Alberdi et al. (1998) considered *E. stehlini* as a subspecies of *E. senezensis* (*Equus senezensis stehlini*) based on the cranium morphology and multivariate morphometric analyses on postcranial elements (metapodials, calcanei, astragali, first phalanges). The authors propose that *E. stehlini* possibly originated from populations of *E. senezensis* instead of *E. stenonis*. Cirilli

(2022) supports this evolutionary hypothesis, but also supports Azzaroli's (1965) original recognition of *E. stehlini* as a distinct species.

Equus altidens von Reichenau, 1915

Equus altidens is a medium-sized slender stenonoid horse, larger than *E. stehlini* and smaller than *E. stenonis* and *E. suessenbornensis*. The cranium is moderate in size with a short muzzle and with the nasal notch incised to P2 mesostyle (Bernor et al. 2021). The preorbital fossa is not clearly delimited. The cheek teeth morphology is typically stenonoid with lingually flattened (usually) short protocone and somewhat deep postprotoconal groove. The shape of the protocone is variable (usually triangular shaped), while the linguaflexid is V-shaped and the ectoflexid is deep on molars. The limb bones of *Equus altidens* are more elongated and much slenderer (especially the metapodials) than *E. stenonis* and *E. senezensis* (Alberdi et al. 1998). *Equus altidens* is recorded in Europe from post-Olduvai times to the early Middle Pleistocene (Alberdi and Palombo 2013a; 2013b; Palombo 2014, 2016a, 2016b; Bernor et al. 2021).

This species was originally described by von Reichenau (1915), who based on a few isolated teeth from the early Middle Pleistocene site of Süssenborn (dated at ~0.65Ma: Kahlke 2014). Later, Musil (1969) included several isolated teeth and slender metapodials from the same locality into this species. Recently, Bernor et al. (2021) attributed a well-preserved complete equid cranium (Dm53/59.3.B1gl.192, Bernor et al. 2021: Fig. 5, p. 5) from Dmanisi (Georgia) to *E. altidens*. The cranium resembles in size and general morphology the holotype of '*E. stenonis mygdoniensis*' from Gerakarou (Bernor et al. 2021: Fig. 7a). Their results on cluster analysis have shown that the crania from Dmanisi and Gerakarou are morphometrically similar to *E. quagga* and *E. hemionus* (Bernor et al. 2021).

The chronological distribution of *E. altidens* ranges between 1.85-0.60 Ma (Alberdi and Palombo 2013a). However, some cranial and postcranial elements found at the site of Mosbach, dated at 0.5 Ma, resemble the ones from Süssenborn (Eisenmann 2008). Apart from Süssenborn, the species is also recorded at Voigstedt (Germany) (Musil 1965; Forstén 1986, 1988) and in several other European localities: in Italy at Pirro Nord (*E. altidens altidens*), Selvella-Gioiella, Slivia, Ponte Galeria (Alberdi and Palombo 2013) and Venosa-Loreto (Alberdi and Palombo 2013); in Spain at Huescar-1, Cullar de Baza-1 (Alberdi and Ruiz Bustos 1989; Alberdi et al. 1998), Sima del Elefante, Gran Dolina, Penal (*E.* cf. *altidens*), in Atapuerca TD8 (Van der Made et al.

2017) and possibly Atapuerca TE9 (Van der Made 2013). *E. altidens altidens* is also reported at Cueva Victoria (Piñero and Alberdi 2015) dated at 0.9–0.8Ma (Gibert et al. 2016), but Eisenmann mentions it could be *E. a. granatensis*. The species is known in France at Bois de Riquet (Bourguignon et al. 2016; Lozano-Fernández et al. 2019) and Soleihlac (Prat, 1980; Lacombat, 2005) and in UK at Pakefield (Lister et al. 2010). In Greece, the species is reported at Libakos and Gerakarou (Forstén 1999; Gkeme 2016; Gkeme et al. 2017; Bernor et al. 2021; Koufos et al. 2022). *E. altidens* is associated with *E. suessenbornensis* in most cases.

Still, the systematic position and evolutionary relationships of *E. altidens* have been extensively debated by many equid specialists (von Reichenau 1915; Musil 1969; Alberdi et al. 1998; Forstén 1999; Eisenmann 2006, 2010; Alberdi and Palombo 2013a, b; Palombo and Alberdi 2017; Boulbes and Van Asperen 2019; Bernor et al. 2019; Cirilli et al. 2021). von Reichenau (1915) originally described three species in the site of Süssenborn: *E. altidens* von Reichenau, 1915, *E. marxi* von Reichenau, 1915 and *E. suessenbornensis* Wüst, 1900, though many researchers argue about the exact number of equid species present due to the heterogeneity of the material and the long-time deposits in Süssenborn (Musil 1969; Forstén 1986; Eisenmann 2008; Alberdi and Palombo 2013; Eisenmann and Boulbes 2020). According to some authors, *E. marxi* is not differentiated enough from *E. altidens* and thus it is considered as a synonym of the latter (Forstén 1986; Bonadonna and Alberdi 1987; Caloi and Palombo 1990; Alberdi and Palombo 2013). In contrast, according to Eisenmann and Boulbes (2020) both species, *E. altidens* and *E. marxi*, should carefully be used by scholars, due to their poor definition despite the fact that many European equids have been referred to *E. altidens* or *E.* cf. *altidens*. Although Eisenmann and Boulbes (2020) mention that, the dental features of *E. altidens* from Süssenborn do not resemble "Sussemiones", Eisenmann (2010) includes *E. altidens* into the subgenus *Sussemionus* [=*Equus* (*Sussemionus*) *altidens*] based on a few metapodials (one metacarpal and one metatarsal). Alberdi et al. (1998) split *E. altidens* into two subspecies, the nominotypical subspecies and *E. altidens granatensis* from Venta Micena (formerly described as *E. stenonis granatensis* Alberdi and Ruiz Bustos, 1985), however they could be different ecomorphotypes of *E. altidens* (Palombo and Alberdi 2017). Even though Eisenmann (1999, 2010) acknowledges the resemblance between the Süssenborn's slender species and the one from Venta Micena (Spain), she gives to the latter a full species rank (=*E. a. granatensis*) due to the relatively shorter protocones in relation to *E. altidens* from

Süssenborn. In their revision on the equids from Dmanisi (Georgia, 1.85–1.76 Ma), Bernor et al. (2021) do not distinguish multiple subspecies of *E. altidens*, including *E. altidens altidens*, *E. altidens granatensis* and '*E. stenonis mygdoniensis*'. Forstén (1999) included also *Equus hipparionoides* Vekua, 1962 from the Early Pleistocene site of Akhalkalaki, Georgia (1.0 Ma to 0.8 Ma: Vekua 1986) into *E. altidens* (also in Boulbes and Van Asperen 2019). Bernor et al. (2019) includes the slender medium-sized equids from Dmanisi, Gerakarou, Pirro Nord, Farneta and Venta Micena under the name *E. altidens* with no subspecific rank distinction.

Scholars argue whether *E. altidens* dispersed from Asia (Chinese lineage of *E. qingyangensis*; Eisenmann and Deng 2005) and/or from an Early Pleistocene African incomer dispersed shortly after 1.8Ma to Europe (Guerrero-Alba and Palmqvist 1997) (evolved from *E. tabeti*, *E. numidicus*) (e.g., Eisenmann 1992; Guerrero-Alba and Palmqvist 1997; Fleagle et al. 2010), or may have evolved within Europe by a stenonoid stock (sees e.g., Forstén 1986b, 1999; Azzaroli 1990, 1992; Alberdi et al. 1998; Alberdi and Palombo 2013a, b; Van der Made 2013; Van der Made et al. 2017 for a discussion). As mentioned earlier, Eisenmann (2010) included this species into the subgenus "*Sussemionus*", that probably originated from North America and thus it is not related to the stenonoid group. This scenario is not followed by other authors who include this species into the stenonoid group (Forstén 1986, 1999a; Azzaroli 1990, 1992; Alberdi et al. 1998; Alberdi and Palombo 2013; Palombo and Alberdi 2017; Bernor et al. 2019; Cirilli et al. 2021). Palombo and Alberdi (2017) support the European origin of *E. altidens* by ''*an anagenetic evolutionary process within the stenonian linage as a response to the changing climatic and environmental conditions*'' and that with a general tendency from robust to gracile, this species could represent the latest form of the stenonoid group (Alberdi et al. 1998; Piñero and Alberdi 2015). Bernor et al. (2019) seems to favor the taxonomic implications of *E. altiden*s with the slender Epivillafranchian equids *E. wuesti* from Untermassfeld (Germany; Musil 2001) and *E. hipparionoides* from Akhalkalaki (Georgia; Vekua 1986), based on their morphological and morphometrical resemblance as stated earlier by other authors (Forstén 1999; Palombo and Alberdi 2017; Boulbes and Van Asperen 2019; Eisenmann and Boulbes 2020). In addition, Bernor et al. (2019) support Azzaroli's (1990) hypothesis that *E. altidens* was a member of the clade of *E. hemionus* that at the same time shared more distant relationships with Grévy's zebra (Cirilli et al. 2021a). *Equus altidens* has been also considered as a probable ancestor of *Equus hydruntinus* by several scholars (Musil

1969; Forstén 1986, 1990, 1999a; Azzaroli 1992; Eisenmann 1992; Alberdi et al. 1998; Alberdi and Palombo 2013) based on assemblages of intermediate size and chronology, such as Petralona (Greece), Cullar de Baza-1 (Spain) and Venosa (Italy) (Van der Made et al. 2017).

Equus altidens granatensis Alberdi and Ruiz Bustos, 1985

Originally described as a subspecies of *E. stenonis*, *Equus altidens granatensis* is a slender medium-sized stenonoid equid from the site of Venta Micena, Orce, Granada (dated at ~1.5 Ma according to Martínez-Navarro et al. 2011). The upper cheek teeth morphology is typically stenonoid with always short protocones (often without an anterior part contrary to the type species) that vary in shape. On the lower cheek teeth, the linguaflexid is V-shaped and varies from the typically stenonine pattern (deep and pointed lingual valleys) to hemionine pattern (shallow valleys, elongated metaconid: Figure 2.1) (Eisenmann 1999). The ectoflexid is very deep on molars reaching and flattening the linguaflexid (Figure 2.1); it may also be deep on premolars (p3, p4). The metapodials are slender like those of *E. altidens*, and more elongated than *E. stenonis*.
The species is mainly recorded in several sites in the Guadix-Baza basin in southern Spain, dating from 1.5 to 0.8 Ma, such as Venta Micena, Lachar, Fuensanta, Fuente Nueva 3, Barranco León 5 (Marín, 1987; Alberdi and Ruiz Bustos 1989; Alberdi et al. 1998; Alberdi 2010) and according to Eisenmann in Cueva Victoria (0.9–0.8Ma, Gibert et al. 2016) where however the same equid remains were described by Alberdi and Piñero (2015) as *Equus altidens altidens*. In Italy, Alberdi and Palombo (2013) identified this species in Selvella-Gioiella and Pirro Nord. The dental remains of *E. altidens* from the Epivillafranchian site Vallparadis (~0.85 Ma, Duval et al. 2015) resemble *E. altidens granatensis* on the short protocones (Aurell-Garrido et al. 2010).
As in the case of *E. altidens*, the taxonomy and phylogeny of *E. altidens granatensis* is still matter of debate (Alberdi et al. 1998; Eisenmann 2004, 2010; Boulbes and Van Asperen 2019; Bernor et al. 2021 and references therein). Eisenmann (1999, 2004, 2010) includes '*E. a. granatensis*' to the subgenus '*Sussemionus*' and considers it as a valid species not phylogenetically linked to the stenonoid group. Alberdi et al. (1998) included the equid from Venta Micena into *E. altidens* although distinguishing it from the typical sample at the subspecies level. (*E. a. granatensis*). Later, Palombo and Alberdi (2017) referred that "*Whether "E. a. granatensis" was a primitive representative of the E. altidens lineage or merely an ecomorphotype mainly present in*

Spain, and maybe in France (Sainzelles), is unclear", although favoring the idea of the ecomorphotypes. Boulbes and Van Asperen (2019) following Eisenmann's (1999) opinion on that matter, consider *E. a. granatensis* as a valid species. Bernor et al. (2021) includes '*E. a. granatensis*' into *E. altidens* with no subspecific discrimination. Whether *E. altidens granatensis* is a valid species/subspecies or not, is outside the scope of this study and needs further investigation. For this reason, the present author follows Alberdi et al.'s (1998), Palombo and Alberdi 's (2017) and Bernor et al. 's (2021) nomenclature including it into *E. altidens*.

Equus suessenbornensis Wüst, 1900

Equus suessenbornensis is a large sized stenonoid equid, larger than *E. stenonis* and *E. livenzovensis*, but smaller than *E. major*; these large equids (*Equus suessenbornensis* and *E. major*) are sometimes referred to as the so-called "*Equus bressanus-Equus suessenbornensis* group" (Palombo and Alberdi 2017). *E. suessenbornensis* is diagnosed by its highly plicated enamel (wrinkled) especially on the upper cheek teeth. *E. suessenbornensis* exhibits both stenonoid and caballoid features. The upper cheek teeth have elongated protocones with concave lingual borders, wide mesostyles and grooves on the styles of premolars (at least closely to the crown), while on molars the styles are faintly grooved or simple (Alberdi et al. 1998). The pli caballin is long, multiple, and wide based. The lower cheek teeth have protostylids and consistently very deep ectoflexid often in contact with the linguaflexid on molars. The metapodials are very long (MC1=274.9 mm, MT1=327 mm, pers. measurements). While some authors refer to *Equus suessenbornensis* as the first archaic true equid (true *Equus* and not *Allohippus/Plesippus* either genus or subgenus) or an evolutionary intermediate between stenonoids and caballoids (Gromova 1949), others do not support this hypothesis based on the shape of the double knot, which is indeed more advanced than in *E. stenonis*; however very different from the U-shaped on the caballoids (Forstén 1986, 1999a; Alberdi et al. 1998; Palombo and Alberdi 2017). *E. verae* Sher, 1971 from the north-eastern Siberia (Chukochya, dated around the Jaramillo event), could be a junior synonym of *E. suessenbornensis* (Forstén 1999), or a closely related species (Eisenmann and Kuznetsova 2004), based on the similar cheek teeth morphology and the identical proportions of the metapodials (in the same group belongs also the cranium of *E. coliemensis* Lazarev, 1980 from the northeast Siberia dated at late Early Pleistocene; Eisenmann 2010: Figs. 3, 4A).

E. suessenbornensis is reported in many sites in Europe. In Western Europe, it is known from several Spanish sites such as Barranco León-5 (BL-5), Cueva Victoria (CV), Fuente Nueva-3 (FN-3), Huéscar- 1 (HU-1), Cúllar de Baza-1 (CB-1) (Alberdi and Ruiz Bustos 1989; Alberdi et al. 1998; Alberdi 2010; Alberdi and Piñero 2015). In France, it is reported at the sites Bois de Riquet, Nauterie, Solilhac (SOL) (Prat and Thibault 1976; Prat 1980; Lacombat 2005; Bourguignon et al. 2016), also at Ceyssaguet according to Prat (1980) [later revised by Aouadi (2001) and Aouadi and Bonifay (2003) to "*E. bressanus*"] and Chagny (the MTIII according to Eisenmann 2017); Forstén (1986) argued however that this species was not present in France. In the UK the species is known at the Cromer Forest Bed Formation of England (Azzaroli 1996; Lister et al. 2010). In Central Europe, beside Süssenborn, *E. suessenbornensis* is reported in the Middle Pleistocene site of Voigtstedt (Germany) (Musil 1965) and in Stranska Skala (Czech Republic) (Musil 1972). In Italy, it is reported is several sites such as Pirro Nord, Selvella-Gioiella, Slivia, Bucine, Monte Tenda and Venosa-Loreto in the Farneta or Pirro Nord FU dated between the latest Villafranchian to the middle Galerian (*E.* cf. *stenonis* in De Giuli 1986; Caloi and Palombo 1987; Alberdi et al. 1988; Alberdi and Palombo 2013a, 2013b). Although the occurrence of *E. suessenbornensis* in the Farneta and Pirro Nord FU (Pirro Nord and Selvella sites) could represent the oldest datum of the species in Western-Central Europe, its presence in Pirro Nord is questioned because of the relatively smaller body size of the Pirro Nord sample (variability of the MT1 between 269 and 282.7 mm, meas. taken from Alberdi and Palombo 2013b) contra to the best-known sample from Akhalkalaki (variability of the MT1 between 301 and 330 mm, meas. taken from Eisenmann 2017). In Eastern Europe, *E. suessenbornensis* is also reported in Georgia at Akhalkalaki representing the best-known collection for the species (Vekua 1986), in Ukraine at Tiraspol (Gromova and Dubrovo 1975), in Romania (Samson 1975) and possibly in Turkey at Denizli Basin (*E.* aff. *suessenbornensis* according to Erten et al. 2005), but Boulbes et al. (2014) refers to the larger species as *E.* cf. *apolloniensis*. Taking into consideration the presence of the species in all the mentioned European localities, the chronological distribution of *Equus suessenbornensis* is between the end of Early Pleistocene around 1.2 and 0.6 Ma (Boulbes and Van Asperen 2019).

The mix of stenonoid and caballoid dental features in *E. suessenbornensis* led several authors to a debate about its phylogeny; it could be an intermediate (more advanced) species between stenonoids and caballoids, or a stenonoid equid with some advanced

characters that converge towards the caballoids (Grossouvre and Stehlin 1912; Gromova 1949; Musil 1969, 1992; Nobis 1971; Gromova and Dubrovo 1975; Samson 1975; Azzaroli 1984; Alberdi et al. 1998; Forstén 1999; Alberdi et al. 2001; Aouadi and Bonifay 2008; Eisenmann 2010; Alberdi and Palombo 2013; Palombo and Alberdi 2017). Some authors consider *E. suessenbornensis* as a descendant of *E. major* (Grossouvre and Stehlin 1912; Alberdi et al. 1998; Forstén 1999; Aouadi and Bonifay 2008; Palombo and Alberdi 2017). In particular, Alberdi et al. (1998) endorsed *E. suessenbornensis* to a secondary lineage of *E. major*-*E. suessenbornensis* likely originated from the ancestral European populations of *E. livenzovensis*. Other authors, consider *E. suessenbornensis* a direct descendant of *E. stenonis* (Nobis 1971; Samson 1975, Azzaroli 1984), while others reject any affinity between *E. stenonis* and *E. suessenbornensis* (Musil 1969, 1992), considering *E. suessenbornensis* either an archaic caballoid equid or a 'true' caballine (Gromova 1949a, b), based on the advanced dental features (such as complicated enamel pattern and long protocones with concave lingual borders on the upper and protostylids on the lower cheek teeth). However, Alberdi et al. (1998) stated that *E. suessenbornensis* can be regarded as a true 'stenonoid equid', more than an intermediate or convergent species to stenonoids (also in Alberdi and Palombo 2013), based on the stenonoid V-shaped linguaflexid on the lower cheek teeth. This opinion is also embraced by Forstén (1999), who included the species into the stenonoid group and not the caballoid or the 'true equid' group. Eisenmann (2010) on the other hand, includes this species into the new subgenus "Sussemionus", *E.* (*Sussemionus*) *suessenbornensis*, based on some features such as peculiar plis caballin with very large base, complicated enamel on the upper cheek teeth, the presence of protostylids, shape of the double-knot and very deep ectoflexid on the lower.

Equus major Depéret,
in Delafond and Depéret 1893, ex Boule

Equus major (*=E. bressanus =E. robustus*) is described from the middle Villafranchian of Chagny (Saône-et-Loire, France) (revised by Viret 1954). This species is the largest stenonoid equid, larger and heavier than *E. livenzovensis* and *E. suessenbornensis* (Alberdi et al. 1998; Alberdi and Palombo 2013). *E. major* shows stenonoid dental characters on the upper cheek teeth (e.g., short protocones and well developed pli caballin) and some more advanced features (e.g., teeth large in size, more derived plication on the enamel, longer distal part of the protocone) (Alberdi et al. 1998). The

metaconid is elongated on the lower cheek teeth, the linguaflexid is V-shaped (shallow) and the ectoflexid is relatively deep on the molars (in Boulbes and Van Asperen 2019: Fig. 3B-b). The cranium FP1-2001-0371 from Fonelas P-1 (Cuenca De Guadix, Granada) that is assigned to *Equus* cf. *major* is large with its maximal length (M6) at ~670 mm (see Garrido 2008 for detailed descriptions). *E. major* was almost double the body mass of *E. livenzovensis* (Alberdi et al. 1998). The limb bone morphology of *E. major* is similar to the stenonoids in most of the parts, with some features also resembling the caballoids. The limb bones are large (radius=401 mm, tibia=407 mm taken from Alberdi et al. 1998), the largest among the other stenonoid equids and the metapodials are long (MC1=271 mm, MT1=329 mm, averages taken from Alberdi et al. 1998). The most recognisable difference from other stenonoid equids is exhibited on the dimensions of the phalanges (PhA1=106.24 mm, see also Alberdi et al. 1998) rather than on the metapodials.

Apart from Chagny (Viret 1954), the species is also recorded in other French localities such as Pardines (together with *E. stenonis*), Le Coupet, Senèze, Blassac, (Pratt 1980), La Malouteyre (Bout 1970, 1976) and possibly in Ceyssaguet ("*E. bressanus*": Aouadi 1999; Aouadi and Bonifay 2001). The species ("*E. bressanus*") is also described by Azzaroli (1983, 1990, p. 346, 1996) from East Runton, Norfolk of England, but Caloi and Palombo (1987) believe that it is better resembling *E. suessenbornensis* based on the richly plicated enamel of the cheek teeth. In Romania, *E. major* is present at Oasele and Malusteni [=*Plesippus* (*Allohippus*) *major euxinicus* (Samson 1975, p. 202); *Equus euxinicus* according to Eisenmann 2017]. The species is also recorded in the Netherlands at Tegelen (Viret 1954) and probably in Upper Valdarno (Italy: Azzaroli 1990) and in Schernfeld (Germany: Musil 1992).

The chronological distribution and taxonomic status of *E. major* are not well defined. Musil (1992) gave a range of distribution between 2.2-1.7 Ma for "*E. bressanus*". However, the origin of specimens described by Boule *in* Parandier (1891) are coming from two different sites (Chagny and Perrigny) as stated by Depéret (in Delafond and Depéret 1893, p. 236). Furthermore, the exact stratigraphic position is uncertain since there are two fossil-bearing stratigraphic layers in Chagny (Chagny I and II) dated at Early Pleistocene and (?)late Early Pleistocene respectively (Chaline and Michaux 1969; Azzaroli et al. 1988). Azzaroli 1990 supports a restricted early Pleistocene age for *E. major*. However, based on the biochron and estimated body size, small equids are younger than the largest ones and *E. major* is larger than the older *E. livenzovensis*

(Alberdi et al. 1998). The possible presence of the species in Ceyssaguet ("*E. bressanus*") can expand its range up to 1.5 Ma (Aouadi 1999; Aouadi and Bonifay 2001).

The taxonomic situation is also debated. Pomel (1853) assigned the name *E. robustus* for some specimens from Auverge, and later for some other from Le Coupet. Viret (1954) replaced the names *E. robustus* Pomel, 1853, and *E. stenonis major* Boule *in* Parandier, 1891 by the name *E. bressanus* for the large equids from Chagny, Senèze and Tegelen. Depéret (in Delafond and Depéret 1893, p. 235), following Boule's designation, used the name "*E. stenonis* race *major*" suggesting that it is a distinct species however including it at that time into the *E. stenonis* group. The same author referred to Boule's designation (1891, p. 801 and 815), who proposed the presence of a larger equid than the typical *E. stenonis* at Le Coupet (France). Azzaroli (1990) refers that "Boule's *Equus major* represents the same species as Viret's *Equus bressanus*" and accepts *E. bressanus* as a valid species. Alberdi et al. (1998), following the ICZN nomenclature rules, consider *E. robustus* as a nomen dubium and *Equus bressanus* a junior synonym of *E. major* (Palombo and Alberdi 2017).

From a phylogenetic point of view, the *E. major-E. suessenbornensis* monophyletic group may have stemmed from *E. livenzovensis* according to Alberdi et al. (1998), while Azzaroli (1992) suggests that *E. major* may have stemmed from *E. stenonis* and that *E. suessenbornensis* is possibly closely related to this lineage.

Equus wuesti Musil, 2001

Equus wuesti has originally been described from the Epivillafranchian fauna of Untermassfeld (Thuringia, Germany) dated at the beginning of the Jaramillo chron (~1.07 Ma: Ellenberg and Kahlke 1997; Kahlke 2000; Kahlke and Gaudzinski 2005; Kahlke 2006). According to Musil (2001), this species exhibits both primitive and advanced features and it is close to, yet different from, *E. altidens* von Reichenau, 1915. Eisenmann and Boulbes (2020) revised the old and described the new material from Untermassfeld which mainly comprises by postcranial elements, a few teeth (most of them are decidual), but no crania whatsoever. On the upper cheek teeth, the protocone is short with not very deep postprotoconal groove, the inner fossettes are plicated and the pli caballin is normally developed (Eisenmann and Boulbes 2020). The lower cheek teeth exhibit stenonoid pattern, with V-shaped linguaflexid, lingually pointed metastylid and deep ectoflexid on molars (Eisenmann and Boulbes 2020; Fig. 4). The

metapodials are slender (however more robust than the ones of *E. altidens*) with deeper diaphysis and very strong distal tuberosities (Eisenmann and Boulbes 2020).

Forstén (1999) considered the slender *Equus* from Untermassfeld as a stenonoid equid (also Palombo and Alberdi 2017) similar to *E. altidens*, suggesting some relationship with the slender equid identified by her at Livenzovka or with the Asian equids e.g., from Nalaikha (Mongolia) and Nihowan (China) (but see Eisenmann and Kuznetsova 2004). Other authors, consider *Equus wuesti* as the ancestor of *E. altidens* (Musil 2001; Lister et al. 2010). This scenario is questioned though since the latter species (*E. altidens*) is present at many fossiliferous European localities older than Untermassfeld (Palombo and Alberdi 2017). According to Eisenmann and Boulbes (2020), *Equus wuesti* belongs to the Sussemione group close to, but different from, *Equus altidens granatensis* from Venta Micena and *Equus hipparionoides* from Akhalkalaki, representing an important link between the older Venta Micena in the West and the younger Akhalkalaki in the East. Whether *E. wuesti* originated from an Asian species or from a local population of *E. stenonis* or represent a local morphotype of the *E. altidens* sensu lato, still needs to be answered.

Equus apolloniensis Koufos, Kostopoulos and Sylvestrou, 1997

(Modified from Gkeme et al.'s 2021 emerged diagnosis) *Equus apolloniensis* is a large-sized equid that was originally described and figured by Koufos et al. (1997) from the Epivillafranchian fauna of Apollonia-1 (Mygdonia Basin, 1.2–0.9 Ma, Kahlke et al. 2011). This species exhibits both caballoid and stenonoid features like *E. suessenbornensis*. Unlike *E. stenonis*, *E. apolloniensis* has a short narial notch that ends above the distal lobe of the P2 (Figure 5.52e). The buccinator fossa is well-developed and the braincase is rather small like in *E. stenonis*. The facial crest is shorter than *E. stenonis*. The choanae are more elongated than any other stenonoid horse and the palate is relatively shorter. The protocone is more elongated (Figure 5.52e) than the typical *E. stenonis*, resembling *E. stenonis vireti* in this feature and the parastyle is occlusally notched on the upper cheek teeth, while the double knot is typically stenonoid (V-shaped) and the ectoflexid is shallow even on molars in most cases (Figure 5.52e). The metapodials are larger and slenderer than *E. stenonis*, and shorter than *E. major* and *E. suessenbornensis*.

Apart from Apollonia-1, *Equus apolloniensis* is also reported in Alykes (1.6 Ma, Athanassiou 2002; Kahlke et al. 2011) and Volos (Magnesia, Greece) (Gkeme et al.

2021; Koufos et al. 2022) and according to Konidaris et al. (2015) possibly in Tsiotra Vryssi and Platanochori-1 (Mygdonia Basin). This species is possibly present in Turkey in the upper travertines of the Denizli Basin dated between 1.6 and 1.1Ma (Boulbes et al. 2014; Lebatard et al. 2014).

Like in *E. suessenbornensis*, the unique mix of stenonoid and caballoid features of *E. apolloniensis* led several authors to a debate about its exact taxonomic position and its phylogenetic relationships to or within the stenonoid lineage (Koufos et al. 1997; Eisenmann and Boulbes 2020; Palombo and Alberdi 2017; Eisenmann and Kuznetsova 2004; Boulbes and Van Asperen 2019; Gkeme et al. 2021; Eisenmann 2022; Koufos et al. 2022). According to Koufos et al. (1997), *E. apolloniensis* represents a transitional form from the typical (archaic) stenonoid horses (*E. stenonis*) to the more advanced *E. suessenbornensis*, and thus it is linked to the stenonoid group. In their latest review on *E. apolloniensis*, Gkeme et al. (2021) favor this scenario. On the contrary, according to Eisenmann and Kuznetsova (2004), *E. apolloniensis* is considered a "true" *Equus* and it is distinguished from the primitive *Plesippus* and *Allohippus* based on their cranial morphology and morphometrics, hence it is likely the oldest occurrence of a true *Equus* (non caballine) in Europe. Eisenmann and Boulbes (2020) point out great similarities of the dental elements and general proportions of the metapodials between *E. apolloniensis* and the extant wild asses (*E. africanus*). In her recent review, Eisenmann (2022) includes *E. apolloniensis* in the group of Asses, *E. (Asinus) apolloniensis* Koufos et al., 1997. The possible phylogenetic scenarios are going to be analyzed in detail later in this work.

Equus petraloniensis Tsoukala, 1989

Equus petraloniensis was described and figured by Tsoukala (1989) from the Middle-Late Pleistocene of Petralona Cave (Chalkidiki, Central Macedonia). The type specimen is a third metacarpal (PEC-500) stored in the Museum of Geology-Palaeontology-Palaeoanthropology of the Aristotle University of Thessaloniki (Tsoukala 1989: pl. XXVII, fig. a). The species is characterized by its gracile and slender metapodials. The cheek teeth are typically stenonoid, with short protocones on the upper, V-shaped linguaflexid on the lower, and deep ectoflexid on the molars.

The taxonomic and phylogenetic position of *Equus petraloniensis* are still debated. According to Tsoukala (1989), *Equus petraloniensis* is possibly an intermediate form between *E. stenonis* and *E. hydruntinus*. Forstén (1999) refers the gracile equid from

Petralona as *E*. cf. *altidens*, resembling the equids from Libakos, Krimni-1 and Gerakarou. Eisenmann et al. (2008) and Eisenmann et al. (2022) include *E. petraloniensis* within the variation of *Equus hydruntinus* and they refer it as *'E. (Hemionus) hydruntinus petraloniensis'*, the largest subspecies of *E. hydruntinus* (see Fig. 10 in Eisenmann et al. 2008).

Equus graziosii Azzaroli, 1979

This species was described by Azzaroli (1979) from the Middle-Late Pleistocene of Maspino and Chiana valley (near Arezzo, eastern Tuscany) (Azzaroli 1966, 1979). The species shares common features with *E. asinus* with only a few different details at the muzzle and thus it is closely related to asses (Azzaroli 1979; Eisenmann and Kuznetsova 2004; Eisenmann 2006); the postcranial elements are typically asinine. The type cranium of *E. graziosii* shows a combination of *E. grevyi* and Ass features (Eisenmann 2006: Fig. 8); it resembles *E. nalaikhaensis* (Nalaikha quarry, Mongolia) in face and muzzle proportions, although it is much smaller (Eisenmann and Kuznetsova 2004: Fig. 8), and the frontal is wide as in the case of *E. grevyi* (Eisenmann and Kuznetsova 2004: Fig. 7; Annexe: Table 2). There is no mandible associated with the cranium, however Azzaroli (1979: pl.7) includes a mandible that according to Eisenmann and Kuznetsova (2004) looks rather caballine. The morphology of the upper cheek teeth is hemionine and asinine with deep postprotoconal grooves and lack of plis caballins (Eisenmann 2006: Fig. 9-1). The upper cheek teeth also resemble those of *E. hydruntinus davidi* (Boulbes and Van Asperen 2019, Fig. 13F). The ectoflexid on the lower molars is deep or moderately deep although in most asses it is shallow (Eisenmann 1981). According to Eisenmann and Kuznetsova (2004), this species belongs to a 'true' *Equus* based on its basicranial proportions.

4.2 CABALLOID EQUIDS

There is agreement between equid specialists that at the beginning of the Middle Pleistocene (Forstén 1998), caballoids emerged and dispersed into Europe and gradually replaced the stenonoid equids. Usually, they were of larger body size than the stenonoid equids. Their wide skeletal plasticity enabled them to survive in an extensive range of environments and climatic conditions from interglacial forests to grass-steppes (Van Asperen 2010; Saarinen et al. 2016) and sometimes adopt a diversified diet (e.g., Van Asperen 2010, 2012; Moncel et al. 2011; Rivals et al. 2010; Rivals and Lister 2016; Saarinen et al. 2016). Due to their abundance in many palaeontological and

archaeological sites, caballoids were extensively studied by many authors both by means of taxonomy (Von Reichenau 1915; Gromova 1949; Prat 1968; Nobis 1971; Eisenman et al. 1985; Eisenmann 1988, 1991a,b; Eisenmann and David 2002; Forstén 1973, 1999b; Forstén and Moigne 1998; Musil 1975, 1977, 1978, 1984, 1990, 1991; Guadelli 1987, 1991) and biostratigraphy (e.g., Eisenmann 1988, 1991a,b; Forstén 1998b; Cramer 2002; Boulbes 2010; Van Asperen 2011, 2012, 2013a; Uzunidis 2017).

Equus ferus Boddaert, 1785

After many decades of debate, the systematics of the caballoid equids have been redefined. *Equus ferus* Boddaert, 1785, was proposed to be used for the living wild caballine horse species by the International Commission on Zoological Nomenclature (ICZN 2003; also reported by Van Asperen 2010), distinguishing it from the domestic species *Equus caballus* Linnaeus, 1758 (Gentry et al. 2004), in order to underline the existing differences between these two equine forms (domestic and wild).

This species first appeared in Europe in the early Middle Pleistocene (Galerian, ca. 0.7–0.6 Ma), originating probably from earlier forms from central Asia and Mongolia (Azzaroli 1983; Forstén and Sharapov 2000). Boddaert (1785) did not refer to any holotype or lectotype of the species, but he gave a detailed description of its anatomical characters (Boddaert 1785, p. 159). From a taxonomic viewpoint, *E. ferus* has been questioned mainly because the species split into many chronological and geographical varieties, which have been used either as subspecies or different species [*E. mosbachensis* von Reichenau, 1915; *E. mosbachensis tautavelensis* Crégut-Bonnoure, 1980; *E. mosbachensis campdepeyri* Guadelli and Prat, 1995; *E. mosbachensis palustris* Bonifay, 1980; *Equus mosbachensis micoquii* Langlois, 2005; *E. steinheimensis* von Reichenau, 1915; *E. torralbae* Prat, 1977; *E. achenheimensis* Nobis, 1971; *E. ferus taubachensis* Freudenberg, 1911; *E. ferus piveteaui* David and Prat, 1962; *E. ferus germanicus* Nehring, 1884; *E. ferus antunesi* Cardoso and Eisenmann, 1989; *E. ferus gallicus* Prat, 1968; *E. ferus latipes* Gromova, 1949; *E. ferus arcelini* Guadelli, 1991, and *E. caballus* Linnaeus, 1758 (see also Boulbes and Van Asperen 2019 and references therein)] in order to identify the Middle and Late Pleistocene fossil samples of the caballine equids.

These samples/taxa were distinguished by their size or skeletal proportions and they exhibit a wide range of morphological variability within the same lineage (for these differences see Boulbes and Van Asperen 2019). Forstén (1986) acknowledged

morphological and morphometrical resemblance between *E. ferus germanicus*, *E. ferus orientalis* and *E. ferus chosaricus*, and proposed that they represent different populations of a single widespread species *E. ferus*. These different forms or subspecies have been considered to be chrono species by Eisenmann and Kuznetsova (2004). Eisenmann et al. (1985) suggested that such differences in cranial variations cannot be accounted as an individual age variation nor by any intraspecific variation; they could be a result to climatic adaptations (Allen's law accounting for short muzzles) leading to more or less speciations. Van Asperen (2010) noted that the observed differences are not more variable than those on modern ponies or highly homogeneous groups such as Arabian equids or *E. przewalskii*. The variation observed between assemblages follows certain patterns that can be interpreted as ecomorphological variation of the same species, and the resulting groups are best referred to as ecomorphs, or, at most, subspecies of *E. ferus* (Boulbes and Van Asperen 2019). Studies of equid genetic variation conducted by Weinstock et al. (2005) and Orlando et al. (2009) support the genetic variation of the Middle and Late Pleistocene caballine horses.

Taking all this into account, the author of the thesis follows the ICZN 2003 (see also Cramer, 2002; Van Asperen 2013b; Boulbes and Van Asperen 2019), where all European late Middle Pleistocene and Upper Pleistocene caballoid equids are being referred to *Equus ferus* Boddaert, 1785, even though this taxon, commonly chosen for Pleistocene wild horses, remains questionable (Guadelli and Delpech 2000; Eisenmann 2006b).

In Greece, the species is referred in Aggitis in Eastern Macedonia (=*E. caballus* in Koufos 1981), in Peneios Valley in Thessaly (Athanassiou 2002, 2011), as well as in several prehistoric places. *E. ferus* cf. *germanicus* (=*E. caballus* cf. *germanicus* in Tsoukala 1992) is referred in the cave of Agios Georgios (Kilkis, Central Macedonia) and *E. ferus piveteaui* (=*E. caballus piveteaui* in Tsoukala 1989) in the Petralona cave.

Equus mosbachensis Von Reichenau, 1915

This taxon was instituted by Von Reichenau (1915) based on the material from the fossiliferous sites of Mosbach (~0.5Ma) in Germany. It was originally described as *E. caballus mosbachensis* due to the resemblance of dental characters to *E. caballus* [=*E. ferus* according to ICZN (2003)]. This species, also known as *E. ferus mosbachensis*, is considered as the first 'true horse' (caballine *sensu lato*) in Europe. It is perhaps the only equid regarded widely as a true species (Eisenmann 1979, 1980, 2020; Bonifay

1980; Crégut 1980; Eisenmann et al. 1985; Guadelli and Prat 1995; Langlois 2005; Boulbes 2010; Palombo 2014; Palombo and Alberdi 2017; Uzunidis et al. 2017; Boulbes and Van Asperen 2019). Its cranial dimensions are very large, and its snout is long (Eisenmann et al. 1985). Although, *E. mosbachensis* shares common features with *E. ferus*, it also exhibits some "archaic" (stenonine) morphological characters: large size and slender/heavy(?) general build, presence of the tendon insertion of the anterior brachialis muscle on the inner edge of the diaphysis of the radius and strong supraarticular tuberosities on metapodials (Bonifay 1980; Crégut-Bonnoure 1980; Eisenmann 1991a; Guadelli and Prat 1995; Hadjouis 1998; 143 Langlois 2005; Boulbes and Van Asperen 2019). The variation of the protoconal index (low and sub-equal between P4 and M1) is diagnostic.

Various subspecies of *E. mosbachensis* have been recognized from the Middle Pleistocene archaeological sites in France: *E. mosbachensis tautavelensis* Crégut-Bonnoure, 1980 from the Arago Cave (Pyrénées-Orientales), *E. mosbachensis campdepeyri* Guadelli and Prat, 1995 from the Camp-de-Peyre: (Sauveterre la Lémance, Lot-et-Garonne), *E. mosbachensis palustris* Bonifay, 1980 from the caves of Lunel-Viel (Hérault, France) and *Equus mosbachensis micoquii* Langlois, 2005 from the archaeological site of "La Micoque" (Les Eyzies-de-Tayac, Dordogne).

E. mosbachensis is identified in Mauer (Nobis 1971), dated at 609 ± 40 ka (Wagner et al. 2011) and in the eponymous site of Mosbach 2. Also in Germany, (0.64–0.62Ma, Kahlke 2014) a few caballine teeth in Süssenborn could represent some of the oldest evidence the species (Forstén 1986; Eisenmann 2008). The species is present in many regions of southern and western Europe at the beginning of the Middle Pleistocene (Lister et al. 2010; Aurell-Garrido et al. 2010; Madurell-Malapeira et al. 2010; Martínez et al. 2014; Van der Made 2013; Palombo 2014). *Equus mosbachensis* could extend to the end of Middle Pleistocene during MIS 6 (Guadelli 2007; Uzunidis 2017), although there is no chronological consensus on its last appearance due to the numerous regional and chrono/ecotype variations.

4.3 THE EUROPEAN WILD ASS

Equus hydruntinus Regalia, 1907

Equus hydruntinus was described by Regalia (1907) based on the equid material collected from the Upper Palaeolithic (Epigravettian, Sardella et al. 2018) cave site Grotta Romanelli in Italy. An extensive analysis of this species has been conducted by

Stehlin and Graziosi (1935). *E. hydruntinus* is characterized by slender limbs, cursorial proportions, and relatively short teeth. The upper cheek teeth of *E. hydruntinus* have short protocones, while the lower exhibit V-shaped linguaflexid and deep ectoflexid especially on molars. The crania from the Late Pleistocene Emine-Bair-Khosar Cave (Crimea, Ukraine), belonging to *E. hydruntinus* (crania no. Ba2 384 and Bc 141 in Van Asperen et al. 2012: Figs. 3.1 and 3.2 respectively), are small in size with short but broad muzzles. Other cranial elements are known from the Middle Palaeolithic site Kabazi II (Crimea) (Burke et al. 2003; Patou-Mathis and Chabai 2003), however most of the given measurements are estimated from images or damaged regions of the specimens (Burke et al. 2003). They are characterized by their significant wide muzzles (M14, M15) and their very short naso-incisival notch (M30). Cranial fragments from Lunel-Viel, also attributed to *E. hydruntinus*, are smaller in size than the ones from Emine-Bair-Khosar Cave, morphologically resembling each other (although the muzzle is relatively shorter); *E. hydruntinus minor* proposed by Bonifay (1991). Eisenmann (1992, p. 166) pointed out the resemblance of the cranium LVIV 18698 from Lunel-Viel with the hemiones: "the skull shape of the small equid from Lunel-Viel is closer to hemiones than any other equid species" despite the fact that the metapodials are more robust than the hemiones.

Equus hydruntinus spread over Eurasia during the Pleistocene; its oldest appearance in the European fossil record seems to be at the Middle Pleistocene of Vallparadís (Spain) (=*E.* cf. *hydruntinus*, level 11, EVT3), dated slightly later than 0.6Ma (Aurell-Garrido et al. 2010; Madurell-Malapeira et al. 2010; Martínez et al. 2014) and not as previously assumed at the late Middle Pleistocene site of Lunel-Viel (oldest appearance in France) which is dated ca. 300 Ka (Bonifay 1991; Orlando et al. 2006); this is because the dispersion of the species throughout Europe was diachronous. The species probably became extinct at the beginning of the Holocene/middle Holocene, and it might possibly have been present at historical times in Portugal (Antunes 2006). The species is also recorded in other sites of Spain such as Gran Dolina (*E.* cf. *hydruntinus*, Saladié et al. 2018) (complex of the Sierra de Atapuerca) and at Galeria (Rodríguez et al. 2011; Van der Made 2013). It also known in Italy at Grotta Romanelli and San Teodoro, in Germany at Schöningen (Van Kolfschoten et al. 2015) and Steinheim (Forstén 1999b), in Greece at Agios Georgios (Tsoukala 1992) and in many other sites in France, Germany, Britain, Portugal, Russia, Hungary, Israel and Spain. There are also some

dental and postcranial elements that are resembling those of *E. hydruntinus* in Africa at Haua Fteah Cave (Libya, Blanc 1956) and Salé (Morocco).

Subspecies or ecomorphotypes of *Equus hydruntinus*

Several forms of *E. hydruntinus* have been described over the years besides the type species from Grotta Romanelli, *E. hydruntinus hydruntinus*, described by Stehlin and Graziosi (1935). *Equus hydruntinus minor* from Lunel-Viel (France) was described by Bonifay (1991) and it is the smallest, oldest (dated ca. 300 Ka, Bonifay 1991), yet less typical, form of the species. Although the description is based on a rich material, including a fragmentary cranium, the relationships of this form with *E. hydruntinus* is questioned by some authors (Azzaroli 1990; Van der Made et al. 2017). *Equus hydruntinus danubiensis* is described by Samson (1975) from Romania and it represents a large-sized form of the species. Eisenmann et al. (2008) and Eisenmann (2022) included the equid from Petralona (*E. petraloniensis*, Tsoukala 1991) into the species, representing one of its largest forms '*E. hydruntinus petraloniensis*'. Alimen (1946) created another form from the Mousterian site of Saint-Agneau (Charente), *Equus hydruntinus davidi*, based on a single tooth with longer protocone. Forstén (1999) refers that the equid from Venosa shares common features with *E. hydruntinus*, however it is considered by other authors one of the last representatives of *E. altidens* (Alberdi et al. 1988; Alberdi and Palombo 2013).

The systematic position *E. hydruntinus* has been a long matter of debate and its phylogeny was puzzling for equid specialists. This species is molecularly linked to extant hemiones (Asian wild ass) (Orlando et al. 2006), and only after the beginning of the twenty-first century that was unveiled by genetical analyses (study of ancient DNA); though it differs by some cranial and dental features (Eisenmann and Mashkour 1999; Burke et al. 2003).

There are manifold hypotheses regarding the phylogenetic traits of *E. hydruntinus*: it was either included into the subgenus *Asinus* (Regalia 1907; Stehlin and Graziosi 1935; Gromova 1949), or *Hemionus* (Azzaroli 1992), placed close to zebras (Davis 1980; Bonifay 1991), considered as the last stenonoid (Forstén 1986, 1990, 1999a; Forstén and Ziegler 1995) or even included into a separate genus *Hydruntinus* (Radulesco and Samson 1965). These diverse hypotheses are based on the mosaic of features (archaic + derived) found on the dental and postcranial elements of the species: gracile limb bones with cursorial adaptation like the hemiones, short protocones like the stenonoids,

deep ectoflexids like on zebras (Eisenmann and Mashkour 1999) and cranial morphology (crania from Kabazi II, Crimea) close to the hemiones (Burke et al. 2003). The extraction of ancient DNA from the samples of Crimea (*E. hydruntinus*) and Iran (*E.* cf. *hydruntinus*) supported the proximity of the species to hemiones and rejected any proximity to zebras (*E. burchelli*) or asses that was proposed based on the tooth morphology (Orlando et al. 2006, 2009).

Recent palaeogenetic studies allow the possibility of *E. hydruntinus* to be conspecific with *E. hemionus* and not a distinct species (Orlando et al. 2009; Bennett et al. 2017). From a morphometrical and morphological point of view, there are several dental and cranial differences between *E. hydruntinus* and *E. hemionus* based on the study of the crania coming from the sites from Crimea (Kabazi II and Emine-Bair-Khosar cave). On *E. hydruntinus*, the palatal length is greater, the muzzle is very short and wide and the naso-incisival incision is significantly much shorter (Burke et al. 2003; Orlando et al. 2006; Eisenmann et al. 2008; Van Asperen et al. 2012).

E. hydruntinus is often characterized by microdonty, meaning that the cheek teeth are relatively small proportionally to the postcranial skeleton, although it is also featured by a high degree of hypsodonty (Stehlin and Graziosi 1935; Eisenmann and Baryshnikov 1995; Palombo and Alberdi 2017; Eisenmann et al. 2008). The occlusal surfaces (length + width / 2) of P3–P4 and M1–M2 are small compared to the length of metapodials (MC1 and MT1) except *E. hydruntinus minor* from Lunel-Viel. Also, the mesio-distal length of the M3 is always shorter than the mesio-distal length of the M2 (Bonifay 1991; Boulbes 2009: Fig.4, p. 454). Another difference is the increment of the protoconal index within the tooth row from the P4 to the M1 at the case of *E. hydruntinus* (Eisenmann and Patou 1980; Cardoso 1995; Boulbes 2009: Fig.4, p. 454). Nevertheless, Eisenmann (2022) underlines the resemblance of these dental features (e.g., short protocones) of *E. hydruntinus* with the late Villafranchian–early Galerian equids (e.g., Pirro Nord, Italy and Aïn Hanech, Africa). The same author also refers: "Morphologically, *E. hydruntinus* could easily be considered a close relative or even a descendant of these taxa if they belonged to *Equus* instead of *Allohippus* or *Plesippus* as is commonly accepted (Alberdi and Palombo 2017)", although "the crania from Pirro and Aïn Hanech are unknown, and the cranium from Kabazi is close to the extant *Equus* (*Hemionus*)".

Regarding the skeleton, the general proportions are close to those of hemiones, although it seems that the third metacarpal is shorter than the third metatarsal (Eisenmann et al.

2008: Figs. 2, 9; Eisenmann 2022). The diaphysis of both metacarpals and metatarsals of *E. hydruntinus* are more robust (M3 relative to M1) and deeper (M4) (Eisenmann et al. 2008: Fig. 11, p. 171; Van Asperen et al. 2012). The epiphyses (M5) relative to the maximal length (M1) are less developed (Boulbes and Van Asperen 2019: Fig. 12), while to distal keel (M12) is in proportion less developed. Other primitive distinctive characters on the skeleton are discussed in Bonifay (1966, 1991), Prat (1968) and Boulbes and Rillardon (2010).

As mentioned earlier, *E. hydruntinus* had been considered as a descendant of *E. altidens* (Musil 1969; Forstén 1986, 1990, 1999) based on the intermediate size and age of some assemblages (Venosa, Petralona, Cullar de Baza 1) (Van der Made et al. 2017). *E. petraloniensis* is considered an intermediate form between the two in the morphometrics of metacarpals and phalanges and also the chronology (Van der Made et al. 2017). Similarities with the African *E. tabeti* (Aïn Hanech) and *E.* cf. *tabeti* (Oubeidiyeh) (Guerrero-Alba and Palmqvist 1997; Eisenmann 1999) have been acknowledged likewise. Another scenario is that the species arrived from Asia and dispersed into Europe, occupying the ecological niche that was not occupied by *E. altidens* (Palombo and Alberdi 2017). This scenario rejects the hypothesis of *E. hydruntinus* being linked to the stenonoid lineage and supports its hemionine origin from Asian species (Palombo and Alberdi 2017).

CHAPTER 5. THE GREEK QUATERNARY *EQUUS*

5.1 SYSTEMATIC PALAEONTOLOGY

Order Perissodactyla Owen, 1848

Family Equidae Gray, 1821

Genus *Equus* Linnaeus, 1758

***Equus stenonis* Cocchi, 1867**

Localities.

Danfero-1 (DFN), Aliakmon Basin, Western Macedonia

Dafnero-3 (DFN3), Aliakmon Basin, Western Macedonia

Volax (VOL), Drama Basin, Eastern Macedonia

Sésklo (SES), Magnesia, Thessaly

Krimni-1 (KRI), Mygdonia Basin, Central Macedonia

Riza-1 (RIZ), Mygdonia Basin, Central Macedonia

Material.

Dafnero-1. Part of cranium DFN-112; maxilla with P1-M3 sin/dex DFN-108; fragment of maxilla with dP2-dP4 sin DFN-88; in situ dP3-dP4 sin DFN-198; in situ dP2-dP4 dex DFN-147; in situ P2-P4 dex DFN-77; dP3/4 sin: DFN-72, 98, 126; dP3/4 dex: DFN-96, 97,133; C sin DFN-81; P2 sin: DFN-40, 79; P3/4 sin DFN-101, 131, 208 (fragment); M1/2 sin: DFN-132, 161, 208 (fragment); P3/4 dex: DFN-13, 32 (fragment), 130; M1/2 dex: DFN-18, 34 (fragment), 210 (fragment); mandibular fragment with di2, c, dp2-dp4, m1 sin and di1-di3, c, dp2-dp4, m1 dex DFN-183; fragment of mandibular ramus with p2-p4 sin DFN-62; fragment of mandibular ramus with p3-m3 sin (+ in situ p3-m2 dex) DFN-67; fragment of mandibular ramus with p2-

p4 dex DFN-182; i (lower?) dex DFN-99; dp2 sin DFN-160; dp3 sin DFN-204 in situ p2-p4 dex DFN-148; in situ m1-m3 dex DFN-67; p2 sin DFN-15; p3/4 dex DFN-14; third metacarpals with fragmentary accessories: DFN-91, 113, 114, 153, 163, 164 (juv.?) 165; proximal part of third metacarpal with accessory DFN-9; distal parts of third metacarpals: DFN-60, 206; distal part of tibia DFN-155; astragali: DFN-31, 35, 36, 37, 38, 90, 115, 170; third metatarsals: DFN-10, 29, 30, 106 (fragment), 151, 152, 154, 166 (fragment), 169, 179 (with fragmentary accessories), 195; proximal part of third metatarsal DFN-180; distal parts of third metatarsals DFN-107; distal epiphysis of third metapodial DFN-57; first phalanges: DFN-46, 65, 89, 171; second phalanges: DFN-115, 181; third phalanx DFN-66.

Dafnero-3. Cranium DFN3-334; maxilla with P2-M3 sin/dex DFN3-121; part of muzzle with I1-I3 sin/dex DFN3-286; in situ dP2-dP4 sin DFN3-3, 283; fragment of maxilla with dP3-dP4, M1 dex DFN3-66; dP2 dex DFN3-249; dP3 dex DFN3-246; dP3,4 dex DFN3-289, 331; P3/4 dex DFN3-296; M1/2 sin DFN3-284; M3 dex DFN3-288; part of muzzle with di1-di3 sin/dex DFN3-326; fragment of mandibular ramus with dp2-dp4 sin DFN3-290, 292; fragment of mandibular ramus with di2-di3, dp2-dp4 dex DFN3-118; fragment of mandibular ramus with dp2-dp4 dex DFN3-99; fragment of mandibular ramus with dp4 dex DFN3-332; fragment of mandibular ramus with p2-m1 dex DFN3-287; in situ m2-m3 dex DFN3-147; p2 dex DFN3-15, 16; p3/4 dex DFN3-17, 18; proximal part of radioulna DFN3-222, 236; distal parts of humeri DFN3-253 (juv.?), 310; scaphoid DFN3-131; pisiform DFN3-311; third metacarpals: DFN3-73 (with accessories), 82, 83, 84 (with accessories), 93 (juv.?), 96, 137, 215, 240 (juv.) (with accessories), 268 (fragment), 293 (with accessories), 294, 306, 309 (with accessories), 320(with accessories); proximal parts of third metacarpals: DFN3-56, 74 (fragment, no measurements), 75 (with accessory) 76, 81, 90, 104 (fragment); distal parts of third metacarpals: DFN3-301a, distal parts of tibia DFN3-92, 95, 103 (epiphysis), 114, 124 (fragment), 243, 247 (juv.?), 262, 271 (fragment), 265 (epiphysis juvenile), 327 (fragment); astragali DFN3-54 (fragment), 58, 59, 61, 62 (fragment), 63, 140, 216, 217 (fragment), 218, 219, 220, 221, 232, 233 (fragment), 238, 242, 254 (fragment), 270, 303, 304, 305, 314, 316; fragmentary parts of astragali DFN3-244, 245; calcaneum DFN3-60, 65, 145 (fragment), 237 (fragment), 250 (fragment), 256, 315; distal part of calcaneum DFN3-275; navicular DFN3-144; third metatarsals: DFN3-68 (fragment), 85 (juv.?), 86, 87, 88, 89, 94, 97 (juv.?), 100, 139, 257, 259, 260, 261, 267, 269, 308 (with accessories), 318, 337, 338; proximal parts of third metatarsals

DFN3-55, 239, 258 (with accessories), 272 (fragment, no measurements), 276, 277; distal parts of third metatarsals DFN3-141, 339; distal parts of third metapodials DFN3-235, 266, 279, 329; first phalanges: DFN3-9 (fragment), 57, 134, 138 (fragment), 143, 227, 228, 229, 230 (fragment), 252, 248, 264, 307; proximal part of first phalanges: DFN3-317; distal parts of first phalanges: DFN3-11, 25 (juv.?), 231; second phalanges: DFN3-12, 30, 234 (fragment), 281 (fragment), 282 (fragment), 321, 323; third phalanges: DFN3-10 (juv.?, fragment),135, 223, 224 (fragment), 225, 226 (fragment), 231 (fragment with sesamoid), 263, 298, 299 (fragment), 319, 322 (fragment).

In articulation: distal part of humerus (b) + radioulna (a) dex DFN3-297; scaphoid + lunatum + pyramidal + pisiform + magnum + sesamoid + proximal part of third metacarpal with accessories dex DFN3-301; distal part of tibia (b) + astragalus (a) sin DFN3-142; distal part of tibia (a) + astragalus (b) dex DFN3-302; distal part of tibia (c) + astragalus (a) + calcaneum (b) dex DFN3-122; astragalus (a) + calcaneum (b) dex DFN3-313; astragalus (b) + calcaneum (a) + big cuneiform (d) + small cuneiform (e) + cuboid (d) + navicular (c) dex DFN3-136; fragment of astragalus + big cuneiform (d) + small cuneiform (e) + cuboid (d) + navicular (c) + proximal part of third metatarsal sin DFN3-328; distal part of tibia (b) + astragalus (c) + calcaneum (d) + big cuneiform (e) + cuboid (e) + navicular (e) + third metatarsal (a) sin DFN3-336; astragalus (b) + calcaneum (c) + big cuneiform (d) + fragment of small cuneiform + navicular (d) + third metatarsal (a) dex DFN3-330; navicular + third metatarsal with accessories (a) + first phalanx (b) + second phalanx (b) + fragment of third phalanx with sesamoid dex DFN3-312; first phalanx (a) + fragment of second phalanx (b): DFN3-274.

Sésklo. Fragments of crania with I1-I3, C, P2-M3 sin/dex ΣA-1, 3; fragment of cranium with C, P2-M3 sin/dex Se-2; fragment of cranium with P3-M3 sin/ dex ΣA-4; fragment of cranium with C sin, I2-I3 sin, I2-I3 dex, P2-M3 sin, P2-P4 dex Σ-203; fragment of maxilla with M3 sin Σ-71; part of maxilla with P2-M2 sin Σ-170; part of maxilla with P2-M3 sin Σ-194; part of maxilla with P4-M1 sin Σ-197; fragment of maxilla with P2 dex Σ-198; part of maxilla with P2-M3 dex Σ-199; part of maxilla with P2-M3 sin, P2-P4 dex Σ-203; part of maxilla with P2-P4 sin, P2-P4 dex Σ-383; fragment of maxilla with P3-M3 dex Σ-916; fragment of maxilla with M3 sin Σ-953; fragment of maxilla with P3-M1 dex Σ-1029; fragment of maxilla with M1-M2 sin Σ-1203; fragment of maxilla with P3-M3 sin S1220; part of mandibular ramus dex Σ-951; part of mandible with i1-i3, c, p2-m3 sin/dex Σ-1026; mandibular ramus with dp2 dex Σ-1226; humerus dex (without number); proximal parts of humeri sin: Σ-123, 1236, 1247; distal parts of

humeri sin: Σ-166, 210, 281, 315, 342; distal parts of humeri dex: Σ-209, Σ-211, Σ-265, Σ-666, Σ-667, Σ-668, Σ-1031, Σ-1235; parts of humerus, radius and ulna sin: Σ-99, 356; proximal parts of radius sin: Σ-352, 672, 1238, 1241; proximal part of radius dex: Σ-333, 671, 673, 1032; distal parts of radius sin: Σ-86, 373, 375, 376, 663, 665, 930; distal parts of radius dex: Σ-662, 664, 1240, 376; third metacarpal with accessories dex Σ-87; third metacarpal with McIV sin Σ-114; third metacarpals with McII sin: Σ-108, Σ-113; proximal parts of third metacarpals: Σ-36, 64, 69, 87, 125, 127, 128, 137, 138, 140, 142, 143, 147, 206, 309, 310, 329, 336, 409, 551, 578, 579, 588, 964, 1253, 1254, 1255); distal part of third metacarpals: Σ-106, 117, 118, 119, 120, 121, 122, 123, 124, 130, 134, 164, 165, 205, 303, 307, 311, 317, 583, 584, 585, 1219); first anterior phalanges: Σ-88, 1003, 1005, 353, 624); distal parts of anterior phalanx Σ-622; second phalanges: Σ-89, 204; third phalanges Σ-604, 634; proximal parts of femur: Σ-231, Σ-351; distal parts of femur: Σ-212, 374, 705, 1246); proximal parts of tibiae: Σ-234, 1244, 2016; distal parts of tibiae: Σ-52, 61, 223, 237, 264, 282, 316, 332, 334, 348, 349, 360, 361, 362, 378, 381, 606, 650, 651, 652, 653, 654, 655, 656, 657, 658; 659, 660, 661, 1250, 2012); astragali: Σ-188, 226, 227, 228, 238, 250, 284, 301, 312, 323, 609, 611, 612, 615, 613, 614, 634, 1030, 1034); calcanei: Σ-57, 193, 215, 239, 294, 377, 504, 505, 600, 610, 617, 616, 635, 1046); third metatarsal with accessories sin Σ-109; third metatarsals: Σ-112, 126, 177, 192, 202; proximal parts of third metatarsals with accessories: (Σ-47, 149, 144, 160, 244); proximal parts of third metatarsals: Σ-65, 141, 150, 151, 218, 225, 267, 283, 314, 352, 353, 571, 577, 1252); distal parts of third metatarsals: Σ-105, 116, 129, 135, 136, 187, 201, 308, 581, 582, 586, 587, 982, 983, 1257, 1045, 1218, 1256); first posterior phalanges: Σ-602, 1042; proximal parts of first posterior phalanges: Σ-605, 980, 1043, 1044, 1262, 1266, 1280); second phalanges Σ-295, 603; third phalanges: Σ-186, 318, 321, 340, 341, 623, 978, 982, 1263.

In articulation: second and third phalanges Σ-180, 979; distal part of tibia + astragalus sin Σ-18 (juv.); distal part of tibia + astragalus + calcaneum dex Σ-345 (juv.); distal part of tibia + astragalus + calcaneum + navicular + cuboid + cuneiform medial + cuneiform lateral + third metatarsal with accessories dex Σ-363; distal part of tibia + astragalus + calcaneum + navicular + cuboid + cuneiform medial + cuneiform lateral sin Σ-1251; astragalus + calcaneum + navicular + cuboid + cuneiform medial + cuneiform lateral + proximal part of third metatarsal with accessories sin Σ-22; navicular + cuboid + cuneiform medial + cuneiform lateral + third metatarsal with accessories dex Σ-107, 115; astragalus + calcaneum + navicular + cuboid + cuneiform medial + cuneiform

lateral dex Σ-625; astragalus + calcaneum: Σ-502, 601, 608; distal part of third metatarsal + first phalanx + second phalanx + third phalanx sin Σ-157; distal part of third metatarsal + first phalanx + second phalanx dex Σ-981.

Volax. Maxilla with P2-M3 sin/dex VOL-203; in situ P2 dex VOL-209; P3/4 VOL-207; M3 sin VOL-208; mandible with i1-i3, c (sin), p2-m3 sin/dex VOL-202; distal parts of humerus: VOL-172, 173 (fragment), 174, 175, 177; radius VOL-170; proximal parts of radius: VOL-167, 168 (+fragmentary ulna); distal part of radius VOL-169; third metacarpals: VOL-152 (fragment), 153 (fragment), 155; distal part of third metacarpal VOL-156 juv.?; astragali: VOL-196 (fragment), 197; proximal part of tibia VOL-163; body of tibia VOL-162; distal parts of tibiae: VOL-160, 161, 164, 166 (juv.); first phalanges: VOL-181, 182 (juv. fragment), 183, 185 (fragment); second phalanges: VOL-186, 187; third phalanges: VOL-188, 189, 190 (fragment), 191.

Krimni-1. in situ P3-M3 dex KRI-21; in situ P4-M1 (fragment) KRI-43.

Description.

The majority of *E. stenonis* remains come from Dafnero and Sésklo and they were originally described earlier by Koufos and Kostopoulos (1993) and Athanassiou (1996, 2001) respectively. Both localities have yielded crania with the best-preserved cranium coming from DFN3 site. All the DFN3 and some of the SES material is unpublished; the new crania from Sésklo were unofficially labelled by the present author [ΣA-X (number of specimen)]. The crania from Sésklo are either deformed or extremely damaged.

Cranial remains.

DFN3-334. The cranium is almost complete and well-preserved despite a slight dorsoventral deformation; it lacks the narial notch, the occiput and the right zygomatic (Figure 5.1a-b). It belongs to an adult horse and bears small canines (only the left one is preserved) indicative of a female individual. All cheek teeth are in wear and the Galvayne's groove is halfway down on I3 giving an average individual age of 15 years old. The cranium is long and not high. The nasal bones are missing and the depth of the narial notch cannot be counted. The muzzle is long typical of *E. stenonis*. The index 'Breadth of the muzzle x 100 / Length of the muzzle' (M15 x 100 / M1) is 50.4. The palate is rather long and relatively narrow and the mean palatal breadth at the limit between P4 and M1 is 74.97 mm (M13). The choanae are oval-shaped and its anterior margin is situated at the limit between M2 and M3. The major palatine foramen is

placed at the middle of M3. The medial border of the retroarticular process is almost straight. The orbits are more or less elliptical, and they are situated well behind the third molar. The facial crest is well-developed, and its anterior margin is placed above the limit between P4-M1. No preorbital fossa can be observed with certainty due to the deformation of the cranium. The infraorbital foramen is not preserved. The retroarticular process is relatively long and it outreaches the articular surface of the fossa mandibularis. On the dorsal view, the suture of the nasal bones forms a groove along their sagittal plane. The greatest breadth of the cranium is calculated behind the orbits. The zygomatic process is strong and significant broad, and the supraorbital foramen is rather short and elliptical.

On occlusal view, P1 is present on the right toothrow. It is short, without reaching the occlusal level of P2 and it has a triangular shape. The anterostyle on P2 is relatively long and rounded. Protocone is relatively short except for M3 where it is more elongated. The lingual border of the protocone is almost straight on P2 and M1 and slightly concave on the other cheek teeth. Pli caballin is single, short, and always present on all cheek teeth. All fossettes are closed. The plication of the fossettes is rudimentary to simple: on all cheek teeth the plications are short and only a few (one or two plications) with an exception on the 'plis prefossette and plis protoconule' of P2 and M3 where it is simple (five or six plications). Hypoconal constriction is strong on M3; on all the other cheek teeth it is either absent or rudimentary. No hypoconal islet is formed on M3.

DFN-112. The cranium was described and figured earlier by Koufos and Kostopoulos (1993). It is laterally compressed. The muzzle, the palate, the left cheek, orbit and zygomatic and the braincase are missing. P2-M3 dex is preserved (Figure 5.1c-d). On lateral view, the narial notch is deep and its hind margin is caudally situated above the middle of P3. The distance between the hinder margin of the narial notch and the posterior point of the orbit is ~160 mm. The facial crest is well-developed, but it is not very strong, and its anterior margin is placed above the anterior half of M1. The (right) orbit is elliptical and it is situated well behind the third molar. A short and shallow preorbital fossa is observed in front of the orbit; however, its margins are not clear. The distance between the hind margin of the fossa and the anterior border of the orbit is ~31.6 mm. The infraorbital foramen is large, and it is situated above the level of the mesostyle of M1.

In occlusal view, the major palatine foramen is possibly located at the middle of M3.

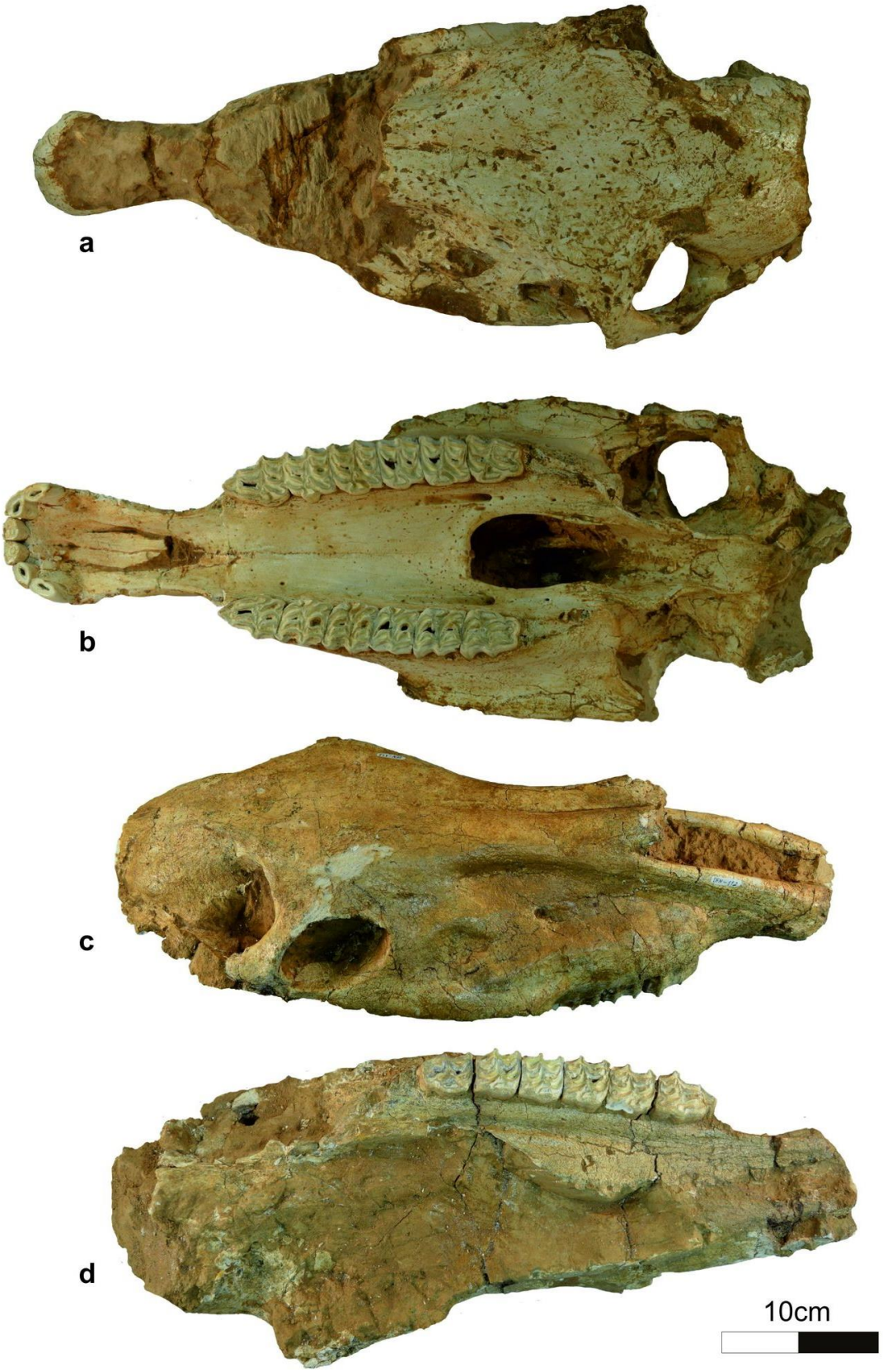

Figure 5.1. Crania of *Equus stenonis*. DFN3-334: (a) dorsal view, (b) ventral view; DFN-112: (c) dorsal view, (d) ventral view.

The protocone is always short on the cheek teeth except for M3 where it is more elongated. The shape of the protocone is squarish on P2 and P3 and its lingual border is straight. On P4-M2, it is semilunar-shaped, while its lingual border is concave at the middle of the protocone. On M3, protocone is elliptical and its lingual border is straight. The postprotoconal groove is shallow on all cheek teeth. On P2, the parastyle is wide and round while the mesostyle is notched. On the other teeth, it is more or less rounded. The hypocone is elliptical and the hypoconal groove is pointed and relatively wide; on P3, the hypoconal groove is isolated as an islet. Pli caballin is always present and it is short. All fossettes on all cheek teeth are isolated and closed and their lateral borders are poorly plicated.

Σ-246. The cranium has already been described by Athanassiou (1998, 2001). It preserves parts of the forehead, nasal bones, zygomatics and occiput and it is deformed. Unfortunately, only a few anatomical characters can be observed, such the posterior margin of the narial opening and the distance between that and the anterior border of the orbit.

Σ-203. The cranium has already been described by Athanassiou (1998, 2001). Only a part of the maxilla and muzzle are preserved. The cranium belongs to an old individual (incisors and all cheek teeth are extremely worn) possibly female based on the size of the preserved left canine. The muzzle is relatively long. The index 'Breadth of the muzzle x 100/ Length of the muzzle' (M15 x 100 / M1) is 46.4. The palate is rather long and relatively narrow and the mean palatal breadth at the limit between P4 and M1 is 84.1 mm (M13).

Σ-203 preserves the lateral incisors which are fragmentary, the left series P2-M3 and right P2-P4. The protocone is short and the postprotoconal groove is shallow. The inner fossettes are worn. On M3, the hypoconal constriction is apparent and an islet is formed on the hypocone.

SE-2. The cranium is fairly preserved in relation to the other crania from Sésklo; it lacks the narial frontal bones, the occiput, a part of the left zygomatic and it is laterally compressed (Figure 5.2). The cranium belongs to a male adult equid; cheek teeth and canines are in full wear. The narial notch is deep, situated above the mesostyle of P3. The nasal bones form a small groove between them. The muzzle is relatively long. The index 'Breadth of the muzzle x 100/ Length of the muzzle' (M15 x 100 / M1) is 47. The palate is rather long and the mean palatal breadth at the limit between P4 and M1 is more than 77 mm (M13). The choanae are relatively large and elliptical and their

anterior border is situated at the anterior border of M3. The facial crest is well-developed, and its anterior border is situated at the P4/M1 contact.

Se-2 preserves both canines, and all cheek teeth while all incisors are missing (Figure 5.2b). Both P1 are missing, but their alveoli verify their presence. The anterostyle on P2 is wide and relatively elongated. The protocone is triangular-shaped or elliptical-shaped on all cheek teeth; the lingual border of the protocone is straight and the post-protoconal groove is rather deep on P3 and P4. The hypoconal groove is pointed and relatively deep and, in some cases, the hypocone is isolated as an islet (P3 sin, P4 and M3). The inner fossettes are simply plicated and pli caballin is either rudimentary or single.

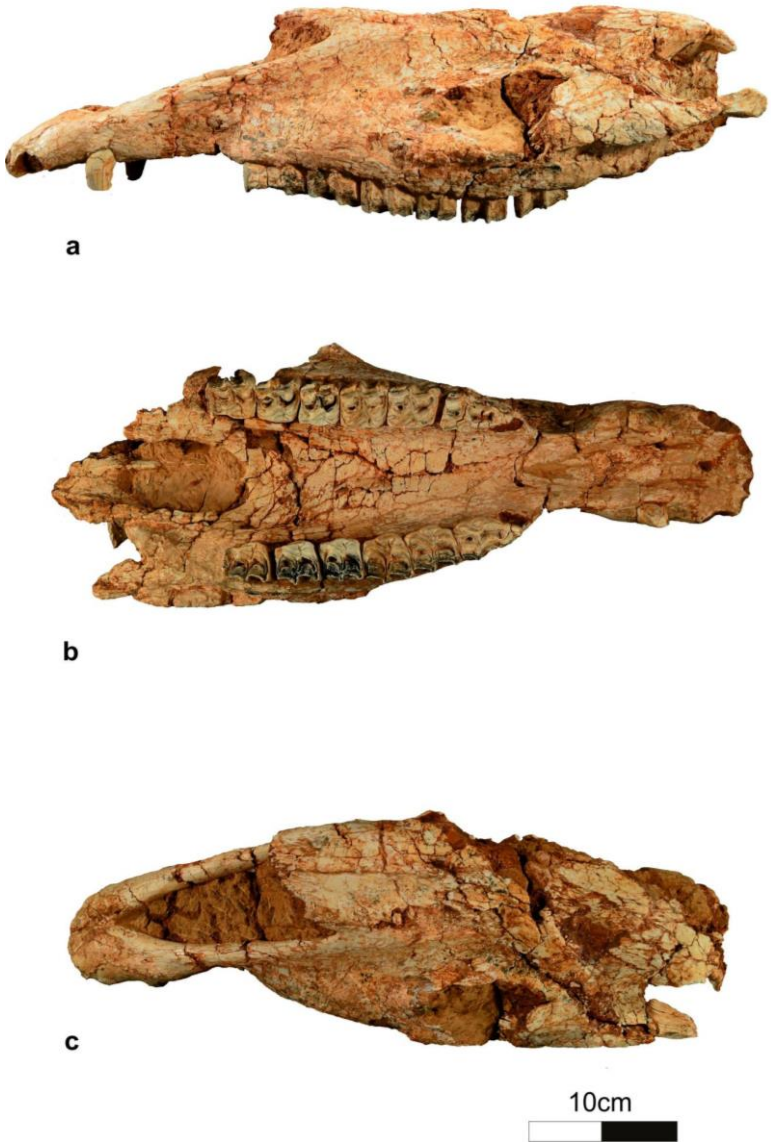

Figure 5.2. *Equus stenonis*. SE-2. (a) Left lateral view, (b) ventral view, (c) dorsal view.

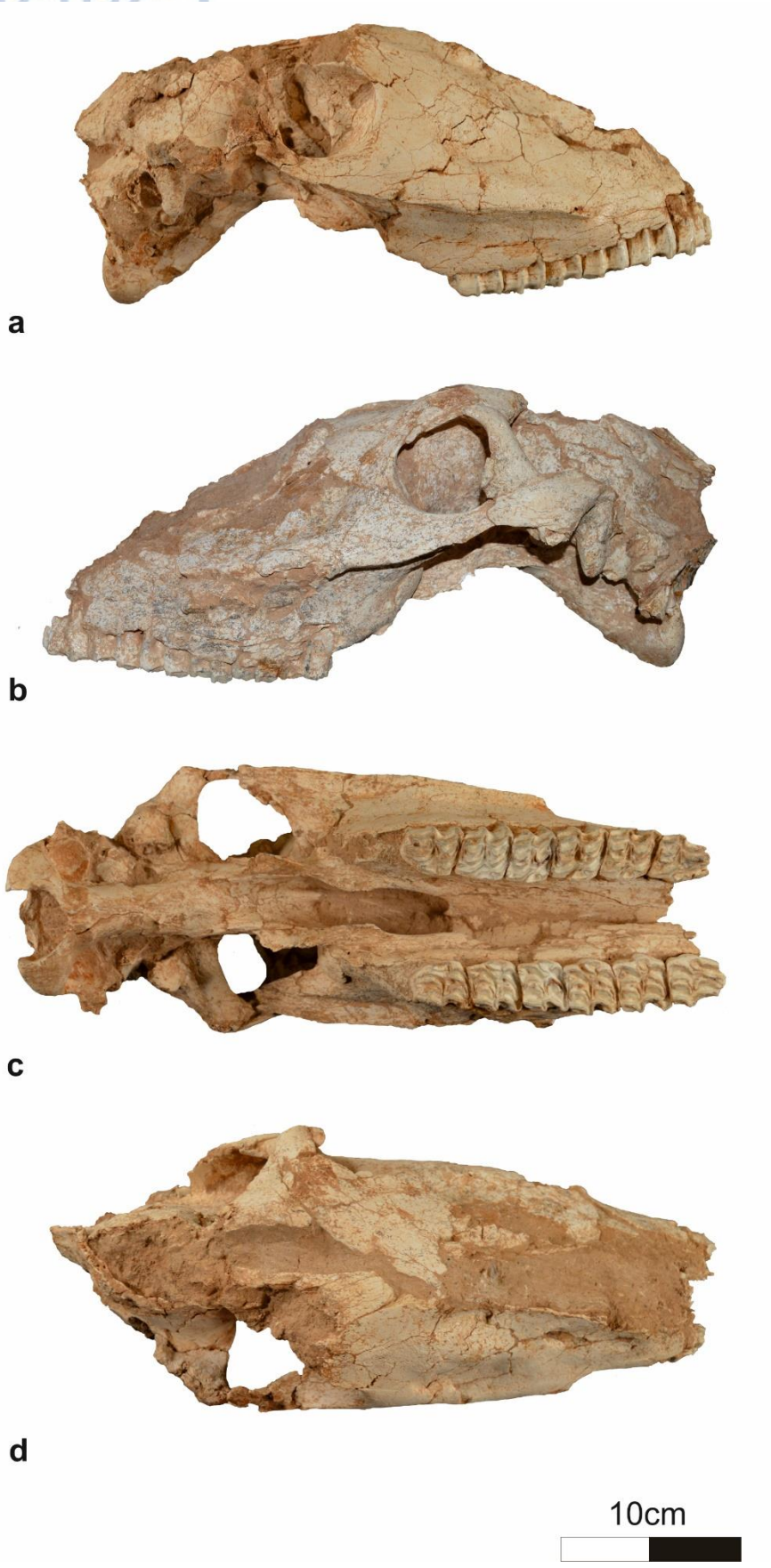

Figure 5.3. *Equus stenonis*. ΣΑ-1. (a) Right lateral view, (b) left lateral view (c) ventral view, (d) dorsal view.

ΣΑ-1. The cranium lacks the muzzle, the nasal bones, a part of the right zygomatic and occiput and it is laterally compressed (Figure 5.3). It belongs to an adult individual (M3 in full wear). The anterior border of the choanae is situated at the posterior half of M2. The major palatine foramen is located at M2M3 contact. The upper profile of the skull seems wavy. The facial crest is well-developed, strong, and slightly wavy on profile view, and its anterior border is above the posterior half of P4. The retroarticular processes are strong, laterally outreaching the level of the articular surface of the mandibular fossa (Figure 5.3a-b). On the right side, there is an elliptical-shaped preorbital fossa.

ΣΑ-1 preserves all cheek teeth (Figure 5.3). The anterostyles on P2 are not preserved. The protocone is short and semilunar or elliptical-shaped and its lingual border is straight or slightly convex. The post-protoconal groove is rather shallow on all cheek teeth. The hypoconal groove is short and, in some cases, the hypocone is isolated as an islet (P3, P4). The fossettes are simply plicated and pli caballin is single and short.

ΣΑ-3. The cranium is moderately preserved, and it lacks the frontal nasal bones and most of the part behind the last molars (Figure 5.4). The cranium belongs to a male adult equid; all teeth are in full wear. The narial opening is deep and the narial notch is situated above the mesostyle of P3. The muzzle is relatively long. The index 'Breadth of the muzzle x 100/ Length of the muzzle' (M15 x 100 / M1) is 50.6. The palate is rather long and the mean palatal breadth at the limit between P4 and M1 is 80.82 mm (M13). The choanae are elliptical and their anterior border is situated at the anterior border of M3. The facial crest is well-developed, and its anterior border is situated at the P4/M1 contact.

The dentition is completely preserved on both sides of ΣΑ-3 (Figure 5.4b), while both P1 are present and elliptical-shaped. The anterostyle on P2 is wide and elongated. The protocone is semilunar-shaped or elliptical-shaped on all cheek teeth; its lingual border is straight or slightly convex and the post-protoconal groove is rather deeper on premolars than on molars. The hypoconal groove is short and, in some cases, the hypocone is isolated as an islet (P3, P4 dex and M3). The inner fossettes are simply plicated and pli caballin is either rudimentary or single and short.

ΣΑ-4. The cranium lacks the muzzle, a part of nasal bones and both P2 and it is laterally compressed (Figure 5.5). It belongs to an adult (or young adult) individual (M3 in wear). The choanae are compressed, but their anterior border seems to be situated at the anterior border of M3. The facial crest is well-developed, and its anterior border is

situated at the P4/M1 contact. The orbit is placed far behind M3. No preorbital fossa can be observed. The zygomatic process of the frontal bone is strong and relatively broad. The nasal bones form a smooth groove along their sagittal suture (dorsal view). ΣΑ-4 preserves P3-M3 teeth rows; however, the left series are poorly preserved (Figure 5.5a). The protocone is short and semilunar-shaped or elliptical-shaped; its lingual border is straight or slightly concave. The post-protoconal groove is rather deep on all cheek teeth. The hypoconal groove is pointed and deep. The inner fossettes are moderately plicated and the pli caballin is single.

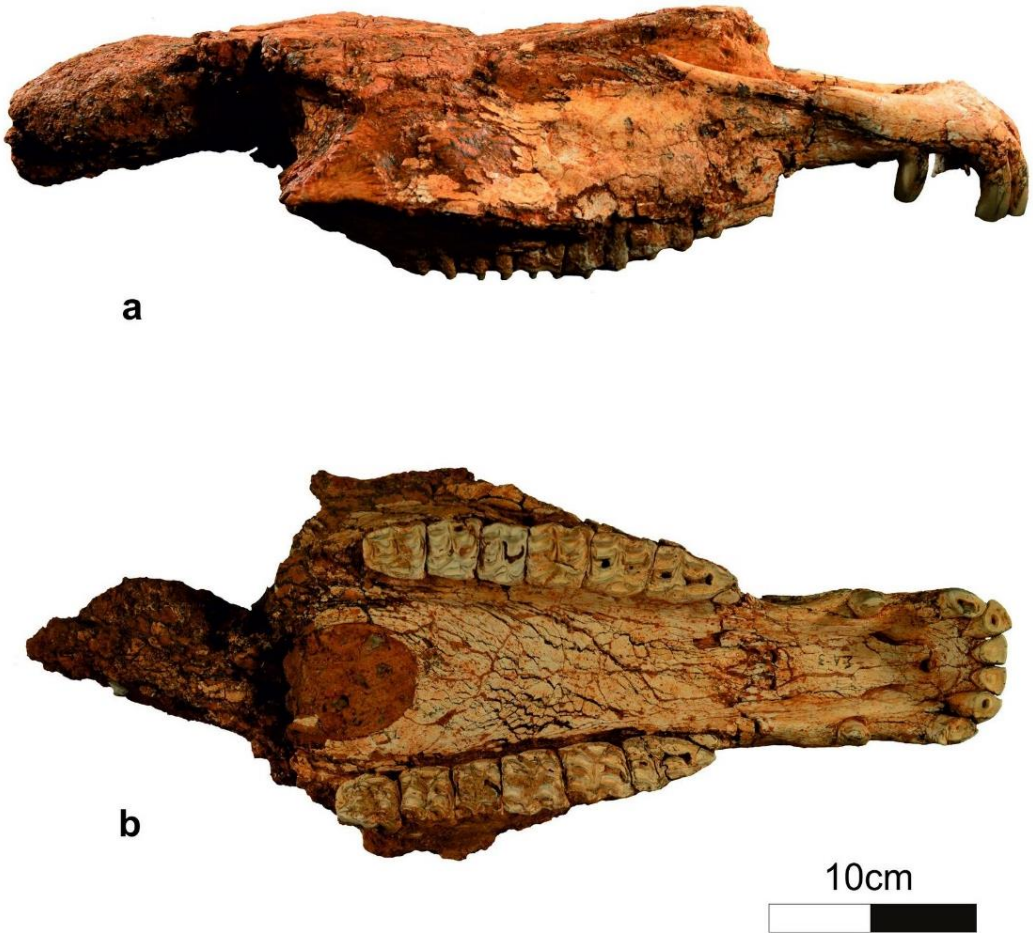

Figure 5.4. *Equus stenonis*. ΣΑ-3. (a) Right lateral view, (b) ventral view

Mandible. There is a moderately preserved mandible (Σ-1026) from Sésklo described by Athanassiou (1996, 2001), but the rami are missing (Figure 5.5a-b). It belongs to an old male individual; incisors, canines and cheek teeth are very worn. The diastema is relatively long. The morphology of the cheek teeth is typically stenonine with a V-

shaped linguaflexid. The ectoflexid does not penetrate the isthmus on molars. Most of the mandibular remains from Dafnero sites belong to juveniles with deciduous dentition. However, based on some fragments (DFN-62, 182), the cheek teeth morphology is stenonine (V-shaped linguaflexid). The ectoflexid is moderately deep on molars, penetrating in some cases the isthmus. VOL-202 from Volax is also missing both rami (described by Koufos and Vlachou 1997). It belongs to a male adult equid. The diastema is long, and the vascular notch is apparent (Figure 5.5c-d). The morphology of the cheek teeth resembles DFN and SES equids. There is an angle forming at the junction of the interalveolar border with the border of p2, in a way that the junction forms an angle of almost 90 degrees.

Upper cheek teeth. The studied material consists of many toothrows and isolated teeth coming mostly from Sésklo and Dafnero sites. The length of the upper tooth row (M9) from Volax is 185.6 (n=1), while for Sésklo it ranges from 175.1-206.4 mm (mean=190.1 mm; n=9) and for Dafnero from 186.5-193.5 mm (mean=189.5 mm; n=4). The ratio molar length (M8)/premolar length (M7) % on average is 82.8, 85.3 and 84.9 for Sésklo, Dafnero and Volax respectively. The anterostyle on P2 is relatively short and wide. The parastyle is wider than the mesostyle and it is projected labially. The mesostyle is narrow especially on molars. Neither of them is not notched expect for the mesostyle of P2 on the cranium DFN-112. The fossettes are closed except for the slightly worn teeth. The enamel of their lateral borders is simply to moderately plicated and it depends on the stage of wear; on the little worn teeth the plication is more intense. A pli caballin is always present, well-developed, and single on the little to moderately worn teeth (stages of wear 1-3), while it is absent or rudimentary on the worn ones. The length of the pli caballin reduces by the stage of wear. The number of plications is given in Table S11 (Appendix 1). The protocone is mainly short (on M3 is more elongated), triangular to semilunar on premolars and more elliptical on molars (Figures 5.1b, 5.1d, 5.2b, 5.3c, 5.4b). Its lingual border is either straight (Figure 5.1b), or slightly convex or slightly concave (Figure 5.1d). The postprotoconal groove is relatively shallow; on the little worn teeth is deep (ΣΑ-3; Figure 5.4b). The hypocone is elliptical shaped, the hypoconal groove is either rounded or pointed and reduces by wear. In some cases, hypocone is isolated and forms an islet usually on the P3, P4 and M3; on the same individual it can be observed on the one series and not on the other (P3 sin, Figure 5.1b). The hypoconal constriction can be observed either none, weak or strong depending on the stage of wear and the kind of tooth.

Figure 5.5. *Equus stenonis*. ΣΑ-4. (a) Ventral view, (b) left lateral view (c) dorsal view.

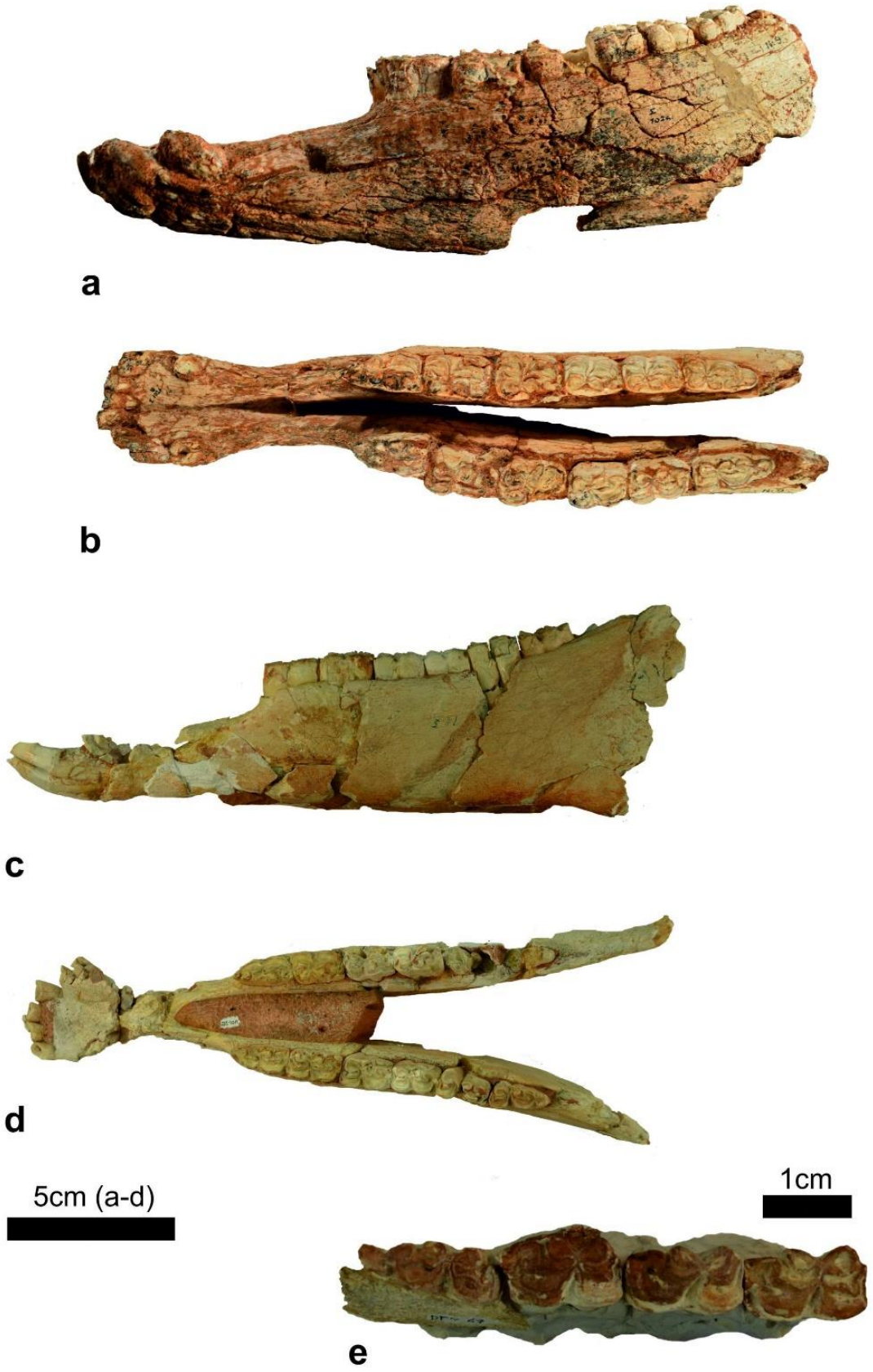

Figure 5.6. Fragments of mandibles of *Equus stenonis*. Σ-1026: (a) Left lateral view, (b) ventral view; VOL-202: (c) left lateral view, (c) ventral view; DFN-67: (e) ventral view.

Lower cheek teeth. Most of the studied material comes here from Sésklo and Dafnero, even though most of the specimens from the latter locality belong to juveniles. The length of the lower tooth row (M5) is 190.2 (n=1) for Volax and 191.7 (n=1) for Sésklo, while for Dafnero it ranges between 175-183 mm (mean=179 mm; n=2). The linguaflexid is typically stenonine with a V-shaped morphology (Figures 5.6b, d, e). The metaconid is relatively wide, rounded, and cyclic or more elliptical-shaped. The metastylid is slightly smaller than metaconid and its lingual posterior border tends to be more pointed on premolars than on molars. The entoconid is squarish on premolars, while on molars is more elliptical. The ectoflexid is not very deep; it reaches the mesio-lingual corner of the postflexid without, however, penetrating the isthmus (Figure 5.6b). Only on the third molars of the toothrows DFN-67, the ectoflexid penetrates the isthmus (Figure 5.6e). Pli caballinid is either absent, rudimentary, or single; on the same series (Figure 5.6b), pli caballinid is well-developed on the premolars, while it is absent or rudimentary on molars. The enamel of the postflexid is not plicated. Protostylids are not observed.

Third metacarpals. The third metacarpals from Dafnero sites are slightly shorter than the ones from Sésklo and Volax. The morphology of the articular surfaces for the lateral metacarpals is variable. The slenderness index (SI 2), distal maximal articular breadth (M11)/maximal length (M1) % ranges from 20.9–21.6 (n = 4; mean = 21.4) and 19.4–21.9 (n = 9; mean = 21.1) for Dafnero-1 and Dafnero-3 respectively, from 19.4–21.3 (n = 4; mean = 20.6) for Sésklo and from 20.1–20.5 (n = 2; mean = 20.3) for Volax. The keel index varies between 125.1–128.9 (n = 4; mean = 126.6) and 124.0–137.0 (n = 10; mean = 131.1) for Dafnero-1 and Dafnero-3 respectively, for Sésklo between 127.9–131.6 (n = 4; mean = 130.3) and for Volax between 127.3–129.9 (n = 3; mean = 128.3).

Third metatarsals. The third metatarsals from Dafnero sites are also slightly shorter than the ones from Sésklo and Volax. The slenderness index (SI 2), distal maximal articular breadth (M11)/maximal length (M1) % ranges from 18.0–19.1 (n = 8; mean = 18.4) and 15.8–18.8 (n = 17; mean = 18.0) for Dafnero-1 and Dafnero-3 respectively, from 16.2–17.5 (n = 7; mean = 17.1) for Sésklo and from 16.7–17.2 (n = 2; mean = 17.0) for Volax. The keel index varies between 130.6–142.3 (n = 7; mean = 135.4) and 129.0–144.4 (n = 15; mean = 136.7) for Dafnero-1 and Dafnero-3 respectively, for Sésklo between 131.2–138.7 (n = 9; mean = 136.0) and for Volax between 128.9–137.9 (n = 3; mean = 132.4).

Comparison and discussion.

The morphological and morphometric analyses show that the equids from Dafnero, Sésklo and Volax belong to a large stenonoid *Equus*. The cranial morphology and morphometry exhibit typical characters of *E. stenonis* [generally long snout, deep nasal notch etc. as described earlier by several authors Prat (1964, 1980); Azzaroli (1965, 1982); De Giuli (1972); Boeuf (1986); Forstén (1986); Alberdi et al. (1991); Caloi (1997) among others and Cirilli et al.' s (2021) emended diagnosis] and thus can safely attributed to this species. The cranial morphometric comparisons of the Greek *E. stenonis* with subspecies of the European *E. stenonis* and other Pleistocene and extant equids are shown in Figures 5.7 and 5.8 respectively. Although most of the crania from Sésklo and Dafnero are poorly or relatively preserved, they clearly belong to *Equus stenonis*. The morphological characters of the DFN and DFN3 crania are in general similar to *E. stenonis*; they are long (M6; >520mm without the braincase on DFN3-334), the cheek teeth are stenonine, but none of them is completely preserved. The narial opening from the cranium DFN-112 from Dafnero-1 is extending above the third molar (Figure 5.1c), a diagnostic feature of *E. stenonis*, while it is not preserved on the DFN3-334. On DFN-112, a preorbital fossa is observed (Figure 5.1c), but it is shallower than the one in the holotype of *E. stenonis* (IGF560) from Upper Valdarno. The type cranium of *E. stenonis guthi* (CH3-1978-CS-5760), although it is partially preserved, displays a deep preorbital fossa like the specimen IGF560. In lateral view, the morphology (facial crest, orbit and stenonoid cheek teeth morphology) and the length of the cheek teeth row resemble both crania from the Dafnero sites. Eisenmann (2017; fig. 1) separates stenonoid (*Allohippus*) equids based on their muzzle length; the typical *E. stenonis* and *E. stenonis vireti* have long muzzles, while *E. stenonis pueblensis* has shorter muzzle. The crania of *E. stenonis pueblensis*, PUE 3280 and PUE 3279 (Eisenmann 1980; pl. X) exhibit short muzzles therefore resembling DFN3-334. The groove of the nasal bones that is formed along the sagittal plane and the development of the facial crest are typical of *E. stenonis* (Azzaroli 1968; De Giuli 1972). The morphology and dimensions of the crania from Sésklo (Figures 5.2-5.5) suggest a large sized *Equus* that shares great similarities (deep narial opening, long snout, stenonoid pattern teeth etc.) to *E. stenonis* and they are close to the size from Saint-Vallier (*E. stenonis vireti*), and La Puebla de Valverde (*E. stenonis pueblensis*) as mentioned earlier by Athanassiou (2001). In all cranial elements from Sésklo, the muzzle is long like the typical *E. stenonis* and *E. stenonis vireti*. The fragmentary maxilla from Volax

also resembles *E. stenonis* in size and in the pattern of the cheek teeth. The different cranial variations on the length of the muzzles in the Greek sample could be a result to (local) climatic adaptations (Allen's law accounting for short muzzles in Eisenmann et al. 1985) that leads to more or less speciations.

In the Figure 5.8, the crania of *E. stenonis* from Greece are being compared to other European Pleistocene equids. The length of the muzzle (M1) of *E. stenonis* from Dafnero is shorter than the one from Sésklo; the latter resembles in size *E. stenonis vireti* and *E. stenonis olivolanus* (plots between them). The palatal length (M2) is similar between *E. stenonis* from Dafnero and *E. stenonis vireti*. The length of the premolar and molar toothrows and their proportions are similar between Dafnero and Sésklo close to E. *s. vireti*, and longer than *E. s. guthi*. *E. s. olivolanus* displays similar analogies, slightly smaller in size and *E. s. guthi* holotype has shorter molar toothrow. The ratio of the length naso-incisival notch (M30) and cheek length (M31) are similar between *E. s. vireti* and *E. s. olivolanus*. The cheek length is relatively shorter than *E. apolloniensis* in relation to the naso-incisival notch. The proportions between the minimal muzzle breadth (M14) and maximal muzzle breadth (M15) on the crania from Sésklo are slightly smaller yet similar to *E. s. vireti* from Saint-Vallier. The orbit of *E. stenonis* from Dafnero (Figures 5.7) shows shorter dimensions (M29) than all the other equids, but that can be due to the deformation of the cranium. As it seems in Figure 5.8, all *E. stenonis* crania (subspecies/populations) are quite larger in overall dimensions than the ones of '*E. stenonis mygdoniensis*' from Gerakarou; the latter is well separated due to its moderate size, quite shorter cranium (M6) and slenderer muzzle.

Figure 5.9 presents the bivariate analysis between the length of the P2-P4 (M7) versus the length M1-M3 (M8) of the various living and extinct equids. *E. stenonis* from Dafnero, Volax and Sésklo plot within the range of *E. stenonis vireti* and *E. stenonis olivolanus*. Two specimens from Sésklo, belonging to the same individual (SE-2), exhibit longer tooth rows and they plot within the range of *E. eisenmannae*. This however is explained due to the distortion of the cranium SE-2. Here too, '*E. stenonis mygdoniensis*' is well separated from *E. stenonis* subspecies/populations and it is included within the variability of *E. senezensis* and *E. altidens* from Dmanisi.

The mandibles of *E. stenonis* subspecies/populations are large in size. The vascular notch is strong on 20.163362A and less apparent on 20.163361A (both specimens from Saint-Vallier), while on the holotype of *E. stenonis*, IGF560 the notch is relatively shallow but perceptible (Cirilli et al. 2021: Fig. 5).

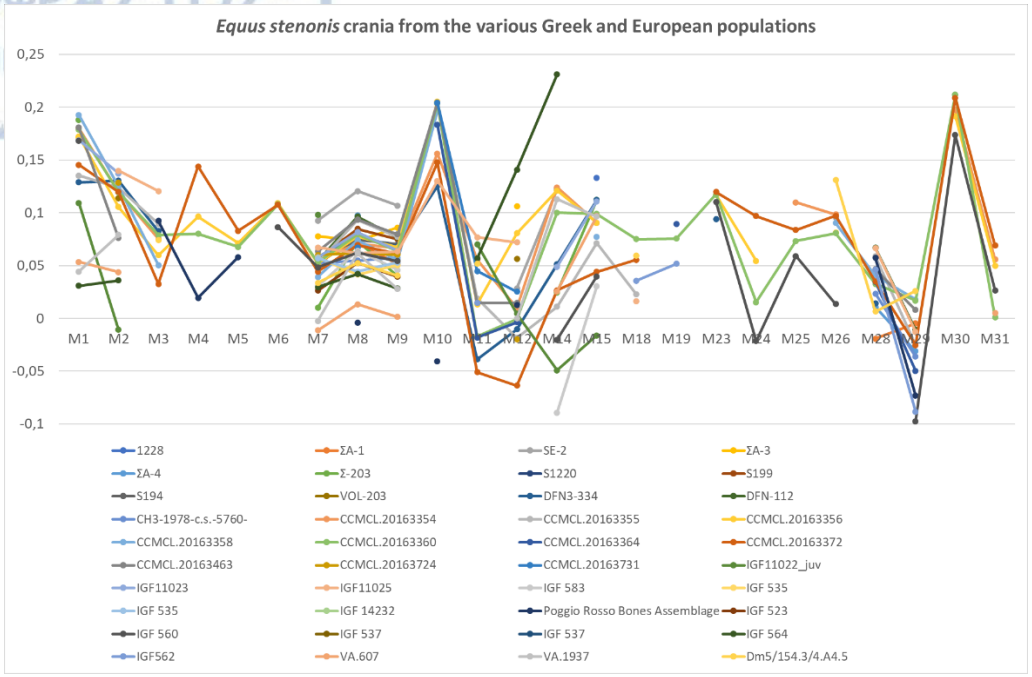

Figure 5.7. Simpson's log ratio diagrams comparing the cranial dimensions of *E. stenonis* from Greece (ΣA, S, SE, VOL, SES, DFN/DNF3), Saint Vallier (CCMCL), Upper Valdarno (VA, IGF), Dmanisi (DM) and Chilhac (CH3). Standard: *Equus hemionus onager*. Data from Bernor et al. (2021) and personal dataset.

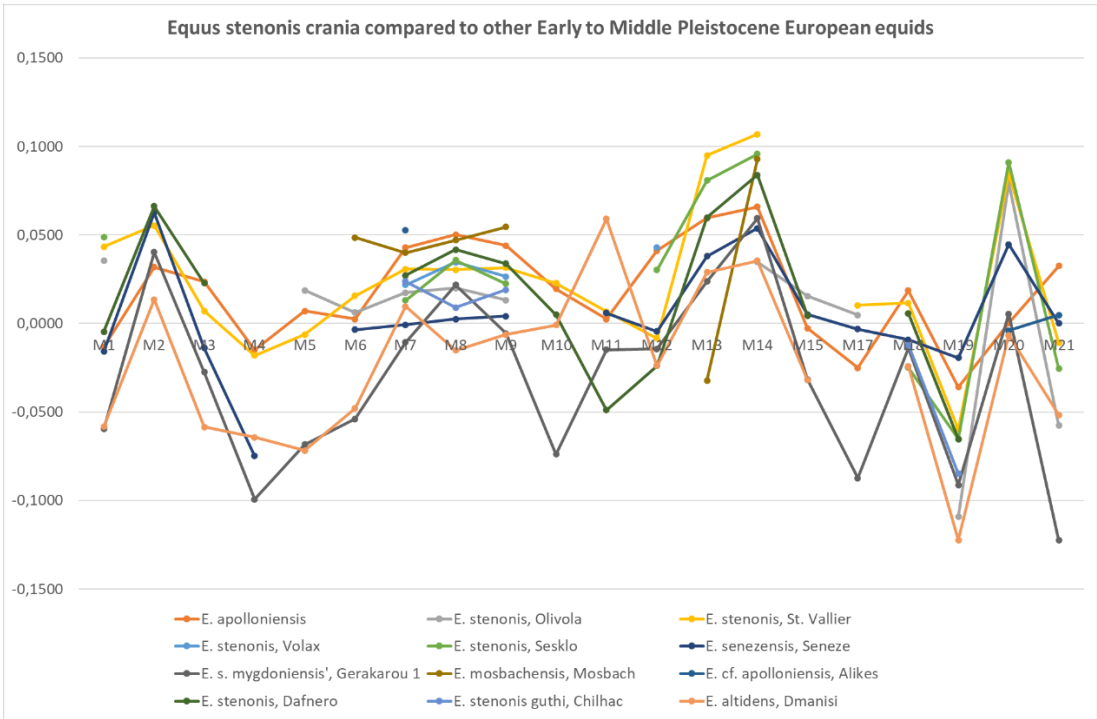

Figure 5.8. Simpson's log ratio diagrams comparing the average cranial dimensions of *E. stenonis* from Dafnero, Volax and Sésklo with several Early Pleistocene equids from Europe. Standard: *Equus grevyi*. Data from Bernor et al. (2021), Eisenmann (2008a, b, 2017) and personal dataset. Additional data for *E. senezensis* from Eisenmann (2017).

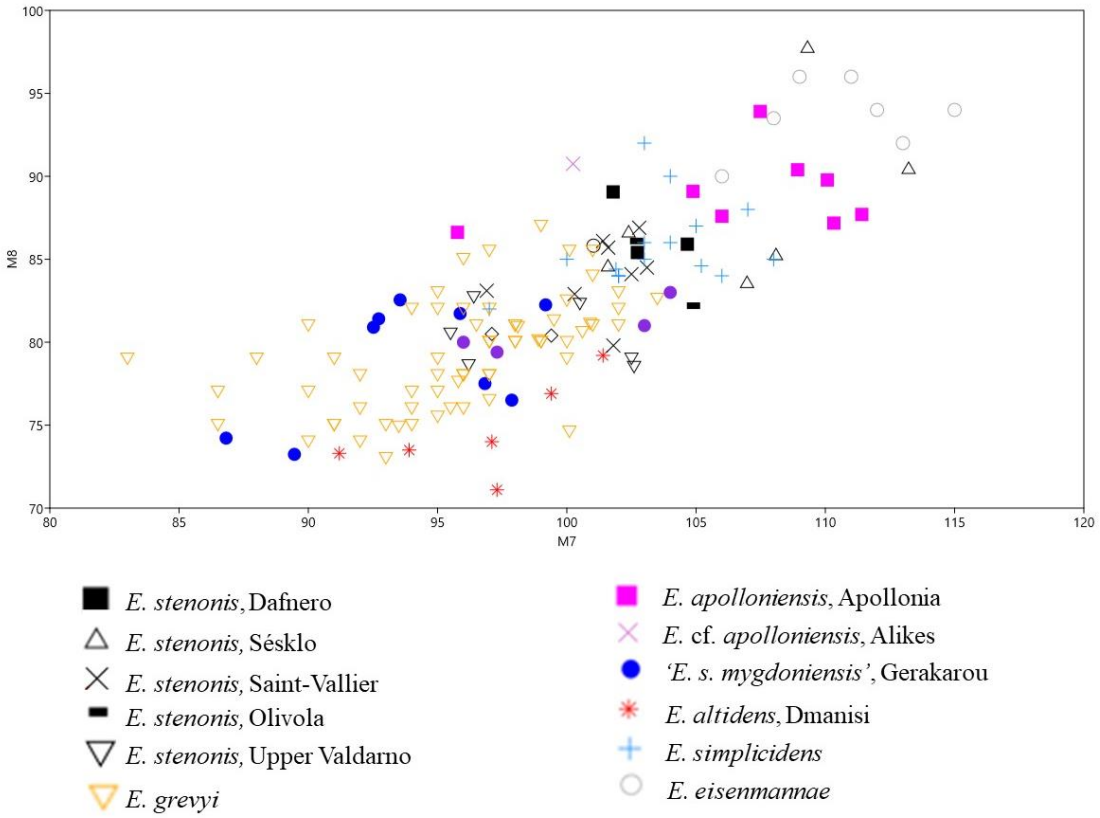

Figure 5.9. Bivariate plots comparing upper premolar (M7) and molar (M8) tooth rows length of the various *Equus stenonis* subspecies/populations (black), *Equus altidens* (red), *E. apolloniensis* (pink) and other Early Pleistocene and extant equids. Data from Alberdi and Piñero (2012), Piñero and Alberdi (2015), Bernor et al. (2021), Eisenmann (2017) and personal dataset. Also, additional data from Cirilli et al. (2021) and Cirilli (2022a).

Unfortunately, there is no complete mandible of *E. stenonis* in the Greek sample. Almost all the specimens from Dafnero belong to juveniles or juvenile adults and they are fragmentary. Comparing the mandible VOL-202 from Volakas to other known specimens of *E. stenonis* (Figure 5.10), it seems to have rather shorter snout (M2, M13) compared to *E. stenonis vireti*. The snout in Σ-1026 is more robust (lower values in M2, M13 in relation to higher values in M14) compared to *E. stenonis vireti* resembling IGF11024 from Olivola. VOL-202 appears to have slenderer snout (M14) than Σ-1026, although possibly due to the deformation. The length of the cheek toothrows (M3, M4, M5) of the Greek specimens resembles *E. stenonis vireti* (Figures 5.10). The ratio of the premolar/molar tooth row length is variable. On IGF538 and CCMCL 20.163362(a, b) the molar tooth row length is greater than the premolar tooth row length vice versa on *E. stenonis guthi*. This could be explained as the result of different wear stages within

a single species/subspecies. Figure 5.11 plots the length of p2-p4 versus the length of m1-m3 of *E. stenonis* and other Pleistocene European equids. The *E. stenonis* subspecies/populations plot between *E. apolloniensis-E. suessenbornensis* (Pirro Nord) and *E. senezensis*. '*E. stenonis mygdoniensis*' is well separated from all *E. stenonis* subspecies/populations and plots in the range of *E. senezensis*, *E. stehlini*, *E. altidens* from Pirro Nord and Dmanisi.

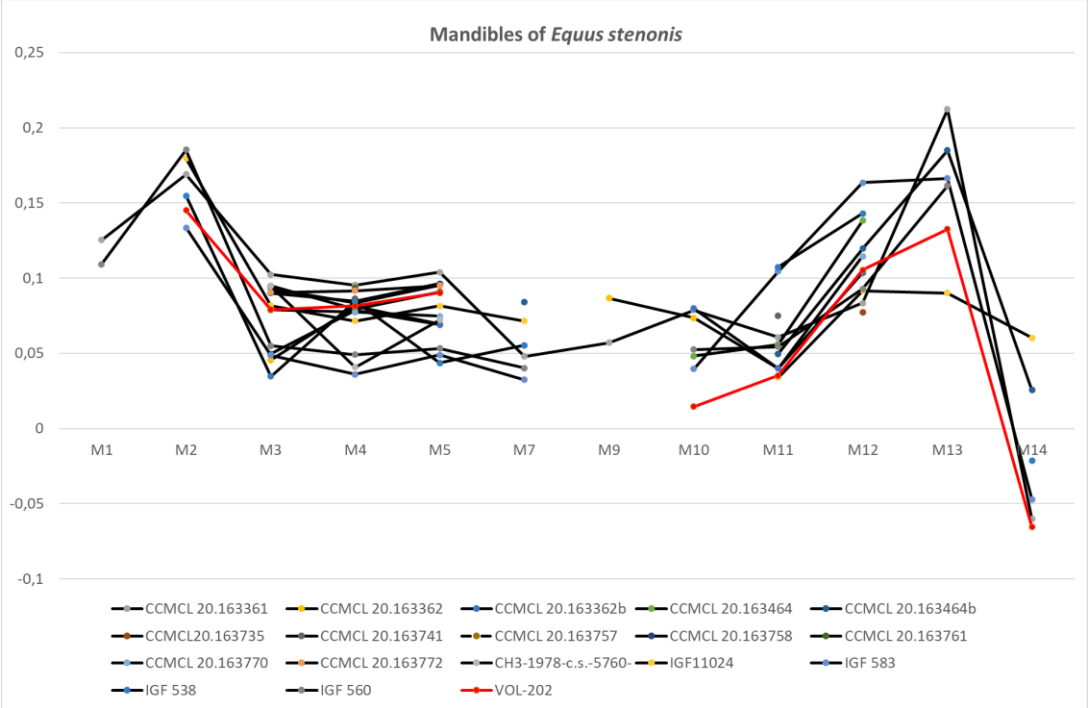

Figure 5.10. Simpson's log ratio diagrams comparing the mandibular dimensions of *E. stenonis* from Saint-Vallier (CCMCL), Chilhac (CH3), Upper Valdarno (IGF) and Volax (VOL). Standard: *Equus hemionus onager*. Data from Cirilli et al. (2021) and personal dataset.

The morphology of the upper and lower dentition is typical of *E. stenonis*. The protocone on the upper cheek teeth is usually short; the protocone on the DFN, DFN3 and VOL cheek teeth exhibit short protocones like *E. stenonis* from Italy, while on the teeth from Sésklo it is usually more elongated resembling *E. stenonis vireti* (Figure 5.57). The length versus the breadth at the base (1 cm above the roots) is plotted in Figure 5.12. The data are limited due to the fact that most teeth were in situ and not isolated. Premolars and molars from DFN and DFN3 plot with *E. stenonis guthi* and *E. stenonis vireti*. A single P3,4 from Volax exhibits slightly higher value on Lb (Figure 5.12), but it plots within the range of *E. stenonis guthi*. *E. stenonis* from Ceyssaguet (Figure 5.12) appears to have larger dimensions than all the other specimens.

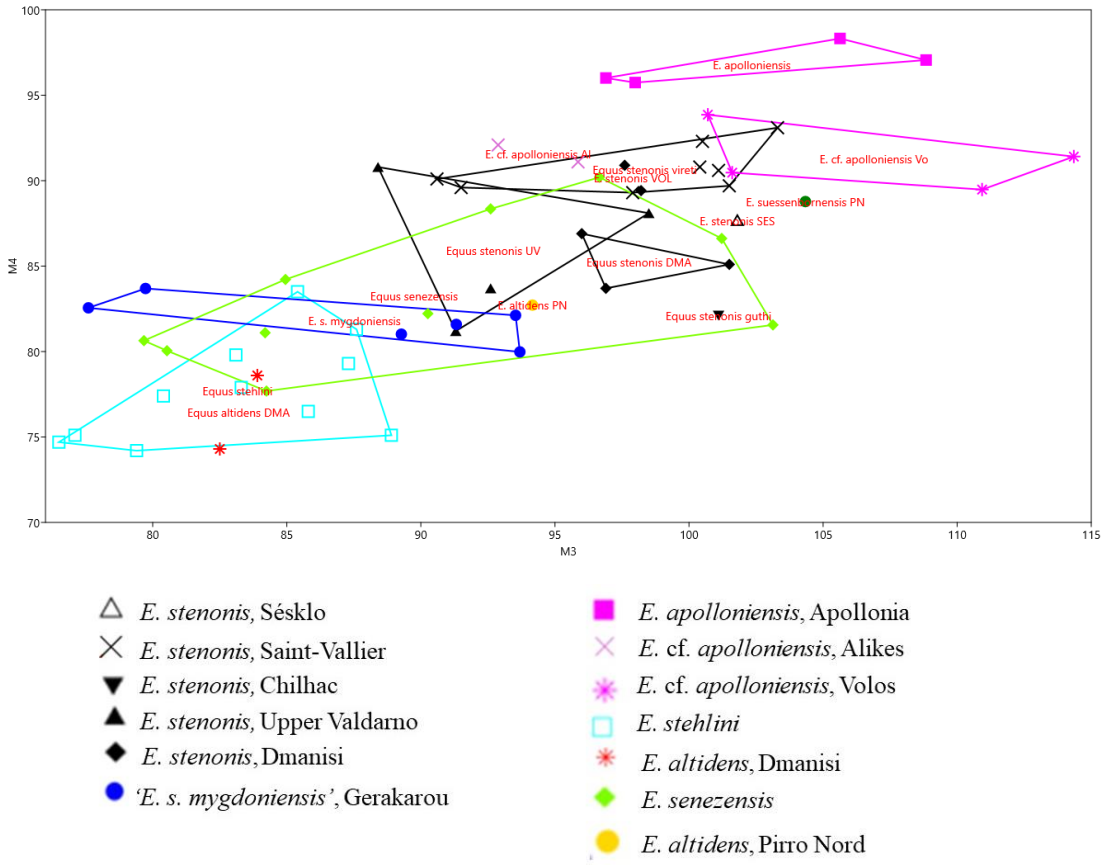

Figure 5.11. Bivariate plots comparing lower premolar (M3) and molar (M4) teeth rows length of the various *Equus stenonis* subspecies/populations, *Equus altidens* subspecies/populations, *E. apolloniensis* and other Early Pleistocene and extant equids. Data from Alberdi and Piñero (2012), Piñero and Alberdi (2015), Bernor et al. (2021), Eisenmann (2017) and personal dataset. Also, additional data from Cirilli et al. (2021) and Cirilli (2022a) for *E. stehlini* and *E. stenonis* (Upper Valdarno).

The morphology of the cheek teeth is typical of *E. stenonis* (Viret 1954; De Giuli 1972; Eisenmann 1981) with a V-shaped double knot. The double knot is separated by a pointed and usually deep linguaflexid and an ectoflexid that varies from shallow on molars or deep (penetrating the isthmus). The bivariate analysis of the occlusal length versus the length of the double knot of the lower cheek teeth is demonstrated in Figure 5.13. The length of the double knot of *E. stenonis* from Sésklo and Volax plot in range of *E. stenonis vireti* and *E. apolloniensis*, exhibiting longer double knot and slightly more elongated occlusal length. *E. stenonis* from the Dafnero sites are close to *E. senezensis* and the GER equid. The range of variability of *E. stenonis* subspecies/populations is large with *E. stenonis* vireti to show the greater variability.

E. senezensis appears to have the same level of variability. The bivariate analysis of the length versus the breadth at the base (1cm from the roots) of the lower cheek teeth is demonstrated in Figure 5.14. The data here too are limited. However, it appears that all samples (Saint-Vallier, Dafnero, Chilhac, Ceyssaguet) are close. Only on p2, Dafnero is broader (higher values on Bb than on Lb).

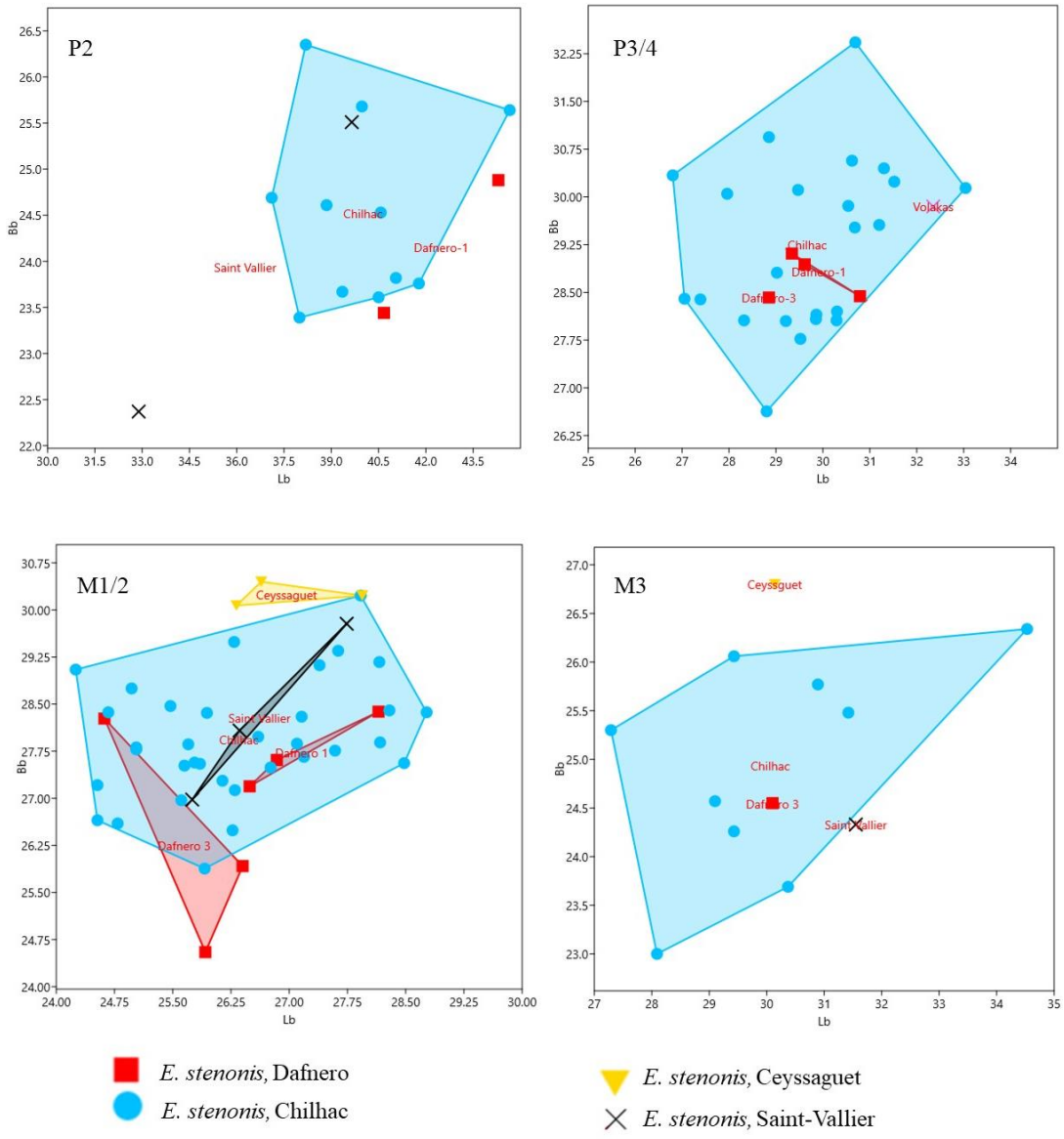

Figure 5.12. Bivariate plots comparing the length versus the breadth at the base (1 cm above the roots) of the upper cheek teeth of *E. stenonis* from Dafnero, Volax, Chilhac, Ceyssaguet and Saint-Vallier.

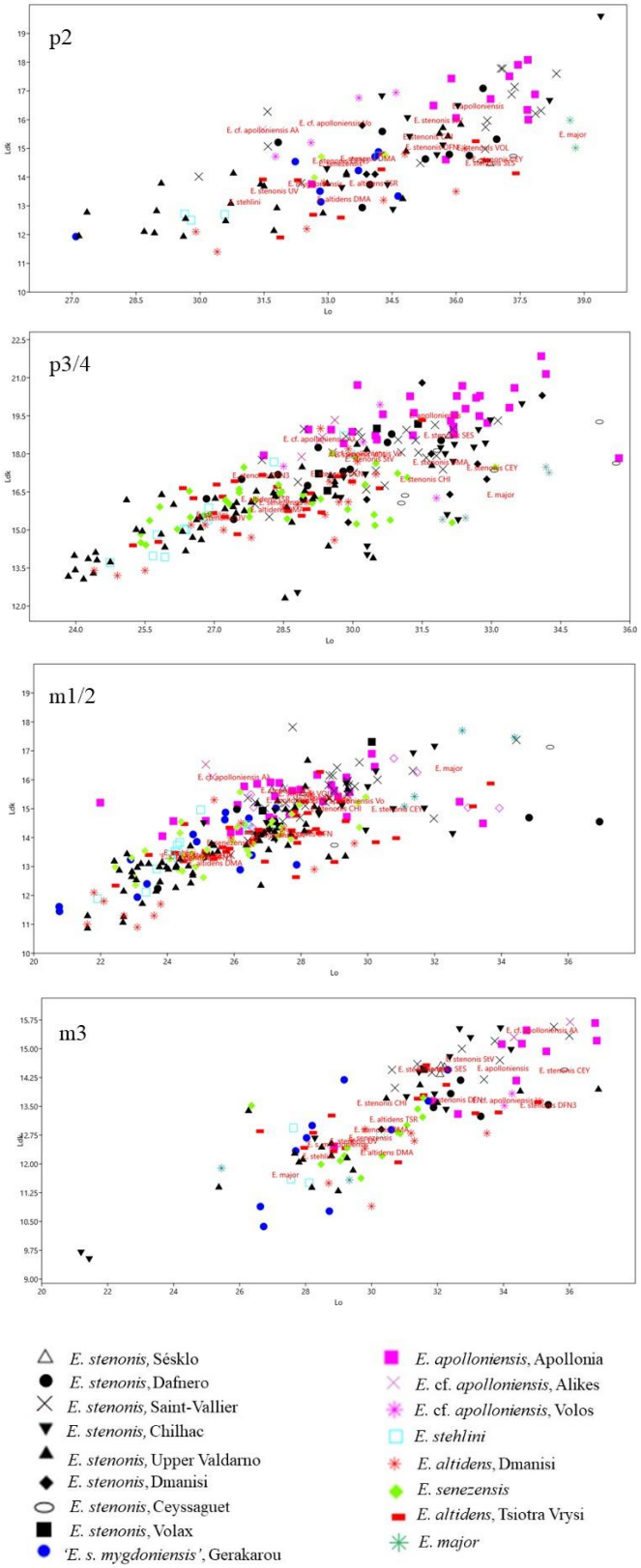

Figure 5.13. Bivariate plots of the occlusal length versus the length of the double knot of the lower cheek teeth of *E. stenonis* samples/populations compared to other Early Pleistocene

Greek and European equids. Data from Bernor et al. (2021), Eisenmann (2008a, b, 2017) and personal dataset.

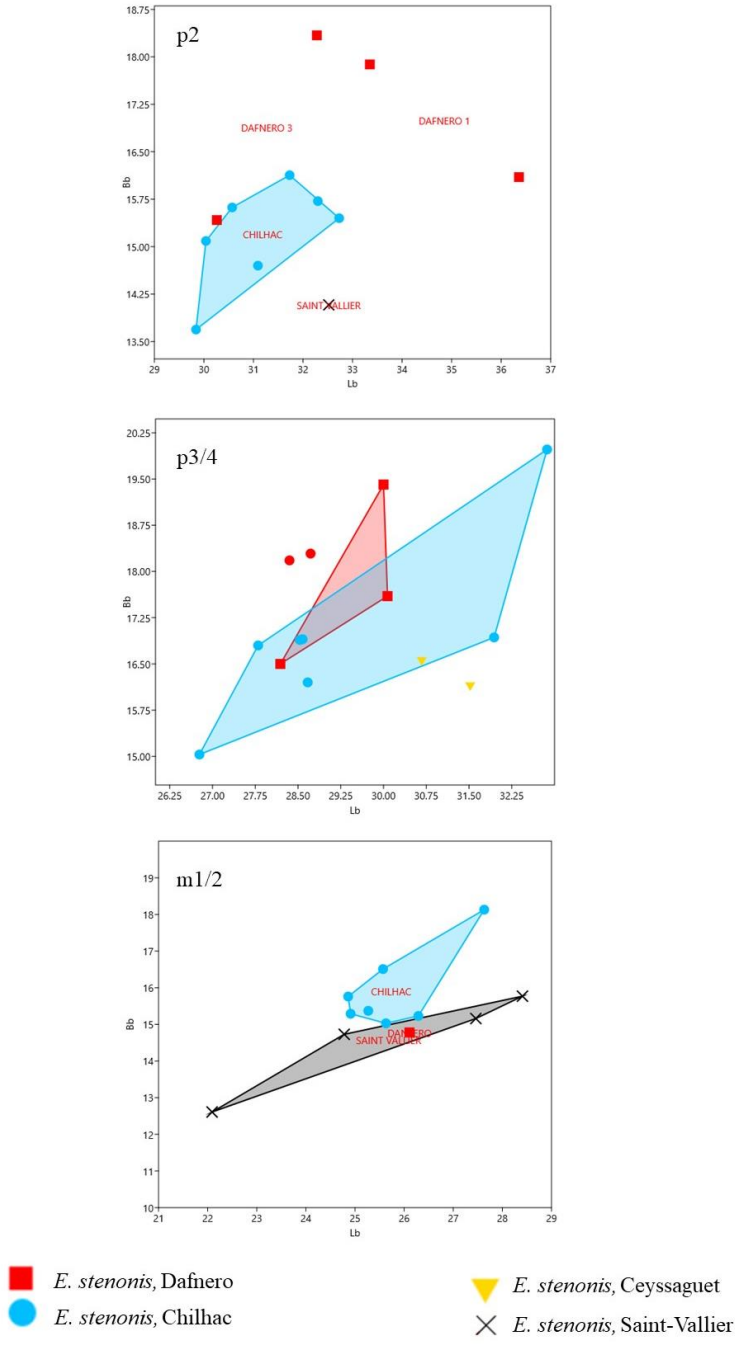

Figure 5.14. Bivariate plots of the length versus the breadth at the base (1cm above the roots) for the lower cheek (p2, p3,4, m1/2) tooth of *Equus stenonis* Dafnero sites, Chilhac and Saint-Vallier.

Simpson's log ratio diagrams for the third metacarpals of the various *E. stenonis* samples from Greece and Europe are given in Figure 5.15. The McIII from Sésklo and

Dafnero are more robust (M3) than Volax possibly because the small sample size of the latter (n=3). The distal keel is moderately developed in all Greek samples resembling *E. stenonis* morphology (Gromova 1949; De Giuli 1972). The distal supra-articular breadth at the tubercles (M10) of *E. stenonis* from Sésklo is greater than at the trochlea (M11), a typical feature of the species (e.g., *E. stenonis* from Chilhac, Saint-Vallier, Olivola). In Dafnero, the analogies between M10-M11 are similar to *E. stenonis* from La Puebla de Valverde, while in Volax the DAP at the trochlea (M11) is slightly greater than at the tubercles (n=3). The metacarpal from Saint-Vallier has the most robust distal epiphysis. In particular, the metacarpals from Dafnero resemble the ones from La Puebla de Valverde and Chilhac (Figure 5.15, 5.16). *E. stenonis* from La Puebla de Valverde and Chilhac seem to have similar proportions. *E. stenonis guthi* has the shortest metacarpal (M1) (Figure 5.15, 5.16) than all subspecies of *E. stenonis*. However, the overall proportions of third metacarpals from Dafnero seem to be similar with both *E. stenonis* from Chilhac and La Puebla de Valverde.

In Figure 5.17, PC1 and PC2 accounted for 89.14% for the variance (PC1 = 70.86% and PC2 = 18.28/%). The various *E. stenonis* samples from Dafnero, Volax, Sésklo, Saint Vallier, Chilhac, Olivola, Matassino, Upper Valdarno and Dmanisi overlap; *E. stenonis* from Saint Vallier here too shows a more robust morphology when compared to the other samples.

Simpson's log ratio diagrams for the third metatarsals of the various *E. stenonis* samples from Greece and Europe are given in Figure 5.18. As in case of the third metacarpals, the third metatarsals exhibit similar bauplan between various subspecies/ecomorphotypes of *E. stenonis* (Figure 5.18) except for '*E. s. mygdoniensis'* from Gerakarou (Figure 5.18). The length (M1) of the metatarsals shows variability. *E. stenonis guthi* has the shortest metatarsals of all *E. stenonis* subspecies (Figure 5.18, 5.19), although close to *E. stenonis* from Dafnero sites. The metatarsals from Volax and Sésklo are somehow longer (M1) resembling those from Olivola.

The proportions of the distal articular breadth are similar, but in relation to maximal length, *E. s. guthi* is slightly more robust (M1, M10, M11, M12, M13, M14). The metatarsals of *E. stenonis* from Dafnero (Figure 5.18, 5.19) is similar to *E. stenonis guthi*, but it shows higher maximal length (M1) and a relatively larger articular facet for the fourth tarsal (M8) in Dafnero sample. *E. stenonis guthi* has also the shortest metatarsal (M1) (Figure 5.18, 5.19) than all subspecies of *E. stenonis*, and they are overall slender.

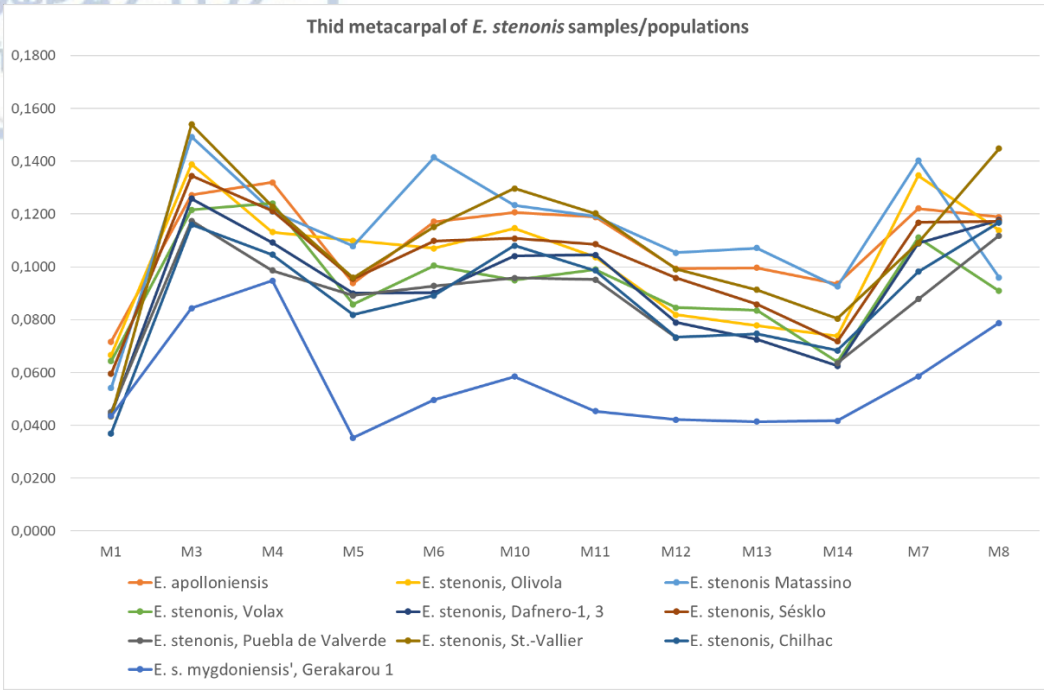

Figure 5.16. Simpson's log ratio diagram comparing the third metacarpals of *E. stenonis* subspecies/populations from Greece and the rest of Europe. Standard: *Equus hemionus onager*. Data from Eisenmann (1980) and personal dataset. Additional data for the Italian *E. stenonis* from Bernor et al. (2021).

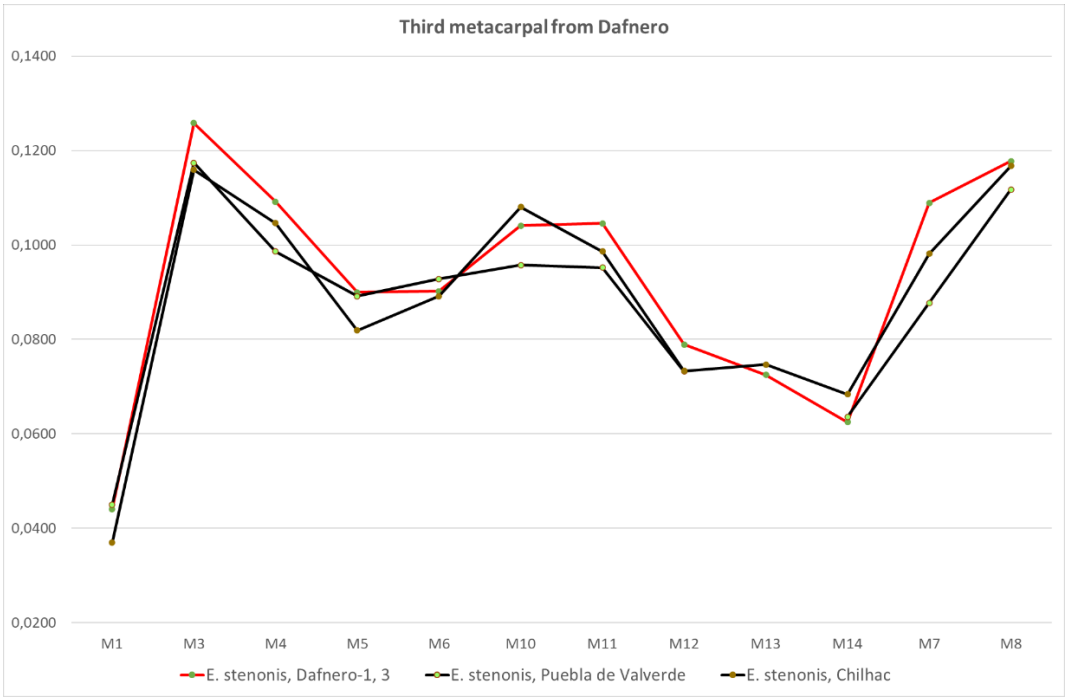

Figure 5.16. Simpson's log ratio diagram comparing the third metacarpal of *E. stenonis* from Dafnero to *E. stenonis* from La Puebla de Valverde and Chilhac. Standard: *Equus hemionus onager*. Data from Eisenmann (1980) and personal dataset.

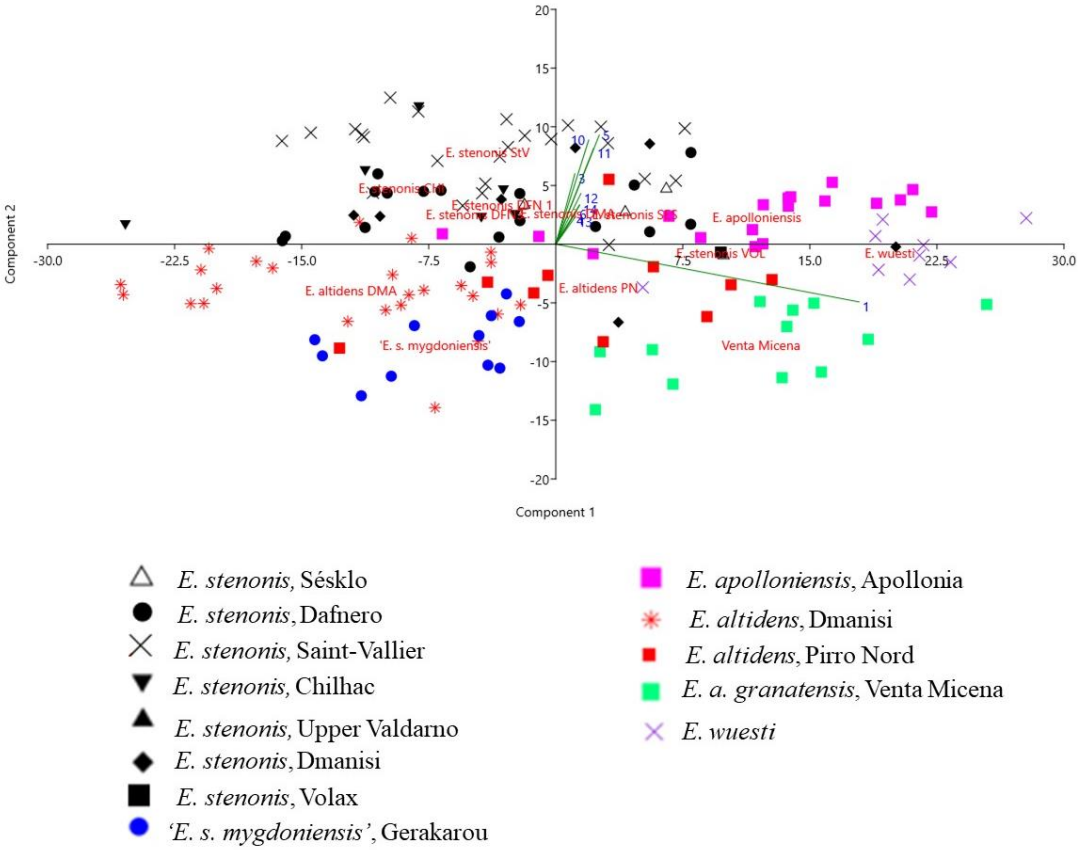

Figure 5.17. PCA plot on selected measurements of the third metacarpal of several Early Pleistocene equids from Greece and the rest of the Europe. Data from Eisenmann and Boulbes (2020), Bernor et al. (2021) and personal dataset.

E. s. pueblensis and *E. stenonis* from Dmanisi are quite similar in morphometry (Figure 5.19). *E. stenonis pueblensis* and *E. stenonis* from Dafnero have similar maximal length (M1) and same distal articular dimensions (M10, M11, M12, M14), but *E. s. pueblensis* shows slightly wider proximal articular dimensions (M5, M6). The overall proportions of metatarsals of both *E. s. guthi* and *E. s. pueblensis* just like with the metacarpals. The metatarsals from Sésklo and Volax resemble in maximal length (M1) *E. stenonis* from Olivola. *E. stenonis* from Sésklo shows similar proportions of the distal articular facet (M10, M11, M12, M13, M14) with *E. stenonis* from Olivola, but the latter shows greater midshaft width (M3) lower midshaft depth (M4). The distal maximal supra-articular breadth at the tubercles (M10) is, more or less, greater than at the trochlea (M11) on the metatarsals from all *E. stenonis* samples apart from Volax (n=3).

In Figure 5.20, PC1 and PC2 accounting for 88.5% for the variance (PC1 = 60.31% and PC2 = 28.19%). The various *E. stenonis* samples exhibit a wide variability; *E. stenonis*

from Saint Vallier here too shows a more robust morphology when compared to the other samples. *E. stenonis* from Dafnero plots between Olivola and Chilhac.

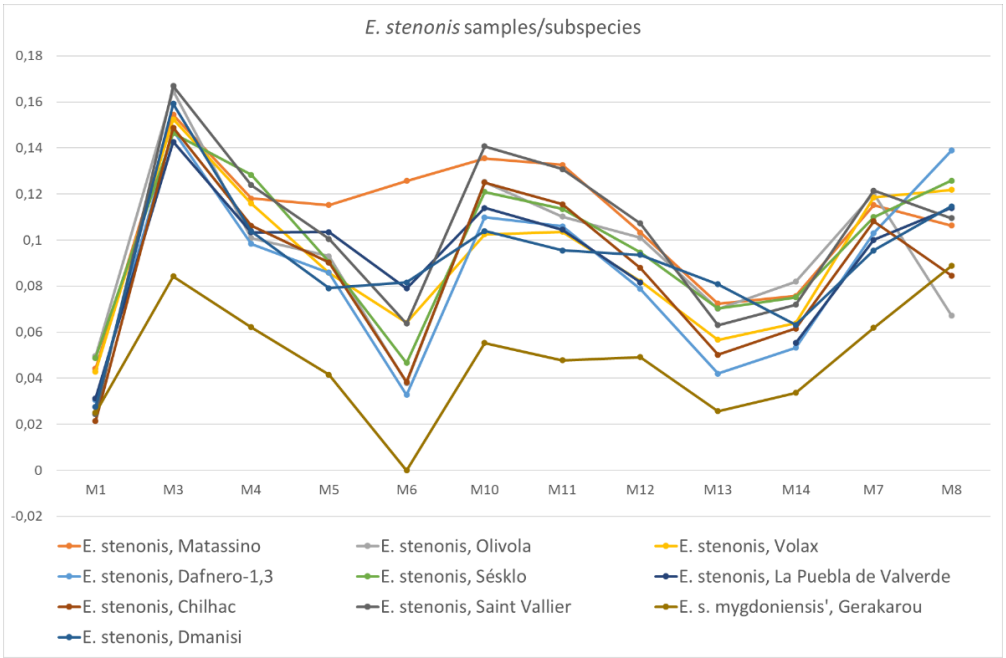

Figure 5.18. Simpson's log ratio diagram comparing the third metatarsal of *E. stenonis* subspecies/populations from Greece and the rest of Europe. Standard: *Equus hemionus onager*. Data from Bernor et al. (2021), Eisenmann (1980) and personal dataset.

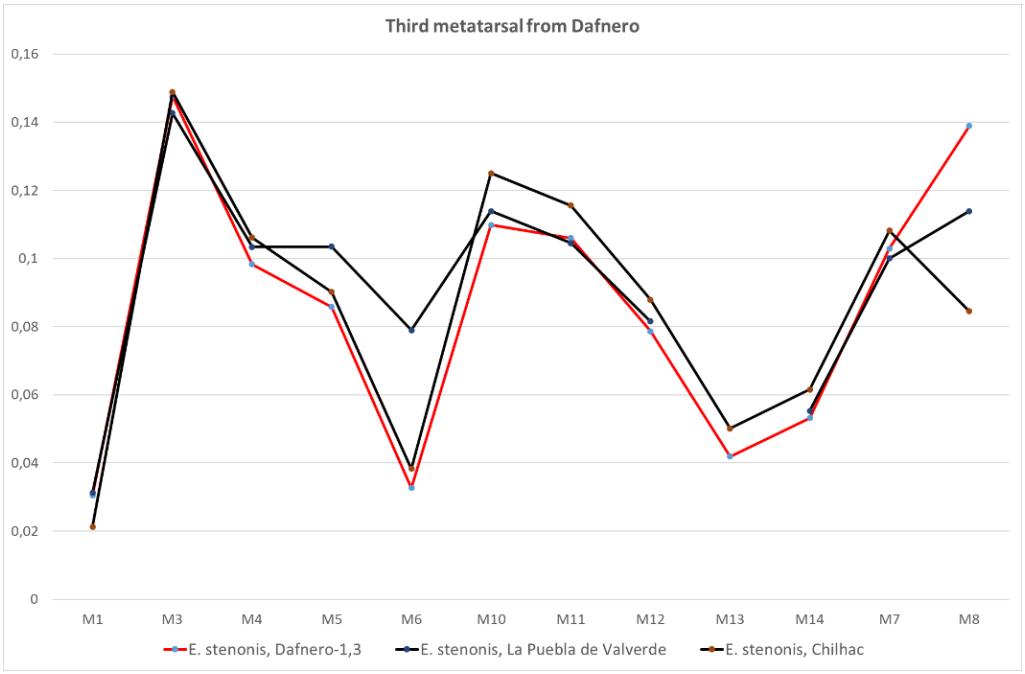

Figure 5.19. Simpson's log ratio diagram comparing the third metatarsals of *E. stenonis* from Dafnero sites to those from La Puebla de Valverde (*E. s. pueblensis*) and Chilhac (*E. s. guthi*). Standard: *Equus hemionus onager*. Data from Eisenmann (1980) and personal dataset.

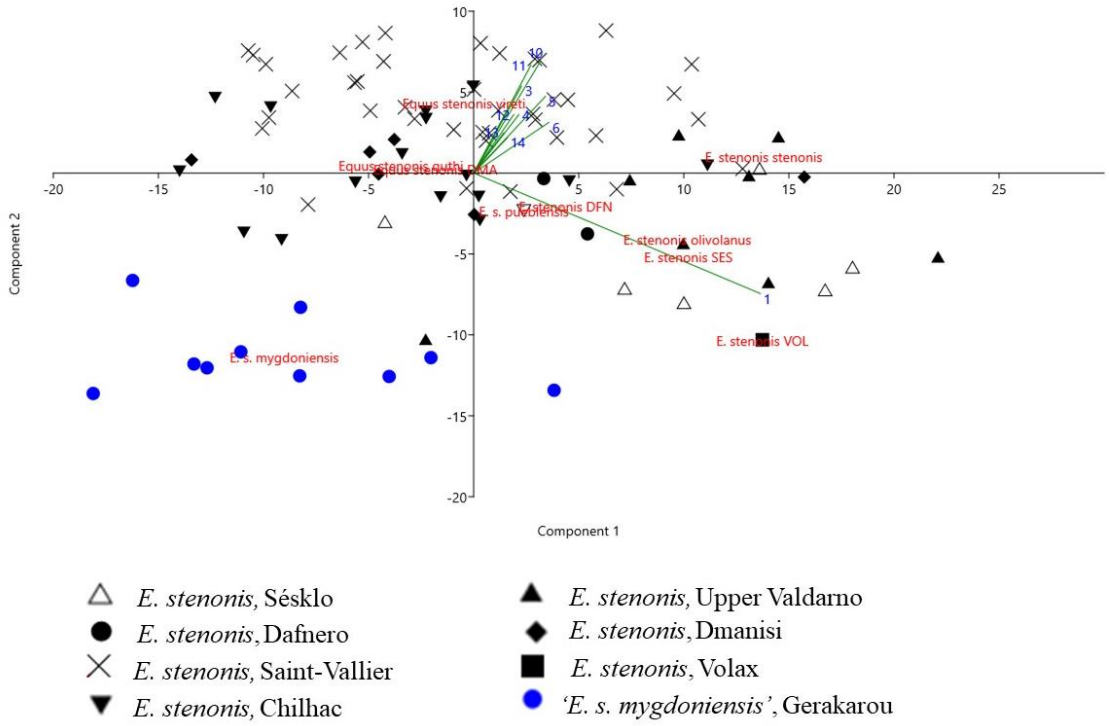

Figure 5.20. PCA plot on selected measurements of the third metatarsal of the several *E. stenonis* samples/populations. Data from Bernor et al. (2021) and personal dataset.

The PERMANOVA results for both metacarpals and metatarsals indicate significant differences between *E. stenonis vireti* and *E. stenonis* from Dafnero, while no statistical differences were identified between the latter and *E. stenonis guthi*. The metacarpals from Sésklo do not show any statistical difference with the ones of *E. apolloniensis* (in agreement with PCA results), while metatarsals indicate significant differences between the two of them. Metapodials of *E. stenonis* from both Sésklo and Volax do not have any statistical differences with *E. stenonis* from Olivola.

The tibia of the *various E. stenonis* subspecies/populations exhibit similar morphometry at the distal part of the epiphysis (M7, M8; Figure 5.21) and they are mainly overlapping; *E. stenonis vireti* shows greater range of variability and slightly larger dimensions. The Greek specimens from Dafnero plot closer to *E. stenonis guthi*, while the ones from Sésklo plot closer to Upper Valdarno and the lower measurements of *E. stenonis vireti*.

The astragali of *E. stenonis* samples from the Greek (Dafnero, Sésklo, Volax) and the European (Saint-Vallier, Matassino, Olivola, Upper Valdarno) localities show a broad range of variability. Figure 5.22a exhibits the bivariate analysis of the maximum length

(M1) versus maximum width (M4) of the astragali of the various *E. stenonis* subspecies. There is a linear regression between these two variables (Figure 5.22a). The astragali from Dafnero-1, Volax and Sésklo plot together with *E. s. guthi* and *E. s. pueblensis*, while *E. s. vireti* show quite larger dimensions and wider range of variability. The astragali of *E. stenonis* from Dafnero-3 are slightly shorter and they are plotted close to *E. stenonis* from Dmanisi, yet again within the range from Dafnero-1, Volax and Sésklo.

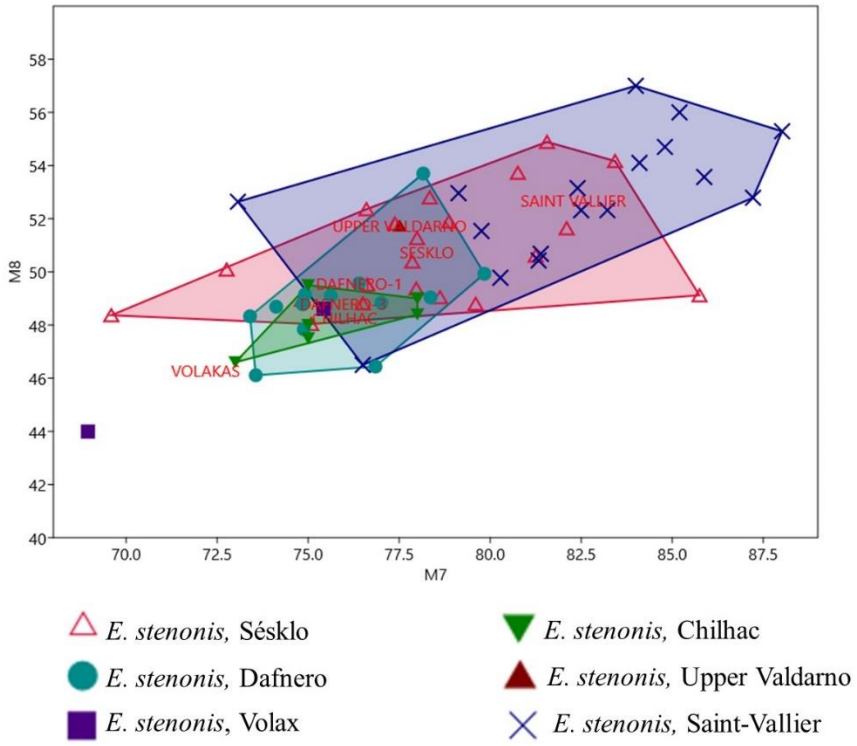

Figure 5.21. Bivariate plot of the distal maximal breadth (M7) versus the distal maximal depth (M8) of the tibiae of the various *E. stenonis* samples/populations. Data from Bernor et al. (2021) and personal dataset.

Although the equine calcanei are usually fragmentary or broken, there are plenty specimens in the material that could benefit some further information about the tarsal bones. The bivariate plot of M1 (maximal length) and M6 (maximal breadth) for the calcanei is reported in Figure 5.22b. The results support the previous interpratations based on the postcranial elements (third metacarpals, third metatarsals, astragali). The astragali from Dafnero plot together with *E. stenonis guthi*, while *E. stenonis vireti* appears to have larger dimensions and a greater range of variability.

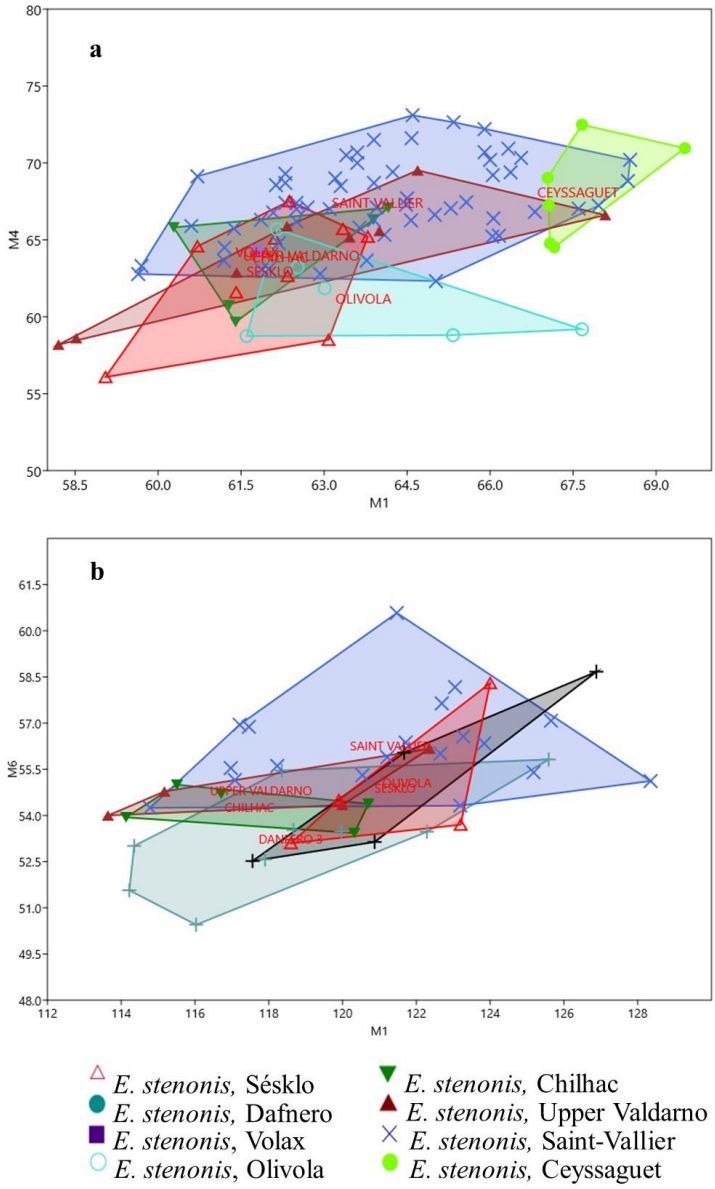

Figure 5.22. Bivariate plot of the (a) maximum length (M1) versus maximum width (M4) of the astragali and (b) maximum length (M1) versus maximum breadth (M6) of the calcaneum of the various *E. stenonis* samples/populations. Data from Bernor et al. (2021) and personal dataset.

The PCA results for the first phalanx (anterior and posterior) of *E. stenonis* subspecies/populations compared to other Pleistocene European equids are presented in Figure 5.23. PC1 and PC2 account for the 83.83% of the total variance (PC1 = 64.12%; PC2 = 19.71%). The results are consistent with those for the third metacarpal and third metatarsal, with all *E. stenonis* subspecies being clustered together although appearing a wide range of variability. '*E. stenonis mygdoniensis'* is being clustered separately from all *E. stenonis* subspecies due to its small and slenderer dimensions.

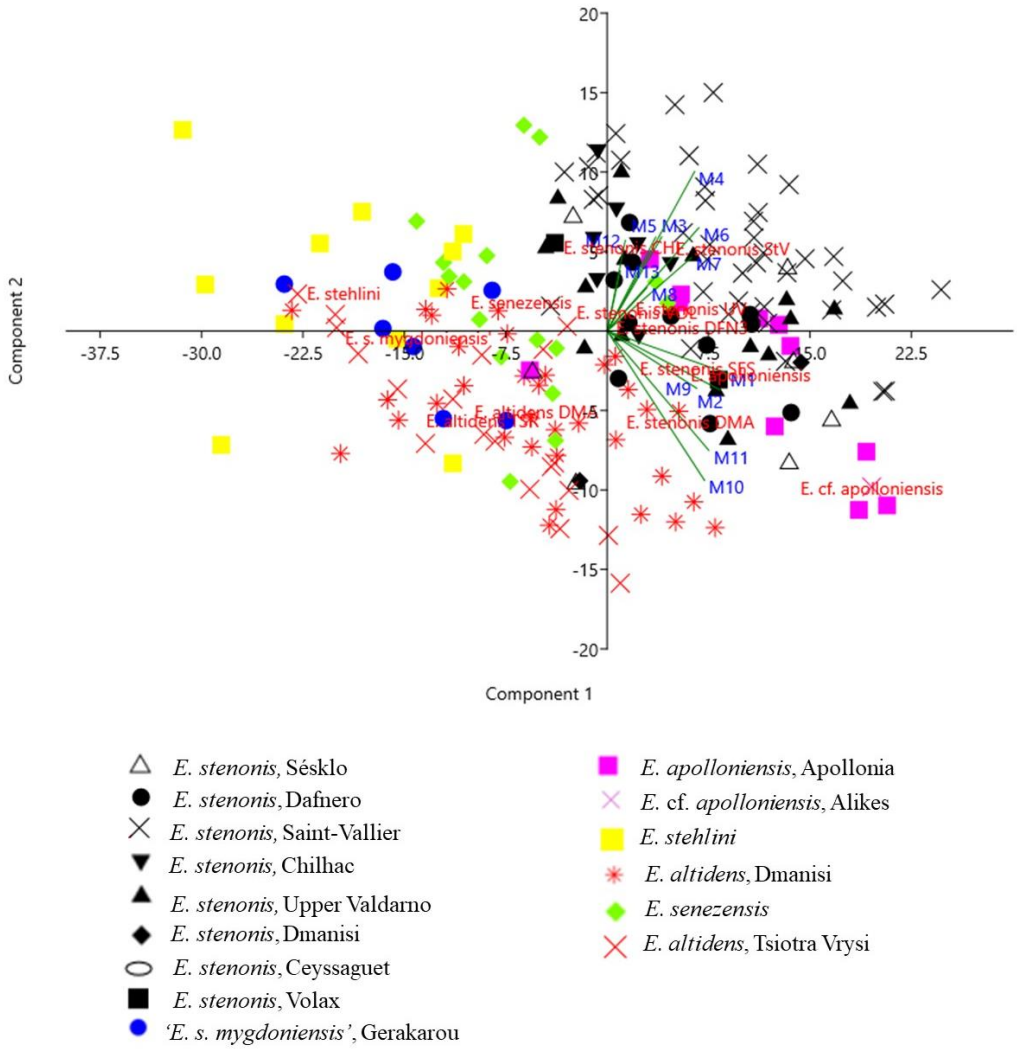

Figure 5.23. Principal component analysis of the first phalange. *E. stenonis* (black) is compared to other Early Pleistocene Greek and European equids. Data from Van Asperen et al. (2012), Eisenmann (2017), Bernor et al. (2021), Cirilli (2022), https://vera-eisenmann.com/, and personal dataset.

The results of the present analyses could potentially improve the taxonomic status of *E. stenonis*. Summarising the description and comparison, the *E. stenonis* sample from Dafnero, Sésklo and Volax belong to a large equid with cranial morphometry and morphology similar to *E. stenonis* sensu lato, stenonoid dental characters and long and robust limb bones. The cranial elements from Sésklo resemble in morphometry those from La Puebla de Valverde, Saint-Vallier, Olivola and Volax (Athanassiou 2001) with long muzzle. The cranial elements from Dafnero, which is more or less contemporary to Sésklo, do not exhibit any significant morphometrical differences except for the

shorter muzzle a feature that is closer to *E. stenonis pueblensis* [the muzzle of *E. stenonis guthi* is unknown although Eisenmann (2017) includes it to stenonoid equids with short muzzles], yet all of them (DFN, SES and VOL) they are larger and heavier than '*E. stenonis mygdoniensis*' and *E. senezensis*. In general, the metapodials from Dafnero are shorter and heavier resembling those of *E. stenonis guthi* and *E. stenonis pueblensis*, while those from Sésklo are slenderer (yet more robust than those of *E. apolloniensis*) resembling *E. stenonis* from Olivola and *E. stenonis vireti* (partim). The cranium from Dafnero-3 belongs to an equid with shorter muzzle closer to *E. s. pueblensis* and *E. stenonis guthi*. The results of the present morphometric and statistical analysis show that in majority European *E. stenonis* samples (Greek and European sample) have homogeneous dimensions of the metapodials, tibia (see also Cherin et al. 2020), astragali and calcaneum (also in Cirilli et al. 2021) with the exception of '*E. stenonis mygdoniensis*'.

The several subspecies of *E. stenonis* that have been erected by Prat (1964, 1980), De Giuli (1972), Boeuf (1986), Alberdi and Ruiz Bustos (1985), Koufos (1992) and Caloi (1997) were based on some minor morphometric differences. They have been revised by several authors over the last 50 years. In addition, due to the scarcity of complete cranial remains, the lack of crania associated to limb bones and the mixing of old collections from key localities, the various *E. stenonis* populations were split into different subspecies (that shared a common bauplan) that were many times delimited only to a single locality (i.e., type locality) (Cherin et al. 2020). That means that the material from the type locality of *E. stenonis* (Terranuova, Upper Valdarno Basin) referred to the nominotypical subspecies *E. s. stenonis* (De Giuli 1972), would be different from *E. stenonis vireti* from Saint-Vallier (Prat 1980), *E. stenonis guthi* from Chilhac (Boeuf 1986), *E. stenonis pueblensis* from La Puebla de Valverde (Caloi 1997), *E. stenonis olivolanus* from Olivola (Caloi 1997), *E. stenonis senezensis* from Senèze (Prat 1964, 1980; "*E. senezensis senezensis*" in Alberdi et al. 1998; *E. (Allohippus) senezensis* in Eisenmann 2017), and *E. stenonis mygdoniensis* from Gerakarou-1 (Koufos 1992). Although Alberdi et al. (1998) acknowledged three subspecies of *E. stenonis* (*E. s. stenonis*, *E. s. vireti*, *E. s. guthi*) and Eisenmann (2017) erected all subspecies of *E. stenonis* to species rank (*Allohippus vireti*, *Allohippus guthi* etc), the present analysis rather supports the hypotheses by Forstén (1999), Athanassiou (2001), Alberdi and Palombo (2013a), Palombo and Alberdi (2017), Bernor et al. (2019), Cirilli et al. (2020a) Cherin et al. (2021) and Cirilli et al. (2021), in which *E. stenonis*

subspecies are recognized as ecomorphotypes (or else ecomorphs) of a single species; the morphological and morphometrical differences may have not any taxonomical significance. According to this hypothesis, local specific ecological conditions may have triggered the appearance/differentiation of ecomorphs (regarded also as geographical subspecies due to geographical vicariance) (Palombo and Alberdi 2017), and that these forms exhibit intraspecific variation of a single widespread long-lasting species that is *E. stenonis*.

The present analyses support Cirilli et al.'s (2021) work suggesting a wide inter- and intraspecific variability between the subspecies of *E. stenonis* including the samples from Saint-Vallier, Olivola, Matassino, Chilhac, La Puebla de Valverde, Dafnero, Sésklo and Volax into a single species with the exception of '*E. stenonis senezensis'* and '*E. stenonis mygdoniensis'*. The later will be analyzed later in this work. Further, the medium sized *Equus* from Senèze, according to its cranial and postcranial elements could be acknowledged as a valid different species (*E. senezensis* in Alberdi et al. 1988 and Eisenmann 2017). Whether it is a valid species or not it is beyond the scope of this thesis.

***Equus altidens* von Reichenau, 1915**

Synonyms: *Equus stenonis mygdoniensis* in Koufos 1992

Equus petraloniensis in Tsoukala 1989

Localities.

Gerakarou-1 (GER), Mygdonia Basin, Central Macedonia

Tsiotra Vrysi (TSR), Mygdonia Basin, Central Macedonia

Krimni-1, 2, 3 (KRI, KRM, KMN), Mygdonia Basin, Central Macedonia

Libakos (LIB), Aliakmon Basin, Western Macedonia

Polylakkos (POL), Aliakmon Basin, Western Macedonia

Siatista-E (E-SIA), Aliakmon Basin, Western Macedonia

Petralona Cave (PEC), Chalkidiki peninsula, Central Macedonia

Material.

Gerakarou. Crania GER-8, 9, 31, 122; fragment of cranium with dP1-dP4 GER-37; fragments of maxilla with dP2-dP4 sin/dex GER-114, 115; fragment of maxilla with dP2-dP4 sin GER-113, 114; fragment of maxilla with P2-M2 sin GER-36; fragment of

maxilla with P2-M3 sin GER-35; fragment of maxilla with dP3-M2 sin GER-10; P2 sin GER-116; 2 M1,2 dex GER-117, 118; fragment of mandible with dp2-dp4 dex GER-181; part of muzzle with i2-i3, c sin/dex GER-73; mandible with i1-i3, p2-m3 sin/dex GER-32; mandible with i1-i3, p2-m3 sin/dex (broken sinistral ramus) GER-33; mandible (broken rami) with i1-i3 sin, i2-i3 dex, c and p2-m3 sin/dex GER-34; fragment of mandible with p2-m3 sin/dex GER-70; fragmentary body of mandible with p2 dex GER-72; fragmentary body of mandible with p2-m3 dex: GER-11, 71; fragmentary body of mandible with m2-m3 sin GER-12; humerus GER-54; proximal part of humeri GER-55 (fragment); distal parts of humeri GER-86, 128; radioulna GER-87; proximal part of radioulna GER-16; proximal part of radius GER-354 (juv.); distal part of radius GER-120; lunatum GER-112; third metacarpals GER-17, 63, 64, 88, 89, 90, 91, 92, 93, 98, 176; proximal part of third metacarpal GER-18; proximal part of third metacarpal GER-18; distal part of third metacarpal GER-19; sesamoid GER-100; fragment of pelvis GER-351; distal parts of femur GER-38? (fragment), 39; tibia GER-352; proximal parts of tibiae: GER-27 (fragment), 129 (fragment); distal parts of tibiae: GER-28, 29, 30, 40, 41, 42, 56, 74, 75, 76, 77, 78, 85, 121, 125, 126, 127 (fragment), 178; astragali: GER-58, 80, 105, 106, 107, 177; calcaneum GER-79; third metatarsals: GER-21, 22, 23, 65, 66, 94, 95, 96, 99, 101, 102, 103, 104, 123, 124; proximal parts of third metatarsals: GER-24, 25, 67, 82, 97; distal parts of third metatarsals: GER-68 (juv.?), 69; first phalanges GER-59, 60; proximal parts of first phalanges GER-108, 179 (fragment); second phalanx GER-83; third phalanges GER-61, 62, 84, 109, 110 (fragment), 111 (fragment).

In articulation: magnum + third metacarpal GER-100; distal part of tibia + astragalus + calcaneum + navicular + cuboid GER-57; astragalus + big cuneiform GER-81.

Libakos. Upper teeth series P2-M3 sin, LIB-317-322 (+dP2, dP4: LIB-315, 316 respectively); P2-M3 dex, LIB-287, 289, 290a, 288, 286a-b (+dP3, dP4: LIB-291, 290b respectively); P2 sin: LIB-203, 210, 211, 401; P2 dex: LIB-204, 205, 206, 207, 208, 209; P3,4 sin: LIB-188, 192, 193, 194, 296, 297, 299, 300, 301, 303, 304, 310, 550, 551, 552, 553, 554, 555, 588, 590, 591, 592, 680, 681, 712; P3,4 dex: LIB-186, 187, 190, 191, 195, 196, 197, 198, 199, 200, 201, 202, 305, 306, 307, 308, 311, 312, 313, 556, 557, 558, 589, 629, 630; M1,2 sin: LIB-189, 293a-b, 530, 531, 532, 533, 534, 537, 615, 631, 632, 633, 634, 635, 711, 715, 716, 721, 722, 723, 724, 725, 726; M1,2 dex: LIB-294, 295, 298, 535, 536, 538, 539, 614, 616, -617, 636, 637, 638, 639, 640, 641, 642, 643, 644, 645, 646, 647, 648, 649, 650, 713, 714, 719, 720; M3 sin: LIB-619, 620,

628, 705, 706, 707, 708, 710; M3 dex: LIB-621, 622, 623, 624, 625, 626, 627, 709; mandibular fragment with m1-m3 sin, LIB-529; mandibular fragment with m2-m3 sin, LIB-593; mandibular fragment with p2-m2 dex, LIB-540; mandibular fragment with m3 dex, LIB-674; mandibular fragments with p2-p3 dex, LIB-528, 727; p2 sin: LIB-594-569, 598, 654, 656, 657, 658, 659, 660, 661, 662, 663, 664; p2 dex: LIB-571, -578, 597, 599, 651, 652, 653, 655, 665, 666, 667; p3,4 sin: LIB-326, 327, 328, 329, 330, 331, 332, 344, 345, 347, 354, 355, 356, 357, 358, 359, 360, 361, 362, 422, 428, 429, 430, 431, 432, 433, 434, 435, 436, 487, 493, 495, 572; p3,4 dex: LIB-333, 334, 335, 337, 338, 339, 340, 341, 342, 343, 348, 349, 350, 351, 352, 363, 380, 385, 386, 405, 406, 407, 408, 409, 410, 411, 412, 413, 414, 415, 416, 417, 418, 419, 420, 421, 573, 579, 580; m1,2 sin: LIB-382, 383, 384, 387, 398, 483, 484, 485, 491, 492, 494, 496, 574, 575; m1,2 dex: LIB-371, 372, 373, 374, 377, 378, 381, 393, 394, 395, 396, 397, 399, 488, 489, 490, 581, 582; m3 sin: LIB-375, 546, 563, 564, 565, 566, 567, 675; m3 dex: LIB-56, 376, 379, 541, 542, 543, 544, 545, 547, 548, 560, 562, 568; distal parts of humerus: LIB-516, 524, 512; diaphysis of humerus LIB-691; radius: LIB-853, 862, 881, 882, 884; proximal parts of radius: LIB-521, 522, 525; distal parts of radius with fragmentary ulna: LIB-511, L519, 518, 513, 517; parts of ulna LIB-609, 735, 736; lunatum LIB-600; second metacarpals: LIB-748, 749; third metacarpals with second metacarpal: LIB-833, 836, 861; third metacarpals: LIB-824, 835, 837, 852, 855, 859, 865, 866, 867, 869, 871, 872, 876, 877, 879; proximal parts of metacarpals: LIB-874, LIB-843; distal parts of metacarpals LIB-830, 833, 834, 842, 844, 848, 849, 850, 851, 875, 880; first phalanges LIB-773, 768, 769; proximal part of first phalanx (anterior/posterior) LIB-772; third phalanges (anterior/posterior): LIB-602 LIB-608; parts of third phalanges (anterior/posterior): LIB-603, LIB-604 (fragment), LIB-605, LIB-606 (fragment), LIB-607 (fragment); distal part of femur LIB-601; tibiae LIB-765+POL-18; proximal parts of tibia LIB-737 juv.(?); distal parts of tibia LIB-690, 728, 729, 730 (fragment), 738 (juv.?), 763, 764, 766, 767, 788 (juv.?), 784, 785, 786, 787 (fragment), 789, 790, 791, 801, 802, 803, 804 (+two specimens without number); calcaneum LIB-702, 703, 731, 733; proximal parts of calcaneum LIB-704, 732, 734; astragali LIB-692, 693, 694, 695, 696, 697, 698, 701; parts of astragali: LIB-699, 700; navicular: LIB-757, 758, 759, 760, 761, 762; cuboid: LIB-775, 776, 777, 778, 779, 780; big cuneiform LIB-753, 754 (fragment), 755, 756 (fragment); proximal parts of third metacarpals LIB-750-752; third metatarsals with second metatarsal: LIB-856, 857; third metatarsals: LIB-774, 781, 782, 783, 805, 806, 807, 808, 809, 810, 811, 812, 813,

814, 815, 816, 822 (juv.), 823, 825, 826, 827, 829, 838, 839, 840, 854, 858, 860, 863, 864, 868, 870; proximal parts of third metatarsals: LIB-793, 794, 795, 796, 797, 799, 800, 819, 820, 821, 846, 873, 878; distal part of third metatarsal: LIB-847; proximal parts of forth metatarsals: LIB-739, 740, 741, 742, 743, 744, 745, 746, 747; first posterior phalanges: LIB-770, 771.

In articulation/in situ: third metacarpal, first phalanx, second phalanx, third phalanx LIB-4, 3, 2, 1 respectively.

Polylakkos. Proximal parts of humeri POL-3, 4; proximal part of radius POL-1; tibia POL-18+LIB-765; distal part of tibia POL-2; proximal parts of third metatarsals POL-6, 7.

Siatista-E. M3 sin E-SIA-18; m3 sin: E-SIA-12, 13; m1,2 sin: E-SIA-17, -16; third metacarpal E-SIA-22; first anterior phalanx E-SIA-26.

Tsiotra Vryssi. Fragment of cranium TSR-162 (juvenile); maxilla with dP1, P2-M3 sin and P2-M1 dex TSR-H23-13; maxilla with dP2- dP4 dex TSR-186; fragment of mandible with p2-m2 sin TSR-136; fragments of mandibles with p2-m3 sin D18-17, D20-17, D20-33, F20-27, fragment of mandible with p3-m3 sin TSR-D17-39, F19-5, fragment of mandible with p2-p4 sin TSR-191, fragment of mandible with p2-m3 dex TSR-G21-46; fragment of mandible with p2-m2 dex TSR-E19-6, F20-15; fragment of mandible with p2-p4 dex TSR-E19-46; fragment of mandible with p2-p3 dex TSR-H18-14; fragment of mandible with p3-m3 dex TSR-D20-9; fragment of mandible with p3-m2 dex TSR-F17-10; fragment of mandible with p4-m2 dex TSR-F17-14; fragment of mandible with m2-m3 dex TSR-E19-36; fragment of mandible with m2 dex TSR-E17-16; fragment of mandible with m3 dex TSR-F17-25; isolated P2: TSR-G19-17, E19-29, G21-1, E21-41, D18-12; isolated P3/4: TSR-E13-13, F20-37, G21-2, D16-45, E20-21, G20-2, E21-7, F19-12, F20-2, D21-15, D21-6, E19-25, G17-21, F20-3; isolated M1/2: TSR-G21-52, C14-4, E21-46, E20-22, E20-23, E20-30, G22-10, E17-2, E17-4, H17-11; isolated M3: TSR-G21-28, D14-11, E20-7, E19-28, TSR-63; isolated p2: TSR-F17-5, D16.3-I20-1; isolated p3/4: TSR-F16-1, G19-16; isolated m1/2: TSR-E20-4, F17-6, G21-54, F17-4, F16-2, G21-53, F15-1, E19-43, E19-43, F17-5, G20-50, G21-49, F15-2; isolated m3: TSR-F17-25, G17-18, G21-51, 195, D18-4, E19-14; humeri: TSR-G20-7, TSR-F19-31, TSR-C18-12; distal parts of humeri: TSR-G20-6, 130; diaphysis of humerus: TSR-F19-21, TSR-I20-5, TSR-142; radius: TSR-E16-3; proximal parts of radius: TSR-E19-57, TSR-132; distal parts of radius: TSR-E21-65; diaphysis of radius TSR-G21-83; third metacarpals: TSR-G21-63, TSR-C17-53, TSR-

C21-3, TSR-D13-15, TSR-D19-11, TSR-E16-20 (with accessories), TSR-E21-37, TSR-F21-4, TSR-F22-7, TSR-G21-63, TSR-H23-12 (with accessory); proximal parts of third metacarpals TSR-G23-3; distal parts of third metacarpals: TSR-G23-4, TSR-107; diaphysis of third metacarpals TSR-11; distal parts of femur TSR-H21-11; diaphysis of femur: TSR- G20-15, TSR-F18-39, TSR-F16-21, TSR-H18-39; tibia: TSR-C16-22; distal parts of tibia: TSR-G20-52, TSR- G20-49, TSR-G17-20, TSR-C16-25, TSR-D15-8, TSR-E20-15, TSR-F17-32, TSR-G19-6, TSR-G22-5, TSR-52, TSR-180, TSR-193; diaphysis of tibia. TSR-F15-10, TSR-I19-1; third metatarsals: TSR-F18-54 (with accessories), TSR-F18-49 (with accessories), TSR-D16-37, TSR-D20-20, TSR-E19-31, TSR-F17-13, TSR-F17-12, TSR-34, TSR-98, TSR-166 (with accessories); proximal parts of third metatarsals: TSR-8; distal part of third metatarsals TSR-E12-1; diaphysis of third metatarsals TSR-10; calcaneum: TSR-F19-22, TSR-C16-9, TSR-F14-4, TSR-F17-36, TSR-H19-38; astragali: TSR-F18-2, TSR-E16-22, TSR-64, TSR-153; first phalanges: TSR-C17-25, TSR-E21-8, TSR-F20-28, TSR-G19-23, TSR-H18-23; second phalanges: TSR-G18-42, TSR-H21-10; third phalanges: TSR-C17-13, TSR-C17-33, TSR-C18-2, TSR-D14-16, TSR-F17-20, TSR-G19-21, TSR-G21-2, TSR-H16-1, TSR-12, TSR-69, TSR-199; distal parts of third metapodials: TSR-6, 67 (juv.), TSR-E15-2 (juv.?), TSR-E21-1, TSR-H17-3 (JUV.?), TSR-E17-28, TSR-H17-3, TSR-6, TSR-9, TSR-67.

In articulation/in situ: scapula + humerus + radioulna + carpals + third metacarpal + first phalanx +second phalanx + third phalanx +sesamoids TSR-152; humerus (e) + radioulna (d) + carpals (c) + third metacarpal (b) +first phalanx (a) TSR-E16-15; third metacarpal with accessories, carpals TSR-D18-76 + first phalanx TSR-D18-77 + second phalanx TSR-D18-78 + third phalanx TSR-D18-49; radius (b) + carpal (a) TSR-F18-70; humerus (a) + radioulna (b) TSR-G19-14; third metacarpal with accessories (a) + first phalanx (b) TSR-G19-11; distal part of radius (f) + carpals, sesamoids (e) + third metacarpal with accessories (a) + first phalanx (b) + second phalanx (c) + third phalanx (d) TSR-F18-58, sesamoid (a) + sesamoid (b) + first phalanx (c) + second phalanx (d) + third phalanx (e) TSR-F18-53 (possibly articulates with third metacarpal with accessories TSR-F18-68 and radius TSR-F18-66); distal part of humerus (e) + radius with fragmentary ulna (d)+ carpals + sesamoids (c), third metacarpal with accessories (b) + first phalanx (a) TSR-E16-15; carpals + third metacarpal with accessories + third phalanx + sesamoid TSR-62; third metacarpal (a) + accessories (b, c) + first phalanx (d) + sesamoids (e, f) TSR-G19-20; first phalanx with sesamoids +

second phalanx TSR-F18-54; first phalanx TSR-21-57 + second phalanx TSR-21-53 + third phalanx TSR-21-54; first phalanx + second phalanx TSR-G19-18; first phalanx + second phalanx +third phalanx TSR-66; femur (a) + tibia (b) TSR-E18-8; tibia (a) + tarsals (e) +astragalus (b) + calcaneum (c) + third metatarsal with accessories (d) TSR-C18-11; tarsal (b) + tarsal (c) + astragalus (a) TSR-F17-35; distal part of tibia (a) + tarsals, sesamoids, + astragalus + calcaneum (f) + third metatarsal with accessories (b) + first phalanx (c) + second phalanx (b)+ third phalanx (e) TSR-E17-7; third metatarsal with accessories (d) + first phalanx (c) + second phalanx (b)+ third phalanx, sesamoids (a) TSR-F17-31; third metatarsal with accessories (d) + first phalanx (c) + second phalanx (b)+ third phalanx (a) + sesamoids (e) TSR-F17-31; tarsal + third metatarsal with accessories + sesamoid TSR-65; distal part of tibia (h) + tarsals (e) + astragalus (g) + calcaneum (f) + third metatarsal with accessories (b) + first phalanx (b) + second phalanx (a)+ sesamoids (c) TSR-F17-29; distal part of tibia (a) + tarsals (e) + calcaneum (f) + astragalus (g) + third metatarsal with accessories (d) + first phalanx (c) + second phalanx (b) + third phalanx (a) TSR-G20-4; distal part of tibia (h) + tarsals, sesamoids (e) + calcaneum (f) + astragalus (g) + third metatarsal with accessories (d) + first phalanx (c) + second phalanx (b)+ third phalanx (a) TSR-F18-60; distal part of tibia (e) + tarsal (b) + tarsal (c) + tarsal (d) + calcaneum (f) + astragalus (g) + third metatarsal (a) TSR-F18-41; calcaneum (a) + astragalus (b) + second and third metatarsal (c) + first phalanx (d) + sesamoids (e) TSR-G17-23; tarsal + first phalanx + second phalanx TSR-35; first phalanx + second phalanx + third phalanx TSR-97.

Krimni 1. Fragment of cranium with P3-M1 sin/dex KRI-1; in situ dP3-dP4 KRI-7; in situ M1-M2 sin KRI-2; P2 dex KRI-3; P3/4 dex: KRI-5, 42 (fragment); M1/2: KRI-4(sin), 41 (dex, fragment); proximal parts of radius with fragmentary ulna KRI-11, 12, 32; third metacarpals KRI-8, 16; proximal part of third metacarpal KRI-17; distal part of third metacarpal KRI-40 (fragment); fragmentary astragali KRI-14, 15; third metatarsal KRI-9, 19 (a+b); proximal part of third metatarsals KRI-18; distal parts of third metatarsals KRI-20, 22 (fragment / no measurements), 23 (fragment / no measurements).

Krimni 2. p3,4 dex KRM-3; distal part of tibia KRM-4; calcaneum KRM-5; navicular KRM-6; third metatarsal KRM-1; proximal part of third metatarsal KRM-2; first phalanges KRM-7, 8 (fragment); second phalanges KRM-9, 10 (fragment), 11.

Krimni 3. Cranium KMN-50; dp4 dex KMN-29; p2 sin KMN-92; p3,4 dex KMN-30; radius KMN-56; distal part of tibia KMN-16; astragalus KMN-19; calcaneum KMN-

15; proximal part of third metapodial KMN-14; accessories KMN-33; first phalanx KMN-24; third phalanx KMN-25.

In articulation: atlas (a) + axis (b) + cervical vertebrae (c) KMN-45; humerus (a) + radioulna (b) KMN-48; humerus (a) + radioulna (b, c) + scaphoid, lunatum, magnum, sesamoids (d), third metacarpal with accessories (e) KMN-10; distal part of humerus (a) + ulna (fragment) (b) + radius (c) + scaphoid, lunatum, pyramidal, pisiform, magnum, sesamoids (d) KMN-2; third metacarpal with accessories (a) + first phalanx (b) + second phalanx (c) + sesamoids (d) KMN-8; distal part of femur (a) + tibia (b) + astragalus (c) + calcaneum (d) + big cuneiform + navicular, big cuneiform, cuboid small cuneiform (e) + third metatarsal (f) + accessories (g) + first phalanx (h) + second phalanx (i) + sesamoids (j) KMN-43; femur (a) + tibia (b) + astragalus (c) + calcaneum (d) + big cuneiform, navicular (e) + third metatarsal (f) + accessory (g) + first phalanx (h) + second phalanx (i) + third phalanx (j) + sesamoids (k) KMN-44; third phalanx (a) + sesamoid (b) KMN-70 (possibly articulated with KMN-8); possibly articulated: distal part of tibia + astragalus + lunatum KMN-22, 20, 23 respectively.

Petralona. Fragment of maxilla with P1-P3 sin PEC-1700; fragment of maxilla with M1-M3 sin PEC-1701; fragment of maxilla with P4-M1 sin PEC-1885; fragmentary mandibular body with p3-m1 sin PEC-701; fragmentary mandibular ramus with p2-p4 dex PEC-700; DP2 sin: PEC-1858, 1859; DP3,4 sin: PEC-815, 816, 817, 818, 819, 820; DP3,4 dex: PEC-808, 809, 810, 811, 812, 813, 814; isolated P2 sin: PEC-1841, 1844, 1845, 1846, 1850, 1851, 1853, 1857; isolated P2 dex: PEC-1840, 1842, 1843, 1847, 1848, 1849, 1852, 1854, 1855, 1856, 1860, 1861, 1862; isolated P3/4 sin: PEC-1702, 1703,1704, 1706, 1714, 1715, 1718, 1722, 1724, 1725, 1726, 1727, 1728, 1731,1736,1737, 1739, 1740, 1741, 1743, 1745, 1749, 1750, 1752, 1755, 1757, 1759, 1761, 1762, 1763, 1765, 1768, 1769, 1770, 1773, 1823, 1826; isolated P3/4 dex: PEC-1705, 1710, 1713, 1716, 1717, 1720 1721, 1723, 1729, 1732, 1733, 1734, 1735, 1738, 1742, 1744, 1746, 1747, 1748, 1753, 1754, 1758, 1760, 1764, 1772, 1774, 1825, 1827, 1828, 1829, 1830; isolated M1/2 sin: PEC-1707, 1711, 1756, 1766, 1767, 1775, 1779, 1781, 1782, 1783, 1785, 1786, 1789, 1790, 1791, 1792, 1793, 1794, 1794, 1795, 1798, 1799, 1800, 1802, 1803, 1805, 1807, 1809, 1813, 1814, 1815, 1816, 1818, 1819, 1820, 1821, 1824, 1833, 1835; isolated M1/2 dex: PEC-1708, 1709, 1712, 1719, 1730, 1751, 1776, 1777, 1778, 1780, 1784, 1787, 1788, 1796, 1797, 1801, 1804, 1806, 1808, 1810, 1811, 1812, 1817, 1822, 1831, 1832, 1834; isolated M3 sin: PEC-1865, 1869, 1871,

1876, 1877, 1881, 1882, 1883; isolated M3 dex: PEC-1863, 1864, 1866, 1867, 1868, 1870, 1872, 1873, 1874, 1875, 1878, 1884; dp2 sin PEC-692; dp2 dex: PEC-785, 789; dp3 sin PEC-784; dp3 dex: PEC-783, 786; dp4 sin: PEC-788, 795; dp4 dex PEC-787; isolated p2 sin: PEC-682, 683, 684, 685, 686, 687, 688, 689, 690, 691, 693, 694, 697; isolated p2 dex: PEC-680,681, 695, 696; isolated p3/4 sin: PEC-698, 699, 703, 704, 705, 708, 710, 713, 717, 718, 719, 720, 721, 723, 724, 725, 726,728, 729, 730, 731, 732, 734, 763,770, 771, 779, 780, 781; isolated p3,4 dex: PEC-706,707, 709, 711, 712, 714, 715, 716, 722, 727, 735, 736, 737, 742,748, 782; isolated m1/2 sin: PEC-744, 745, 746, 747, 750, 751, 756, 757, 758, 760, 761, 764, 768, 772, 776, 777, 778, 791, 793, 794; isolated m1/2 dex: PEC-740, 741, 743, 749, 752, 753, 754, 755, 759, 762, 765, 766, 767, 769, 773, 774, 775, 790, 792; isolated m3 sin: PEC-796, 797, 798, 800, 801, 802, 805,807; isolated m3 dex: PEC-799, 803, 804, 806; distal parts of humeri PEC-662, 663, 664, 665 (or 554? fragment); proximal part of radius PEC-669; distal parts of radius: PEC-665, 666, 667, 668; scaphoid PEC 599 (fragment); third metacarpals: PEC-500, 501, 502, 503 juv, 504, 505, 506, 507, 508, 509, 510; proximal parts of third metacarpals: PEC-511, 512, 513, 514, 515, 516; distal parts of third metacarpals: PEC-517, 518, 519, 520, 521, 522, 523, 524, 525, 526, 604, 605, 606, 607, 608, 609; fragments of accessories PEC-670, 671, 672; distal parts of tibiae: PEC-620, 621, 622, 623, 624, 625, 626, 627, 628, 629, 630, 631 632, 633, 634, 635, 636, 637, 638, 639, 640, 641; astragali: PEC-593, 594, 595, 596; calcanei: PEC-600 juv., 601; big cuneiforms: PEC-597, 598; third metatarsals: PEC-540, 541, 542, 543, 544, 545, 546, 547, 548, 549, 550, 551, 552, 553, 554, 555, 563+532 602; proximal parts of third metatarsals: PEC-527, 528, 529, 530, 531, 533, 534, 535, 536, 537, 610, 611, 612, 613, 614, 615, 616; fragments of accessories: PEC-673, 674, 675, 676, 677, 678; first phalanges: PEC-565, 566, 567, 568, 569, 570, 571, 572, 573, 574, 575, 576, 577, 578; second phalanges: PEC-579, 580, 581, 582, 583, 617; third phalanges: PEC-584, 585, 586, 587, 588, 589, 590, 591, 618.

Description.

GER-8. Described earlier by Koufos (1992). This is the better well-preserved cranium from Gerakarou. Only the frontal nasal bones and the occipital crest are missing (Figure 5.24). The cranium is slightly laterally compressed. The presence of large canines indicates a male individual. The muzzle seems to be rather slender, however it is slightly compressed. The index 'Breadth of the muzzle x 100/ Length of the muzzle'

(M15 x 100 / M1) is 47.6 mm. The palate is relatively wide and the mean palatal breadth at the level of P4-M1 is >65mm (slightly compressed); its posterior margin is situated at the M2-M3 contact. The major palatal foramen is located at the half of M3. The narial notch is very deep; its hinder margin is placed above the level of the mesostyle of P3. The nasal bones form a groove along their sagittal suture; the frontal nasal bones are missing. The facial crests are well-developed, and their anterior margins are placed at the level of the P4-M1 contact. In lateral view, they are straight. The infraorbital foramens are not preserved on either side. The orbits are rounded-elliptical. There is only one supraorbital foramen, and it is relatively large. No preorbital fossa can be observed with certainty due to the deformation of the maxillary sinuses. The medial border of the retroarticular process is almost straight. The zygomatic process of the frontal bone is relatively short (breadth 23.9 mm). The dorsal edge of the zygomatic arch is directed horizontally at a point behind the orbit. The external acoustic meatus points dorsoventrally at an angle of about 45^{o}. The occipital crest is missing possible due to carnivore attack. The external occipital protuberance is represented by a rough, raised area which is surrounding by a V-shaped depression. The foramen magnum appears as a rectangular opening with its long axis in the horizontal plane. The dorsal border of the foramen magnum is almost straight (it is not notched). In dorsal aspect, the greatest breadth of the cranium is behind the orbits. The mean width of the frontal bones is 157.36 mm.

GER-8 preserves all dentition, and all teeth are in wear (Figure 5.24b). The Galvayne's groove on I3 appears at gum line giving the individual an average age of 10 years old. P1 is still present on the left side, and it is elliptical. Protocone is short on all cheek teeth; on premolars is squarish-shaped while on molars it is elliptical. The lingual border of the protocone is either almost straight (premolars) or slightly convex at the middle (molars). Postprotoconal groove is deeper on premolars than on molars. Hypocone is elliptical and no hypoconal constriction is observed; the hypoconal grooves are deeper on premolars than on molars. Fossettes are always closed. The enamel of their lateral borders is poorly plicated. Pli caballin is present on premolars (on P2 is short, on P3-P4 is rudimentary), while on it disappears on molars.

GER-9. Described earlier by Koufos (1992). The cranium belongs to a young adult (Figure 5.25); all cheek teeth at first stage of wear, canines are slightly worn and the absence of Galvayne's groove on I3 gives an average age between 4-5,5 years old.

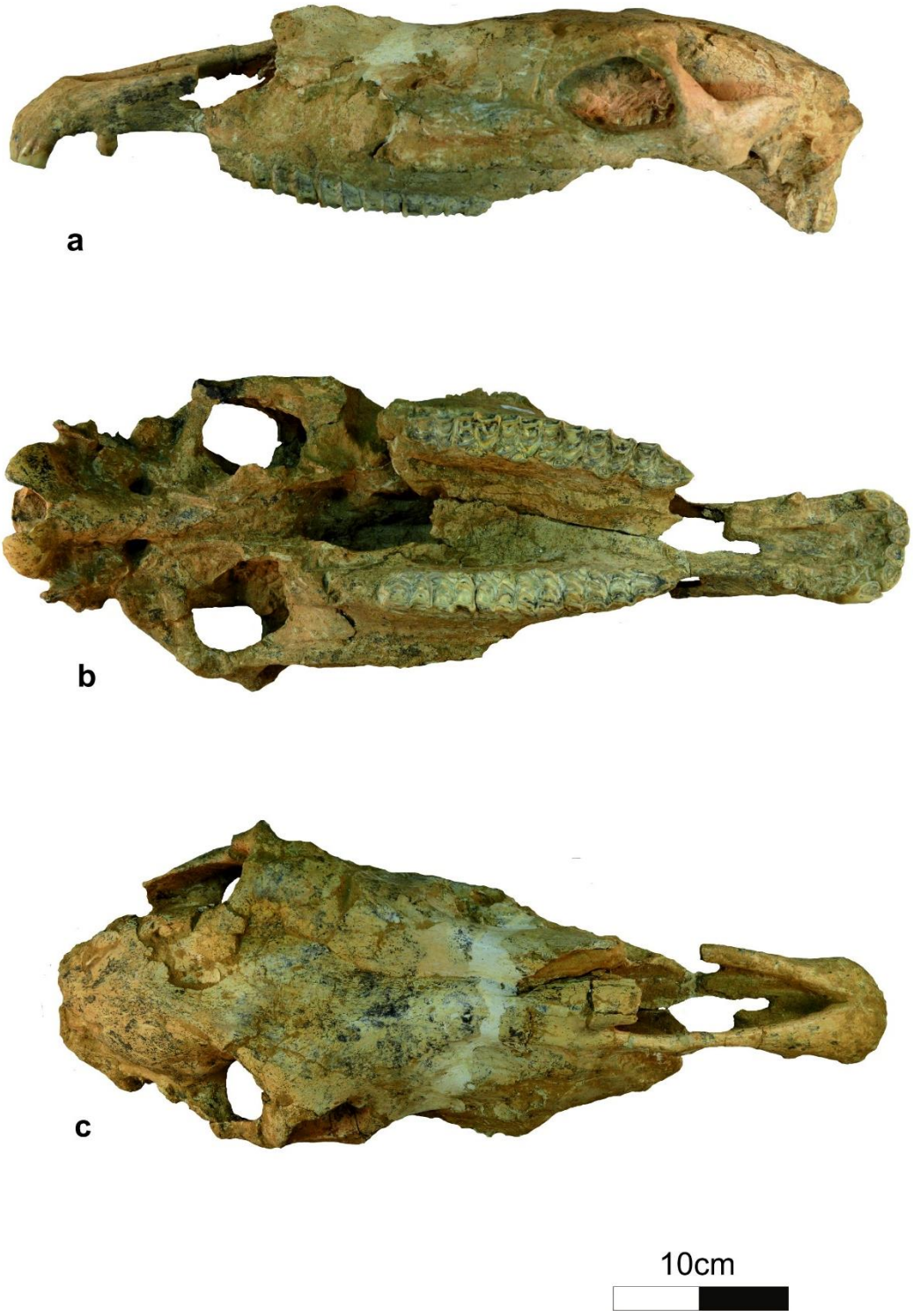

Figure 5.24. *Equus altidens*. GER-8, (a) Left lateral view, (b) ventral view, (c) dorsal view.

The presence of large canines indicates a male individual. It is mediolaterally compressed and lacks the zygomatic arches, the braincase, and the frontal nasal-maxillary bones. The muzzle is short. The index 'Breadth of the muzzle x 100 / Length of the muzzle' (M15 x 100 / M1) is 45.6. The palate and choanae are compressed and the mean palatal breadth at the limit between P4-M1 cannot be measured. The major palatine foramen is possible situated at the anterior half of M3. The facial crests are less developed than all other GER cranium; they do not project laterally. Their anterior border is placed above the P4-M1 contact and on lateral view, they are straight. The depth of the narial notch cannot be measured. The infraorbital foramen is only preserved on the left side of the cranium and is placed above the P4-M1 contact. The orbits are broken on both sides. There is only one elliptical supraorbital foramen, and it is relatively large (5.6 mm). An extremely shallow preorbital fossa is observed in front of the orbits but its margins are not clear. Dorsally, the frontonasal suture forms an angle meeting rostrally in the median plane.

GER-9 preserves all dentition (Figure 5.25b). P1 is present on the left toothrow, but it is half broken. Fossettes are closed and they are simply plicated. Pli caballin is single and short on premolars, on M1 it is absent and on M2-M3 is rudimentary. The anterostyle is rounded on P2. Protocone is short on all cheek teeth and the lingual border is either straight or more convex; its shape varies from squarish (premolars) to elliptical (molars). The postprotoconal groove is very deep especially on premolars. Hypocone is elliptical and on M3 it is isolated forming a circular islet. The hypoconal constriction is rudimentary (premolars, M2) or absent (M1, M3).

GER-31. Described earlier by Koufos (1992). The cranium is well-preserved despite the slight dorsoventrally compression; only the snout is missing (Figure 5.26). It is the only cranium from Gerakarou where the entire occiput is preserved. It belongs to an old individual. The narial notch is deep and its posterior border is situated above the mesostyle of M3. The groove that forms along the sagittal suture of the nasal bones is rather deep. The palate is relatively wide. The mean palatal breadth at the limit between P4-M1 is 73.6 mm. The choanae is large and oval-shaped and its anterior margin is situated at the parastyle of M3. The major palatine foramen is placed at the middle of M3. The facial crests are well-developed, and they strongly projected laterally; their anterior border is placed at the middle of M1. The orbits are extremely elliptical possibly due to the deformation of the cranium. There are two supraorbital foramina: a minor foramen that is minute and a major foramen that is twice that (5.4 mm). No

preorbital fossa can be observed. The medial border of the retroarticular process is almost straight. The zygomatic process of frontal bone is relatively short (breadth 24.9 mm). The dorsal edge of the zygomatic arch is directed horizontally at a point behind the orbit. The external acoustic meatus points dorsoventrally at an angle of about 45^{o} like on GER-8.

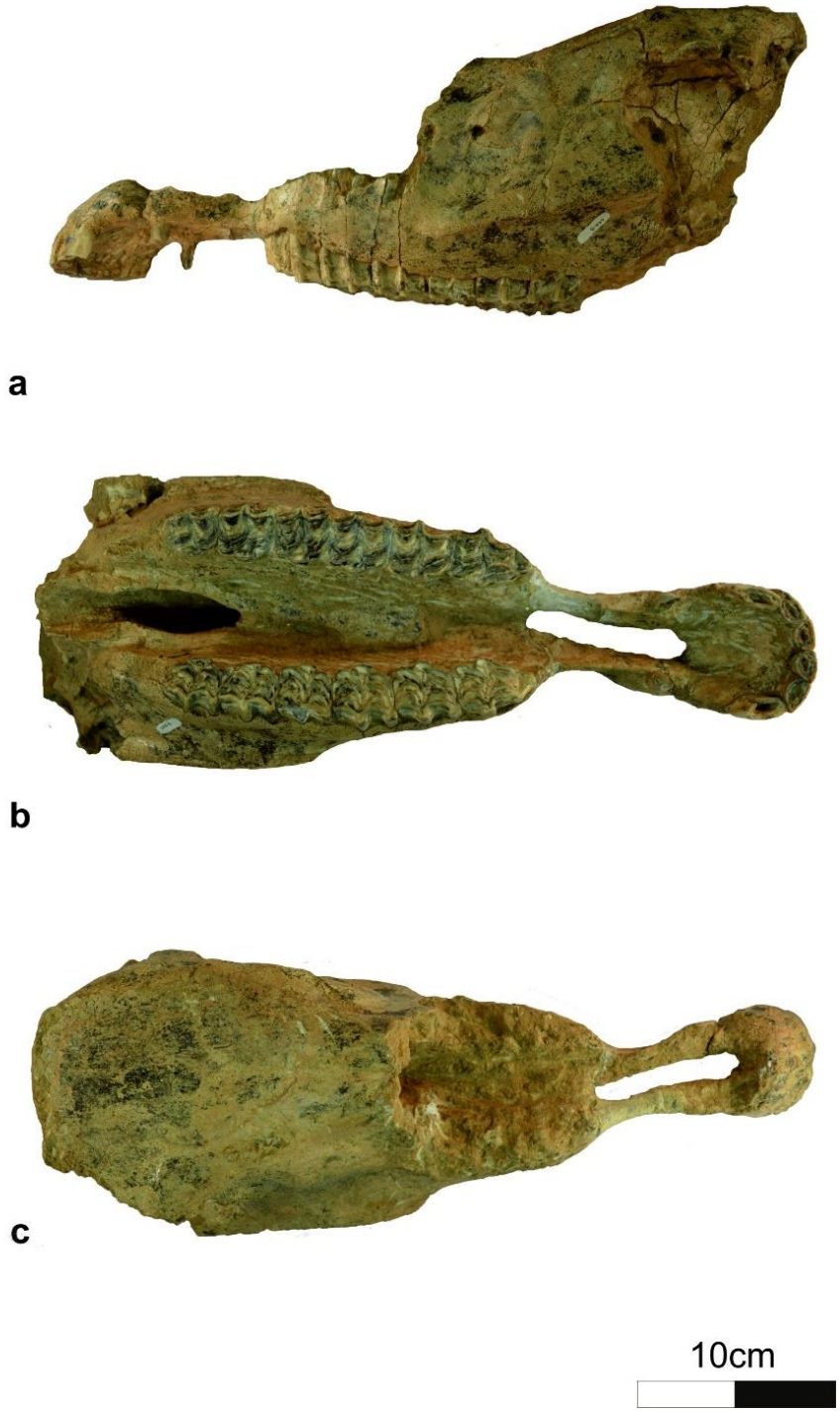

Figure 5.25. *Equus altidens*. GER-9, (a) Left lateral view, (b) ventral view, (c) dorsal view.

The external occipital protuberance is represented by a rough, raised area which is surrounding by a V-shaped depression like on GER-8. The external occipital process is strongly projecting posteriorly and overcomes the posterior margin of the occipital condyles. It is a typical feature of donkeys and of some hybrids (Barone 1976, Arloing 1882; Hanot et al. 2017). The foramen magnum appears as a rectangular opening with its long axis in the horizontal plane. The dorsal border of the foramen magnum is almost straight. In dorsal aspect, the face is wide, and the greatest breadth of the cranium is behind the orbits. The mean width of the frontal bones is 167.36mm.

Fossettes are closed, the enamel is poorly plicated and on M1 completely worn. Protocone is short and its lingual border varies from convex to straight; on premolars it is squarish while on molars it is elliptical-triangular. Postprotoconal groove is relatively shallow on all cheek teeth. Hypocone islets are formed on P2, P3 and M3.

GER-122. Described earlier by Koufos (1992). The cranium is dorsoventrally compressed, and the braincase is missing (Figure 5.27). It belongs to a male adult (M3 and canines are in full wear). The narial opening is very deep; its hinder margin situated above the mesostyle of P3 on the left and a bit further on the right side (parastyle of P4). This slightly 'reposition' of the opening occurs because of the distortion of the cranium. The muzzle is short and slightly broader than the other GER crania, especially at the posterior borders of I3 (M 15). The index 'Breadth of the muzzle x 100/ Length of the muzzle' is 55, versus 47.6 and 45.6 on GER-8 and GER-9, respectively. The palate is relatively wide. The mean palatal breadth at the limit between P4-M1 is 74.1 mm. The choanae is oval-shaped and its anterior border is situated at the anterior half of M3. The major palatine foramen is placed at the middle of M3. The facial crest is well-developed, and its anterior border lies on the limit of P4-M1 contact. Orbits are rounded and they are placed posteriorly enough of the third molar. No preorbital fossa can be observed with certainty. The zygomatic arches run parallel to the sagittal plane of the cranium.

The Galvayne's groove on I3 is at its full length giving the individual an average age of 20 years old. P1 is present, short, and elliptical and is does not reach the occlusal level of P2. The anterostyle on P2 is relatively short and pointed. Protocone is short and its lingual border is always straight (Figure 5.27): on P2 it is rounded, on P3-M2 it is 'squarish' to semilunar and on M3 it is atractoid. M1 lacks pli caballin while on all the other cheek teeth it is rudimentary. The plication of the fossettes is simple on all cheek teeth.

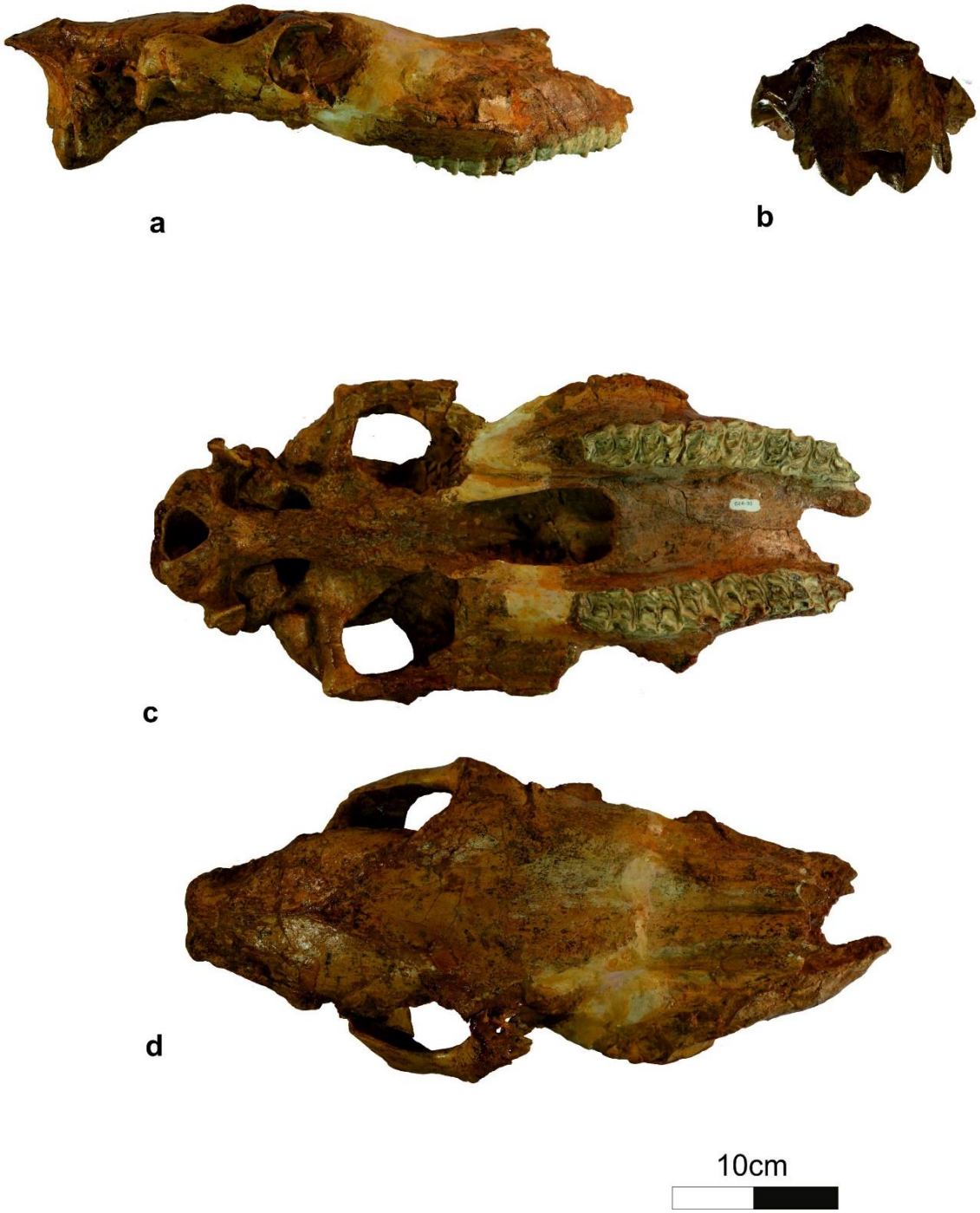

Figure 5.26. *Equus altidens*. GER-31, (a) Right lateral view, (b) occiput, (c) ventral view, (d) dorsal view.

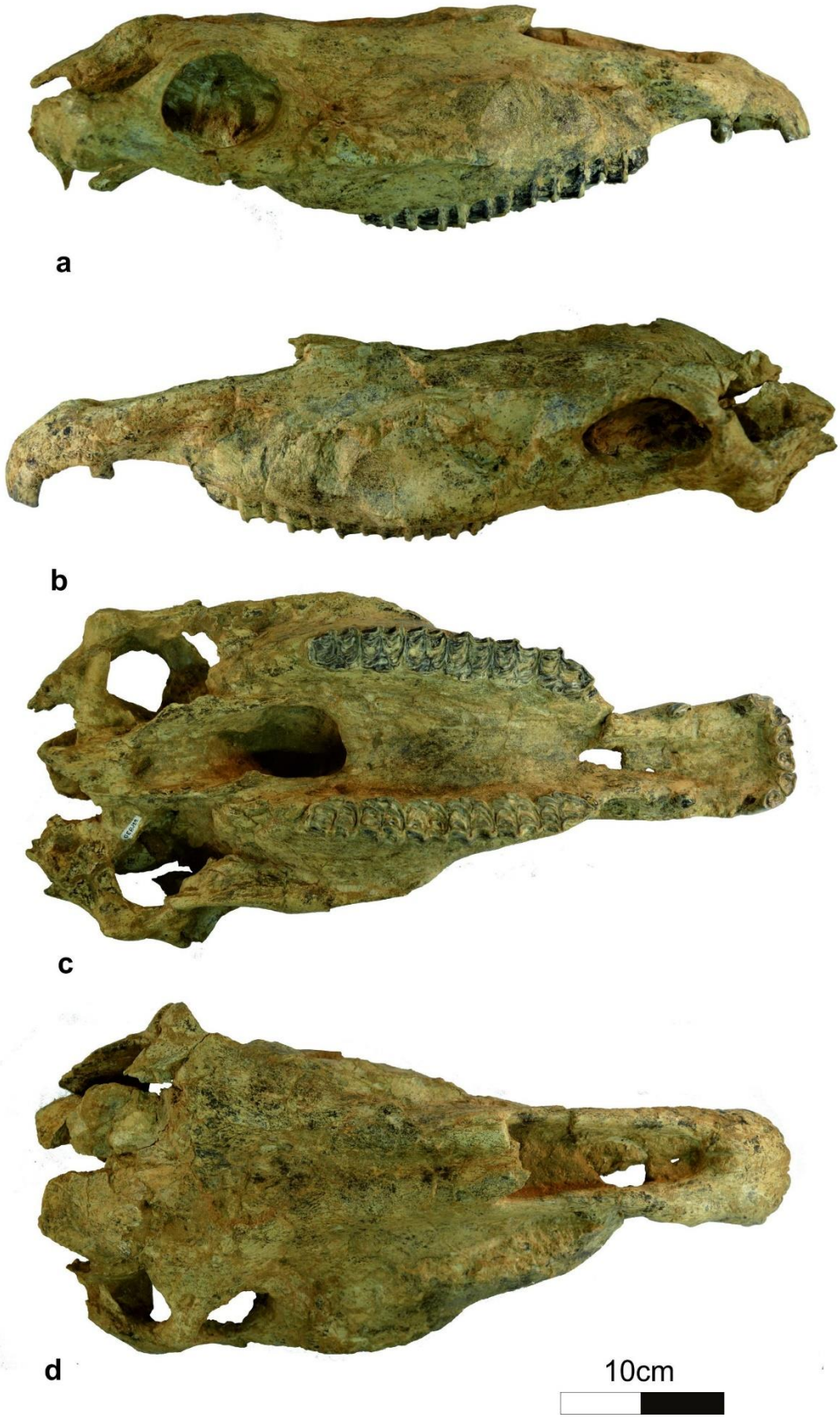

Figure 5.27. *Equus altidens*. GER-122, (a) Right lateral view, (b) left lateral view, (c) ventral view, (d) dorsal view.

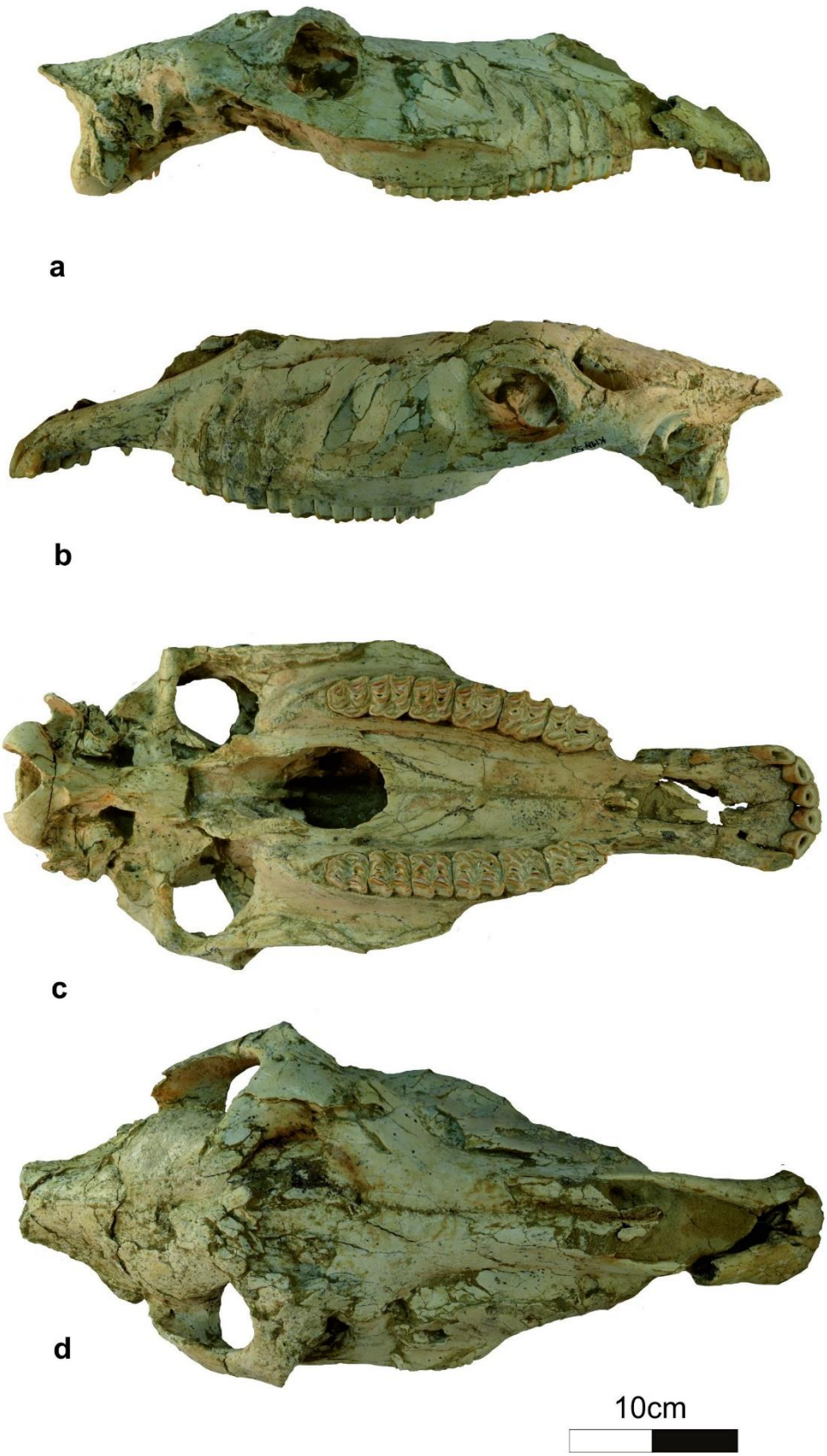

Figure 5.28. *Equus altidens*. KMN-50, (a) Right lateral view, (b) left lateral view, (c) ventral view, (d) dorsal view.

KMN-50. The cranium is complete and incredibly well-preserved with a slightly dorsoventrally compression (Figure 5.28); only the nasal bones (rostral processes) are damaged during the excavation. The cranium belongs to a young individual up to 5 years old; M3 is in wear, canine is unworn and no Galvayne's groove is observed on I3. The presence of the canines indicates that it belongs to a male individual; the right canine is fully emerged, while the left canine is remarkably rudimentary. The narial notch is deep and its hinder margin is situated above the anterior half of P3. A groove runs along the sagittal suture of the nasal bones. The muzzle is short and wide. The index 'Breadth of the muzzle x 100/ Length of the muzzle' is 171.5. The palate is relatively wide. The palatal breadth at the level of P4-M1 is 85.1 mm. The major palatine foramens are placed at the anterior half of M3. The choanae are oval-shaped and their anterior margin is situated at the middle of M2. The medial border of the retroarticular process is almost straight. The facial crest is well-developed; its anterior border is placed caudally at the level of P4-M1 contact; in the profile view, the crest is almost straight. The infraorbital foramen is situated slightly posteriorly above the parastyle of M1. The orbits are rounded. There is only one supraorbital foramen, and it is relatively large (5.4 mm). No preorbital fossa can be observed with certainty due to the crashed maxillary sinuses. The greatest breadth of the cranium is behind the orbits. The retroarticular process is relatively short laterally at the same level with the articular surface of the fossa mandibularis. The zygomatic process is strong and significantly broad (breadth 32.16 mm) (unlike *E. quagga burchelli*) and the supraorbital foramen is rather short and elliptical. The dorsal edge of the zygomatic arch is directed horizontally at a point caudal to the orbit. The frontonasal sutures meet at an angle rostrally in the median plane. The external sagittal crest is relatively long. The occiput is complete. The foramen magnum is wide (resembles a rectangular) and internally it is elliptical. The nuchal crest of the occiput is placed horizontally. The dorsal border of the foramen magnum is almost straight [like on *E. quagga burchelli*, unlike *E. zebra* on which there is a distinct median notch (Berry 2020)]. The external occipital protuberance consists of a rough, projected laterally area which is surrounded by a V-shaped depression like on GER crania (Smuts and Penzhorn 1988). The paracondylar processes have broken edges and they are not outreaching the level of the condyles.

P1 are present on both sides with rectangular-elliptical shape, and they are remarkably long (Figure 5.28). They both reach the occlusal level of P2. The anterostyle on P2 is rounded and relatively elongated. Protocone is short on all cheek teeth; its shape varies

from triangular to semilunar/elliptical. Postprotoconal groove is relatively shallow. The lingual border of the protocone is either straight or slightly convex. Fossettes are closed and the plication is simple. Pli caballin is rudimentary on premolars and absent on molars.

Mandible. There are three more or less complete mandibles from Gerakarou (GER-32, 33, 34) originally described by Koufos et al. (1992), several mandibular remains from Gerakarou, Libakos and Tsiotra Vryssi, but none from the Krimni sites. GER-33 (Figure 5.29a) is complete and only the left coronoid process and condyle are missing. The mandible belongs to a male adult individual based on the presence of large canines and the stage of the attrition (m3 in wear, canines not in wear). The rami are slightly reflected distally (they are not vertical). GER-32 belongs to an old female individual; preserves all dentition, there are no canines and cheek teeth are very worn. The ramus and a part of the left body and the right coronoid process and condyle. are missing. GER-34 belongs to a young adult male: unworn canines, m3 in wear, the muzzle is preserved and parts of the bodies. In both GER-32 and GER-33, the rami are slightly reflected distally (they are not vertical), the vascular notch is apparent, the mental foramen is single and there is no acute angle at the junction of the interalveolar border with the border of p2 (observed also in GER-33) (Figure 5.29a). The morphology of the cheek teeth is typically stenonoid with V-shaped linguaflexids (Figure 5.29c). The ectoflexid in molars is always penetrating the isthmus and sometimes reaches and flattens the linguaflexid. The metaconids are rounded and the lingual border of the metastylids tends to be more pointed on premolars than on molars. In Tsiotra Vryssi, most of the mandibular remains are extremely fragmentary, because they derive from the upper layers of the site and only the lengths of the premolars and molars can be measured. In the muzzle, TSR-E21-58, the presence of the canines indicates a male individual. In TSR-D20-17, there is no acute angle at the junction of the interalveolar border with the border of p2 like in the GER samples.

Although the cheek teeth in many mandibular remains are fragmentary, they exhibit the following characters: V-shaped linguaflexid, often flattened by the ectoflexid on molars, usually shallow to intermediate ectoflexid on premolars, while on molars is always deep, penetrating the isthmus between the inner fossettes. In LIB-727, the interalveolar border with the border of p2 join in a way that the junction forms an angle of almost 90 degrees unlike the GER and TSR samples and LIB-540. The cheek teeth are similar in morphology with Gerakarou.

Figure 5.29. *Equus altidens*. (a) Mandible, GER-33: (a1) right lateral view, (a2) left lateral view, (a3) occlusal view; (b) mandibular fragment, GER-71: (b1) occlusal view, (b2) left lateral; (c) mandibular fragment, PEC-697: (c1) occlusal view, (c2) left lateral.

Upper cheek teeth. The morphology of the upper cheek teeth from Gerakarou and Krimni-1 were originally described by Koufos et al. (1992), from Libakos and Polylakkos by Steensma (1988) and Gkeme (2016) and from Petralona Cave by Tsoukala 1989. The anterostyle on P2 is relatively short and rounded (GER-36, KRI-3). The fossettes are closed and they do not communicate except for the slightly worn

teeth. The enamel of their borders is simply up to moderate plicated. The parastyle is well-developed, relatively wide, and strongly projected labially, while the mesostyle is also well-developed, less wide than the parastyle and projecting labially. The protocone is short on all cheek teeth (on molars is slightly more elongated) and the lingual border is either straight or more convex; its shape varies from squarish (premolars) to semilunar-elliptical (molars) (Figure 5.28c). The postprotoconal groove is relatively deeper on premolars on the first stages of wear (Figure 5.24b); on the same series, the postprotoconal groove is deeper on premolars than on molars (GER-8, GER-122). The hypocone is rounded and elliptical shaped; on M3, it can be isolated and form an islet (LIB-, TSR-E20-7, TSR-G21-28). The hypoconal constriction is either rudimentary, slightly stronger, or absent. The hypoconal groove is more or less pointed and relatively deeper on premolars than on molars. The pli caballin is usually short and single on all cheek teeth, and it disappears on very worn teeth; on the slightly worn teeth it can be longer or multiplied.

Lower cheek teeth. Most of the material comes from Libakos (mostly with isolated teeth) originally described by Steensma (1988) and later by Gkeme (2016) and Petralona Cave (Tsoukala 1989). The material from Tsiotra Vryssi (Konidaris et al. 2015) and Gerakarou (Koufos et al. 1992) mainly consisted of cheek teeth series, while only three isolated premolars are available from the Krimni sites. The morphology of the linguaflexid is typically stenonoid (V-shaped and pointed) (Figures 5.29a3, b1, c1). The ectoflexid is shallow on premolars, while on molars it is deeper penetrating the isthmus formed between the inner fossettes; in many cases, the linguaflexid is flattened by the ectoflexid (e.g., GER-12, TSR-D20-17, TSR-G17-19 among others). The metaconid is rounded and the metastylid rounded (cyclic or elliptical-shaped) and its lingual border tends to be more pointed on premolars than on molars. The entoconid is squarish on premolars, while on molars is more elliptical. In some cases, there is a pli on the lateral part of the preflexid (e.g., TSR-G21-46) and the post flexid is occasionally slightly wrinkled (e.g., TSR-D20-17). The pli caballinid is usually absent rudimentary or single on premolars, while on molars it is absent. On GER-71, there is a single pli protostylid on p2.

Third metacarpals. The slenderness index (SI 2) for Gerakarou ranges from 17.9–18.8 (n = 10; mean = 18.4), for Libakos from 17.3–20.0 (n = 16; mean = 18.6), for Tsiotra Vrysi from 17.6–18.9 (n = 16; mean = 18.1), and for Petralona Cave from 17.9–19.5 (n = 8; mean = 18.3). For Krimni-1 the slenderness index is calculated 17.5 (n=1) and

Krimni-3 ranges between 18.7-18.8 (n=2) respectively. The keel index varies between 125.1–131.9 (n = 11; mean = 128.2) for Gerakarou, between 120.2–137.5 (n = 25; mean = 129.5) for Libakos, between 121.7–129.4 (n = 16; mean = 125.2) for Tsiotra Vrysi, for Polylakkos the keel index is calculated 136.8 (n = 1), from 128.9–191.2 (n = 2; mean = 124.1) and 127.7–128.8 (n = 2; mean = 128.2) for Krimni-1 and Krimni-3 respectively, and for Petralona Cave from 121.6–132.4 (n = 17; mean = 127.3).

Third metatarsals. The slenderness index (SI 2) for Gerakarou ranges from 14.7–17.0 (n = 13; mean = 15.7), for Libakos from 15.0–17.2 (n = 32; mean = 16.2), for Tsiotra Vrysi from 15.3–17.4 (n = 11; mean = 15.9) and for Petralona Cave from 14.6–16.7 (n = 16; mean = 15.5). The slenderness index (SI 2) for Krimni-1 varies from 16.2 - 16.4 (n = 2; mean =16.3), Krimni-2 is calculated 15.3 (n = 1) and Krimni-3 ranges between 15.8-15.9 (n = 2; mean = 15.85). The keel index varies between 131.1–140.8 (n = 13; mean = 136.7) for Gerakarou, between 123.7–144.5 (n = 29; mean = 136.1) for Libakos, for Petralona Cave from 123.9–141.3 (n = 32; mean = 131.4), for Tsiotra Vrysi from 125.2–138.3 (n = 13; mean = 132.7). The keel index for Krimni-1 is calculated 131.4 (n = 1), for Krimni-2 ranges between 129.5 – 136.4 (n = 3; 134.9) and Krimni-3 ranges between 130.1-133.5 (n = 3; mean = 132.0).

Comparison and discussion.

The crania from Gerakarou are moderate in size and they are shorter in length (M6) than all subspecies of *E. stenonis* and *E. senezensis*, but longer than *E. stehlini*. The facial crest on every cranium from Gerakarou, unlike *E. stenonis* (where it is concave), it is almost straight resembling *E. simplicidens* (Figures 4b, d in Cirilli et al. 2019). The occiput forms a depression like in *E. simplicidens* (Bernor et al. 2019), Grévy's zebra and unlike *E. apolloniensis* (Figure 5d in Gkeme et al. 2021). The depth of the narial opening is shorter, at the anterior half or parastyle of P3, while in *E. senezensis* and *E. stehlini* it is retraced to P3 mesostyle. The length of naso-incisival notch (M30) is longer in *E. stehlini* showing the same specialization with *E. senezensis*, while the length of the cheek is shorter (M31). The muzzle of the Gerakarou crania is slenderer. The forehead of *E. stehlini* is transversally undulated, while in the case of GER crania it is almost straight.

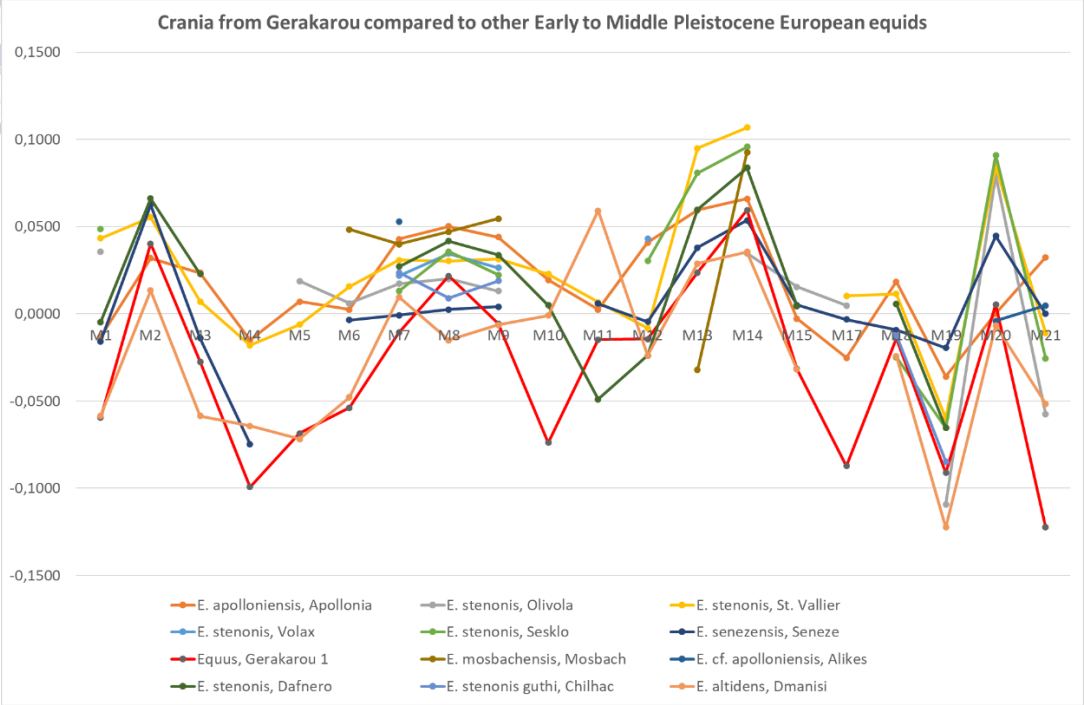

Figure 5.30. Simpson's log ratio diagrams comparing the cranial dimensions of *E. stenonis mygdoniensis* with other equids from Greece and Europe. Standard: *Equus grevyi* (Eisenmann 2007). Data from Bernor et al. (2021) and personal dataset.

The crania from Gerakarou in comparison with *E. stenonis* are much shorter and slenderer than all *E. stenonis* subspecies from Greece and the rest of Europe (Figure 5.30). The crania of the GER equid are characterized by shorter naso-incisival notch (M30) and shorter cheek length (M31), but the ratio is rather similar (Figure 5.30). The naso-incisival notch (M30) is slightly deeper on *E. senezensis*. The GER equid seems to have the shortest muzzle (M1) than all stenonoid equids. The cheek teeth length (M9) and the premolar length (M7) are similar to those of *E. senezensis*, while the molar length is relatively larger (M8); the dimensions are quite smaller than all *E. stenonis* subspecies and larger than *E. stehlini* (Figure 5.31). The analogies of the palatal length (M2), vomerine length (M3) and post-vomerine length (M4) are similar between the GER equid and *E. senezensis* with the ones from the latter being slightly larger. If according to Eisenmann and Baylac (2000), the post-vomerine length (M4) can be interpreted as an estimation of the brain case, the GER equid has a short braincase compared the basilar length (M6), shorter than *E. stenonis* and slightly greater than *E. senezensis* (Figure 5.30).

The new cranium from Krimni-3 (KMN-50; Figure 5.28) is similar in size and morphology with those from Gerakarou and thus they belong to the same species. The

cranium KMN-50 resembles in length (M6) the cranium GER-8. The muzzle is short like the latter. The narial opening is relatively deep like in the GER crania. Both crania, exhibit a depression on the occiput, unlike the APL crania. The post-vomerine length (M4) compared to the basilar length (M6) is short like the case of crania from Gerakarou. The crania from Gerakarou and Krimni-3 are quite similar in size and morphology (Figure 5.31) with the cranium Dm53/59.3.B1gl.192 from Dmanisi that was recently attributed to the species, *E. altidens* by Bernor et al. (2021); those authors' cluster analysis has shown that the crania from Dmanisi and Gerakarou are grouped together, and they are morphometrically similar to *E. quagga* and *E. hemionus*. There are some morphological differences between the GER, KMN and DMA crania. The most recognisable difference lies on the depth of the narial opening; in the Greek samples the narial notch is deep extending above the anterior half or parastyle of P3, while the one from Dmanisi (*E. altidens*) is slightly shallower, reaching above the mesostyle of P2 (Figure 5A in Bernor et al. 2021); this feature is found in all crania from Gerakarou and the one from Krimni-3. Furthermore, in *E. altidens* the dorsal edge of the zygomatic arch is directed dorsoventrally in contrast to its horizontal position in the Greek sample. Another difference is the slightly wider palate (M13) and possibly wider muzzle (M15) of the GER crania. The retroarticular processes seem similar on both *E. altidens* and the GER equid, slightly laterally outreaching the level of the articular surface of the mandibular fossa. The nuchal crest is extending backwards further in KMN-50 (Figure 5.28). The position of the external acoustic meatus is the same for both samples. On all crania from Gerakarou the length of the molars (M8) is always greater than the length of the premolars (M7), while on KMN-50 (Krimni-3) is analogous to *E. altidens* from Dmanisi; however, the one from Krimi-3 belongs to a young adult while the one from Dmanisi to an old individual. The ratio between the length of the cheek (M30) and the narial opening (M31) is rather analogous.

In Figure 5.32, PCA was conducted on selected cranial measurements based on Bernor et al. (2021) analysis. PC1 (76,14%) separates species by their basilar length (M6) from negative to positive values (less elongated crania to more elongated), while PC2 (9.26%) clusters species by their post-vomerine length (M4) and post-palatal length (M5) from negative to positive (more to less elongated). The European *E. stenonis* (Upper Valdarno, Saint-Vallier) is closely related to *E. grevyi* and *E. koobiforensis*. *Equus apolloniensis* is clustered with *E. simplicidens* by its reduced M4 values. *Equus senezensis* is closely related to *E. stenonis* but the cranium is much less elongated. The

equid from Gerakarou is closely related to hemiones and *E. altidens* from Dmanisi (Georgia) and it is well separated from *E. senezensis* and the European *E. stenonis*. The cranium from Krimni-3 (KMN-50) is also closely related to those from Gerakarou with a slightly wider palate (M2). No complete crania of *E. stehlini* and *E. a. granatensis* makes the comparisons rather difficult.

The mandibles originally attributed to '*E. stenonis mygdoniensis'* are few. There is a complete mandible from Gerakarou (GER-34) and several fragments of mandibles (badly preserved) from Gerakarou and Tsiotra Vrysi. The vascular notch is present in the GER equid (Figure 5.29a2), *E. stehlini* and *E. altidens* from Dmanisi. Comparing the mandibles of the GER equid to those of *E. stenonis* (Figure 5.33), the latter clearly displays larger dimensions, and the teeth rows are quite longer. The specimens TSR-E19-7 and TSR-154 from Tsiotra Vrysi exhibit long cheek tooth rows (M3, M4, M5) analogous to *E. apolloniensis* and Volos samples (Figure 5.33). The GER equid and *E. altidens* from Dmanisi are shorter in general size from all the other stenonoid species.

In Figure 5.34, the mandibles from Gerakarou and Tsiotra Vrysi are being compared to *E. altidens* from Dmanisi, *E. altidens granatensis* from Venta Micena and *E. stehlini* from several sites of Italy. The mandibles from Gerakarou are resembling *E. altidens* on the height of the jaw between p4-m1 (M11) and in front of the p2 (M12), while the height posterior of m3 is shorter in Gerakarou's samples. The lengths of the premolars and molars is slightly shorter in *E. altidens*. The samples from Venta Micena are larger from both *E. altidens* and GER equid, but the general proportions are quite similar (lines are parallel to one another). In most cases, *E. stehlini* samples are shorter in overall dimensions (especially at the lengths of the cheek tooth rows). As it seems, the mandibles TSR-E19-7 and TSR-154 from Tsiotra Vrysi are quite larger than all mandibles from Gerakarou with longer cheek tooth rows (M3, M4, M5) and thus larger teeth. The mandible TSR-G21-46 is intermediate in size, close to *E. a. granatensis* lower cheek teeth lengths (M3, M4, M5).

The morphology of the upper and lower dentition is this taxon is typical stenonoid. '*E. stenonis mygdoniensis'*, *E. senezensis* and *E. altidens* (including *E. a. granatensis*) display rather short protocones similarly to *E. stenonis* (Alberdi et al. 1988; Eisenmann 2017; Koufos 1992a), while *E. stenonis vireti* and *E. apolloniensis* display slightly longer protocone on the premolars. The protocone on the upper cheek teeth is short like *E. altidens* from Dmanisi, *E. stenonis* from Dafnero sites and *E. a. granatensis*: the latter appears to have the shortest protocone together with Gerakarou (Figure 5.57).

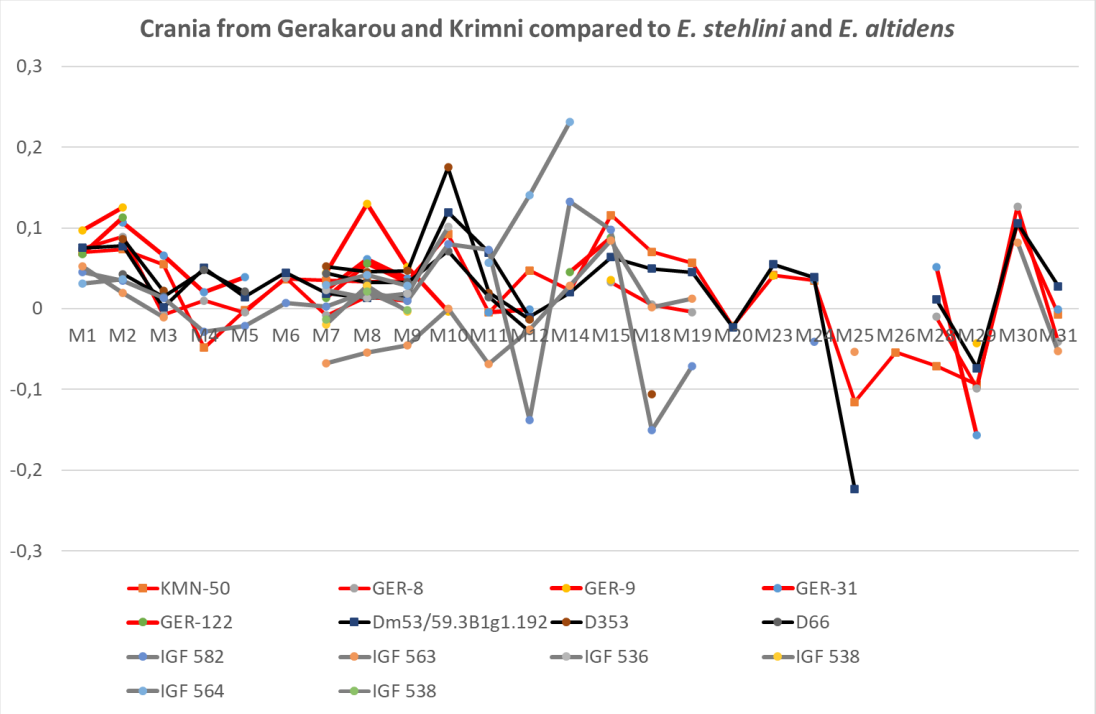

Figure 5.31. Simpson's log ratio diagrams comparing the crania from Gerakarou and Krimni-3 (red) to *E. altidens* (black; Dmanisi) from Dmanisi and *E. stehlini* (grey; Le Ville, Terranuova, Valdarno indet.). Standard: *Equus hemionus onager*. Data from Bernor et al. (2021) and personal dataset. Additional data for *E. stehlini* from Cirilli (2022).

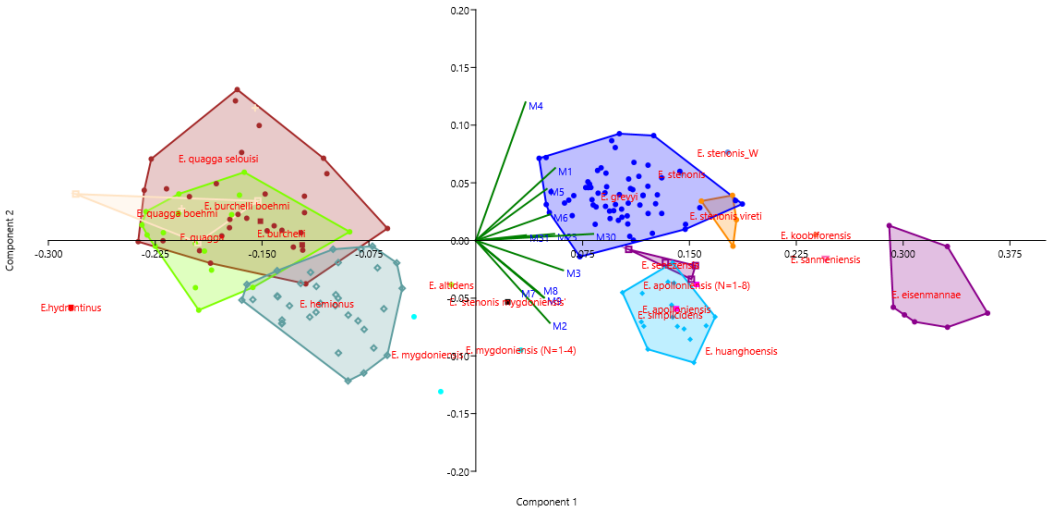

Figure 5.32. Principal component analysis (PCA), loading selected cranial measurements (based on Bernor et al. (2021) analysis) of the crania from Gerakarou and Krimni-3 compared to *E. apolloniensis* (Apollonia), *E. altidens* (Dmanisi) and various extant and fossil equids. Data from Bernor et al. (2021), Cirilli (2022), Van Asperen et al. (2012), https://vera-eisenmann.com/, and personal dataset.

The protocone of the Krimni-1,3 is also short on both molars and premolars, however a single larger specimen from Krimni-1 (fragment of maxilla, KRI-21) attributed to *E.* cf. *stenonis* exhibits slightly longer protocone on the premolars. The protocone length of the equids from Tsiotra Vrysi, Libakos and Petralona Cave is rather similar to each other (Figure 5.57). *E. apolloniensis* appears to have the longest protocone on the premolars similar to *E. stenonis vireti*. The length versus the breadth at the base (1 cm from the roots) is plotted in Figure 5.35. The data from Gerakarou, Tsiotra Vrysi and Krimni is limited because most of the teeth are in situ and not isolated. However, in Libakos and Petralona there are plenty of isolated teeth. There are no significant differences between the dimensions of the cheek between equids with more or less similar size. The premolars (P2, P3/4) of the GER equid overlap with those of *E. altidens* from Süssenborn and Dmanisi and the PEC equid, while *E. senezensis* exhibits slightly larger dimensions although within the range of *E. altidens*. The GER equid overlaps with *E. stehlini* in both premolars and molars. The larger teeth from Tsiotra Vrysi and a single specimen from Vassiloudi plot close to *E. suessenbornensis* although outside its range of variability. *E. apolloniensis* appears to have similar dimensions with *E. suessenbornensis*, yet wider.

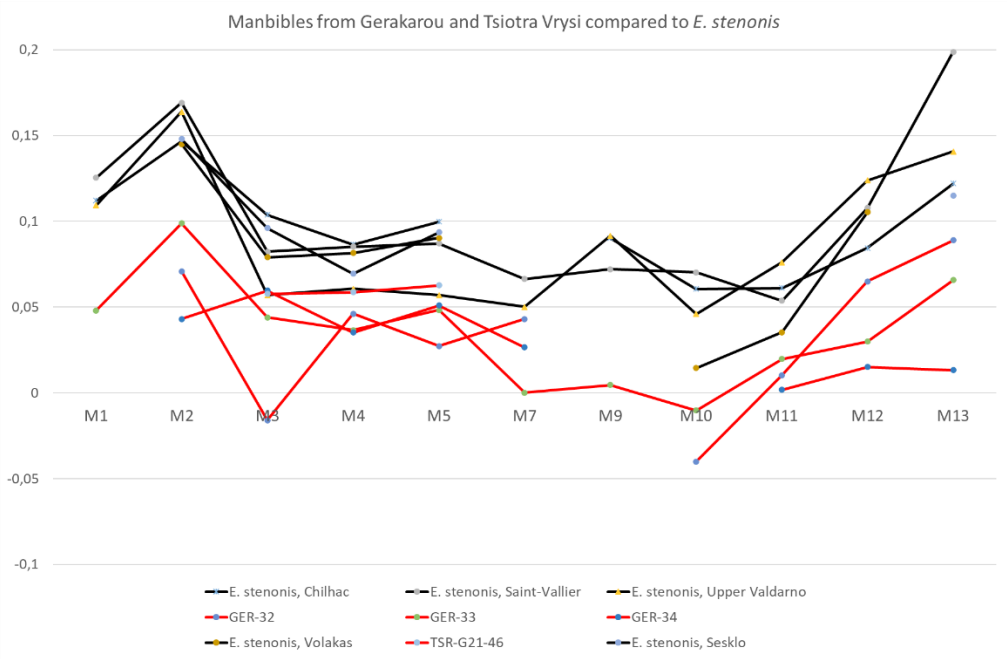

Figure 5.33. Simpson's log ratio diagrams comparing the mandibular dimensions of the equids from Gerakarou and Tsiotra Vrysi to *E. stenonis* (Chilhac, Volax, Sésklo, Saint-Vallier, Upper Valdarno). Standard: *Equus hemionus onager*. Data from Bernor et al. (2021), Van Asperen et al. (2012) and personal dataset.

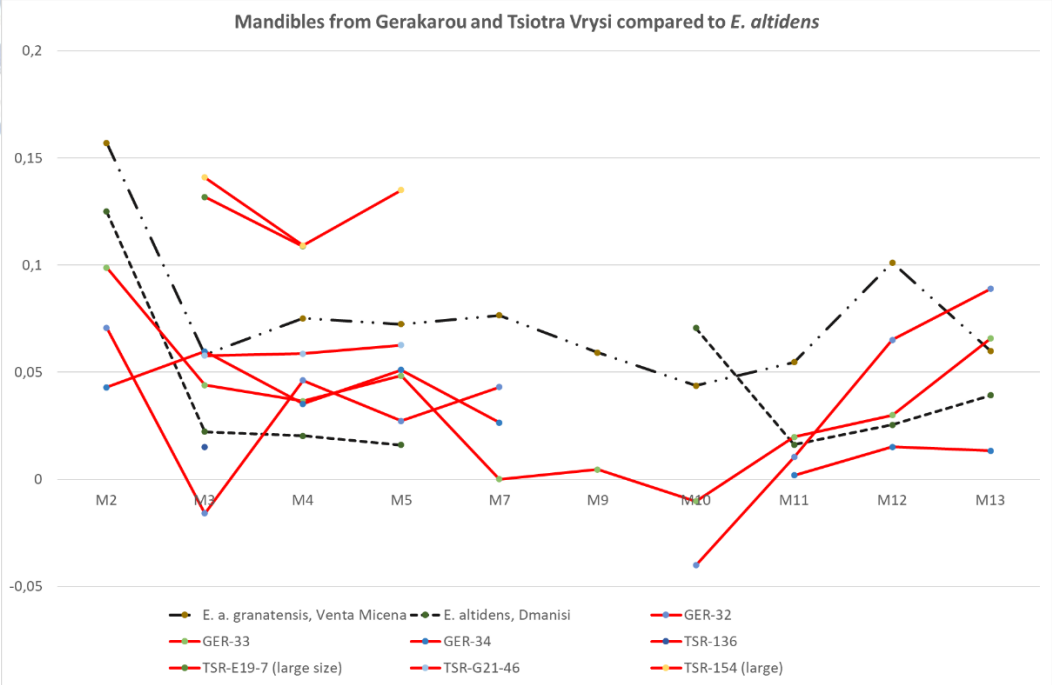

Figure 5.34. Simpson's log ratio diagrams comparing the mandibular dimensions of the equids from Gerakarou and Tsiotra Vrysi to *E. stenonis* (Chilhac, Volax, Sésklo, Saint-Vallier, Upper Valdarno). Standard: *Equus hemionus onager*. Data from Bernor et al. (2021), Van Asperen et al. (2012) and personal dataset.

The bivariate plots of the length of premolar row (M3) versus the length of the molar row (M4) of the lower cheek teeth are demonstrated in Figure 5.11. *E. stehlini* exhibits the shortest dimensions among the entire sample along with two specimens from Dmanisi. *Equus senezensis* and Tsiotra Vrysi (partim) mainly exhibit intermediate dimensions between the *E. stenonis* from Upper Valdarno Basin and the smaller *E. altidens* and *E. stehlini*. The equid from Gerakarou exhibits intermediate dimensions between *E. senezensis* and *E. stehlini*, though mainly overlapping with *E. senezensis* and *E. altidens* from Pirro Nord. *E. apolloniensis* from Apollonia and Volos exhibit larger dimensions even from *E. stenonis vireti*. The two specimens from Tsiotra Vrysi that belong to a larger *Equus*, plot close to *E. apolloniensis*, but not within its range.

The shape of the double knot is typically V-shaped. The double knot belonging to medium sized species such *E. senezensis*, *E. altidens* and *E. stehlini* is rather similar in length. Figure 5.36 demonstrates the bivariate analysis of the length versus the breadth at the base for each tooth for several Early to Middle Pleistocene European equids. The GER equid overlaps with the PEC equid, *E. stehlini* and *E. senezensis* (partim). Tsiotra Vrysi mostly plots together with *E. senezensis* and *E. altidens* from Süssenborn, yet in the range of the GER equid.

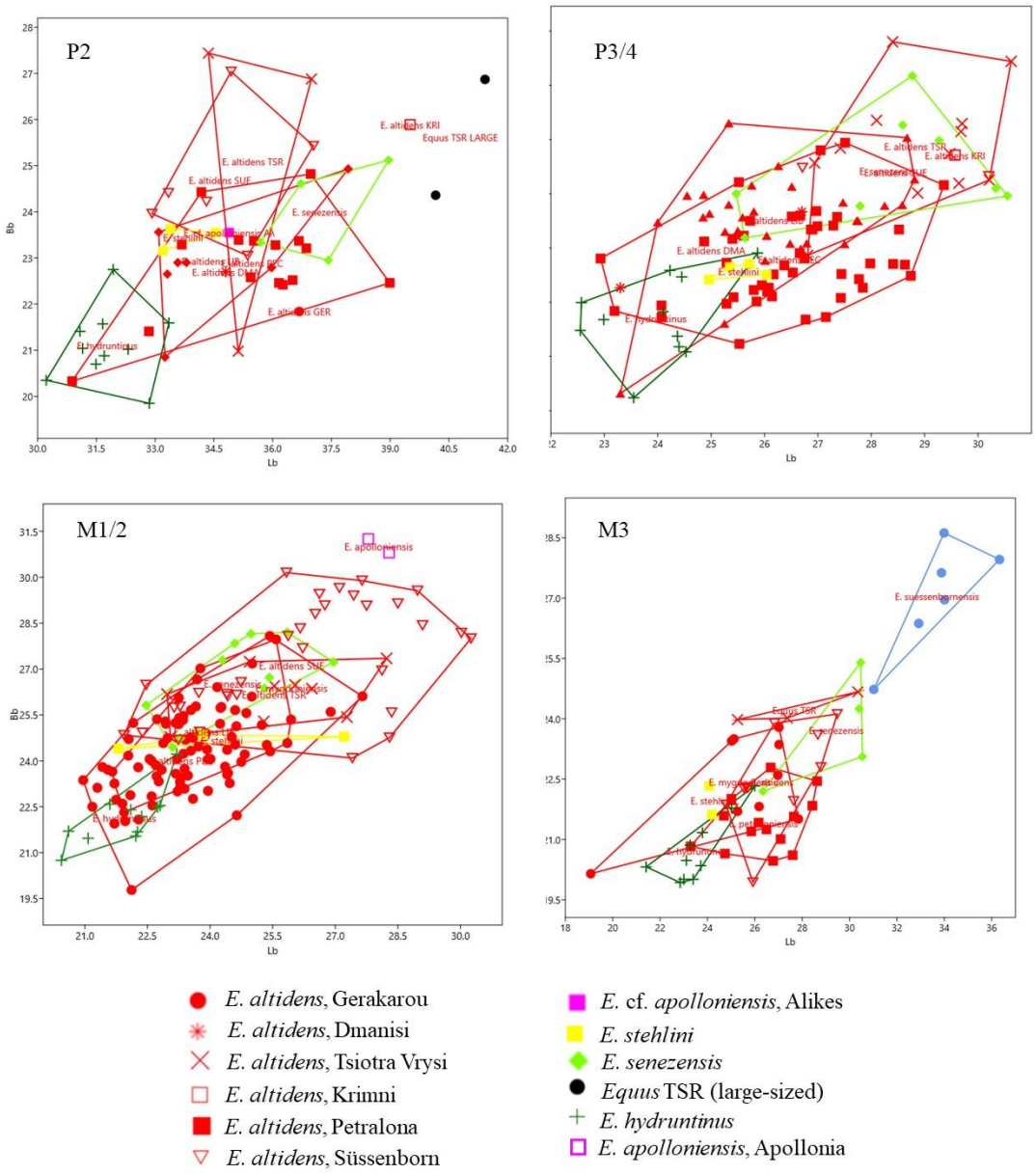

Figure 5.35. Bivariate plots comparing the length versus the breadth at the base (1cm from the roots) for each upper cheek tooth from Gerakarou, Krimni, Tsiotra Vrysi, Petralona and other Early to Middle Pleistocene stenonoid equids. Data from Eisenmann (2017a, b, c) and personal dataset.

In Figures 5.37 and 5.38, the third metacarpals from Gerakarou and Libakos are being compared to *E. stenonis* and *E. altidens* subspecies/populations. The metacarpals from Libakos are completely identical to those from Gerakarou. The third metacarpals from both Gerakarou and Libakos have deeper and narrower metacarpal diaphysis (M3,4) than *E. stenonis* subspecies/populations (Figure 5.37a), they exhibit slenderer distal epiphysis (M10, M11). In addition, both Gerakarou and Libakos are distinguished from

E. senezensis and *E. stehlini* which are much shorter (M1) and robust (Figure 5.39). The distal supra-articular breadth (M10) on the GER equid is higher than the distal articular breadth at the tubercles (M11) like on *E. altidens granatensis* and *E. altidens* from Dmanisi (Figures 5.37b, 5.38). This feature is vice versa on *E. altidens* from Pirro Nord and Selvella.

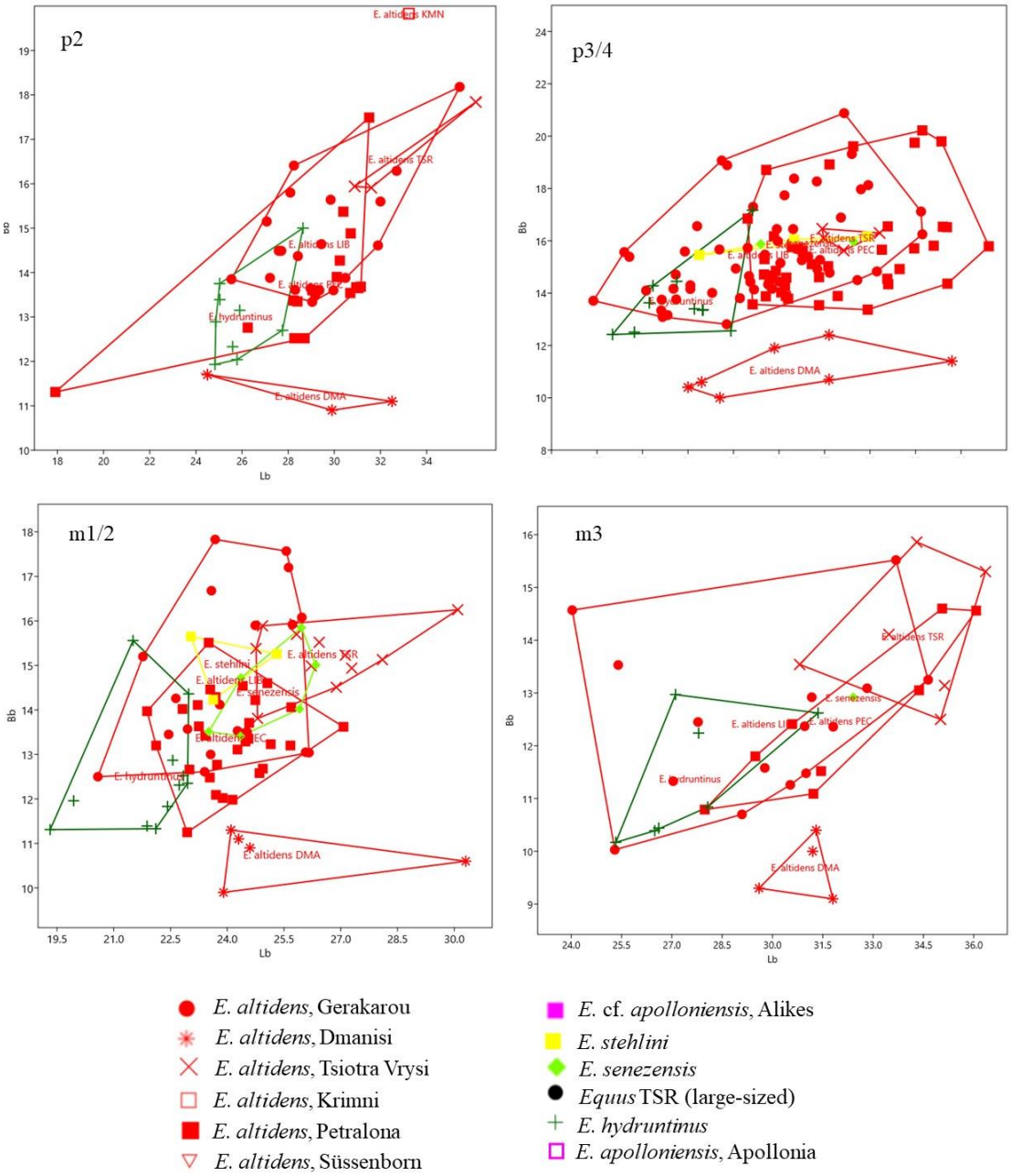

Figure 5.36. Bivariate plots comparing the length versus the breadth at the base (1cm from the roots) for each lower cheek tooth from Gerakarou, Krimni, Tsiotra Vrysi, Petralona and other Early to Middle Pleistocene stenonoid equids. Data from Eisenmann (2017a, b, c) and personal dataset.

The third metacarpals of the medium sized species from TSR share common affinities with the ones from Gerakarou, Libakos and Venta Micena (Figures 5.41a and 5.40a respectively). They seem to be slightly longer (M1) than GER and LIB (Figure 5.41a), but evenly slender. The metacarpals of the medium sized equid fall within the range of Libakos, and Venta Micena and they are slenderer than of the ones of *E. apolloniensis* (Figure 5.40); the metacarpals of *E. altidens granatensis* and *E. apolloniensis* are similar in maximal length, but the latter is more robust.

The third metacarpals from Krimni share common features with those of the medium sized equid from Tsiotra Vrysi. In Krimni 1 and 3, all metapodials are slender; in Krimni 1, they are slightly shorter than the ones from Krimni-3. The mean values of the KRI and KMN fall within the range of *E. a. granatensis*, and the longer KMN McIIIs are similar to the average of *E. a. granatensis* (Figure 5.42a). KRI is distinguished from *E. apolloniensis* based its small dimensions, while KMN is close to the shortest (minimum values) of *E. apolloniensis* (Figure 5.42b). Both KRI and KMN fall within the range of Libakos (Figure 5.41b), while the later falls outside the maximum values of the GER equid.

PC1 and PC2 account for 93.93% of the total variance (82.61% and 11.32%, respectively; Figure 5.43). PC1 separates species by maximal length (M1) from negative to positive, whereas PC2 expresses the slenderness from negative to positive values (from wide to narrow). The third metacarpals from Krimni-3 (KMN) and Tsiotra Vrysi fall into the convex hull of *E. a. granatensis*. *E. altidens* from Gerakarou overlaps with Krimni, Petralona, Libakos and *E. altidens* from Dmanisi.

The third metacarpals from Petralona are close to those from Gerakarou and Libakos, but they are slightly slenderer than both of them (Figure 5.38). Although the maximal length (M1) of the metacarpals from Petralona are similar with Gerakarou, Libakos and Dmanisi, the dimension of the diaphysis (M3, M4) is always much slenderer, and the distal part (M10, M11, M12, M13, M14) are also slenderer in relation to its maximal length. The average of Petralona overlaps with Libakos and Gerakarou's minimum. Comparing the slender equid from Petralona to *E. hydruntinus* samples, the average value from Petralona Cave is close to the maximum measurements of *E. hydruntinus*. Their lines are quite similar expect for the M12-13 ratio.

a

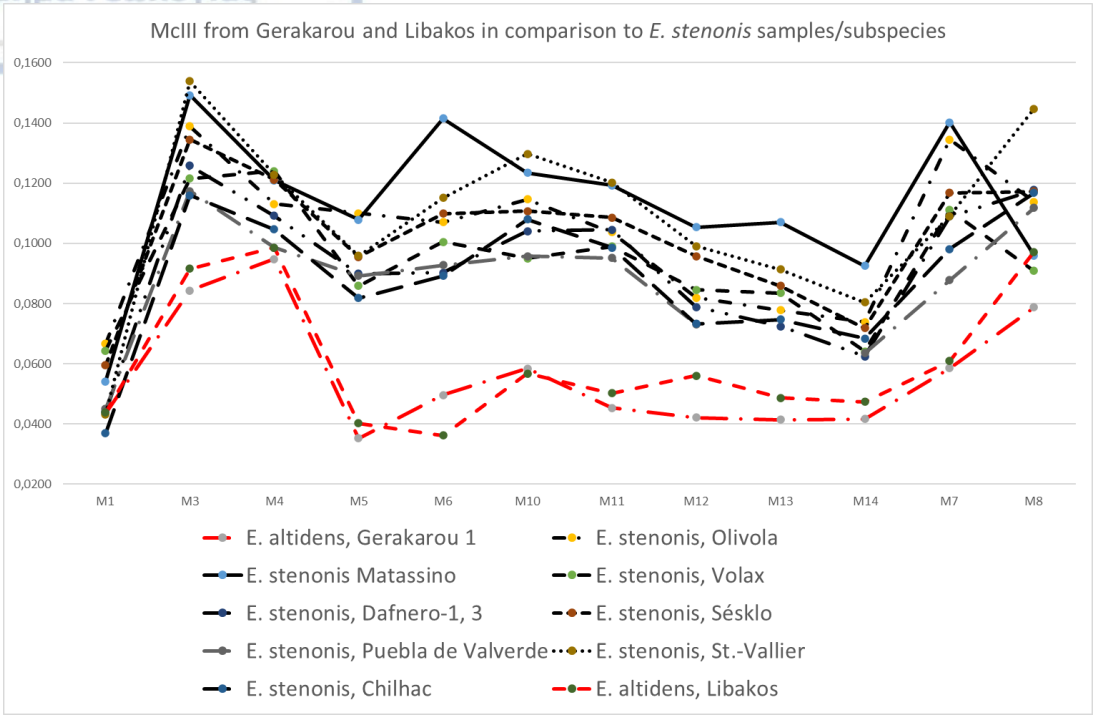

b

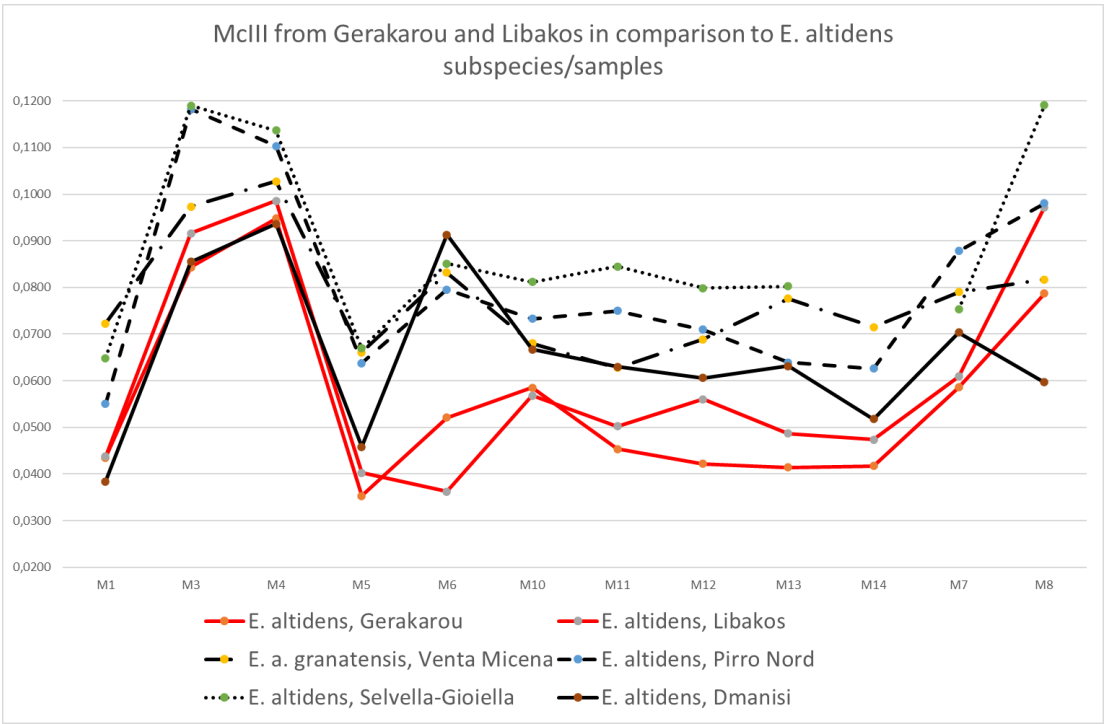

Figure 5.37. Simpson's log ratio diagram comparing the third metacarpals from Gerakarou and Libakos to the (a) Greek and European *E. stenonis* subspecies/populations and (b) the European *E. altidens* samples. Standard: *Equus hemionus onager*. Data from Bernor et al. (2021) and personal dataset.

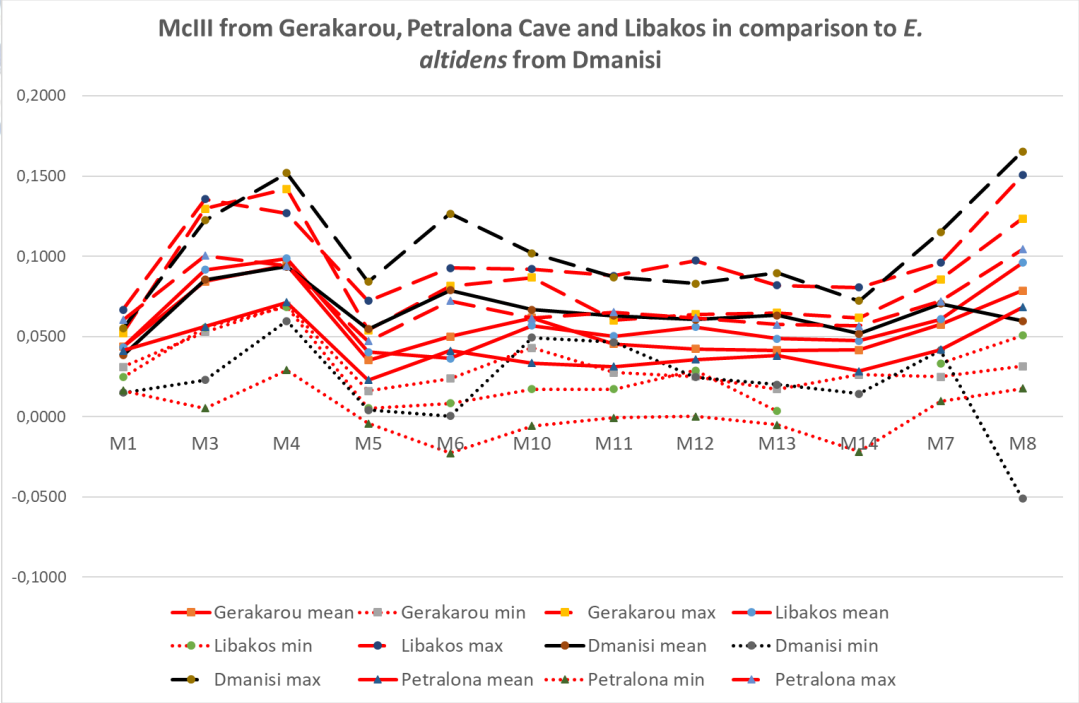

Figure 5.38. Simpson's log ratio diagram comparing the third metacarpals from Gerakarou, Petralona Cave and Libakos to *E. altidens* from Dmanisi. Standard: *Equus hemionus onager*. Data from Bernor et al. (2021) and personal dataset.

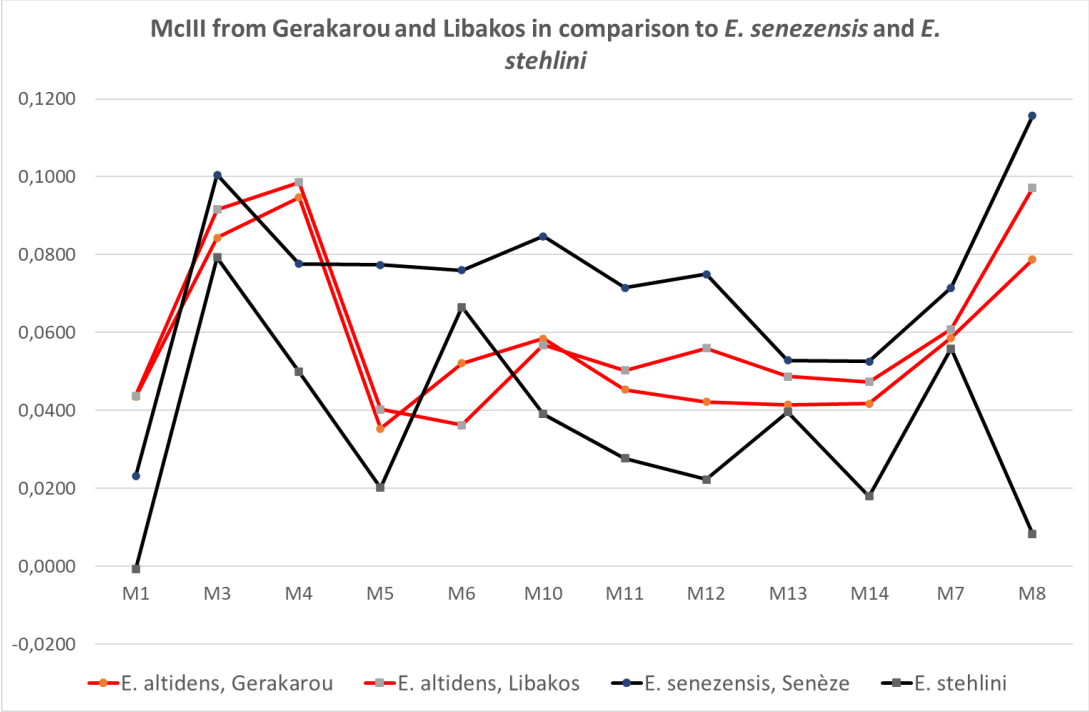

Figure 5.39. Simpson's log ratio diagram comparing the average values of the third metacarpals from Gerakarou and Libakos to the average values of *E. senezensis* from Senèze and *E. stehlini* from Casa Frata. Standard: *Equus hemionus onager*. Data from Bernor et al. (2021) and personal dataset.

a

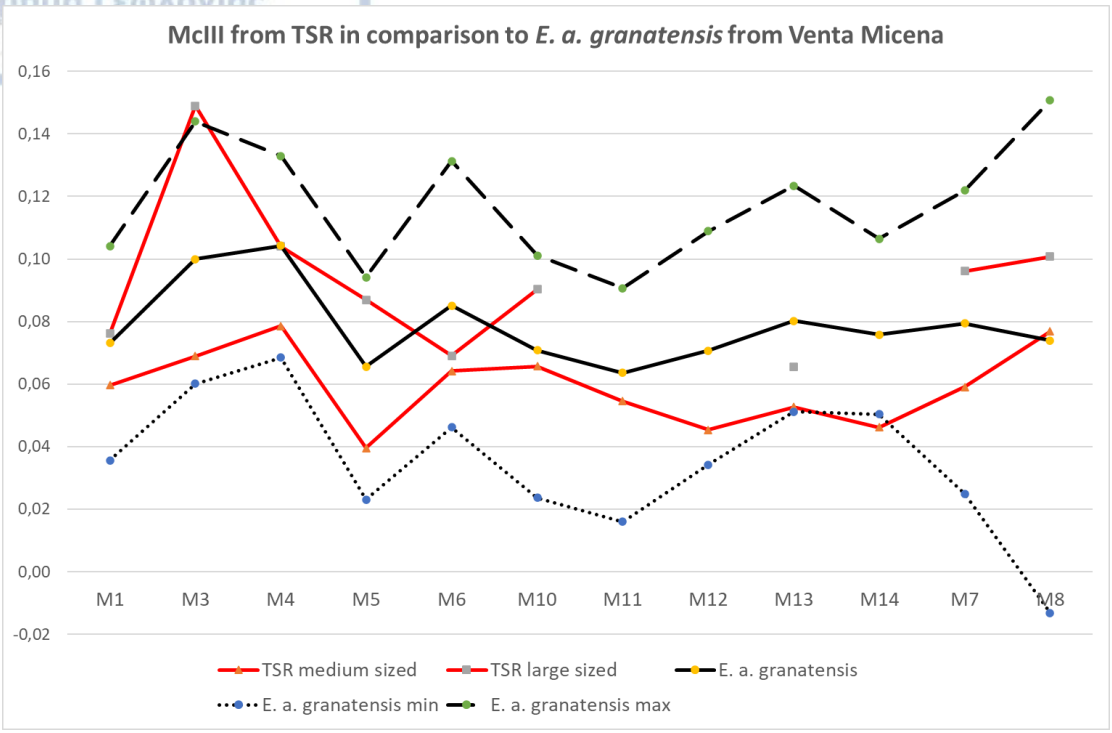

b

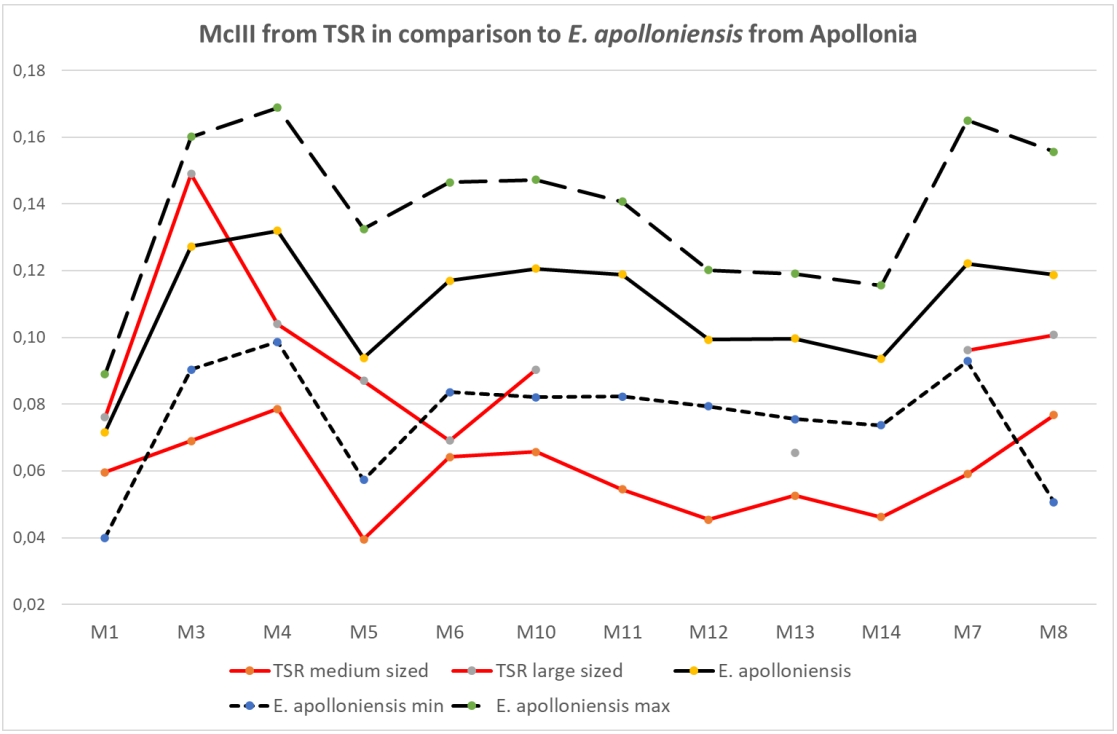

Figure 5.40. Simpson's log ratio diagram comparing the average values of the third metacarpals from Tsiotra Vrysi to (a) *E. altidens granatensis* from Venta Micena and (b) *E. apolloniensis*. Standard: *Equus hemionus onager*. Data from Eisenmann (2018) and personal dataset.

a

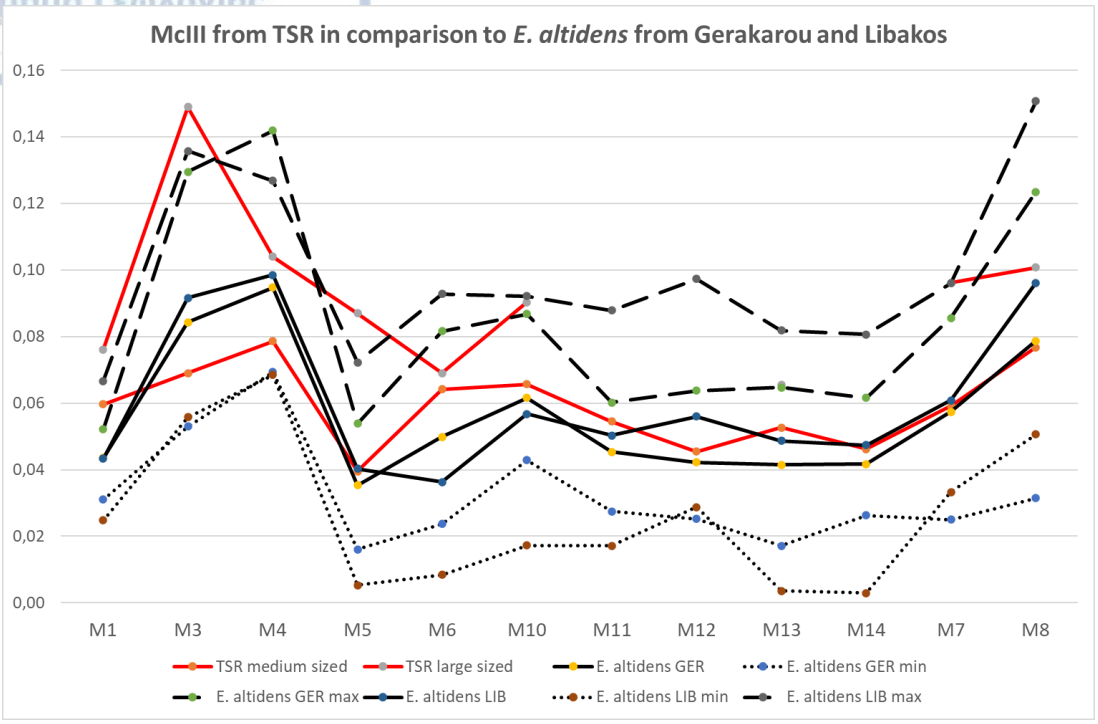

b

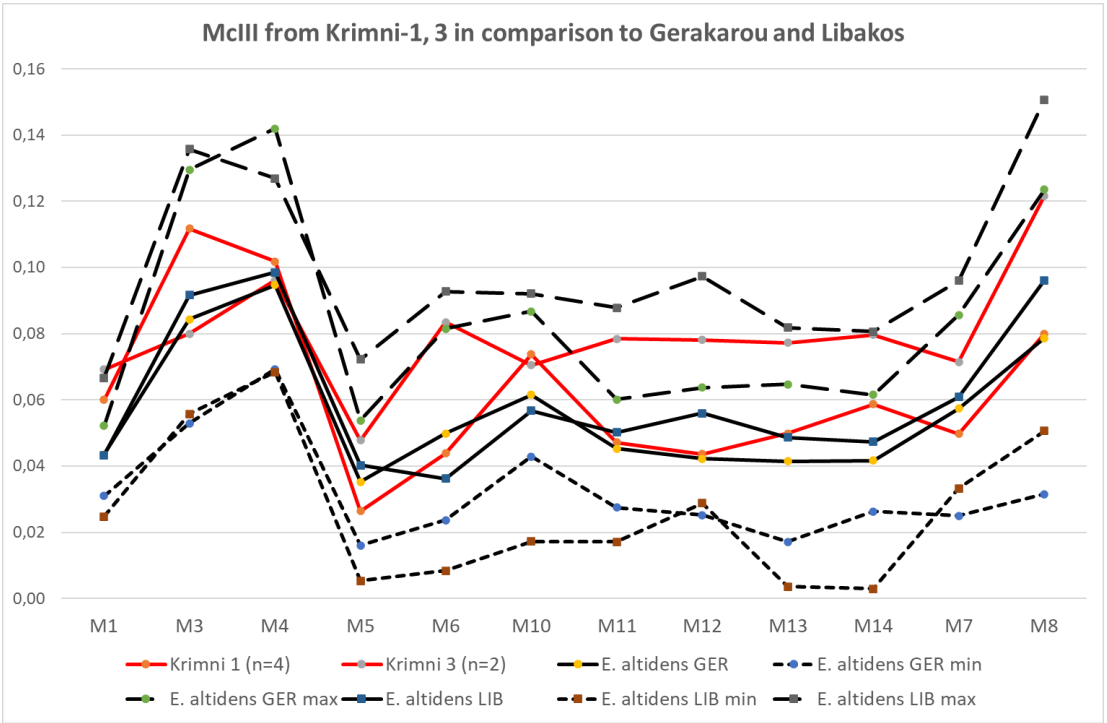

Figure 5.41. Simpson's log ratio diagram comparing the average values of the third metacarpals from (a) Tsiotra Vrysi and (b) Krimni to *E. altidens* from Gerakarou and Libakos. Standard: *Equus hemionus onager*.

a

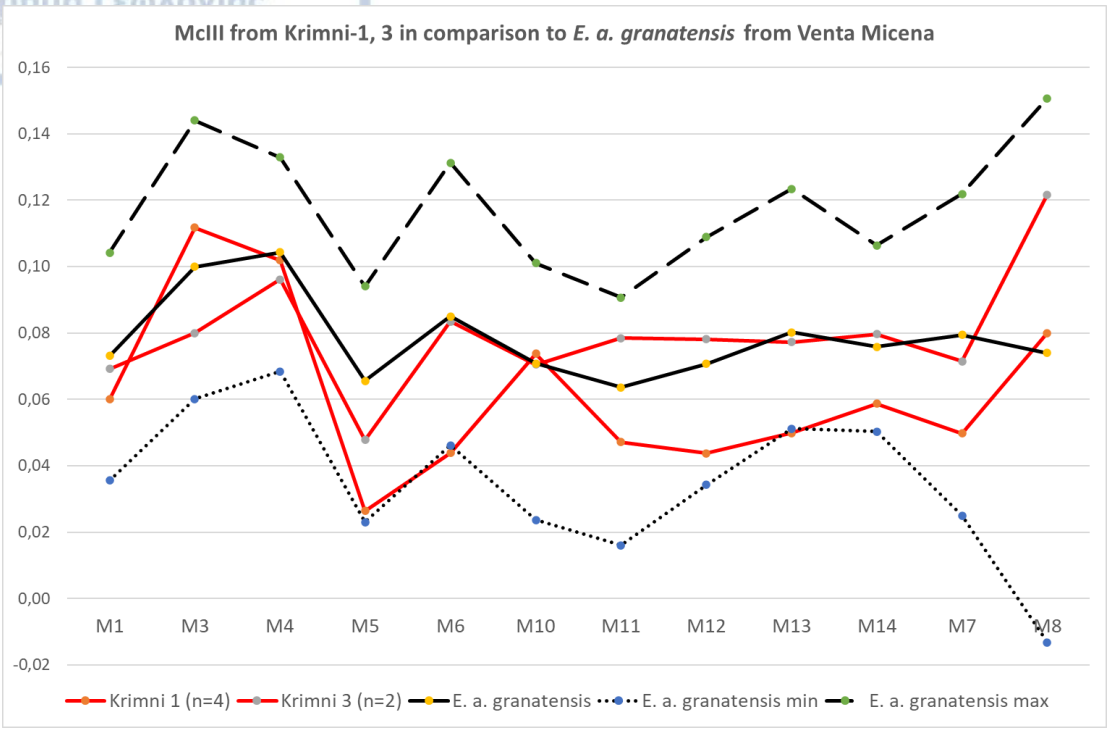

b

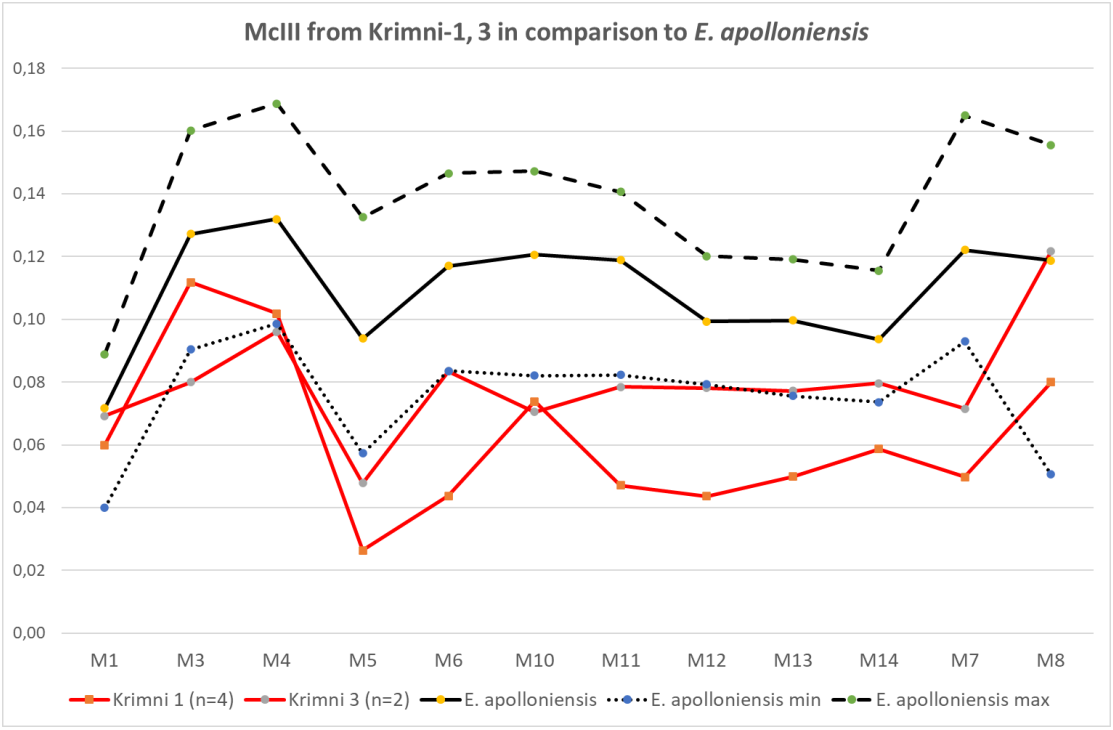

Figure 5.42. Simpson's log ratio diagram comparing the average values of the third metacarpals from Krimni to (a) *E. altidens granatensis* from Venta Micena and (b) *E. apolloniensis* from Apollonia-1. Standard: *Equus hemionus onager*. Data from Eisenmann (2018) and personal dataset.

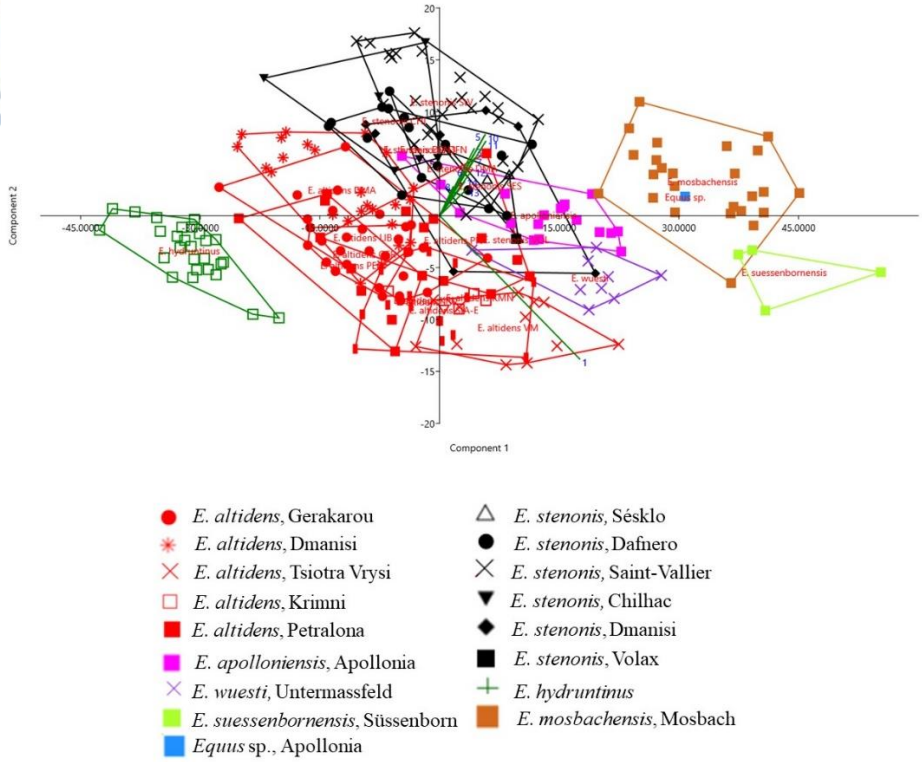

Figure 5.43. PCA analysis on selected measurements of the third metacarpals from Gerakarou, Krimni, Tsiotra Vrysi, Petralona Cave and several Early to Middle Pleistocene European equids. Data from Bernor et al. (2021), Cirilli et al. (2021), Boulbes and Eisenmann (2020), Eisenmann (2017) and personal dataset.

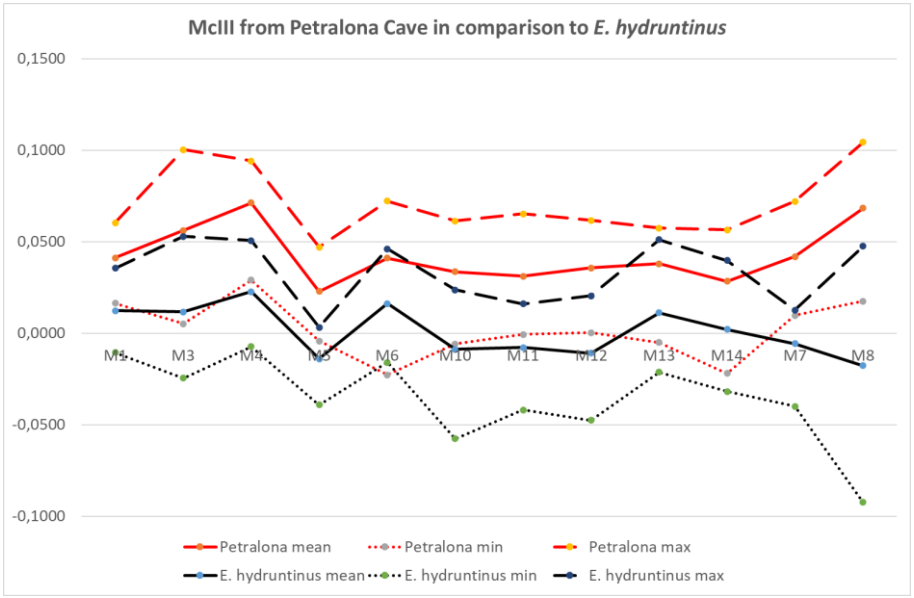

Figure 5.40. Simpson's log ratio diagram comparing the third metacarpals from Gerakarou and Libakos to *E. hydruntinus* samples from Grotta Romanelli, Staroselie, San Sidero, Rotenberg, Agios Georgios, Berlin Senzig, Magnano. Standard: *Equus hemionus onager*. Data from Tsoukala (1992), Eisenmann (2017a, b, c) and personal dataset.

The third metatarsals from Libakos and Gerakarou are identical to each other, and they are short and slender (Figures 5.41). It seems that they are as short as *E. stenonis guthi*, yet they are much slenderer (they are deeper M3 and narrower M4). Another significant difference is that the specimens from Gerakarou and Libakos display stronger (more developed) distal keel (M12) than *E. stenonis* from Volax, Dafnero-1 and -3 and Sésklo, as well as from all European *E. stenonis*, resembling in this feature *E. simplicidens, E. senezensis, E. a. granatensis* and *E. altidens* from Selvella and Pirro Nord (Figures 5.42). Further, the PERMANOVA results (Supplementary Table) for the metatarsals indicate significant differences between Gerakarou and all *E. stenonis* samples. Thus, it is well separated from all known *E. stenonis* populations. The samples from Gerakarou and Libakos are resembling in maximal length the third metatarsals of *E. altidens* from Selvella and Pirro Nord, while those from Dmanisi are slightly shorter. *E. a. granatensis* exhibits the longest third metatarsals along with *E. apolloniensis* and the large-sized *Equus* from Tsiotra Vrysi. The distal supra-articular breadth (M10) of the GER equid is higher than the distal articular breadth (M11) like in *E. altidens* from Selvella but unlike *E. altidens* from Pirro Nord.

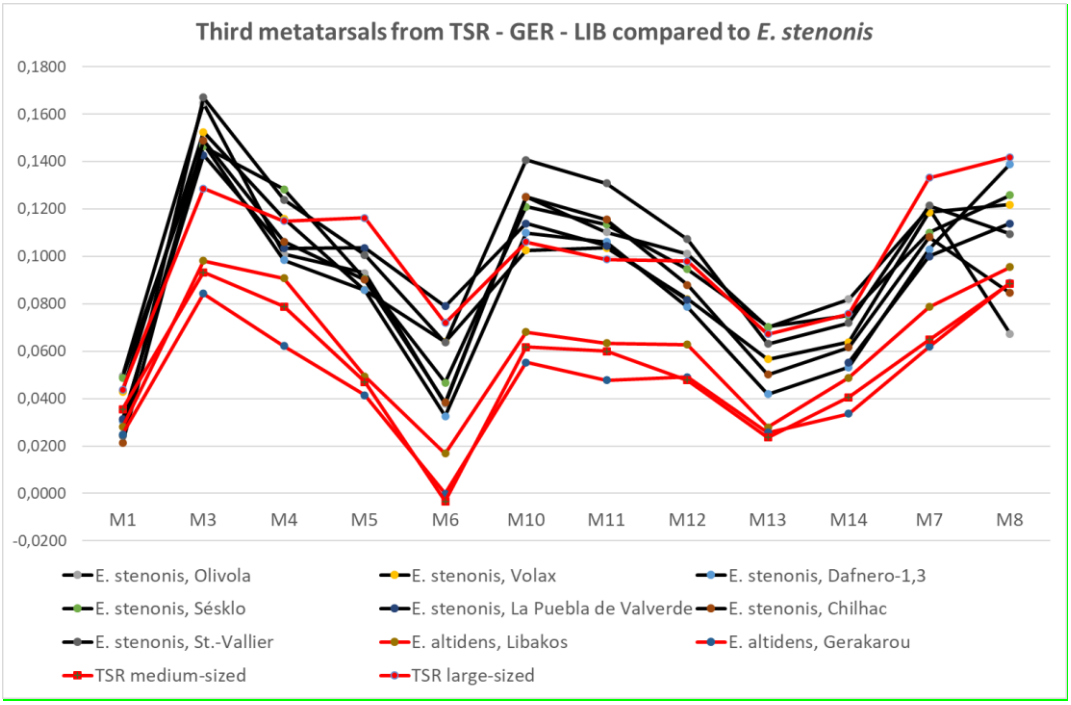

Figure 5.41. Simpson's log ratio diagram comparing the average values of the third metatarsals from Tsiotra Vrysi, Gerakarou and Libakos to *E. stenonis* subspecies/populations from Greece and the rest of Europe. Standard: *Equus hemionus onager*. Data from Bernor et al. (2021), Eisenmann (1980) and personal dataset.

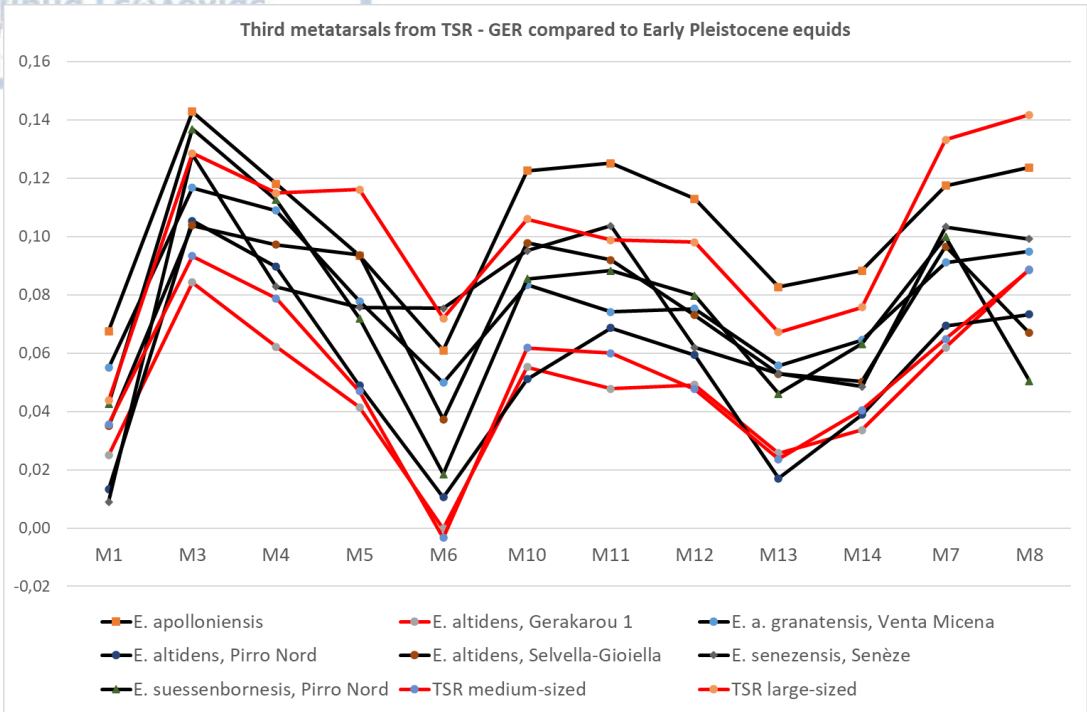

Figure 5.42. Simpson's log ratio diagram comparing the average values of the third metatarsals from Tsiotra Vrysi and Gerakarou Libakos to compared to other Early Pleistocene equids. Standard: *Equus hemionus onager*. Data from Bernor et al. (2021), Eisenmann (1980) and personal dataset.

The third metatarsals of the medium sized equids from Tsiotra Vrysi are resembling in overall dimensions those from Gerakarou and Libakos (Figure 5.41). In Figure 5.43b, the third metatarsals from Tsiotra Vrysi are being compared to *E. a. granatensis* from Venta Micena. It seems the medium-sized equid from TSR is within the range of variability of the sample from Venta Micena. The metatarsals from Krimni are within the range of those from Gerakarou and Libakos (Figure 5.44a), although the specimens from Krimni-3 are slightly longer and larger in overall dimensions but as slender as those from Gerakarou. The specimens from KMN are close to the minimum values of *E. apolloniensis* (Figure 5.44b) and the specimens from TSR, they are in the range of variability of *E. a. granatensis* (Figure 5.45). The metatarsals from Petralona are identical to those from Gerakarou (Figure 5.46).

Figure 5.47 exhibits the PCA results for the third metatarsal of the medium sized equids from Libakos, Gerakarou, Petralona, Krimni sites, and Tsiotra Vrysi compared to other Early Pleistocene European equids. PC1 separates species by maximum length, longer to shorter metapodials (from negative to positive values), whereas PC2 indicates a

slenderer built from positive to negative values. The equid from Gerakarou plots together with Libakos, Petralona and Tsiotra Vrysi (well-separated from all *E. stenonis* samples), while the two specimens from Krimni-3 are plotting within the range of variability of *E. a. granatensis*.

The tibiae of the Greek/European small/medium sized equids are also overlapping (M7, M8; Figure 5.48a). The tibiae from Gerakarou overlap with Petralona and Libakos showing no morphometric differences. The specimens from Tsiotra Vrysi exhibit a wider range of variability (Figure 5.48a); the medium sized *Equus* from TSR overlaps with Gerakarou, Petralona and Libakos, including those from Senèze. The specimen TSR-G19-6 exhibits larger proportions. The specimen Pgl.2 from Pyrgos plots along with *E. senezensis*, while the specimen Pgl.14 plots within the average range of *E. altidens* from Gerakarou and Petralona Cave. The specimens from the Krimni sites (KRI, KMN) overlap with the Tsiotra Vrysi, Libakos, Polylakkos and Gerakarou; KMN-44 exhibits unusual deeper distal epiphysis (M8).

The astragali from Gerakarou are separated from all *E. stenonis* subspecies (Figure 5.48b), while the astragali from Libakos are falling within the range of the shortest astragali from Dafnero and they are slightly wider (M4) than the ones from Gerakarou. The three specimens (GER-105, GER-107, GER-58) from Gerakarou that are quite shorter than the other may belong to young individuals, or to a smaller species. There is no evidence of a smaller species in the rest of the cranial or postcranial material, but there is a larger one (*Equus* sp. B herein); thus, acknowledging more than two different species is arbitrary. As it seems, *E. stehlini* has the shortest and widest astragali from all stenonoid equids including *E. senezensis*, albeit with a remarkable overlay of the specimens from Gerakarou, Petralona and Dmanisi (Figure 5.48b). The astragali from Libakos, Tsiotra Vryssi and Krimni (KRI and KMN) plot mostly within the range of *E. altidens* from Pirro Nord, Dmanisi and Gerakarou. The European populations of *E. altidens* sensu lato exhibit a wide metrical variability (Figure 5.48b). *E. hydruntinus* exhibits the smallest astragali in overall dimensions from all the other equids in comparison (Figure 5.48b).

a

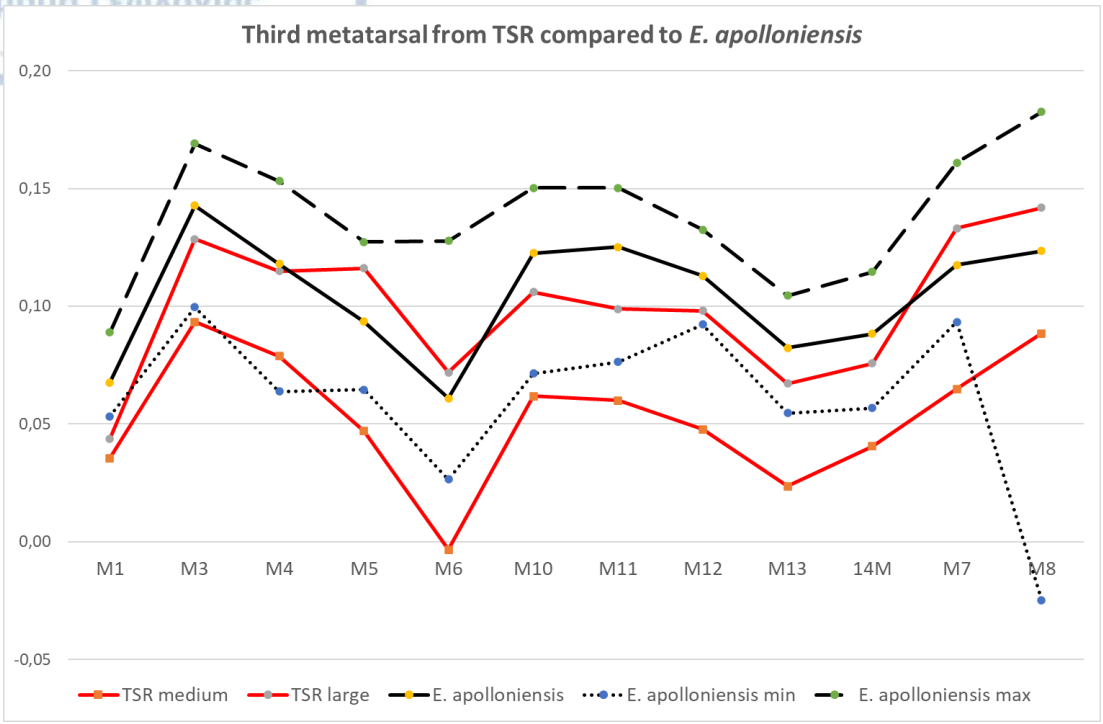

b

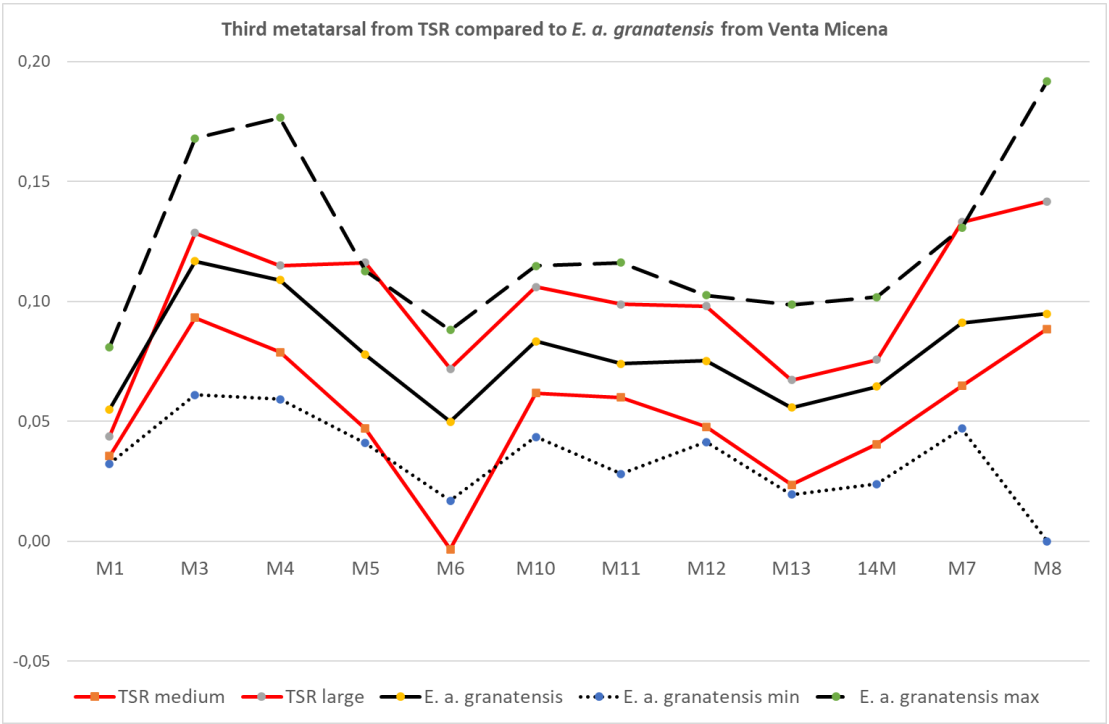

Figure 5.43. Simpson's log ratio diagram comparing the third metatarsals from Tsiotra Vrysi to those of (a) *E. apolloniensis* and (b) *E. altidens granatensis* from Venta Micena. Standard: *Equus hemionus onager*. Data from Eisenmann (1980, 2018) and personal dataset.

a

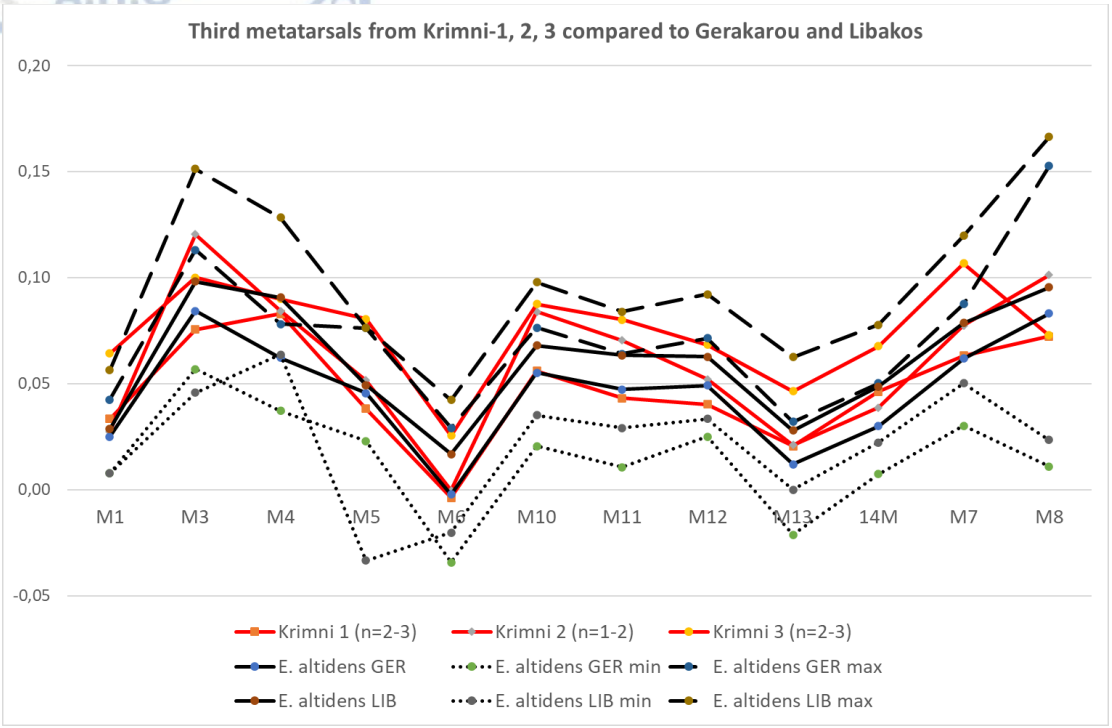

b

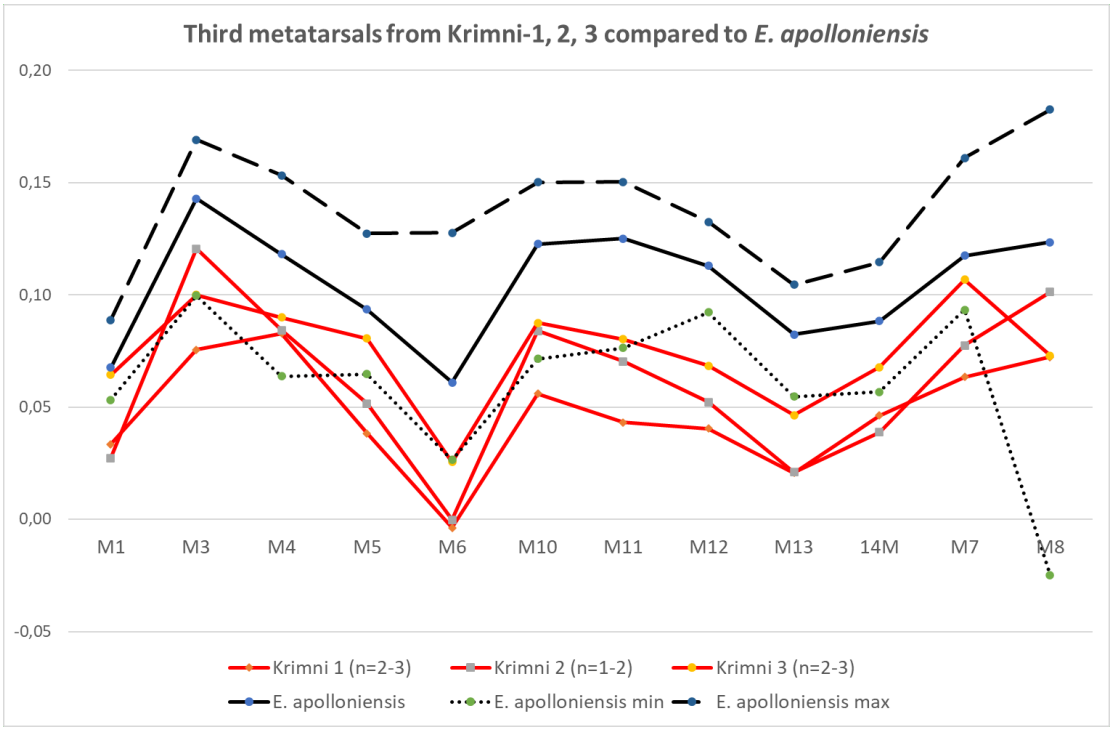

Figure 5.44. Simpson's log ratio diagram comparing the third metatarsals from Krimni to those from (a) Gerakarou and Libakos (*E. altidens*), and (b) Apollonia-1 (*E. apolloniensis*). Standard: *Equus hemionus onager*. Data from Eisenmann (1980) and personal dataset.

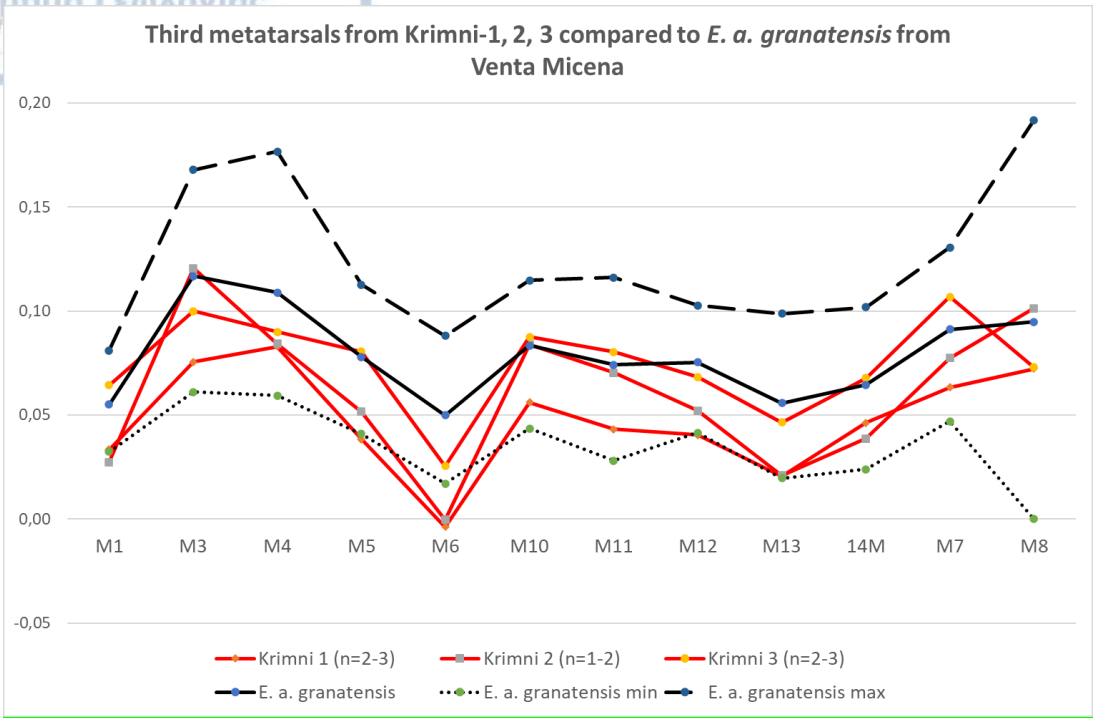

Figure 5.45. Simpson's log ratio diagram comparing the third metatarsals from Krimni to those of *E. altidens granatensis* from Venta Micena. Standard: *Equus hemionus onager*. Data from Eisenmann (1980) and personal dataset.

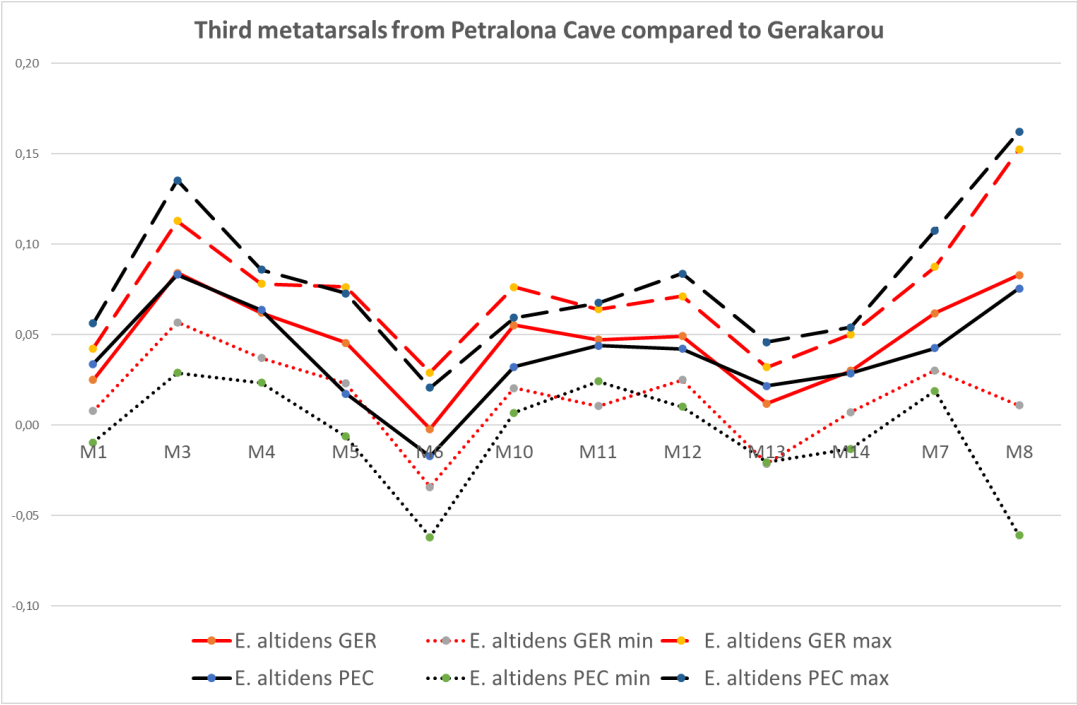

Figure 5.46. Simpson's log ratio diagram comparing the third metatarsals from Petralona Cave to those from Gerakarou. Standard: *Equus hemionus onager* (Eisenmann 1980).

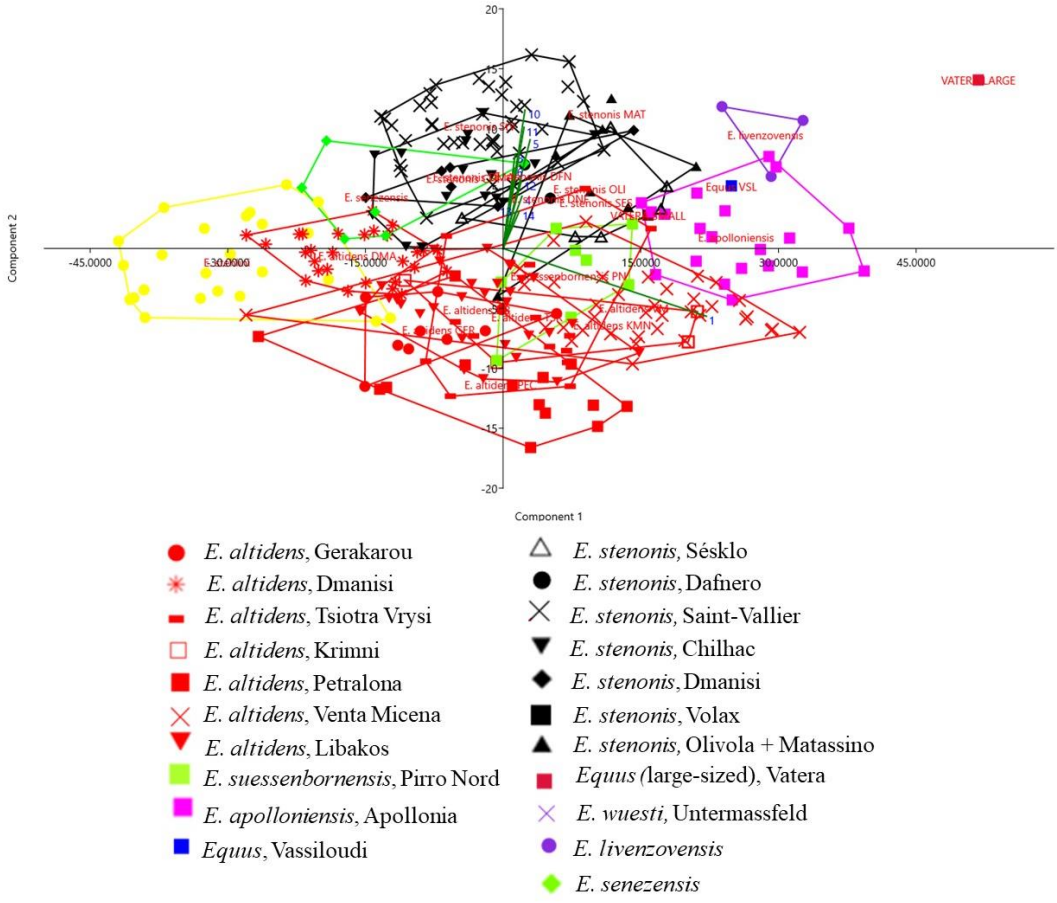

Figure 5.47. PCA analysis on selected measurements of the third metatarsal of several Early to Middle Pleistocene European equids. Data from Bernor et al. 2021; Cirilli et al. 2021; Eisenmann 2017; Eisenmann 2015 and personal dataset.

Although the calcanei are usually fragmentary or broken, there are plenty specimens in the material that could benefit some further information about the tarsal bones. In the PCA analysis of the calcaneum, PC1 and PC2 account for 88.12% of the total variance (PC1 = 79.76; PC2 = 8.36; Figure 5.49). PC1 separates species by maximal length (M1) from negative to positive (less to more elongated calcanei), whereas PC2 expresses the slenderness from negative to positive values (wide to narrow). The results support the previous interpretation that the equid from Gerakarou is separated from all *E. stenonis* subspecies and plots close to *E. altidens* from Dmanisi and Libakos and *E. stehlini*. The specimens from Krimni sites (KRI and KMN), and Tsiotra Vrysi plot between the slenderer equids from Dmanisi and Gerakarou and *E. stenonis-E.apolloniensis* resembling the dimensions of *E. senezensis*.

a

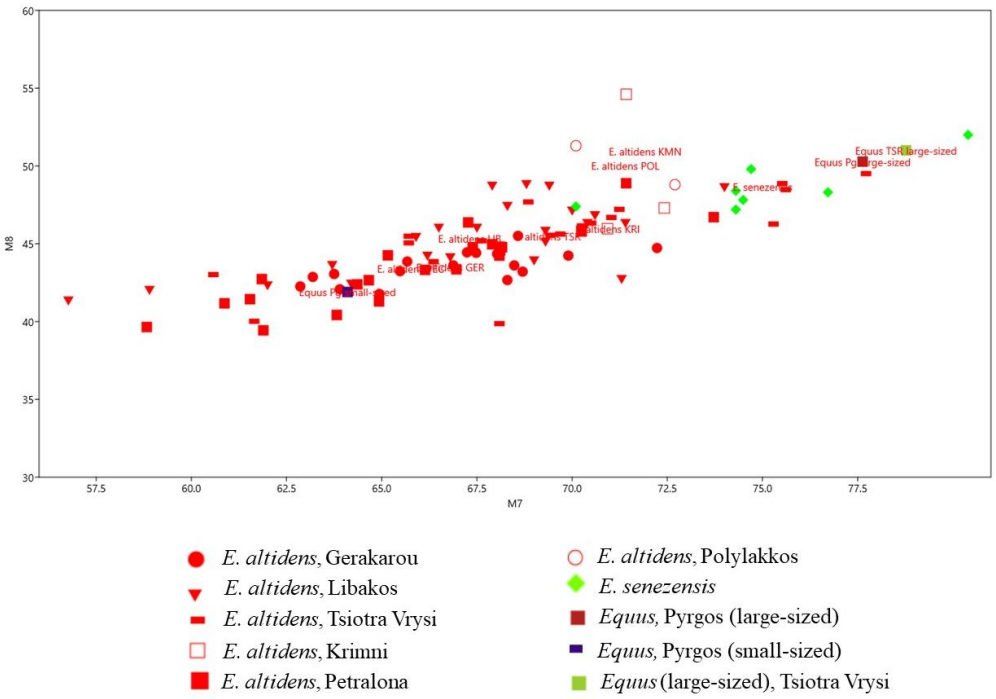

b

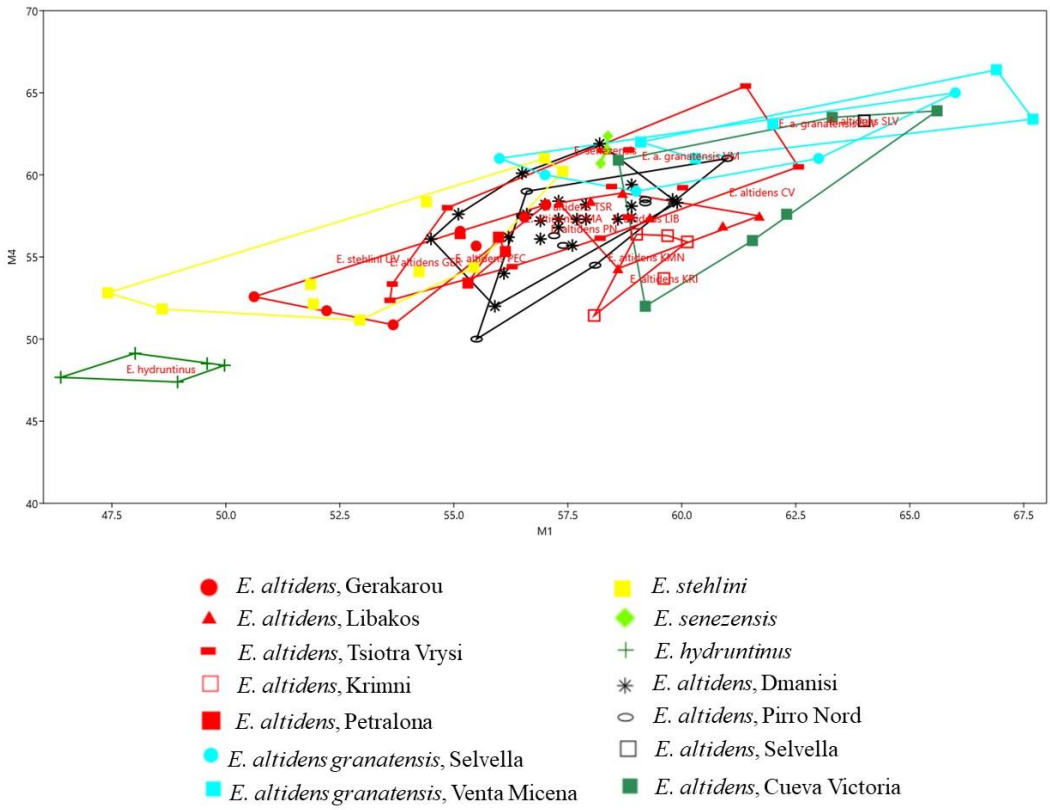

Figure 5.48. Bivariate plot of the (a) distal maximal breadth (M7) versus the distal maximal depth (M8) of the tibiae and (b) the maximum length (M1) versus maximum width (M4) of the astragali of several small/medium sized and/or gracile European Early Pleistocene equids. Data from Eisenmann (2017) and personal dataset.

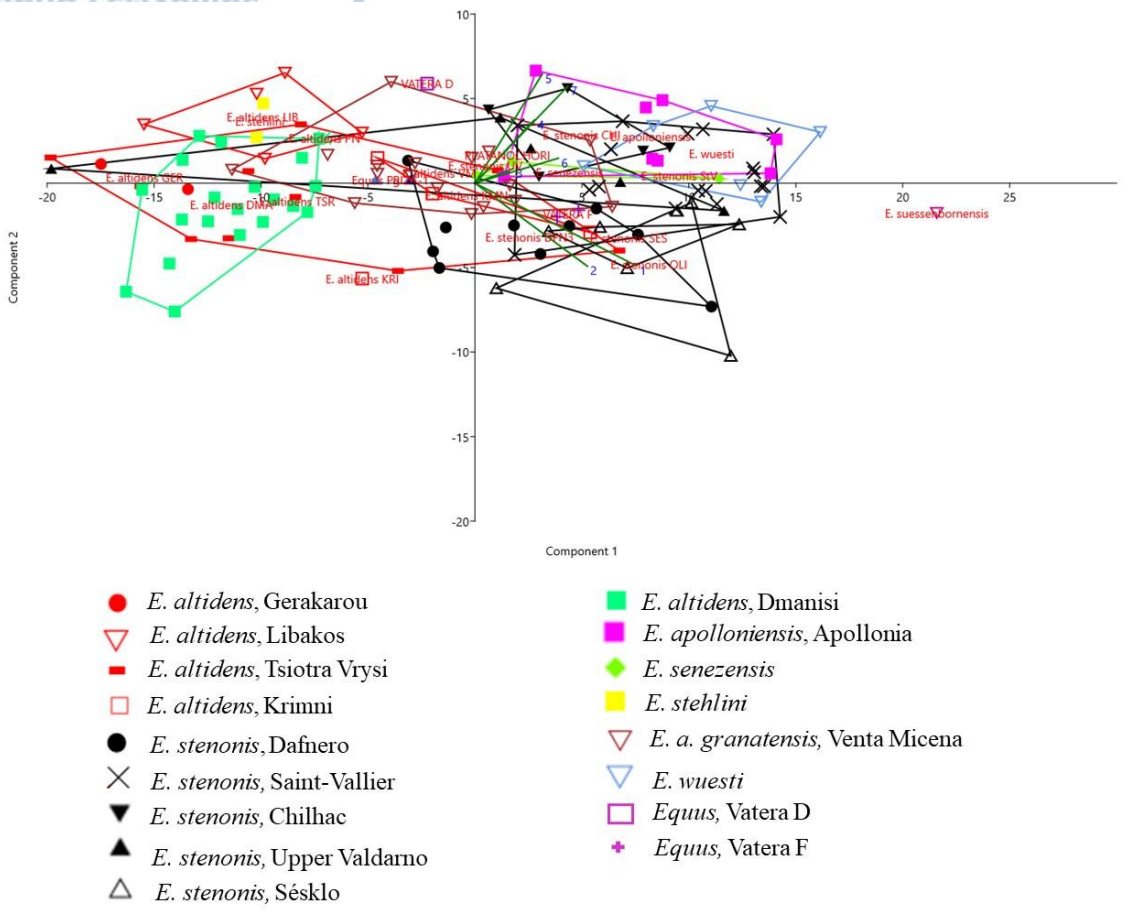

Figure 5.49. Principal component analysis on the calcanei of several Early to Middle Pleistocene European equids. Data from Bernor et al. (2021), Cirilli (2022), Van Asperen et al. (2012), https://vera-eisenmann.com/, and personal dataset.

The first results of the first anterior phalanges are in accordance with the metapodials and the tarsals. In the PCA analysis, the phalanges from Gerakarou, Petralona, Tsiotra Vrysi, Libakos and Krimni are slenderer than those of *E. stenonis* The Greek sample is close to *E. altidens* from Pirro Nord and Dmanisi. The phalanges of *E. hydruntinus* are close to those from Petralona Cave although they are slightly slenderer. *E. stehlini* overlaps with Gerakarou (partim).

To sum up, the GER equid is characterized by its slender third metapodials, phalanges and its small and slender cranium (Koufos 1992), and it is remarkably different from all the other European *E. stenonis* subspecies/populations. The morphological, morphometric, and statistical results, herein, showed significant differences between the equid from Gerakarou and *E. stenonis* subspecies/populations.

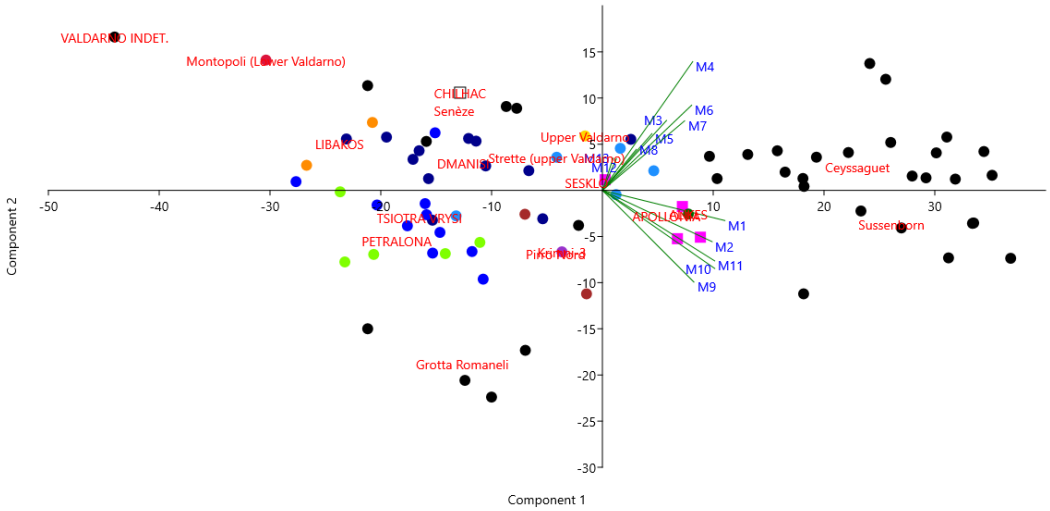

Figure 5.50. Principal component analysis (PCA) on the calcanei of several Early to Middle Pleistocene European equids. Data from Bernor et al. (2021), Cirilli (2022), Van Asperen et al. (2012), https://vera-eisenmann.com/, and personal dataset.

As the dimensions of the several *E. stenonis* subspecies/populations of the metapodials are generally homogenous, '*E. stenonis mygdoniensis*' should be excluded as a subspecies from the *E. stenonis* group (see also Cherin et al. 2020; Bernor et al. 2021). The taxonomy of '*E. stenonis mygdoniensis*' has been a matter of debate among equid specialists (Koufos 1992; Forstén 1999; Gkeme et al. 2017a, b; Eisenman 2017; Cherin et al. 2019; Palombo and Alberdi 2017; Cirilli et al. 2020; Bernor et al. 2021 and references therein) and its relationship to *E. altidens* has been questioned. The results herein are in accordance with Forstén' s (1999) original suggestion, embraced later by Gkeme et al. (2017) and Koufos et al. (2022), that the equids from Gerakarou, Krimni, Libakos and Petralona should be all included under the name *E. altidens* due to their slenderness. Until recently, no crania of *E. altidens* were acknowledged. Bernor et al. (2021) attributed a well-preserved complete equid cranium (Dm53/59.3.B1gl.192) from Dmanisi to *E. altidens*. The cranium belongs to a female adult. The cranium resembles in size and general morphology the crania from Gerakarou and Krimni-3 (Bernor et al. 2021). Their results on cluster analysis have shown that the crania from Dmanisi and Gerakarou are clustered together, and they are morphometrically similar to *E. quagga* and *E. hemionus*. The results herein rather support this idea. The resemblance of the crania from Gerakarou and Krimni-3 with the cranium of *E. altidens* from Dmanisi is clear, based on the Log10 dimensions and the multivariate analysis

(PCA). These crania share common features like the length of the snout, position of the orbit behind the M3, position and length of the lateral maxillary crest, slender palatine process, and the upper cheek tooth enamel morphology (Bernor et al. 2021). However, some macroscopic morphological dimensions could reflect (or acknowledged as) subspecific taxonomic differences (depth of the narial opening). As for the postcranial elements, no statistical differences were acknowledged between the Italian, Spanish and Georgian *E. altidens*, and '*E. stenonis mygdoniensis'* as already stated by Bernor et al. (2021). They refer *E. s. mygdoniensis* as a junior synonym of *E. altidens*. In their results, Bernor et al. (2021) do not distinguish multiple subspecies of *E. altidens*, including *E. altidens altidens, E. altidens granatensis* and '*E. stenonis mygdoniensis'*. The recent findings from Krimni-3 could give some new insight on this matter. The cranium KMN-50 from Krimni-3 was found near an in situ equine skeleton (back legs, pelvis, some vertebra etc). These legs are quite longer than those from Gerakarou. The question rises whether they could belong to the same individual with the cranium or not. Given the fact that most of the material from this site was in situ, the author believes that they belong to the same individual. If this is correct, another question arises: to which species do they belong, because the legs are identical to the sample from Venta Micena and the cranium to the GER equid. This observation supports Bernor at al.' s (2021) suggestion that *E. altidens granatensis* and '*E. stenonis mygdoniensis'* belong to the same species and should be included in *E. altidens*. It also rejects Eisenmann's (2010) subgenus *Sussemionus*. If the cranium and partial skeleton from KMN belong to two different individuals, then they would probably belong to two different taxa. This hypothesis favours Eisenmann (1995, 2006, 2010) model recognising *E. a. granatensis* as a valid taxon (species or subspecies). In case of different individuals, three species should be described at Krimni-3. However, the recognition of three species based on a few specimens is rather impossible.

Eisenmann suggests using the name '*Equus altidens*' with caution. The present author agrees to that at some point. *E. altidens* is a species created by von Reichenau 1915 based on isolated teeth from Süssenborn. The latter author acknowledged three different species in the material: *E. altidens*, *E. marxi* and *E. suessenbornensis*. Although, *E. suessenbornensis* is easily recognized (richly plicated inner fossettes or wrinkled fossettes, larger size), the distinction between the other two is not clear. Some authors believe that they belong to the same species (Alberdi et al. 1998; Palombo and Alberdi 2017). The present author agrees to the latter authors.

Apart from *E. altidens*, the GER equid exhibits similarities to *E. stehlini*. So, another question arises, why '*E. stenonis mygdoniensis'* is not included in *E. stehlini*. Although, the equid from Gerakarou is close to both *E. stehlini* and *E. altidens*, the crania fit better with Dmanisi's *E. altidens* (Bernor et al. 2021).

Equus apolloniensis Koufos, Kostopoulos and Sylvestrou, 1997

Locality.

Apollonia-1 (APL), Mygdonia Basin, Central Macedonia

Material.

Apollonia-1. Crania: APL-147, 148, 518 (fragment), 519 (fragment), 605 (fragment), 858 juv. (fragment), 871, 842; fragment of occipital bone APL-813; maxilla with P4-M3 sin and P2-M3 dex APL-129; part of muzzle with I1-C APL-268, parts of muzzle with I1-I3: APL-314, 574; 646, 812; fragment of muzzle with dI1-I3 sin and dI1-I2 dex APL-873; fragment of maxilla with M1 APL-816; fragment of juvenile maxilla with dP2-dP4 APL-825; fragment of juvenile maxilla with dP2-dP4 sin and dP1-dP4 dex APL-863; fragment of juvenile maxilla with dP2-dP4 dex APL-601; in situ dP2-dP3 dex APL-573; in situ dP3-dP4 dex APL-229, 228 respectively; in situ dP3-dP4 dex APL-607, 647; dP3 sin APL-842; dP3 dex APL-223; APL-341; in situ P3-P4 APL-343; incisors APL-303, 461; P2: APL-138; P3,4: APL-469; M1,2: APL-142, 471, 500, 564; M3: APL-154, 830, 558, 566, 626 874; mandible: APL-570 (complete), fragment of mandibular ramus with dP2-dP4, M1-M2 dex APL-572; fragment of mandibular ramus with dI3, dP2-dP4 sin and dP2-dP4 dex APL-317; mandibular fragment with dI1-I3, dP2-dP4 sin/dex APL-318; mandibular fragment with dI2, dP2-dP4 sin and dI1-I2, dP2-dP4 dex APL-571; mandibular fragment with dP2- dP4 sin/dex APL-857; fragment of mandibular body and ramus with dP2-dP4, M1-M2 sin APL-870; fragment of mandibular body with I1-I3, C, P2-M3 sin/dex APL-785; fragment of mandibular body with I1-I3, C, P2-M2 sin and I1-3, C, P2-P4 dex APL-633; fragment of mandibular body with I1-I3, C, P2-M2 sin and I1-I3, C, P2-M2 dex APL-792; fragment of mandibular body with P3-M3 sin APL-424; fragment of mandibular body with P2-M3 sin APL-355; fragment of mandibular body with P2-M3 dex APL-606; fragment of mandibular body and ramus with P4-M3 sin APL-295; fragment of mandibular body with M1-M3 dex APL-486; fragment of mandibular body with P3-M2 sin APL-315;

fragment of mandibular body with P3-M3 dex APL-557; mandibular fragment with M3 sin APL-26; mandibular fragment with P2-P3 sin APL-250, 834; mandibular fragment with P2-P4 dex APL-622; fragment of mandibular ramus (condyle) APL-640; in situ p2-p3 sin APL-598; milk incisors APL-252; in situ p2-p3 sin APL-311; in situ p4-m3 sin APL-319; in situ p4-m1 dex APL-345; p2 sin APL-562; p2 dex APL-88 (fragment), 138, 186, 470, 563 (fragment); p3/4 sin APL-623; m1/2 sin APL-119 (fragment), 137, 185, 609; p3/4 dex APL- 608; m1/2 dex APL-139, 345, 153, 369, 496, 587, 140; m3 sin APL-561; m3 dex APL-301; atlas: APL-642, 485; scapula: APL-881; distal parts of humeri: APL-57, 204, 423, 481, 566, 818; radius: APL-799; radius with fragmentary ulna: APL-350, 785, 866, 796, 808; proximal parts of radius 371, 783; distal parts of radius:APL-75, 363 juv., 392, 404, 427, 457, 460, 468, 740, 791; ulna: APL-288 (broken), 368 (broken), 431 (fragment); magnum APL-631, 643; pisiform APL-644; third metacarpals:APL-612, 635, 776, 777, 778, 787, 788, 793, 861; proximal parts of McIII APL-396, 637, 807, 850; distal parts of McIII APL-636, 851; femur. APL-F?, 638 juv.; distal part of femur APL-814; tibiae: APL-406,798; distal parts of tibia: APL-93, 98 juv., 209, 280 !, 316, 324, 329, 353, 389, 393, 398 juv., 405 451, 581, 619, 620, 639, 780, 797, 844, 855, cuboid APL-628; navicular APL-545; astragali: APL-42, 54, 55, 57, 86, 171, 172, 173, 174, 175, 256, 324, 329, 387, 388, 575, 629, 632, 641 (fragment), 811, 826, 827, 852; calcanei**:** APL-52, 53, 168, 169, 170 juv., 287 juv.?, 331, 337, 450, 575, 588, 596 juv., 630, 829 juv., 853; third metatarsals: APL-610, 611, 621, 634, 789, 790, 794, 846, 848; proximal parts of MtIII: APL- C, 81, 167, 248, 362 (fragment), 476 (fragment), 517, 739, 805, 854, 859; distal parts of MtIII: APL-166 (fragment), 608, 779, 860, distal parts of third metapodials: APL-63, 584, 627 juv., 741, 810; first phalanges: APL-56, 177, 336, 349 juv.?, 364 juv.?, 803 (broken), 804, 831; second phalanges: APL-145, 365, 395, 409, 410, 599 juv.?, 856, third phalanges: APL-251, 394, 411, 426 (fragment), 802, 832, 869;

In articulation/in situ: atlas + axis APL-786; distal part of humerus + proximal part of radius APL-304 (juv.?); distal part of tibia + astragalus + calcaneum + navicular + cuboid + small cuneiform + big cuneiform + proximal part of third metatarsal with accessories APL-324; distal part of tibia + navicular + big cuneiform calcaneum + astragalus APL-329; navicular + big cuneiform APL-50; astragalus (a) + distal part of calcaneum (b) + navicular + cuboid + small cuneiform + big cuneiform (c) + third metatarsal with accessories (d) + first phalanx (e) + second phalanx (f) + third phalanx (g) + sesamoids (h) APL-877; tibia (a) + astragalus (b) APL864; calcaneum + astragalus

APL-386; calcaneum + astragalus APL-552, 553 respectively (juv.?); calcaneum + astragalus APL-554, 555 respectively; distal part of third metatarsal + first phalanx + second phalanx + third phalanx + sesamoids APL-267; first phalanx + second phalanx APL-340, 365, 330; second phalanx (a) + third phalanx (b) + sesamoid (c) APL-868;

Description.

APL-148. It is the holotype of *E. apolloniensis* and it was originally described by Koufos et al. (1997) and recently by Gkeme et al. (2021). The cranium is almost complete, but it is laterally compressed (Figure 5.51). It belongs to a young adult individual; canines are not in wear while M3 is slightly worn suggesting an age between 3.5-4 years (Levine 1982). The large canines indicate of a male individual. The cranium is elongated, and the muzzle is rather short and wide. The ratio: breadth of the muzzle x 100/ length of the muzzle (M15 x 100/ M1) is 49.2 mm. The palate is probably wide, but the mean palatal breadth (M13) cannot be measured due to the compression. The major palatine foramen is located at the level of the mesial half of M2. The choanae are large and elliptical; their anterior border is situated between the border of M1/M2. The medial border of the retroarticular process is almost straight (on profile view). The narial notch riches almost the mesostyle of P2. The infraorbital foramen is quite large (diameter=13 mm) and deep and is situated above the level the parastyle of P4. The anterior border of the facial crest is located at the mesostyle of M1. The facial crests are well-developed, and they are wavy above the last molars (Figure 5.51). No preorbital fossa is observed. The orbits are quite large and rounded. Foramen magnum is quite large, less wide, and pentagon shaped. The retroarticular processes are quite large and strong and they are laterally outreaching the level of the articular surface of the mandibular fossa. The greatest length of the cranium is probably at the zygomatic arches. The occipital region is partially preserved (possibly due to carnivore attack). The external occipital protuberance is represented by a vertical crest.

The dentition is completely preserved on both sides (Figure 5.51a). Both P1 are missing, but their alveoli verify their presence. On lateral view, the cheek teeth are remarkably elongated. The anterostyle on P2 is elongated but not very wide. Parastyle and mesostyle on P2 and P3 are notched. The protocone is relatively elongated. Its lingual border is concave except for P2 and M3 (where it is almost straight). The hypoconal groove is always deep, elongated and pointed. The pli caballin is long and

multiple on premolars, while on molars, it is short and single. The plication of the inner fossettes is moderate.

APL-147. The cranium (Figure 5.52) was originally described by Koufos et al. (1997) and recently by Gkeme et al. (2021). It belongs to an old individual (cheek teeth at fourth stage of wear). The muzzle is missing, and it is mediolaterally compressed. The palate is wide, but the mean palatal breadth (M13) cannot be measured due to the deformation. The major palatine foramen is located at the posterior half of M2. The choanae are large and elliptical and their anterior border is situated at the M1/M2 contact. The narial notch is situated above the parastyle of P2. The facial crest is well-developed, but the sinuses on both sides are crushed. The anterior border of the facial crest is located at the level between the P4/M1 contact on the left side, and at the anterior half of M1 on the right side. The crest, on the lateral view, is wavy like on the other APL crania. The right infraorbital foramen is situated above the posterior half of P4. No preorbital fossae can be distinguished with certainty. The orbits are oval-shaped due to the deformation, and their anterior border is far behind the M3. The retroarticular processes are quite large and strong and they are laterally outreaching the level of the articular surface of the mandibular fossa. The dorsal edge of the zygomatic arch is directed horizontally at a point caudal to the orbit. The zygomatic process of the frontal bone is strong and relatively broad (breadth 28.42 mm). The nasal bones form a smooth groove along their sagittal suture (dorsal view). The greatest length of the cranium is behind the orbits. The frontonasal suture is almost a straight line like on *E. zebra* (Smuts and Penzhorn 1988). The foramen magnum and paracondylar processes resemble those of APL-148. The crest of the occipital bone is missing. The external occipital protuberance is represented by a vertical crest and no depression are formed (Figure 5.52d).

APL-147 preserves the tooth rows P3-M3 sin and P2-M3 dex (Figure 5.52e). The anterostyle of P2 is rounded and relatively short. The hypoconal groove is always shallow and rounded; on the right M3, the hypocone is isolated as an islet. The protocone is relatively long on all teeth; except for P2. The lingual border of the protocone is almost straight on P2 and M3, while on all the other cheek teeth it is concave. Pli caballin is absent. The inner fossettes are simply plicated. The enamel of the buccal side of the fossettes is wrinkled (Figure 5.52e).

APL-519. The cranium was originally described by Koufos et al. (1997). Only the right part of the cranium is preserved; the palate is completely missing. The M3 is on wear

(slightly) indicating of a young adult. The facial crest is not preserved. The infraorbital foramen is situated caudally at the P3/P4 contact. The orbit (dex) is quite larger than all other APL crania and it is elliptical; it is situated almost at the posterior border of M3. The zygomatic process of the frontal bone is slightly less broad than on other APL crania (breadth 23.87 mm).

APL-519 preserves only the right P3-M3 series. The protocone is more or less elliptical and it is relatively short; its lingual border is slightly concave or flat. The plication of the fossettes is simple. Pli caballin is present on P3 and P4.

APL-605. The cranium is lacking the muzzle, orbits, braincase and occipital bones and it is dorsoventrally compressed. It belongs to a young individual between 2-4 years old; P4 is slightly worn while M3 just erupted, but it is still unworn. The palate is less wide than on the other APL crania and it is a bit convex perpendicularly. The palatal breadth at the level of P4-M1 (M13) is approximately 83,74 mm. The choanae are well-preserved and their anterior border is situated at the posterior half of M1. The anterior part of the vomer and the pterygoid bones are also preserved. The major palatine foramens are placed at the middle of M2. The facial crests are well-developed, and their anterior border is situated above the middle of the posterior half of P4; a slightly curving is also observed at the anterior half of the crest. The left infraorbital foramen is possibly situated at the level of the mesostyle of P4. No preorbital fossae can be distinguished with certainty on neither side; the cranium is dorsally compressed and the region above and anteriorly of the crests is squeezed. The groove that is observed along the sagittal suture of the nasal bones, it is quite steep due to the dorsally compression of the cranium.

P1 is present on the left toothrow but it is remarkably short with ‘atractoid’ shape; the right one is missing. The protocone on the cheek teeth is relatively short just like on APL-519 and APL-871; its lingual border is concave except on P2 where it is convex. The enamel of the fossettes is moderately plicated.

APL-518. The cranium was originally described by Koufos et al. (1997). The cranium is laterally compressed and poorly preserved; only the muzzle, the palate, and a part of the maxilla with the zygomatic bone are preserved. It belongs to a male individual. M3 and canines are in wear and the Galvayne’s groove appears at the gum line indicating an individual of ~10 years old. The muzzle is relatively wide. The facial crest is well-developed with its anterior margin to be placed at the middle of M1; it is ‘wavy’ just like all the other APL crania. The hinder margin of the narial notch is located above the

posterior half of P2. The orbit is placed well behind M3, it is relatively large and possibly oval-shaped.

Figure 5.51. *Equus apolloniensis*, cranium APL-148; (a) ventral view, (b) dorsal view, (c) right lateral view, and (d) left lateral view.

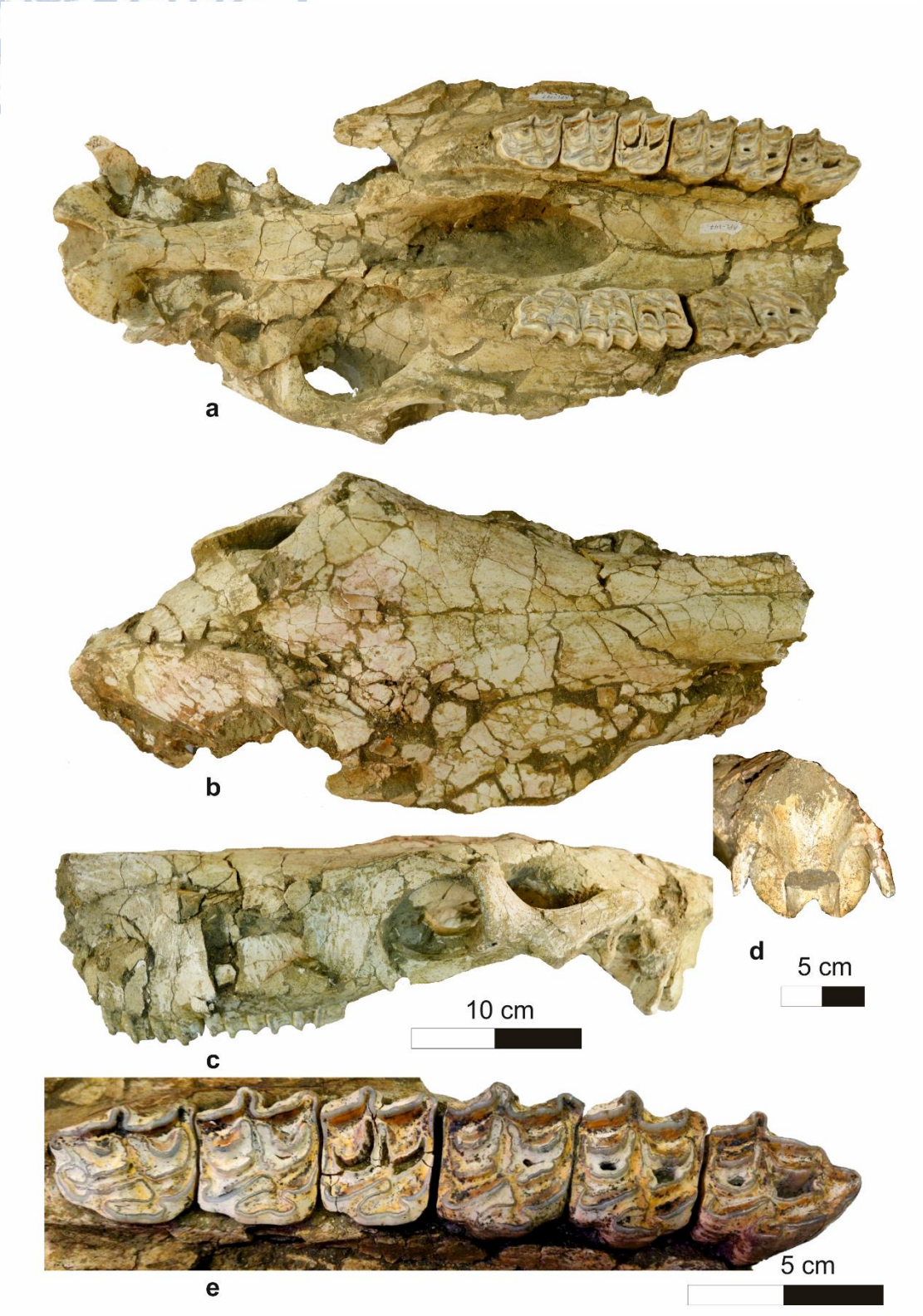

Figure 5.52. *Equus apolloniensis*, cranium APL-147; (a) ventral view, (b) dorsal view, (c) left lateral view, (d) occipital view and (e) right tooth row, occlusal view.

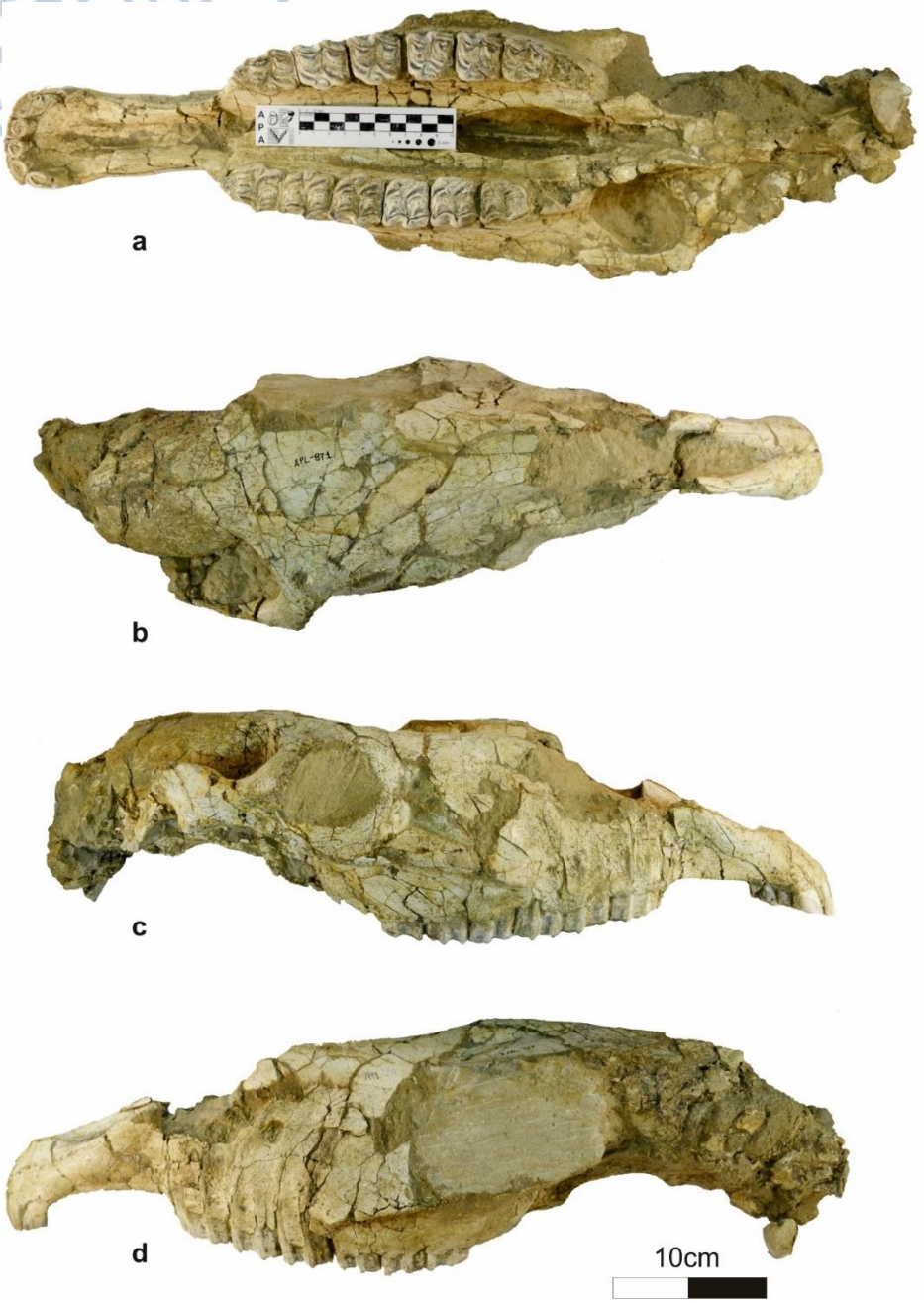

Figure 5.53. *Equus apolloniensis*, cranium APL-871; (a) ventral view, (b) dorsal view, (c) right lateral view, and (d) left lateral view.

APL-518 preserves all incisors, right canine and the tooth rows P2-M1(half broken) sin and P2-M3 dex. The protocone is relatively long and its lingual border is convex on P2 and concave on the other cheek teeth. The hypoconal constriction is always apparent, but not deep. The pli caballin is single and relatively elongated on all cheek teeth; on M3 it is double. The enamel of the fossettes varies from moderately to simply plicated with more or less shallow plications. All fossettes are closed and they don't communicate with each other.

APL-871. The cranium is described by Gkeme et al. (2021). It is almost complete, but laterally compressed; only the frontal nasal bones, the left zygomatic and temporal bones are missing (Figure 5.53). It lacks canines or alveoli for them indicating that it is a female individual. In ventral view, the muzzle is rather short, and it is laterally compressed. The palate is not very long but relatively wide. The choanae are large, elliptical-shaped and their anterior margin seems to be above the M1/M2 contact. The infraorbital foramen is large, and it is situated at the level of the parastyle of P4. The facial crest is slightly wavy, well developed; its left anterior border is situated caudally above the P4/M1 contact, while the right one is located above the posterior half of P4. The orbit is relatively short, elliptical and its anterior border is placed above the posterior margin of M3. The greatest breadth of the cranium seems to be behind the orbits. The zygomatic arch runs almost parallel to the sagittal plane of the cranium.

The check tooth rows are parallel to each other (Figure 5.53). The P1 is present on both sides; they are quite 'tall' reaching the occlusal level of P2. They are quite elongated and elliptical-shaped. The anterostyle on P2 is wide and rounded. The protocone is relatively short on all cheek teeth; its lingual border is more or less concave. The fossette margin is moderately plicated.

APL-872. The cranium is described by Gkeme et al. (2021). It is mediolaterally compressed, and lacks the frontal nasal bones, the right maxillary sinuses and both orbital fossae; only a part of the braincase is preserved, and the occiput is completely missing (Figure, Appendix). It possibly belongs to a female individual, relatively old; the Galvayne's groove on I3 is at its full length giving an average age 20 years old. The muzzle is relatively short and wide. The ratio muzzle breadth (M15) / muzzle length (M1) % is 50.4 mm. The palate is relatively short and wide. The major palatine foramens are placed at the anterior half of M3. The choanae are elongated and elliptical; their anterior border is situated approximately at the middle of M2. The left orbit is partially preserved; it is possibly rounded with its anterior border is far behind M3. The facial crest is well-developed, but it is not projecting very strongly laterally as on the other APL crania; its anterior border is placed above the mesostyle of M1, and it is slightly wavy like on all the other APL crania.

The wolf teeth are absent. The anterostyle on P2 is rounded and relatively wide. Protocone is relatively long and elliptical on all cheek teeth apart from P2; its lingual border is always more or less concave (on P2 it is straight to convex). The second and

third premolars are very worn and most of the enamel of the inner fossettes is gone. On the other cheek teeth, the plication is simple.

APL-858. The cranium belongs to a very young individual. The deciduous I3 is unworn, the deciduous premolars are slightly worn which gives an age between 7 to10 months old according to Levine (1982). The choanae are relatively short and oval-shaped; their anterior margin is placed at the middle of dP4. The facial crest is not well-developed; its anterior margin is placed above the middle of dP4. The deciduous cheek teeth are elongated. The lingual border of the protocone is straight on DP2 and concave on DP3, DP4. The posterior margin of the prefossette is always open posteriorly as well as the posterior margin of the postfossette on DP4. Hypoconal constriction is present on all teeth. The wolf teeth are present on both sides, but they are not worn.

Maxilla. Only one maxilla is preserved, APL-129, and it belongs to a very old individual with P4-M3 and P2-M3 on the left and right side respectively. On ventral view, the choanae are elliptical-shaped and remarkably wider than all other APL crania. This may be explained as a result to its perfect preservation; there is not any lateral deformation/compression; its anterior margin is situated at the middle of M3. The palate is relatively wide; the mean palatal breadth at the limit between P4 and M1(M13) is 88.21 mm. The major palatine foramens are situated at the middle of M3. On the pterygoid bone, the left hamulus is preserved and is strongly projected ventrally.

On occlusal view, the cheek teeth are large and extremely worn. On P4 and M2 only the prefossette is worn, while on P3 and M1 both fossettes (prefossette and postfossette) are completely worn. The anterostyle on P2 is wide and rounded. Protocone on all cheek teeth is relatively long (except on P2) while on M3 is extremely elongated. The lingual border of the protocone is concave with the exception on P2 and M3 where it is almost straight. On M3 the hypocone is isolated and forms an elliptical islet. A rudimentary pli caballin is observed on the right P2, P4 and M3; no pli caballin is observed on the left side on these teeth. Furthermore, the enamel of the fossettes on M3 are simple plicated.

Mandible. There is one almost complete mandible (APL-570) that has already been described by Koufos et al. (1997) and many fragments of bodies with more or less complete dentitions. APL-570 is slightly laterally compressed and only the left condyle and the right coronoid process are missing (Figure 5.54a). No canines are present which is indicative of a female individual. It seems that the vascular notch is apparent on APL-570, while on APL-792 it is quite shallow. The mental foramen is relatively large and single. On APL-570 and 633, there is no acute angle at the junction of the interalveolar

border with the border of p2 (Figure 5.53a3-4), while on APL-792 and 785, they join in a way that the junction forms an angle of almost 90 degrees. On APL-792, hypoplasia is observed on molars (Figure 5.53c).

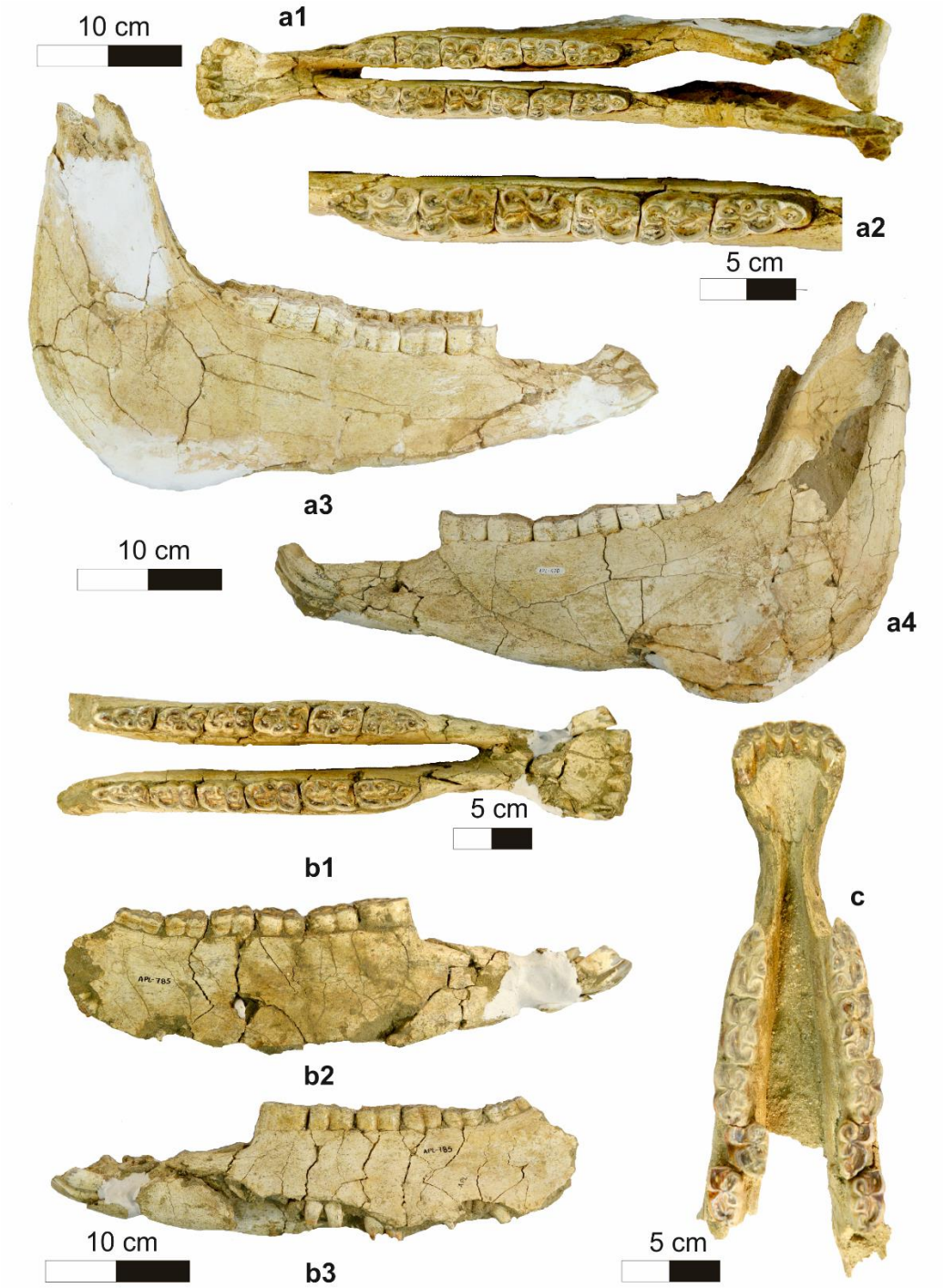

Figure 5.54. *Equus apolloniensis*, (a1–a4) mandible, APL-570: (a1) occlusal view, (a2) left tooth row, (a3) right lateral view, (a4) left lateral view; (b1–b3) partial mandible, APL-785: (b1) occlusal view, (b2) right lateral view, (b3) left lateral view; (c) partial mandible, APL-792: occlusal view.

Upper cheek teeth. Both premolars and molars are very long and large. Anterostyle on P2 is relatively long and wide. Fossettes are closed and they do not communicate. Parastyle is wide and well-developed and strongly projected labially. Mesostyle is also well-developed and wide projecting labially. On APL-148 (Figure 5.51a), the mesostyle of the right premolars is strongly notched, while on the left side it is not that clear. Fossettes are always closed, and they do not communicate except for the slightly worn teeth. The enamel of their borders is moderate plicated. On APL-147 (Figure 5.52e), the enamel of the buccal side of the fossettes is wrinkled resembling the pattern of *E. suessenbornensis*. Protocone is relatively long while on the worn teeth on APL-147 is more elongated (especially on M3). On APL-519, it is relatively shorter. The shape of the protocone varies from more elongated-elliptical to semilunar-elliptical; on M3 it can be atractoid. The lingual border of the protocone is more or less concave expect on P2 where it is straight or convex. The anterior border off the protocone is usually longer on molars than on premolars. On the same series, the postprotoconal groove is deeper on premolars than on molars (APL-148). Hypocone is rounded and elliptical shaped. On M3 it can be isolated and form an islet (APL-147, Figure 5.52e). Hypoconal constriction can be observed either none, weak or strong. The hypoconal groove is more or less pointed and relatively deeper on premolars than on molars. Pli caballin is usually present and single on all cheek teeth, and it disappears on very worn teeth; on premolars it is more elongated than on molars.

Lower cheek teeth. The linguaflexid is V-shaped. Metaconid is relatively wide, rounded, and cyclic-shaped. Metastylid is slightly smaller than metaconid, but also rounded (cyclic or elliptical-shaped) and its lingual border tends to be more pointed on premolars than on molars. Entoconid is squarish on premolars, while on molars is more elliptical. Postflexid on premolars is longer than preflexid, while on molars is less long. Parastylid is usually half open except for the quite worn teeth (APL-355) where it is closed. Ectoflexid is shallow on premolars more or less pointed, while on molars it is deeper reaching the mesio-lingual corner of postflexid without however penetrating the isthmus. Only on APL-355 (fragmentary ramus with p2-m3), ectoflexid of the second and third molar is very deep penetrating the isthmus. Pli caballinid is usually absent except for some slightly unworn molars (APL-139, 137, 345, 369) and premolars and molars on the mandible APL-785, where it is simple to rudimentary (slightly worn cheek teeth). On the same series, the enamel of the postflexid on premolars can be slightly plicated while no plication appears on molars. On APL-785 (first stage of

wear), the enamel on the postflexid is more plicated than the rest of the specimens. A single pli on the preflexid is observed on: p4 of APL-345, p4 of APL-295, m3 of APL-785 and the isolated m3 APL-301. Protostylid is present on molars and more frequent on premolars, it is not isolated, but appears as a simple and shallow plication; it is notable but not well-developed (rather weak). On the same series (mandible APL-570), the left m1 and m2 it is present, while on the right series it is extremely weak (m1) or even absent (m2).

Metapodials. The third metapodials are long and relatively robust. The slenderness index, distal maximal articular breadth (M11) / maximal length (M1) % ranges from 19.8–20.9 (n = 16; mean = 20.5) for the third metacarpals, and from 16.1–18.1 (n = 23; mean = 17.1) for the third metatarsals. The morphology of the articular surfaces for the lateral metapodials is variable. The distal maximal supra-articular breadth at the tubercles (M10) is slightly greater than at the trochlea (M11) on the metacarpals, while on the metatarsals the distal maximal supra-articular breadth at the trochlea (m11) is greater than at the tubercles (m10). The distal keel is well developed; the keel index varies between 125.1 and 132.9 (n = 20; mean = 128.1) for the third metacarpals, and from 127.5–146.0 (n = 28; mean = 134.6) for the third metatarsals.

Comparison and discussion.

One of the most important differences between *E. apolloniensis* and *E. stenonis* is the depth of the narial notch (Koufos et al. 1997; Gkeme et al. 2021). In Apollonia 1 crania, the narial notch is shallow and its hinder margin is situated above the mesostyle of P2. Furthermore, no preorbital fossa is traced in APL crania, unlike the typical cranium of *E. stenonis* (IGF 560), where it is clearly developed (Azzaroli 1965, 1990; Bernor et al. 2019). A depression on the occiput of APL crania is also lacking unlike in *E. stenonis* and *E. altidens* from Gerakarou and Krimni. Unfortunately, the supraoccipital crest, which could give more information is missing from all crania of *E. apolloniensis*. Moreover, as the distance between the vomerine notch and the basion (M4) can be interpreted as an estimation of the brain case (Eisenmann and Baylac 2000), the braincase of *E. apolloniensis* seems to be relatively larger than that of *E. stenonis vireti* compared to the basilar length (M6). The cranium of *E. apolloniensis* is distinguished easily from that of *E. altidens* from Gerakarou and *E. altidens* from Dmanisi (Bernor et al. 2021) by its larger dimensions (Figure 5.30, 5.55).

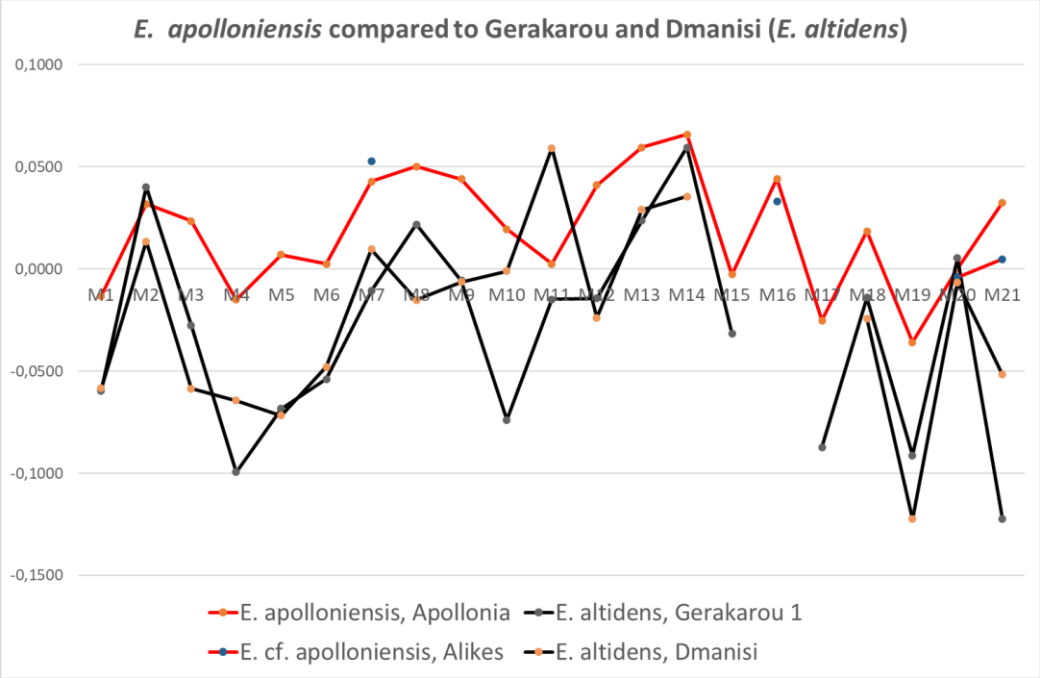

Figure 5.55. Simpson's log ratio diagrams comparing the cranial dimensions of *E. apolloniensis* with *E. altidens* from Dmanisi and Gerakarou. Standard: *Equus grevyi* (Eisenmann 2007). Data from Bernor et al. (2021) and personal dataset.

In comparison with *E. stenonis*, the cranium of *E. apolloniensis* is characterized by shorter muzzle and palatal length (M1, M2), wider choanae (M12), longer cheek tooth rows (M7, M8, M9), narrower muzzle (M14, M15), quite shorter naso-incisival notch (M30) and longer cheek length (M31) (Figure 5.30). The length of the cheek tooth rows (M7, M8, M9) of *E. apolloniensis* are quite similar with those from Alykes and Volos. *E. apolloniensis* resembles *E. senezensis* in the basilar length and the short muzzle (M6, M1), but it differs, by having larger cheek tooth rows (M7, N8, 9), wider choanae (M12), wider muzzle (M14, M15), shorter naso-incisival notch (M30), and remarkably longer cheek length (M31). Unfortunately, the lack of adult crania of *E. a. granatensis*, *E. suessenbornensis* and *E. wuesti* does not permit any further comparison.

In Figure 5.32, PCA was conducted on selected cranial measurements based on Bernor et al. (2021) analysis. PC1 (76.14%) separates species by their basilar length (M6) from less elongated crania to more elongated (negative to positive values), while PC2 (9.26%) clusters species by their post-vomerine length (M4) and post-palatal length (M5) from negative to positive (more to less elongated). *Equus apolloniensis* is clustered with *E. simplicidens* by its reduced M4 values and it is separated from *E. stenonis* sensu lato.

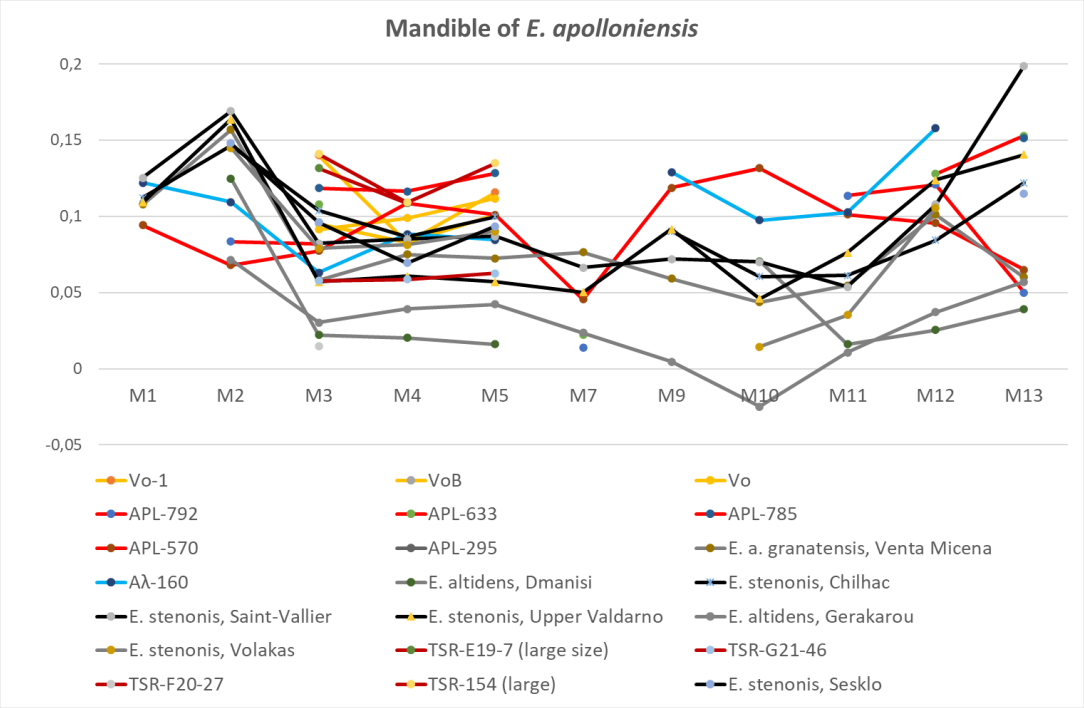

Figure 5.56. Simpson's log ratio diagrams comparing the mandibular dimensions of *E. apolloniensis* to those from Volos, Alykes, Tsiotra Vrysi, Volakas and other Early Pleistocene European equids. Standard: *Equus hemionus onager*. Data from Eisenmann (2018), Bernor et al. (2021) and personal dataset.

The mandible of *E. apolloniensis* is large in size (Figure 5.54, 5.56). The vascular notch on APL-570 from Apollonia and also on IGF560 (holotype of *E. stenonis*) is relatively shallow, but perceptible, while on NHML20.163362A it is strong and less apparent on NHML20.163361A (both specimens from Saint-Vallier). The vascular notch is also present in *E. altidens* from Gerakarou, Krimni and Dmanisi and *E. stehlini*. The mandibles from Alykes and Volos are large and rather similar to each other (general morphology, presence of the vascular notch), and they both resemble the ones from Apollonia. The length of the mandible (M1) from Alykes is larger than most of *E. stenonis* subspecies/populations and *E. altidens granatensis* (Figure 5.56), and also longer than the one from Apollonia because the latter is slightly broken at the condyles. The corpus of the jaw (M10, M11, M12) on APL and Aλ specimens is higher than *E. altidens* from Dmanisi, *E. stenonis* subspecies/populations and *E. a. granatensis*. The specimens TSR-E19-7 and TSR-154 from Tsiotra Vrysi exhibit long cheek tooth rows (M3, M4, M5) analogous to *E. apolloniensis*.

The teeth of *E. apolloniensis* are more elongated than those of *E. stenonis* and *E. altidens*. The occlusal surface of the cheek teeth of *E. apolloniensis* is large, close to

that of *E. suessenbornensis* from Cueva Victoria; they are similar in breadth, but the latter has more elongated occlusal surfaces. The lingual border of the protocone is concave on *E. apolloniensis* (see also Koufos et al. 1997), Alykes (Athanassiou 1998) and Volos and its distal part is clearly more pronounced like in *E. altidens* and *E. suessenbornensis*, though not far from the condition seen in *E. s. vireti*. The length of the protocone is similar to *E. stenonis vireti* (Figure 5.57). The postprotoconal groove of *E. apolloniensis* is deeper than in *E. stenonis*. Like *E. suessenbornensis*, the buccal side of the fossettes in APL-147 (teeth at fourth stage of wear) is wrinkled (Figure 5.52e). On *E. apolloniensis*, the pli caballin is present; on APL-148 (teeth at first stage of wear), pli caballin is multiple on the premolars with a very large base, resembling sussemiones (Eisenmann 2010); however, it reduces in size by the progressive attrition and disappears at the final wear stages. The shape of the double knot varies from typically rounded stenonoid, separated by a pointed and deep linguaflexid (APL-295, 570, 785) to a rather hemionine type with an elongated metaconid and pointed metastylid separated by a shallow and wide linguaflexid (APL-633, 792). The length of the double knot is slightly longer in relation to its occlusal length than all *E. stenonis* samples (Figure 5.58). In these features, the APL equid resembles *E. a. granatensis* (Eisenmann 1999), from which (and sussemiones in general) differs in the shallow ectoflexid on the molars that recall for hemiones and asses. The ectoflexid on APL-355 (on m2 and m3) and APL-369 is very deep penetrating the isthmus. These specimens could belong to the second species identified in Apollonia 1; however, no other differences in the morphology or size were observed in order to assign them to a separate taxon. The presence of a 'bridge' on the first molar of APL-295 is a character that appears on both wild asses and hemiones (https://vera-eisenmann.com/, 20-12-2020). The presence of the pli protostylid on the lower premolars and molars (except on p2) is a character that is usually occur in the sussemiones (Eisenmann 2010, https://vera-eisenmann.com/, 20-12-2020).

The third metacarpal of *E. apolloniensis* is distinguished from *E. altidens, E. senezensis* and Libakos (Figure 5.59a), due to its larger dimensions and from *E. suessenbornensis* and *E. mosbachensis* due to its smaller dimensions (Figure 5.59b). *E. apolloniensis* has longer metacarpals (M1) than all *E. stenonis* samples except for Olivola, and the isochronous, to *E. apolloniensis, E. a. granatensis* which both seem rather similar to those from Apollonia. However, *E. apolloniensis* has deeper and narrower metacarpal diaphysis (M3,4) than *E. stenonis* from Greece and Europe (Figure 5.59a).

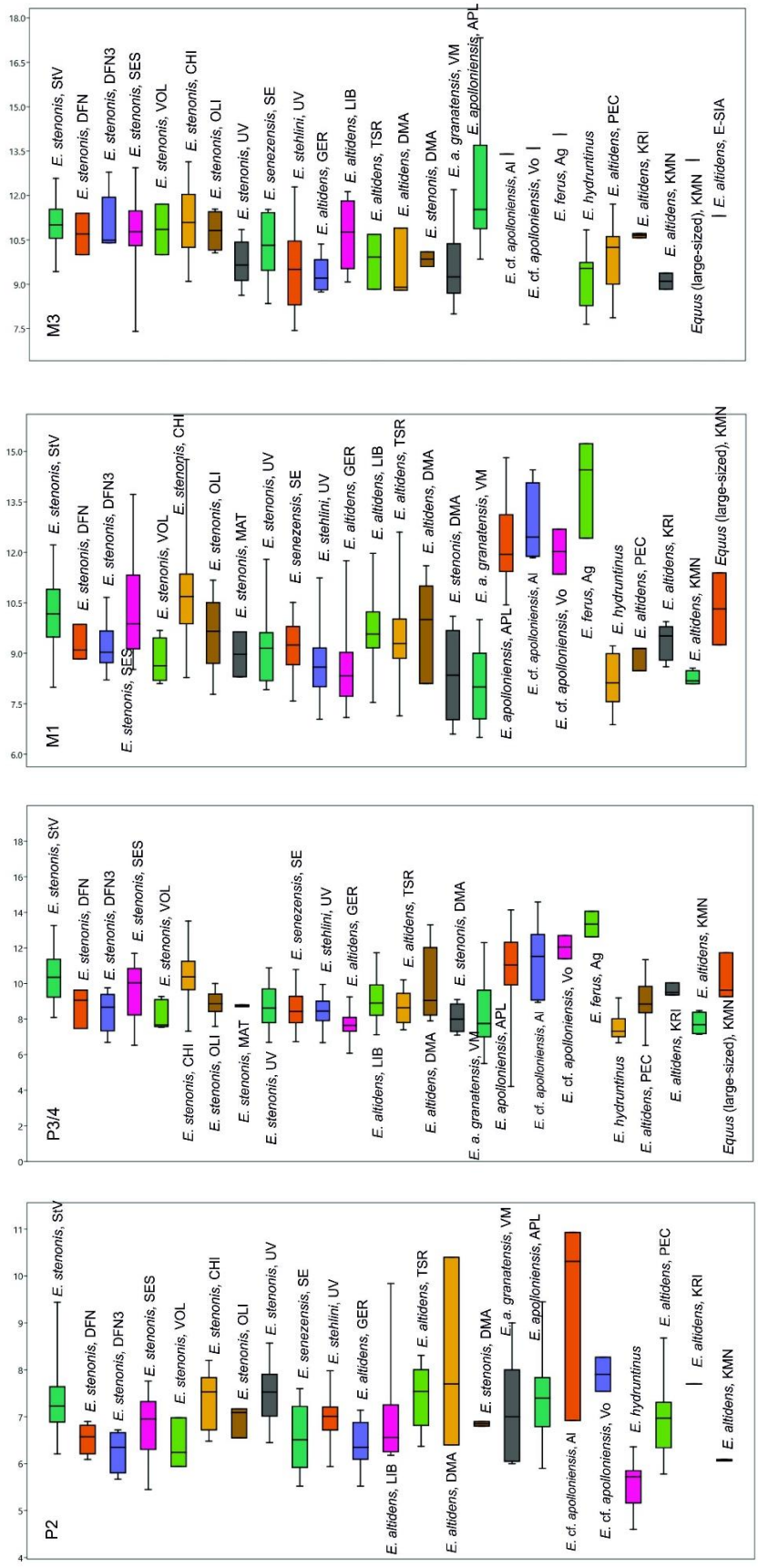

Figure 5.57. Boxplots of the protocone length of each upper cheek tooth of various Greek and European Early to Middle Pleistocene equids. Data from Bernor et al. (2021) and pers. dataset.

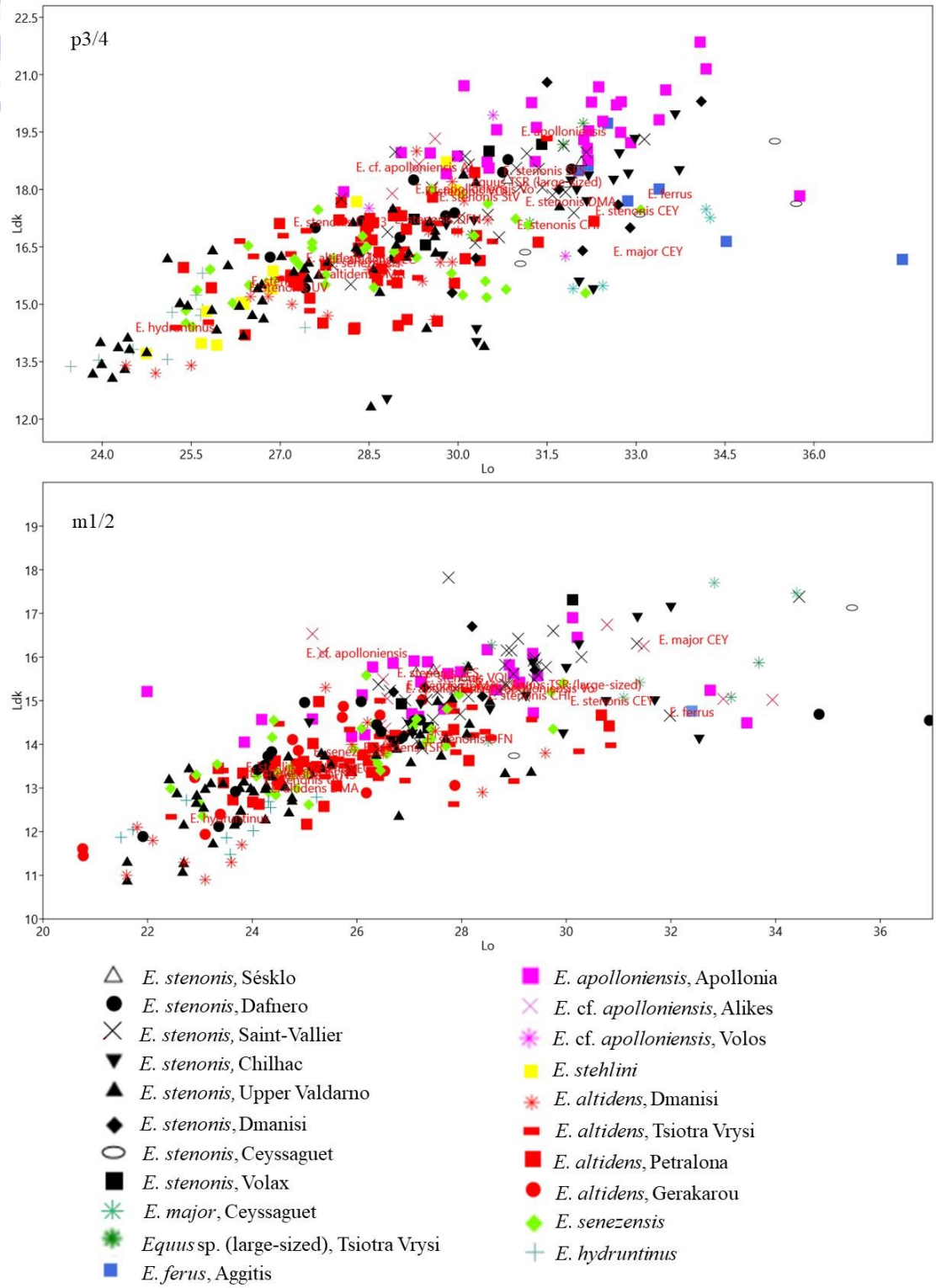

Figure 5.58. Bivariate plots of the length of the double knot (Ldk) versus the occlusal length (Lo) of the p3,4 and m1,2 of *E. apolloniensis* compared to other Early to Middle Pleistocene European equids. Data from Eisenmann and Boulbes (2020), Eisenmann (2017a, b, c), Bernor et al. (2021), Cirilli et al. (2021) and personal dataset.

This means a relatively slenderer metacarpal unlike all *E. stenonis* samples, except for that from Volax; this is probably due to the small number of specimens from the latter site (only three). Some more differences are seen in the distal epiphysis. The metacarpal of the Volax equid is wider with slightly stronger keel and deeper trochlea (M10-M14). The metacarpal proportions of *E. apolloniensis* seems to be closer to those of *E. stenonis vireti*, from which it differs in the greater maximal length (M1), the narrower diaphysis (M3), the less wide breadth at the tubercles (M10), the deeper trochlea (M13, M14), the larger articular facet for os magnum, and the quite larger articular facet for os hamatum (M8) (Figure 5.59a). Although the maximal length of the third metacarpal of *E. apolloniensis* is close to those of the European taxa *E. a. granatensis* and *E. altidens* all the other dimensions are quite larger, distinguishing it well from them and suggesting for it a more robust appearance (Figure 5.59b). The third metacarpal of *E. apolloniensis* and *E. wuesti* seem to have similar proportions, but the latter is significantly longer (M1). Thus, the metacarpal of *E. wuesti* appears slenderer with narrower trochlea (M11), weaker keel (M12), and considerably wider articular facet for the os hamatum (M8) than those of *E. apolloniensis* (Figure 5.59b).

The third metatarsal of *E. apolloniensis* is longer (M1) than all *E. stenonis* samples from Greece and Europe (Figure 5.59a). Along with *E. wuesti*, it seems intermediate between the metatarsals of *E. stenonis* and the middle Pleistocene equids *E. suessenbornensis* and *E. mosbachensis* (Figure 5.59b). Its diaphysis and proximal epiphysis have similar proportions with *E. stenonis*, except for *E. stenonis* from Dafnero 1, 3, which is characterized by a less deep diaphysis (M4) and from Sésklo and Dafnero 1, 3, both showing a less deep proximal articular facet (M6). Furthermore, the articular breadth at the trochlea (M11) is greater than the suprarticular breadth at the tubercles (M10) unlike all *E. stenonis* except for Dafnero 1, 3 and Volax (Figure 5.59a). Comparing with the European *E. stenonis*, *E. apolloniensis* has longer metatarsal (M1) with deeper trochlea (M13, M14), and larger articular facet for cuboid (M8) (Figure 5.59a).

Like third metacarpals, the third metatarsal of *E. apolloniensis* is close to *E. stenonis* from Saint-Vallier, but its remarkably shorter maximal length (M1) distinguishes it well from the latter taxon (Figure 5.59a). The third metatarsal of *E. a. granatensis*, *E. altidens*, and *E. senezensis* are smaller than that of *E. apolloniensis* (Figure 5.59a, b).

a

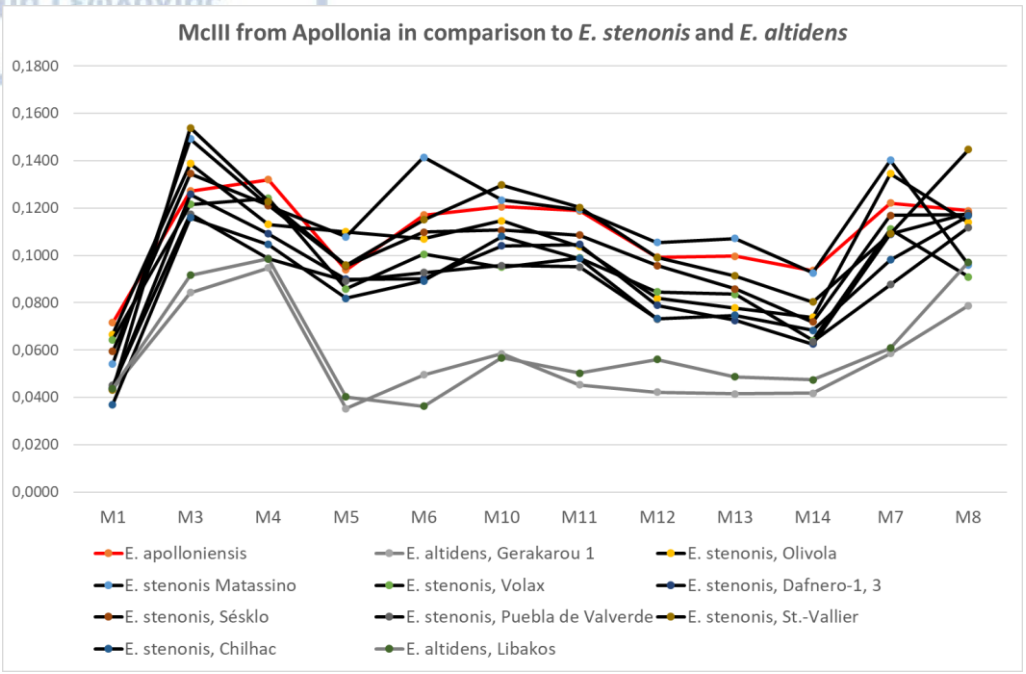

b

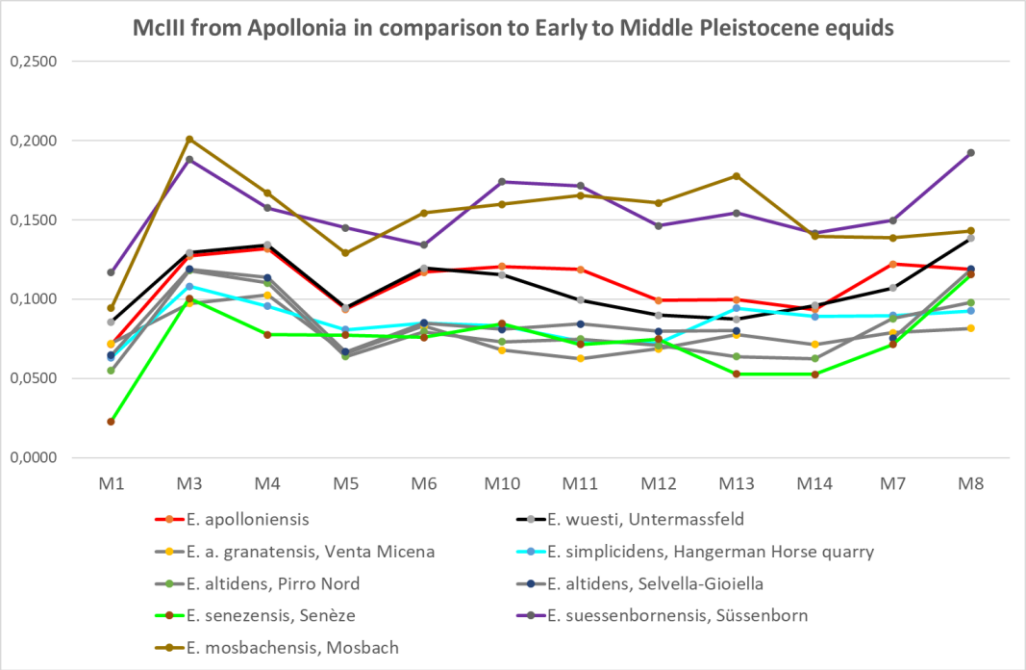

Figure 5.59. Simpson's log ratio diagrams comparing the third metacarpal of *E. apolloniensis* to (a) E. stenonis samples/populations and the Greek E. altidens, (b) Early to Pleistocene European and North American equids. Standard: *Equus hemionus onager*. Data from Eisenmann (2017, 2018), Eisenmann and Boulbes (2020), Bernor et al. (2021), Cirilli et al. (2021) and personal dataset.

E. wuesti is slightly longer (M1) than *E. apolloniensis* but it clearly differs in the larger proximal articular dimensions (M5, 6) and the considerably larger articular facets for cuneiform and cuboid (M7, 8). *E. apolloniensis* and *E. suessenbornensis* metatarsals have similar proportions but the latter species has significantly larger third metatarsal (Figure 5.59a). In both taxa, the distal articular breadth (M11) seems larger relatively to the suprarticular breadth at the tubercles (M10). The third metatarsals of *E. apolloniensis* are well separated from those of *E. mosbachensis* and *E. suessenbornensis* by their quite smaller size (Figure 5.59a).

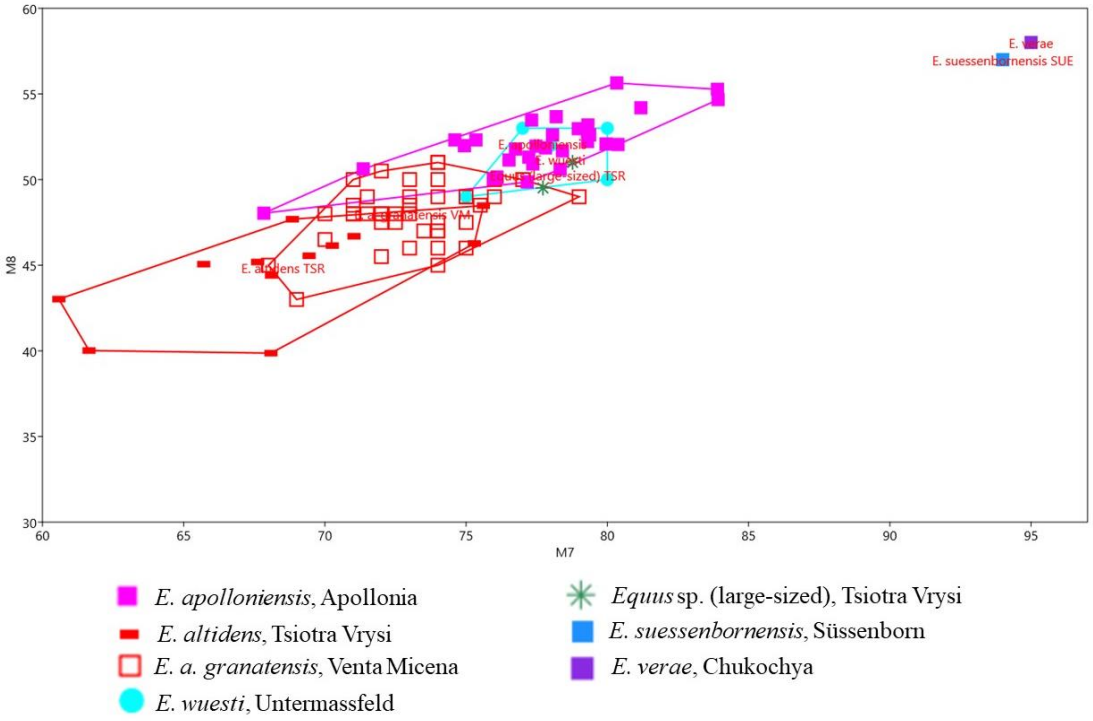

Figure 5.60. Bivariate plots of the length of the distal maximal breadth (M7) versus the distal maximal depth (M8) of the tibia of *E. apolloniensis* compared to other Early to Middle Pleistocene European equids. Data from Eisenmann and Boulbes (2020), Eisenmann (2017a, b, c, 2018), Bernor et al. (2021), Cirilli et al. (2021) and personal dataset.

The tibiae are less longer than those of *E. suessenbornensis*, and close to *E. wuesti* (Figure 5.60). The astragali of *E. apolloniensis* are generally longer than *E. stenonis* sensu lato (Figure 5.61), while the latter is wider (M4). The specimens from Platanochori and the single astragalus from Riza-1 fall within the range of *E. apolloniensis*. The three specimens from Vatera-F (PO496F, PO101, PO095) overlap with both *E. stenonis* sensu lato and *E. apolloniensis*, while the single specimen from

Vatera-E (PO001E) is seems to belong to a gigantic equid close to *E. major* from Senèze and Ceyssaguet and larger than *E.* cf. *livenzovensis*.

The calcaneum of *E. apolloniensis* (Figure 5.49) overlaps with those of *E. wuesti*, *E. stenonis vireti* and *E. stenonis* from Sesklo and Olivola. All of them are well-separated from all medium sized equids (Gerakarou, Libakos, Petralona, Dmanisi, Tsiotra Vrysi, *E. stehlini*, *E. senezensis*). The three specimens from Vatera (F and D) (PO129F, PO604D5, PO096F) overlap with both *E. stenonis* subspecies and *E. apolloniensis*.

In the PCA analyses of the first phalanx (Figures 5.23, 5.49), PC1 separates species by maximal length (M1) from negative to positive (less to more elongated phalanges), whereas PC2 expresses the slenderness from negative to positive values (wide to narrow). The results support the previous interpretation that *E. apolloniensis* is close to *E. stenonis* from Sésklo (mainly because Olivola and Sésklo exhibit slender built than the typical *E. stenonis*).

Recently the species *E. apolloniensis* was considered as a valid taxon by Gkeme et al. (2021). The exact taxonomic position of *E. apolloniensis* and its phylogenetic relationships to the stenonoid equids is a matter of debate (Koufos et al. 1997; Palombo and Alberdi 2017; Eisenmann and Boulbes 2020; Eisenmann and Kuznetsova 2004; Boulbes and Van Asperen 2019). *Equus apolloniensis* was originally described as a species with both stenonoid and caballoid features (Koufos et al. 1997). The shorter muzzle, the more elongated protocones (which occurred at 1.2–0.7 Ma, Boulbes and Van Asperen 2019) and the slender metapodials (slenderer than the archaic *E. stenonis*) indicate an advanced species adapted to dry-cool habitats. According to Koufos et al. (1997), *E. apolloniensis* could "*represent a transitional form from the typical* E. stenonis *to the middle Pleistocene horses* (Equus *ex gr.* E. suessenbornensis). According to Eisenmann and Boulbes (2020), *E. apolloniensis* shares great similarities in the morphology of the teeth and the general proportions of the metapodials with extant wild asses (*E. africanus*), and thus it could represent "*a step within the lineage of asses soon after their differentiation*". Furthermore, similarities with *E. altidens* from Gerakarou, Venta Micena and Pirro Nord, and *E. wuesti* on either the metapodials and/or the tooth morphology make relationships of *E. apolloniensis* more complicate.

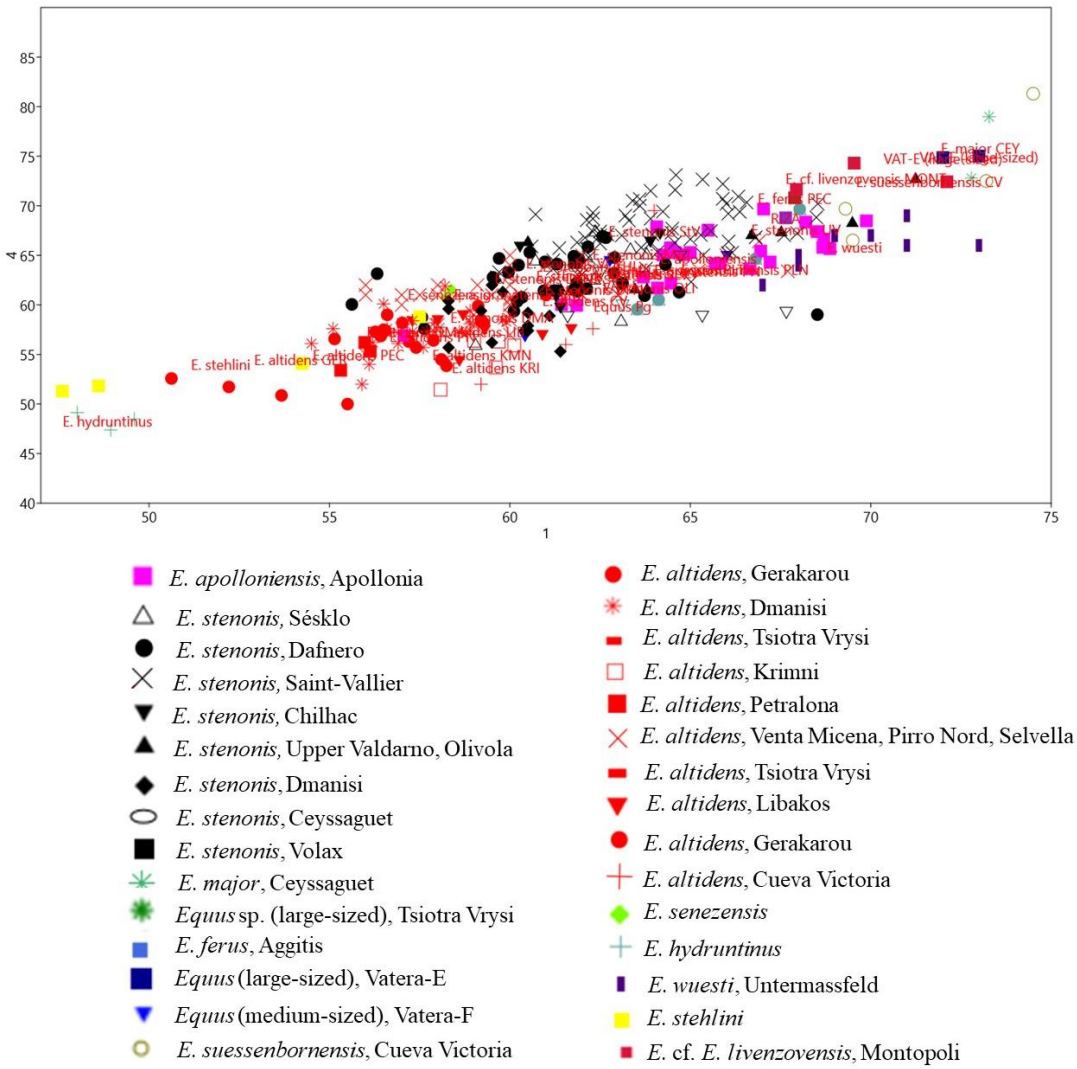

Figure 5.61. Bivariate plot of the maximum length (M1) versus maximum width (M4) of the astragalus of *E. apolloniensis* compared to several Early to Middle Pleistocene European equids. Data from Eisenmann and Boulbes (2020), Eisenmann (2017a, b, c, 2018), Bernor et al. (2021), Cirilli et al. (2021) and personal dataset.

Based on the basicranial proportions, Eisenmann and Kuznetsova (2004) and Eisenmann and Boulbes (2020) consider *E. apolloniensis* as a true *Equus* along with *E. suessenbornensis* and other equids. Eisenmann (2006) and Eisenmann and Baylac (2000) distinguish the crania of true *Equus* from the primitive *Plesippus* and *Allohippus*, using Franck's index [vomerine length (M3) / post-vomerine length (M4) %] and the palatal index [palatal length (M2) / vomerine length (M3) %]. In the best-preserved specimen APL-148, Franck's index is 112, indicating that vomerine length is longer than post-vomerine one, contrary to the true horses, and it is similar to asses and donkeys (Eisenmann and Baylac 2000). On the other hand, the palatal index on APL-

148 and APL-872 is 103 and 104.3, respectively, indicating a slightly longer palate than vomerine length, a character of true *Equus*. Consequently, *E. apolloniensis* must be assigned to *Equus*, though not to the caballine forms. It is likely the oldest occurrence of a cranium belonging to a true *Equus* (non caballine) in Europe (Eisenmann and Kuznetsova 2004; Boulbes and Van Asperen 2019), while *E. mosbachensis* von Reichenau, 1915 dated at 0.5 Ma, is believed to be the first evidence of a caballine equid (Eisenmann 2006; Maul et al. 2000). Considering all mentioned above, the following hypotheses could be formulated:

(a) *E. apolloniensis* could be an intermediate form between *E. stenonis* and the middle Pleistocene equid, *E. suessenbornensis*. Although the general size of the metapodials of *E. apolloniensis* is similar to those of *E. stenonis*, the proportions fit better with the slender but smaller *E. altidens* from Pirro Nord and Gerakarou. In other words, there is an obvious proportional analogy associated with a size increase through time from the metapodials of *E. altidens* from Gerakarou and Pirro Nord to those of *E. apolloniensis* (see also Koufos et al. 1997). *E. apolloniensis* may originate from an *E. altidens* stock-keeping similar proportions on the metapodials but increasing in size. Palombo (2016) suggested that the equid from Gerakarou, and perhaps *E. wuesti* and *E. apolloniensis* could represent different local species or ecomorphotypes of the same lineage. Although this scenario cannot be ruled out with the available data, differences on the crania (at least with the better-known from Gerakarou) contradict the hypothesis of local ecomorphotypes and rather support the idea of different species from the same lineage. The affinities with *E. suessenbornensis* at the distal articulations of the metapodials (analogies between M10–11) could also support a link between the two species. This hypothesis rather supports the idea that both species, *E. suessenbornensis* and *E. apolloniensis*, evolved in Europe from a stenonoid lineage.

(b) Based on similarities of both upper and especially lower teeth and metapodials, Eisenmann and Boulbes (2020) noted affinities between *E. apolloniensis* and the modern wild asses (*E. africanus*). If indeed, as these authors state, *E. apolloniensis* represents an early step in the lineage of asses, it cannot be linked to stenonoid s. s. and *E. suessenbornensis* (Boulbes and Van Asperen 2019). Although the lower teeth of the mandible APL-570 are ass-like, the revised description of both old and new material suggests that *E. apolloniensis* resembles asses as much as hemiones.

Considering all mentioned above, the similarities with the stenonoid equids and the proportional similarities of its metapodials to those of *E. altidens* from Pirro Nord and

Gerakarou rather support the first hypothesis. However, the relationship of *E. apolloniensis* to the other European Early Pleistocene equids will be examined in the Chapter 6 (Phylogeny).

Equus cf. *E. apolloniensis*

Localities.

Alykes (Aλ), Magnesia, Thessaly

Volos (Vo), Magnesia, Thessaly

Material.

Alykes. Fragment of cranium Aλ-20; fragment of maxilla P2-M3 sin Aλ-171; isolated M1/2 dex Aλ-270; mandible Aλ-160; distal part of radius Aλ-21; third metatarsal Aλ-269; first anterior phalanx Aλ-32; second anterior (?) phalanx Aλ-23.

Volos. Fragment of maxilla with P2 dex Vo-2; fragment of maxilla with P2-M3 sin Vo-3; fragments of mandibular bodies with p2, p4-m3 sin and dex Vo-1; fragment of mandibular body with p2-m3 sin Vo; fragment of mandibular body with p2, p4-m3 dex Vo; isolated p3/4 sin Vo-28; proximal parts of radius sin Vo-32, 34; proximal and distal part of third metacarpal sin Vo-27; third metatarsal sin Vo-4; first anterior(?) phalanx Vo-26.

Description.

Aλ. The material from Alykes was originally described by Athanassiou (1998) referring the equid as *Equus* sp. and later as *Equus* cf. *apolloniensis* (Athanassiou 2002). The cranium Aλ-20 (Figure 5.62) belongs to a young adult equid 3-4 years old; incisors are worn but the degree is unknown, and premolars are slightly worn. Only a part of the maxilla and muzzle is preserved. The narial notch riches the mesostyle of P2. The facial crest is well developed, and its anterior margin is situated above the half of M1. There is no preorbital fossa. The upper cheek teeth are incredibly large in lateral view (Figure 5.62b). The premolar length is 106.87. For Aλ-171, the length of premolars (M7) and molars (M8) is 100.24 and 90.75 respectively. The protocone is elongated, especially on M1; its anterior border is more pronounced anteriorly. The lingual border of the protocone is concave except for P2 where it is convex and for M3 where it is straight. The parastyle of P3 and P4 and the mesostyle on P4 in Aλ-171, is slightly notched. The plication is simple, while pli caballin is single or absent.

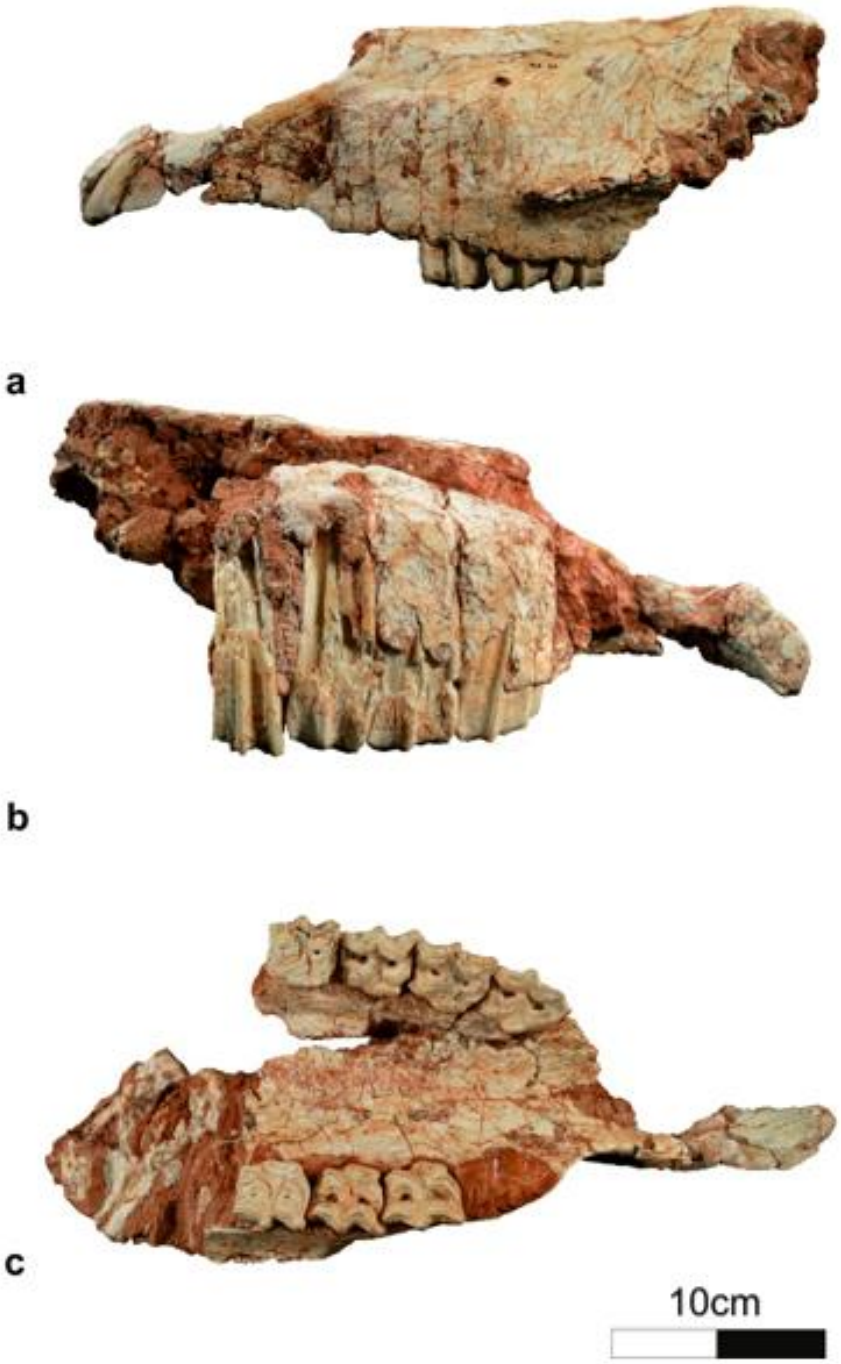

Figure 5.62. *Equus* cf. *apolloniensis*, cranium Αλ-20; (a) left lateral view, (b) right lateral view, (c) ventral view; (d) occlusal view.

The complete mandible Αλ-160 is compressed laterally, and only small parts of the condyles and processes are missing (Figure 5.63a). The mandible belongs to an old individual. The mandibular corpus is high. The vascular notch is apparent. There is no

acute angle at the junction of the interalveolar border with the border of p2. The p1 is absent. The lower cheek teeth are relatively large (Figure 5.63) and typically stenonoid (V-shaped linguaflexid). The ectoflexid is shallow on premolars, while on molars it is deeper, penetrating the isthmus (Figure 5.63b). Metaconid is relatively wide, with round occlusal outline, while the metastylid is slightly smaller, but also rounded (round or elliptical-shaped) and its lingual border tends to be more pointed on premolars than on molars. The entoconid is squarish on premolars, while on molars is more elliptical. Pli caballinid is usually absent or rudimentary. Protostylid is present on molars and more frequent on premolars, it is not isolated, but appears as a simple, shallow, rather weak, plication. For the third metatarsal Aλ-269, the proximal flatness (PF), proximal articular breadth (M5)/proximal articular depth (M6), is 1.28.

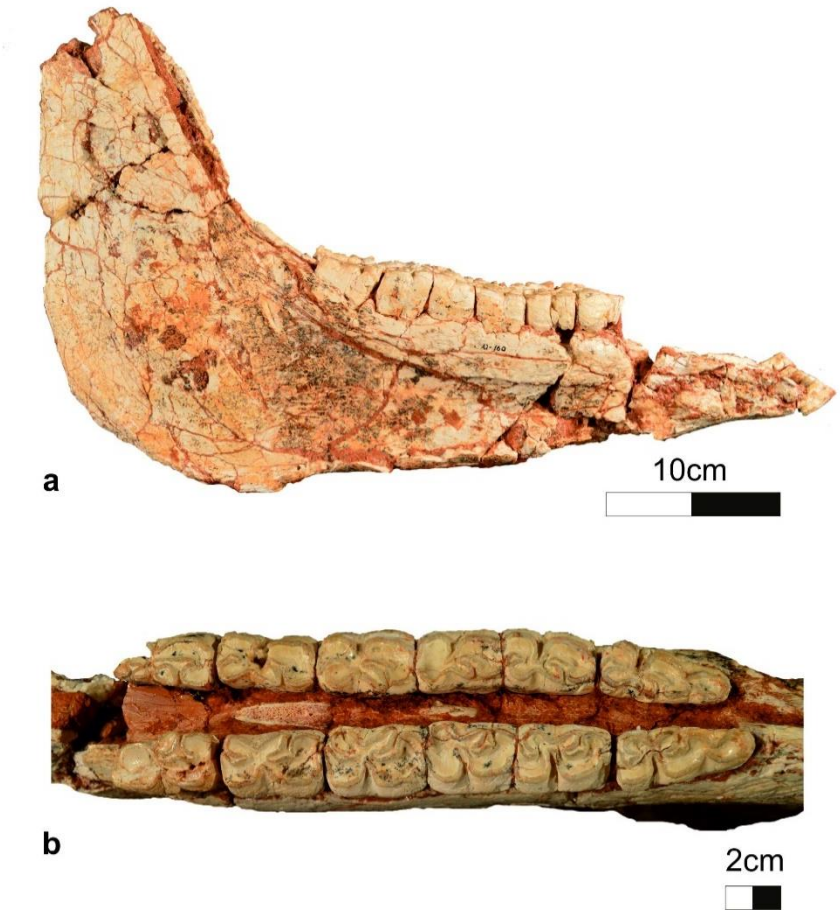

Figure 5.63. *Equus* cf. *apolloniensis*, mandible Aλ-160; (a) right lateral view, (b) occlusal view.

Vo. The upper cheek teeth on Vo-3 are large and elongated in profile view (Table 2a, Appendix 2). The protocone is elongated; its anterior border is more pronounced anteriorly. The lingual border of the protocone is concave except for P2 where it is

convex and for M3 where it is straight. The postprotoconal groove is relatively deep on premolars. The plication is moderate, while pli caballin is single or absent. On the lower cheek teeth, the linguaflexid is V-shaped (typically stenonoid) and the ectoflexid is shallow on premolars more or less pointed, while on molars it is deeper, penetrating the isthmus, reaching, and flattening the linguaflexid. Metaconid is relatively wide and rounded. Metastylid is slightly smaller than metaconid, but also rounded and its lingual border is pointed; on premolars it tends to be more pointed than on molars. Entoconid is squarish on premolars, while on molars is more elliptical. Pli caballinid is usually absent or rudimentary. A single pli on the preflexid is occasionally observed. Protostylid is not isolated but appears as a simple and shallow plication; it is notable but not well-developed (rather weak).

Comparison and discussion.

The crania-maxilla from Alykes and Volos resemble in size and general morphology of *E. apolloniensis*. Al-20 exhibits similar morphology and morphometry (Figures 5.55, 5.64), to *E. apolloniensis*; the length of the muzzle (M1) is similar, while the ratio of the cheek length (M30) and narial opening (M31) is rather close. On Al-20, the length of the tooth row (M9) was estimated (M2, M3 are missing): it is shorter than *E. apolloniensis*. The protocone is elongated like *E. apolloniensis*. On Aλ and Vo upper cheek teeth, plication ranges from moderate to simple based on the stage of the dental wear. The length of the lower cheek tooth row (M3, M4, M5) from Alykes is slightly shorter than *E. apolloniensis* and Volos samples, because the mandible belongs to an old individual and cheek teeth are very worn (Figure 5.56). On Vo-3, the length of the premolars (M7) is greater than molars (M8) which is vice versa on *E. apolloniensis*. This could be justified due to the fact that Vo-3 belongs to a young adult and the molars are slightly worn. Moreover, the length of the cheek teeth resembles that of the cheek teeth of *E. apolloniensis*. The shape of the double knot varies from typically stenonoid to a rather hemionine type with an elongated metaconid and pointed metastylid separated by a shallow and wide linguaflexid. The dimensions of the third metacarpal and first anterior phalanx from Volos and Alykes coincide to those of *E. apolloniensis*.

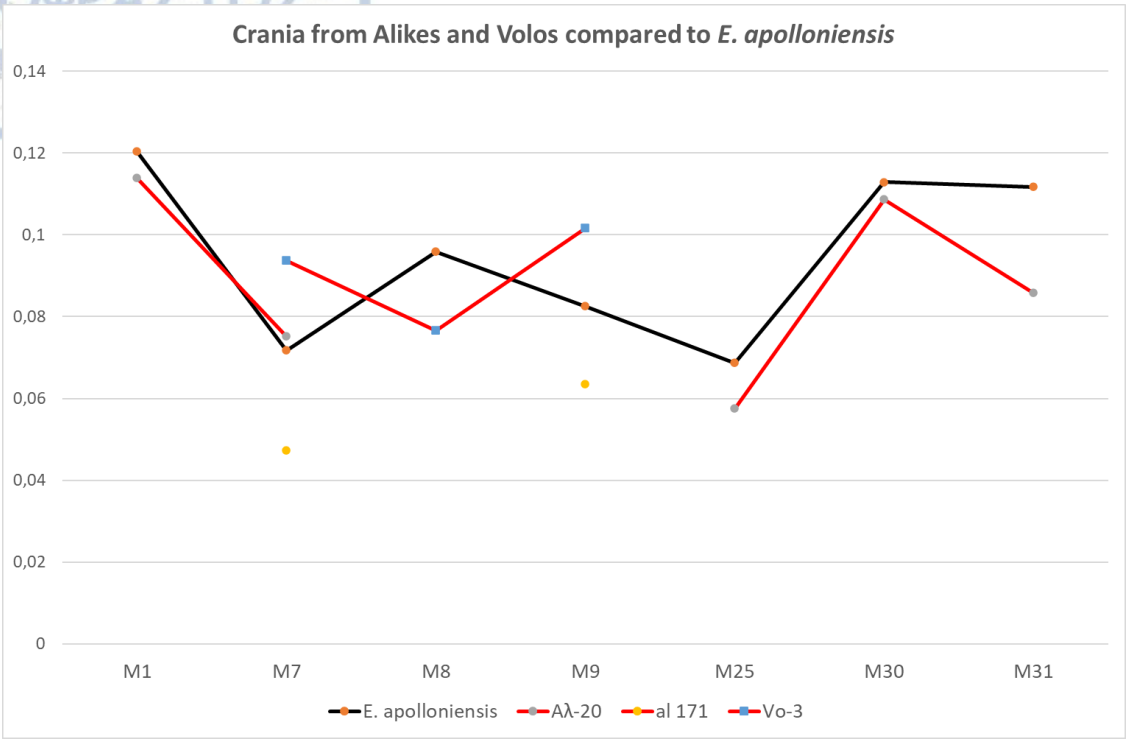

Figure 5.64. Simpson's log ratio diagrams comparing the cranial elements from Alykes and Volos to *E. apolloniensis* (Apollonia). Standard: *Equus hemionus onager*.

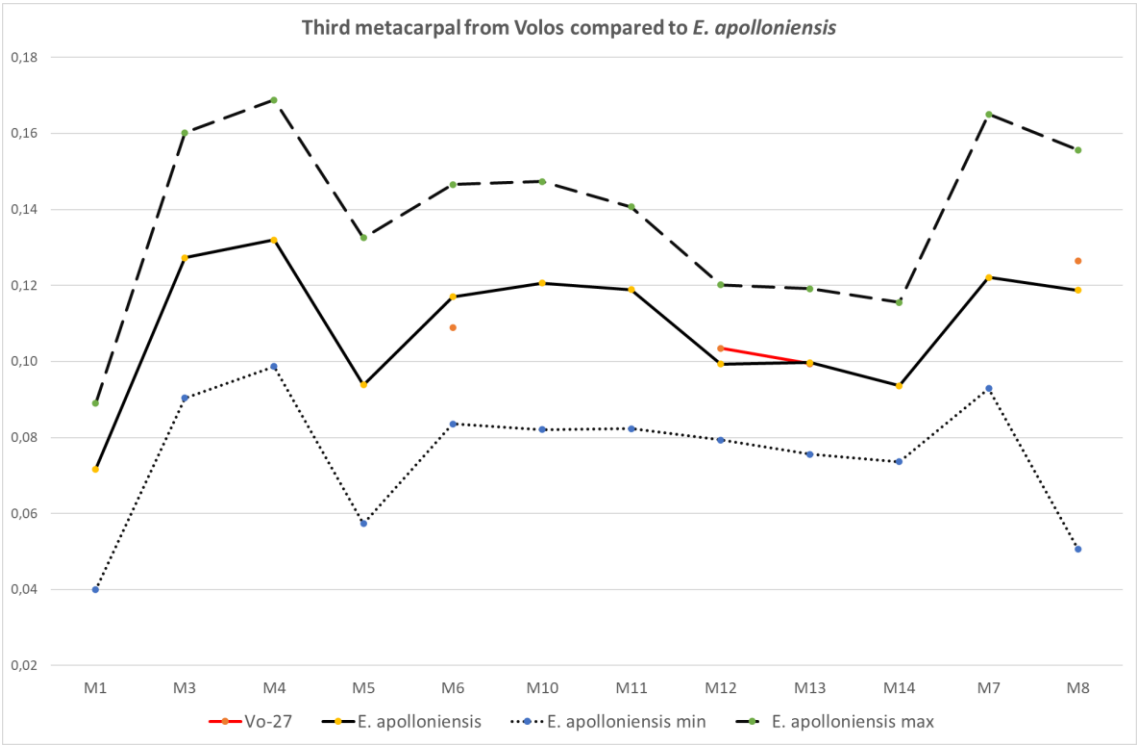

Figure 5.65. Simpson's log ratio diagrams comparing the third metacarpal from Volos to *E. apolloniensis* (Apollonia). Standard: *Equus hemionus onager*.

Equus* aff. *E. suessenbornensis

Locality.

Vassiloudi-1 (VSL), Mygdonia Basin, Central Macedonia

Material.

Vassiloudi. P3,4 dex VSL-12; distal part of humerus VSL-5; third metacarpal VSL-22; distal parts of tibia VSL-3, 8, 9 (juv.); third metatarsal VSL-1, 4; distal part of third metapodial VSL-2.

Description.

VSL. The material is incredibly scarce and mediocre preserved; there is only one isolated upper P3,4 (VSL-8) and a few postcranial elements. The lingual border of protocone (half broken) seems to be slightly concave in the middle. The hypoconal groove is relatively deep and the hypoconal constriction is weakly developed. The hypocone is elliptical and the hypoconal groove is deep and pointed. The pli caballin is short and single and the plication of the inner fossettes is simple. The metapodials are long. The distal maximal supra-articular breadth at the tubercles (M10) is greater than at the trochlea (M11) on both third metacarpals and third metatarsals. The slenderness index SI 1 is 16.1 (n=1) for the third metacarpal and 14.3 (n=1) for the third metatarsal. The slenderness index SI 2 is 7.7 (n=1) and 16.6 (n=1) for the third metacarpal and third metatarsal respectively, whereas the keel index is 128.1 (n=1) and 130.8 (n=1) for the third metacarpal and third metatarsal respectively. The distal part of the tibia is large with its maximal breadth and depth to be 78.11 mm (n=1) and 47.8 mm (n=2) respectively.

Comparison and discussion.

Comparing the third metacarpals from Vassiloudi to *E. stenonis* from Olivola, although they both exhibit long metacarpals, it seems that the VSL is much slenderer (Figure 5.66a). The bauplan shared by all *E. stenonis* samples is not shared by this equid, so it does not belong to the same species. It is also slenderer than *E. apolloniensis* (Figure 5.66b) and the proportions of the diaphysis (M3, M4) are significantly different. Comparing the third metatarsal with those of *E. suessenbornensis* from Pirro Nord, it seems that they are identical. *E. suessenbornensis* from Pirro Nord is much smaller than

the typical from Süssenborn (Figure 5.67). The VSL sample fits better with this species. Due to the fact there are no dental elements the equid from Vassiloudi is referred to as *E.* aff. *E. suessenbornensis*.

a

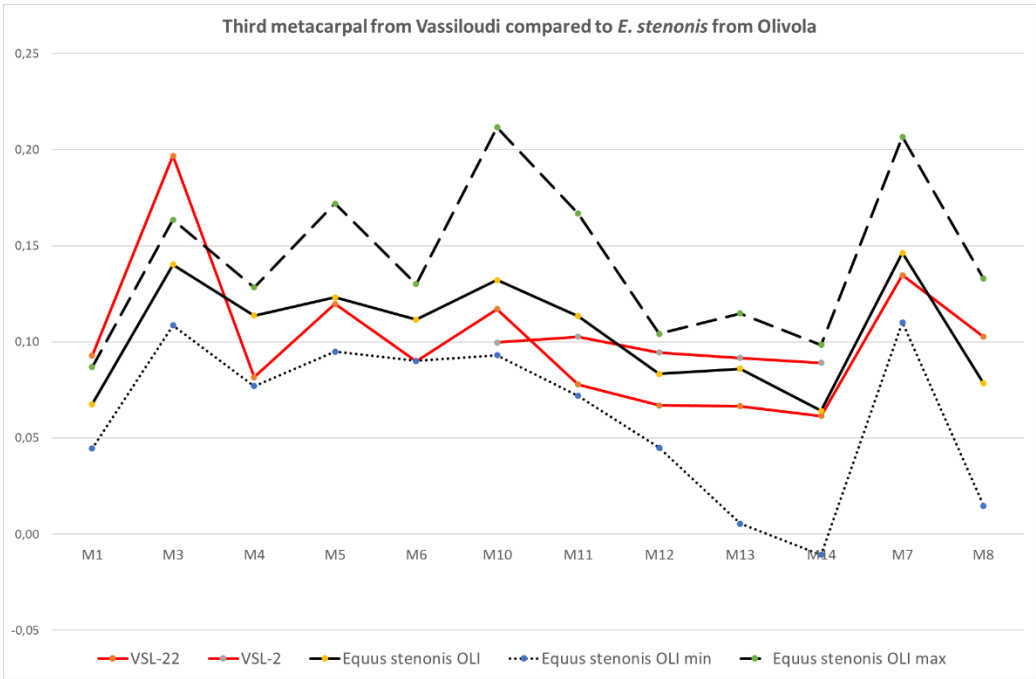

b

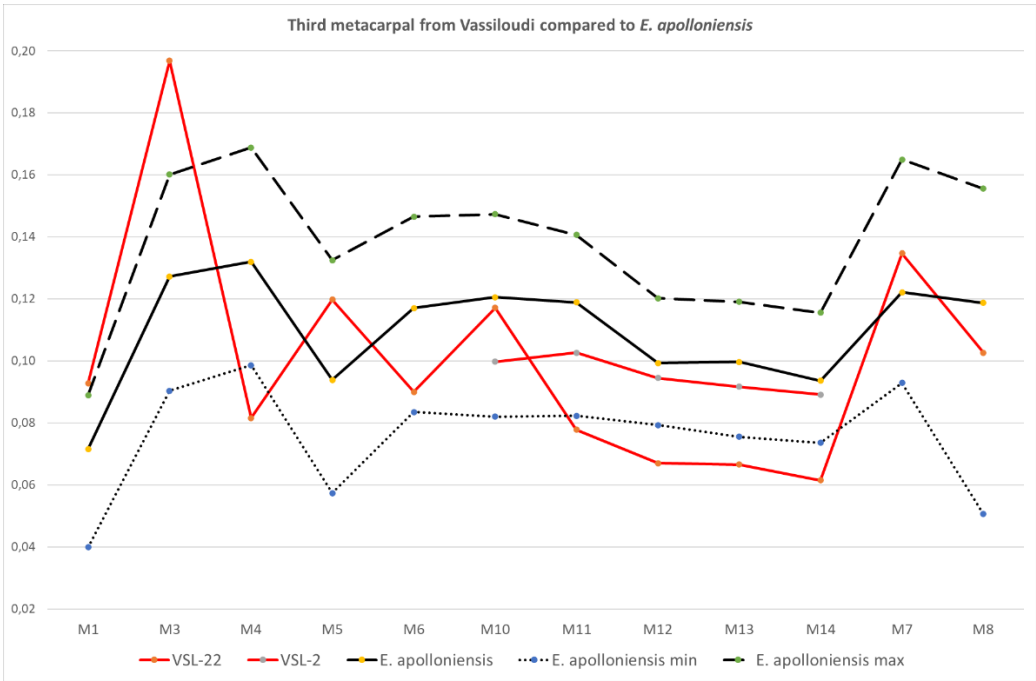

Figure 5.66. Simpson's log ratio diagrams of the third metacarpal from Vassiloudi compared to (a) *E. stenonis* from Olivola and (b) *E. apolloniensis*. Standard: *E. hemionus onager*.

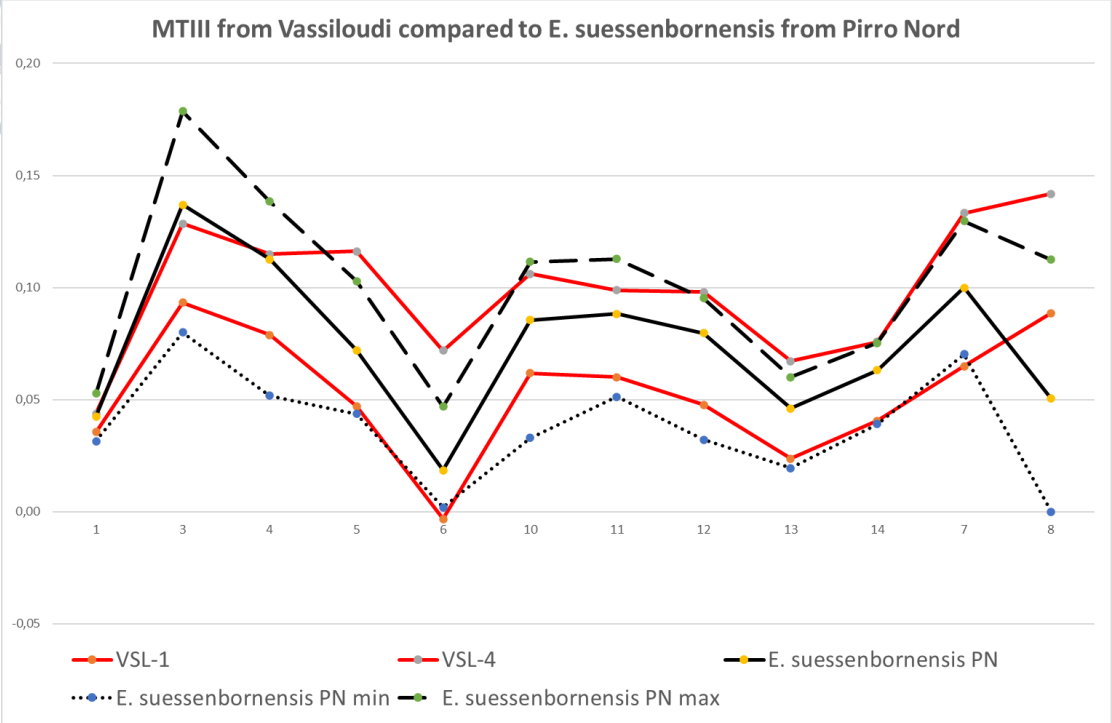

Figure 5.67. Simpson's log ratio diagrams of the third metatarsal from Vassiloudi compared to *E. suessenbornensis* from Pirro Nord. Standard: *E. hemionus onager*.

Equus aff. *E. a. granatensis*

Localities.

Platanochori-1 (PLT), Mygdonia Basin, Central Macedonia

Tsiotra Vryssi (TSR), Mygdonia Basin, Central Macedonia

Material.

Platonochori-1. radius PLN-11; third metacarpal PLN-19; proximal parts of third metacarpal: PLN-2, 38; calcaneum PLN-9, 26 (fragment juv.?); astragali: PLN-3, 7, 21, 22; proximal parts of third metatarsal PLN-28, 36; distal parts of metapodials: PLN-8, 23, 24.

Tsiotra Vrysi. Fragment of mandibular body with P2-M3 sin TSR-E19-7; fragment of mandibular body with P2-M2 sin and P2-M2 dex, TSR-E19-6 (same individual); fragmentary mandibular body TSR-154 sin; fragment of mandible with p2-m3 sin TSR-154; isolated P2: TSR-G21-1, TSR-E21-41, TSR-D21-23, TSR-G19-17; M3: TSR-D20-20; Third metacarpals: TSR-D13-15 sin, TSR-D19-11 dex, TSR-F20-13 dex, TSR-F21-4 dex; distal part of McIII TSR-107; tibia: D18-114; F20-26.

In articulation: tibia (a) + astragalus (b) + calcaneum (c) TSR-C18-14 + third metatarsal TSR-179; tibia (a) + tarsals, astragalus, calcaneum (b) + third metatarsal (c) TSR-D16-41.

Description.

PLN. The material from Platanochori is scanty. Unfortunately, there are no cranial or dental remains. No morphological differences have been traced with the material from Apollonia, except for the slightly longer metacarpal PLN-19. The slenderness index 1, SI 1, for the single complete metacarpal PLN-19 is 13.4. The diaphysis flatness (DF) for the metacarpals, anteroposterior diameter of diaphysis (M4) / minimal breadth of the diaphysis (M3) ranges between 0.79-0.81. The proximal flatness (PF), proximal articular breadth (M5) / proximal articular depth (M6) ranges between 1.5-1.55 and 1.23-1.26 for the metacarpals and metatarsals respectively.

TSR. The material from the large-sized equid from Tsiotra Vryssi comprises a few dental and postcranial elements. The linguaflexid in deep on molars in all lower cheek teeth. The most significant specimens are the mandibular bodies TSR-E19-7 and TSR-E19-6 that belong to the same individual: they exhibit peculiar features like those of described by Eisenmann (2010) as common features of the *Sussemionus* subgenus, such as elongated metaconid, very deep linguaflexid on molars and sometimes also on premolars, presence of plis protostylid (not separated though) etc. The third metapodials are long and slender. For the third metacarpals, the slenderness index 1 (SI 1) ranges between 13.9–16.1 (n = 4; mean = 15.0). For the third metatarsals, the same index ranges between 11.8–13.0 (n = 3; mean = 12.2). The slenderness index SI 2 ranges between 16.7–17.4 (n = 3; mean = 17.0). The keel index varies between 132.5–137.0 (n = 3; mean = 134.7).

Comparison and discussion. In figure 5.68, the third metacarpals from Platanochori are compared to *E. apolloniensis* and *E. a. granatensis*. In seems that the PLT specimens are resembling both species. The morphometry is rather similar although the single complete third metacarpal is longer than the maximal values of *E. apolloniensis*, and close to the maximal values of *E. a. granatensis* (marginally without its range). The third metatarsals do not share any further information as they are fragmentary. They are included in the range of variability of *E. apolloniensis* (Figure 5.68a).

a

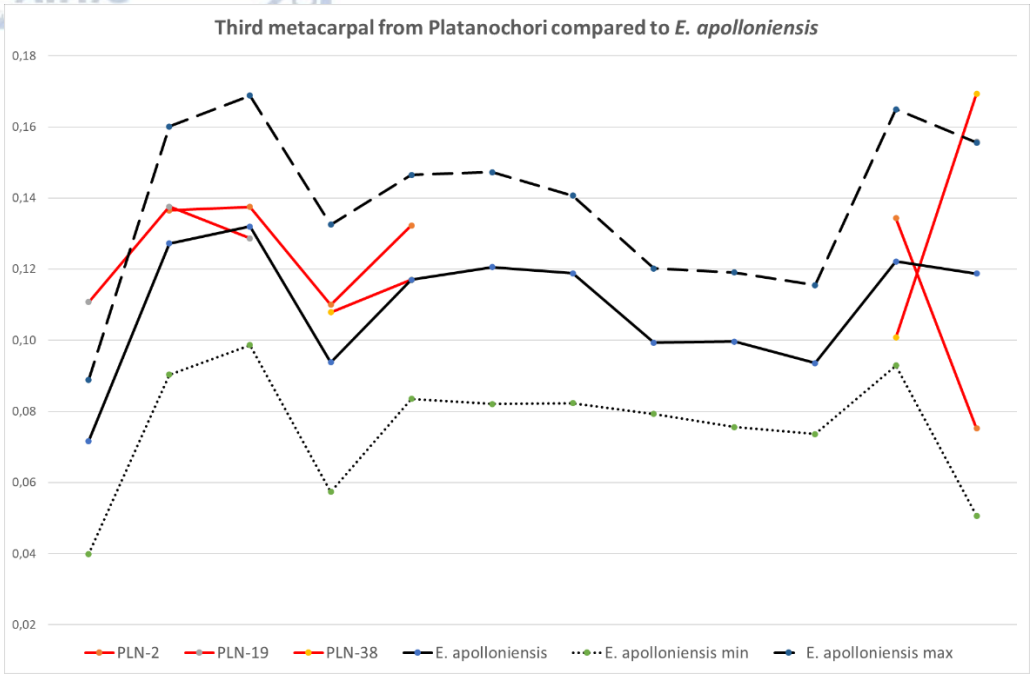

b

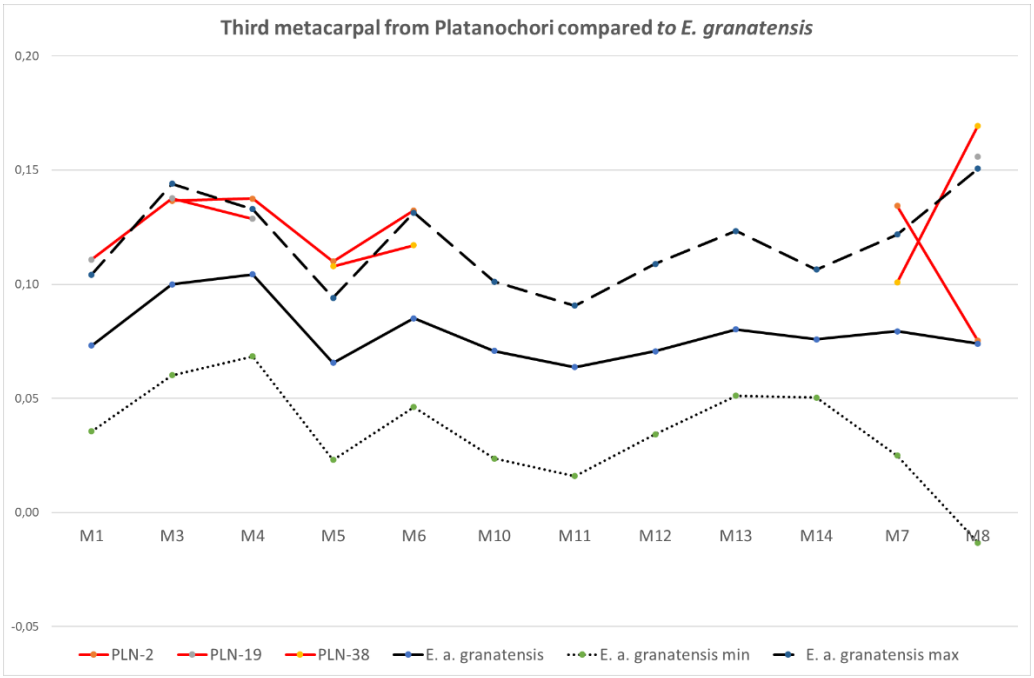

Figure 5.68. Simpson's log ratio diagrams of the third metacarpal from Platanochori compared to (a) *E. apolloniensis* and (b) *E. a. granatensis* from Venta Micena. Standard: *E. hemionus onager*. Data from Eisenmann (2017b) and personal dataset.

The dental elements of the large-sized equid from Tsiotra Vryssi exhibit same features that according to Eisenmann (2017c, 2010) are diagnostic of sussemiones as mentioned earlier. Those features in the TSR sample (TSR-E19-7 and TSR-E19-6) are the more elongated metaconid, the very deep linguaflexid on molars and sometimes also on premolars and the presence of plis protostylid. These features are closer to *E. a. granatensis* rather than to *E. apolloniensis* where the linguaflexid is usually shallow even on molars (except on some specimens). However, these features are not constant on the same individual. As it seems on the same mandible the depth of the linguaflexid at the left and right bodies is not constant: at the right series on P3,4 it is shallow and on the left deep. The TSR third metapodials are resembling both species (at least the third metatarsals). The third metacarpals belonging to the larger equid in TSR are fragmentary. Their length is similar to both taxa (*E. apolloniensis* and *E. a. granatensis*) (Figure 5.68). The main difference from both of them is the depth (M4) of the McIII and the analogies between length and breadth of the diaphysis (M3, M4). The third metatarsals are, however, similar to both taxa (they seem to slightly better fit to *E. apolloniensis*) (Figure 5.69). Thus, the TSR sample belongs either to *E. apolloniensis* or *E. a. granatensis*.

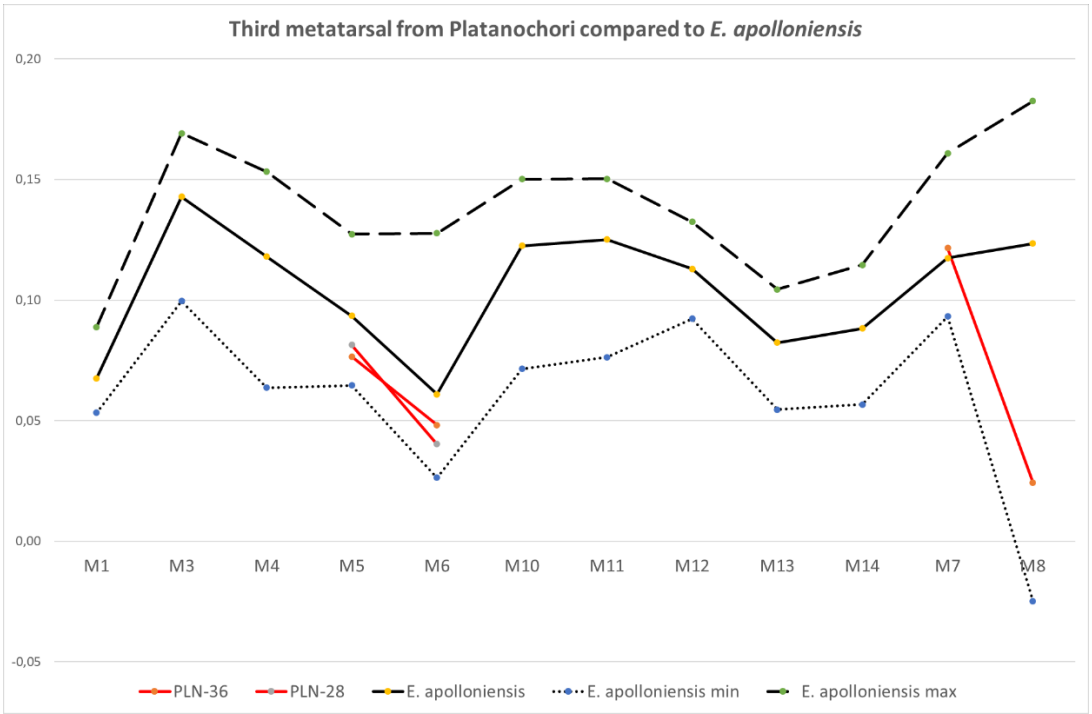

Figure 5.69. Simpson's log ratio diagrams of the third metatarsal from Platanochori compared to *E. apolloniensis*. Standard: *E. hemionus onager*.

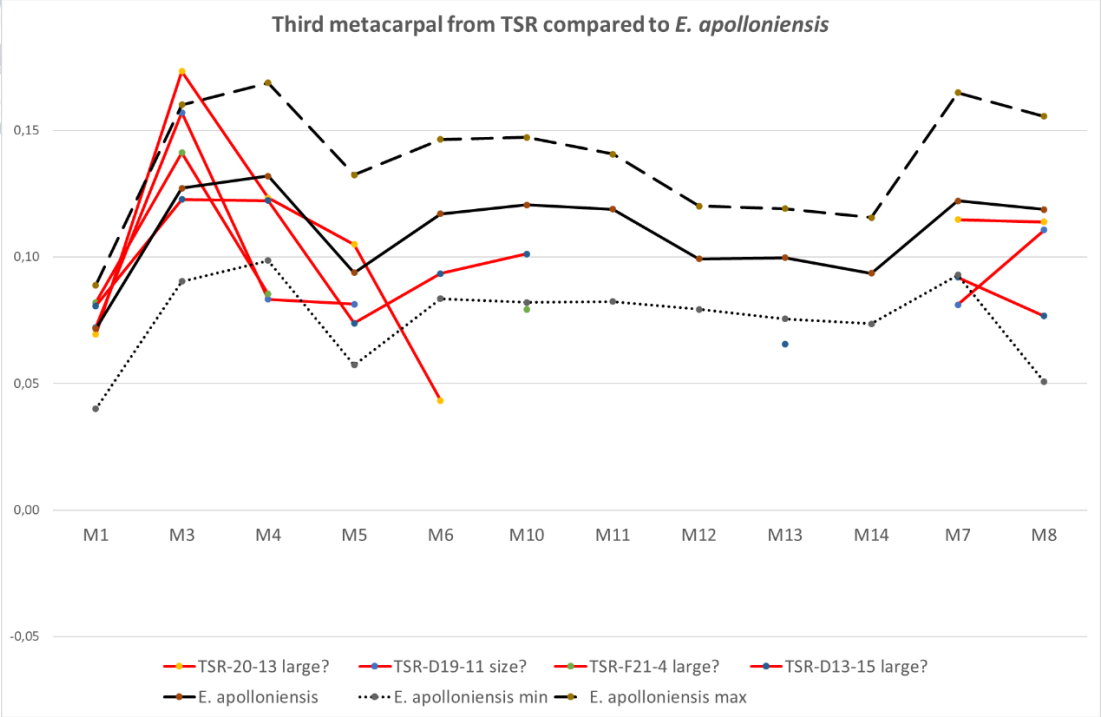

Figure 5.70. Simpson's log ratio diagrams of the third metacarpal from Tsiotra Vrysi compared to *E. apolloniensis* from Apollonia. Standard: *E. hemionus onager*.

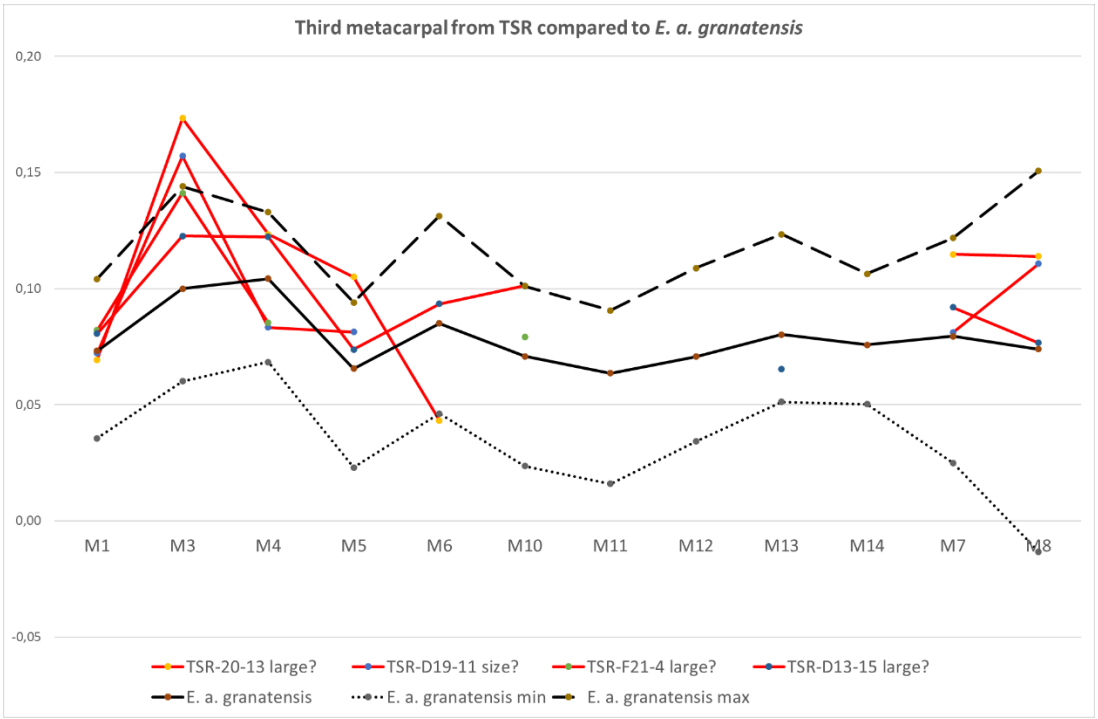

Figure 5.71. Simpson's log ratio diagrams of the third metacarpal from Tsiotra Vrysi compared to *E. a. granatensis* from Venta Micena. Standard: *E. hemionus onager*. Data from Eisenmann (2017b) and personal dataset.

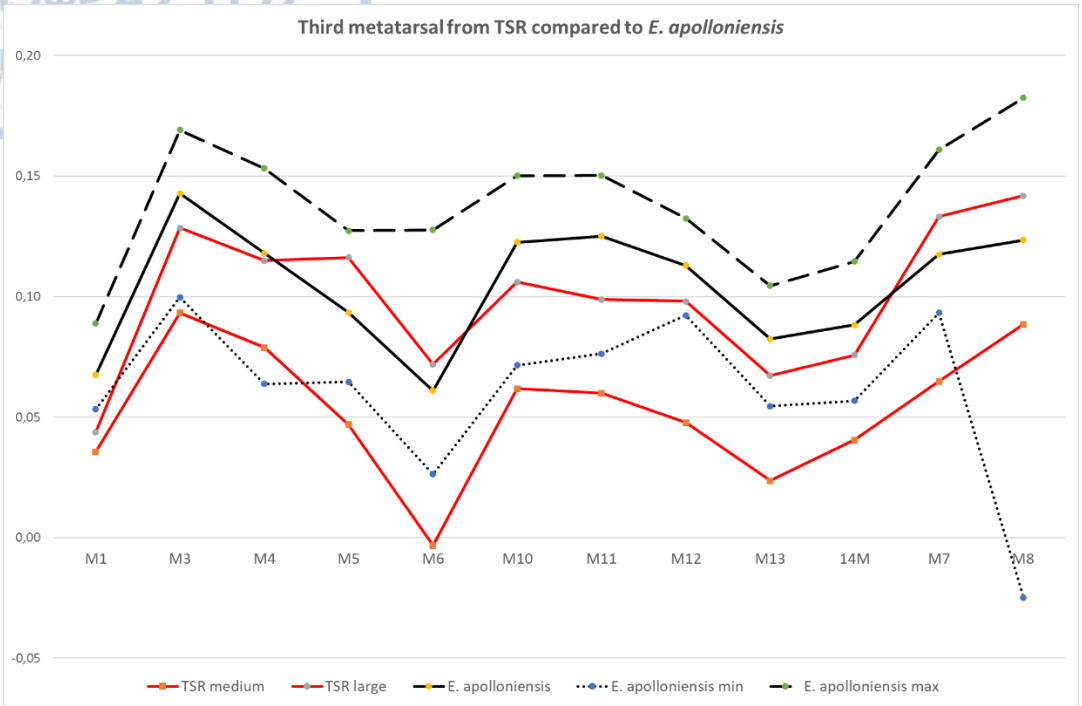

Figure 5.72. Simpson's log ratio diagrams of the third metatarsal from Tsiotra Vrysi compared to *E. apolloniensis* from Apollonia. Standard: *E. hemionus onager*.

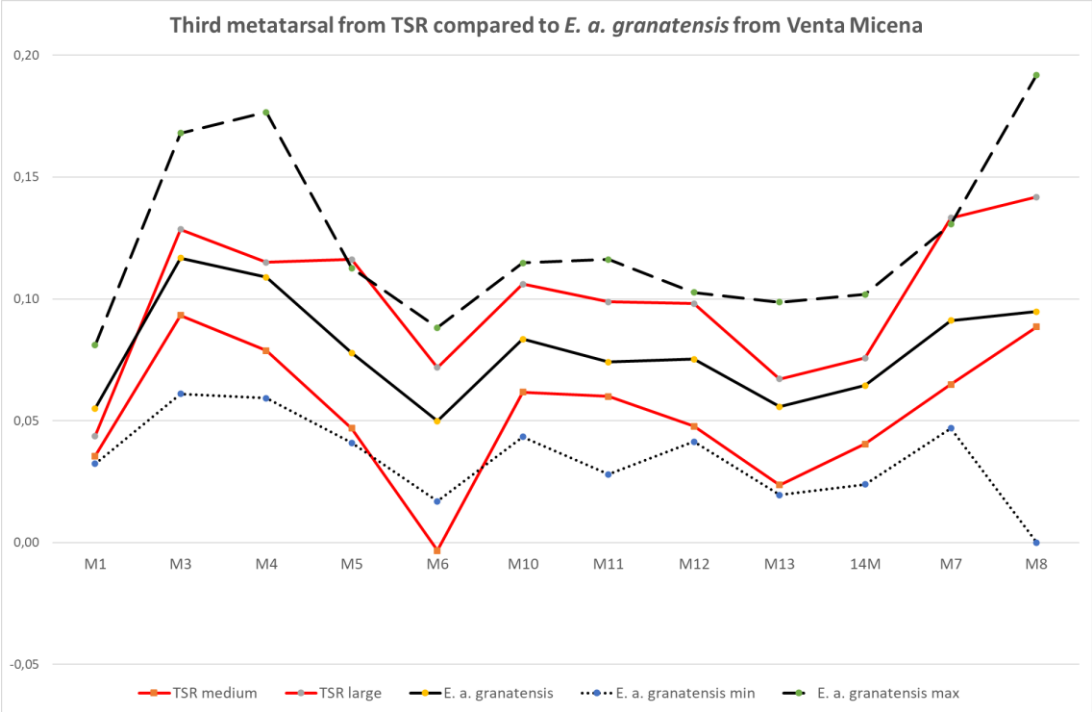

Figure 5.73. Simpson's log ratio diagrams of the third metacarpal from Tsiotra Vrysi compared to *E. a. granatensis* from Venta Micena. Standard: *E. hemionus onager*. Data from Eisenmann (2017b) and personal dataset.

Equus* cf. *E. senezensis

Locality.

Pyrgos **(**PgI), Peloponnese, ?MNQ 18

Material.

Pyrgos. Distal parts of tibia PgI.2, PgII.3(?); astragalus sin PgI.3; calcaneum sin PgI.4; third metatarsal PgI.7; proximal part of third metatarsal PgI (without number).

Description.

The material is sparse, and it comes from the site Pyrgos-1. The material has been pulled under the name *E*. cf. *stenonis* by Van der Meulen and Van Kolfschoten (1986), without any descriptions. The third metatarsal (PgI.7) is short and robust. The distal maximal supra-articular breadth at the trochlea (M11) is greater than at the tubercles (M10). The slenderness index (SI 1), minimal breadth at the middle of the diaphysis (M3) / maximal length (M1) % is calculated 14.2 (n = 1). The slenderness index (SI 2), distal maximal articular breadth (M11)/maximal length (M1) % is calculated 18.8 (n = 1). The keel index, distal maximal anteroposterior diameter of the keel (M12)/ distal minimal DAP of the lateral condyle (M13) % is calculated 140.0 (n = 1). The diaphysis flatness (DF), caballine index (CI), and proximal flatness (PF) are calculated 84.4 (n = 1), 98.4 (n = 1) and 130.0 (n = 1) respectively.

Comparison and discussion

The third metatarsal PgI.7 exhibits similar proportions to *E. senezensis* (Figure 5.744a), and *E. stehlini* (Figure 5.74b). They are short, flat, and relatively robust like *E. senezensis* and *E. stehlini*. The tarsals (astragalus, calcaneum) from Pyrgos are resembling those of *E. senezensis* (Figure 5.75). The astragalus Pgl.3 exhibits similar morphometry to *E. senezensis*: it plots on the average values of the latter species. The same applies for calcaneum. The specimen Pgl.4 plots on the average values of *E. senezensis*, while on the bivariate analysis it is plotted within the range of variability of latter species. Thus, in the present thesis, all these specimens from Pyrgos they are refered to as *E.* cf. *senezensis*.

a

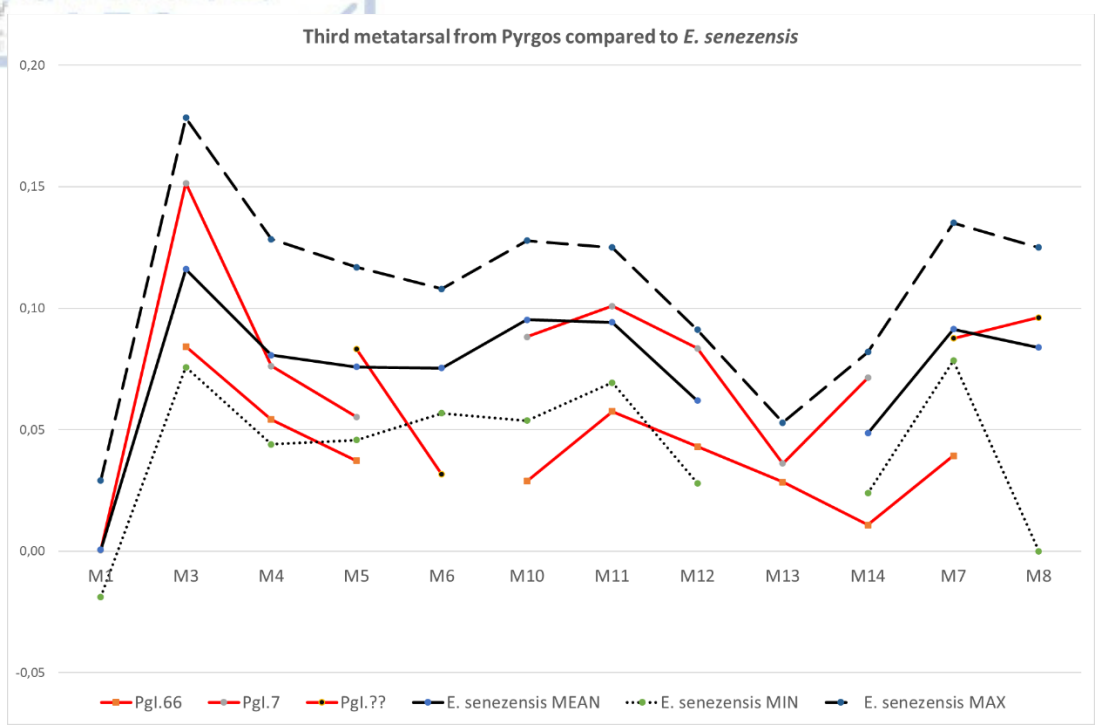

b

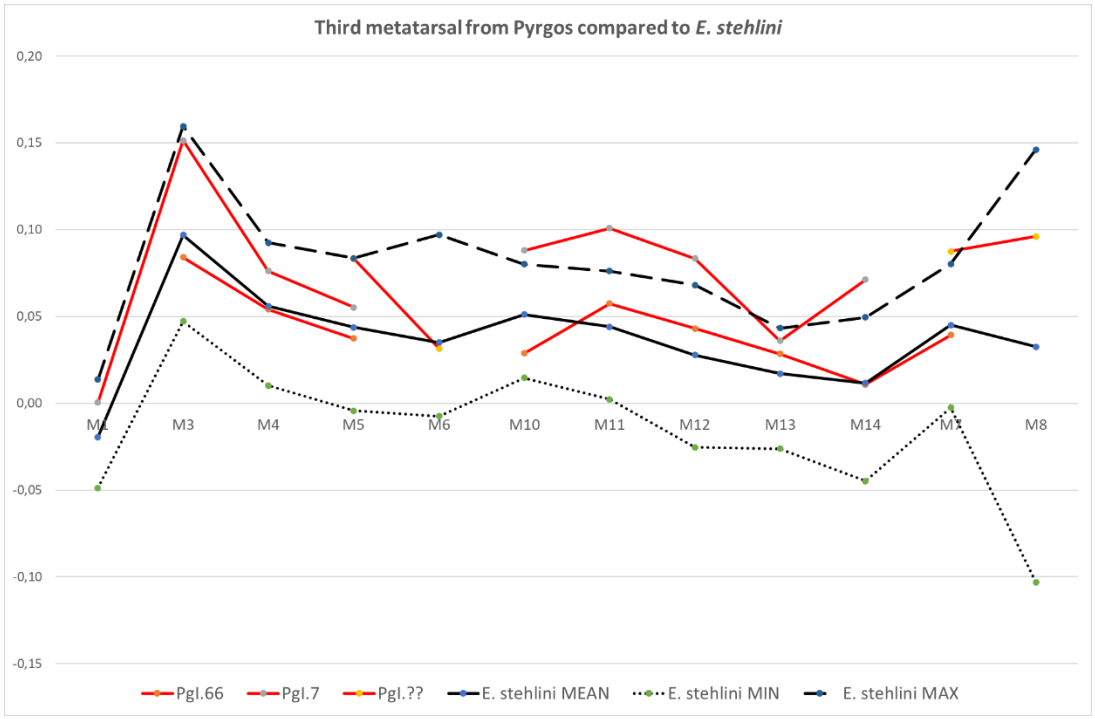

Figure 5.74. Simpson's log ratio diagrams of the third metatarsal from Pyrgos compared to (a) *E. senezensis* and (b) *E. stehlini*. Standard: *E. hemionus onager*. Data from Eisenmann (2017b) and personal dataset.

a

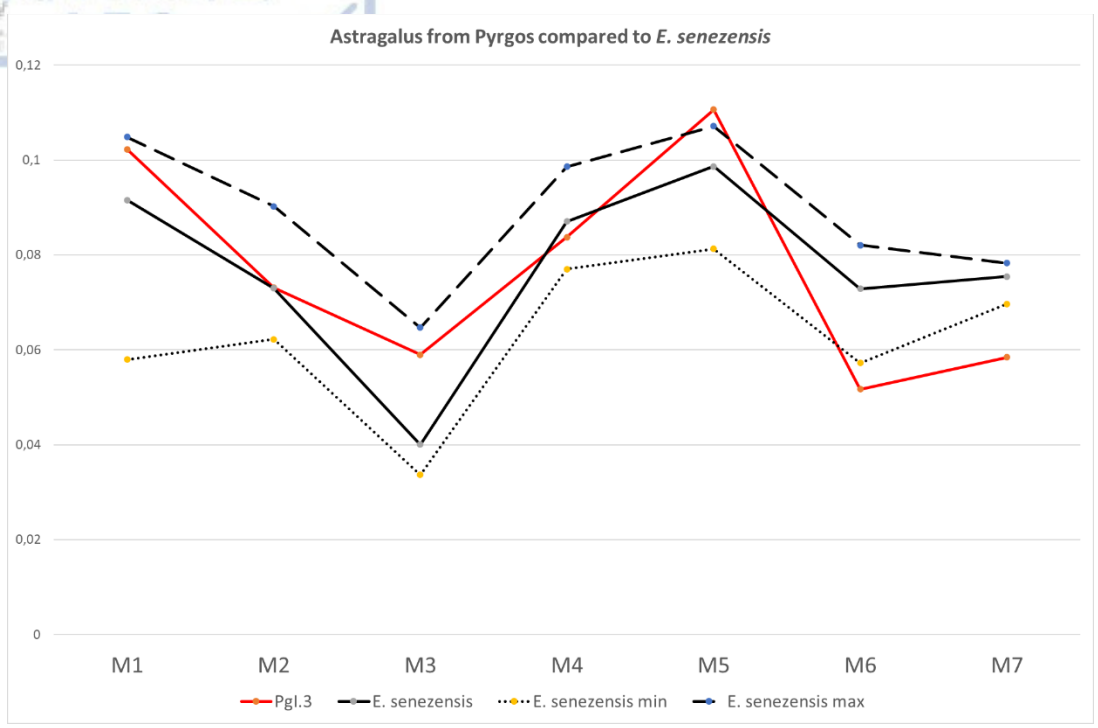

b

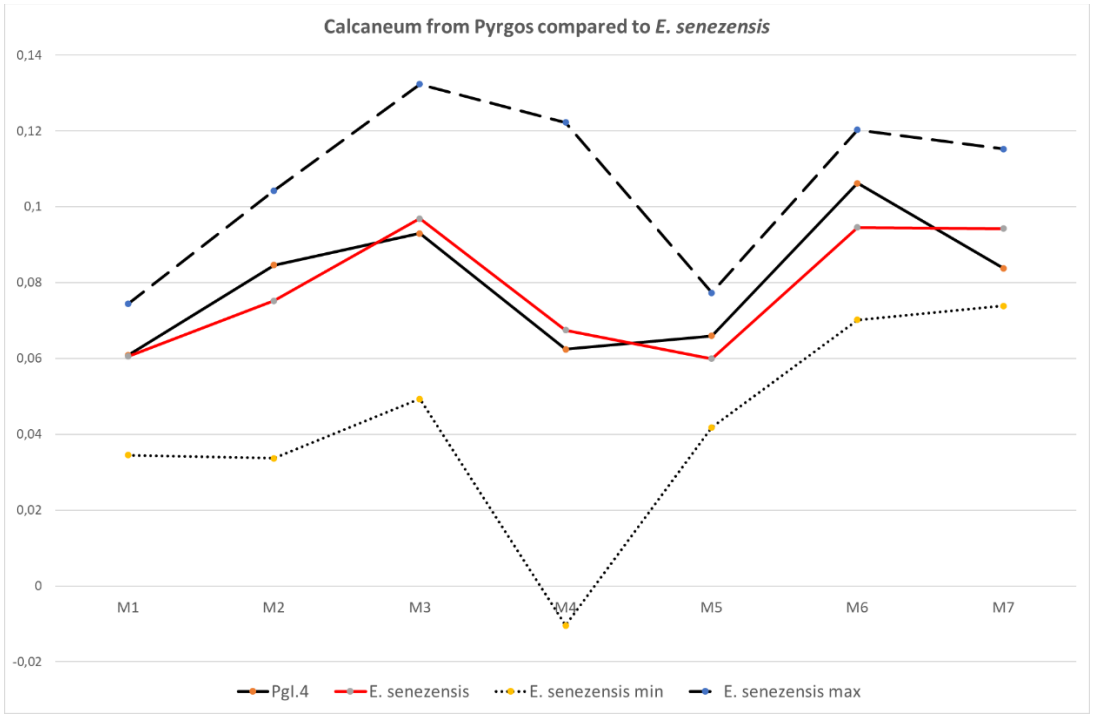

Figure 5.75. Simpson's log ratio diagram comparing the (a) astragalus and (b) calcaneum from Pyrgos to *E. senezensis*. Standard: *Equus hemionus onager*. Data from Eisenmann (2017) and personal dataset.

Equus* aff. *E. stehlini

Locality.

Pyrgos (PgI), Peloponnese, ?MNQ 18

Material.

Distal parts of radius PgI.21, 25; distal part of third metapodial PgI.23; distal part of tibia.3(?), 14; distal part of third metatarsal PgI.66.

Description.

The material is incredibly scanty, without any cranial or dental remains, and it only consists of two distal parts of metapodials and two distal parts of radius and tibia. Van der Meulen and Van Kolfschoten (1986) referred to this material as *E.* cf. *stehlini*, probably due to the differences in size from the second species (*E.* cf. *stenonis* = *E.* cf. *senezensis* herein), but there is no description whatsoever. The third metapodials are short and slender. The distal maximal supra-articular breadth at the trochlea (M11) is greater than at the tubercles (M10) on the third metatarsal (PgI.66) and vice versa on the third metapodial (PgI.33). The keel index for PgI.66 and PgI.33 is 129.81 and 86.23 respectively.

Comparison and discussion

The third metatarsals from Pyrgos exhibit similar proportions (short and flat) to *E. stehlini* (Figure 5.74b), while the tarsals are resembling those of *E. senezensis* (Figures 5.75). These specimens could belong to different stratigraphic layers, or they could belong to one single taxon/species. Although at the present moment, the material from Pyrgos is limited, it is distinguished into two different species *Equus* cf. *E. senezensis* and *Equus* aff. *E. stehlini* based on their morphometry. According to Eisenmann (2002), the presence of two or more species of *Equus* was uncommon during the middle Early Pleistocene. According to Alberdi et al. (1998), *E. stehlini* is a subspecies of *E. senezensis* (=*E. senezensis stehlini*), or it could be a local population of the latter species. However, Cirilli (2022) established *E. stehlini* as a distinct species derived from *E. senezensis*.

Equus sp. B, large-sized (Gerakarou)

Locality.

Gerakarou-1 (GER), Mygdonia Basin, Central Macedonia

Material.

Distal part of radius GER-44.

Description.

The distal part of radius, GER-44, is much larger than the rest of the other radii from Gerakarou. The breadth of the distal articular facet (M8) is 70.43mm versus 57.16mm (n=1), while the breadth of the distal epiphysis (M10) is 83.01mm versus 68.26 (n=2; min=65.69mm, max=70.83mm). It is better to separate GER-44 from the sample of *E. altidens* from Gerakarou and refer to it as *Equus* sp. B large-sized.

Equus sp. large-sized (Krimni-3)

Locality.

Krimni-3 (KMN), Mygdonia Basin, Central Macedonia

Material.

In articulation: Humerus + radius KMN-48.

Description and comparison.

These two specimens from Krimni-3 are large in size and they exhibit different features than those of the other specimens that belong to *E. altidens* from the same site. The intermediate tubercle on distal humerus is quite stronger. They could belong to *E. stenonis* since it is present in Krimni-1. However, humeri and radii are not so common as specific markers (especially when it comes to fossils). So, at the present moment, these two specimens from Krimni-3 separate this sample from *E. altidens* and they are referred to as *Equus* sp., waiting for more material.

***Equus* sp. B, large-sized (Apollonia)**

Locality.

Apollonia-1 (APL), Mygdonia Basin, Central Macedonia

Material.

Radioulna APL-796; third metacarpal APL-74; third phalanges APL-394, 429, 868.

Description.

Among the Apollonia 1 metacarpals, APL-74 is quite larger than the mean of *E. apolloniensis*. The slenderness index SI 1 is 21.2 for APL-74 versus 20.4 (n=16, min= 19.6, max=20.9) on average for *E. apolloniensis*, indicating a more robust metacarpal. The keel index is 121.4 for APL-74 versus 128.2 (n=23, min=125.1, max=132.9) for *E. apolloniensis* indicating a relatively less developed keel.

Comparison and discussion.

These features of APL-74 are closer to *E. mosbachensis* and *E. suessenbornensis*. Nevertheless, compared to *E. mosbachensis* APL-74 has similar maximal length (M1) and proportions, but narrower diaphysis, deeper proximal articular facet (M6), less developed keel (M12) and wider articular facets for the os magnum and os hamatum (M7, M8). In comparison with *E. suessenbornensis*, APL-74 is shorter with narrower diaphysis (M3), and distal epiphysis (M10, M11). APL-74 could belong to one of these large equids, but the poor material cannot allow going any further. Furthermore, three third phalanges were separated from *E. apolloniensis* because they are much wider. Their maximal breadth is 72.6 (n=3, min=69.8, max=74.5) versus 63.31 (n=7, min=62.19, max=64.75) in *E. apolloniensis.* Besides these specimens, there are some more postcranial fragments which also have larger size and could belong to the same equid taxon. Thus, it is better to separate this sample from *E. apolloniensis*, waiting for more material.

***Equus* aff. *E. stenonis* (F-site Vatera)**

Locality.

F-site Vatera (VAT-F), Lesvos Island

Material.

Fragment of humerus (without number); third metacarpals PO 444F, PO 121F; third metacarpal with crushed distal epiphysis PO 450F; astragali PO 095F, PO, 496F calcanei PO 096F, PO 129F, PO 151F (missing the calcanean tuber), PO 604D5; third metatarsals PO 110F, PO 136F (juv.); distal epiphysis of third metapodial PO 089F; first phalanges PO 092F, PO 093F, second phalanges PO 112F, PO 132(?).

In articulation: first phalanx +second phalanx + third phalanx PO 419F (possibly in articulation with radius PO 444F + third metacarpal PO 444F; astragalus PO 101F possibly in articulation with third metatarsal PO 118F.

Description.

The material comes from the E-site from Vatera, and it was described by Eisenmann (2002) and De Vos et al. (2002), also referred in Dermitzakis et al. (1991) and in Lyras and Van der Geer (2007). In De Vos et al. (2002) and in Lyras and Van der Geer (2007), it is pulled under the name *E.* cf. *stenonis*, based on its stenonoid affinities, yet slenderer morphology on the third metapodials than the typical *E. stenonis*. The metapodials are long and slender. The slenderness index SI 1 is 20 and 20.2 for the third metacarpals PO 121F and PO 444F respectively. The slenderness index SI 2 ranges between 14.0-15.1 (n=3, mean=14.4). The keel index is 129.9 and 133.0 for PO 121F and PO 444F respectively. For the third metatarsals, the slenderness index SI 1 is 17.4 and 16.9 for PO 110F and PO 118F respectively. The keel index ranges between 134.4-138.2 (n=2, mean=136.3).

Comparison and discussion.

The third metapodials from the Vatera F-site are resembling *E. stenonis* from Olivola and Sésklo and *E. apolloniensis* in some features (Figures 5.76, 5.77). The third metacarpals from Vatera F are long like those of *E. stenonis olivolanus* but slenderer than all the other *E. stenonis* samples/populations (Figure 5.76a). In comparison to *E. apolloniensis*, they exhibit similar slenderness (Figure 5.76b). The third metatarsals are

close to the morphometry of both *E. stenonis* from Sésklo (Figures 5.77a) and also *E. apolloniensis* (Figure 5.77b). The third metatarsals from Vatera F-site are also within the range of variability of *E.* aff. *major* (Figure 5.78a), the small-sized form of *E. verae* from Siberia (Figure 5.78b) and *E. livenzovensis* from Liventsovka (Figure 5.79).

a

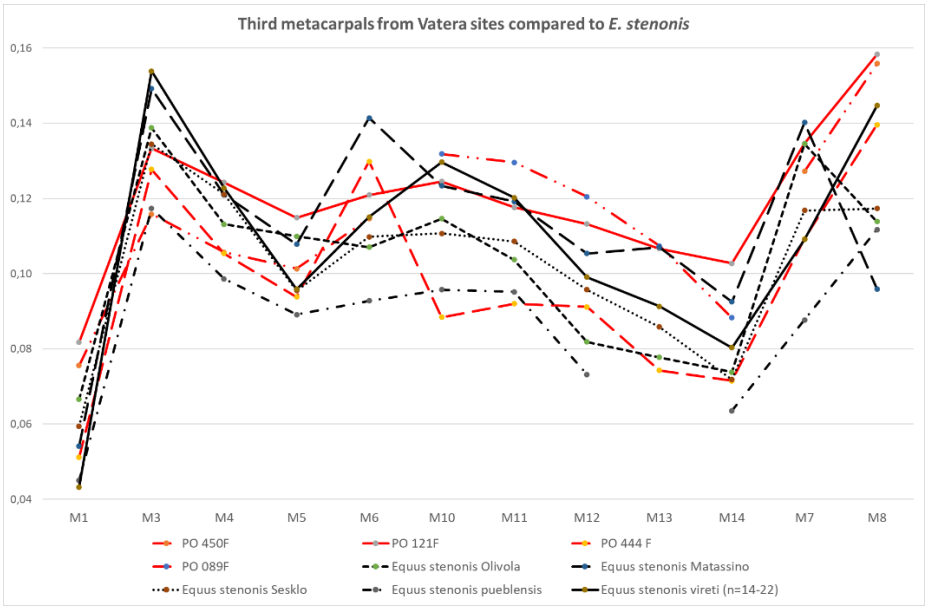

b

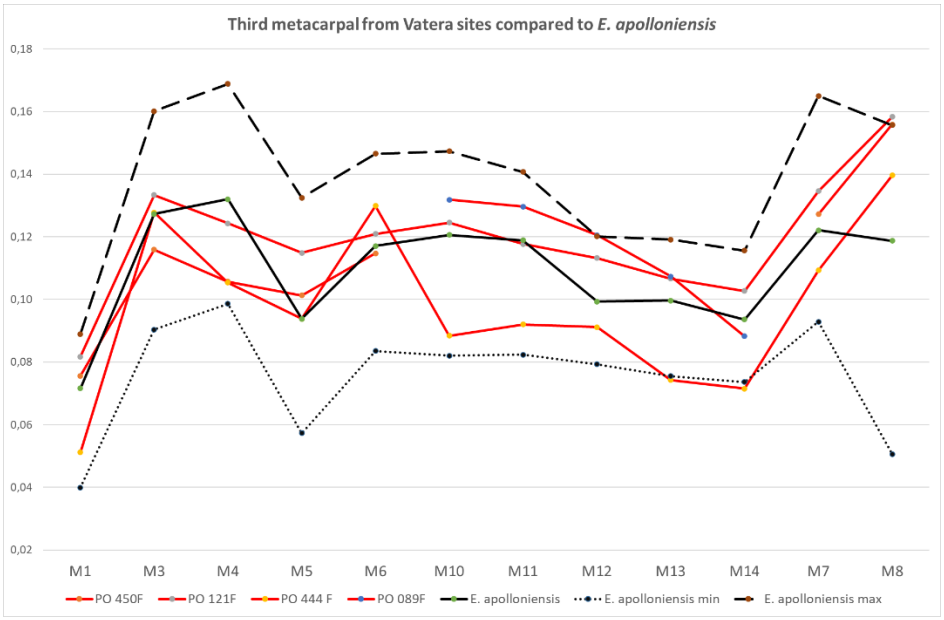

Figure 5.76. Simpson's log ratio diagram comparing the third metacarpal from Vatera to *E. stenonis* samples/populations. Standard: *Equus hemionus onager*. Data from Eisenmann (2017) and personal dataset.

a

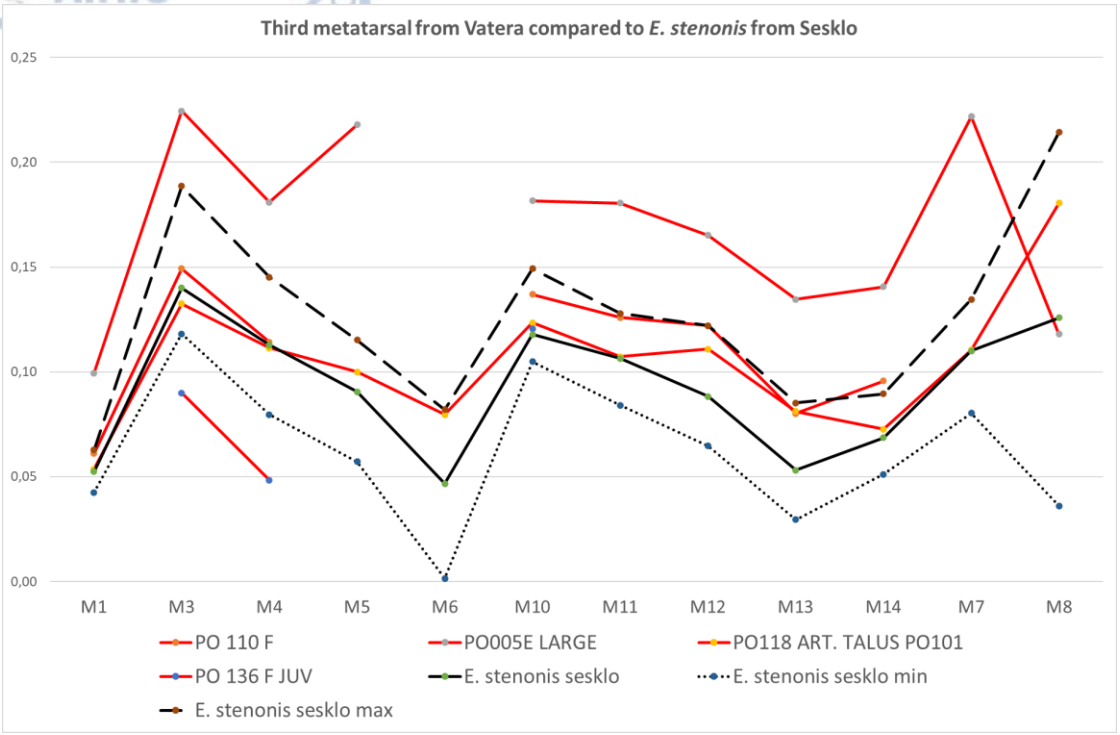

b

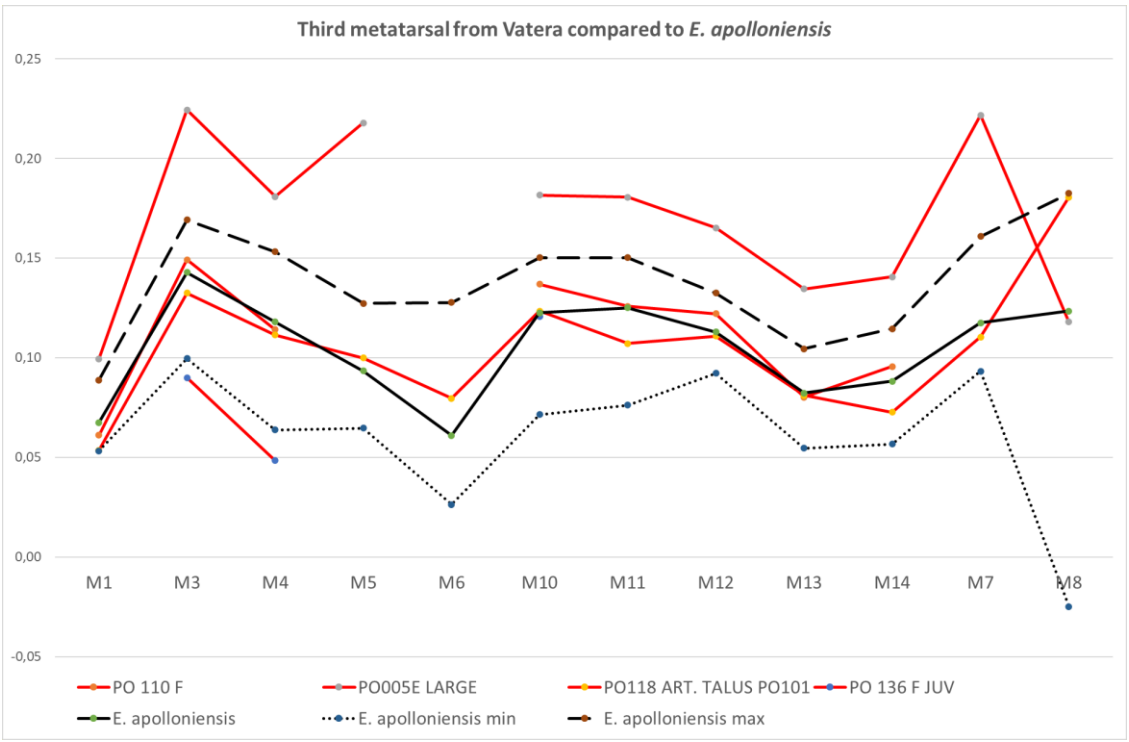

Figure 5.77. Simpson's log ratio diagram comparing the third metatarsal from Vatera to (a) *E. stenonis* from Sésklo and (b) *E. apolloniensis* from Apollonia. Standard: *Equus hemionus onager*.

a

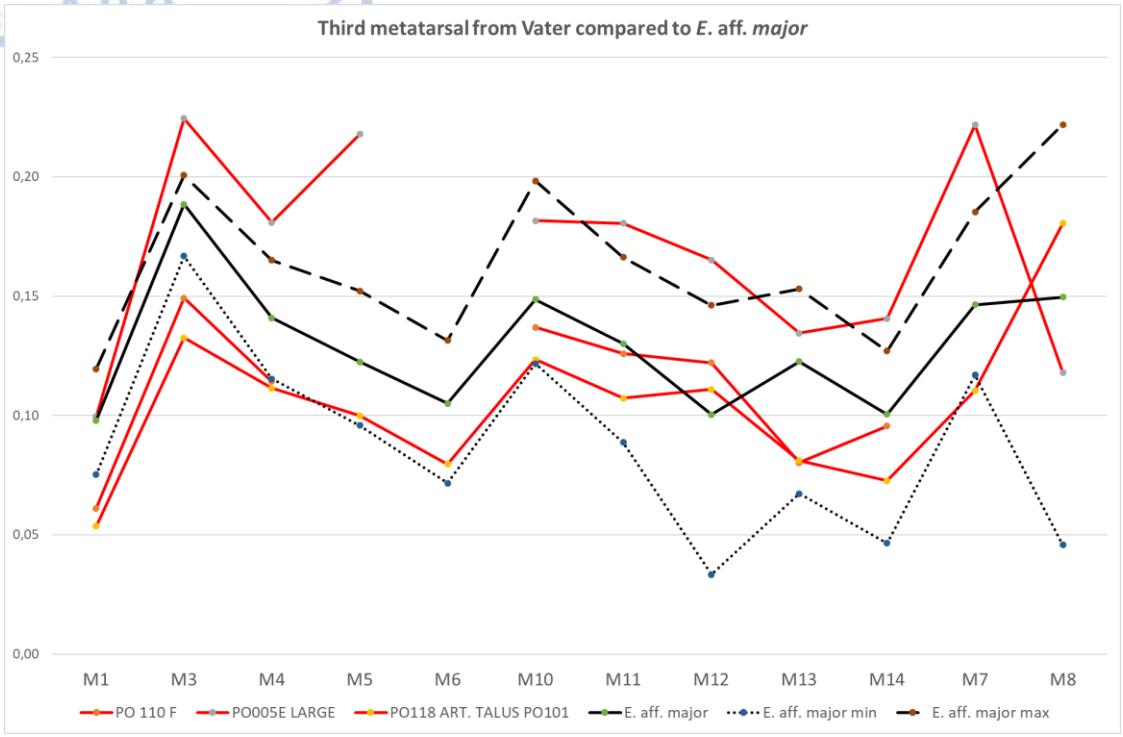

b

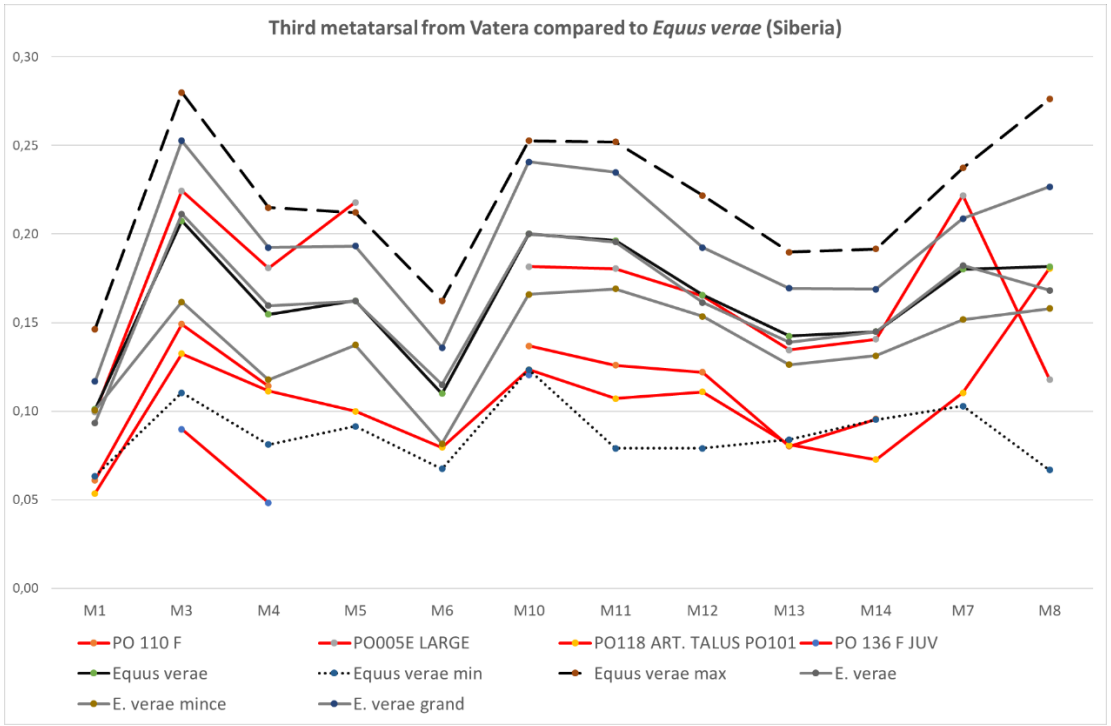

Figure 5.78. Simpson's log ratio diagram comparing the third metatarsal from Vatera to (a) *E.* aff. *major* and (b) *E. verae* from Siberia. Standard: *Equus hemionus onager*. Data from Eisenmann (2011) and personal dataset.

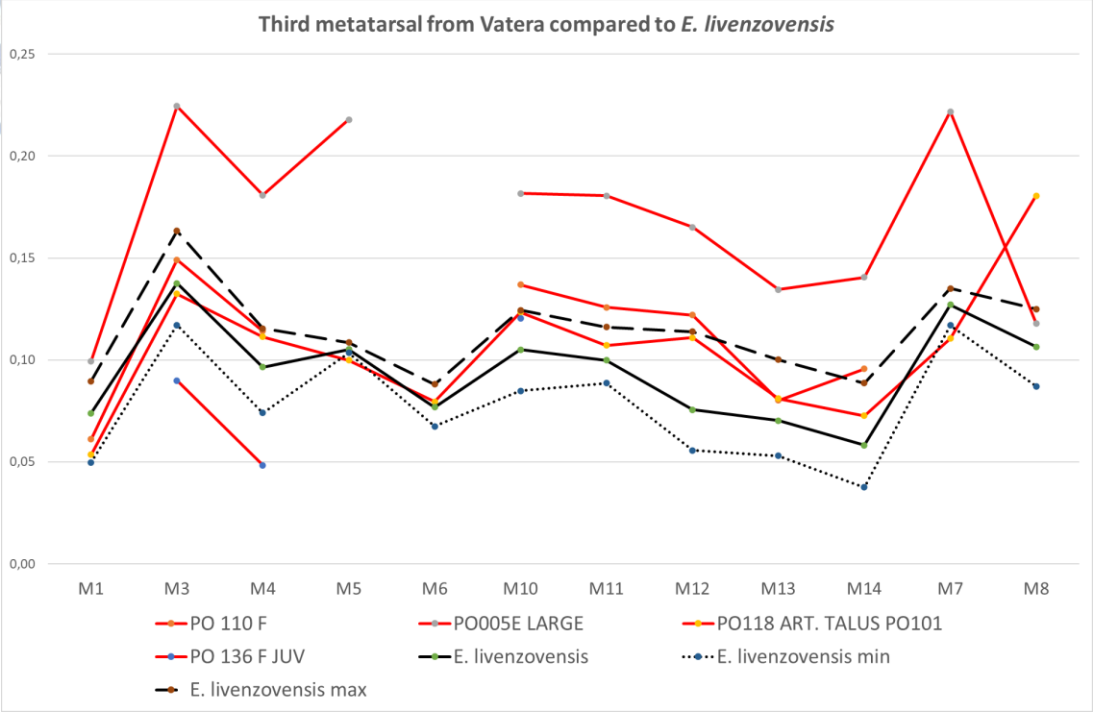

Figure 5.79. Simpson's log ratio diagram comparing the third metatarsal from Vatera to *E. livenzovensis* from Liventsovka. Standard: *Equus hemionus onager*. Data from Eisenmann (2011) and personal dataset.

Equus sp. B, large-sized (Vatera)

Locality.

E-site Vatera (VAT-E), Lesvos Island

Material.

Third metatarsal PO 005E; astragali PO 001E, 123(?)

Description.

The material comes from the E-site from Vatera, and it was described by Eisenmann (2002) and De Vos et al. (2002), also referred in Dermitzakis et al. (1991). There are two astragali (PO 001, 123) quite larger than the others; only PO 001 was measured, because the other one was missing. Their maximal length (M1) is 72.5 mm (n=2, min=72, max=73) versus 63.1 mm (n=3, min=60.42, max=66.01). The third metatarsal (PO 005) is enormous, much greater in length (M1 = 315.11 mm) and proportions than the other metatarsals (e.g., PO 110, 118). The slenderness index SI 1 % is calculated at 18.0 for PO 005 versus 17.2 (n=2, min= 16.9, max=17.4) for the other VAT metatarsals.

The distal maximal supra-articular breadth at the tubercles (M10) is slightly greater than at the trochlea (M11). The keel is well developed, and the keel index is calculated at 134.7. The depth index (diaphysis flatness: M4/M3) is 90.8, which is within the range of stenonine forms according Eisenmann (2002).

Comparison and discussion.

The third metatarsal PO 005E is enormous. It is probably the longest third metatarsal of all the Early Pleistocene equids of Greece so far. It is close to the proportions of *E. major* (Figure 5.80), yet it is slightly slenderer than the latter. As it seems in Figure 5.81, the size and general proportions are similar to the typical *E. suessenbornensis* with the only obvious difference at the maximal length of the proximal articular facet (M5). Eisenmann (2017a) mentions that "For these reasons I have placed the MTIII of "*E. bressanus*" from Chagny and a large specimen from Vatera, Greece, together with the *E. suessenbornensis* group." The astragali are close to the dimensions of *E. suessenbornensis* although the breadth of the trochlea (M3) is shorter in the Vatera E-site sample. Due to the scantiness of the material and the absence of any dental or cranial elements, the gigantic equid from Vatera-E is referred herein as *Equus* sp. B.

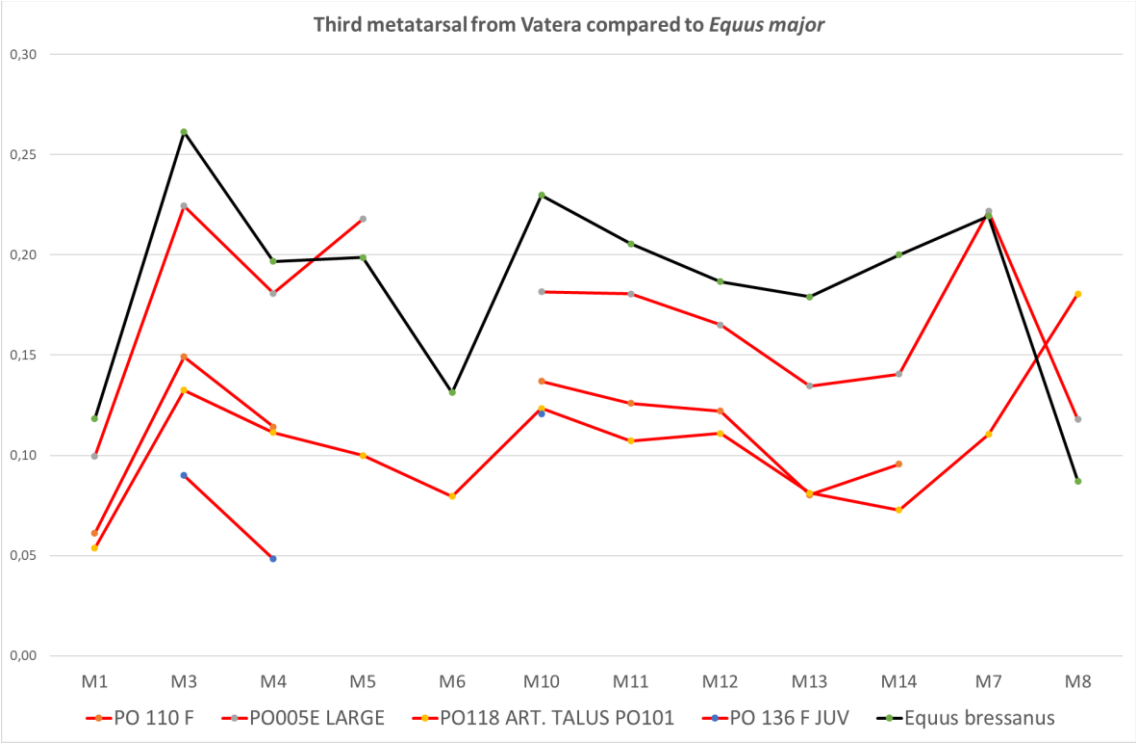

Figure 5.80. Simpson's log ratio diagram comparing the third metatarsal from Vatera to the average values of *E. major* after Alberdi et al. (1988). Standard: *Equus hemionus onager*.

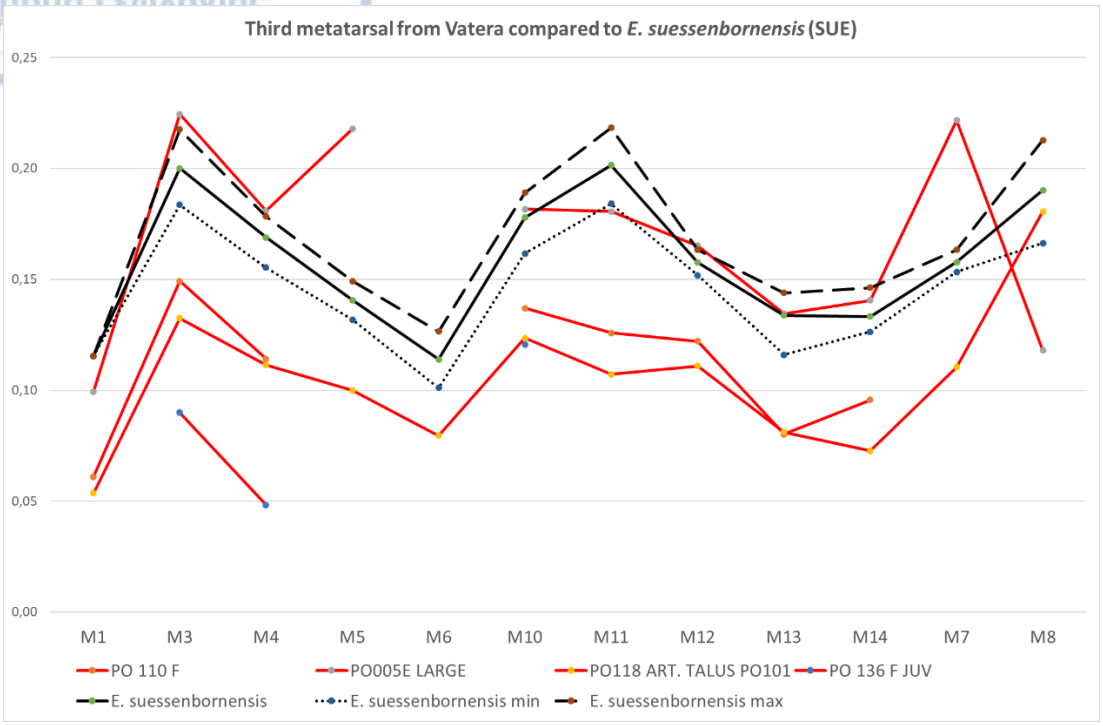

Figure 5.81. Simpson's log ratio diagram comparing the third metatarsal from Vatera to *E. suessenbornensis* from Süssenborn. Standard: *Equus hemionus onager*.

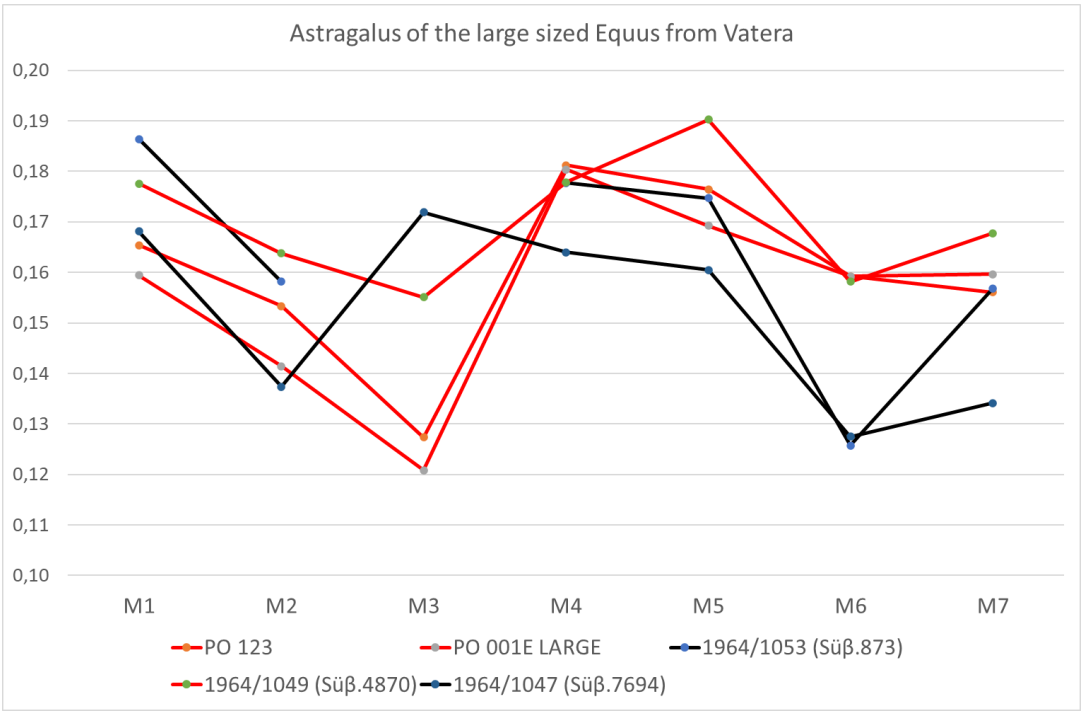

Figure 5.82. Simpson's log ratio diagram comparing the astragalus from Vatera to the typical *E. suessenbornensis* from Süssenborn. Standard: *Equus hemionus onager*.

***Equus ferus* Boddaert, 1785**

Localities.

Aggitis (Ag), Drama Basin, Eastern Macedonia

Petralona Cave (PEC), Chalkidiki Peninsula, Central Macedonia

Material.

Aggitis. in situ M1-M2 dex AG-3, 3a respectively; M1/2 sin: AG-4, 5; M3 dex AG-12; P3/4 sin AG-6, 13, without number; fragment of mandibular body with p2-p4 sin, AG-1; in situ p3, p4 m1 sin, AG-2; 2a, 2b; tibia AG-21; distal part of tibia (without number); proximal part of third metatarsal AG-11; distal parts of metapodials (possibly third metacarpals): AG-9, 10; third phalanx (without number).

Petralona Cave (old collection). Distal part of humerus PEC-661; distal part of third metacarpal PEC-539; astragalus PEC-592; third phalanx PEC-619.

Description.

Aggitis. The material was originally described by Koufos (1981). The upper cheek teeth are large and high. The inner fossettes are isolated except for the little worn teeth, where they communicate with each other; the enamel of these fossettes is low plicated. The protocone is shorter on the third and fourth premolars (P3/4) than on the first and second molars (M1/2). The protocone is notched in the middle and its posterior border is always more pronounced posteriorly. The hypocone is elliptical and the hypoconal constriction is more or less apparent. The hypoconal groove is deep on all cheek teeth. The pli caballin is simple and relatively elongated.

The lower cheek teeth are large and high. The shape of the double knot is typically caballoid with a U-shaped linguaflexid which is either concave or angulated. The protostylids are well-developed; no pli protostylid is observed. The metaconid is rounded (cyclic-shaped) and the metastylid is pointed. The entoconid is rectangular on premolars and squarish on molars. On the buccal side of the protoconid and hypoconid, the enamel is slightly notched at the middle. The ectoflexid is shallow on premolars and intermediate on molars (stops at the beginning of the isthmus without penetrating it). The isthmus is always narrow on both cases. The enamel on the postflexid is rudimentary plicated or absent. Occasionally, there is a single pli preflexid (AG-7). The pli caballinid is single and short on premolars.

The third metapodials are robust. The distal maximal supra-articular breadth at the trochlea (M11) is greater than at the tubercles (M10) on the third metapodials (AG-9, 10). The distal keel is well/moderate developed; the keel index varies between 126.9-137.4 (n= 2; mean=132.1). The third phalanx is relatively large, and its maximal breadth is 63.8 mm.

Petralona Cave. The material was originally described by Tsoukala (1989) and was attributed to *Equus ferus piveteaui* David and Pratt, 1962 (=*E. caballus piveteaui*). It is poorly represented in the related fauna. Unfortunately, there are no cranial or dental remains in the collection. All the postcranial remains are large and robust. The distal maximal supra-articular breadth at the trochlea (M11) is greater than at the tubercles (M10) for the metapodial. The keel index KI is 131.4 (n= 1). The third phalanx is relatively large, and its maximal breadth is 63.8 mm.

Comparison and discussion

The studied postcranial material of caballoid equids is scanty. The third metatarsals are close to *E. ferus piveteaui* and *E. ferus germanicus*. There are no significant differences on the proportions of *E. mosbachensis* and the various *E. ferus* populations. The samples from Petralona Cave and Aggitis belong to *E. ferus* but a subspecific attribution is not possible at the moment.

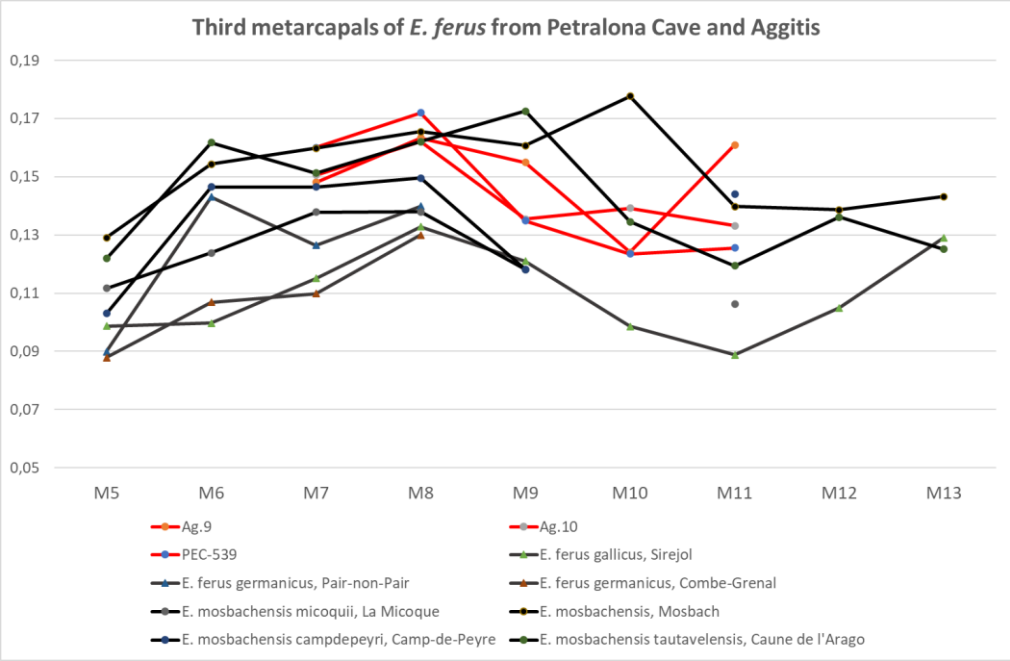

Figure 5.83. Simpson's log ratio diagrams comparing the third metacarpal of *E. ferus* from Petralona and Aggitis to the various *E. ferus* and *E. mosbachensis* subspecies. Standard: *Equus hemionus onager*. Data from Eisenmann (2017a, b, c, d) and personal dataset.

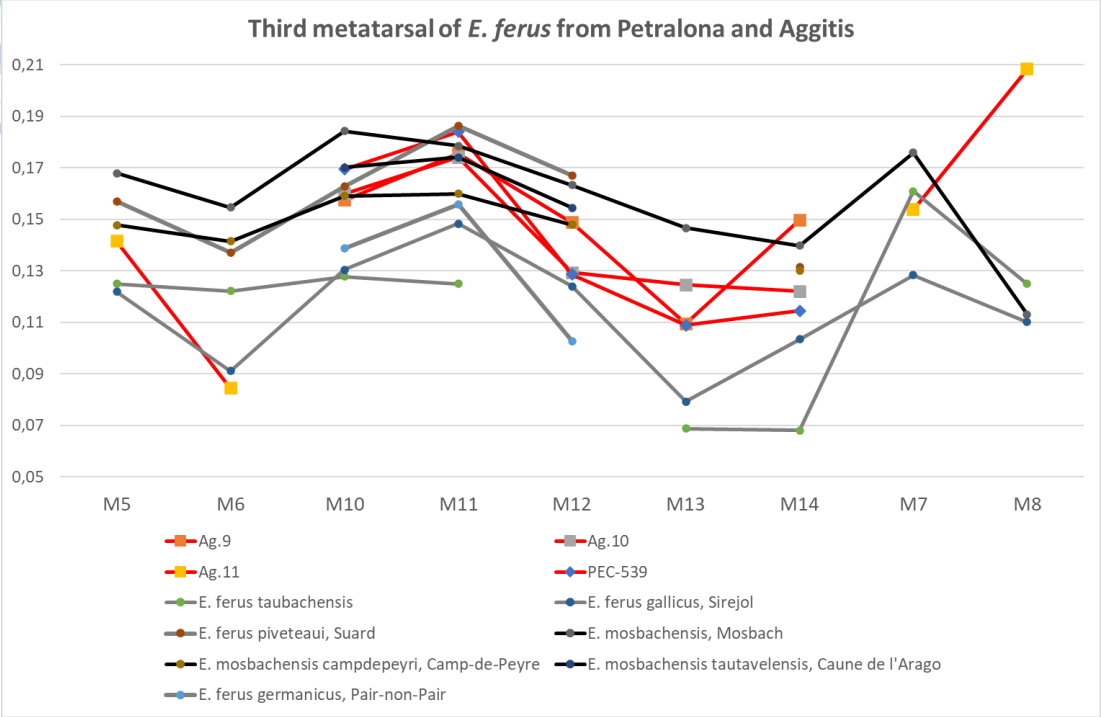

Figure 5.84. Simpson's log ratio diagrams comparing the third metatarsal of *E. ferus* from Petralona and Aggitis to the various *E. ferus* and *E. mosbachensis* subspecies. Standard: *Equus hemionus onager*. Data from Eisenmann (2017a, b, c, d) and personal dataset.

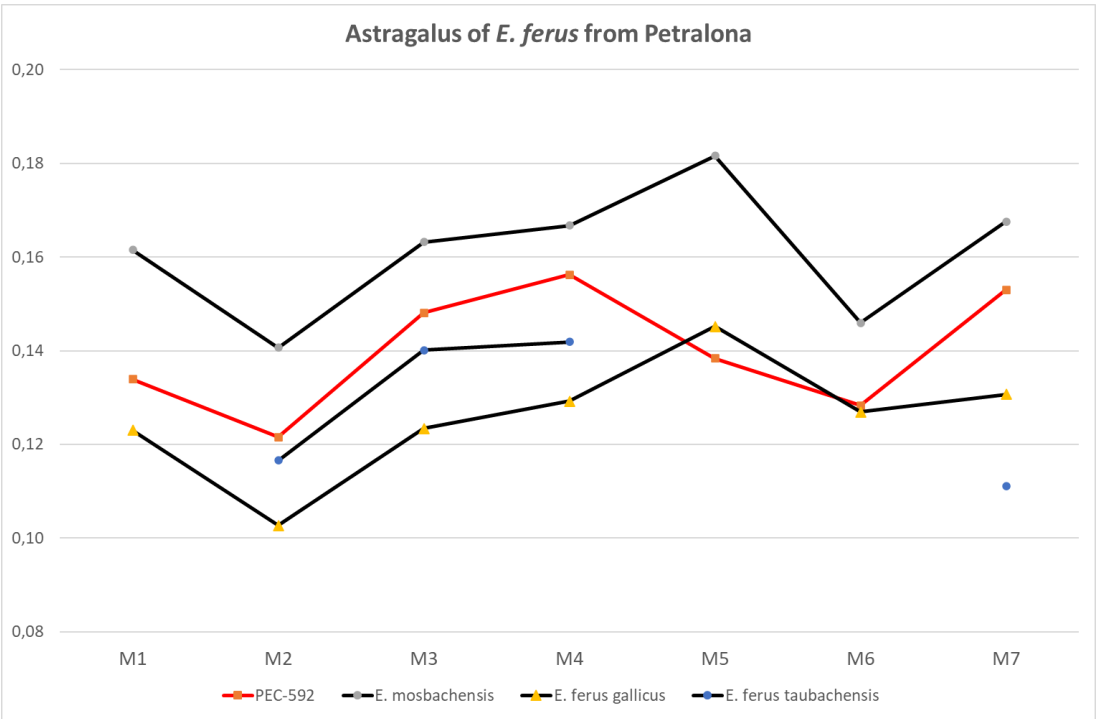

Figure5.85. Simpson's log ratio diagrams comparing the astragalus of *E. ferus* from Petralona to the various *E. ferus* and *E. mosbachensis* subspecies. Standard: *Equus hemionus onager*. Data from Eisenmann (2017a, b, c, d) and personal dataset.

CHAPTER 6. PHYLOGENY

Although the evolution of the Old World *Equus* and its living species has been of a particular interest among palaeontologists and biologists, opinions still remain controversial. Several species of *Equus* were acknowledged in the Quaternary of North and South America, Eurasia, and Africa, only seven of them remain today. Most scholars consider *Equus simplicidens* (=*Plesippus shoshonensis* = *Equus shoshonensis*) as the possible ancestor of *Equus*, *E. livenzovensis* the phylogenetic root of all the European stenonoid species (Azzaroli 1992; Alberdi et al. 1998; Palombo and Alberdi 2017; Bernor et al. 2018) whereas *Dinohippus mexicanus* (4.8 Ma, Carranza-Castañeda et al. 2013) from Mexico is suggested as the closest sister taxon of primitive *Equus.* However, at the present moment, there is no consensus on either taxonomic status or the phylogeny of *Equus*. Recent studies (Cirilli et al. 2021) reject the recognition of the taxa *Plesippus* and *Allohippus* (as either distinct genera or subgenera) and suggest that all Plio-Pleistocene species are grouped into as a single clade of *Equus* in accordance with Bennett's (1980) phylogenetic analysis, followed by many equid specialists (Palombo and Alberdi 2017 and references therein; Sun and Deng 2019; Cirilli et al. 2022 among others). Others, however, support the segregation of the Plio-Pleistocene equids into three distinct genera (Eisenmann and Baylac 2000; Eisenmann and Kuznetsova 2004; Eisenmann and Deng 2005; Eisenmann 2006, 2017; Barrón-Ortiz et al. 2019). This segregation is based only on the size of the cranium (brain box) (Eisenmann and Baylac 2000; Eisenmann 2002). Species that were previously assigned in *Allohippus* and they are included in the present cladistic analysis are: *Equus livenzovensis*, *Equus senezensis*, *Equus stenonis*, *Equus koobiforensis*, and *Equus sanmeniensis* (Samson 1975; Eisenmann 2004, 2006, 2017). Samson (1975) regarded *Allohippus* as a subgenus of *Plesippus* for the European Early Pleistocene equids

[namely *Plesippus* (*Allohippus*) *livenzovensis* and *Plesippus* (*Allohippus*) *stenonis*]. Species that were assigned to *Plesippus* and included in the present analysis are: *Equus simplicidens*, and *Equus qingyangensis* (Eisenmann and Deng 2005). Species that were assigned to *Equus* (true horses) are: *Equus apolloniensis*, *Equus altidens*, and *Equus eisenmannae* (Musil 1969; Eisenmann and Kuznetsova 2004; Weng and Deng 2011; Gkeme et al. 2021).

6.1 RESULTS AND DISCUSSION

The cladistic analysis yielded one most parsimonious tree which is presented in Figure 6.1 (Tree Length = 437). 13 unambiguous synapomorphies define the family of Equidae (node 38). *Cormohipparion* appears as the sister taxon of *Merychippus*, and these tridactyl genera (node 39) are defined by 6 unambiguous synapomorphies that separated them from the monodactyl genus. The genus *Equus* is modelled as a single clade (node 45; Figure 6.1) being supported by 18 unambiguous synapomorphies (Table 6.1). *Equus* clade includes species that were attributed to the genera *Allohippus* and *Plesippus* (e.g., *E. stenonis*, *E. senezensis*, *E. livenzovensis*, *E. simplicidens* etc). This result supports the monophyly of the genus *Equus* as claimed by Bennett's (1980) and Cirilli's (2021) phylogenetic analyses and identifies the genus *Dinohippus* as a paraphyletic group to the clade that includes all species of *Equus*. Within *Equus* clade phylogenetic resolution is mostly low and several polytomies appear. Nevertheless the North American *Equus simplicidens* appears as the sister taxon of the Chinese *Equus qingyangensis* (node 44); *Equus senezensis* forms a clade with *Equus stenonis* (node 51); *Equus altidens* from Dmanisi groups with *Equus altidens* from Gerakarou and Krimni-3 (node 53); *Equus apolloniensis* is included in the European wild ass *Equus hydruntinus* clade (node 63); the extant *Equus ferus* clusters with Przewalski's horse and the Asiatic wild Asses together(node 63); the Tibetan *Equus kiang* groups with the hemione *Equus hemionus* (node 60). According to Cirilli et al. (2021) these subgroups in the *Equus* clade (node 38) do not represent other genera but may indicate morphological differences that are insignificant between these species being scored with similar character states. In particular, *E. altidens* from Dmanisi and *E. altidens* from Gerakarou and Krimni are defined by a single synapomorphy, the depth of the narial opening (slightly more pronounced on the DNA sample).

In the present phylogeny (Figure 6.1), the extant wild African ass *Equus asinus* is regarded as a sister species of *E. hydruntinus-E. apolloniensis* clade. This result seems

to favor the scenario proposed by Eisenmann and Boulbes (2020) that *Equus apolloniensis* is an ass (also stated by Eisenmann and Kuznetsova 2004) and that this species could represent a step within the lineage of asses soon after its differentiation. On the other hand, this outcome could indicate a morphological convergence in skeleton (cranial, dental, postcranial) as a result of ecological pressure. The extant *Equus quagga* is regarded as sister species to the *Equus kiang- Equus hemionus* clade (also in the parsimony tree of Cirilli et al. 2021). This outcome is in contrast to recent phylogenomics (Orlando et al. 2009; Vilstrup et al. 2013; Jónsson et al. 2014), where plain zebras and wild Asian asses are clustered as distinct clades signifying an important difference in their genome sequences.

Table 6.1. List of unambiguous synapomorphies of the *Equus* clade (node 45 in Fig. 6.2).

Character number	Character description	Character state
CH1	Length of the cranium	3
CH2	Lateral outline of the cranium	0
CH16	Buccinator fossa	1
CH27	Orbits position related to the upper third molar	3
CH55	Lingual margin of the protocone	2
CH60	Protocone shape of the upper second premolar	1
CH61	Hypocone shape of the upper third and fourth premolar	1
CH62	Pli caballin shape of the upper third and fourth premolar	2
CH63	Protocone shape of the upper third and fourth premolar	1
CH64	Hypocone shape of the upper first and second molar	1
CH71	Upper premolar cheek teeth length	2
CH91	Morphology of the metaconid-metastylid complex	2
CH92	Morphology of the lingual side of the metastylid	2
CH114	Functional morphology of foot	2
CH116	Elongation of the lateral second metacarpal	3
CH118	Elongation of the lateral fourth metacarpal	3
CH122	Elongation of the lateral second metatarsal	3
CH124	Elongation of the lateral fourth metatarsal	3

As reported earlier, there are mainly two morphology-based phylogenetic scenarios for the origin of *Equus*; the one that *Equus* integrates a monophyletic group (including species formerly attributed to either *Allohippus* or *Plesippus*) and the other that is not. Eisenmann and Baylac (2000) and recently Barron-Ortiz et al. (2019) support the discrimination between modern (extant and recent) equids (subgenus *Equus*) and old plesippine (*Plesippus*) and stenonine (*Allohippus*) equids. According to this scenario,

the modern pattern possibly related to bigger braincase (true horses) appears in the fossil record in less than 1.5 Ma and it is closely related to Grévy's zebra, plains zebra and horses. According to Bennett's (1980) phylogenetic analysis, *Equus* is a monophyletic taxon including all the Plio-Pleistocene and extant equids and it could only be divided into two (and only two) subgenera, *Equus* (*Equus*) and *Equus* (*Asinus*), each of which is characterized by a suite of autapomorphic features. Recent cladistic analysis conducted by Cirilli et al. (2021) and the present one, further support the monophyly of the Plio-Pleistocene and extant *Equus*.

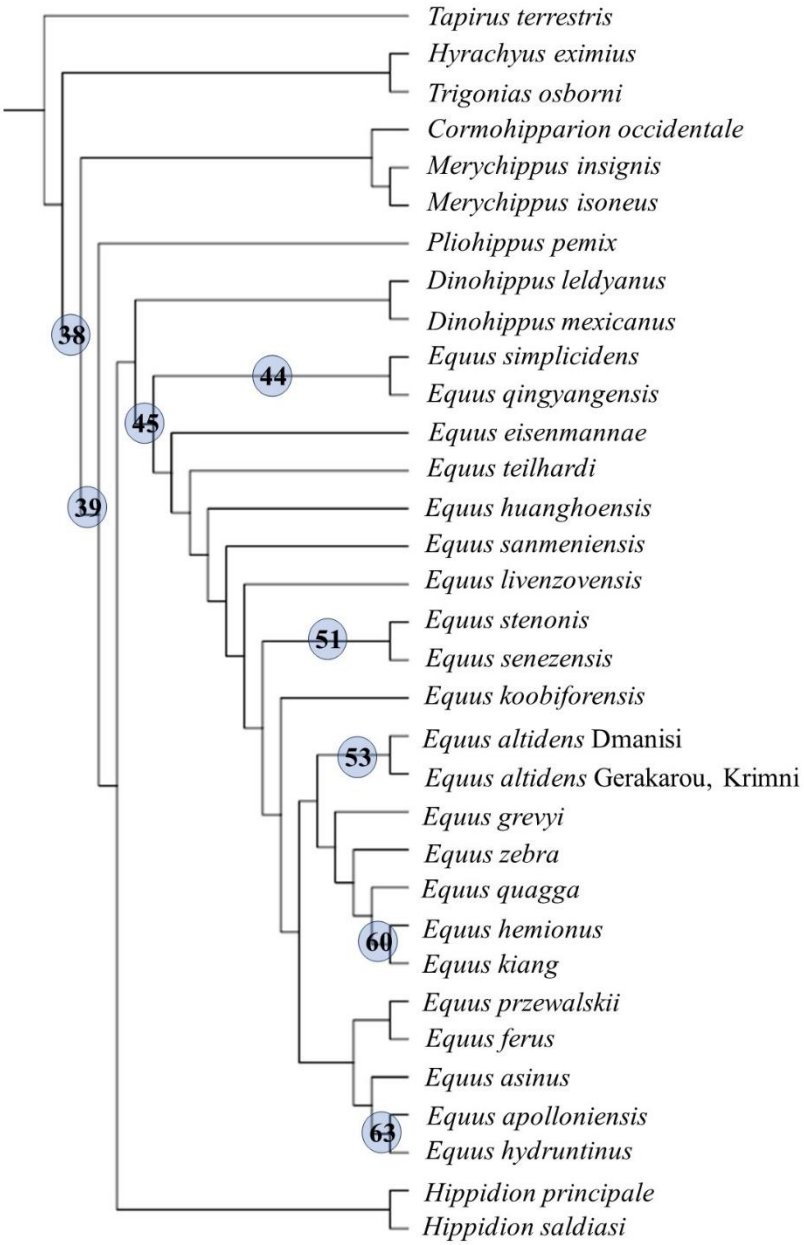

Figure 6.1. Most parsimonious tree of the cladistic analysis (33 taxa; 129 characters; Length = 437) recovered by TNT1.6.

The phylogenetic analysis provided some further insights on the relationships of the Early Pleistocene Greek equids and their relationship to the Old World *Equus* (Early-to-early Middle Pleistocene Eurasian non-caballine *Equus*) and to the zebra-ass clade. Based on the resulted tree and morphological characters described in chapter 4.1 (The Early Pleistocene and Galerian European *Equus*), *E. livenzovensis* has more primitive cranium traits than *E. stenonis* (all included populations) and closer to *E. simplicidens*. *E. stenonis* has reduced vomer length and longer post vomerine length than *E. livenzovensis*. These traits (reduction of the vomer length and elongation of the post vomerine length) as well as the reduction of the preorbital fossa and the reduction on the depth of the narial opening represent evolutionary steps within *Equus* (Cirilli et al. 2021 and references therein). The results on *E. apolloniensis* support its attribution to primitive forms of modern equids based on its derived characters (such as visually absent POF) and increased hypsodonty (cheek tooth crown height). The asinine dental characters of this species place it within the *E. asinus* subclade.

CHAPTER 7. BIOSTRATIGRAPHY–BIOCHRONOLOGY

The stratigraphic value of the different species of *Equus* has been a matter of debate among equid specialists. According to Forstén (1998), *Equus* species/subspecies should be used with caution in biostratigraphy, as different species do not succeed one another in time but occur and co-occur at ages. Alberdi et al. (2001) on the other hand following Vera's (1994) outline, believes that *Equus* species are suited best for bio-stratigraphic analysis because of their wide range of distribution, the high rate of evolution, and their good representation in the rock strata; the chronological issues are caused by equid specialists rather than by equids (due to the different taxonomic opinions on the same populations/localities).

The results of the taxonomy and phylogeny of the Greek equid fossil record provide further confirmation of the biochronological correlation of the studied localities. There is no doubt that stenonoid equids arrived in Eurasia and consequently Greece at the lower boundary of Quaternary. It can be confirmed that at least three stenonoid species appeared simultaneously in Europe at 2.5Ma (Figure 7.1), with *E. livenzovensis* and *E. major* arriving slightly earlier than *E. stenonis*. At least five more species in China (*E. qingyangensis, E. huanghoensis, E. eisenmannae, E. sanmeniensis* and *E. yunnanensis*) have been recognized at the same time frame at about 2.5Ma (Azzaroli 1982; Eisenmann 1975; Deng and Xue 1999a; Sun and Deng 2019 and references therein). It is not peculiar that several different species appeared in Eurasia at the same time, since equids are all highly cursorial and they are able to migrate very long distances in a relatively short time (Sun and Deng 2019). The time difference of their dispersal and arrival in Europe and Asia was negligible on the geochronological scale (Sun and Deng 2019). According to Sun and Deng (2019), there were at least two dispersal events of the genus *Equus* from North America into the Old World, with the second event leading

to the radiation of the *Equus* in China. Cirilli et al. (2021: p. 19, Figure 3) proposed a new biochronologic outline of the Early and Middle Pleistocene European *Equus* of Europe: the early-middle Early Pleistocene is characterized by the presence of *E. livenzovensis*, *E. stenonis*, *E. major*, *E. senezensis* and *E. stehlini* and the late Early Pleistocene by *E. stenonis*, *E. altidens*, *E. suessenbornensis* and *E. apolloniensis*, with *E. altidens* and *E. suessenbornensis* to extend their chronological ranges until the Middle Pleistocene.

Based on Cirilli et al. 's (2021) outline, the two large sized stenonoid equids *E. livenzovensis* and *E. major* have not been documented (or at least described) in the Greek fossil record and only *E. stenonis* (DFN, SES, VOL, KRI partim) and possible *E. senezensis* and *E. stehlini* (PYR) are acknowledged at the early-middle Early Pleistocene of Greece. During the late Early Pleistocene of Greece *E. stenonis* is replaced by *E. altidens* and *E. apolloniensis*. *E. altidens* extends its chronological range until the Middle Pleistocene with its last appearance in Petralona Cave.

Considering the evolutionary history of the European Early Pleistocene equids, *Equus stenonis* can be considered as the most iconic species in the Early Pleistocene of Europe, as it is the most common equid in European middle-late Villafranchian faunas. The biochronologic range of *E. stenonis* is between 2.45-1.2 Ma, from its first appearance in Saint Vallier to its last occurrence in Ceyssaguet (ca. 1.2 Ma; Aouadi 1999; Aouadi and Bonifay 2008). The species appears also in the Italy (Upper Valdarno Basin), Greece (Dafnero, Sésklo, Volax) and Georgia (Dmanisi) (Koufos and Kostopoulos 1997; Bernor et al. 2021).

The rich faunal deposits from Dafnero (DNF, DFN3), Sésklo and Volakas represent a slightly later period during the late middle Villafranchian mainly containing typical faunal elements of this period such as *Gallogoral meneghinii*, *Gazella bouvrainae*, *Gazellospira torticornis*, *Palaeotragus inexpectetus* and *Equus stenonis* though *Nyctereutes* is represented by *N. megamastoides* and *N. tingi* (a species that was previously reported in the Early Pliocene Megalo Emvolon fauna in northern Greece, Tamvakis et al. 2023) and *Ursus etruscus* makes its first appearance (Koufos and Kostopoulos 1997; Koufos 2014; Kostopoulos et al. 2019); *Homotherium latidens* and *Paradolichopithecus* aff. *arvernensis* are also present in the DFN3 faunal assemblage (Kostopoulos et al. 2019; Koufos et al. 2020). The analyzed cranial and postcranial elements from Dafnero (DFN, DFN3) show clear morphometric similarities with the middle Villafranchian *E. stenonis* records from Saint Vallier (~2.5 Ma, Nomade et al.

2014) and in particular with La Puebla de Valverde (~2.2 Ma; Sinusía et al. 2004) and Chilhac (~2.4 Ma). Based on that the Dafnero mammal assemblage corresponds to a middle-late Villafranchian age, European Land Mammal zone MN17b (Kostopoulos et al. 2019), while results on magnetostratigraphy suggest a better match within C2r (i.e., within post-Olduvai Matuyama Chron) (Benami et al. 2020). On the other hand, while taking into consideration the morphological homogeneity found within the *E. stenonis* populations, the samples from Sésklo and Volax show greater similarities with *E. stenonis* from Olivola (~2.0 Ma), which is characterized by its larger dimensions. The LFA's of Dafnero, Volakas and Sésklo (Thessaly) keep strong affinities with contemporaneous mammal communities from SW Europe and W Asia, suggesting the establishment of a rather homogeneous and characteristic South Alpine mammal palaeocenosis (Kostopoulos et al. 2019). The possible presence of *E. stenonis* in Krimni-1 (partim) presents the last occurrence of the species in Greece. Krimni-1 could be correlated to the early late Villafranchian between Gerakarou (~2 Ma, Koufos 1992; Koufos and Kostopoulos 2016) and Libakos (1.6 Ma interval, Kahlke et al. 2011; Gkeme 2016; Gkeme et al. 2017).

A similar faunal assemblage to those of DFN, SES, VOL is recorded at the Vatera sites, where *Paradolichopithecus* and *Homotherium* are also present (de Vos et al. 2002; Lyras and Van der Geer 2007). However, Vatera equids exhibit morphometric differences from *E. stenonis* populations. *Equus* from Vatera-F (*Equus* aff. *E. stenonis* var. *E. apolloniensis* herein) shares some similarities with *E. stenonis* from Olivola (~2.0 Ma), but also with the slenderer *E. apolloniensis* (~1.2-0.9 Ma). Furthermore, the similarities of *Equus* sp. B from Vatera-E with the middle Villafranchian *E. suessenbornensis* rather than *E. major* may support Eisenmann's (2006a, 2010, 2017) scenario of a common origin within the branch of *Equus* for certain equids (sussemiones), at least from 1.5 Ma and maybe soon before around 2.5 Ma, just above the Gauss-Matuyama limit (Vatera Formation, Greece). However, due to the inadequate material from Vatera sites and the lack of cranial/dental elements, this scenario requires further investigation.

The analyzed postcranial elements from Pyrgos indicated the possible presence of two species of *Equus* (*Equus* cf. *E. senezensis* and *Equus* aff. *E. stehlini*) based on the morphometry at least. However, according to Eisenmann (2002) the sympatry of two or more species of *Equus* was uncommon during the middle Early Pleistocene. These fossils could belong to different stratigraphic layers, or they could belong to one single

taxon/species. According to Alberdi et al. (1998) *E. stehlini* is a subspecies of *E. senezensis* (=*E. senezensis stehlini*). However, Cirilli (2022) established *E. stehlini* as a distinct species derived from *E. senezensis*. The latter species is recorded at Senèze (2.093 Ma±10 ka to 2.206 Ma± 21 ka, Nomade et al. 2014), while *E. stehlini* is recorded in several late Villafranchian Italian faunas (Azzaroli 1965; Alberdi et al. 1998; Cirilli 2022), with the oldest to be that from Coste San Giacomo (~2.2Ma). During the second half of the Early Pleistocene, *E. stehlini* replaced *E. stenonis* in Italy (Azzaroli 1965). In Pyrgos, the presence of *Leptobos* sp. and *Gazellospira torticornis* (Koufos 2016) indicate a middle-late Villafranchian age and the fauna is correlated probably to the Olivola FU.

Equus altidens succeeded *Equus stenonis* during the late Early Pleistocene. Because of the many disagreements among the equid specialists regarding the taxonomic status of this species, it is rather difficult to trace a reliable biochronology. The most extensive biochronological scenario suggests the concurrent arrival of *E. altidens* in Eastern Europe in Dmanisi (Georgia) (Lordkipanidze et al. 2007; Bernor et al. 2021) and Southeastern Europe around 1.8-2.0 Ma (Gkeme 2016; Gkeme et al. 2017). The species is a common element of late Early Pleistocene European faunas, dated at 1.6-0.6 Ma (Guerrero-Alba and Palmqvist 1997; Alberdi and Palombo 2013a, b; Madurell-Malapeira et al. 2014). The first appearance of *E. altidens* in Greece is recorded at Gerakarou LFA, and slightly later in Italy around 1.5 Ma (Selvella and Pirro Nord LFAs) (Alberdi and Palombo 2013a, b). The identification of the species in Petralona Cave extends its chronological range to ~0.4 Ma (Kahlke et al. 2011) and possibly marks its last occurrence in Eastern Europe. The presence of *E. altidens* from the Spanish locality of Venta Micena (ca. 1.5 Ma, Guerrero-Alba and Palmqvist 1997; Madurell-Malapeira et al. 2014) as a distinct subspecies (*E. altidens granatensis*) is questioned by the several authors. Based on the latest taxonomic analyses by Bernor et al. (2021) and also herein, no statistical differences were shown between the Italian, Spanish, Greek and Georgian fossil record of *E. altidens*. The material coming from Gerakarou, Libakos, Polylakkos, Krimni-1, Krimni-3, Tsiotra Vrysi and Petralona supports this taxonomic conclusion. In particular, the postcranial elements from Tsiotra Vrysi and Krimni-3 showed clear morphometric similarities with those of Venta Micena, resembling also Gerakarou with yet slightly larger dimensions. The presence of a complete cranium from Krimni-3 identical to those of Gerakarou favors the

taxonomic status originally proposed by Forstén (1988), later by Gkeme et al. (2017) and recently by Bernor et al.'s (2021).

Gerakarou is the oldest than all *E. altidens*-bearing Greek fossiliferous localities because of the presence of *Leptobos* and the co-occurrence of the two hyenas *Pliocrocuta perrieri* and *Pachycrocuta brevirostris* and it is correlated to the Olivola FU. Libakos and Polylakkos correlate at the 1.8-1.2 interval (Kahlke et al. 2011). The Libakos LFA contains *Leptobos* and *P. brevirostris* and is correlated to the Italian Tasso faunas, while in Krimni two species of *Equus* are present and the earliest *Bison* appears [*Bison* (*Eobison*) cf. *degiulii;* Koufos and Kostopoulos 1997; Kostopoulos et al. 2018; Maniakas 2019)] and the last appearance of *E. stenonis* (together with *E. altidens*). The Krimni sites are possibly slightly older (at the beginning of the time interval; Kahlke et al. 2011); KMN is intermediate between the faunas from Tsiotra Vryssi and Apollonia-1, within the 1.8–1.5 Ma time frame (Kostopoulos et al. 2022). The presence of *P. brevirostris*, *C. etruscus* and *Bison* (*Eobison*) in the TSR fauna clearly indicates a late Villafranchian age (Konidaris et al. 2015) and is correlated with Pirro FU [oldest occurrence of *Bison* (*Eobison*) in south-western Europe (Arzarello et al. 2012; Pavia et al. 2012; Masini et al. 2013)] and Dmanisi (1.77 Ma, Lordkipanidze et al. 2007; Akbar Khan et al. 2010). Based on these faunal elements and the magnetostratigraphy of the site and cosmogenic radionuclides, TSR is dated between 1.78 and ~1.5 Ma (within the first part of the late Villafranchian) (Konidaris et al. 2021), chronologically between GER-VSL (middle/late Villafranchian boundary, ~1.8-2.0 Ma) and APL [latest Villafranchian, ~1.2 Ma). Petralona Cave is the youngest site with the presence of *E. altidens*. The presence of *Equus ferus*, *Bos primigenius*, *Bison priscus*, *Sus scrofa* and *Felis silvestris* (Tsoukala 1989, 1991; Baryshnikov and Tsoukala 2010; Tsoukala and Guérin 2016) indicate a Middle Pleistocene age (probably middle Galerian).

Equus apolloniensis appears during the latest Villafranchian and Epivillafranchian of Greece. During that period more primitive equids (*E. stenonis*, *E. senezensis*, *E. stehlini*) are being replaced by more advanced species such as *E. apolloniensis* likely adapted to the open landscapes (Koufos and Kostopoulos 2016; Gkeme et al. 2021). In Southwestern Europe, primitive equids were replaced at about 1.5–1.4 Ma by the slender *E. altidens* (Venta Micena LFA, Spain and Selvella, Pirro Nord LFA, Italy), while the larger *E. suessenbornensis* also occurred in Selvella and Pirro Nord (Italy) and Barranco León 5 and Fuente Nueva 3 (Spain) (Alberdi 2010; Alberdi and Palombo 2013). The chronological and geographical distribution of *E. apolloniensis* seems to be

rather limited in southeastern Europe (Eastern Mediterranean). The species is reported in the *Homo erectus* bearing Kocabas-Denizli mammal locality (1.3–1.1 Ma; Boulbes et al. 2014; Lebatard et al. 2014) originally referred to as *Equus* aff. *suessenbornensis* (Erten et al. 2005). The presence of *E. apolloniensis* in Alykes (~1.6 Ma, Athanassiou 2002), as well as its possible occurrence also in Tsiotra Vryssi (1.78–1.5 Ma; Konidaris et al. 2015, 2021) and Platanochori-1 (Konidaris et al. 2015) could possibly mark its first occurrences.

Alykes and Volos have probably the same age because of their geographic proximity and geological similarity (Athanassiou 2002). Their faunal lists are quite similar including common faunal elements of the late Villafranchian. The faunal assemblage from Alykes contains *Gazellospira torticornis*, *Panthera gombaszoegensis*, and two canids (*C. arnensis* and *C. etruscus*) (Athanassiou 2002; Koufos 2014), while *Canis lupus* and *Panthera gombaszoegensis* are reported in Volos fauna. Concerning the PLN fauna, the presence of *Stephanorhinus hundsheimensis*, *Bison* (*Eobison*) and *Pontoceros ambiguous* indicate close affinities with Apollonia and a similar age is quite possible for it (Konidaris et al. 2015). The occurrence of *Stephanorhinus hundsheimensis* is a strong indicator of a latest Villafranchian age. The PLN bison resembles those from Venta Micena, Pirro Nord and APL indicating also a similar latest Villafranchian age (Konidaris et al. 2015). The possible presence of *E. apolloniensis* confirms this age, although further material is necessary to clarify its taxonomic status. The equid from Vassiloudi shares some common affinities with *E. suessenbornensis* from Pirro Nord, however due to the scarcity of the material, it is arbitrary its definite attribution to this species. The VSL fauna is likely older than the Pirro Nord FU and estimated at the early late Villafranchian (1.8 Ma) correlating to the Olivola FU. This locality (together with Gerakarou) is chronologically placed between the sites of Senèze and Olivola (Koufos and Kostopoulos 1997).

The stenonoid equids have gradually been replaced by the caballoids, the lineage of true horses; there is consensus among equid specialists that true equids emerged at the beginning of Middle Pleistocene in Europe (Forstén 1998b), from when onwards have been an important component of the large vertebrate faunas. Their extensive skeletal plasticity led to the recognition of several subspecies which were later interpreted as ecomorphological adaptations (Van Asperen 2010; Saarinen et al. 2016). Following the guidelines of the ICZN 2003 (see also Van Asperen 2013b), the author attributed the caballoids from Petralona Cave and Aggitis to *Equus ferus*.

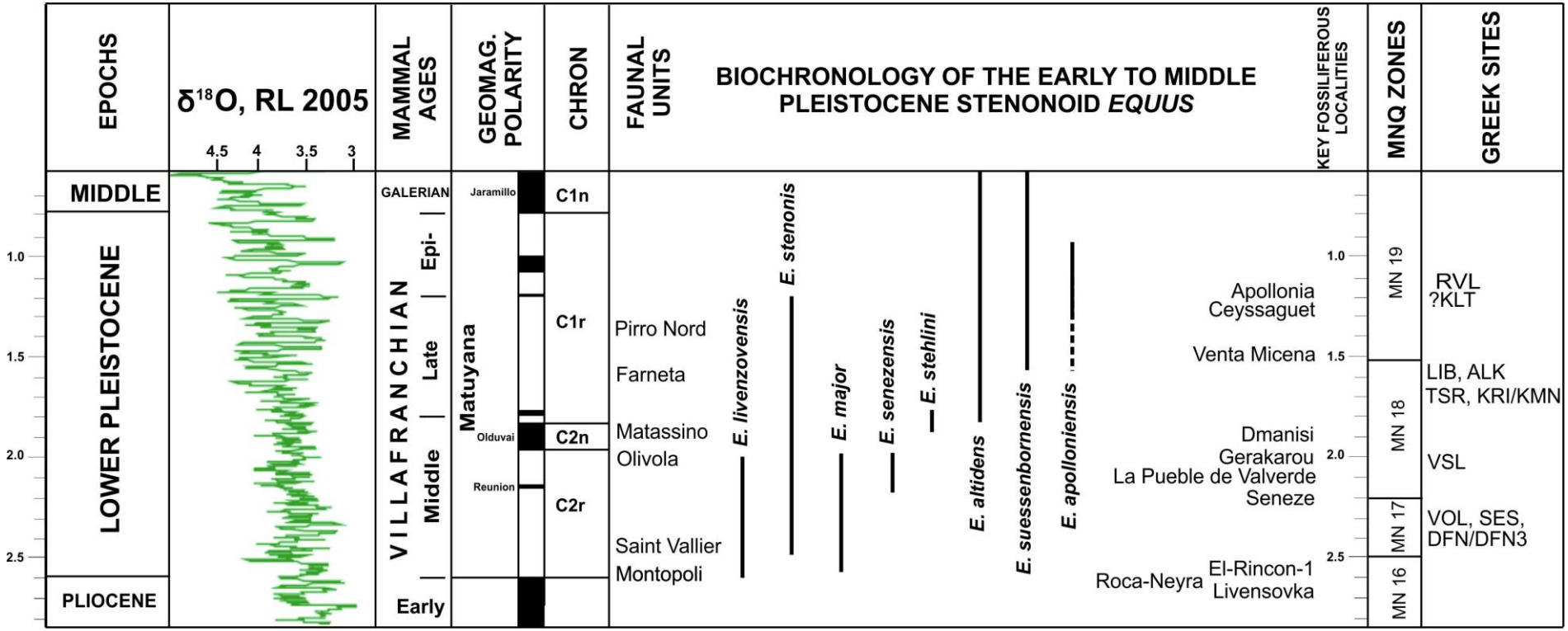

Figure 7.1. Biochronological record of the European Early Pleistocene *Equus* and age of the related LFAs.

CHAPTER 8. PALAEOECOLOGY

8.1 ECOLOGY AND BODY SIZE OF *EQUUS*

Many studies have established that *Equus* is an ecologically flexible genus which can live in a wide range of environments and occasionally adopt a diversified diet (Prat 1968; Forstén 1993; MacFadden 1999; Smith and Pearson 2005; Van Asperen 2010; Rivals and Lister 2016 among others). Extant wild equids are predominantly grazers inhabiting mostly open, grass or shrub-dominated habitats (Rubenstein 1989; Bauert al. 1994; Moehlman 2002). Although they are predominantly grazers, there is a large variation in their diets and body size as a response to different habitat preferences, social strategies, and available food resources. Different species, with very similar ecological requirements, have a high interspecific competition when they share the same geographical range (Hutchinson 1957). Przewalski's equids are adapted to mesic steppe habitats with a preference to riparian and oasis vegetation (water sources) (Kaczensky et al. 2008). Grévy's zebra, which is the largest extant zebra species, occupy semi-arid savannah regions and is considered to be hyper-grazer, meaning that they eat only grass and no browse (herbaceous or woody plants) at all (Fischoff et al. 2007; Sundaresan et al. 2007). The plains zebras (*Equus quagga*) have similar social and feeding habits to Grévy's zebras (Kleine 2010). They are almost exclusively grazers and consequently they are strongly associated with grasslands and savanna woodlands (Hack et al. 2002); they inhabit in both tropical and temperate climates, and they avoid deserts, dense forests, and permanent wetlands. Some of these zebras are resident populations, while some others are migratory depending on the food resource availability (Hack et al. 2002) or else in response to predation danger (Fischhoff et al. 2007). The mountain zebras (Cape Mountain zebra and Hartmann's mountain zebra) inhabit slopes and

plateaus in mountainous areas; their diet primarily consists of grass but also includes browse (Penzhorn 1988). The Asian wild ass *Equus hemionus*, that weights approximately 200–260kg, is adapted to several climatic conditions and its dietary habits change depending on the season (temporal feeding behaviour); they are predominately grazers when grass if plentiful (wet season) but in a drier season they browse most of their diets (Feh et al. 2002). Kiangs, which are larger than *Equus hemionus*, occupy open terrain, of plains, basins, broad valleys, and hills, anywhere grass and sedge are abundant (Shah 2002). They occur in alpine meadows and steppes and also in desert steppe and other arid habitats (Schaller 1998). The African wild ass (*Equus asinus*) occupies semi-desert grasslands, preferring rocky hills to sandy areas (Kingdon 1997; Smith and Pearson 2005) and it is predominantly a (nocturnal) grazer rather than a browser (Haltenorth and Diller 1988).

Diet and habitat preferences are connected with body size patterns in equids (Bauer et al. 1994; Cosyns et al. 2001) (for purposes herein body size is synonymous with body mass). There is a strong correlation between a high body mass and open habitats in fossil North American equids (MacFadden 1986). Large-sized extant zebras live in open habitats dominated by herbaceous vegetation developed upon soft soils (Durets 1926; Gromova 1949; Eisenmann and Karchoud 1982; Eisenmann 1984; Eisenmann and Guerin 1984).

While one of the most striking features apparent in evolutionary history of Equidae is the increase of body size (Cope's rule), there is a trend toward decreasing body size through time in stenonoid equids probably related to the climatic-environmental changes that occurred from the middle Villafranchian to the early Galerian, following the inverse direction of Cope's rule (Prat 1968; Alberdi et al. 1998); the middle Villafranchian large stenonoids were associated to open and dry habitats (steppes), whereas the late Villafranchian to earliest Galerian smaller species lived in more closed and wet habitats (savannah-mosaic, woodlands) (Alberdi et al. 1998). During the Middle Pleistocene, equids present various morphometrical features (including size) that were results as a response to climatic changes. Their extensive plasticity enabled them to survive in interglacial forests to grass-steppes during glacial periods (Boulbes and Van Asperen 2019). Equids underwent a size decreasing initiated throughout the Upper Pleistocene that has already been started by the end of the Middle Pleistocene (Boulbes and Van Asperen 2019). After the Last Glacial Maximum (LGM), equid populations of Europe were led to fragmentation (Boulbes and Van Asperen 2019).

The present results on body mass estimations are shown in Figures 8.1 and 8.2 based on the selected measurements on the third metacarpals and third metatarsals respectively. Based on Saarinen et al.'s (2021) body size classes, the Greek and European populations of *E. stenonis* mainly belong to the medium sized equids (380–450 kg), while *E. altidens* populations, *E. senezensis* and *E. stehlini* are all included in the small sized equids (<380 kg). The primitive *E. simplicidens* and *E. livenzovensis* share similar size, medium to large. The body size increases from *E. livenzovensis* to the group composed by *E. major, E. suessenbornensis* and probably *E. apolloniensis*; the gigantic *E. major* was double the body mass of *E. livenzovensis* (Alberdi et al. 1988).

In the same group, the gigantic equid from Vatera (the large-sized *Equus* sp. B) and the large sized *E.* aff. *E. suessenbornensis* from Vassiloudi are also included. *E. livenzovensis* probably lived in open habitats with soft soils, under cold and dry climates (Alberdi et al. 1988), such as steppe or steppe-like environments inferred for this time in Western Europe (see Guerin 1984; Alberdi et al. 1991). The body size increases from *E. livenzovensis* to the group composed by *E. stenonis, E. senezensis, E. stehlini* and *E. altidens* (Alberdi et al. 1988) (Figures 8.1, 8.2). According to Sanchez Chil1on et al. (1994), the Spanish *E. stenonis* (*E. s. pueblensis*) lived in cold temperate climates, landscapes savannas but with some intervals of forest dominance. The small sized *Equus senezensis* and *E. stehlini* (Figures 8.1, 8.2) were adapted to cold-temperate and wet climate in Central to Western Europe occupying woodlands-savannas (Alberdi et al. 1988; Boulbes and Van Asperen 2019). According to Sainchez Chillon et al. (1994) the *E. altidens* from Venta Micena lived under warm or warm-temperate climatic conditions occupying woodlands or woodland-savannas. During that period the climates were predominantly warm and wet in Western Europe (Meon et al. 1980; Guerin 1984; Bonifay 1990; Boulbes and Van Asperen 2019; Kahlke et al. 2011 among others).

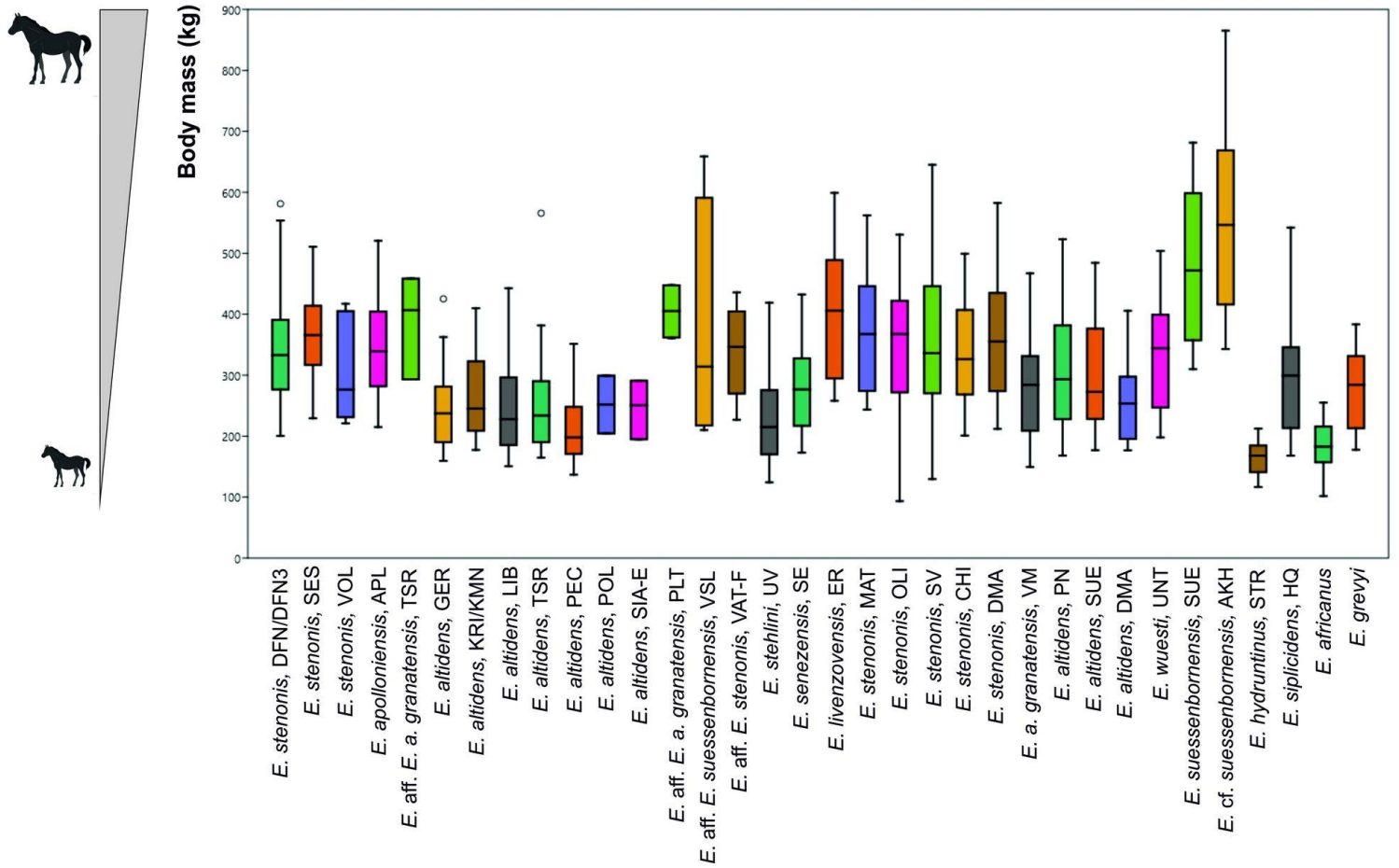

Figure 8.1. Box plot of the estimated weight in kilograms of the Early to Middle Pleistocene equids of Greek and European equids, the North American *E. simplicidens*, the European wild ass *E. hydruntinus* and the extant *E. africanus* and *E. grevyi* based on metacarpal measurements (MC3, MC5 and MC11 of Scott 1983). Data were taken from Eisenmann 2017a,b; Bernor et al. 2021; Cirilli et al. 2022; 2021; Eisenmann and Boulbes 2020 and personal data set.

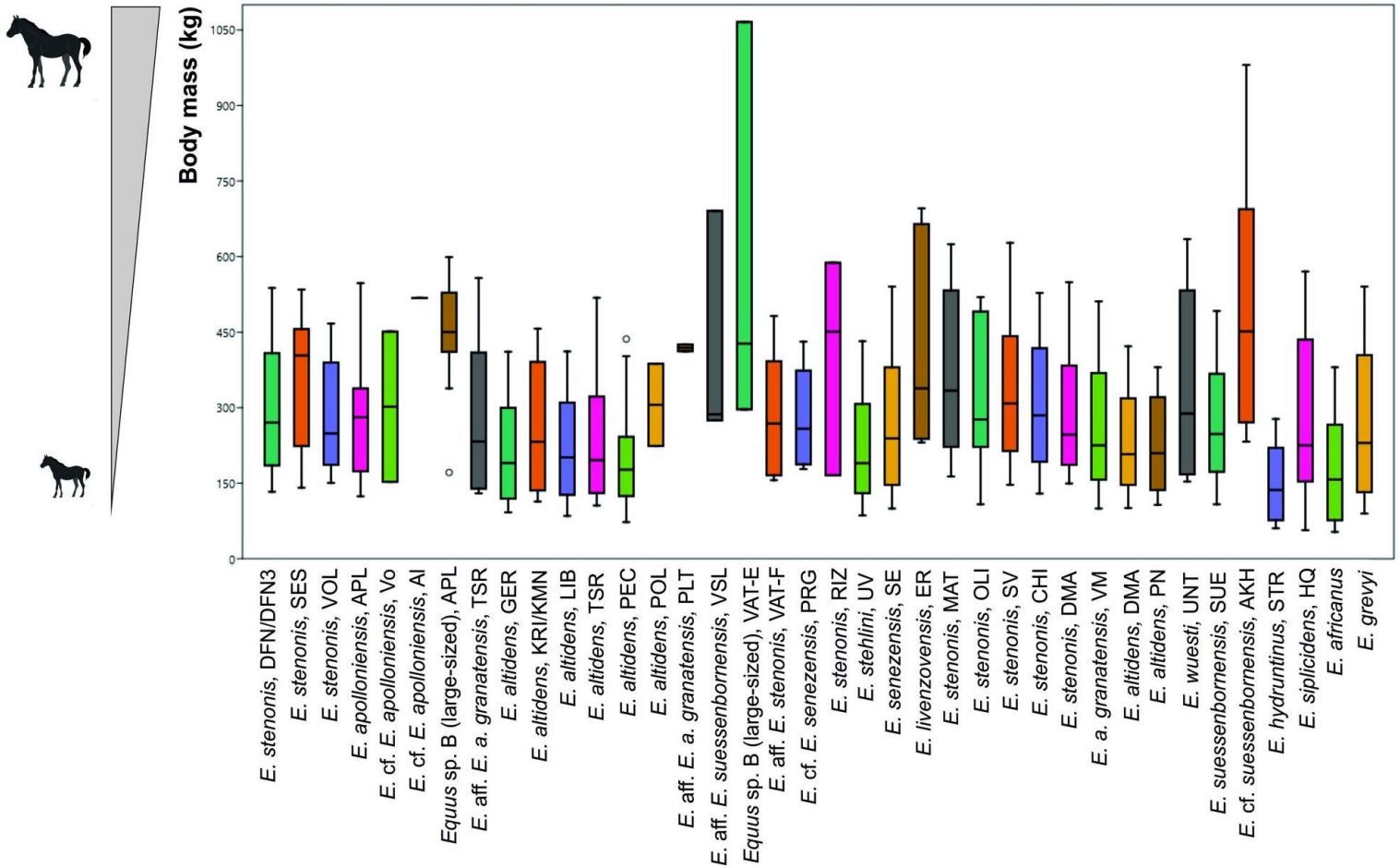

Figure 8.2. Box plot of the estimated weight in kilograms of the Early to Middle Pleistocene equids of Greek and European equids, the North American *E. simplicidens*, the European wild ass *E. hydruntinus* and the extant *E. africanus* and *E. grevyi* based on metatarsal measurements (MT3, MT5 and MT11 of Scott 1983). Data were taken from Eisenmann 2017a, b; Bernor et al. 2021; Cirilli et al. 2022; 2021; Eisenmann and Boulbes 2020 and personal data set.

8.2 MESOWEAR

The results of the mesowear analysis based the Mihlbachler et al.'s (2011) scale are plotted in Figure 8.3. For all localities/taxa, all the series provide mesowear scores higher than 4 (Figure 8.3) including the Middle Pleistocene French equids, while reference taxa of extant ungulates exhibit low scores. In comparison to the reference data on extant ungulates (Mihlbachler et al.'s 2011; Figure 2.11), the high values of the mesowear scores of the studied Greek sites generally shows that these equids were preferentially grazers, with food dominated by abrasive plants such as grasses and occasionally mixed feeders possibly due to the different food resources or seasonal differences (scores close to 4).

E. altidens from Gerakarou has a grazing mesowear score: that means that the equid from Gerakarou consumed abrasive foods like hay (more abrasive than foliage, less than grasses), fresh grass or even forbs/herbs. However, it has also a mixed feeding signal (scores close to 4) with the consumption of less abrasive grasses that have a lower concentration of phytoliths, comparable to dicot shrubs and herbs (Tsartsidou et al. 2007). *E. altidens* from Libakos, Krimni and Petralona exhibit both grazing and mixed feeding signal. They were probably more mixed feeders than grazers. Saarinen et al. (2021) indicated that *E. altidens* from Süssenborn had a grazing mesowear signal. The difference between the German and Greek sample of *E. altidens* populations could be interpreted due to the different food resources available or the seasonal differences. *E. apolloniensis* from Apollonia has similar mesowear score like the LIB-GER-KRI *E. altidens* indicating a more mixed feeding mesowear signal than a grazing one, but it was mainly using as food sources fresh-small grasses, herbs, forbs, etc., depending on the availability. *E.* cf. *apolloniensis* from Alykes and Volos show a more grazing signal. The available data on the Greek *E. stenonis* are limited due to the either bad preservation or the lack of worn teeth at the middle stages of wear. However, generally the mesowear signal is that of grazing. The reference taxa *Capreolus capreolus*, *Cervus elaphus* and *Rupicapra rupicapra* exhibit the lowest scores indicating strictly browsing habits, while *Ovis ammon* also exhibits mixed feeding habits.

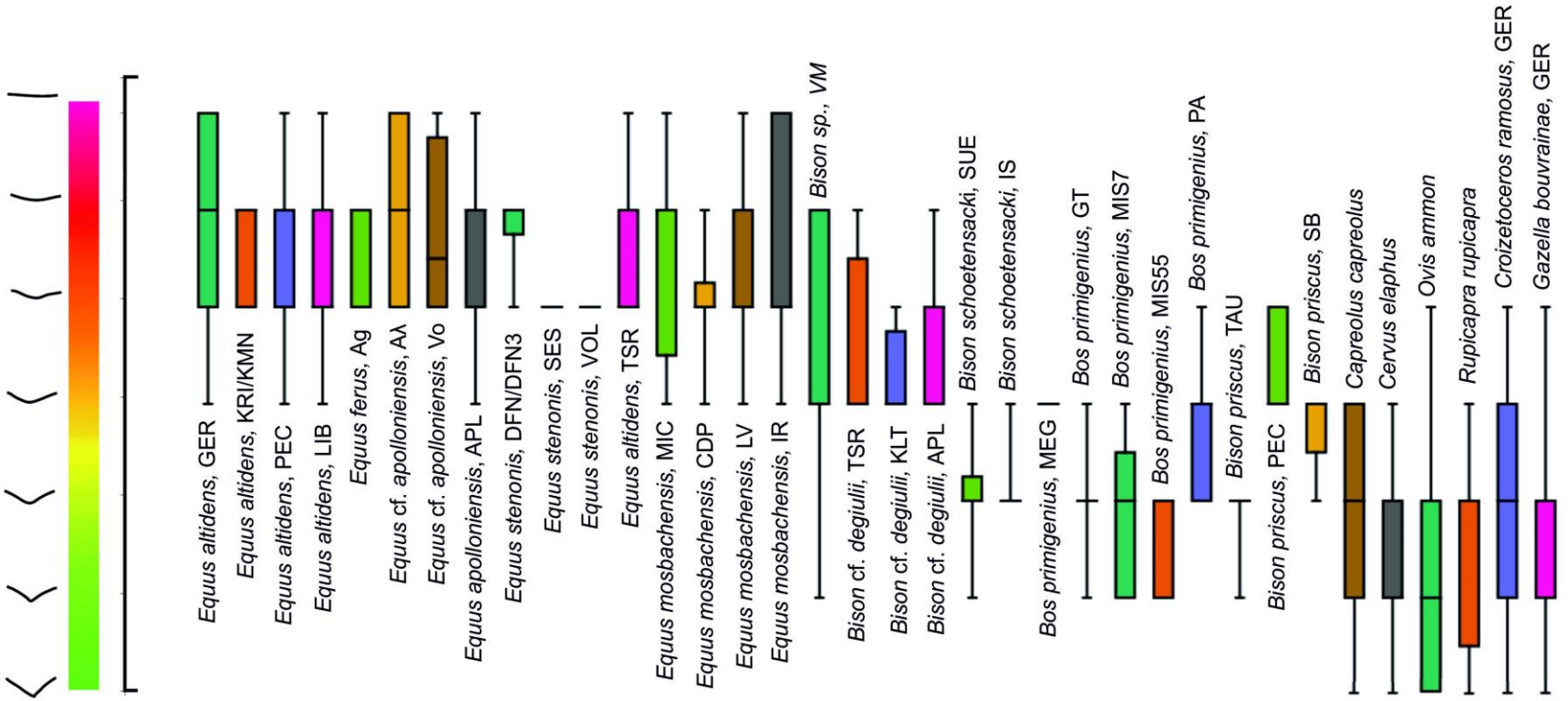

Figure 8.3. Mesowear score according to Mihlbachler et al.'s (2011) scale for the samples from Gerakarou (*E. altidens*), Krimni (*E. altidens*), Petralona (*E. altidens*), Libakos (*E. altidens*), Aggitis (*E. ferus*), Alykes (*E.* cf. *apolloniensis*), Volos (*E. apolloniensis*), Apollonia (*E. apolloniensis*), Dafnero (*E. stenonis*), Sésklo (*E. stenonis*), Volax (*E. stenonis*) and Tsiotra Vrysi (*E. altidens*) compared the Middle Pleistocene French equids from La Micoque (*E. mosbachensis micoquii*), Camps-de-Peyre (*E. mosbachensis campdepeyri*), Lunel-Viel (*E. mosbachensis palustris*) and Igue des Rameaux sites (*E. mosbachensis* ssp.), several species of bovids and extant ungulates. The data of French equids was taken from Uzunidis et al. (2017) and from bovids and extant ungulates from Maniakas (2019)

8.3 MICROWEAR

The results of the Kruskal-Wallis test (on Phase II facets), for the fossil and extant species, revealed significant differences ($p<0.05$; Table S) between species for all SSFA variables [Asfc, epLsar and heterogeneities Hasfc9, Hasfc36, Hasfc81]. Biplots (Figure 8.4) represent each species dispersion for epLsar-Asfc and HAsfs9- HAsfs81.

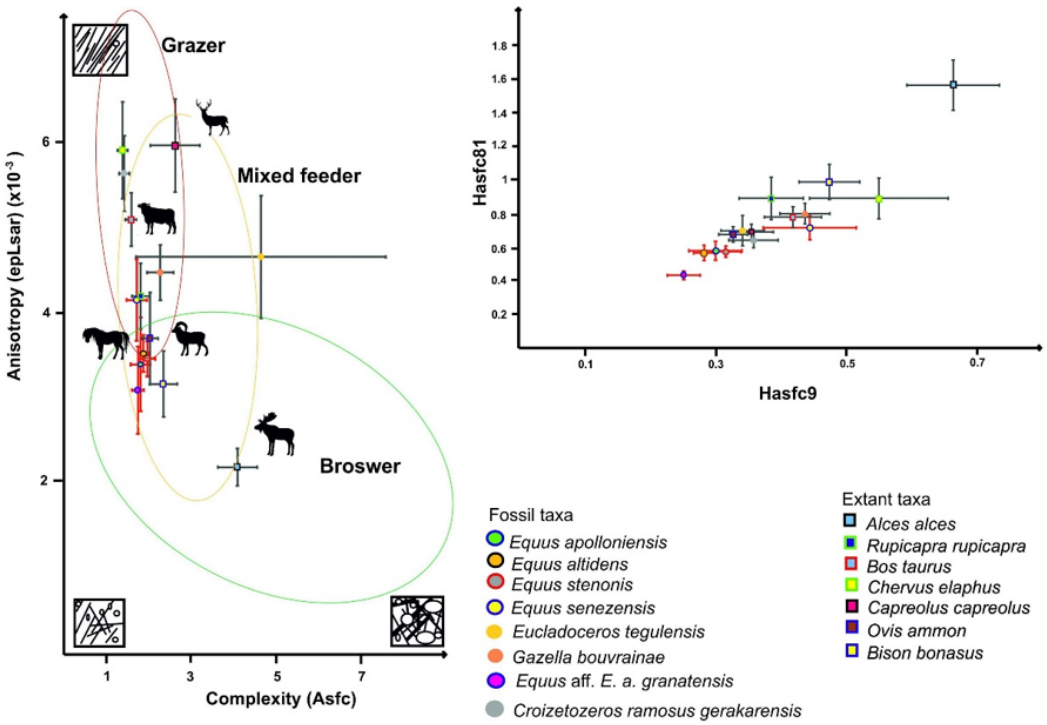

Figure 8.4. Bivariate plots (means with 95% conf. interval) of complexity (Asfc) versus anisotropy (epLsar) and on the Heterogeneities of Asfc (9 cells versus 81) on Phase II of the Greek and European Early to Middle Pleistocene equids (red crosses), the referenced extant taxa and the fossil taxa (black crosses), using their mean values (Table SI 1); red circle is for grazers, light orange circle is for mixed feeders and dark green circle is for browsers. Each point represents the mean (Table SI 1). Uncertainty crosses represent the 95% CI of the standard error (Table SI 1).

The pairwise comparisons using the Bonferroni corrected p values of the DMTA SSFA between species are given in Table 8.2. Comparing the dental microwear texture of equids to the reference taxa (extant species): *E. stenonis* differs from all extant species except for *R. rupicapra* and *Ovis ammon*, while *E. senezensis* only differs from *A. alces*. *E. altidens* differs from all extant species apart from *Ovis ammon*. The species differs mostly from *Bos taurus* and *Bison bonasus* in anisotropy and heterogeneities of

anisotropy. *Equus apolloniensis* differs only from *Alces alces*, while *Equus* aff. *E. a. granatensis* differs from the extant *Bison bonasus*, *Ovis ammon* and *Alces alces*. There are no significant differences among equids. Further, it is worth mentioning that the reference populations of the extant species, *Alces alces* differs from all the extant species differs and mostly from the domestic cattle *B. taurus*, while there are no differences from *Bison bonasus*.

Anisotropy (epLsar): Among equids, *E. senezensis* has the highest values of anisotropy, while the lowest belongs to *Equus* aff. *E. a. granatensis*. All the other equid species plot between them having intermediate epLsar values (Figure 8.4). Further, the means of all equids plot are close to the wild sheep *Ovis Ammon*. *Alces alces* has the lowest anisotropy of all extant and fossil species. The highest values of anisotropy belong to the red deer and *Capreolus capreolus*. In general, equids are plotted between the moose and the domestic cattle indicating mixed feeders.

Complexity (Asfc): All equids including the red deer (*Cervus elaphus*), Bos taurus and *Rupicapra rupicapra* have the lowest values of Asfc. *Croizetoceros ramosus gerakarensis* has the highest values of complexity from all fossil and extant taxa including the moose *Alces alces* (Figure 8.4). Among the extant species, the latter has the highest values. That is expected because the moose feeds on hard items (browser, Figure 8.4).

Heterogeneities of Asfc (HAsfc9, HAsfc36, HAsfc81): Equids have the lowest values of HAsfc9 and HAsfc81 except for *Equus senezensis* which is plotted close to *Bos taurus*. The lowest values from both extant and fossil taxa belong to *Equus* aff. *E. a. granatensis*. Here too, *Alces alces* has the highest values of both heterogeneities from all extant and fossil taxa is typical of the browsing dietary category; all the other taxa plot close to each other (Figure 8.4).

Taxa		SSFA Parameters				
		Asfc	epLsar (×10-3)	Hasfc9	Hasfc36	Hasfc81
E. apolloniensis	n	13	13	13	13	13
	Mean	1,79	3,45	0,3	0,43	0,58
	SE	0,23	0,56	0,04	0,05	0,06
	SD	0,84	2,01	0,15	0,17	0,2
E. stenonis	n	67	67	67	67	67
	Mean	1,95	3,52	0,32	0,45	0,58
	SE	0,19	0,21	0,02	0,03	0,03
	SD	1,53	1,72	0,19	0,23	0,28
E. altidens	n	72	72	72	72	72
	Mean	1,86	3,58	0,28	0,44	0,57
	SE	0,12	0,22	0,02	0,04	0,05
	SD	1	1,85	0,13	0,33	0,39
E. aff. E. a. granatensis	n	8	8	8	8	8
	Mean	1,73	3,15	0,25	0,36	0,44
	SE	0,14	0,52	0,02	0,02	0,02
	SD	0,4	1,47	0,07	0,06	0,07
E. senezensis	n	14	14	14	14	14
	Mean	1,7	4,22	0,45	0,59	0,72
	SE	0,25	0,48	0,07	0,07	0,07
	SD	0,92	1,81	0,27	0,25	0,27
Bos taurus	n	44	44	44	44	44
	Mean	1,57	5,17	0,42	0,58	0,78
	SE	0,14	0,32	0,04	0,04	0,06
	SD	0,95	2,1	0,29	0,28	0,41
Bison bonasus	n	24	24	24	24	24
	Mean	2,34	3,22	0,48	0,73	0,99
	SE	0,33	0,39	0,05	0,08	0,1
	SD	1,6	1,91	0,23	0,38	0,51
Rupicapra rupicapra	n	21	21	21	21	21
	Mean	1,79	4,26	0,39	0,6	0,9
	SE	0,21	0,39	0,05	0,07	0,13
	SD	0,97	1,78	0,22	0,31	0,58
Ovis ammon	n	22	22	22	22	22
	Mean	2,02	3,76	0,33	0,48	0,68
	SE	0,19	0,55	0,02	0,03	0,04
	SD	0,88	2,56	0,1	0,12	0,21
Cervus elaphus	n	21	21	21	21	21
	Mean	1,36	5,99	0,55	0,7	0,9
	SE	0,13	0,57	0,11	0,09	0,12
	SD	0,57	2,63	0,48	0,43	0,56
Capreolus capreolus	n	18	18	18	18	18
	Mean	2,61	6,05	0,36	0,52	0,7
	SE	0,59	0,55	0,05	0,03	0,05
	SD	2,49	2,34	0,14	0,14	0,2
Alces alces	n	48	48	48	48	48
	Mean	4,1	2,23	0,67	1,04	1,57
	SE	0,47	0,22	0,07	0,09	0,15
	SD	3,25	1,54	0,49	0,64	1,04
Gazella bouvrainae	n	31	31	31	31	31
	Mean	2,26	4,54	0,44	0,65	0,8
	SE	0,32	0,33	0,04	0,05	0,06
	SD	1,77	1,82	0,21	0,27	0,33
Croizetoceros ramosus gerakarensis	n	33	33	33	33	33
	Mean	1,4	5,72	0,36	0,52	0,65
	SE	0,12	0,45	0,04	0,04	0,04
	SD	0,69	2,58	0,21	0,25	0,26
Eucladoceros tegulensis	n	7	7	7	7	7
	Mean	4,66	4,73	0,34	0,51	0,7
	SE	2,98	0,73	0,03	0,06	0,09
	SD	7,88	1,92	0,09	0,17	0,24

Table 8.1 Mean, standard error (SE) and standard deviation (SD) for the European fossil equids, fossil artiodactyls and extant ungulates; Asfc = Area-scale fractal complexity, epLsar = exact proportion length-scale anisotropy of relief, Hasfc9, 36, 81 = Heterogeneity of area-scale fractal complexity on 9, 36 and 81 cells respectively. Statistics of fossil artiodactyls and extant ungulates were calculated from Alifieri's (2021) data set.

SPECIES	EAPOL	ESTE	EALTI	ESENEZ	BTAUR	BBONA	RRUPI	OAMMO	CELAPH	CCAPRE	AALC	GBOUVR	CRUMGE	EUTEGU	EAFFGRA
EAPOL	-														
ESTE		-													
EALTI			-								Asfc				
ESENEZ				-											
BTAUR		epLsar	EpLsar Hasfc36 Hasfc81		-						Asfc, epLsar				
BBONA		Hasfc9 Hasfc36 Hasfc81	Hasfc9 Hasfc36 Hasfc81			-									Hasfc81
RRUPI			Hasfc81				-				epLsar				
OAMMO						epLsar		-							
CELAPH		epLsar, Hasfc36, Hasfc81	epLsar Hasfc36 Hasfc81			epLsar			-		epLsar				Hasfc81
CCAPRE		epLsar	epLsar							-	epLsar				
AALC	Hasfc9 Hasfc36 Hasfc81	Asfc Hasfc9 Hasfc36	Hasfc9	Asfc	Hasfc9 Hasfc36 Hasfc81		Asfc	Hasfc36 Hasfc81	Asfc	Hasfc36, Hasfc81	-	Hasfc81	Asfc Hasfc9 Hasfc36 Hasfc81	Hasfc9 Hasfc3 Hasfc81	Hasfc81
GBOUVR		Hasfc9 Hasfc36 Hasfc81	Hasfc9, Hasfc36, Hasfc81								epLsar	-			Hasfc36 Hasfc81
CRUMGE		EpLsar	epLsar			epLsar					epLsar		-		
EUTEGU														-	
EAFFGRA															-

Table 8.2. Significant differences between species using Kruskal-Wallis tests for medians, showing the statistically significant parameters from the Dunn's post hoc tests when using the Bonferroni corrected p values. Fossil equids EAPOL=*Equus apolloniensis*, ESTE= *Equus stenonis*, EALTI= *Equus altidens*, ESENEZ=*Equus senezensis*, EAFFGRA = *Equus* aff. *E. a. granatensis*; fossil artiodactyls GBOUVR=*Gazella bouvrainae*, CRUMGE=*Croizetoceros ramosus gerakarensis*, EUTEGU=*Eucladoceros tegulensis*; reference taxa (extant species) BTAUR=*Bos taurus*, BBONA=*Bison bonasus*, RRUPI=*Rupicapra rupicapra*, OAMMO=*Ovis ammon*, CELAPH=*Cervus elaphus*, CCAPRE=*Capreolus capreolus*, AALC= *Alces alces*. Data of extant data and fossil artiodactyles were taken from Alifieri (2021).

8.4 HABITAT SCORES

The results of the habitat analysis (Figures 8.5, 8.6) showed that the metapodials (both McIII and MtIII) of *Equus grevyi* are placed in open plains habitats, while those of *Equus africanus* are also indicating light cover habitat.

The archaic large-sized stenonoid *E. livenzovensis* suggests habitats between heavy cover to plains based on the third metacarpals, more or less similar to the North American *Equus simplicidens* (intemediate between light cover and plains).

The metapodials of the various *Equus stenonis* populations mainly indicate habitats of light cover and heavy cover; the Italian population from Matassino also indicates marginally plains (McIII) while the French population of *Equus stenonis* from Chilhac is mostly indicative of a heavy cover habitat (similar to the *Hipparion* fauna from Howenegg). The metapodials of *Equus stenonis* from Saint Vallier are grouped mostly in heavy cover habitats. *Equus senezensis* and *Equus stehlini*, although close in morphometry, they designate habitats with light cover and heavy cover respectively.

The populations of *Equus altidens* indicate mainly habitats from heavy cover to plains. The highest scores belong to the populations coming from Tsiotra Vrysi and Krimni (KRI, KMN), resembling mostly those of *Equus apolloniensis* from Apollonia and *Equus altidens* from Venta Micena (particurarly the MtIII) indicating open habitats. The sample of the third metacarpals from Tsiotra Vrysi and Dmanisi are grouped together between the light cover habitat category and plains category. The sample from Petralona has a wider range of scores indicating heavy and light cover up to plains.

The metapodials of *Equus apolloniensis* (which are latger than *E. altidens*) are grouped in plains habitat, incicating open landscapes. The metapodials of *Equus wuesti* which in moprhometry are close to *E. apolloniensis*, indicate intermediate habitat between light cover (McIII) and plains (MtIII). These is a slight difference between the analysis conducted on the third metacarpals and on third metatarsals. As it seems, the third metacarpals of *Equus suessenbornensis* from Sussenborn and Akhalkalaki are grouped light cover and plains habitats. On the hand, the third metatarsals are catergorized in plains habitat indicating open landscapes similar ro *Equus apolloniensis*.

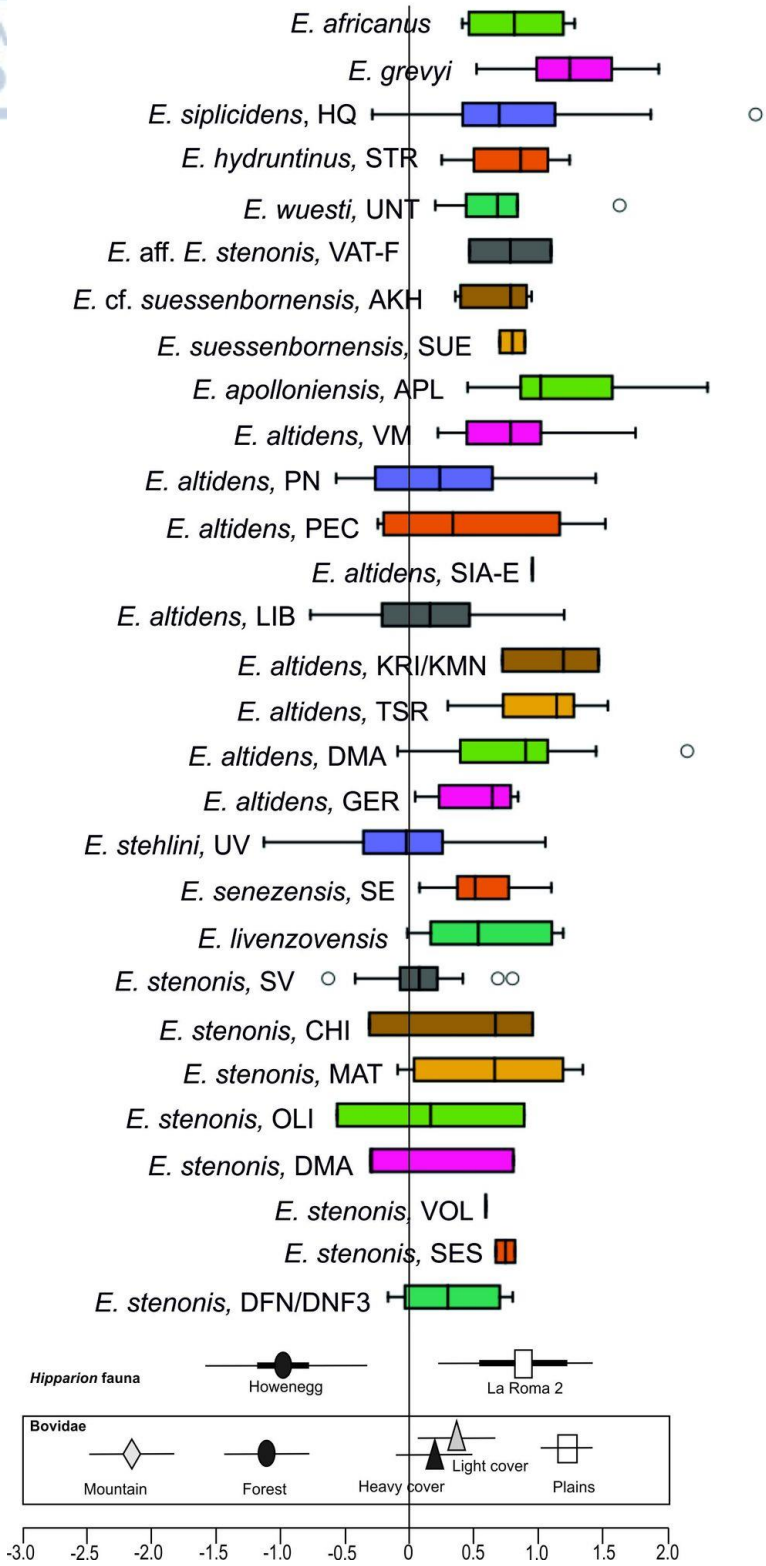

Figure 8.5. Habitat scores of the third metacarpals of the Early to Middle Pleistocene Greek and European equids, the North American *E. simplicidens* and the extant *E. grevyi* and *E. africanus* based on Scott's (2004) method. The Hipparion faunas Höwenegg and La Roma 2 represent closed and open habitats respectively (Scott 2004). Data from Eisenmann (2017a, b, 2018), Eisenmann and Boulbes (2020) and personal dataset.

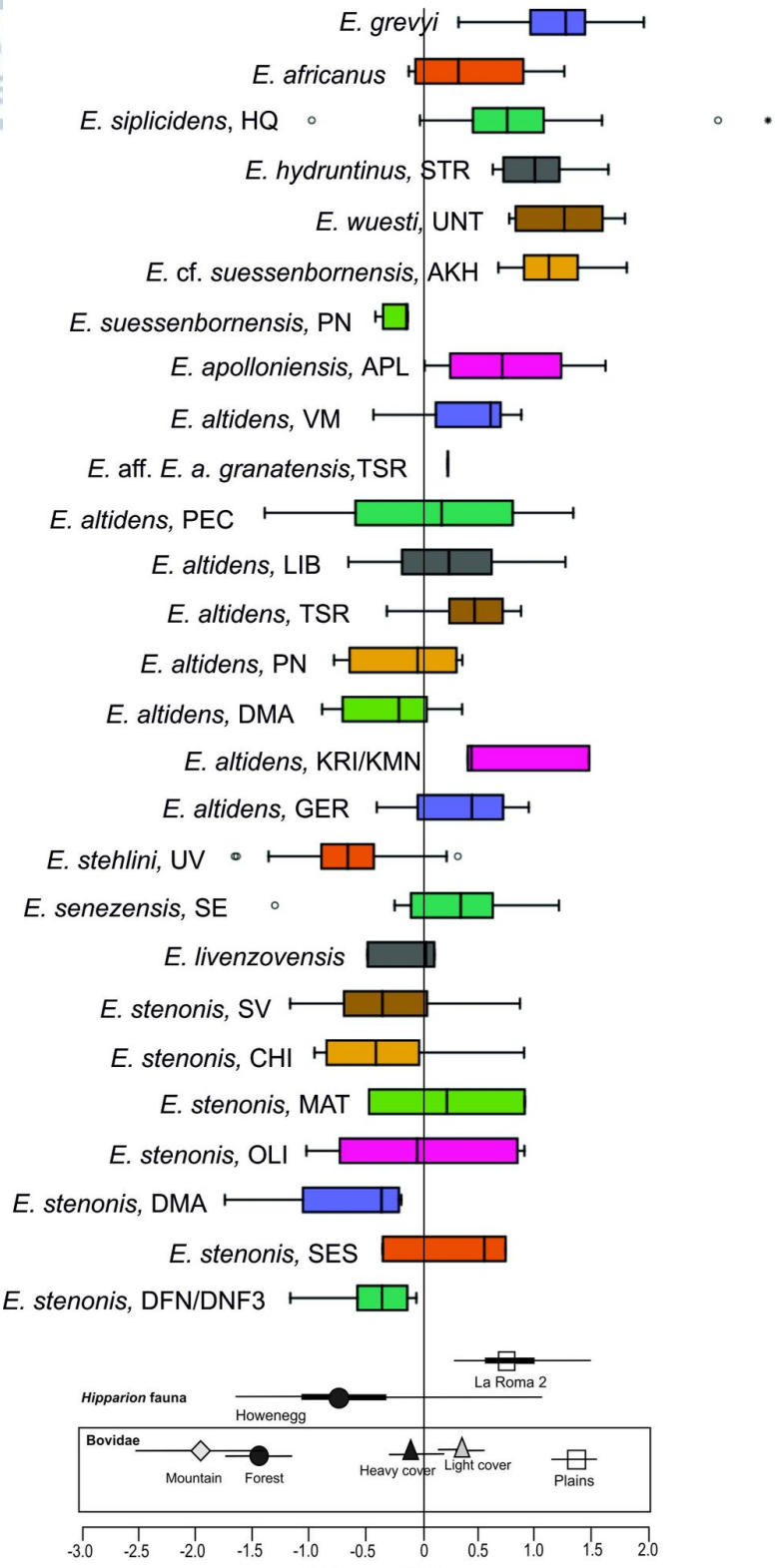

140

141 **Figure 8.6.** Habitat scores of the third metatarsals of the Early to Middle Pleistocene Greek and
142 European equids, the North American *E. simplicidens* and the extant *E. grevyi* and *E. africanus*
143 based on Scott's (2004) method. The Hipparion faunas Höwenegg and La Roma 2 represent
144 closed and open habitats respectively (Scott 2004). Data from Eisenmann (2017a, b, 2018),
145 Eisenmann and Boulbes (2020) and personal dataset.

8.5 REMARKS AND DISCUSSION

When compared with the values for the reference populations categorizing browsing to grazing dietary categories (Table; Figure 8.4), the dental textures of the Early to Middle Pleistocene equids (*E. stenonis, E. senezensis, E. altidens, E. apolloniensis* and *E.* aff. *E. a. granatensis*) reflect mainly mixed feeding diet, while *E. senezensis* also reflects a slightly more grazing behavior. This feeding behavior is well-known for Pleistocene species at this time because most *Equus* taxa showed dietary flexibility, alternating between browse and grass (Semprebon et al. 2019). However, there are some differences between the two approaches of dental wear analysis. Feeding habits reconstructions based on mesowear analysis indicate a high level of abrasion of all equids as demonstrated by *Equus stenonis* from Sésklo, Volax and Dafnero, by *Equus altidens* from Gerakarou, Krimni (KRI/KMN), Petralona, Libakos and Tsiotra Vrysi and by *Equus apolloniensis* from Apollonia. Although, *Equus altidens* has originally been acknowledged as a strictly "grazer", it is classified as either grazer or seasonal mixed feeder based on the microwear scores, while based on the mesowear is strictly grazer on recent studies (Valli et al. 2012; Rivals and Lister 2016; Strani et al. 2019; Alifieri 2021). That is in agreement with the present results (both microwear and mesowear), where *Equus altidens* is acknowledged as a mixed feeder with grazing tendencies (also in Alifieri 2021). A similar case is exhibited by the rest of the fossil equids (*E. stenonis, E. senezensis, E. apolloniensis* and *E.* aff. *E. a. granatensis*); they exhibit high abrasion patterns in mesowear grazing diet and also a microwear mixed feeding behavior. It is worth mentioning, that in Tsiotra Vrysi where two (probably) sympatric species of equids were described, the large-sized tends to have higher browsing dietary signal (see Calandra and Merceron 2015). The feeding habits of the Early to Middle Pleistocene European equids are closer to those of extant asses which are not exclusively grazers, e.g. *Equus hemionus*, a species living in several climatic conditions with dietary habits changing depending on the season (temporal feeding behaviour) (Feh et al. 2002) and the mixed feeder *Equus asinus africanus* [supported by both mesowear (Merceron 2007) and microwear scores (Calandra and Merceron 2015)] rather than those of zebras, Prezwalskii horses or semi-wild horses.

Combining the body mass and the locomotor behaviors/locomotor substrates of the Early to Middle Pleistocene to track palaeoenvironmental differences between *Equus* local samples from Greece, it seems that the more robust species (such as *E. stenonis* from Dafnero, also Dmanisi and Chilhac, *E. stehlini* from Upper Valdarno) with stocky

limbs were adaptive to woodlands-savannas (Alberdi et al. 1988; Boulbes and Van Asperen 2019); however, other local populations of *E. stenonis*, such those from Sésklo and Olivola indicate slightly more open habitats. The slenderer and (highly) cursorial species, such as *E. altidens* and *E. apolloniensis* were adaptive to more open habitats occupying savanna-like and or like steppe biotopes.

Taking into account the palaeoecological results and the faunal elements that compose each studied Greek fossiliferous locality, the following palaeoenvironmental implications can be expressed:

During the middle Villafranchian of Greece (DFN/DFN3, VOL and especially in SES) the predominance of mixed feeders and grazers suggest that equids inhabited in predominately open landscapes and savannah-like woodland environment (also in Koufos and Kostopoulos 2000; Kostopoulos et al. 2019). During that time, the climate in Europe changed from warm-temperate during late middle Villafranchian (Meon et al. 1980; Guerin 1984; Bonifay 1990) to cold-temperate and wet in Western Europe (Chillón et al. 1994; Alberdi et al. 1988; Boulbes and Van Asperen 2019); although the faunas from Spain, France, and Italy are quite similar to those from Greece, species with browsing dietary preferences are more abundant than the grazers, indicating some intervals of forest dominance (particularly during late Villafranchian) in Western Europe (Alberdi et al. 1998). The large sized species were adapted to temperate climates (Alberdi et al. 1998).

At the beginning of the late Villafranchian, there are no significant differences on the faunal elements of Greece with those of middle Villafranchian. However, equids are marked by the trend towards size-reduction (*Equus altidens* from Gerakarou) and a possible second trend towards size-increasing (*Equus* aff. *E. suessenbornensis* from Vassiloudi). During that time, mixed feeders were dominant (supported herein also by microwear analysis), while browsers balance with grazers indicative of open landscapes and savannah-like woodland environment (see also Kostopoulos and Koufos 2000). Probably simultaneously to the West, the two different trends towards size-reduction (and slenderness-increasing) and size-increasing in Vatera (*Equus* aff. *E. suessenbornensis* and *Equus* aff. *E. stenonis*) indicate open landscapes and warm-temperate humid climatic conditions (see Drinia et al. 2002). At the same time to the South, the presence of two equids (*E. senezensis* and *E. stehlini*) in Pyrgos, with short and flat metapodials indicate more local forestrial landscapes.

During the late Villafranchian, the presence of slender mixed feeding equids in the landscapes of Tsiotra Vrysi, Krimni (KRI, KRM, KMN), Libakos, Siatista-E and Alykes-Volos indicating open and savannah-like environments.

At the latest Villafranchian-Epivillafranchian of Greece, the predominance of two large equids, *Equus apolloniensis* and *Equus* sp. (large sized), in Apollonia (Mygdonia Basin) as well as the primacy of bovids instead of cervids suggests more open landscapes (Kostopoulos and Koufos 1998; Kostopoulos and Koufos 2000; Gkeme et al. 2021) and the presence of rhinos and hippos indicate grassland-like environment.

In the Middle Pleistocene, the presence of the large caballoid equid *Equus ferus* in Petralona Cave and Aggitis, the last appearance of the slender *Equus altidens* in Petralona and the predominance of large mammals in the related faunas (Tsoukala 1989) are indicative of both open and forested habitats that are Mediterranean-influenced interglacial climates and mosaic-like environments (Kahlke et al. 2011).

CHAPTER 9. CONCLUSION

The present thesis offers important updated information on the systematics and evolution of the Quaternary equids (genus *Equus*) that contributes to the biostratigraphy and palaeoecology of the Greek fossil record. The thesis deals with the study of more than 8000 equine specimens. The studied material comes from the following Quaternary fossiliferous localities: Dafnero (DNF, DFN3), Sésklo, Vatera (VAT-E, VAT-F, VAT-D), Volax, Vassiloudi, Gerakarou, Libakos, Polylakkos, E-Siatista, Kapetanios, Krimni (KRI, KRM, KMN), Riza-1, Tsiotra Vryssi, Apollonia, Alykes, Volos, Platanochori-1, Petralona Cave (old collection) and Aggitis. The study mainly focused on the detailed description of the available specimens including many new fossils and nearly all the previously published ones (some remains were not traced or were not available for revision). Evolutionary hypotheses were discussed and biostratigraphic contribution has been investigated. The palaeoecological adaptations of Pleistocene equids of the Greek and European fossil record were also examined. The conclusions on each objective listed in the introduction are provided below:

Palaeontological conclusions

The equid fossil assemblages of Greece are represented by the genus *Equus*, including stenonoid and caballoid species (Table 9.1). Stenonoid equids constitute the majority of the studied material. *E. stenonis* has been identified at Sésklo, Dafnero, Volax and Krimni-1. The revision of the material from old collections and the description of new material agrees with past results. *Equus stenonis* from Dafnero shares common features and morphometric characteristics with other European stenonoid equids such as *E. stenonis guthi* (Chilhac, France) and *E. stenonis pueblensis* (La Puebla Valverde, Spain).

Table 9.1. List of the taxonomic results (species attributions) on the studied Greek localities containing *Equus* fossils in comparison to earlier publications. References of previous publications: 1. Koufos (1981); 2. Tsoukala (1989); 3. Koufos (1992); 4. Konidaris et al. (2015); 5. Koufos et al. (1997); 6. Gkeme et al. (2021); 7. Van der Meulen and Van Kolfschoten (1988); 8. Athanassiou (2002c); 9. Steensma (1988); 10. Gkeme (2016); 11. Konidaris et al. (2022); 12. Koufos and Kostopoulos (1997); 13. De Vos et al. (2002); 14. Koufos and Vlachou (1997); 15. Athanassiou (2001); 16. Koufos and Kostopoulos (1993); 17. Kostopoulos et al. (2019).

Locality	**Age**	**Previous publications**	**Present thesis**
Aggitis Cave	Middle Pleistocene	*E. caballus* cf. *germanicus*[1]	*E. ferus*
Petralona Cave	Middle Pleistocene	*E. petraloniensis*[2]	*E. altidens*
		E. caballus piveteaui[2]	*E. ferus*
Riza-1	Villafranchian	*E. stenonis*[3]	*E. stenonis*
Platanochori-1	latest Villafranchian	*E. apolloniensis*[4]	*E.* aff. *E. a. granatensis*
Apollonia-1	latest Villafranchian	*E. apolloniensis*[5]	*E. apolloniensis*
		Equus sp. B. (large-sized)[6]	*Equus* sp. B. (large-sized)
Volos	late Villafranchian	*E.* cf. *marxi*[7] *Equus* sp.[8]	*E.* cf. *E. apolloniensis*
Alykes	late Villafranchian	*Equus* sp.[8]	*E.* cf. *E. apolloniensis*
Kapetanios	?late Villafranchian	*Equus* sp.[9]	*Equus* sp.
Polylakkos	late Villafranchian	*E. stenonis* cf. *senezensis*[9] *E. altidens*[10]	*E. altidens*
Libakos	late Villafranchian	*E. stenonis* cf. *senezensis*[9] *E. stenonis* cf. *mygdoniensis*[3] *E. altidens*[10]	*E. altidens*
Krimni-3	late Villafranchian	*E. altidens*[11]	*E. altidens*
		-	*Equus* sp. (large-sized)
Krimni-1	late Villafranchian	*E. stenonis* cf. *mygdoniensis*[3]	*E. altidens*
		-	*E. stenonis*
Tsiotra Vrysi	late Villafranchian	*Equus* sp. (medium-sized) [4]	*E. altidens*
		Equus sp. (large-sized) [4]	*Equus* sp. B (large-sized)
Pyrgos	?late Villafranchian	*E.* cf. *stenonis*[7]	*E.* cf. *E. senezensis*
		E. cf. *stehlini*[7]	*E.* aff. *E. stehlini*
Vassiloudi	late Villafranchian	*E. stenonis*[12]	*E.* aff. *E. suessenbornensis*
Gerakarou-1	late Villafranchian	*E. stenonis mygdoniensis*[3] *E. altidens*[10]	*E. altidens*
		-	*Equus* sp. B (large-sized)
Vatera E-site	middle/late Villafranchian	*Equus* sp. B[13]	*Equus* sp. B (large-sized)
Vatera F-site	middle/late Villafranchian	*E.* cf. *stenonis*[13]	*E.* aff. *E. stenonis*
Volax	middle/late Villafranchian	*E. stenonis* cf. *vireti*[14]	*E. stenonis*
Sésklo	middle/late Villafranchian	*E. stenonis*[15]	*E. stenonis*
Dafnero-3	middle/late Villafranchian	*E. stenonis* cf. *vireti*[16]	*E. stenonis*
Dafnero-1	middle/late Villafranchian	*E. stenonis* cf. *vireti*	*E. stenonis*

Equus stenonis from Sésklo and Volax share common morphometry (longer muzzle and longer metapodials) with *E. stenonis vireti* (Sanit Vallier) and *E. stenonis olivolanus* (Olivola). The range of variability between the various "subspecies" of *E. stenonis* is not adequate to discriminate them as separate taxa (subspecies) but would appear to be assignable to population variability of a single species over time.

Equus cf. *E. senezensis* (= *E.* cf. *stenonis*) from Pyrgos is the first record of *E. senezensis* in Greece and the second record outside Senèze, providing new insights on the evolution of the Villafranchian small-medium sized equids. The presence of *Equus* aff. *E. stehlini* is also reported in Pyrgos; it shares common morphometry to *Equus stehlini* from Casa Frata.

The presence of *Equus altidens* in the localities of Gerakarou, Krimni (KRI, KMN), Libakos, Tsiotra Vryssi and E-Siatista is here confirmed. *E. altidens* (=*E. s. mygdoniensis*) from Gerakarou and Libakos shares common features with *E. altidens* from Pirro Nord and Dmanisi. *E. altidens* from Krimni and Tsiotra Vrysi shares common features with both *E. altidens* from Dmanisi and *E. altidens granatensis* from Venta Micena. This attribution is also supported by Bernor et al. (2021), who rejected the distinction of multiple subspecies of *E. altidens*, including *E. altidens altidens*, *E. altidens granatensis* and, '*E. stenonis mygdoniensis'*, to a single species. The equid from Petralona Cave (=*E. petraloniensis*) that shares common morphology and morphometry to that from Gerakarou has also been included here to *E. altidens*. The presence of *E. altidens* in Petralona probably marks its last occurrence in Eastern Europe.

The fossil remains from Vassiloudi show great similarities with *E. suessenbornensis* from Pirro Nord. However, its presence is questioned in Pirro Nord due to its smaller size. The possible presence of *E. suessenbornensis* in Vassiloudi marks its first identification in the Greek fossil record and perhaps in Vatera-E where it may indicate the oldest occurrence of the species in Eastern Europe.

E. apolloniensis is recorded in Apollonia, Volos and Alykes. The new material from Apollonia gave further insights on the taxonomy of *E. apolloniensis* considering it as a valid species. The large sized *Equus* from Tsiotra Vrysi resembles *E. apolloniensis* in some features (morphometry of the metapodials). Further, the possible presence of the species in Vatera-E is also discussed. The equid shows great similarities with both *E. apolloniensis* and *E. stenonis olivolanus*. However, due to the scarcity of material in Vatera-E and Tsiotra Vrysi, its attribution remains uncertain.

The caballoid species *E. ferus* has been acknowledged in Petralona Cave and Aggitis but a subspecific attribution is not possible at the moment.

The phylogenetic analysis of the Greek *Equus* focused only on taxa that include cranial, dental, and postcranial elements, i.e.: *Equus altidens* (Gerakarou, Krimni), *Equus apolloniensis* (Apollonia) and *Equus stenonis* (Sésklo, Dafnero). The results on *E. apolloniensis* support its attribution to primitive forms of modern equids based on its derived characters (such as visually absent POF) and increased hypsodonty (cheek tooth crown height). The asinine dental characters of this species place it within the *E. asinus* subclade. Further, the results also verify the close phylogenetic relationship of *E. altidens* from Gerakarou and Dmanisi.

Biostratigraphic-biochronological conclusions

The results of the taxonomy and phylogeny of the Greek equid fossil record provide further confirmation of the biochronological correlation of the studied localities. Following Cirilli et al. 's (2021) outline on the biochronology of the European *Equus*, the two large sized stenonoid equids *E. livenzovensis* and *E. major* have not been documented (or at least described) in the Greek fossil record and only *E. stenonis* (DFN, SES, VOL, KRI partim) and possible *E. senezensis* and *E. stehlini* (PYR) are acknowledged at the early-middle Early Pleistocene of Greece. During the late Early Pleistocene of Greece *E. stenonis* is still present along with *E. altidens* and *E. apolloniensis*. *E. altidens* extends its chronological range until the Middle Pleistocene with its last appearance in Petralona Cave.

The biochronologic range of *E. stenonis* is between 2.45-1.2 Ma, from its first appearance in Saint Vallier to its last occurrence in Ceyssaguet (ca. 1.2 Ma). The species appears also in the Italy (Upper Valdarno Basin), Greece (Dafnero, Sésklo, Volax) and Georgia (Dmanisi).

The similarities of *Equus* sp. B from Vatera-E with the middle Villafranchian *E. suessenbornensis* rather than *E. major* may support the scenario of a common origin within the branch of *Equus* for certain equids (sussemiones), at least from 1.5 Ma and maybe soon before around 2.5 Ma, just above the Gauss-Matuyama limit (Vatera Formation, Greece). However, due to the inadequate material from Vatera sites and the lack of cranial/dental elements, this scenario requires further investigation.

During the second half of the Early Pleistocene, *E. stehlini* replaced *E. stenonis* in Italy. *E. senezensis* is recorded at Senèze (~2.1-2.20 Ma), while *E. stehlini* is recorded in

several late Villafranchian Italian faunas, with the oldest to be that from Coste San Giacomo (~2.2Ma). The presence of both species at Pyrgos indicate a late Villafranchian age and the fauna is correlated probably to the Olivola FU, although the sympatry of two or more species of *Equus* during the middle Early Pleistocene was uncommon.

Equus altidens succeeded *Equus stenonis* during the late Early Pleistocene. The most extensive biochronological scenario suggests the concurrent arrival of *E. altidens* in Eastern Europe in Dmanisi (Georgia) and Southeastern Europe around 1.8-2.0 Ma. The species is a common element of late Early Pleistocene European faunas, dated at 1.6-0.6 Ma. The first appearance of *E. altidens* in Greece is recorded at Gerakarou LFA, and slightly later in Italy around 1.5 Ma (Selvella and Pirro Nord LFAs). The identification of the species in Petralona Cave extends its chronological range to ~0.4 Ma and possibly marks its last occurrence in Eastern Europe.

Equus apolloniensis appears during the latest Villafranchian and Epivillafranchian of Greece. During that period more primitive equids (*E. stenonis, E. senezensis, E. stehlini*) are being replaced by more advanced species. In Southwestern Europe, primitive equids were replaced at about 1.5–1.4 Ma by the slender, middle sized '*E. altidens granatensis*' (Venta Micena LFA, Spain) and *E. altidens* (Selvella, Pirro Nord LFA, Italy), while the larger *E. suessenbornensis* also occurred in Selvella and Pirro Nord (Italy) and in Barranco León 5 and Fuente Nueva 3 (Spain). The chronological and geographical distribution of *E. apolloniensis* seems to be rather limited in southeastern Europe (Eastern Mediterranean). The presence of *E. apolloniensis* in Alykes (~1.6 Ma) could possibly mark its first occurrence.

At the beginning of Middle Pleistocene in Europe, the stenonoid equids have gradually been replaced by the caballoids, the lineage of true horses (*E. ferus*).

Palaeoecological conclusions

The results of the mesowear analysis indicated grazing habits for all the Early to Middle Pleistocene Greek and European equids. The results of the dental textures indicated mixed feeding diet for the Early to Middle Pleistocene equids (*E. stenonis, E. senezensis, E. altidens, E. apolloniensis* and *E.* aff. *E. a. granatensis*). *E. senezensis* also reflects a slightly more grazing and the larger equid from Tsiotra Vrysi more browsing behavior.

During the middle Villafranchian of Greece the predominance of mixed feeders and grazers suggest that equids inhabited in predominately open landscapes and savannah-like woodland. During that time, the climate in Europe changed from warm-temperate during late middle Villafranchian to cold-temperate and wet in Western Europe.

At the beginning of the late Villafranchian, mixed feeders were dominant, while browsers balance with grazers indicative of open landscapes and savannah-like woodland environment. During the late Villafranchian, the presence of slender mixed feeding equids indicated open and savannah-like environments. At the latest Villafranchian-Epivillafranchian of Greece, the predominance of the large sized *Equus apolloniensis* suggests more open landscapes.

ABSTRACT

The present thesis deals with the study of more than 8000 equine specimens and offers an important updated information on the systematics and evolution of the Greek Quaternary equids (genus *Equus*) that contributes to the biostratigraphy and palaeoecology of the Greek fossil record. The studied material comes from the following Quaternary fossiliferous localities: Dafnero (DNF, DFN3), Sésklo, Vatera (VAT-E, VAT-F, VAT-D), Volax, Vassiloudi, Gerakarou, Libakos, Polylakkos, E-Siatista, Kapetanios, Krimni (KRI, KRM, KMN), Riza-1, Tsiotra Vryssi, Apollonia, Alikes, Volos, Platanochori-1, Petralona Cave and Aggitis. The study mainly focused on the detailed description of the available specimens including many new fossils and nearly all the previously published ones. Evolutionary hypotheses were discussed and biostratigraphic contribution has been investigated. The palaeoecological adaptations of Pleistocene equids of the Greek and European fossil record were also examined.

E. stenonis has been identified at Sésklo, Dafnero, Volax and Krimni-1 (partim). The range of variability between the various "subspecies" of *E. stenonis* is not adequate to discriminate them as separate subspecies but would appear to be assignable to population variability of a single species over time. *Equus* cf. *E. senezensis* and *Equus* aff. *E. stehlini* have been identified in Pyrgos. *Equus altidens* has been identified in Gerakarou, Krimni (KRI, KMN), Libakos, Tsiotra Vryssi, Petralona and E-Siatista. The presence of *E. altidens* in Petralona probably marks its last occurrence in Eastern Europe. The fossil remains from Vassiloudi show great similarities with *E. suessenbornensis* from Pirro Nord. *E. apolloniensis* is recorded in Apollonia, Volos and Alikes. The large sized *Equus* from Tsiotra Vrysi resembles both *E. apolloniensis* and *Equus altidens granatensis*. The equid from VAT-F resembles both *E. apolloniensis* and *E. stenonis olivolanus*, while the gigantic equid from VAT-E resembles the typical *E. suessenbornensis* and *E. major*. The caballoid *E. ferus* has been identified in Petralona Cave and Aggitis.

The phylogenetic analysis of the Greek *Equus* focused only on species that include cranial, dental, and postcranial elements. The results of the cladistic analysis on *E. apolloniensis* support its attribution to primitive forms of modern equids based on its derived characters and increased hypsodonty. The asinine dental characters of this species place it within the *E. asinus* subclade. Further, the results also verify the close phylogenetic relationship of *E. altidens* from Gerakarou and Dmanisi.

The results of the taxonomy and phylogeny of the Greek equid fossil record provided further confirmation of the biochronological correlation of the studied localities. During the early-middle Early Pleistocene *E. stenonis*, *E. senezensis* and possible *E. stehlini* are present in Greece. *Equus altidens* succeeded *Equus stenonis* during the late Early Pleistocene. *Equus apolloniensis* appears during the latest Villafranchian and Epivillafranchian of Greece. At the beginning of Middle Pleistocene in Europe, the stenonoid equids have gradually been replaced by the caballoids, the lineage of true horses (e.g., *E. ferus*). The results of the palaeoecological analyses (mesowear, microwear, ecomorphology-habitat scores) suggested grazing habits for all the Early to Middle Pleistocene Greek and European equids, indicative of open landscapes and savannah-like woodland environments.

ΠΕΡΙΛΗΨΗ

Αντικείμενο της παρούσας διδακτορικής διατριβής αποτελεί η συστηματική, φυλογενετική, βιοστρωματογραφική και παλαιοοικολογική μελέτη των απολιθωμένων Τεταρτογενών (2,5 εκ. χρόνια πριν έως σήμερα) ιπποειδών (γένος *Equus*) της Ελλάδας. Το υλικό μελέτης αποτελείται από ~8.000 απολιθώματα κρανιακού, οδοντικού και μετακρανιακού υλικού προερχόμενα από 20 απολιθωματοφόρες θέσεις σε όλη την επικράτεια: Κεντρική Μακεδονία: Γερακαρού, Βασιλούδι, Ριζά-1, Κρήμνη (KRI, KRM, KMN), Τσιότρα Βρύση, Πλατανοχώρι, Απολλωνία, Σπήλαιο των Πετραλώνων, Δυτική Μακεδονία: Δαφνερό (DFN, DFN3), Λίβακος, Καπετάνιος, Πολύλακκος, Σιάτιστα-Ε, Ανατολική Μακεδονία: Βώλακας, Αγγίτης, Θεσσαλία: Σέσκλο, Αλυκές, Βόλος, Πελοπόννησος: Πύργος, Βόρειο Αιγαίο: Βατερά Λέσβου (VAT-F, VAT-E). Τα απολιθωμένα ιπποειδή κατά κοινή ομολογία αποτελούν το συντριπτικό ποσοστό αυτών των ελληνικών πανίδων θηλαστικών του Τεταρτογενούς σε αριθμό ευρημάτων.

Η Οικογένεια των Equidae αντιπροσωπεύεται από ένα εξαιρετικά μεγάλο αρχείο απολιθωμάτων σχεδόν σε όλο τον κόσμο. Εξαιτίας της μεγάλης γεωγραφικής τους εξάπλωσης, τα τελευταία 56 εκ. χρόνια, τα άλογα αποτέλεσαν ίσως το πιο χαρακτηριστικό παράδειγμα μάκρο-εξέλιξης στην ιστορία της παλαιοντολογίας σπονδυλωτών. Η εξελικτική πορεία των ιπποειδών περιλαμβάνει διαδοχικά γεγονότα εξαφανίσεων και μεταναστεύσεων από τη Β. Αμερική στην Ευρασία και αντίστροφα, λόγω κλιματικών αλλαγών και τεκτονικών κινήσεων. Η τελευταία μετανάστευση της οικογένειας των ιπποειδών από την Β. Αμερική στην Ευρασία έγινε πριν από 2,5 εκ. χρόνια με την άφιξη του σύγχρονου αλόγου (γνωστή ως «*Equus* event»), το τελευταίο μέλος της εξελικτικής γραμμής των ιπποειδών.

Παρά το πλούσιο ευρωπαϊκό αρχείο απολιθωμένων αλόγων και τον μεγάλο αριθμό μελετών, τόσο η ταξινόμηση και η φυλογένεση, όσο και η χρονολογική κατανομή των διαφόρων ειδών, εξακολουθούν να αποτελούν αντικείμενο συζήτησης-αντιπαράθεσης πολλών ερευνητών. Η συστηματική ταξινόμηση της Οικογένειας των Equidae περιέχει σύγχρονα και απολιθωμένα είδη, πολλά από οποία βασίζονται ωστόσο σε αποσπασματικά ευρήματα ή έχουν ελλιπείς περιγραφές. Η έρευνα πάνω στις φυλογενετικές σχέσεις των αλόγων διατηρεί επίσης πολλά κενά, καθώς παραδοσιακά βασίστηκε στη μορφολογική ομοιότητα των απολιθωμένων ιπποειδών, χωρίς, μέχρι πρόσφατα, να γίνεται διάκριση των εμπλεκόμενων χαρακτήρων με βάση την

εξελικτική τους σημασία, με αποτέλεσμα σε αρκετές περιπτώσεις να μην αντανακλάται ο βαθμός πραγματικής συγγένειας μεταξύ των ειδών.

Το ελληνικό αρχείο απολιθωμένων ιπποειδών παρότι άφθονο, μελετήθηκε αποσπασματικά κυρίως στις αρχές της δεκαετίας το 1990. Στο διάστημα των 30 ετών που μεσολάβησαν έως σήμερα, σημαντικά νέα ευρήματα ήλθαν στο φως από πλήθος ανασκαφών, ενώ παράλληλα νέα δεδομένα και προσεγγίσεις παρουσιάστηκαν στη διεθνή βιβλιογραφία, όσον αφορά τη συστηματική, βιοστρωματογραφία, εξελικτική ιστορία και παλαιοοικολογία των ιπποειδών.

Οι Τεταρτογενείς πανίδες θηλαστικών της Ελλάδας αποτελούνται από το γένος *Equus* που αποτελεί το συντριπτικό ποσοστό των θηλαστικών. Η πρώτη εμφάνιση του γένους βρίσκεται στη θέση Δαμάτρια (Ρόδος). Πρόσφατα, ιππάρια (γένος *Plesiohipparion*) και άλογα (*Equus stenonis*) αναγνωρίστηκαν στην απολιθωματοφόρο θέση Σέσκλο (Μαγνησία) η οποία χρονολογείται στο κατώτερο Βιλλαφράγκιο (MNQ 16). Το είδος *Equus stenonis* αναγνωρίστηκε επιπλέον στις θέσεις Δαφνερό (λεκάνη Αλιάκμονα), Βώλακας (Δράμα) και Κρήμνη-1 (Μυγδονία λεκάνη). Το *Equus stenonis* από το Δαφνερό έχει κοινά μορφολογικά χαρακτηριστικά (σχετικά κοντά και εύρωστα μεταπόδια, κοντό μουσούδι) και παρόμοιες διαστάσεις/αναλογίες του μετακρανιακού σκελετού με το *E. stenonis guthi* (Chilhac, Γαλλία) και *E. stenonis pueblensis* (La Puebla Valverde, Ισπανία). Το *Equus stenonis* από το Σέσκλο και τον Βώλακα έχουν παρόμοια μορφολογία και διαστάσεις (πιο επιμήκη μεταπόδια) με το *E. stenonis vireti* από το Sanit Vallier της Γαλλίας και το *E. stenonis olivolanus* από την Olivola της Ιταλίας. Τα διάφορα υποείδη του είδους *E. stenonis* παρουσιάζουν ένα μορφολογικό εύρος το οποίο όμως βασίζεται σε ένα κοινό «μορφολογικό πλαίσιο» (bauplan). Αυτές οι μικρές διαφορές στη μορφολογία δεν είναι επαρκείς ώστε να μπορούν να τα διαχωρίσουν σε ξεχωριστά taxa (υποείδη), αλλά πιθανώς αποτελούν τοπικούς πληθυσμούς ενός κοινού είδους μέσα στον χρόνο και οι οποίοι προσαρμόστηκαν σε διαφορετικές περιβαλλοντικές συνθήκες και διατροφικές ανάγκες.

Στη θέση Πύργος (Πελοπόννησος) αναγνωρίστηκαν δύο είδη αλόγων, το *Equus* cf. *E. senezensis* (= *E.* cf. *stenonis*) και το *Equus* aff. *E. stehlini*. Είναι η πρώτη φορά που αναγνωρίζεται το *E. senezensis* στην Ανατολική Ευρώπη, εκτός της τυπικής του θέσης (Senèze). Τα δύο άλογα από τον Πύργο διαχωρίζονται κυρίως λόγω μεγέθους (παρότι είναι πολύ κοντά μορφολογικά). Ωστόσο, η συνύπαρξη δύο ειδών αλόγων κατά το Κατώτερο Πλειστόκαινο δεν είναι συχνή. Η συστηματική των δύο ειδών από το Senèze και Casa Frata (*Equus stehlini*) είναι υπό συζήτηση: παλαιότερες έρευνες τα

αναγνώριζαν κάτω από ένα κοινό είδος αποτελώντας δύο διαφορετικούς τοπικούς πληθυσμούς. Πρόσφατες έρευνες θεωρούν και τα δύο είδη ως «valid».

Στις θέσεις της Μυγδονίας Λεκάνης, Γερακαρού, Κρήμνη και Τσιότρα Βρύση καθώς και στις θέσεις της Λεκάνης του Αλιάκμονα, Λίβακος, Πολύλακκος και Ε-Σιάτιστα αναγνωρίστηκε το *Equus altidens*. Παρότι το άλογο από την Γερακαρού αρχικά είχε αναγνωριστεί ως ένα ξεχωριστό υποείδος του *E. stenonis* (= *E. s. mygdoniensis*), διαφέρει σημαντικά από όλους τους υπόλοιπους πληθυσμούς του είδους. Τόσο το κρανίο, όσο και οι μετακρανιακός σκελετός είναι πολύ πιο λεπτεπίλεπτα και παρουσιάζουν μορφολογικές και μορφομετρικές ομοιότητες με το *E. altidens* από το Pirro Nord (Ιταλία) και το Dmanisi (Γεωργία). Τα κρανία από την Γερακαρού και την Κρήμνη έχουν κοινή μορφολογία με αυτό από το Dmanisi. Το άλογο από την Κρήμνη και την Τσιότρα Βρύση έχει ελαφρώς πιο επιμήκη μεταπόδια που είναι κοντά στις αναλογίες του Ισπανικού *E. altidens granatensis* από τη Venta Micena. Οι μικρές διαφορές στη μορφολογία δεν επιτρέπουν στον διαχωρισμό τους σε διαφορετικά υποείδη, αλλά σε τοπικούς πληθυσμούς ενός είδους. Το άλογο από τα Πετράλωνα αν και είχε αρχικά αναγνωριστεί ως ένα ξεχωριστό είδος, *E. petraloniensis* (μορφολογικά ενδιάμεσα από το *E. stenonis* και το *E. hydruntinus*) παρουσιάζει κοινή μορφολογία με αυτό της Γερακαρούς και για το λόγω αυτό συμπεριλαμβάνεται στο ίδιο είδος. Η παρουσία του *E. altidens* στο Σπήλαιο των Πετραλώνων πιθανώς να σηματοδοτεί την τελευταία εμφάνιση του είδους στην Ανατολική Ευρώπη.

Το υλικό από το Βασιλούδι (Μυγδονία Λεκάνη) παρότι είναι εξαιρετικά περιορισμένο, παρουσιάζει ομοιότητες με το *E. suessenbornensis* από το Pirro Nord. Ωστόσο, η παρουσία του τελευταίου στο Pirro Nord είναι υπό συζήτηση, καθώς το μέγεθός του είναι πολύ μικρότερο από αυτό της τυπικής θέσης του *E. suessenbornensis* (Süssenborn, Γερμανία). Το γιγαντιαίο άλογο από τη θέση Βατερά-Ε (Λέσβος) παρουσιάζει κοινό μέγεθος και παρόμοια μορφολογία με το τυπικό *E. suessenbornensis* αλλά και με το *E. major*. Ωστόσο, το υλικό είναι ελάχιστο και η έλλειψη κρανιακών υπολειμμάτων δεν ευνοούν στην περαιτέρω αναγνώριση του αλόγου.

Το *E. apolloniensis*, εκτός της τυπικής του θέσης στη λεκάνη της Μυγδονίας (Απολλωνία), αναγνωρίστηκε και στις θέσεις Βόλος και Αλυκές (Μαγνησία). Το μεγαλόσωμο άλογο από τη θέση Τσιότρα Βρύση παρουσιάζει ομοιότητες με αυτό της Απολλωνίας (μορφολογία μεταποδίων), αλλά η μορφολογία των δοντιών της κάτω γνάθου είναι ίδια με την αντίστοιχη του *E. altidens* από τη Venta Micena. Το άλογο αυτό αναφέρεται εδώ, ως *Equus* aff. *E. a. granatensis*.

Το άλογο από τη θέση Βατερά-F έχει μορφομετρικές ομοιότητες με αυτό της Απολλωνίας και του *E. stenonis olivolanus* από τη θέση Olivola (Ιταλία). Αν και βιοχρονολογικά το *E. stenonis olivolanus* ταιριάζει καλύτερα στην ηλικία των Βατερών, το άλογο στην παρούσα διατριβή αναφέρεται ως *Equus* aff. *E. stenonis*.

Στις θέσεις Πετράλωνα και Αγγίτης (Δράμα) αναγνωρίστηκε το *E. ferus*. Δεν έγινε περαιτέρω ανάλυση σε επίπεδο υποειδών εξαιτίας του εξαιρετικά ελάχιστου διαθέσιμου υλικού.

Η φυλογενετική ανάλυση των ιπποειδών της Ελλάδας έγινε αποκλειστικά σε είδη από θέσεις με κρανιακά ευρήματα, δηλ. *Equus altidens* (Γερακαρού, Κρήμνη), *Equus apolloniensis* (Απολλωνία, Αλυκές) and *Equus stenonis* (Σέσκλο, Δαφνερό). Τα αποτελέσματα τις κλαδιστικής ανάλυσης επιβεβαιώνουν την κοινή φυλογεντική σχέση των αλόγων από την Γερακαρού και το Dmanisi. Το *E. apolloniensis* σχετίζεται φυλογενετικά με τον υποκλάδο του *E. asinus*.

Τα αποτελέσματα τις συστηματικής και φυλογενετικής ανάλυσης συνέβαλαν την χρονολογική διάρθρωση των χερσαίων αποθέσεων του Τεταρτογενούς της Ελλάδας και την χρονολόγηση των υπό μελέτη απολιθωματοφόρων θέσεων με βάση τα ιπποειδή. Κατά τις αρχές του Κατώτερου Πλειστόκαινου (early-middle Early Pleistocene) στην Ελλάδα εμφανίζονται το *E. stenonis* (DFN, SES, VOL, KRI), το *E. senezensis* και το *E. stehlini* (PYR). Περί το τέλος του Κατωτέρου Πλειστόκαινου της Ελλάδας το *E. stenonis* εξακολουθεί να υπάρχει, ενώ την άφιξή τους έχουν κάνει το *E. altidens* και το *E. apolloniensis*. Το *E. altidens* εμφανίζεται έως και το Μέσο Πλειστόκαινο (Πετράλωνα).

Το βιοχρονολογικό εύρος του *E. stenonis* υπολογίζεται μεταξύ 2.45-1.2 εκ. χρόνια, με την πρώτη του εμφάνιση στο Saint Vallier της Γαλλίας και την τελευταία του στο Ceyssaguet (~ 1.2 εκ. χρόνια). Το είδος εμφανίζεται επιπλέον στην Ιταλία, τη Γεωργία και την Ελλάδα.

Η πιθανή παρουσία του *E. suessenbornensis* στα Vatera-E (Μέσο Βιλλαφράγκιο) υποστηρίζει το σενάριο ιπποειδών (sussemiones), με «ιδιόμορφα» χαρακτηριστικά δοντιών, να αποτέλεσε έναν κλάδο ξεχωριστό υποκλάδο στο *Equus* τουλάχιστον περί τα 1.5 εκ. χρόνια ή και ακόμα παλαιότερα πάνω από το όριο Gauss-Matuyama (Σχηματισμός Βατερών).

Κατά το Ανώτερο Πλειστόκαινο, το *E. stehlini* αντικατέστησε το *E. stenonis* στην Ιταλία, με την παλαιότερη εμφάνισή του στο Coste San Giacomo (~2.2 εκ. χρόνια). Το *E. senezensis* εμφανίζεται στο Senèze περί τα ~2.1-2.20 εκ. χρόνια. Η παρουσία και

των δύο stenonoid μορφών στον Πύργο υποδεικνύει μία ηλικία ανώτερου Βιλλαφραγκίου (late Villafranchian).

Το *Equus altidens* διαδέχτηκε το *Equus stenonis* στο τέλος του Κατώτερου Πλειστοκαίνου (late Early Pleistocene). Πιθανολογείται ότι έφτασε σχεδόν ταυτόχρονα στην Ανατολική Ευρώπη (Dmanisi, Γεωργία) και την Κεντρική και Νότια Ευρώπη (Γερακαρού) περί τα 1.8-2.0 εκ. χρόνια. Η πρώτη εμφάνιση του είδους στην Ελλάδα καταγράφεται στην Γερακαρού, ενώ λίγο αργότερα κάνει την εμφάνισή του στην Ιταλία περί τα 1.5 Ma (Selvella και Pirro Nord). Το είδος αυτό έχει αναγνωριστεί σε πολλές θέσεις του Ανώτερου Πλειστοκαίνου (late Early Pleistocene) μεταξύ 1.6-0.6 εκ. ετών. Η αναγνώριση του *Equus altidens* στα Πετράλωνα επεκτείνει την χρονολογική του εξάπλωση στα ~0.4 σηματοδοτώντας πιθανώς την τελευταία του εμφάνιση στην Ανατολική Ευρώπη.

Το *Equus apolloniensis* εμφανίζεται στο τέλος του ανώτερου Βιλλαφραγκίου και Επιβιλλαφραγκίου της Ελλάδας. Την ίδια περίοδο στην Νοτιοδυτική Ευρώπη, τα αρχαϊκά άλογα αντικαθίστανται από πιο εξελιγμένα όπως το *E. altidens granatensis* (Venta Micena) και το *E. altidens* (Selvella, Pirro Nord, ενώ το *E. suessenbornensis* εμφανίζεται στη Selvella και το Pirro Nord (Italy) της Ιταλίας, αλλά και στην Ισπανία στις θέσεις Barranco León 5 και Fuente Nueva 3. Η γεωγραφική του εξάπλωση τού *Equus apolloniensis* είναι σχετικά μικρή και περιορίζεται κυρίως στην Ελλάδα, αλλά και την Τουρκία.

Τέλος, στην έναρξη του Μέσου Πλειστοκαίνου της Ευρώπης, τα αρχαϊκά «stenonoid» άλογα σταδιακά αντικαταστάθηκαν από τα πιο εξελιγμένα «caballoid» άλογα.

Τα αποτελέσματα της μεσοτριβής των δοντιών έδειξαν για τα άλογα της Ελλάδας να προτιμούν τη βόσκηση σε γρασίδι (grazing habits). Τα αποτελέσματα της μικροτιβής έδειξαν ότι τα Κάτω Πλειστοκαινικά άλογα είχαν ενδιάμεσες διατροφικές προτιμήσεις (mixed feeders), υποδεικνύοντας ένα μωσαϊκό περιβάλλον με ανοικτά δάση-δασώδεις σαβάνες (open forest-savanna woodland).

REFERENCES

Ackermans, N. L., Martin, L. F., Codron, D., Hummel, J., Kircher, P. R., Richter, H., Kaiser, T. M., Clauss, M. and Hatt, J. M., 2020. Mesowear represents a lifetime signal in sheep (*Ovis aries*) within a long-term feeding experiment. *Palaeogeography, Palaeoclimatology, Palaeoecology*, 553, 109793.

Ackermans, N. L., Winkler, D. E., Schulz-Kornas, E., Kaiser, T. M., Martin, L. F., Hatt, J. M. and Clauss, M., 2021. Dental wear proxy correlation in a long-term feeding experiment on sheep (*Ovis aries*). *Journal of the Royal Society Interface*, 18(180), 20210139.

Alberdi, M. T., 2010. Estudio de los caballos de los yacimientos de Fuente Nueva-3 y Barranco León-5 (Granada). In: Toro, I., Martínez-Navarro, B., Agustí, J., Monografías, A., de Andalucía, J. and de Cultura, C. (eds) *Ocupaciones Humanas En El Pleistoceno Inferior y Medio de La Cuenca de Guadix-Baza*. Editorial Junta de Andalucia: Sevilla, Spain, 221–306.

Alberdi, M. T., Cerdeno, E., Lopez-Martínez, Morales, J. and Soria, M. D., 1997. La fauna villafranquiense de El rincon-1 (Albacete, Castilla-La Mancha). *Estudio Geologico* (Madr.) 53, 69e93.

Alberdi, M. T., Ortiz-Jaureguizar, E. and Prado, J. L., 1998. A quantitative review of European stenonoid horses. *Journal of Paleontology*, 72(2), 371-387.

Alberdi, M. T. and Palombo, M.R., 2013. The Early to early Middle Pleistocene stenonoid horses from Italy. *Quaternary International*, 288, 25–44.

Alimen, H., 1946. Remarques sur *Equus hydruntinus* Regalia. *Bulletin de la Société Géologique de France*, 5, 585–595.

Antunes, M. T., 2006. The Zebro (Equidae) and its extinction in Portugal, with an Appendix on the noun zebro and the modern "zebra". *9th ICAZ Conference, Durham 2002*. In: Mashkour, M. (eds) *Equids in Time and Space*. Oxbow Books, Oxford, UK, 2006, 17, 211–236.

Aouadi, N., 1999. Étude préliminaire des restes crâniens de chevaux villafranchiens (Ceyssaguet, Haute-Loire). *Bulletin du Musée d'anthropologie préhistorique de Monaco*, 40, 23–43.

Aouadi, N., 2001. Equidés pléistocènes non caballins en Europe du Sud. *Thèse de doctorat*, Université d'Aix-Marseille, Marseille, France.

Aouadi, N. and Bonifay, M. F., 2008. Les métapodes des chevaux de Ceyssaguet: études morphologique et biométrique. *Bulletin du Musée d'Anthropologie Préhistorique de Monaco*, 48, 17–29.

Arloing, J., 1882. Caractères ostéologiques différentiels de l'âne, du cheval et de leurs hybrides. *Recueil de Médecine Vétérinaire*, 53(1), 312–332.

Athanassiou, A., 1994. First results of the palaeontological study of the fissure fillings of the area of Halykes, Magnesia. *Bulletin de la Société Spéleologique de Grèce*, 21, 318–329.

Athanassiou, A., 2001. New data on the *Equus stenonis* Cocchi, 1867 from the Late Pliocene locality of Sésklo (Thessaly, Greece). *Geodiversitas*, 23(3), 439–469.

Athanassiou, A., 2002a. A new gazelle species (Artiodactyla, Bovidae) from the Late Pliocene of Greece. *Annales Géologiques des Pays Helléniques*, 39(A), 299–310.

Athanassiou, A., 2002b. *Euthyceros thessalicus*, a new bovid from the Late Pliocene of Sésklo (Thessaly, Greece). *Neues Jahrbuch für Geologie und Paläontologie, Monatshefte*, 2, 113–128.

Athanassiou, A., 2002c. Neogene and Quaternary mammal faunas of Thessaly. *Annales Géologiques des Pays Helléniques*, 39, 279–293

Athanassiou, A., 2014. New girafid (Artiodactyla) material from the Lower Pleistocene locality of Sésklo (SE Thessaly, Greece): evidence for an extension of the genus *Palaeotragus* into the Pleistocene. *Zitteliana*, 71–89.

Auguste, P., 1995. *Cadres biostratigraphiques et paléoécologiques du peuplement humain dans la France septentrionale durant le pléistocène: apports de l'étude paléontologique des grands mammifères du gisement de Biache-Saint-Vaast (Pas-de-Calais)* (Doctoral dissertation). Muséum National d'Histoire Naturelle, Paris, France.

Azzaroli, A., 1982. On Villafranchian palaeoarctic equids and their allies. *Palaeontographia Italica*, 72, 74–97.

Azzaroli, A., 2000. On *Equus livenzovensis* Baigusheva 1978 and the "stenonid" lineage of Equids. *Palaeontographia Italica*, 87, 1e17.

Azzaroli, A., De Giuli, C., Ficcarelli, G. and Torre, D., 1988. Late Pliocene to Early Mid-Pleistocene mammals in Eurasia: Faunal succession and dispersal events. *Palaeogeography, Palaeoclimatology, Palaeoecology*, 66, 77–100.

Azzaroli, A. and Voorhies, M. R., 1993. The genus *Equus* in North America. The Blancan species. *Palaeontographia Italica*, 80, 175e198.

Baigusheva, V. S., 1978. The large horse from the Khapryc omplex on North-Eastern Azov Sea region. Izv. Severo-Kavkazkogo Nauchnogo Zentra Vysshej Shkoly, Estestvennye Nauki, 1, 98–102. (In Russian)

Baryshnikov, G. F. and Tsoukala, E., 2010. New analysis of the Pleistocene carnivores from Petralona Cave (Macedonia, Greece) based on the Collection of the Thessaloniki Aristotle University. *Geobios*, 43, 389-402

Barone, R., 1986. Anatomie comparée des mammifères domestiques. Tome 1: Ostéologie. *Vigot Frères*, Paris.

Barrón-Ortiz, C. I., Avilla, L. S., Jass, C. N., Bravo-Cuevas, V. M., Machado, H. and Mothé, D. 2019. What is *Equus*? Reconciling taxonomy and phylogenetic analyses. *Frontiers in Ecology and Evolution*, 7, 343.

Bauer, I. E., McMorrow, J. and Yalden, D. W., 1994. The historic range of three equid species in north-east Africa: a quantitative comparison of environmental tolerances. *Journal of Biogeography*, 21, 169–182.

Benammi, M., Aidona, E., Merceron, G., Koufos, G. D. and Kostopoulos, D. S., 2020. Magnetostratigraphy and Chronology of the Lower Pleistocene Primate Bearing Dafnero Fossil Site, N. Greece. *Quaternary*, 3(3), 22.

Bennett, D. K., 1980 Stripes do not a zebra make, Part I: A cladistic analysis of *Equus*. *Systematic Zoology*, 29, 272–287.

Berlioz, E., Leduc, C., Hofman-Kamińska, E., Bignon-Lau, O., Kowalczyk, R. and Merceron, G., 2022. Dental microwear foraging ecology of a large browsing ruminant in Northern Hemisphere: The European moose (*Alces alces*). *Palaeogeography, Palaeoclimatology, Palaeoecology*, 586, 110754.

Bernor, L., Tobien, H., Hayek, L.-A. C. and Mittmann, H.-W., 1997. *Hippotherium primigenium* (Equidae, Mammalia) from the Late Miocene of Howenegg (Hegau, Germany). *Andrias*, 10, 1–230.

Bernor, R. L., Armour-Chelu, M., Gilbert, H., Kaiser, T. M. and Schulz, E., 2010. Equidae. In: Werdelin, L. and Sanders, W.L. (eds) *Cenozoic mammals of Africa* (Berkeley, CA: University of California Press), 685–721.

Bernor, R. L., Cirilli, O., Bukhsianidze, M., Lordkipanidze, D. and Rook, L., 2021. The Dmanisi *Equus*: Systematics, biogeography, and palaeoecology. *Journal of Human Evolution*, 158, 103051.

Berry, H. H., 2020. Anatomical comparison between crania and mandibles of Hartmann's zebra *Equus zebra hartmannae* and Burchell's zebra *E. burchellii* antiquorum in Namibia. *Namibian Journal of Environment*, 4, A-27.

Boeuf, O., 1986. L' Equide u site Villafranchien de Chilhac (Haute- Loire, France). *Annales de Paléontologie (Vertebrate)*, 72, 29–67.

Bolomey, A., 1965. Die Fauna zweier villafrankischer Fundstellen in Rumanien. *Berichte der Geologischen Gesellschaft DDR*, 10, 77–88.

Bonifay, M.F., 1980. Le Cheval du pléistocène moyen des grottes de Lunel-Viel (Hérault) *Equus mosbachensis palustris* n.ssp. *Gallia Prehistoire*, 23, 2, 233–281.

Bonifay, M.F., 1991. *Equus hydruntinus* Regalia *minor* n.ssp. from the caves of Lunel-Viel (Hérault, France). In: Meadow, R. H., Uerpmann, H.-P. (eds) *Equids in the Ancient World*. Beihefte zum Tübinger Atlas des Vorderen Orients, Reihe A (Naturwissenschaften), Nr. 19/2; Dr Ludwig Reichert Verlag: Wiesbaden, Germany, 1991; Volume 2.

Boulbes, N., 2009. Étude comparée de la denture d' *Equus hydruntinus* (Mammalia, Perissodactyla) dans le sud-est de la France. Implications biogéographiques et biostratigraphiques. *Quaternaire. Revue de l'Association française pour l'étude du Quaternaire*, 20(4), 449–465.

Boulbes, N. and Rillardon, M., 2010. Révision paléontologique et analyse archéozoologique d' *Equus hydruntinus* (Mammalia, Perissodactyla) de la Baume de Valorgues (St-Quentin-La-Poterie, Gard) et remarques sur l'évolution de la taille de cette espèce du Pléistocène moyen à l'Holocène. In: Gardeisen, A., Furet, E. and Boulbes, N. (eds) *Histoire d'Equidés, des textes, des images et des os Monographies d'Archéologie Méditerranéenne*, Hors-sérien, 4, 9–27.

Boulbes, N., Mayda, S., Titov, V. V. and Alçiçek, M. C., 2014. Les grands mammifères du Villafranchien supérieur des travertins du Bassin de Denizli (Sud-Ouest Anatolie, Turquie). *L'Anthropologie*, 118(1), 44–73.

Boule, M., 1899. Observations sur quelques Equides fossiles. *Bulletin de la Société Geologique de France*, 27, 531–542.

Bout, P., 1970. Absolute ages of some volcanic formations in the Auvergne and Velay areas and chronology of the European Pleistocene. *Palaeogeography, Palaeoclimatology, Palaeoecology*, 8, 95–106.

Boyde, A. and Fortelius, M., 1991. New confocal LM method for studying local relative microrelief with special reference to wear studies. *Scanning*, 13, 429–430.

Brünnacker, K., Jäger, K. D., Hennig, G. J., Preuss, J. and Grün, R., 1983. Radiometrische Untersuchungen zur Datierung milleleuropäischer Travertinvorkommen. *Ethnographisch-Archaeologische Zeitschrift*, 24, 217-266.

Burke, A., Eisenmann, V. and Ambler, G., 2003. The systematic position of *Equus hydruntinus*, an extinct species of Pleistocene equid. *Quaternary Research*, 59, 459–469.

Calandra, I. and Merceron, G. 2016. Dental microwear texture analysis in mammalian ecology. *Mammalian Review*, 46, 215–228.

Calandra, I., Bob, K., Merceron, G., Blateyron, F., Hildebrandt, A., Schulz-Kornas, E., Souron, A. and Winkler, D. E., 2022. Surface texture analysis in Toothfrax and MountainsMap® SSFA module: Different software packages, different results?. *Peer Community Journal*, 2, e77.

Caloi, L., 1997. New forms of equids in Western Europe and palaeoenvironmental changes. *Geobios*, 30(2), 267-284.

Caloi, L. and Palombo, M.R., 1990. Osservazioni sugli equidi italiani del Pleistocene medio inferiore. *Geologica Romana*, 26 (1987), 187e221.

Carranza-Castañeda, O., Aranda-Gómez, J. J., Wang, X. and Iriondo, A., 2013. The early-late Hemphillian (Hh2) Fauna assemblage from Juchipila Basin, state of Zacatecas, México, and its biochronologic correlation with other Hemphillian Faunas in Central México. *Contributions in Science*, 521, 13–49.

Cerling, T. E., Harris, M. J., MacFadden, B. J., Leakey, M. G., Quade, J., Eisenmann, V. and Ehleringer, J. R., 1997. Global vegetation change through the Miocene/Pliocene boundary. *Nature*, 389:153–158.

Chaline, J. and Michaux, J., 1969. Evolution et signification stratigraphique des Arvicolidés du genre *Mimomys* dans le Plio-Pleistocene de France. *Comptes Rendus Académie Science*, 268, 3029-3032.

Cherin, M., 2020. *Equus stenonis* (Equidae, Mammalia) from the Early Pleistocene of Pantalla (Italy) and the dispersion of stenonine horses in Europe. *Bollettino della Società palaeontologica italiana*, 60(1).

Chillón, B. S., Alberdi, M. T., Leone, G., Bonadonna, F. P., Stenni, B. and Longinelli, A., 1994. Oxygen isotopic composition of fossil equid tooth and bone phosphate: an archive of difficult interpretation. *Palaeogeography, Palaeoclimatology, Palaeoecology*, 107(3-4), 317–328.

Cibien, C., 1984. Variations saisonnières de l'utilisation de l'espace en fonction des disponibilités alimentaires chez le chevreuil (*Capreolus capreolus* L.). Université François Rabelais, Académie de Tours-Orléans, Tours, France.

Cirilli, O., 2022. *Equus stehlini* Azzaroli, 1964 (Perissodactyla, Equidae). a revision of the most enigmatic horse from the Early Pleistocene of Europe, with new insights on the evolutionary history of European medium- and small-sized horses. *Rivista Italiana di Paleontologia e Stratigrafia*, 128(1), 241–265.

Cirilli, O., Machado, H., Arroyo-Cabrales, J., Barrón-Ortiz, C. I., Davis, E., Jass, C. N. and Bernor, R. L., 2022. Evolution of the Family Equidae, Subfamily Equinae, in North, Central and South America, Eurasia and Africa during the Plio-Pleistocene. *Biology*, 11(9), 1258.

Cirilli, O., Pandolfi, L. and Bernor, R.L., 2020a. The Villafranchian perissodactyls of Italy: knowledge of the fossil record and future research perspectives. *Geobios* 63, 1e21.

Cirilli, O., Pandolfi, L., Rook, L. and Bernor, R. L., 2021. Evolution of Old World *Equus* and origin of the zebra-ass clade. *Scientific reports*, 11(1), 1–11.

Cirilli, O., Saarinen, J., Pandolfi, L., Rook, L. and Bernor, R. L., 2021. An updated review on *Equus stenonis* (Mammalia, Perissodactyla): New implications for the European early Pleistocene *Equus* taxonomy and palaeoecology, and remarks on the Old World *Equus* evolution. *Quaternary Science Reviews*, 269, 107155.

Conover, W. J. and Iman, R. L., 1981. Rank transformations as a bridge between parametric and nonparametric statistics. *The American Statistician*, 35(3), 124–129.

Cornelis, J., Casaer, J. and Hermy, M., 1999. Impact of season, habitat and research techniques on diet composition of roe deer (*Capreolus capreolus*): a review. *Journal of Zoology*, 248(2), 195–207.

Cosyns, E., Degezelle, T., Demeulenaere, E. and Hoffmann, M., 2001. Feeding ecology of Konik horses and donkeys in Belgian coastal dunes and its implications for nature management. *8th Benelux congress of zoology*, 131, 2, 111–118, Koninklijke Belgische Vereniging voor Dierkunde,

Cransac, N., Cibien, C., Angibault, J.-M., Morrelet, N., Vincent, J.-P. and Hewison, A.J.M., 2001. Variations saisonnières du régime alimentaire du chevreuil (*Capreolus capreolus*) selon le sexe en milieu forestier à forte densité (forêt domaniale de Dourdan). *Mammalia*, 65, 1–12.

Crégut-Bonnoure, E., 1980. *Equus mosbachensis tautavelensis* nov. subsp., un nouvel Equidae (Mammalia, Perissodactyla) du gisement pléistocène moyen anté-rissien de la Caune de l'Arago (Tautavel, Pyrénées Orientales, France). *Geobios*, 13(1),121–127.

Crégut-Bonnoure, E. and Tsoukala, E., 2005. The Pleistocene bovids from the Petralona Cave (Macedonia, Greece): new interpretations and biostratigraphical implications. *Quaternaire, Supplement*, 2, 161–178.

Cucchi, T., Mohaseb, A., Peigné, S., Debue, K., Orlando, L. and Mashkour, M., 2017. Detecting taxonomic and phylogenetic signals in equid cheek teeth: towards new palaeontological and archaeological proxies. *Royal Society open science*, 4(4), 160997.

De Vos, J., Van der Made, J., Athanassiou, A., Lyras, G., Sondaar, P. Y. and Dermitzakis, M. D., 2002. Preliminary note on the Late Pliocene fauna from Vatera (Lesvos, Greece). In *Annales géologiques des Pays helléniques* (Vol. 39, No. 3).

Delafond, F. and Depéret, C., 1893. Les Terrains Tertiaires de la Bresse et Leurs Gites de Lignites et de Minerais de fer. Etudes des Gites Mineraux de France. Paris, Imprimerie Nationale, 332.

Deng, T. and Xue, X., 1999. Chinese Fossil Horses of *Equus* and Their Environment. China Ocean Press, Beijing.

Dermitzakis, M. D. and Drinia, H., 1999. The presence of fossil mammals in Lesvos Island, NE Aegean Sea, and their palaeobiogeographical implications. *Deinsea*, *7*(1), 113-120.

DeSantis, L. R. G., 2016. Dental microwear textures: reconstructing diets of fossil mammals. *Surface Topography: Metrology and Properties*, 4, 023002.

DeSantis, L. R. G., Scott, J. R., Schubert, B. W., Donohue, S. L., McCray, B. M., Van Stolk, C. A., Winburn, A. A., Greshko, M. A. and O'Hara, M. C., 2013. Direct comparisons of 2D and 3D dental microwear proxies in extant herbivorous and carnivorous mammals. *PLoS One*, 8, e71428.

Eisenmann, V., 1975. Nouvelles interpretations des restes d'équidés (Mammalia, Perissodactyla) de Nihowan (Pléistocène inférieur de la Chine du Nord): *Equus teilhardi* nov. sp. *Geobios*, 8, 125–134. doi: 10.1016/S0016-6995(75)80009-X

Eisenmann, V., 1979. Les métapodes d'*Equus* sensu lato (Mammalia, Perissodactyla). *Geobios*, 12(6), 863–886.

Eisenmann, V., 1980. Caractères spécifiques et problèmes taxonomiques relatifs a certains hipparions africains. *Proceedings of the 8th Panafrican congress of prehistory and quaternary studies*, 76–81.

Eisenmann, V., 1981. Analyses multidimensionnelles des cranes d'Equides actuels: Methodes et resultats. In: Table Ronde MNHN Mai 1981, Paris, 21–22.

Eisenmann, V., 1986. Comparative osteology of modern and fossil horses, half-asses, and asses. 67–116. In: Meadow, R. H. and Uerpmann, H. P. (eds) *Equids in the ancient world.* Wiesbaden, Germany.

Eisenmann, V., 1995. What metapodial morphometry has to say about some Miocene hipparions. In: Vrba, E. S., Denton, G. H., Partridge, T. C. and Burckle, L. H. (eds) *Palaeoclimate and Evolution, with Emphasis on Human Origins*. New Haven: Yale University Press, 148–163.

Eisenmann, V., 1999. *Equus granatensis* of Venta Micena and evidence for primitive non stenonid horses in the Lower Pleistocene. In: *The Hominids and Their Environment During the Lower and Middle Pleistocene of Eurasia. Proceedings of the International Conference of Human Palaeontology*, eds J.

Eisenmann, V., 2002. The primitive horses of the Vatera Formation (Lesbos, Greece). *Proceedings of the 1st International Workshop "On Late Plio/Pleistocene Extinction and Evolution in the Palearctic. The Vatera site". Annales Géologiques des Pays Helléniques, 1ère série*, 39(A), 131–153.

Eisenmann, V., 2004. Les équidés (Mammalia, Perissodactyla) de Saint-Vallier (Drôme, France) et les équidés plio-pléistocènes d'Europe. *Géobios*, 37, 279–305. doi: 10.1016/S0016-6995(04)80019-6

Eisenmann, V., 2006a. Discriminating *Equus* crania: the Franck's index and the new palatal index. *Equids in time and space: papers in honour of Véra Eisenmann. Oxford: Oxbow Books*, 172–182.

Eisenmann, V., 2006b. Pliocene and Pleistocene Equids: Palaeontology versus Molecular Biology. In: Kahlke, R.-D., Maul, L. C. and Mazza, P. (eds.): Late Neogene and Quaternary biodiversity and evolution: Regional developments and interregional correlations. *Proceedings volume of the 18th International Senckenberg Conference (VI International Palaeontological Colloquium in Weimar)*, 25th-20th April 2004. *Courier Forschungsinstitut Senckenberg*, 256, 71–89.

Eisenmann, V., 2006c. Pliocene and Pleistocene Equids: Palaeontology versus molecular biology. *Courier Forschungsinstitut Senckenerg*, 256, 71–89

Eisenmann, V., 2007, 2008. Mosbach et *E. mosbachensis*. https://vera-eisenmann.com/. Published 2008. Available online at: https://vera-eisenmann.com/main-caballine-crania-morphs

Eisenmann, V., 2008a. *Equus hemionus onager*. https://vera-eisenmann.com/. Published 2008. Available online at: https://vera-eisenmann.com/main-caballine-crania-morphs

Eisenmann, V., 2008b. *Equus verae* et formes proches. https://vera-eisenmann.com/. Published 2008. Available online at: https://vera-eisenmann.com/main-caballine-crania-morphs

Eisenmann, V., 2008c. Hagerman, Idaho: *Plesippus shoshonensis*. https://vera-eisenmann.com/. Published 2009. Accessed December 10. 2022

Eisenmann, V., 2008d. Siréjol, *E. gallicus*. https://vera-eisenmann.com/. Published 2008. Available online at: https://vera-eisenmann.com/main-caballine-crania-morphs

Eisenmann, V., 2013. Preorbital Fossa: one possible cause. Available online at: https://vera-eisenmann.com/main-caballine-crania-morphs

Eisenmann, V., 2014. Main Caballine Crania Morphs. Available online at: https://vera-eisenmann.com/main-caballine-crania-morphs

Eisenmann, V., 2017. Seneze Text. Available online at: https://vera-eisenmann.com/main-caballine-crania-morphs

Eisenmann, V., 2018a. *Equus hydruntinus* Romanelli. Available online at: https://vera-eisenmann.com/main-caballine-crania-morphs

Eisenmann, V., 2018b. *Equus hydruntinus* Roterberg. Available online at: https://vera-eisenmann.com/main-caballine-crania-morphs

Eisenmann, V., 2018c. *Equus hydruntinus* San Sidero. Available online at: https://vera-eisenmann.com/main-caballine-crania-morphs

Eisenmann, V., 2018d. *Equus hydruntinus* Senzig Available online at: https://vera-eisenmann.com/main-caballine-crania-morphs

Eisenmann, V., 2018e. *Equus hydruntinus* Straroselie and Tchokurcha. Available online at: https://vera-eisenmann.com/main-caballine-crania-morphs

Eisenmann, V., 2020. Caballines Nomenclature. Available online at: https://vera-eisenmann.com/main-caballine-crania-morphs

Eisenmann, V., 2022a. Old World Fossil *Equus* (Perissodactyla, Mammalia), Extant Wild Relatives, and Incertae Sedis Forms. *Quaternary*, 5(3), 38.

Eisenmann, V., 2022b. The equids from Liventsovka and other localities of the Khaprovskii Faunal Complex, Russia: A revision. *Geobios*, 70, 17-33.

Eisenmann, V., Alberdi, M. T., De Giuli, C. and Staesche, U., 1988. Methodology. In: Woodburne, M. and Sondaar, P. Y. (eds.) *Studying Fossil Horses*. EJ Brill Press, Leiden, 1–71.

Eisenmann, V. and Boulbes, N., 2020. New results on equids from the Early Pleistocene site of Untermassfeld. *The Pleictocene of Untermassfeld Near Meiningen (Thüringen, Germany), Part 4*, 40(4), *Monographien des Römisch-Germanischen Zentralmuseums Mainz*, 1295–1321.

Eisenmann, V. and Mashkour, M., 1999. The small equids of Binagady (Azerbaidjan) and Qazvin (Iran): *E. hemionus binagadensis* nov. subsp., and *E. hydruntinus*. *Géobios*, 32, 105–122.

Ellenberg, J., and Kahlke, R.-D., 1997. Die quartärgeologische Entwicklung des mittleren Werratals und der Bau der unterpleistozänen Komplexfundstelle Untermassfeld. In: Kahlke, R.-D. (Ed.), *Das Pleistozän von Untermassfeld bei Meiningen (Thüringen). Teil 1. Monographien des Römisch-Germanischen Zentralmuseums* 40, 1, 29–62.

Erten, H., Sen, S., and Özkul, M., 2005. Pleistocene mammals from travertine deposits of the Denizli basin (SW Turkey). In *Annales de Paléontologie*, 91, 3, 267–278.

Evans, A. R., Wilson, G. P., Fortelius, M. and Jernvall, J., 2007. High-level similarity of dentitions in carnivorans and rodents. *Nature*, 445, 78–81

Feh, C., Shah, N., Rowen, M., Reading, R. and Goyal, S. P. 2002. Status and action plan for the Asiatic wild ass (*Equus hemionus*). *Equids: zebras, asses and horses*, 62–71.

Fischhoff, I. R., Sundaresan, S. R., Cordingley, J. and Rubenstein, D. I., 2007. Habitat use and movements of plains zebra (*Equus burchelli*) in response to predation danger from lions. *Behavioral Ecology*,18(4), 725–729.

Forstén, A., 1986. A review of the Süssenborn horses and the origin of *Equus hydruntinus* Regalia. *Quatärpalaläontologie*, 6, 43–52.

Forstén, A., 1993. Size Decrease in Late Pleistocene-Holocene Caballoid Horses (Genus *Equus*), Intra-or Interspecific Evolution? A Discussion of Alternatives. *Quaternary International*, 19, 71–75.

Forstén, A., 1997. The fossil horses (Equidae, Mammalia) from the Plio-Pleistocene of Liventsovka near Rostov-don, Russia. *Geobios*, 31, 645–657.

Forstén, A., 1999. A review of *Equus stenonis* Cocchi (Perissodactyla, Equidae) and related forms. *Quaternary Science Reviews*, 18(12), 1373–1408.

Forstén, A., 1999. The horses (genus *Equus*) from the Middle Pleistocene of Steinheim, Germany. In: *Haynes G., Klimovicz J. and Reumer J.W.F. (eds) – Mammoths and the Mammoth fauna: studies of an extinct ecosystem*, *Deinsea*, 6, 147–154.

Forstén, A. and Eisenmann, V., 1995. *Equus (Plesippus) simplicidens* (Cope), not *Dolichohippus*. *Mammalia* 59 (1), 85–89.

Forsyth Major, C., 1885. On the mammalian fauna of the val d'Arno. *Quarterly Journal of the Geological Society*, 41, 1e8.

Fortelius, M. and Solounias, N., 2000. Functional characterization of ungulate molars using the abrasion-attrition wear gradient: a new method for reconstructing palaeodiets. *American Museum Novitates*, 3301, 1–36.

Galbany, J., Martínez, L. M., López-Amor, H. M., Espurz, V., Hiraldo, O., Romero, A., de Juan, J. and Pérez-Pérez, A., 2005. Error rates in buccal-dental microwear quantification using scanning electron microscopy. *Scanning*, 27, 23–29.

Garrido, G., 2008. Los perisodáctilos [*Equus* cf. *major* Depéret, 1893 y *Stephanorhinus etruscus* (Falconer, 1859)] del yacimiento Plioceno Superior Terminal De Fonelas P-1 (Cuenca De Guadix, Granada). *Cuadernos del Museo Geominero*, 10, 553–595.

Gazin, C.L., 1936. A study of the fossil horses remains from the Upper Pliocene of Idaho. *Proceedings of the United States National Museum*, 83, 281e320.

George, M. Jr. and Ryder, O. A., 1986. Mitochondrial DNA evolution in the genus *Equus*. Molecular Biology and Evolution, 3(6), 535–546.

Giddley, J. W. 1930. A new Pliocene horse from Idaho. *Journal of Mammalogy*, 11, 300–303.

Giusti, D., Konidaris, G. E., Tourloukis, V., Marini, M., Maron, M., Zerboni, A., Thompson, N., Koufos, G. D., Kostopoulos, D. S. and Harvati, K. 2019. Recursive anisotropy: a spatial taphonomic study of the Early Pleistocene vertebrate assemblage of Tsiotra Vryssi, Mygdonia Basin, Greece. *Boreas*, 48(3), 713–730.

Gkeme, A. G., Koufos, G. D. and Kostopoulos, D. S., 2017. The Early Pleistocene stenonoid horse from Libakos (Western Macedonia, Greece): Biochronological

and palaeoecological implications and dispersal events. *15th RCMNS Congress Athens, Abstracts*.

Gkeme, A. G., Koufos, G. D. and Kostopoulos, D. S., 2021. Reconsidering the equids from the Early Pleistocene fauna of Apollonia 1 (Mygdonia Basin, Greece). *Quaternary*, 4(2), 12. https://doi.org/10.3390/ quat4020012

Goloboff, P. A., Farris, J. S. and Nixon, K. C., 2008. TNT, a free program for phylogenetic analysis. *Cladistics*, 24(5), 774–786.

Goloboff, P. A. and Morales, M. E. 2023. TNT version 1.6, with a graphical interface for MacOS and Linux, including new routines in parallel. *Cladistics*, 39(2), 144–153.

Gregory, W. K., 1912. Notes on the principles of quadrupedal locomotion and of the mechanism of the limbs in hoofed animals. *Annals of the New York Academy of Sciences*, 22, 267–294.

Grine, F. E., Ungar, P. S. and Teaford, M. F., 2002. Error rates in dental microwear quantification using scanning electron microscopy. *Scanning*, 24, 144–153.

Grossouvre, A., and Stehlin, H. G., 1912. Les sables de Rosieres, près Saint-Florent (Cher). *Bulletin de la Société Géologique de France*, 4, 194–212.

Groves, C. P., 2002. Taxonomy of living Equidae, Report 8, 94–107. Gland, Switzerland, and Cambridge, IUCN/SCC Equid Specialist Group, IUCN.

Guadelli, J. L., 1991. Les Chevaux de Solutré (Saône-et-Loire, France). In *Datation et Caractérisation des Milieux Pléistocènes. Actes des Symposiums 11 et 17 de la 11ème RST, Clermont-Ferrand, 1986*, 16, pp. 261-336. Cahiers du Quaternaire, CNRS Editions.

Guadelli, J. L. and Prat, F. 1995. Le cheval du gisement pléistocène moyen de Camp-de-Peyre (Sauveterre-la-Lémance, Lot-et-Garonne) [*Equus mosbachensis campdepeyri* nov. ssp.]. *Paléo, Revue d'Archéologie Préhistorique*, 7(1), 85–121.

Hack, M. A., East, R. and Rubenstein, D. I. 2002. Status and action plan for the plains zebra (*Equus burchellii*). *Equids: zebras, asses and horses. Status survey and conservation action plan*, 43–60.

Haltenorth, T. and Diller, H., 1988. *The Collins field guide to the mammals of Africa: Including Madagascar*. S. Greene Press.

Hanot, P., Guintard, C., Lepetz, S., and Cornette, R. 2017. Identifying domestic horses, donkeys, and hybrids from archaeological deposits: a 3D morphological investigation on skeletons. *Journal of Archaeological Science*, 78, 88–98.

Haupt, R. J., DeSantis, L. R. G. Green, J.L., and Ungar, P. S., 2013. Dental microwear texture as a proxy for diet in xenarthrans. *Journal of Mammalogy*, 94, 856–866.

Heinrich, W. D., 1990. Review of fossil arvicolids (Mammalia, Rodentia) from the Pliocene and Quaternary in the German Democratic Republic. *International symposium evolution, phylogeny and biostratigraphy of arvicolids (Rodentia, mammalia)*, 183–200.

Hermier, R., Merceron, G. and Kostopoulos, D. S., 2020. The emblematic Eurasian Villafranchian antelope *Gazellospira* (Mammalia: Bovidae): New insights from the Lower Pleistocene Dafnero fossil sites (Northern Greece). *Geobios*, 61, 11–29. https://doi.org/10.1016/j.geobios.2020.06.006

Hoffman, J. M., Fraser, D. and Clementz, M. T. 2015. Controlled feeding trials with ungulates: a new application of in vivo dental molding to assess the abrasive factors of microwear. *Journal of Experimental* Biology, 218, 1538–1547. doi: 10.1242/jeb.118406

Hopwood, A. T. 1936. The former distribution of caballine and zebrine horses in Europa and Asia. *Proceeding Zoological Society of London*, 1936, 897–912.

Hutchinson, G. E. 1957. Concluding remarks. *Cold Spring Harbor Symposium on Quantitative Biology*, 22, 415–427.

Jónsson, H., Schubert, M., Seguin-Orlando, A., Ginolhac, A., Petersen, L., Fumagalli, M. and Orlando, L. 2014. Speciation with gene flow in equids despite extensive chromosomal plasticity. *Proceedings of the National Academy of Sciences*, 111(52), 18655–18660.

Jungers, W. L., Falsetti, A. B. and Wall, C. E., 1995. Shape, relative size, and size-adjustments in morphometrics. *Yearbook of Physical Anthropology*, 38, 137–161.

Kaczensky, P., Ganbaatar, O., Von Wehrden, H. and Walzer, C. 2008. Resource selection by sympatric wild equids in the Mongolian Gobi. *Journal of Applied Ecology*, 45(6), 1762–1769.

Kahlke, R. D., 2000. The Early Pleistocene (Epivillafranchian) Faunal Site of Untermassfeld (Thuringia, Central Germany): Synthesis of New Results. In: Lordkipanidze, D., Bar-Yosef, O. and Otte, M. (eds.) *Early Humans at the Gates of Europe. Proceedings of the first International symposium Dmanisi, Tbilisi (Georgia), Septembre 1998*. Etudes et Recherches Archéologiques de l´Université Liège, 92, 123–138.

Kahlke, R. D., 2006. Untermassfeld. A late Early Pleistocene (Epivillafranchian) fossil site near Meiningen (Thuringia, Germany) and its position in the development of the European mammal fauna British Archaeological Reports, International Series 1578. Oxford. in this volume. Excavation progress and research at the Early Pleistocene site of Untermassfeld during the years 1997–2015, 1031–1078

Kahlke, R. D., 2014. The origin of Eurasian mammoth faunas (*Mammuthus–Coelodonta* faunal complex). *Quaternary Science Reviews*, 96, 32-49.

Kahlke, R. D., Garcia N., Kostopoulos, D. S., Lacombat, F., Lister, A. M., Mazza, P. P. A., Spassov, N. and Titov, V. V., 2011. Western Palaearctic palaeoenvironmental conditions during the Early and early Middle Pleistocene inferred from large mammal faunal communities, and implications for hominin dispersal in Europe. *Quaternary Science Review*, 30, 1368–1395.

Kahlke, R. D. and Gaudzinski, S., 2005. The blessing of a great flood: differentiation of mortality patterns in the large mammal record of the Lower Pleistocene fluvial site of Untermassfeld (Germany) and its relevance for the interpretation of faunal assemblages from archaeological sites. *Journal of Archaeological Science*, 32, 1202–1222.

Kaiser, T. M. and Solounias, N. 2003. Extending the tooth mesowear method to extinct and extant equids. *Geodiversitas*, 25(2), 321–345.

Kaiser, T. M., 2002. Functional significance of ontogenetic gradients in the enamel ridge pattern of the upper cheek dentition of the Miocene hipparionine horse *Cormohipparion occidentale* (Equidae, Perissodactyla). *Senckenbergiana Lethaea*, 82, 167–180.

Kaiser, T. M. and Fortelius, M., 2003. Differential mesowear in occluding upper and lower molars: opening mesowear analysis for lower molars and premolars in hypsodont horses. *Journal of Morphology*, 258(1), 67–83.

Kleine, L., 2010. Stable isotope ecology of the endangered Grevy's zebra *(Equus grevyi*) in Laikipia, Kenya. *Writing Excellence Award Winners*. Paper 13.

Koliadimou, K. K., 1996. *Palaeontological and Biostratigraphical Study of the Neogene-Quaternary Micromammals from Mydgonia Basin*. PhD thesis, University of Thessaloniki, 612 p.

Konidaris, G. E., Kostopoulos, D. S., and Koufos, G. D. 2020. *Mammuthus meridionalis* (Nesti, 1825) from Apollonia-1 (Mygdonia Basin, Northern Greece)

and its importance within the Early Pleistocene mammoth evolution in Europe. *Geodiversitas*, 42(6), 69–91.

Konidaris, G. E., Kostopoulos, D. S., Koufos, G. D., Tourloukis, V. and Harvati, K., 2016. Tsiotra Vryssi: a new vertebrate locality from the early Pleistocene of Mygdonia Basin (Macedonia, Greece). In: *XIV Annual Meeting of the European Association of Vertebrate Palaeontologists*. Koninklijke Nederlandse Akademie Van Wetenschappen, p. 37. Haarlem, The Netherlands.

Konidaris, G. E., Kostopoulos, D. S., Maron, M., Schaller, M., Ehlers, T.A., Aidona, E., Marini, M., Tourloukis, V., Muttoni, G. and Koufos, G. D., 2021. Dating of the Lower Pleistocene vertebrate site of Tsiotra Vryssi (Mygdonia Basin, Greece): Biochronology, magnetostratigraphy, and cosmogenic radionuclides. *Quaternary*, 4, 1.

Konidaris, G. E., Tourloukis, V., Kostopoulos, D. S., Thompson, N., Giusti, D., Michailidis, D., Koufos G. D. and Harvati, K., 2015. Two new vertebrate localities from the Early Pleistocene of Mygdonia Basin (Macedonia, Greece): preliminary results. *Comptes Rendus Palevol*, 14(5), 353–362.

Kostopoulos, D. S., Aidona, E., Benammi, M., Gkeme, A., Grasset, L., Guy, F. and Merceron, G., 2019. The Lower Pleistocene primate-bearing fossil site of Dafnero (W. Macedonia, Greece): New data from classic and innovative approaches. In: *15th International Congress of the Geological Society of Greece*. *Bulletin of the Geological Society of Greece*, Special Publication 7, Extended Abstract GSG2019-024.

Kostopoulos, D. S., Konidaris, G.E., Amanatidou, M., Chitoglou, K., Fragkioudakis, E., Gerakakis, N., Giannakou, V., Gkeme, A., Kalaitzi, C., Tsakalidis, C. and Tsatsalis, V., 2022. The new fossil site Krimni-3 in Mygdonia Basin and the first evidence of a giant ostrich in the Early Pleistocene of Greece. *PalZ*, 97(1), 147–161.

Kostopoulos, D. S. and Koufos, G. D. 2000. Palaeoecological remarks on Plio-Pleistocene mammalian faunas. *Bulletin of the Geological Society of Greece, Special Publication*, 9, 139–150.

Kostopoulos, D. S. and Koufos, G. D., 1998. Palaeoecological remarks from the Villafranchian mammalian faunas of Macedonia, Greece. *Romanian Journal of Stratigraphy, 78*, 83–90.

Koufos, G. D., 1981. A new late Pleistocene (Würmian) mammal locality from the basin of Drama (Northern Greece). *Scientific Annals, Faculty of Physics and Mathematics, University of Thessaloniki, 21*, 129–148.

Koufos, G. D., 1992. Early Pleistocene equids from Mygdonia basin (Macedonia, Greece). *Palaeontographia Italica*, 79, 167–199.

Koufos, G. D., 2001. The Villafranchian mammalian faunas and biochronology of Greece. *Bollettino Societa Palaeontologica Italiana*, 40(2), 217–224.

Koufos, G. D., 2014. The Villafranchian carnivoran guild of Greece: implications for the fauna, biochronology and palaeoecology. *Integrative zoology*, 9(4), 444–460.

Koufos, G. D., Konidaris, G. E. and Harvati, K., 2018. Revisiting *Ursus etruscus* (Carnivora, Mammalia) from the Early Pleistocene of Greece with description of new material. *Quaternary International*, 497, 222–239.

Koufos, G. D. and Kostopoulos, D. S., 1993. A stenonoid horse (Equidae, Mammalia) from the Villafrnachian of western Macedonia (Greece). *Bulletin of the Geological Society of Greece*, 28(3), 131–143.

Koufos, G. D. and Kostopoulos, D. S., 1997. New carnivore material from the Plio-Pleistocene of Macedonia (Greece) with a description of a new canid. *Münchner Geowissenschaftliche Abhandlungen*, 34, 33–63.

Koufos, G. D. and Kostopoulos, D. S., 2013. First report of *Brachypotherium* Roger, 1904 (Rhinocerotidae, Mammalia) in the Middle Miocene of Greece. *Geodiversitas*, 35(3), 629–641.

Koufos, G. D., Kostopoulos, D. S. and Merceron, G. 2020. The saber-toothed cat *Homotherium latidens* (Owen, 1846) from the lower Pleistocene locality Dafnero, Western Macedonia, Greece. *Geodiversitas*, 42(10), 139–149.

Koufos, G. D., Kostopoulos, D. S. and Sylvestrou, I., 1997. *Equus apolloniensis* n. sp. (Mammalia, Equidae) from the latest Villafranchian locality of Apollonia, Macedonia, Greece. *Palaeontologia i Evolució*, 30(31), 4976.

Koufos, G. D. and Sen, S., 2016. Equidae. In: Sen, S. (eds) Late Miocene mammal locality of Küçükçekmece, European Turkey. *Geodiversitas* 38(2), 225–243.

Koufos, G. D., Syrides, G. and Koliadimou, K., 1989. A new Pleistocene mammal locality from Macedonia (Greece). Contribution to the study of Villafranchian (Villangian) in Central Macedonia. *Bulletin of the Geological Society of Greece*, 23, 113–124.

Koufos, G. D. and Vlachou, T. D., 1993. *Equus stenonis* from the middle Villafranchian locality of Volax (Macedonia, Greece). *Geodiversitas*, 19, 641–657.

Koufos, G. D., Vlachou, T. D. and Gkeme, A. G. 2022. The Fossil Record of Equids (Mammalia: Perissodactyla: Equidae) in Greece. In: Vlachos, E. (eds) *Fossil Vertebrates of Greece Vol. 2: Fossil vertebrates of Greece Vol. 2: Laurasiatherians, artiodactyles, perissodactyles, carnivorans, and island endemics*, Springer, Cham, 351–401.

Langlois, A., 2005. Le Cheval du gisement Pléistocène moyen de La Micoque (Les Eyzies-de-Tayac, Dordogne): *Equus mosbachensis micoquii* nov. ssp. *PALAEO. Revue d'archéologie préhistorique*, 17, 73–110.

Lee-Thorp, J. L. and Van Der Merwe, N. J., 1987. Carbon isotope analysis of fossil bone apatite. *South African Journal of Science*, 83(11),712–715

Lindsay, E.H., and Jacobs, L.L. 1985. Pliocene small mammal fossils from Chihuahua, Mexico. *Palaeontologia Mexicana*, Universidad Nacional Autonoma de Mexico, Instituto de Geologia, 51, 1–53.

Linnaeus, C., 1758. *Systema naturae perregna tria naturae, secundum classes, ordines, genera, species cum characteribus, differentiis, synonymis, locis*. Editio decima, reformata. Stockholm, Laurentii Salvii, 824 p.

Lisiecki, L. E. and Raymo, M. E., 2005. A Pliocene-Pleistocene stack of 57 globally distributed benthic d18O records. *Palaeoceanography* 20, PA1003. doi:10.1029/2004PA001071

Lundelius, E. L., Churcher, C. S., Downs, T., Harington, C. R., Lindsay, E. H., Schultz, G. E., Semken, H. A., Webb, S. D. and Zakrzewski, R. J. 1987. The North American Quaternary sequence. In: Woodburne, M. O. (eds) *Cenozoic Mammals of North America*. University of California Press, Berkeley, 211–235

Lyras, G. A., and Van der Geer, A. A. 2007. The Late Pliocene vertebrate fauna of Vatera (Lesvos Island, Greece). *Cranium*, 24(2), 11–24.

MacFadden, B. J., 1992. Fossil horses. Systematics, palaeobiology, and evolution of the family Equidae. Cambridge University Press, New York.

MacFadden, B. J., 2005. Diet and habitat of toxodont megaherbivores (Mammalia, Notoungulata) from the late Quaternary of South and Central America. *Quaternary Research*, 64, 113–124.

MacFadden, B. J., Solounias, N., and Cerling, T. E., 1999. Ancient diets, ecology, and extinction of 5-million-year-old horses from Florida. *Science*, 283(5403), 824–827.

Maddison, W. P. and Maddison, D. R., 2023. Mesquite: a modular system for evolutionary analysis. Version 3.81 http://www.mesquiteproject.org

Magniez, P. and Boulbes, N., 2014. Environment during the Middle to Late Palaeolithic Transition in Southern France: The Archaeological Sequence of Tournal Cave (Bize-Minervois, France). *Quaternary International*, 337, 43–63.

Marchand, P., Redjadj, C., Garel, M., Cugnasse, J.-M., Maillard, D. and Loison, A., 2013. Are mouflon *Ovis gmelini musimon* really grazers? A review of variation in diet composition. *Mammal Revision*, 43, 275–291.

Masini, F., Palombo, M. R. and Rozzi, R., 2013. A reappraisal of the Early to Middle Pleistocene Italian Bovidae. *Quaternary International*, 288, 45–62.

McDonald, H., 1996. "opulation structure of the Late Pliocene (Blancan) zebra *Equus simplicidens* (Perissodactyla: Equidae) from the Hagerman Horse Quarry, Idaho in *Palaeoecology and Palaeoenvironments of Late Cenozoic Mammals: Tributes to the Career of CS (Rufus) Churcher*, eds K. M. Stewart and K. L. Seymour. (Toronto: University of Toronto Press), 134–155.

McGrew, P. O., 1944. An Early Pleistocene (Blancan) fauna from Nebraska. *Field Museum Natural History, Geology*, 9, 33–66.

Merceron, G., Berlioz, E., Vonhof, H., Green, D., Garel, M. and Tütken, T., 2021. Tooth tales told by dental diet proxies: An alpine community of sympatric ruminants as a model to decipher the ecology of fossil fauna. *Palaeogeography, Palaeoclimatology, Palaeoecology*, 562, 110077.

Merceron, G., Blondel, C., Koufos, G. D. and De Bonis, L., 2007. Dental microwear analysis of bovids from the Vallesian (Late Miocene) of Axios Valley in Greece: reconstruction of the habitat of *Ouranopithecus macedoniensis* (Primates, Hominoidea). *Geodiversitas*, 29, 421–433.

Merceron, G., Hofman-Kamińska, E. and Kowalczyk, R., 2014. 3D dental microwear texture analysis of feeding habits of sympatric ruminants in the Białowieża Primeval Forest, Poland. *Forest Ecology and Management*, 328, 262–269.

Merceron, G., Novello, A. and Scott, R. S., 2016. Palaeoenvironments inferred from phytoliths and dental microwear texture analyses of meso-herbivores. *Geobios*, 49(1-2), 135–146.

Merceron, G., Novello, A., and Scott, R.S., 2016. Palaeontology of the Upper Miocene vertebrate localities of Nikiti (Chalkidiki Peninsula, Macedonia, Greece) – palaeoenvironments inferred from phytoliths and dental microwear texture analyses of meso-herbivores. *Geobios*, 49, 135–146.

Merceron, G., Schulz, E., Kordos, L. and Kaiser, T. M., 2007. Palaeoenvironment of *Dryopithecus brancoi* at Rudabánya, Hungary: evidence from dental meso-and micro-wear analyses of large vegetarian mammals. *Journal of Human Evolution*, 53(4), 331–349.

Mihlbachler, M. C. and Beatty, B. L., 2012. Magnification and resolution in dental microwear analysis using light microscopy. *Palaeontologia Electronica*, 15, 25A.

Mihlbachler, M. C., Beatty, B. L., Caldera-Siu, A., Chan, D. and Lee, R., 2012. Error rates and observer bias in dental microwear analysis using light microscopy. *Palaeontologia Electronica*, 15, 12A.

Mihlbachler, M.C., Rivals, F., Solounias, N., and Semprebon, G.M., 2011. Dietary change and evolution of horses in North America. *Science*, 331(6021), 1178–1181.

Moehlman, P.D., 2002. *Equids: Zebras, Asses and Horses*. IUCN Publication Services Unit, Cambridge, UK.

Moncel, M.-H. and Rivals, F., 2011. On the Question of Short-Term Neanderthal Site Occupations: Payre, France (MIS 8-7), and Taubach/Weimar, Germany (MIS 5). *Journal of Anthropological Research*, 67, 47–75.

Musil, R., 1968. Die Equiden aus dem Travertin von Ehringsdorf - Paläontologische *Abhandlungen*, 23, 265–335.

Musil, R., 2001. Die equiden-reste aus dem Unterpleistozän von Untermassfeld. In Das Pleistozän von Untermassfeld Bei Meiningen (Thüringen). Teil 2, Monographien Des. RGZM; Kahlke, R. D. (eds); Verl. d. Römisch-Germanischen Zentralmuseums: Mainz, Germany, 557–587.

Nomade, S., Pastre, J. F., Guillou, H., Faure, M., Guérin, C., Delson, E., Debard, E., Voinchet, P. and Messager, E., 2014. 40 Ar/ 39 Ar constraints on some French landmark late Pliocene to Early Pleistocene large mammalian palaeo-faunas: palaeoenvironmental and palaeoecological implications. *Quaternary Geochronology*, 21, 2–15.

Orlandi-Oliveras, G., Köhler, M., Clavel, J., Scott, R. S., Mayda, S., and Merceron, G. (2022). Feeding strategies of circum-Mediterranean hipparionins during the late

Miocene: Exploring dietary preferences related to size through dental microwear analysis. *Palaeontologia Electronica*, 25(1), 1-45.

Orlando, L., Mashkour, M., Burke, A., Douady C. J. and Eisenmann, V., 2006 Geographic distribution of an extinct equid (*E. hydruntinus*, Mammalia, Equidae) revealed by morphological and genetical analyses of fossils. *Molecular ecology*, 15, 2083–2093.

Orlando, L., Metcal, J. L., Alberdi, M. T., Telles-Antunes, M., Bonjean, D., Otte, M., Marting, F., Eisenmann V., Mashkour, M., Morello, F., Prado, J. L., Salas-Gismondi, R., Shockey, B. J., Wrinn, P. J., Vasil'ev, S. K., Ovodov, N. D., Cherry, M. I., Hopwood, B., Male, D., Austin J. J., Ha¨nni, C. and Cooper, A., 2009. Revising the recent evolutionary history of equids using ancient DNA. *PNAS USA* 106:21754–21759

Osborn, H. F., 1912. Craniometry of the Equidae. *Memoires of the American Museum of Natural History*.

Papamarinopoulos, S., Readman, P. W., Maniatis, Y. and Simopoulos, A., 1987. Palaeomagnetic and mineral magnetic studies of sediments from Petralona Cave, Greece. *Archaeometry*, 29, 50–59.

Parandier, M., 1891. Notice géologique et Paléontologique sur la nature des terrains traversés par le chemin de fer entre Dijon et Chalon-sur-Saone. *Bulletin de la Société Géologique de France*, 19, 794–818.

Penzhorn, B. L., 1982. Age determination in cape mountain zebras *Equus zebra zebra* in the Mountain Zebra National Park. *Koedoe*, 25(1), 89–102.

Penzhorn, B. L., 1988. *Equus zebra*. *Mammalian Species*, 314, 1–7.

Pérez-Barberia, F. J., OliVan, M., Osoro, K. and Nores, C., 1997. Sex, seasonal and spatial differences in the diet of Cantabrian chamois *Rupicapra pyrenaica parva*. *Acta Theriol. (Warsz.)*, 42, 37–46.

Philippe, M., 1975. La faune würmienne du gisement paléontologique de Siréjol à Gignac (Lot). *Bulletin de la Société Scientifique, Historique et Archéologique de la Corrèze*, 97, 1–9.

Pomel, A., 1853. *Catalogue méthodique et descriptif des Vertébrés fossils découverts dans le basin hydrographique supérieur de la loire, et surtout dans la vallée de son affluent principal, l'Allier*. Bailliere, Paris, 123 p.

Prat, F., 1968. Recherches sur les Equidés Pléistocènes en France. *Doctoral Thesis, Bordeaux Faculty of Sciences, Bordeaux*, France.

Psilovikos, A., 1977. Palaeogeographic development of the basin and lake of Mygdonia (Lagada-Volvi area, Greece). *Doctoral Thesis, School of Geology, Aristotle University of Thessaloniki,* Thessaloniki, Greece.

Reed, K. E., 1997. Early hominid evolution and ecological change through the African Plio-Pleistocene. *Journal of Human Evolution* 32, 289–322.

Reed, K. E., 1998. Using large mammal communities to examine ecological and taxonomic structure and predict vegetation in extant and extinct assemblages. *Palaeobiology* 24, 384–408.

Regalia, E., 1907. Sull' *Equus* (*Asinus*) *hydruntinus* Regalia della grotta di Romanelli (Castro, Lecce). *Archivio per l'Antropologia e l'Etnologia*, 37, 375–390.

Repenning, C. 1987. Biochronology of the Microtine rodents of the United States. In: Woodburne, M. O. (eds) *Cenozoic Mammals of North America, Geochronology and Biostratigraphy*. University of California Press, Berkeley, USA, 236–268.

Rivals, F. and Lister, A. M. 2016. Dietary flexibility and niche partitioning of large herbivores through the Pleistocene of Britain. *Quaternary Science Review*, 146, 116–133. doi: 10.1016/j.quascirev.2016.06.007

Rivals, F. and Lister, A. M., 2016. Dietary Flexibility and Niche Partitioning of Large Herbivores through the Pleistocene of Britain. *Quaternary Science Reviews*, 146, 116–133.

Rivals, F., and Semprebon, G., 2010. What can incisor microwear reveal about the diet of ungulates? *Mammalia*, 74, 401–406. doi: 10.1515/mamm.2010.044

Rivals, F., Julien, M.-A., Kuitems, M., Van Kolfschoten, T., Serangeli, J., Drucker, D. G., Bocherens, H., and Conard, N. J., 2015. Investigation of Equid Palaeodiet from Schöningen 13 II-4 through Dental Wear and Isotopic Analyses: Archaeological Implications. *Journal of Human Evolution*, 89, 129–137.

Rivals, F., Mihlbachler, M. C. and Solounias, N., 2007. Effect of ontogenetic-age distribution in fossil samples on the interpretation of ungulate palaeodiets using the mesowear method. *Journal of Vertebrate Palaeontology*, 27, 763–767.

Rivals, F., Mihlbachler, M.C., Solounias, N., Mol, D., Semprebon, G. M., de Vos, J. and Kalthoff, D. C., 2010. Palaeoecology of the Mammoth Steppe Fauna from the Late Pleistocene of the North Sea and Alaska: Separating Species Preferences from Geographic Influence in Palaeoecological Dental Wear Analysis. *Palaeogeography, Palaeoclimatology, Palaeoecology*, 286, 42–54.

Rook, L., Bernor R. L., Avilla, L. S., Cirilli, O., Flynn, L., Jukar, A., Sanders, W., Scott, E. and Wang, X., 2019. Mammal Biochronology (Land Mammal Ages) Around the World from Late Miocene to Middle Pleistocene and Major Events in Horse Evolutionary History. *Frontiers in Ecology and Evolution*, 7, 278. doi: 10.3389/fevo.2019.00278

Rook, L., Cirilli, O. and Bernor, R. L., 2017. A late occurring "*Hipparion*" from the middle Villafranchian of Montopoli, Italy (Early Pleistocene; MN16b; ca. 2.5 Ma). *Bollettino della Società Palaeontologica Italiana*, 56, 333–339.

Rubenstein, D. I., 1989. Life history and social organization in arid adapted ungulates. *Journal of Arid Environments*, 17, 145–156.

Saarinen, J., Cirilli, O., Strani, F., Meshida, K. and Bernor, R. L., 2021. Testing equid body mass estimate equations on modern zebras—With implications to understanding the relationship of body size, diet, and habitats of *Equus* in the Pleistocene of Europe. *Frontiers in Ecology and Evolution*, 9.

Saladié, P., Rodríguez-Hidalgo, A., Marín, J., Vallverdú i Poch, J. and Carbonell, E., 2018. The top of the Gran Dolina (Atapuerca, Spain) sequence: a zooarchaeological and occupational perspective. *Quaternary Science Revision*, 195, 48–71. doi: 10.1016/j.quascirev.2018.07.010

Samson, P., 1975. Les équidés fossiles de Roumanie. *Geologica Romana*, 14, 165-352.

Schaller, G. B. 1998. *Wildlife of the Tibetan Steppe.* The University of Chicago Press, Chicago and London. 373 p.

Scott, K. M., 1990. Postcranial dimensions of ungulates as predictors of body mass. In: Damuth, J. and MacFadden, B. J. (eds) *Body Size in Mammalian Palaeobiology—Estimation and Biological Implications*. Cambridge University Press: New York, NY, USA, 301–355.

Scott, R. S., 2004. The comparative palaeoecology of late Miocene Eurasian hominoids. *Doctoral Thesis*, The University of Texas at Austin.

Scott, R. S., Ungar, P. S., Bergstrom, T. S., Brown, C. A., Childs, B. E., Teaford, M. F. and Walker, A., 2006. Dental microwear texture analysis: technical considerations. *Journal of human evolution*, 51(4), 339-349.

Scott, R. S., Ungar, P. S., Bergstrom, T. S., Brown, C. A., Grine, F. E., Teaford, M. F. and Walker, A., 2005. Dental microwear texture analysis shows within-species diet variability in fossil hominins. *Nature*, 436, 693–695.

Semprebon, G.M., Rivals, F., and Janis, C.M., 2019. The role of grass vs. exogenous abrasives in the palaeodietary patterns of North American ungulates. *Frontiers in Ecology and Evolution*, 7, 65.

Shah, N., 2002. Status and action plan for the kiang (*Equus kiang*). *Equids: zebras, asses and horses. Status survey and conservation action plan (PD Moehlman, ed.). International Union for Conservation of Nature and Natural Resources/Species Survival Commission, Equid Specialist Group, Gland, Switzerland*, 72-81.

Sher, A. V., 1971. Mlekopitaiushchie i Stratigrafia Pleistotsena Krainego Severo-Vostoka SSSR i Severnoi Ameriki. Nauka, Moskva.

Sickenberg, O., 1967. Die Unterpleistozäne Fauna von Wolaks (Griech. - Mazedonien) I. eine neue Giraffe (*Macedonitherium martinii* nov. gen. nov. spec.) aus dem Untern Pleistozän von Griechenland. *Annales Géologiques des Pays Helléniques*, 18, 314–330.

Sickenberg, O., 1968. Die Unterpleistozäne fauna von Wolaks (Griech.-Mazedonien) II. Carnivoren. *Annales Géologiques des Pays Helléniques*, 19, 621–46.

Sickenberg, O., 1968a. Die Pleistozäne knochen brekzien von Volax (Griech. - Mazedonien). *Geologische Jahrbuch*, 85, 33–54.

Sickenberg, O., 1968b. Die Unterpleistozäne Fauna von Wolaks (Griech. - Mazedonien) II. Die Carnivoren. *Annales Géologiques des Pays Helléniques*, 19, 621–646.

Simpson, G. G., 1941. Large Pleistocene felines of North America. *American Museum Novitates*, 1136, 1–27.

Sinusía, C., Pueyo, E. L., Azanza, B. and Pocoví, A., 2004. Datación magnetoestratigráfica del yacimiento palaeontológico de la Puebla de Valverde (Teruel). *Geotemas*, 6, 329–342.

Skinner, M. F. and Hibbard, C. W., 1972. Early Pleistocene pre-glacial and glacial rocks and faunas of north-central Nebraska. *Bulletin of the American Museum of Natural History*, 141(1), 1–148.

Smith, D. G. and Pearson, R. A., 2005. A review of the factors affecting the survival of donkeys in semi-arid regions of sub-Saharan Africa. *Tropical Animal Health and Production*, 37, 1–19.

Smuts, M. M., and Penzhorn, B. L., 1988. Descriptions of anatomical differences between crania and mandibles of *E. zebra* and *E. burchelli* from Southern Africa. *African Zoology*, 23(4), 328–336.

Sokal, S. R. and Rohlf, F. J., 1969. Biometry. W.E. Freeman and Company, New York.

Solounias, N., and Semprebon, G., 2002. Advances in the reconstruction of ungulate ecomorphology with application to early fossil equids. *American Museum Novitates*, 3366, 1–49.

Souron, A., Merceron, G., Blondel, C., Brunetière, N., Colyn, M., Hofman-Kamińska, E. and Boisserie, J. R., 2015. Three-dimensional dental microwear texture analysis and diet in extant Suidae (Mammalia: Cetartiodactyla). *Mammalia*, 79(3), 279–291.

Steensma, K. J., 1988. Plio-Pleistozäne Grossäugetiere (Mammalia) aus dem Beckem von Kastoria/Grevena, südlich von Neapolis-NW Griechenland. *Doctoral Thesis*, Technische Universität Clausthal, Clausthal, Germany.

Storms, D., Aubry, Ph., Hamann, J.-L., Saïd, S., Fritz, H., Saint-Andrieux, Ch. and Klein, F., 2008. Seasonal variation in diet composition and similarity of sympatric red deer *Cervus elaphus* and roe deer *Capreolus capreolus*. *Wildlife Biology*, 14, 237–250.

Strani, F., DeMiguel, D., Alba, D. M., Moyà-Solà, S., Bellucci, L., Sardella, R., et al. 2019. The effects of the "0.9Ma event" on the Mediterranean ecosystems during the Early-Middle Pleistocene transition as revealed by dental wear patterns of fossil ungulates. *Quaternary Science Reviews*, 210, 80–89. doi: 10.1016/j.quascirev.2019.02.027

Strani, F., DeMiguel, D., Bellucci, L. and Sardella, R. 2018b. Dietary response of Early Pleistocene ungulate communities to the climate oscillations of the Gelasian/Calabrian transition in Central Italy. *Palaeogeography, Palaeoclimatology, Palaeoecology*, 499, 102–111. doi: 10.1016/j.palaeo.2018.03.021

Strani, F., DeMiguel, D., Bona, F., Sardella, R., Biddittu, I., Bruni, L., De Castro, A., Guadagnoli, F. and Bellucci, L., 2018a. Ungulate dietary adaptations and palaeoecology of the Middle Pleistocene site of Fontana Ranuccio (Anagni, Central Italy). *Palaeogeography, Palaeoclimatology, Palaeoecology*, 496, 238–247. doi: 10.1016/j.palaeo.2018.01.041

Strani, F., DeMiguel, D., Sardella, R. and Bellucci, L. 2015. Palaeoenvironments and climatic changes in the Italian Peninsula during the Early Pleistocene: evidence from dental wear patterns of the ungulate community of Coste San Giacomo. *Quaternary Science Reviews*, 121, 28–35. doi: 10.1016/j.quascirev.2015. 05.008

Strani, F., Pushkina, D., Bocherens, H., Bellucci, L., Sardella, R. and DeMiguel, D. 2019. Dietary adaptations of Early and Middle Pleistocene equids from the Anagni basin (Frosinone, central Italy). *Frontiers in Ecology and Evolution*, 7, 176.

Stringer, C., Howell, F. C. and Melentis, J., 1979. The significance of the fossil hominid cranium from Petralona, Greece. *Journal of Archeological Sciences*, 6, 235–253.

Sun, B. and Deng, T., 2019. The *Equus* Datum and the Early Radiation of *Equus* in China. *Frontiers in Ecology and Evolution*, 7, 429. doi: 10.3389/fevo.2019.00429

Sundaresan, S. R., Fischoff, I. R., Hartung, H. M., Akilong, P. and Rubenstein, D. I., 2007. Habitat choice of Grevy's zebras (*Equus grevyi*) in Laikipia, Kenya. *African Journal of Ecology*, 46, 359–364.

Symeonidis, N., 1992. Lower Pleistocene (Villafranchian) fossil Mammals from the Sésklo basin (Volos). *Annales Géologiques des Pays Helléniques* 35, 1–41. (in Greek).

Tamvakis, A., Savvidou, A., Spassov, N., Youlatos, D., Merceron, G. and Kostopoulos, D. S., 2022. New insights on Early Pleistocene *Nyctereutes* from the Balkans based on material from Dafnero-3 (Greece) and Varshets (Bulgaria). *Palaeoworld*, 32(3), 55–572.

Teaford, M. F. and Oyen, O. J., 1989. Differences in the Rate of Molar Wear between Monkeys Raised on Different Diets. *Journal of Dental Research*, 68, 1513–1518. https://doi.org/10.1177/00220345890680110901

Teaford, M. F., Ungar, P. S., Taylor, A. B., Ross, C. F. and Vinyard, C. J., 2020. The dental microwear of hard-object feeding in laboratory *Sapajus apella* and its implications for dental microwear formation. *American Journal of Physical Anthropology*, 171, 439–455. https://doi.org/10.1002/ajpa.24000

Titov, V. V., 2008. Late Pliocene large mammals from Northeastern Sea of Azov Region. Managing editor Acad. G.G. Matishov, Rostov-on-Don, SSC RAS Publishing, 264 p.

Tixier, H., Duncan, P., Scehovic, J., Yani, A., Gleizes, M. and Lila, M., 1997. Food selection by a roe deer (*Capreolus capreolus*): effects of plant chemistry, and

consequences for the nutritional value of their diet. *Journal of Zoology*, 242, 229–245.

Tsartsidou, G., Lev-Yadun, S., Albert, R. M., Miller-Rosen, A., Efstratiou, N. and Weiner, S., 2007. The phytolith archaeological record: strengths and weaknesses evaluated based on a quantitative modern reference collection from Greece. *Journal of Archaeological Science*, 34, 1262–1275. https://doi.org/10.1016/j.jas.2006.10.017

Tsoukala, E., 1991. Contribution to the study of the Pleistocene fauna of large mammals (Carnivora, Perissodactyla, Artiodactyla) from Petralona Cave, Chalkidiki (N. Greece). Preliminary report. *Comptes Rendus hebdomadaires des Séances de l'Académie des Sciences de Paris* (2) 312, 331–336.

Tsoukala, E., 1992. The Pleistocene large mammals from the Agios Georgios cave, Kilkis (Macedonia, N. Greece). *Geobios*, 25(3), 415–433.

Tsoukala, E., 2000. Remains of a Pliocene *Mammut borsoni* (Hays, 1834) (Proboscidea, Mammalia), from Milia (Grevena, W. Macedonia, Greece). In *Annales de Paléontologie* Vol. 86, No. 3, 165–191.

Tsoukala, E. and Chatzopoulou, K., 2005. A new Early Pleistocene (Latest Villafranchian) site with mammals in Kalamotó (Mygdonia Basin, Macedonia, Greece) – preliminary report. *Mitt. Komm. Quartärforsch. Österr. Akad. Wiss*. 14, 213–233.

Tsoukala, E. and Guérin, C., 2016. The Rhinocerotidae and Suidae (Mammalia) of Middle Pleistocene from Petralona Cave (Macedonia, Greece). *Acta Zoologica Bulgarica*, 68(2), 243-264.

Ungar, P. S. and Evans, A. A. 2016. Exposing the past: surface topography and texture of palaeontological and archeological remains. *Surface Topography: Metrology and Properties*, 4, 040302. https://doi.org/10.1088/2051-672X/4/4/040302

Ungar, P. S. and Zhou, Z. 2017. Dental biotribology: Wearing away the boundary between biology and engineering. *Biosurface and Biotribology*, 3, 115–118. https://doi.org/10.1016/j.bsbt.2017.11.002

Ungar, P. S., Brown, C. A., Bergstrom, T. S. and Walker, A., 2003. Quantification of dental microwear by tandem scanning confocal microscopy and scale-sensitive fractal analyses. *Scanning*, 25, 185–193.

Ungar, P. S., Merceron, G. and Scott, R. S., 2007. Dental microwear texture analysis of Varswater bovids and early Pliocene palaeoenvironments of Langebaanweg,

Western Cape Province, South Africa. *Journal of Mammal Evolution*, 14,163–181.

Valli, A. M. F., Palombo, M. R. and Alberdi, M. T., 2012. How homogeneous are microwear patterns on a fossil horse tooth? preliminay test on a premolar of *Equus altidens* from Barranco Leon 5 (Spain). *Alpine and Mediterranean Quaternary*, 25, 25–33.

Van Asperen, E. N, 2010. Ecomorphological Adaptations to Climate and Substrate in Late Middle Pleistocene Caballoid Horses. *Palaeogeography, Palaeoclimatology, Palaeoecology*, 297, 584–596.

Van Asperen, E. N., 2012. Late Middle Pleistocene Horse Fossils from Northwestern Europe as Biostratigraphic Indicators. *Journal of Archeological Science*, 39, 1974–1983.

Van Asperen, E. N., Krzysztof, S., Proskurnyak, I. and Ridush, B., 2012. Equids from Emine-Bair-Khosar Cave (Crimea, Ukraine): co-occurrence of the stenonid *Equus hydruntinus* and the caballoid *E. ferus latipes* based on skull and postcranial remains. *Palaeontologia Electronica*, 15, 1, 5A, 28p.

Van der Meulen, A. and Van Kolfschoten, T., 1986. Review of the Late Turolian to Early Biharian mammal faunas from Greece and Turkey. *Società Geologica Italiana*, 31, 201–211.

Van Kolfschoten, T., Buhrs, E. and Verheijen, I., 2015. The larger mammal fauna from the Lower Paleolithic Schöningen spear site and its contribution to hominin subsistence. *Journal of Human Evolution*, 89, 138–153. doi: 10.1016/j.jhevol.2015.09.014

Vilstrup, J. L., Seguin-Orlando, A., Stiller, M., Ginolhac, A., Raghavan M., Nielsen, Sandra, S. C. A., Weinstock, J., Froese, D., Vasiliev, S. K., Ovodov, N. D., Clary, J., Helgen, K. M., Fleischer, R. C., Cooper, A., Shapiro, B. and Orlando, L., 2013. Mitochondrial phylogenomics of modern and ancient equids. *PLoS ONE* 8(2), e55950.

Walker, A., Hoeck, H. N., and Perez, L., 1978. Microwear of mammalian teeth as an indicator of diet. *Science*, 201, 908–910. doi: 10.1126/science.684415

Weinstock, J., Willersley, E., Sher, A., Tong, W. and Ho, SYW, 2005. New world Pleistocene horses: pruning the equid tree. *PLoS Biol*, 3(8):1332–1333

Winkler, D. E., Schulz-Kornas, E., Kaiser, T.M., Codron, D., Leichliter, J., Hummel, J., Martin, L. F., Clauss, M. and Tütken, T., 2020. The turnover of dental

microwear texture: Testing the “last supper” effect in small mammals in a controlled feeding experiment. *Palaeogeography, Palaeoclimatology, Palaeoecology*, 557, 109930. https://doi.org/10.1016/j.palaeo.2020.109930

Wüst, E., 1900. Untersuchungen über das Pliozän und das älteste Pleistozän Thüringens, nördlich vom Thüringer walde und westlich von der Saale. *Abhandlungen der Naturforshgung Gessellschaften zu Halle*, 23, 1–352. doi: 10.5962/bhl.title. 13977

Wüst, E., 1900. Das Pliozän und das älteste Pleistozän Thüringens. Nördlich vom Thüringer Walde und Westlich von der Saale. *Abhandlungen der Naturforshgung Gessellschaften zu Halle*, 23, 1-352.

Ελληνική Βιβλιογραφία

Γκεμέ, Α. Γ., 2016. Μελέτη των Πλειστοκαινικών ιπποειδών της συλλογής Eltgen collection (θέσεις Λίβακος, Καπετάνιος, Πολύλακκος, Δυτική Μακεδονία). *Διατριβή Ειδίκευσης, Τμήμα Γεωλογίας Α.Π.Θ.*, σελ. 119.

Μανιάκας, Ι. Θ., 2019. Συμβολή στη μελέτη των χωροχρονικών μεταβολών της παλαιοοικολογίας των Πλειστοκαινικών Bovini της Ευρώπης με χρήση μορφολειτουργικών και γεωμορφομετρικών μεθόδων. *Διδακτορική Διατριβή, Τμήμα Γεωλογίας Α.Π.Θ., Αριθμός Παραρτήματος Επιστημονικής Επετηρίδας No 192*, σελ. 668.

Τσουκαλά, Ε., 1989. Συμβολή στη μελέτη της παλαιοπανίδας των μεγάλων σπονδυλωτών (Carnivora, Perissodactyla, Artiodactyla) του Σπηλαίου των Πετραλώνων της Χαλκιδικής. *Διδακτορική Διατριβή, Τμήμα Γεωλογίας Α.Π.Θ., Αριθμός Παραρτήματος Επιστημονικής Επετηρίδας No 8*, σελ. 360.

APPENDIX 1

Tables of measurements

Table S1. Crania of *E. stenonis* from Sésklo (Σ, ΣA, SE) and Dafnero 1, 3 (DFN, DFN3).

Crania	Σ-1228	ΣA-1	SE-2	ΣA-3	ΣA-4	Σ-203	DFN3-334	DFN-112
M1			160	154		160	139,76	
M2		{130,2}	{180}		{168}		153,77	
M3		{222,5}					140,36	
M6							>520	
M7			111,265	107,53		92	102	101,79
M8		84,07	94,17	84,48	89,335	84,5	85,41	89,06
M9			204,4	194,8		175,1	186,9	190,67
M10							83,94	
M11							35,48	
M12			50,21	60			45,9	
M13			{83,53}	91,56		84	74,97	
M14			53,87	{71,17}		43	45,64	
M15	74,16		{75,07}	78		70,5	70,53	
M16							73,78	
M17		{178,6}						
M18							>216,16	
M23							425	
M26		{111,5}					71,58	
M28		55,25			60		60,49	68,28
M29		53,45	{99,3}		50,31		33,64	52,73
M30			233,2					
M31			{197,8}	{205,8}				

Table S2. Crania of *E. altidens* from Gerakarou (GER) and Krimni 3 (KMN).

Crania	GER-8	GER-31	GER-122	GER-9	KMN-50
M1	123,3		121,3	129,75	121,98
M2	139,8	145,675	147,7	{152,12}	134,91
M3	114,03	134,89			ca 131,74
M4	103,65	106,16			ca 90,58
M5	214,95	237,85			216,37
M6	472				470
M7	88,14	94,71	92,62	99,48	97,35
M8	73,73	82,14	81,155	96,28	77,01
M9	163,33	174,155	172,2	179,92	172,855
M10		ca 68,39		ca 62,42	77,78
M11		38,38	{34,39}		38,35
M12		46,92	{41,09}		52,4
M13	{64,66}	73,75	{74,14}		85,07
M14	{39,07}		45,11	{39,91}	42,85
M15	58,75		66,7	59,12	71,14
M16	62,88	69,16	73,4		58,1
M17		107,39			113,465
M18	195,92	207,67			227,64
M19	179,42	196,84			206,51
M20		59,46			54,3
M21	100,75	110,99			113,42
M22	{67,58}	69,99			65,9
M23	393			ca 380	381
M24	{171,48}	199,93			199,4
M25					77,865
M26	86,39	74,12		{108,94}	79,08
M27	11,455	12,29			11,355
M28	57,19	65,865			43,49
M29	43,08	37,64		49,01	49,71
M30	188,34				182,48
M31	144,64	158,73			156,43

Table S3. Crania of *E. apolloniensis* from Apollonia (APL).

Crania	APL-871	APL-872	APL-518	APL-605	APL-519	APL-129	APL-858juv.	APL-148	APL-147
M1	136,42	ca 136,73	145				62,45	129,98	
M2	140,98	151		132,465		148,63	111,14	144,53	{135,05}
M3								140,59	{158,32}
M4								125,91	128,8
M5	{ca 272,04}							259,05	277
M6	{542?}							533	
M7	107,465	104,88		109,855		95,77	122,355	110,745	107,48
M8	88,99	89,095	87,26	87,175	88,53	87,985		88,74	93,91
M9	194,57	194,45		193,16		180,7		195,99	201
M10	ca 88,16			85,43			74,36	{92-97}	{ca 97,35}
M11		40,54		39,33					{38,08}
M12		49,62		48,72		61,56	45,57		
M13		>78,54	>85,9	85,26		88,21	73,07		
M14		45,71	{54,72}				38,95		
M15	65,03	72,55	79,29					{69,34}	
M16	59,61	68,95	76,96					68,245	82,59
M17								ca 145,18	147,06
M21									117,29
M22									ca >67,09
M23	415							425	
M26	ca 100,77	111,96			{95,33}			{>96,06}	
M27									
M28	64,21		ca 70,34		73,91			60	63,04
M29	52,69				56,72			57,3	51,645
M30			ca 190					181,61	
M31			{230,98}						

Table S4. Crania of *E. apolloniensis* from Alikes (Aλ).

Crania	Aλ-20	al 171
M7	106,87	100,24
M8		90,75
M9		176,41
M13	{85,41}	
M16	61,1	

Table S5. Mandible of *E. stenonis* from Volax (VOL) and Sésklo (Σ).

Mandible	VOL-202	Σ-1026
M2	131,33	132,23
M3	97,905	101,8
M4	90,16	87,69
M5	190,235	191,7
M7	{69,89}	
M10	103,095	
M11	79,05	
M12	66,475	
M13	{97,69}	93,8
M14	{32,1}	43,1

Table S6. Mandible of *E. altidens* from Tsiotra Vrysi (TSR) and Gerakarou (GER).

Mandible	TSR-136	TSR-G21-46	TSR-D20-33	TSR-F20-27	GER-33	GER-32	GER-34	GER-73
M2					110,7	118,085	103,83	
M3	84,48	93,21	{98,55}	84,41	78,665	90,295	93,61	
M4	-	85,55	{126,77}		83,125	81,305	81,05	
M5	-	178,49	{196,46}		164,55	172,715	173,775	
M6					126,67	119,32		
M7					56,67	51,33	54,55	
M8						199,86		
M10					90,91	97,38		
M11					74,64	76,27	73,2	
M12					60,58	55,87	54	
M13					88,36	83,76	74,24	{75}
M14					35,96	33,71	34,47	36,23

Table S7. Mandible of *Equus* aff. *E. altidens granatensis* var *E. apolloniensis* from Tsiotra Vrysi (TSR).

Mandible	**TSR-E19-7**	**TSR-154**
M3	110,51	112,89
M4	96,01	96,08
M5	{209,54}	210,88

Table S8. Mandible of *E. apolloniensis* from Apollonia (APL).

Mandible	APL-792	APL-633	APL-785	APL-318 juv.	APL-317 juv.	APL-857 juv.	APL-571 juv.	APL-572 juv.	APL-570	APL-295	APL-355	APL-424	APL-606	APL-622
M1									467,5					
M2	113,955			76,925					90,23					
M3	98,505	104,655	107,235	119,47	110,115	123,995	120,37	103,82	97,445		96,54		90,24	92,11
M4			97,69						95,875		94,27	94,58	93,08	
M5			207,87						194,705		195,37			
M6									131,65					
M7	62,08	53,12	{70,96}	52,04					58,15					
M8								183,36	262,3					
M9								166,22	236,22					
M10									134,68	{130,47}				
M11									89,13					
M12	68,97	70,02	{79,4}	55,91	50,17	57,2	52,13		70,995					
M13	80,82	102,41	101,98	68,12	{61,84}		72,41	58,22	83,62					
M14	36,4	41,33	44,85	40,19	39,39	41,13	33,27		41,55					

Table S9. Mandible of *E. apolloniensis* from Alikes (Aλ) and Volos (Vo).

Mandible	Aλ-160	VoB	Vo	Vo-1
M1	506,5			
M2	190			
M3	94,37	101,61	100,7	112,64
M4	91,595	90,47	93,86	90,445
M5	187,8	194,99	199,93	201,745
M6	161,9			
M8	265,5			
M9	253,75			
M10	124,8			
M11	92,325			
M12	75			
M14	{39,43}			

Table S10. Maxilla of *E. stenonis* from Volax (VOL) and Sésklo (S), *E. altidens* from Tsiotra Vrysi (TSR) and Krimni-1 (KRI) and *E. apolloniensis* from Alikes (al) and Volos (Vo).

	E. stenonis					*E. altidens*		*E. apolloniensis*	
Maxilla	VOL-203	DFN-108	S1220	s199	s194	TSR-H23-13	KRI-1	al 171	Vo-3
M2	147,975								
M7		104,66		102,39	101,59	94,12	82	100,24	111,53
M8		85,91	88,69	86,69	84,64	80,86		90,75	85,11
M9		193,49		167,56	187,89	175,01		176,41	201,97
M12	ca 53,55								
M13						{81,54}	82,7		

Table S11. Upper cheek teeth of *E. stenonis* from Sésklo. Lo= occlusal length; Bo= occlusal breadth; Lp= protocone length; Bp= protocone breadth

		n	x	min	max	s	cv	plication
P2	Lo	12	42,93	35,22	48,73	4,09	0,10	1.5, 2.8, 1.3, 1.1 / 0.4
	Bo	11	26,22	23,72	28,69	1,60	0,06	
	Lp	12	6,72	5,45	7,76	0,70	0,10	
	Bp	11	5,74	5,07	6,51	0,50	0,09	
P3/4	Lo	29	31,73	26,20	36,38	2,30	0,07	0.9, 2.4, 1.5, 1.1 / 0.9
	Bo	23	28,63	22,33	30,97	2,00	0,07	
	Lp	27	9,57	6,53	11,70	1,45	0,15	
	Bp	25	5,77	3,65	7,03	0,91	0,16	
M1/2	Lo	28	26,81	23,22	34,51	2,59	0,10	0.5, 2.6, 1.6, 1 / 1
	Bo	25	27,90	26,01	31,17	1,10	0,04	
	Lp	28	10,19	8,52	13,72	1,29	0,13	
	Bp	26	5,55	4,17	6,99	0,86	0,16	
M3	Lo	13	30,63	23,88	35,66	2,91	0,09	0.4, 3.8, 1.5, 1.2 / 1.1
	Bo	14	24,76	15,52	27,39	3,18	0,13	
	Lp	15	10,81	7,41	12,94	1,43	0,13	
	Bp	14	4,78	3,33	7,62	1,08	0,22	

Table S12. Upper cheek teeth of *E. stenonis* from Volax. Lo= occlusal length; Bo= occlusal breadth; Lp= protocone length; Bp= protocone breadth

		n	x	min	max	s	cv	plication
P2	Lo	3	41,03	40,21	41,76	0,78	0,02	1.3, 1, 0.7, 0.7 / 0.7
	Bo	3	27,40	26,98	27,66	0,37	0,01	
	Lp	3	6,39	5,94	6,98	0,54	0,08	
	Bp	3	5,44	5,04	5,83	0,40	0,07	
P3/4	Lo	3	31,72	30,12	34,45	2,38	0,07	1, 5.2, 1.8, 1 / 1
	Bo	3	29,39	28,58	30,18	0,80	0,03	
	Lp	5	8,20	7,54	9,27	0,83	0,10	
	Bp	5	5,39	5,15	6,12	0,41	0,08	
M1/2	Lo	1	31,50					1, 4, 2, 0 / 1
	Bo	3	27,68	22,93	32,72	4,90	0,18	
	Lp	4	8,76	8,10	9,68	0,68	0,08	
	Bp	3	4,42	4,12	4,72	0,30	0,07	
M3	Lo	2	28,00	24,93	31,07	4,34	0,16	1, 7, 2 , 1 / 1
	Bo	1	25,90					
	Lp	2	10,86	10,00	11,71	1,21	0,11	
	Bp	2	3,50	3,43	3,56	0,09	0,03	

Table S13. Upper cheek teeth of *E. stenonis* from Dafnero (DFN, DFN3). Lo= occlusal length; Bo= occlusal breadth; Lp= protocone length; Bp= protocone breadth

		n	x	min	max	s	cv	plication
P2	Lo	7	41,68	39,75	43,32	1,18	0,03	1.4, 3.4, 1.3, 0.8 / 0.6
	Bo	6	26,87	25,58	28,40	1,04	0,04	
	Lp	8	6,40	5,67	6,90	0,39	0,06	
	Bp	8	5,31	4,75	6,28	0,53	0,10	
P3/4	Lo	16	30,15	27,32	32,54	1,71	0,06	0.8, 3.6, 2.2, 0.9 / 0.9
	Bo	16	28,77	27,20	30,98	1,20	0,04	
	Lp	16	8,39	6,69	9,76	1,14	0,14	
	Bp	16	5,31	4,06	6,51	0,74	0,14	
M1/2	Lo	22	27,02	21,42	32,63	2,63	0,10	0.3, 2.6, 1.5, 0.6 / 0.8
	Bo	21	26,26	22,70	29,25	2,04	0,08	
	Lp	20	9,68	8,21	12,53	1,10	0,11	
	Bp	21	4,65	2,77	6,67	1,00	0,21	
M3	Lo	6	29,65	28,41	30,82	0,81	0,03	0.3, 2.9, 1.3, 1.8 / 0.8
	Bo	6	25,32	23,63	28,28	1,89	0,07	
	Lp	6	11,12	10,00	12,79	1,03	0,09	
	Bp	6	4,52	3,48	5,54	0,78	0,17	

Table S14. Upper cheek teeth of *E. altidens* from Gerakarou. Lo= occlusal length; Bo= occlusal breadth; Lp= protocone length; Bp= protocone breadth

		n	x	min	max	s	cv	plication
P2	Lo	10	38,25	36,28	40,40	1,46	0,04	1.8, 3.3, 1.6, 0.8 / 0.9
	Bo	10	25,95	23,21	27,40	1,72	0,07	
	Lp	10	6,40	5,52	7,14	0,49	0,08	
	Bp	10	5,19	4,62	5,75	0,40	0,08	
P3/4	Lo	20	28,48	25,22	31,42	1,68	0,06	0.5, 4.3, 1.8, 0.6 / 0.8
	Bo	20	27,74	25,52	29,67	1,13	0,04	
	Lp	20	7,71	6,08	9,25	0,67	0,09	
	Bp	20	5,38	4,87	6,26	0,37	0,07	
M1/2	Lo	21	25,14	21,59	27,62	1,64	0,07	0.3, 2.3, 1.5, 0,5 / 0.4
	Bo	22	25,42	22,00	27,15	1,24	0,05	
	Lp	22	8,38	7,09	9,68	0,68	0,08	
	Bp	21	4,93	3,89	5,84	0,46	0,09	
M3	Lo	9	27,04	25,65	28,53	1,00	0,04	0.4, 3.5, 1.3, 0.7 / 0.4
	Bo	9	23,70	21,92	25,45	1,23	0,05	
	Lp	9	9,33	8,74	10,36	0,59	0,06	
	Bp	9	4,35	3,51	5,06	0,53	0,12	

Table S15. Upper cheek teeth of *E. altidens* from Libakos. Lo= occlusal length; Bo= occlusal breadth; Lp= protocone length; Bp= protocone breadth.

		n	x	min	max	s	cv	plication
P2	Lo	13	36,55	32,02	39,56	2,00	0,05	2.6, 4, 2.9, 1 / 0.8
	Bo	12	25,08	21,42	27,33	1,43	0,06	
	Lp	9	7,00	6,18	9,84	1,14	0,16	
	Bp	10	5,17	3,65	6,25	0,97	0,19	
P3/4	Lo	45	28,75	26,30	32,78	1,47	0,05	1.5, 4.1, 2.5, 1.1 / 1.1
	Bo	43	26,64	22,24	29,31	1,70	0,06	
	Lp	38	8,99	7,12	11,73	1,23	0,14	
	Bp	37	5,37	3,15	6,76	0,75	0,14	
M1/2	Lo	49	26,00	23,27	31,25	2,10	0,08	1.2, 4, 3, 1.4 / 1.3
	Bo	47	24,30	19,69	28,38	1,93	0,08	
	Lp	42	9,74	5,30	11,97	1,20	0,12	
	Bp	42	4,75	3,44	6,49	0,60	0,13	
M3	Lo	16	24,75	20,64	29,69	2,31	0,09	1.8, 3.8, 2.2, 2 / 1.1
	Bo	15	22,19	18,23	25,56	2,05	0,09	
	Lp	13	10,68	9,08	12,13	1,13	0,11	
	Bp	13	3,90	3,27	5,02	0,54	0,14	

Table S16. Upper cheek teeth of *E. altidens* from Tsiotra Vrysi. Lo= occlusal length; Bo= occlusal breadth; Lp= protocone length; Bp= protocone breadth.

		n	x	min	max	s	cv	plication
P2	Lo	4	37,78	34,56	42,71	3,47	0,09	1.4, 2.5, 1.8, 0.8 / 0.8
	Bo	6	26,69	21,60	30,32	2,93	0,11	
	Lp	5	7,44	6,37	8,31	0,71	0,10	
	Bp	6	5,45	4,34	6,25	0,68	0,13	
P3/4	Lo	24	30,42	26,84	36,00	2,32	0,08	1.2, 3.9, 2.5, 1.1 / 0.9
	Bo	20	27,47	23,39	30,28	1,87	0,07	
	Lp	21	8,69	7,40	10,21	0,88	0,10	
	Bp	20	5,33	2,69	6,47	0,98	0,18	
M1/2	Lo	18	26,94	23,70	31,71	2,52	0,09	0.6, 3.2, 1.9, 1.1 / 0.5
	Bo	19	25,70	23,07	28,48	1,39	0,05	
	Lp	19	9,50	7,14	12,60	1,18	0,12	
	Bp	19	4,94	3,73	5,60	0,54	0,11	
M3	Lo	8	25,86	17,23	29,82	4,05	0,16	0.1, 2.3, 0.9, 0.9 / 0
	Bo	9	22,17	15,67	24,52	2,72	0,12	
	Lp	6	10,07	8,56	11,34	1,17	0,12	
	Bp	8	4,46	3,48	5,65	0,84	0,19	

Table S17. Upper cheek teeth of *E. altidens* from Krimni. Lo= occlusal length; Bo= occlusal breadth; Lp= protocone length; Bp= protocone breadth.

		n	x	min	max	s	cv	plication
P2	Lo	3	38,47	36,83	40,29	1,74	0,05	3, 4, 2, 1 / 1
	Bo	3	27,52	26,45	29,58	1,78	0,06	
	Lp	3	6,62	6,06	7,70	0,94	0,14	
	Bp	3	5,47	5,01	6,03	0,52	0,09	
P3/4	Lo	10	31,00	26,84	33,52	1,95	0,06	1.6, 5.2, 3, 1.2 / 1.1
	Bo	9	28,53	26,65	30,77	1,54	0,05	
	Lp	9	8,99	7,15	11,73	1,43	0,16	
	Bp	10	5,52	4,56	6,78	0,75	0,14	
M1/2	Lo	12	26,04	23,85	28,31	1,41	0,05	0.5, 4.6, 3.2, 0.8 / 0.3
	Bo	12	25,97	24,24	29,07	1,60	0,06	
	Lp	12	9,15	8,09	11,39	0,95	0,10	
	Bp	12	4,88	3,85	5,85	0,61	0,12	
M3	Lo	6	27,21	24,24	31,24	2,84	0,10	0.7, 3.6, 1.7, 1.6 / 0.7
	Bo	6	23,86	21,52	26,61	1,78	0,07	
	Lp	6	10,56	8,83	13,20	1,51	0,14	
	Bp	6	4,46	3,84	4,94	0,49	0,11	

Table S18. Upper cheek teeth of *E. altidens* from Petralona. Lo= occlusal length; Bo= occlusal breadth; Lp= protocone length; Bp= protocone breadth.

		n	x	min	max	s	cv	plication
P2	Lo	22	36,01	31,25	39,31	1,97	0,05	1.3, 3,7, 2.3, 1 / 0
	Bo	25	25,28	21,43	31,72	2,38	0,09	
	Lp	25	9,28	5,78	26,72	6,37	0,69	
	Bp	25	5,94	4,07	12,30	1,93	0,32	
P3/4	Lo	53	28,13	24,30	31,66	1,85	0,07	1.2, 3.1, 1.6, 0.8 / 0.6
	Bo	54	25,30	21,63	28,54	1,39	0,06	
	Lp	53	9,06	6,52	11,34	1,17	0,13	
	Bp	53	5,09	3,39	6,75	0,74	0,14	
M1/2	Lo	72	25,33	19,81	30,11	1,83	0,07	0,8, 2.8, 1.5, 0.8/ 0.5
	Bo	73	23,43	19,21	27,45	1,54	0,07	
	Lp	73	9,46	7,65	11,92	1,15	0,12	
	Bp	73	4,55	2,55	6,52	0,70	0,15	
M3	Lo	23	25,10	20,17	31,14	2,65	0,11	0.6, 2,2, 0.8, 0.6 / 0.4
	Bo	23	21,78	16,92	26,87	2,67	0,12	
	Lp	23	10,20	7,67	20,38	2,52	0,25	
	Bp	23	4,47	3,27	6,08	0,82	0,18	

Table S19. Upper cheek teeth of *E. apolloniensis* from Apollonia. Lo= occlusal length; Bo= occlusal breadth; Lp= protocone length; Bp= protocone breadth.

		n	x	min	max	s	cv	plication
P2	Lo	13	40,64	30,79	43,32	3,26	0,08	2.4. 4.3, 1.7, 0.6 / 0.8
	Bo	13	27,36	14,20	31,11	4,06	0,15	
	Lp	13	7,43	5,90	9,45	1,02	0,14	
	Bp	13	6,01	5,41	7,20	0,51	0,08	
P3/4	Lo	33	32,42	28,79	35,82	1,96	0,06	1.8, 6.5, 2.9, 0.9 / 0.9
	Bo	33	31,06	26,20	34,06	1,85	0,06	
	Lp	33	10,66	4,21	14,14	2,49	0,23	
	Bp	33	5,93	3,95	7,54	0,68	0,12	
M1/2	Lo	34	22,26	32,20	2,07	0,07	27,97	0.9, 5.6, 2.2, 1.1 / 0.6
	Bo	34	24,80	31,32	1,48	0,05	28,86	
	Lp	35	4,10	14,81	2,68	0,24	11,37	
	Bp	33	2,93	7,73	0,87	0,16	5,49	
M3	Lo	15	29,44	23,14	37,21	3,81	0,13	1.2, 4.9, 1.1, 1.3 / 0.6
	Bo	15	25,34	21,72	28,25	2,23	0,09	
	Lp	15	12,34	9,85	17,33	2,24	0,18	
	Bp	15	4,76	3,28	5,98	0,64	0,13	

Table S20. Upper cheek teeth of *E. apolloniensis* from Volos. Lo= occlusal length; Bo= occlusal breadth; Lp= protocone length; Bp= protocone breadth.

		n	x	min	max	s	cv	plication
P2	Lo	2	42,00	41,96	42,04	0,06	0,00	3, 5, 5, 1 / 1
	Bo	2	29,05	28,26	29,83	1,11	0,04	
	Lp	2	7,91	7,54	8,27	0,52	0,07	
	Bp	2	5,76	5,54	5,97	0,30	0,05	
P3/4	Lo	2	34,04	33,18	34,90	1,22	0,04	1, 7, 5, 1 / 0
	Bo	2	29,51	29,24	29,78	0,38	0,01	
	Lp	2	12,05	11,39	12,70	0,93	0,08	
	Bp	2	5,91	5,56	6,26	0,49	0,08	
M1/2	Lo	2	28,53	27,48	29,57	1,48	0,05	1, 2, 2, 1 / 0
	Bo	2	27,68	26,28	29,08	1,98	0,07	
	Lp	2	12,02	11,35	12,69	0,95	0,08	
	Bp	2	5,34	5,13	5,55	0,30	0,06	
M3	Lo	1	25,36					1, 2, ?, 0 / 0
	Bo	1	24,13					
	Lp	1	13,60					
	Bp	1	4,18					

Table S21. Upper cheek teeth of *E. ferus* from Aggitis. Lo= occlusal length; Bo= occlusal breadth; Lp= protocone length; Bp= protocone breadth.

		n	x	min	max	s	cv	plication
P3/4	Lo	2	32,36	30,16	34,61	3,15	0,10	1, 4.5, 3.5, 1 / 1
	Bo	2	29,84	29,33	30,34	0,71	0,02	
	Lp	2	13,34	12,62	14,06	1,02	0,08	
	Bp	2	5,62	5,24	5,99	0,53	0,09	
M1/2	Lo	2	31,56	28,09	34,57	3,21	0,10	1.6, 3, 1, 1.3 / 1
	Bo	2	26,43	23,80	28,70	2,03	0,08	
	Lp	1	14,03	12,42	15,23	1,45	0,10	
	Bp	2	5,16	4,55	5,49	0,42	0,08	
M3	Lo	1	{30,51}	{30,51}	{30,51}			2, 5, 2, 2 / 2
	Bo							
	Lp	1	14,07	14,07	14,07			
	Bp	1	5,04	5,04	5,04			

Table S22. Lower cheek teeth of *E. stenonis* from Sésklo. Lo= occlusal length; Bo ant= anterior occlusal breadth; Bo post= posterior occlusal breadth; Lprfl= preflexid length; Lptfl = postflexid length.

		n	x	min	max	s	cv
p2	Lo	1	36,80				
	Bo ant.	2	13,69	13,55	13,83	0,20	0,01
	Bo post.	1	16,63				
	Lprfl	2	8,18	7,82	8,53	0,50	0,06
	Lptfl	2	15,53	15,35	15,71	0,25	0,02
p3/4	Lo	2	31,46	30,83	32,08	0,88	0,03
	Bo ant.	2	17,74	17,44	18,04	0,42	0,02
	Bo post.	1	18,33				
	Lprfl	3	9,02	8,86	9,15	0,15	0,02
	Lptfl	3	14,12	13,79	14,43	0,32	0,02
m1/2	Lo	4	27,39	26,92	28,06	0,50	0,02
	Bo ant.	2	15,30	15,12	15,47	0,25	0,02
	Bo post.	4	13,67	12,23	14,31	0,97	0,07
	Lprfl	5	8,13	6,78	10,15	1,36	0,17
	Lptfl	5	10,89	9,66	11,63	0,74	0,07
m3	Lo	3	32,13	32,08	32,21	0,07	0,00
	Bo ant.	3	13,40	11,33	14,73	1,82	0,14
	Bo post.	3	11,88	10,48	12,81	1,23	0,10
	Lprfl	3	8,68	8,09	9,76	0,93	0,11
	Lptfl	3	12,39	11,39	13,34	0,98	0,08

Table S23. Lower cheek teeth of *E. stenonis* from Volax. Lo= occlusal length; Bo ant= anterior occlusal breadth; Bo post= posterior occlusal breadth; Lprfl= preflexid length; Lptfl = postflexid length.

		n	x	min	max	s	cv
p2	Lo	2	36,63	36,31	36,95	0,45	0,01
	Bo ant.	2	13,85	13,83	13,86	0,02	0,00
	Bo post.	1	15,91				
	Lprfl	2	8,83	8,79	8,86	0,05	0,01
	Lptfl	2	14,03	13,30	14,76	1,03	0,07
p3/4	Lo	4	30,16	29,26	31,41	1,00	0,03
	Bo ant.	4	16,97	16,78	17,27	0,23	0,01
	Bo post.	4	16,48	16,16	16,88	0,32	0,02
	Lprfl	4	8,70	8,12	9,24	0,47	0,05
	Lptfl	4	12,26	11,66	12,88	0,50	0,04
m1/2	Lo	3	28,11	26,85	30,12	1,76	0,06
	Bo ant.	3	15,07	14,71	15,54	0,43	0,03
	Bo post.	3	14,94	13,72	16,42	1,37	0,09
	Lprfl	3	7,52	7,28	7,83	0,28	0,04
	Lptfl	3	9,20	8,63	9,77	0,57	0,06
m3	Lo	1	31,59				
	Bo ant.	1	14,87				
	Bo post.	1	12,14				
	Lprfl	1	7,30				
	Lptfl	1	9,33				

Table S24. Lower cheek teeth of *E. stenonis* from Volax. Lo= occlusal length; Bo ant= anterior occlusal breadth; Bo post= posterior occlusal breadth; Lprfl= preflexid length; Lptfl = postflexid length.

		n	x	min	max	s	cv
p2	Lo	7	34,52	31,83	36,63	1,57	0,05
	Bo ant.	7	12,02	11,14	12,58	0,49	0,04
	Bo post.	7	15,41	14,11	16,02	0,67	0,04
	Lprfl	7	6,58	3,67	8,66	1,59	0,24
	Lptfl	7	14,42	13,52	15,44	0,63	0,04
p3/4	Lo	13	29,15	26,83	31,91	1,48	0,05
	Bo ant.	13	16,33	13,77	18,96	1,39	0,08
	Bo post.	13	16,07	13,98	19,09	1,21	0,08
	Lprfl	13	7,33	4,20	8,68	1,51	0,21
	Lptfl	13	11,10	7,67	15,04	2,26	0,20
m1/2	Lo	11	27,87	23,71	36,94	4,13	0,15
	Bo ant.	12	14,49	11,10	16,58	1,53	0,11
	Bo post.	11	13,14	11,76	14,10	0,82	0,06
	Lprfl	11	6,11	1,44	11,75	3,60	0,59
	Lptfl	11	9,43	4,92	12,35	2,70	0,29
m3	Lo	5	33,13	31,88	35,36	1,35	0,04
	Bo ant.	5	13,22	12,30	13,93	0,65	0,05
	Bo post.	5	11,67	11,19	12,42	0,48	0,04
	Lprfl	5	7,40	5,79	8,13	0,94	0,13
	Lptfl	5	8,95	7,58	9,90	0,85	0,10

Table S25. Lower cheek teeth of *E. altidens* from Gerakarou. Lo= occlusal length; Bo ant= anterior occlusal breadth; Bo post= posterior occlusal breadth; Lprfl= preflexid length; Lptfl = postflexid length.

		n	x	min	max	s	cv
p2	Lo	10	31,61	26,84	34,64	3,14	0,10
	Bo ant.	10	11,17	9,72	12,78	1,03	0,09
	Bo post.	11	14,24	13,22	14,97	0,56	0,04
	Lprfl	8	7,33	5,56	8,81	1,11	0,15
	Lptfl	11	12,27	6,79	15,78	3,38	0,28
p3/4	Lo	19	25,92	22,33	28,37	1,92	0,07
	Bo ant.	19	14,69	12,72	16,57	0,94	0,06
	Bo post.	19	14,52	13,03	16,02	0,74	0,05
	Lprfl	15	6,37	2,01	8,81	2,21	0,35
	Lptfl	19	8,45	2,77	14,15	3,94	0,47
m1/2	Lo	19	23,63	19,50	27,87	2,73	0,12
	Bo ant.	19	13,77	12,27	15,32	0,88	0,06
	Bo post.	19	12,28	11,16	14,18	0,64	0,05
	Lprfl	11	6,37	2,09	7,34	1,47	0,23
	Lptfl	12	7,27	2,33	9,11	2,08	0,29
m3	Lo	10	28,98	26,63	32,31	1,97	0,07
	Bo ant.	10	12,13	10,36	13,27	0,97	0,08
	Bo post.	10	10,40	9,08	11,50	0,79	0,08
	Lprfl	9	6,58	5,03	7,91	0,89	0,14
	Lptfl	9	6,62	4,07	8,95	1,47	0,22

Table S26. Lower cheek teeth of *E. altidens* from Libakos. Lo= occlusal length; Bo ant= anterior occlusal breadth; Bo post= posterior occlusal breadth; Lprfl= preflexid length; Lptfl = postflexid length.

		n	x	min	max	s	cv
p2	Lo	24	31,44	27,66	33,68	1,52	0,05
	Bo ant.	23	12,77	10,74	14,42	0,98	0,08
	Bo post.	23	14,40	12,11	15,83	0,81	0,06
	Lprfl	23	7,70	5,12	10,66	1,43	0,19
	Lptfl	24	14,24	12,01	17,23	1,26	0,09
p3/4	Lo	67	27,84	23,09	32,56	2,01	0,07
	Bo ant.	64	15,24	10,28	16,89	1,32	0,09
	Bo post.	60	16,92	10,76	144,86	16,85	1,00
	Lprfl	73	7,40	2,51	9,02	1,23	0,17
	Lptfl	72	12,09	5,86	15,93	2,46	0,20
m1/2	Lo	31	25,50	21,24	30,40	2,30	0,09
	Bo ant.	30	13,04	10,15	14,80	1,20	0,09
	Bo post.	30	12,12	8,78	13,47	1,06	0,09
	Lprfl	36	6,61	2,19	8,95	1,44	0,22
	Lptfl	37	7,66	3,81	9,35	1,52	0,20
m3	Lo	21	28,74	21,02	33,03	2,67	0,09
	Bo ant.	23	11,53	6,93	13,51	1,77	0,15
	Bo post.	24	10,42	6,19	12,38	1,49	0,14
	Lprfl	20	6,96	2,85	9,01	1,42	0,20
	Lptfl	22	7,63	3,85	9,60	1,44	0,19

Table S27. Lower cheek teeth of *E. altidens* from Tsiotra Vrysi. Lo= occlusal length; Bo ant= anterior occlusal breadth; Bo post= posterior occlusal breadth; Lprfl= preflexid length; Lptfl = postflexid length.

		n	x	min	max	s	cv
p2	Lo	9	32,97	30,12	36,46	1,86	0,06
	Bo ant.	12	12,33	9,77	13,91	1,06	0,09
	Bo post.	13	14,96	12,98	16,82	1,20	0,08
	Lprfl	13	7,70	4,51	9,47	1,41	0,18
	Lptfl	14	13,97	11,16	16,56	1,66	0,12
p3/4	Lo	23	28,22	25,24	31,50	1,61	0,06
	Bo ant.	22	15,54	13,14	17,56	1,11	0,07
	Bo post.	18	15,41	12,81	17,77	1,32	0,09
	Lprfl	31	7,19	2,48	12,71	2,06	0,29
	Lptfl	32	12,39	5,17	16,61	2,54	0,21
m1/2	Lo	33	26,86	22,45	30,85	1,76	0,07
	Bo ant.	33	13,66	8,90	16,51	1,40	0,10
	Bo post.	32	12,40	8,11	17,05	1,51	0,12
	Lprfl	39	7,06	2,52	26,68	3,47	0,49
	Lptfl	41	8,08	2,74	26,08	3,74	0,46
m3	Lo	14	30,68	26,62	35,05	2,47	0,08
	Bo ant.	13	12,43	10,12	13,71	1,10	0,09
	Bo post.	14	11,10	8,91	12,44	1,11	0,10
	Lprfl	16	7,28	6,37	8,07	0,47	0,06
	Lptfl	16	7,19	5,47	8,91	0,89	0,12

Table S28. Lower cheek teeth of *E. altidens* from Krimni. Lo= occlusal length; Bo ant= anterior occlusal breadth; Bo post= posterior occlusal breadth; Lprfl= preflexid length; Lptfl = postflexid length.

		n	x	min	max	s	cv
p2	Lo	1	> 32,88				
	Bo ant.	1	12,13				
	Bo post.	1	15,39				
	Lprfl	1	5,79				
	Lptfl	1	14,81				
p3/4	Lo	2	31,49	30,16	32,82	1,88	0,06
	Bo ant.	2	13,68	11,19	16,16	3,51	0,26
	Bo post.	2	14,65	12,47	16,82	3,08	0,21
	Lprfl	2	8,40	7,96	8,84	0,62	0,07
	Lptfl	2	16,26	15,18	17,34	1,53	0,09

Table S29. Lower cheek teeth of *E. altidens* from Petralona. Lo= occlusal length; Bo ant= anterior occlusal breadth; Bo post= posterior occlusal breadth; Lprfl= preflexid length; Lptfl = postflexid length.

		n	x	min	max	s	cv
p2	Lo	20	30,69	27,36	33,50	1,67	0,05
	Bo ant.	20	11,72	9,93	15,79	1,40	0,12
	Bo post.	20	13,62	6,43	15,79	1,90	0,14
	Lprfl	20	7,12	3,96	12,78	1,76	0,25
	Lptfl	20	15,70	13,11	33,70	4,33	0,28
p3/4	Lo	47	28,47	24,20	32,29	1,45	0,05
	Bo ant.	47	14,82	10,94	16,90	1,33	0,09
	Bo post.	47	15,04	11,27	16,92	1,10	0,07
	Lprfl	47	7,87	4,03	9,25	1,06	0,13
	Lptfl	47	13,23	5,87	16,46	2,32	0,18
m1/2	Lo	35	25,68	23,35	30,82	1,80	0,07
	Bo ant.	37	13,25	10,71	16,48	1,19	0,09
	Bo post.	36	12,41	10,09	16,40	1,28	0,10
	Lprfl	37	6,89	5,06	8,90	0,83	0,12
	Lptfl	37	8,30	6,01	14,50	1,52	0,18
m3	Lo	12	28,88	21,68	34,48	3,60	0,12
	Bo ant.	11	11,92	9,22	15,79	1,83	0,15
	Bo post.	11	10,68	7,90	15,79	2,11	0,20
	Lprfl	9	6,73	5,98	7,74	0,67	0,10
	Lptfl	9	8,68	6,61	14,50	2,31	0,27

Table S30. Lower cheek teeth of *E. apolloniensis* from Apollonia. Lo= occlusal length; Bo ant= anterior occlusal breadth; Bo post= posterior occlusal breadth; Lprfl= preflexid length; Lptfl = postflexid length.

		n	x	min	max	s	cv
p2	Lo	17	36,22	32,61	39,85	1,94	0,05
	Bo ant.	18	13,63	12,05	14,59	0,77	0,06
	Bo post.	18	16,18	14,61	17,32	0,68	0,04
	Lprfl	18	7,39		11,63	2,62	0,35
	Lptfl	19	15,99	13,81	18,64	1,41	0,09
p3/4	Lo	33	31,95	28,07	35,76	1,78	0,06
	Bo ant.	33	17,84	14,56	20,11	1,23	0,07
	Bo post.	33	17,87	14,98	20,10	0,99	0,06
	Lprfl	35	8,93	1,66	12,36	1,92	0,22
	Lptfl	34	13,63	10,29	17,21	2,09	0,15
m1/2	Lo	38	27,87	21,99	33,45	2,22	0,08
	Bo ant.	39	15,93	12,62	21,85	1,67	0,10
	Bo post.	39	14,35	11,95	17,86	1,08	0,08
	Lprfl	39	8,19	1,80	9,96	1,55	0,19
	Lptfl	40	10,70	6,87	14,00	1,67	0,16
m3	Lo	13	33,95	28,87	36,83	2,38	0,07
	Bo ant.	12	14,65	13,07	16,37	1,05	0,07
	Bo post.	12	12,63	10,84	13,92	0,95	0,08
	Lprfl	13	9,39	7,25	10,98	1,16	0,12
	Lptfl	13	10,39	7,47	12,85	1,56	0,15

Table S31. Lower cheek teeth of *E. apolloniensis* from Volos. Lo= occlusal length; Bo ant= anterior occlusal breadth; Bo post= posterior occlusal breadth; Lprfl= preflexid length; Lptfl = postflexid length.

		n	x	min	max	s	cv
p2	Lo	4	33,17	31,77	34,59	1,24	0,04
	Bo ant.	4	12,96	12,09	14,38	1,01	0,08
	Bo post.	4	16,61	15,47	18,20	1,16	0,07
	Lprfl	4	8,07	7,23	8,93	0,93	0,12
	Lptfl	4	17,77	14,98	19,71	2,22	0,13
p3/4	Lo	3	29,77	28,50	30,59	1,12	0,04
	Bo ant.	2	16,72	16,34	17,10	0,54	0,03
	Bo post.	3	16,80	16,78	16,82	0,02	0,00
	Lprfl	3	8,96	8,59	9,33	0,37	0,04
	Lptfl	3	14,71	14,58	14,80	0,12	0,01
m1/2	Lo	8	29,41	26,45	33,94	3,23	0,11
	Bo ant.	8	14,19	12,86	15,10	0,80	0,06
	Bo post.	7	13,03	12,33	13,75	0,53	0,04
	Lprfl	8	7,54	6,69	8,18	0,59	0,08
	Lptfl	8	10,07	7,68	12,69	2,06	0,20
m3	Lo	2	34,15	34,03	34,26	0,16	0,00
	Bo ant.	2	13,91	13,13	14,69	1,10	0,08
	Bo post.	2	13,00	12,58	13,41	0,59	0,05
	Lprfl	2	8,30	8,22	8,37	0,11	0,01
	Lptfl	2	8,93	8,88	8,97	0,06	0,01

Table S31. Lower cheek teeth of *Equus* aff. *E. a. granatensis* var *E. apolloniensis* from Volos. Lo= occlusal length; Bo ant= anterior occlusal breadth; Bo post= posterior occlusal breadth; Lprfl= preflexid length; Lptfl = postflexid length.

		n	x	min	max	s	cv
p2	Lo	2	37,06	36,71	37,40	0,49	0,01
	Bo ant.	3	11,68	9,22	13,04	2,14	0,18
	Bo post.	3	15,11	12,53	16,59	2,24	0,15
	Lprfl	2	9,38	9,31	9,45	0,10	0,01
	Lptfl	2	15,41	15,30	15,51	0,15	0,01
p3/4	Lo	4	31,33	30,23	32,11	0,82	0,03
	Bo ant.	6	14,76	8,13	17,93	4,38	0,30
	Bo post.	6	14,91	9,99	17,94	3,22	0,22
	Lprfl	4	8,50	7,68	9,27	0,73	0,09
	Lptfl	4	12,84	11,21	14,54	1,47	0,11
m1/2	Lo	1	31,66				
	Bo ant.	2	10,69	8,05	13,33	3,73	0,35
	Bo post.	2	9,19	6,84	11,54	3,32	0,36
	Lprfl	1	8,18				
	Lptfl	1	7,56				
m3	Lo	6	30,20	28,10	33,68	2,52	0,08
	Bo ant.	4	13,68	12,11	15,13	1,41	0,10
	Bo post.	6	12,43	10,03	13,40	1,34	0,11
	Lprfl	6	8,69	8,05	9,83	0,79	0,09
	Lptfl	6	9,27	8,53	10,89	0,98	0,11

Table S32. Lower cheek teeth of *E. ferus* from Aggitis. Lo= occlusal length; Bo ant= anterior occlusal breadth; Bo post= posterior occlusal breadth; Lprfl= preflexid length; Lptfl = postflexid length.

		n	x	min	max	s	cv
p2	Lo	1	37,49				
	Bo ant.	1	13,71				
	Bo post.	1	16,89				
	Lprfl	1	7,36				
	Lptfl	1	19,30				
p3/4	Lo	6	32,92	32,03	34,52	0,92	0,03
	Bo ant.	6	16,75	13,79	18,59	1,99	0,12
	Bo post.	5	16,29	13,24	18,98	2,76	0,17
	Lprfl	5	9,19	8,40	9,87	0,62	0,07
	Lptfl	6	15,32	14,16	16,40	0,87	0,06
m1/2	Lo	1	32,40				
	Bo ant.	1	13,80				
	Bo post.	1	15,46				
	Lprfl	1	8,76				
	Lptfl	1	14,60				

Table S33. Third metacarpal of *E. stenonis* from Sésklo. Measurements according to Eisenmann et al. (1988).

McIII	n	x	min	max	s	cv
M1	4	240,88	234,34	246,82	5,16	0,02
M2	4	230,96	225,99	235,66	3,99	0,02
M3	11	36,20	34,20	38,18	1,20	0,03
M4	9	28,22	26,02	30,19	1,16	0,04
M5	21	53,17	47,14	57,45	2,66	0,05
M6	25	34,74	31,73	37,85	1,67	0,05
M7	22	44,48	39,46	47,13	1,98	0,04
M8	25	16,21	9,49	18,67	1,84	0,11
M16	19	8,59	6,80	10,09	0,92	0,11
M9	5	3,08	2,15	4,74	0,98	0,32
M10	5	50,10	48,70	51,27	1,03	0,02
M11	5	49,50	47,87	51,63	1,43	0,03
M12	5	36,87	35,44	37,85	0,98	0,03
M13	4	28,16	27,68	29,11	0,67	0,02
M14	5	30,47	29,57	31,48	0,74	0,02

Table S34. Third metacarpal of *E. stenonis* from Dafnero. Measurements according to Eisenmann et al. (1988).

McIII	n	x	min	max	s	v
M1	20	232,54	221,41	244,54	6,97	0,03
M2	5	221,14	216,19	226,02	5,87	0,03
M3	7	34,96	34,13	36,69	1,76	0,05
M4	7	27,26	26,62	28,60	1,28	0,05
M5	5	52,52	50,21	54,69	2,08	0,04
M6	4	33,25	31,16	34,47	1,60	0,05
M7	5	43,87	42,10	45,97	1,70	0,04
M8	6	16,15	14,39	17,18	1,27	0,08
M16	3	7,83	6,87	8,69	0,87	0,11
M9						
M10	6	49,81	48,20	51,65	1,70	0,03
M11	5	48,94	45,73	51,01	1,98	0,04
M12	4	35,84	33,67	37,78	1,55	0,04
M13	5	28,23	26,82	29,81	1,05	0,04
M14	5	30,40	28,84	32,18	1,01	0,03

Table S35. Third metacarpal of *E. stenonis* from Volax. Measurements according to Eisenmann et al. (1988).

McIII	n	x	min	max	s	cv
M1	2	243,61	240,54	246,67	4,33	0,02
M2	2	239,14	236,20	242,07	4,15	0,02
M3	3	35,13	34,42	35,55	0,62	0,02
M4	3	28,41	27,10	29,39	1,18	0,04
M5	1	51,24				
M6	1	35,58				
M7	2	43,90	43,38	44,41	0,73	0,02
M8	1	15,25				
M16	2	8,38	8,25	8,50	0,18	0,02
M9						
M10	4	48,32	47,39	49,37	0,82	0,02
M11	4	48,42	47,12	49,60	1,28	0,03
M12	3	35,93	34,38	37,10	1,40	0,04
M13	3	28,01	26,47	29,05	1,36	0,05
M14	3	29,93	28,32	31,40	1,55	0,05

Table S36. Third metacarpal of *E. altidens* from Gerakarou. Measurements according to Eisenmann et al. (1988).

McIII	n	x	min	max	s	cv
M1	12	232,21	225,60	236,87	4,08	0,02
M2	11	224,98	218,21	229,87	4,28	0,02
M3	12	32,25	30,00	35,79	1,71	0,05
M4	12	26,56	25,05	29,61	1,28	0,05
M5	13	46,29	44,28	48,31	1,37	0,03
M6	12	30,26	28,49	32,55	1,28	0,04
M7	13	38,79	36,00	41,40	1,87	0,05
M8	13	14,83	13,30	16,44	0,90	0,06
M16	7	7,75	5,43	8,99	1,26	0,16
M9	2	7,11	6,48	7,74	0,89	0,13
M10	10	44,74	42,85	47,41	1,34	0,03
M11	10	42,79	41,07	44,28	1,02	0,02
M12	11	32,59	31,34	34,25	0,97	0,03
M13	11	25,42	24,04	26,82	0,78	0,03
M14	10	28,43	27,44	29,76	0,76	0,03

Table S37. Third metacarpal of *E. altidens* from Libakos. Measurements according to Eisenmann et al. (1988).

McIII	n	x	min	max	s	cv
M1	19	232,08	222,40	244,90	6,36	0,03
M2	19	222,84	211,80	234,50	6,62	0,03
M3	20	32,80	30,20	36,30	1,62	0,05
M4	20	26,80	25,00	28,60	1,04	0,04
M5	21	46,82	43,20	50,40	1,94	0,04
M6	20	29,33	27,50	33,40	1,37	0,05
M7	17	39,11	36,70	42,40	1,48	0,04
M8	18	15,43	13,90	17,50	1,03	0,07
M16	19	8,67	7,20	10,50	0,90	0,10
M9	9	3,56	2,20	4,50	0,86	0,24
M10	27	44,25	40,40	48,00	1,82	0,04
M11	25	43,28	40,10	47,20	1,91	0,04
M12	25	33,64	31,60	37,00	1,41	0,04
M13	29	25,85	23,30	27,90	1,17	0,05
M14	27	28,80	26,00	31,10	1,28	0,04

Table S38. Third metacarpal of *E. altidens* from Krimni. Measurements according to Eisenmann et al. (1988).

McIII	n	x	min	max	s	cv
M1	4	243,78	237,25	247,17	4,44	0,02
M2	4	236,80	230,70	240,44	4,24	0,02
M3	4	32,95	31,50	35,33	1,66	0,05
M4	4	26,72	26,49	27,03	0,25	0,01
M5	4	46,56	44,54	47,99	1,49	0,03
M6	4	31,55	29,35	33,39	1,68	0,05
M7	3	39,69	38,92	40,32	0,71	0,02
M8	3	15,89	14,94	16,49	0,83	0,05
M16	3	7,11	6,52	7,56	0,53	0,07
M9	1	4,84				
M10	4	45,55	43,53	47,32	1,57	0,03
M11	3	45,11	42,97	46,41	1,87	0,04
M12	4	33,79	30,14	35,41	2,50	0,07
M13	4	26,76	25,29	27,73	1,11	0,04
M14	4	29,77	27,27	31,28	1,78	0,06

Table S39. Third metacarpal of *E. altidens* from Petralona. Measurements according to Eisenmann et al. (1988).

McIII	n	x	min	max	s	cv
M1	9	230,98	218,10	241,43	7,39	0,03
M2	9	223,08	208,50	234,61	8,18	0,04
M3	14	30,23	26,88	33,46	1,96	0,06
M4	14	25,17	22,83	26,52	0,98	0,04
M5	14	44,98	42,26	47,56	1,82	0,04
M6	13	29,66	25,60	31,86	1,90	0,06
M7	14	37,43	34,76	40,12	1,56	0,04
M8	14	14,48	12,88	15,73	1,01	0,07
M16	12	8,48	7,42	12,81	1,55	0,18
M9	3	4,90	3,01	7,26	2,16	0,44
M10	18	41,95	38,31	44,72	1,78	0,04
M11	18	41,43	38,50	44,80	1,72	0,04
M12	17	32,11	29,59	34,08	1,14	0,04
M13	17	25,22	22,84	26,38	0,98	0,04
M14	16	27,58	24,56	29,42	1,32	0,05

Table S40. Third metacarpal of *E. altidens* from Tsiotra Vrysi. Measurements according to Eisenmann et al. (1988).

McIII	n	x	min	max	s	cv
M1	17	240,98	235,06	254,61	5,09	0,02
M2	17	232,22	225,90	243,84	4,66	0,02
M3	19	31,13	27,95	34,45	1,89	0,06
M4	19	25,59	21,35	28,01	1,71	0,07
M5	19	46,74	42,06	51,32	2,37	0,05
M6	18	31,27	29,39	34,04	1,26	0,04
M7	18	38,95	36,78	41,06	1,48	0,04
M8	19	14,76	11,53	18,96	1,60	0,11
M16	11	7,07	4,05	8,77	1,41	0,20
M9	10	3,57	2,36	5,32	0,81	0,23
M10	16	45,07	43,35	49,16	1,60	0,04
M11	16	43,58	41,65	47,06	1,48	0,03
M12	16	32,69	31,13	34,50	0,99	0,03
M13	16	26,02	24,59	27,59	0,89	0,03
M14	17	28,65	27,14	30,10	0,83	0,03

Table S41. Third metacarpal of *E. apolloniensis* from Apollonia. Measurements according to Eisenmann et al. (1988).

McIII	n	x	min	max	s	cv
M1	17	247,77	230,28	257,75	7,32	0,03
M2	17	238,56	221,26	249,80	7,45	0,03
M3	22	35,46	32,62	38,44	1,50	0,04
M4	21	28,82	26,78	31,52	1,20	0,04
M5	23	53,11	48,74	57,87	2,20	0,04
M6	24	35,42	32,74	37,75	1,35	0,04
M7	22	44,95	42,06	48,33	1,84	0,04
M8	22	16,39	13,89	18,51	1,17	0,07
M16	20	9,20	6,92	10,82	1,23	0,13
M9	8	4,90	3,44	5,99	1,00	0,20
M10	21	51,22	46,89	54,51	1,95	0,04
M11	20	50,73	46,59	53,27	1,76	0,03
M12	20	37,30	35,46	38,98	1,17	0,03
M13	21	29,12	27,45	30,35	0,92	0,03
M14	21	32,08	30,61	33,71	0,89	0,03

Table S42. Third metacarpal of *Equus* aff. *E. a. granatensis* var *E. apolloniensis* from Tsiotra Vrysi. Measurements according to Eisenmann et al. (1988).

McIII	n	x	min	max	s	cv
M1	4	250,31	246,46	253,77	3,59	0,01
M2	4	243,63	241,56	245,60	1,82	0,01
M3	4	37,43	35,23	39,59	1,87	0,05
M4	4	27,13	25,87	28,37	1,39	0,05
M5	3	52,14	50,59	54,35	1,97	0,04
M6	2	31,63	29,80	33,45	2,58	0,08
M7	3	42,42	40,97	44,27	1,69	0,04
M8	3	15,60	14,76	16,08	0,73	0,05
M16	2	7,56	7,18	7,94	0,54	0,07
M9	2	3,19	2,97	3,40	0,30	0,10
M10	2	47,81	46,60	49,01	1,70	0,04
M11	1	45,69				
M12	1	35,20				
M13	1	27,22				
M14	1	30,02				

Table S43. Third metacarpal of *Equus* aff. *E. suessenbornensis* from Vassiloudi. Measurements according to Eisenmann et al. (1988).

McIII	n	x	min	max	s	cv
M1	1	260,15				
M2	1	255,98				
M3	1	41,78				
M4	1	25,77				
M5	1	56,23				
M6	1	33,19				
M7	1	46,35				
M8	1	15,67				
M10	2	49,85	48,85	50,84	1,41	0,03
M11	2	47,48	46,12	48,83	1,92	0,04
M12	2	35,64	34,51	36,76	1,59	0,04
M13	2	27,74	26,94	28,54	1,13	0,04
M14	2	30,74	29,76	31,71	1,38	0,04

Table S44. Third metacarpal of *Equus* aff. *E. a. granatensis* var *E. apolloniensis* from Platanochori. Measurements according to Eisenmann et al. (1988).

McIII	n	x	min	max	s	cv
M3	2	36,42	36,37	36,46	0,06	0,00
M4	2	29,02	28,72	29,31	0,42	0,01
M5	2	54,85	54,71	54,98	0,19	0,00
M6	2	35,95	35,32	36,58	0,89	0,02
M7	2	44,59	42,87	46,31	2,43	0,05
M8	3	16,90	14,71	18,27	1,91	0,11
M16	2	10,21	9,18	11,24	1,46	0,14
M9	1	5,60				

Table S45. Third metacarpal of *Equus* aff. *E. stenonis* var *E. apolloniensis* from Vatera. Measurements according to Eisenmann et al. (1988).

McIII	n	x	min	max	s	cv
M1	3	246,61	236,33	253,55	9,08	0,04
M2	3	235,73	225,99	241,34	8,47	0,04
M3	3	35,47	34,68	36,10	0,72	0,02
M4	3	27,63	27,22	28,43	0,69	0,03
M5	3	54,15	52,97	55,60	1,33	0,02
M6	3	35,72	35,13	36,38	0,63	0,02
M7	3	45,21	43,72	46,34	1,35	0,03
M8	3	17,53	17,06	17,81	0,41	0,02
M16	2	10,56	9,66	11,45	1,27	0,12
M9	1	3,41				
M10	3	50,64	47,59	52,60	2,67	0,05
M11	3	50,05	47,65	51,96	2,20	0,04
M12	3	37,96	36,48	39,03	1,33	0,03
M13	3	28,85	27,42	29,59	1,24	0,04
M14	3	31,61	30,45	32,72	1,14	0,04

Table S46. Third metatarsal of *E. stenonis* from Sésklo. Measurements according to Eisenmann et al. (1988).

MtIII	n	x	min	max	s	cv
M1	7	280,40	276,36	289,57	23,28	0,08
M2	7	270,85	265,20	278,44	13,93	0,05
M3	10	35,30	33,08	38,91	1,94	0,06
M4	11	34,00	30,39	35,35	1,47	0,04
M5	22	49,88	46,20	52,81	1,55	0,03
M6	23	39,08	35,22	42,40	1,67	0,04
M7	21	46,25	43,20	48,95	1,35	0,03
M8	22	12,02	9,78	14,74	1,35	0,11
M9	21	7,61	6,17	10,80	0,97	0,13
M10	7	50,20	48,38	53,59	1,98	0,04
M11	6	48,70	45,51	50,35	1,64	0,03
M12	7	37,30	34,82	39,74	1,51	0,04
M13	7	28,10	25,58	29,08	0,95	0,03
M14	6	31,50	29,81	32,57	0,80	0,03

Table S47. Third metatarsal of *E. stenonis* from Dafnero. Measurements according to Eisenmann et al. (1988).

MtIII	n	x	min	max	s	cv
M1	18	268,55	257,78	281,20	8,25	0,03
M2	21	258,84	245,83	273,38	8,37	0,03
M3	24	35,44	32,42	38,35	1,58	0,04
M4	24	31,84	27,90	35,59	1,79	0,06
M5	22	49,41	45,18	52,92	1,93	0,04
M6	22	37,75	32,19	41,29	2,11	0,06
M7	21	45,38	40,90	48,33	1,86	0,04
M8	22	12,55	9,83	15,95	1,43	0,11
M9	23	8,02	6,02	11,38	1,05	0,13
M10	22	48,58	44,00	50,81	1,87	0,04
M11	20	47,78	44,87	50,93	1,89	0,04
M12	15	36,09	32,85	38,91	1,64	0,05
M13	18	26,26	24,30	28,56	1,32	0,05
M14	19	29,99	27,94	32,46	1,21	0,04

Table S48. Third metatarsal of *E. stenonis* from Volax. Measurements according to Eisenmann et al. (1988).

MtIII	n	x	min	max	s	cv
M1	2	276,64	269,80	283,47	9,67	0,03
M2	2	267,94	261,40	274,47	9,24	0,03
M3	5	35,80	33,78	37,01	1,26	0,04
M4	5	33,04	31,10	33,64	1,09	0,03
M5	3	49,35	48,65	50,42	0,94	0,02
M6	3	40,67	40,27	41,31	0,56	0,01
M7	2	47,17	46,82	47,51	0,49	0,01
M8	4	11,92	11,05	12,69	0,85	0,07
M9	1	7,93				
M10	4	48,12	47,08	49,13	0,94	0,02
M11	4	47,60	46,48	49,76	1,48	0,03
M12	4	36,24	34,70	37,91	1,44	0,04
M13	3	27,23	25,17	29,04	1,95	0,07
M14	5	30,69	29,46	31,61	0,86	0,03

Table S49. Third metatarsal of *E. altidens* from Gerakarou. Measurements according to Eisenmann et al. (1988).

MtIII	n	x	min	max	s	cv
M1	13	265,46	255,15	276,35	6,46	0,02
M2	13	257,90	247,71	270,50	6,71	0,03
M3	14	30,60	28,73	32,69	1,04	0,03
M4	14	29,19	27,56	30,29	0,86	0,03
M5	13	44,98	42,70	48,28	1,80	0,04
M6	16	34,93	32,44	37,53	1,65	0,05
M7	13	41,40	38,49	43,92	1,93	0,05
M8	9	10,90	9,23	12,79	1,30	0,12
M9	10	6,79	3,75	8,54	1,40	0,21
M10	17	43,16	39,84	45,31	1,36	0,03
M11	16	41,81	38,43	43,47	1,39	0,03
M12	14	33,60	31,78	35,36	1,13	0,03
M13	15	24,57	22,76	25,73	0,78	0,03
M14	14	28,40	26,95	29,75	0,87	0,03

Table S50. Third metatarsal of *E. altidens* from Libakos. Measurements according to Eisenmann et al. (1988).

MtIII	n	x	min	max	s	cv
M1	32	267,67	255,10	285,40	7,11	0,03
M2	32	259,77	246,60	279,20	7,62	0,03
M3	37	31,59	28,00	35,70	1,71	0,05
M4	37	31,18	29,30	34,00	1,27	0,04
M5	34	45,38	37,50	48,30	2,19	0,05
M6	33	36,49	33,50	38,70	1,31	0,04
M7	38	43,03	40,30	47,30	1,79	0,04
M8	28	11,21	9,50	13,20	1,00	0,09
M9	29	8,67	6,70	10,50	0,94	0,11
M10	33	44,45	41,20	47,60	1,73	0,04
M11	31	43,39	40,10	45,50	1,19	0,03
M12	30	34,67	32,40	37,10	1,24	0,04
M13	33	25,48	23,90	27,60	0,88	0,03
M14	32	29,65	27,90	31,70	1,01	0,03

Table S51. Third metatarsal of *E. altidens* from Tsiotra Vrysi. Measurements according to Eisenmann et al. (1988).

MtIII	n	x	min	max	s	cv
M1	14	271,98	262,12	279,20	6,92	0,03
M2	13	264,25	251,65	275,98	8,40	0,03
M3	15	31,24	26,85	35,22	1,76	0,06
M4	15	30,34	26,95	33,26	1,91	0,06
M5	16	45,13	41,50	47,91	1,75	0,04
M6	15	34,83	31,63	36,84	1,65	0,05
M7	15	41,69	39,40	43,16	1,20	0,03
M8	15	11,03	9,56	14,39	1,20	0,11
M9	13	6,96	4,51	9,25	1,62	0,23
M10	16	43,81	40,89	47,45	2,02	0,05
M11	13	43,05	40,67	45,69	1,55	0,04
M12	13	33,48	30,55	36,72	1,61	0,05
M13	13	25,24	23,88	27,43	1,00	0,04
M14	13	29,09	27,56	30,78	0,92	0,03

Table S52. Third metatarsal of *E. altidens* from Tsiotra Vrysi. Measurements according to Eisenmann et al. (1988).

MtIII	n	x	min	max	s	cv
M1	5	268,15	259,27	274,53	7,93	0,03
M2	5	258,88	250,77	266,98	8,74	0,03
M3	5	33,26	32,77	33,75	1,98	0,06
M4	5	30,72	29,03	32,40	1,42	0,05
M5	5	45,61	44,77	46,44	1,10	0,02
M6	5	35,08	33,24	36,31	1,16	0,03
M7	5	42,91	42,28	43,54	0,95	0,02
M8	5	11,37	11,11	11,62	0,50	0,04
M9	5	5,88	5,57	6,18	0,68	0,12
M10	5	46,10	44,94	47,07	1,68	0,04
M11	5	44,10	42,64	45,12	1,71	0,04
M12	5	33,83	33,17	34,97	0,93	0,03
M13	5	25,09	24,32	25,75	0,59	0,02
M14	5	28,97	28,15	29,51	0,64	0,02

Table S53. Third metatarsal of *E. altidens* from Petralona. Measurements according to Eisenmann et al. (1988).

MtIII	n	x	min	max	s	cv
M1	16	270,94	245,12	285,30	10,47	0,04
M2	17	262,75	236,38	275,94	10,57	0,04
M3	26	30,54	26,93	34,42	1,82	0,06
M4	27	29,42	27,75	30,84	0,93	0,03
M5	22	41,46	26,70	47,91	3,76	0,09
M6	23	33,74	30,43	36,81	1,87	0,06
M7	22	39,61	37,50	45,99	1,96	0,05
M8	19	10,71	7,82	13,08	1,33	0,12
M9	27	7,05	5,56	9,50	0,91	0,13
M10	35	41,36	38,61	56,13	2,97	0,07
M11	34	41,97	39,66	57,28	2,95	0,07
M12	33	33,28	30,71	40,34	1,79	0,05
M13	33	25,29	22,80	30,71	1,32	0,05
M14	33	28,50	25,71	34,49	1,56	0,05

Table S54. Third metatarsal of *E. apolloniensis* from Apollonia. Measurements according to Eisenmann et al. (1988).

MtIII	n	x	min	max	s	cv
M1	21	292,56	282,51	307,52	6,52	0,02
M2	21	271,83	33,86	299,14	54,90	0,20
M3	36	34,95	31,60	37,16	1,43	0,04
M4	35	33,16	29,28	36,17	1,65	0,05
M5	33	50,03	41,32	54,91	2,45	0,05
M6	32	40,48	37,30	47,12	2,00	0,05
M7	29	47,10	44,48	52,03	1,61	0,03
M8	32	11,90	8,51	13,73	1,08	0,09
M9	29	7,97	6,10	10,13	1,08	0,13
M10	31	50,36	44,79	53,69	1,93	0,04
M11	28	49,92	44,74	53,00	1,87	0,04
M12	29	38,89	37,07	40,74	1,02	0,03
M13	29	28,80	25,82	30,37	0,99	0,03
M14	30	32,37	28,73	34,58	1,12	0,03

Table S55. Third metatarsal of *Equus* aff. *E. a. granatensis* var *E. apolloniensis* from Tsiotra Vrysi. Measurements according to Eisenmann et al. (1988).

MtIII	n	x	min	max	s	cv
M1	4	277,18	272,06	283,95	4,95	0,02
M2	3	269,28	267,19	272,79	3,06	0,01
M3	3	33,88	32,17	35,86	1,86	0,05
M4	3	32,97	30,30	34,85	2,37	0,07
M5	2	52,92	52,26	53,58	0,93	0,02
M6	1	41,42				
M7	2	48,79	48,55	49,02	0,33	0,01
M8	4	12,48	11,53	13,64	0,96	0,08
M9	2	9,47	8,96	9,97	0,71	0,08
M10	3	48,51	47,18	49,69	1,26	0,03
M11	3	47,08	45,55	48,16	1,36	0,03
M12	3	37,60	36,65	38,32	0,86	0,02
M13	3	27,90	27,61	28,43	0,46	0,02
M14	3	31,55	30,78	32,30	0,76	0,02

Table S56. Third metatarsal of *Equus* aff. *E. a. granatensis* var *E. apolloniensis* from Platanochori. Measurements according to Eisenmann et al. (1988).

MtIII	n	x	min	max	s	cv
M5	2	48,58	48,31	48,85	0,38	0,01
M6	2	38,87	38,51	39,22	0,50	0,01
M7	1	47,50				
M8	1	9,52				
M9	1	4,87				

Table S57. Third metatarsal of *Equus* aff. *E. stenonis* var *E. apolloniensis* from Vatera. Measurements according to Eisenmann et al. (1988).

MtIII	n	x	min	max	s	cv
M1	2	286,01	283,55	288,46	3,47	0,01
M2	2	274,64	272,72	276,56	2,72	0,01
M3	2	34,86	34,19	35,53	0,95	0,03
M4	2	32,81	32,70	32,91	0,15	0,00
M5	1	50,98				
M6	1	42,16				
M7	1	46,30				
M8	1	13,64				
M9	1	9,38				
M10	2	51,30	50,50	52,09	1,12	0,02
M11	2	49,06	48,00	50,11	1,49	0,03
M12	2	39,24	38,73	39,74	0,71	0,02
M13	2	28,78	28,75	28,81	0,04	0,00
M14	2	32,18	31,33	33,03	1,20	0,04

Table S58. Third metatarsal of *E. ferus* from Aggitis. Measurements according to Eisenmann et al. (1988).

MtIII	n	x	min	max	s	cv
M5	56,1	1,00	56,10	56,10		
M6	42,63	1,00	42,63	42,63		
M7	51,15	1,00	51,15	51,15		
M8	14,54	1,00	14,54	14,54		
M10	54,76	2,00	54,60	54,92	0,23	0,00
M11	56,075	2,00	55,99	56,16	0,12	0,00
M12	41,325	2,00	40,40	42,25	1,31	0,03
M13	31,295	2,00	30,75	31,84	0,77	0,02
M14	36,255	2,00	35,10	37,41	1,63	0,05

Phylogenetic analysis

Abbreviations of the institutions:

AC: Laboratoires d'Anatomie Comparée et des Mammifères du Muséum National d'Historie Naturelle; Paris, France; **AMPG:** Museum of Palaeontology and Geology of the National and Kapodistrian University of Athens; **ANSP:** Academy of Natural Science of Philadelphia, USA; **CMNH**: Carnegie Museum of Natural Histort, Pittsburgh, USA; **D:** Old Dmanisi Collection, S. Janashia Museum of Georgia, Georgian National Museum; Tbilisi, Republic of Georgia; **DLJ:** Dalian Jinyuan Cave, China; **Dm:** New Dmanisi Collection, S. Janashia Museum of Georgia, Georgian National Museum; Tbilisi, Republic of Georgia; **DMNH**: Denver Museum of Natural History, Denver, USA; **FAM:** Frick Collection, American Museum of Natural History; New York, USA.; **FMNH:** Vertebrate Paleonotology (Fossil Mammal) Field Museum of Natural History; Chicago, USA; **HNHM**: Hungarian Natural History Museum, Budapest, Hungary; **HPM**, Hezheng Paleozoological Museum, Hezheng, China; **IGCU:** Instituto de Geología, Ciudad Universitaria; Juriquilla, Mexico; **IGF:** Museo di Storia Naturale, Università di Firenze, Sezione Geologia e Paleontologia; Firenze, Italy; **IGM:** Instituto de Geología; Juriquilla, Mexico; **IVPP:** Institute of Vertebrate Paleontology and Paleoanthropology; Beijing, China; **KNM – ER:** Kenyan Natural History Museum, East Rudolf; Nairobi, Kenya; **L:** Liventsovka, Regional Ethnographic Museum; Rostov – on – Don, Russia; **LGPUT**: Museum of Geology-Palaeontology-Palaeoanthropology of the Aristotle University of Thessaloniki; **MCZ:** Harvard University; Cambridge, USA; **MMP:** Museo de Ciencias 'Lorenzo Scaglia,' Mar Del Plata, Buenos Aires, Argentina; **MNHN:** Muséum National d'Historie Naturelle; Paris, France; **MPGJ:** Museo de Paleontología Geociencias; Juriquilla, Mexico; **MPH:** Museo Municipal 'Punta Hermengo,' Miramar, Argentina; **MSM**: Mesa Southwest Museum,

USA; **MSNF**: Museo di Sotira Naturale, Università di Firenze, sezione di Zoologia "La Specola", Firenze, Italy; **NHML:** Natural History Museum of Lyon; Lyon, France; **NHMUK:** Natural History Museum; London, United Kingdom; **NIH:** Muséum National d'Historie Naturelle, Nihewan collection; Paris, France; **NWUV:** Vertebrate Paleontology of Institute of Cenozoic Geology and Environment, Northwest University; Xian, China; **PMU M:** Museum of Evolution of Uppsala University; Uppsala, Sweden; **RGU:** State University of Rostov; Rostov – on – Don, Russia; **UCBL-FSL:** Université Claude Bernard-1, Paleontological Collection; Lyon, France; **USNM:** National Museum of Natural History, Washington D.C, USA; **YPM:** Yale Peabody Museum, New Haven, USA; **ZIN:** Zoological Institute, Saint Petersburg, Russia; **ZU:** Zoologisches Museum der Universität; Zürich, Switzerland.

The list of taxa and their related specimens used to create the phylogenetic matrix was taken from Cirilli et al. (2021) with additional data on selected specimens by the present author:

Tapirus terrestris
Data: Antoine (2002); Antoine et al. (2010); Cirilli et al. (2021).
Specimens: HNHM 77.299.1; MNHN no code; MSNF no code.

Hyrachyus eximius
Data: Antoine (2002); Antoine et al. (2010) Cirilli et al. (2021).
Specimens: AMNH 5065; AMNH 12354; AMNH 12355; AMNH 12364; AMNH 107978; AMNH 12371.

Trigonias osborni
Data: Antoine (2002); Prothero (2005); Antoine et al. (2010); Pandolfi (2015);.
Specimens: AMNH 9847; CMNH 97; CMNH 897; CMNH 8929; DMNH 890; DMNH 1056; DMNH 1510; DMNH 24800; MSM 97-21

Merychippus insignis
Data: Vera Eisenmann Website https://vera-eisenmann.com/ ; Woodbourne M.O. (2003).
Specimens: FAM 870001; FAM 87003; FAM 87001; FAM 87004; FAM 87005; FAM 87072; FAM 87078; FAM 87080; ANSP 11276; FAM. No 87006; FAM No. 87000; FAM 87002;

Merychippus isoneus

Data: Cirilli et al. (2021).

Specimens: AMNH 14179, complete skeleton (cast housed in the Natural History museum in Florence)

Cormohipparion occidentale

Data: MacFadden (1984); Bernor et al. (2018); Cirilli et al. (2021).

Specimens: FAM71800; FAM71855; FAM71856; FAM71857; FAM71858; FAM71859; FAM71860; FAM71861; FAM71862; FAM71863;

Pliohippus pernix

Data: Cirilli et al. (2021).

Specimens: YPM13007; partial skeleton.

Dinohippus leidyanus

Data: Azzaroli 1986; Cirilli et al. (2021).

Specimens: AMNH 18972; AMNH 87201; AMNH 116129; AMNH 116970; AMNH116134; AMNH 116135; AMNH 87204; AMNH 87208; AMNH 87209; AMNH 87112;

Dinohippus mexicanus

Data: MacFadden, B., and Carranza-Castañada, (2002); Cirilli et al. (2021).

Specimens: IGM 7596; MPGJ 1982; MPGJ 1683; MPGJ 103; MPGJ 5132; MPGJ 1967; IGCU 11503; MPGJ 3987; MPGJ 4040; MPGJ 1982; IGM 7596; MPGJ 856; MPGJ 5129; MPGJ 5126; MPGJ 857; MPGJ 1683

Hippidion principale

Data: MacFadden (1997); Alberdi et al. (1996); Alberdi et al. (2001); Cirilli et al. (2021).

Specimens: Complete skeleton, fig. 2 in MacFadden, 1997; FMNH14200; MPH-P067; MMP-2600.

Hippidion saldiasi

Data: Alberdi et al. (2007); Alberdi et al. (2001); Cirilli et al. (2021).

Specimens: Betecsa 1, AEP1 F(e) 195/1

Equus simplicidens

Data: Cirilli et al. (2021).

Specimens: USNM11989; USNM12481; USNM11989; USNM12501; USNM12522; USNM12528; USNM12535; USNM12538; USNM12542; USNM12543; USNM12546; USNM12547; USNM12548; USNM12573; USNM12576; USNM13793; USNM13835; USNM13841; USNM13841; USNM13842; USNM16785; USNM16982; USNM16985; USNM16987; USNM16995; USNM12522; USNM12538; USNM12546; USNM12570; USNM13791; USNM13792; USNM12793; USNM17000; USNM 16320; USNM 13791; USNM 12573; USNM222034; USNM222041; USNM222025; USNM222036; USNM222029; USNM 13791; USNM 12573; USNM 16320; USNM 13791; USNM 12573; USNM 16320; USNM 13791; USNM 12573

Equus qingyangensis

Data: Deng (1999); Sun et al. (2017); Sun et al. (2020); Cirilli et al. (2021).

Specimens: NWUV1128; NWUV1129; NWUV1134; NWUV1152; NWUV1155; NWUV1128; NWUV DLJ-2016-11-09; NWUV - M 1324

Equus eisenmannae

Data: Personal observations; Qiu et al., 2004 ; Sun and Deng, 2019; Cirilli et al. (2021).

Specimens: IVPP V 13552; HMV1V 1105; HMV 1103; HMV 1105; LDU008; LDL009; LDL012; HZT022; HZT023; HZT024; HZT025; HZT026; HZT027; LDL032; LDL033; LDU013; LDU014; LDL015; LDL016; LDL017; LDL018; LDL019; LDL020; LDL022; HZT028; HZT029; HZU030; HZT031; HZU033; HZT034; HZT035; HZT037; HZT038; LDL035; LDL036; LDL037; LDL038;

Equus sanmeniensis

Data: Personal observations; Kalmiakov, 2015; Sun and Deng, 2019; Cirilli et al. (2021).

Specimens: NIH 002;

Equus huanghoensis

Data: Cirilli et al. (2021).

Specimens: NWUV1403.1, NWUV1403.2; NWUV19039;

Equus teilhardi

Data: Personal observations; Eisenmann, 1975; Sun et al., 2017; Cirilli et al. (2021).

Specimens: M 1321

Equus livenzovensis

Data: Personal observations, Azzaroli, 2000 ; Cirilli et al. (2021)

Specimens: L4; L95; L229; L739; L779; RGU335; RGU570; L291; L860; L1278; RGU11; L911; UCBL-FSL 21173; IGF11074; IGF11075; IGF11224; IGF11225; IGF11226; IGF11236; IGF11275; IGF11276; IGF11277; IGF11282; IGF11285; IGF14689; IGF14690; IGF15371; IGF4093V; IGF954V.

Equus stenonis

Data: Athanassiou (2001); Cirilli et al. (2021) and personal observations.

Specimens: IGF 560; IGF 530; IGF 538; IGF 560; IGF 583; IGF11024; IGF515; IGF 10336; IGF 11039; IGF 11040; IGF 11041; IGF 11044; IGF 11045; IGF 11051; IGF 11057; IGF 11066; IGF 11073; IGF 11314; IGF 11315; IGF 12824; IGF 12825; IGF 12826; IGF 12827; IGF 12828; IGF 12829; IGF 12830; IGF 12831; IGF 1818V; IGF 543; IGF 568; IGF 568; IGF 683/2; IGF 7558V; IGF 7559V; IGF 7608V; IGF11222; IGF11223; IGF11272; IGF11274; IGF11291; IGF11292; IGF11293; IGF4045V; IGF4046V; IGF4047V; IGF 11001; IGF 11005; IGF 11011; IGF 11013; IGF 11014; IGF 11033; IGF 11036; IGF 11037; IGF 11316; IGF 12833; IGF 12834; IGF 12835; IGF 12836; IGF 12837; IGF 1314V; IGF 1315V; IGF 1316V; IGF 13732; IGF 13734; IGF 13735; IGF 14209; IGF 14226; IGF 14227; IGF 15231; IGF 15232; IGF 1817V; IGF 4885V; IGF 544; IGF 548; IGF I567; IGF 569; IGF 7607V; IGF 7715V; IGF 7932V; IGF 8097V; IGF11226; IGF11263; IGF11264; IGF11265; IGF11267; IGF11268; IGF11269; IGF11270; IGF11271; IGF11287; IGF11288; IGF11289; IGF11290; IGF 14232; IGF 523; IGF 535; IGF 537; IGF 564; IGF 583; IGF11023; IGF11025; IGF562; NHML 20.163361; NHML 20.163735; NHML 20.163772; NHML 20.163362; NHML 20.163362b; NHML 20.163464; NHML 20.163464b; NHML 20.163741; NHML 20.163758; NHML 20.163757; NHML 20.163761; NHML 20.163770; NHML 20.163371; NHML 20.163972; NHML 20.163964; NHML 20.163968; NHML 20.163972; NHML 20.163975; NHML 20.163976; NHML 20.163981; NHML 20.163978; NHML 20.163481; NHML 20.163485; NHML 20.163480; NHML 20.163482; NHML 20.163483; NHML 20.163484; NHML 20.163421; NHML 20.163422; NHML 20.163423; NHML 20.163425; NHML 20.163419; NHML 20.163418; NHML 20.163412; NHML 20.163417; NHML 20.163420; NHML 20.163416; NHML 20.163438; NHML 20.163439; NHML 20.163491; NHML 20.163985; NHML 20.163986; NHML 20.163987; NHML 20.163988; NHML 20.163982; NHML 20.163983; NHML 20.163990; NHML 20.163984; NHML 20.163991; NHML 20.163970; NHML 20.163971; NHML 20.163962; NHML 20.163967; NHML 20.163969; NHML 20.163958; NHML 20.163955; NHML 20.163954; NHML 20.163490; NHML

20.163488; NHML 20.163492; NHML 20.163493; NHML 20.163489; NHML 20.163487; NHML 20.163486; NHML 20.163437; NHML 20.163436; NHML 20.163440; NHML 20.163354; NHML 20.163355; NHML 20.163358; NHML 20.163356; NHML 20.163360; NHML 20.163372; NHML 20.163724; NHML 20.163731; NHML 20.163364; NHML 20.163463; LGPUT DFN-112; LGPUT DFN3-334; AMPG Se-2; AMPG ΣA-1; AMPG ΣA-3; AMPG ΣA-4; AMPG Σ-203.

Equus senezensis

Data: Cirilli et al. (2021) and personal observations.

Specimens: NHML SZ30; NHML SZ2; NHML SZ38; NHML SZ5; NHML SZ24; UCBL-FSL 210832; UCBL-FSL 210842; UCBL-FSL 210835; UCBL-FSL 210843; UCBL-FSL 210841; UCBL-FSL 210834; UCBL-FSL 210844; UCBL-FSL 210845; UCBL-FSL 210842; UCBL-FSL 210849; UCBL-FSL 210850; UCBL-FSL 210851; UCBL-FSL 210859; UCBL-FSL 210857; UCBL-FSL 210895; UCBL-FSL 210886; UCBL-FSL 210884; UCBL-FSL 210890; UCBL-FSL 210887; UCBL-FSL 210888; UCBL-FSL 210889; UCBL-FSL 210882; UCBL-FSL 210883; UCBL-FSL 210917; UCBL-FSL 210920; UCBL-FSL 210897; UCBL-FSL 210921; UCBL-FSL 210922; UCBL-FSL 546597; UCBL-FSL 546610; UCBL-FSL 546647; UCBL-FSL 546655; UCBL-FSL 546673; UCBL-FSL 1116

Equus altidens Dmanisi

Data: Cirilli et al. (2021).

Specimens: D2589; D2590; D3697; Dm55/61.1.B1g1.111; D2471; D2620; D3870; D4691; D613; D614; D1350; D1591; D2261; D22618; D2309; D3060; D3152; D3379; D4390; D4864; D529; D5365; D5705; D6851; D717e2; D793; D887; Dm1088; Dm159; Dm50/63i-106; Dm53/59.3.B1g1.178; Dm53/59.3.B1g1.183; Dm61; Dm62; Dm62/63B2a12133; Dm64/64.3B1X48 5620; Dm65/61 VI 43 3066; Dm69/61.2.B1K.67; Dm70/34.3A4.45; Dm8/151.1.A4.26; D2034; D2501; Dm60/5 1I 20; Dm3V246; Dm53/60.3B.Gl.89; Dm64/60Va3918; D3065; D1973; D1838; D1586; D3953; Dm62/62.4B14 174 5640; Dm64/62.381X243 5372; D1235; D1586; D2172; D2172; D2239; D2298; D2311; D2328; D2807; D3344; D335; D3988; D3988; D3993; D3993; D4758; D5200; D5364; D5640; D68; D709; D71; D886; Dm2281; Dm50/62 IV5756 2305; Dm64/63.381x479; Dm64/63.3B1x479 5364; Dm64/63.3blk5407 5144; Dm64/64.1.B1Z.157; Dm65/70.VI.107; Dm66/60 V 162 2622; Dm67/61; Dm67/61 IV 47 3344; Dm68/61 IV 26 2810; Dm7/150.3.B.1; Dm709; Dm71; Dm812; Dm89; DmM6/5.B2.43; D353; D66; Dm53/59.3B1g1.192;

Equus altidens Gerakarou and Krimni

Data: Personal observations.

Specimens: LGPUT GER-8; LGPUT GER-9; LGPUT GER-31; LGPUT GER-122.

Equus koobiforensis

Data: Eisenmann, 1983; Cirilli et al. (2021).

Specimens: KNM-ER1484; KNM-ER5519; KNM-ER5361; KNM-ER2691; KNM-ER2687; KNM-ER4025; KNM-ER1129; KNM-ER1255; KNM-ER2062; KNM-ER2688; KNM-ER1281; KNM-ER1226; KNM-ER1258; KNM-ER1241; KNM-ER1268; KNM-ER5360; KNM-ER333; KNM-ER4026; KNM-ER3986; KNM-ER4015; KNM-ER4027; KNM-ER4046; KNM-ER1275; KNM-ER1276; KNM-ER5358; KNM-ER4052; KNM-ER1275.

Equus apolloniensis

Data: Personal observations.

Specimens: LGPUT APL-147; LGPUT APL-148; LGPUT APL-518; LGPUT APL-519; LGPUT APL-605; LGPUT APL-858 juv.; LGPUT APL-871; LGPUT APL-842; AMPG Aλ-20.

Equus hydruntinus

Data: van Asperen et al. (2012); Eisenmann 2022 and personal observations.

Specimens: 1-05-21 (Kabazi, Russia); MNP-Bonifay LVIV 18698 (Lunel Viel); Ba2 384 Emine-Bair-Khosar, Crimea)

Equus asinus

Data: Vera Eisenmann Website https://vera-eisenmann.com/ and personal observations.

Equus grevyi

Data: Cirilli et al. (2021); Vera Eisenmann Website https://vera-eisenmann.com/ and personal observations.

Specimens: USNM152231; USNM161927; USNM162963; USNM163228; USNM163331; USNM163332; USNM163333; USNM163334; USNM163338; USNM173041; USNM182026; USNM182027; USNM182028; USNM182063; USNM199079; USNM241009; USNM49796; USNM49944.

Equus quagga

Data: Cirilli et al. (2021); Vera Eisenmann Website https://vera-eisenmann.com/ and personal observations.

Specimens: USNM015120; USNM061743; USNM061744; USNM269165; USNMA22977; USNM161928; USNM162950; USNM162951; USNM162952; USNM5342228; USNM534228; USNM534228B; USNM534828; USNM61743; USNMA22870; USNMA22977; USNM161927; USNM162954; USNM162955; USNM162959; USNM162960; USNM162961; USNM162962; USNM162954; USNM163235; USNM163236; USNM163237; USNM163239; USNM164520; USNM164632; USNM181840; USNM252096; USNM259848; USNM38211; USNM38212.

Equus zebra

Data: Cirilli et al. (2021); Vera Eisenmann Website https://vera-eisenmann.com/ and personal observations.

Specimens: USNM197983; USNM270125; USNM270514; AMNH83602; AMNH7691.

Equus hemionus

Data: Cirilli et al. (2021); Vera Eisenmann Website https://vera-eisenmann.com/ and personal observations.

Specimens: USNM327091; USNM521103; USNM541427; USNM581897; USNM581994; MCZ6345; MNHN383; LG19046; LG27139.

Equus kiang

Data: Cirilli et al. (2021); Vera Eisenmann Website https://vera-eisenmann.com/ and personal observations.

Specimens: USNM084081; USNM084088; USNM49493; USNM49796; USNM84083; USNM84088; USNM49493; USNM304614; NHMUK1939.2472; NHMUK1879.11.21.182; NHMUK1905.6.20.1; NHMUK1894.2.8.3; NHMUK1860.4.5.77; NHMUK1851.7.16.4; NHMUK1848.6.11.17; NHMUK1848.6.11.6; NHMUK976.

Equus przewalskii

Data: Cirilli et al. (2021); Vera Eisenmann Website https://vera-eisenmann.com/ and personal observations.

Specimens: AMNH90198; AMNH16234; NHMUK1945.6.11.1; NHMUK1907.5.15.1; AC1926-228; AC1941-332; AC1935-486; AC1932-46; MGU1772; ZIN27089; ZIN27031; ZIN5218; ZIN5214; ZIN5213; ZIN5212; MCZ5108; AMNH21523; AMNH32686; AMNH16234; MA1977.55;

ZU10800; ZU10801; NHMUK1960.2.1.4; NHMUK1902.9.25.1; NHMUK1963.1.25.1; NHMUK1961.5.10.2; AC1896-269; ZIN57/29; MGU1772.

Equus ferus

Data: Cirilli et al. (2021); Vera Eisenmann Website https://vera-eisenmann.com/ and personal observations.

Specimens: USNM399046; ZIN521; AMNH204174; AMNH204210.

Supplementary information (excel files):

SI 1: Data matrix

SI 2: A. List of specimens; B. Microwear ALL SPECIMENS; C. Microwear SELECTED SPECIMENS; C1. SUMMARY; C2. Dunn's post hoc test; D. Mesowear scores

APPENDIX 2

TABLE 1

Equus apolloniensis

(a) fragmentary cranium (juv.) APL: (a1) left lateral view, (a2) ventral view

(b) fragmentary cranium APL-605: (b1) right lateral view, (b2) ventral view

(c) maxilla (occlusal view) APL-129

TABLE 1

a2

a1

b1

b2

c

10cm

TABLE 2

Equus apolloniensis

(a, b) right cheek tooth row Vo-3: (a) occlusal view, (b) lateral view

(c) third metacarpal APL-777

(d) third metacarpal APL-801

(e) third metacarpal APL-157

(f) third metatarsal APL-848

(g) third metatarsal APL-92

(h) third metatarsal APL-237

(i) third metatarsal Vo-4

***Equus* sp. B (Apollonia)**

(j) third metacarpal APL-74

TABLE 2

TABLE 3

Equus altidens

(a) maxilla KRI-1 (occlusal view)

(b) left P4-M1 series KRI-2

(e) third metacarpal KRM-8

(f) third metacarpal KRI-16

(g) third metatarsal KRI-9

(h) third metatarsal KRM-1

Equus stenonis

(c) left P3-M3 series KRI-21

Equus sp. (Krimni-3)

(d) humerus and radioulna in articulation KMN-48

TABLE 3

TABLE 4

Equus altidens

(a) third metacarpal, first anterior phalanx and second anterior phalanx in articulation KMN-8: (a1) third metacarpal, (a2) first phalanx, (a3) second phalanx

(b) third metatarsal KMN-44

(c) astragalus KMN-44d

(d) femur, tibia, tarsals, third metatarsal and posterior phalanges in articulation KMN-44

TABLE 4

TABLE 5

Equus altidens

a) left fragmentary mandibular body with p2-m2 series TSR F20-15

(b) third metacarpal and anterior phalanges in articulation TSR-F18-53

(c) third metacarpal TSR-F17-31a

(d) third metatarsal TSR-F17-12

Equus aff. *E. (a.) granatensis* var. *E. apolloniensis*

(e) third metatarsal TSR-179

TABLE 5

TABLE 6

Equus altidens

(a) third metacarpal PEC-506

(b) third metacarpal PEC-505

(c) third metacarpal PEC-501

(d) third metacarpal LIB-869

(e) third metacarpal LIB-872

(f) third metatarsal LIB-858

(g) third metatarsal LIB-807

TABLE 6

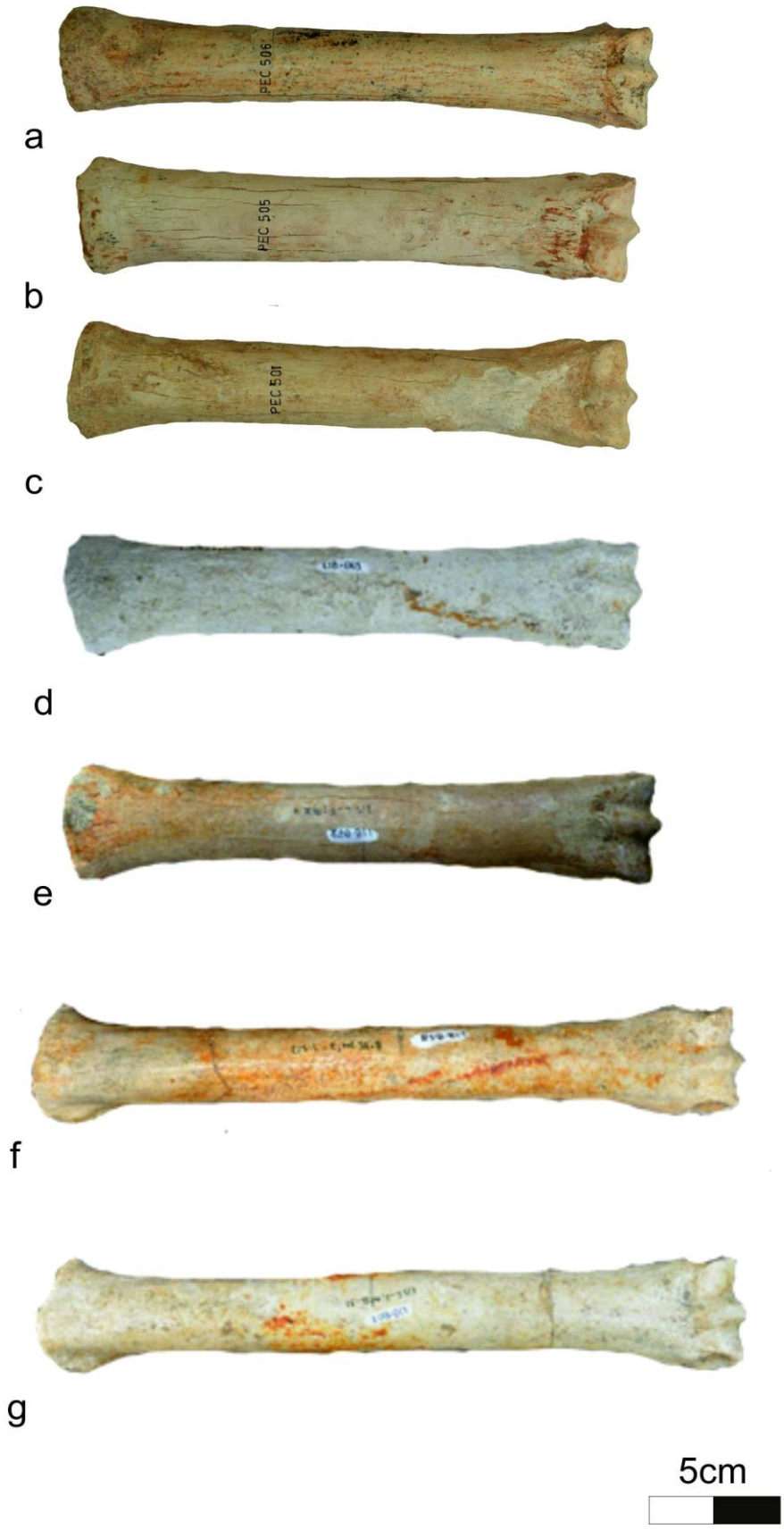

TABLE 7

Equus cf. *E. senezensis*

(a) third metatarsal PgI.7

(b) astragalus PgI.3

(c) calcaneum PgI.4

Equus aff. *E. stehlini*

(d) distal part of third metacarpal PgI.23

Equus aff. *E. stenonis* var. *E. apolloniensis* (Vatera F)

(e) astragalus PO 469 F

(f) calcaneum PO 151 F

(g) third metatarsal PO 136 F